Differentiation of pluripotent stem cells into functional thymic organoids for T cell maturation in vitro

Nathan Provin

▶ **To cite this version:**

Nathan Provin. Differentiation of pluripotent stem cells into functional thymic organoids for T cell maturation in vitro. Médecine humaine et pathologie. Nantes Université, 2022. Français. NNT : 2022NANU1039 . tel-04861105

HAL Id: tel-04861105
https://theses.hal.science/tel-04861105v1

Submitted on 2 Jan 2025

HAL is a multi-disciplinary open access archive for the deposit and dissemination of scientific research documents, whether they are published or not. The documents may come from teaching and research institutions in France or abroad, or from public or private research centers.

L'archive ouverte pluridisciplinaire **HAL**, est destinée au dépôt et à la diffusion de documents scientifiques de niveau recherche, publiés ou non, émanant des établissements d'enseignement et de recherche français ou étrangers, des laboratoires publics ou privés.

THESE DE DOCTORAT DE

NANTES UNIVERSITE

ECOLE DOCTORALE N° 605
Biologie Santé
Spécialité : Immunologie

Par : **Nathan PROVIN**

Différenciation de cellules souches pluripotentes induites en organoïdes thymiques fonctionnels pour la maturation de lymphocytes T *in vitro*

Thèse présentée et soutenue à Nantes, le 15 Décembre 2022
Unité de recherche : CR2TI, UMR1064, CHU Nantes

Rapporteurs avant soutenance :

Anne Galy Directrice de recherche INSERM UMR951, Généthon, EVRY, Directrice de l'Accélérateur de recherche technologique en thérapie génomique, Docteur en Pharmacie

John De Vos Professeur des universités - Praticien hospitalier, CHU de Montpellier, IRMB

Composition du Jury :

Président :	Antoine Toubert	Professeur des universités - Praticien hospitalier, Hôpital Saint-Louis, Paris
Examinateurs :	Antoine Toubert	Professeur des universités - Praticien hospitalier, Hôpital Saint-Louis, Paris
Dir. de thèse :	Matthieu Giraud	INSERM CR1, CR2TI, UMR1064, CHU Hotel Dieu, Nantes

“A process cannot be understood by stopping it. Understanding must move with the flow of the process, must join it and flow with it.”

Frank Herbert, Dune (1965)

Résumé

Le thymus est un organe lymphoïde primaire qui joue un rôle crucial dans l'établissement de la tolérance immunitaire. Les thymocytes y sont sélectionnés par les cellules épithéliales thymiques (TEC). Certaines pathologies congénitales sont causées par une déficience des gènes régulant le développement ou la fonctionnalité des TEC et entraînent un équilibre immunitaire défectueux et une auto-immunité. L'utilisation de cellules souches pluripotentes induites (iPSc) pour la thérapie cellulaire est une approche prometteuse pour traiter ces pathologies. Dans ces travaux, je décris la production de TECs fonctionnelles dérivés d'iPSc exprimant *AIRE* et capables de supporter la maturation de cellules T *in vitro.* Nous avons optimisé un protocole permettant la génération de progéniteurs épithéliaux thymiques (TEP) grâce à une méthode basée sur un design optimal d'expériences et un profilage transcriptomique complet du produit de différenciation. Notre protocole de différenciation dirigée, reposant sur la modulation des voies de signalisation régulatrices de l'organogenèse thymique, a permis d'obtenir des TEP exprimant les marqueurs d'identité thymique. Nous avons ensuite induit leur maturation en TEC par une culture 3D dans un hydrogel en coculture avec des progéniteurs thymiques précoces (ETP) humains, ce qui a permis la formation d'organoïdes thymiques. Ces organoïdes supportent la maturation des ETP en cellules T CD4 ou CD8 simple-positives. La génération in vitro de TEC et d'organoïdes thymiques fonctionnels offre une plateforme prometteuse pour l'étude des interactions cellulaires dans le thymus et ouvre la voie à la production de lymphocytes T pour de futures thérapies cellulaires des patients atteints de maladies auto-immunes.

Abstract

The thymus is a primary lymphoid organ that plays a crucial role in establishing immune tolerance. Thymocytes are selected by thymic epithelial cells (TEC). Congenital pathologies caused by a deficiency in the genes regulating the development or functionality of TECs result in defective immune balance and autoimmunity. The use of induced pluripotent stem cells (iPSc) for cell therapy is a promising approach to treat these pathologies. We describe here the production of functional TECs derived from iPSc expressing AIRE and capable of supporting T cell generation in vitro. We have optimized a protocol for the generation of thymic epithelial progenitors (TECs) using a method based on optimal experimental design and transcriptomic profiling of the differentiation product. Our directed differentiation protocol, based on the modulation of regulatory signaling pathways involved in thymic organogenesis, resulted in TEPs expressing thymic identity markers. We then induced their maturation into TECs by 3D hydrogel coculture with human early thymic progenitors (ETPs), resulting in the formation of thymic organoids. These organoids support the maturation of ETPs into CD4 or CD8 single-positive T cells. The generation of functional TECs and thymic organoids provides a convenient platform for the study of cellular interactions in the thymus and paves the way for future cellular therapies for autoimmune diseases.

Remerciements

Je tiens à remercier sincèrement les membres du jury pour avoir accepté de juger mes travaux de thèse. Merci aux rapporteurs, le Dr. Anne GALY et le Dr. John DE VOS, pour leur travail de relecture et leurs suggestions précieuses pour améliorer cette thèse. Merci au Dr. Antoine TOUBERT pour avoir accepté l'invitation d'être examinateur lors de la soutenance. Je suis honoré de soutenir ma thèse devant un tel collège de scientifiques.

Je remercie mon directeur de thèse, le Dr. Matthieu GIRAUD, pour son encadrement au cours de ses années de thèse. Tu as su m'accorder ta confiance pour mener ce projet, alors que j'arrivais comme un inconnu dans l'équipe. Tu m'as permis de mûrir en tant que scientifique, de donner le meilleur de moi-même et de toujours rester motivé. Je me souviendrai longtemps des journées de réflexions théoriques et d'exploration des possibilités du projet. Pour tout cela je te serai toujours reconnaissant. Je tiens aussi à remercier les membres de mon comité de suivi de thèse, le Dr. Anne CAMUS et Dr. Magali IRLA, pour leur accompagnement depuis la genèse du projet. L'intérêt que vous avez porté à mes travaux, votre soutien et vos conseils m'ont été d'une grande aide.

Je tiens de même à remercier le Pr Régis Josien pour m'avoir accueilli au sein du Centre de Recherche Translationnelle en Transplantation et Immunologie (CR2TI UMR1064).

Merci aussi à tous mes collègues du bureau "des filles et Nathan" à travers toutes ses itérations : Apo, Sonia, Eugénie, Flora, Vanessa, Gwen, Sabrina, Mélanie, les

petits déjeuners du Vendredi ne seront pas oubliés. Merci tout particulièrement à Séverine et Laurence pour votre patience et votre soutien pendant mes nombreux tris du soir à l'ARIA, et les longues discussions scientifiques toujours enrichissantes.

Merci à Laurent et à tous les membres de la plate-forme iPSc pour m'avoir accueilli parmi vous et appris tous les secrets de la culture de ces cellules. Anne, Caro, Isa je n'aurai pas tenu 2 semaines sans votre aide et vos conseils.

Merci également à tous les autres membres de l'équipe 2 et d'autres équipes avec qui j'ai pu collaborer pendant ces quelques années. Merci à mes amis et camarades doctorants avec qui j'ai traversé les épreuves, tout particulièrement l'équipe de l'IRS1, Constance, Alex, Gaël, Dim, Simon, Océane et Eva sur qui j'ai toujours pu compter pour des pauses et de la compagnie pendant les astreintes du week end. Merci à l'équipe originelle, source d'inspiration à la fois au labo et autour d'un jeu de fléchettes : Marine, Alex, Marion, Malo, Pierre, Alice, Anaïs et Eléa. Nos soirées aident vraiment à faire retomber la pression, et la boire. Un immense merci à tous mes amis en dehors du labo que je ne peux pas tous nommer ici. Votre soutien, votre insistance à sortir en semaine et à bouger le week-end m'ont vraiment permis de garder un pied dans le monde réel.

Enfin, un profond merci à mes proches pour leur soutien indéfectible. Merci à tous les membres de ma famille qui m'ont si souvent encouragés, et ont dû se contenter de nos coups de téléphone coutumiers pour rester en contact. Votre aide m'a été indispensable.

Mathilde, merci d'avoir été à mes côtés. Merci d'avoir supporté les sacrifices et d'avoir toujours su être présente ces dernières années.

Table des matières

Liste des abréviations

3PP : 3ème poche pharyngienne

aDC : Activated dendritic cell

ADN : Acide désoxyribonucléique

AGM : aorte-gonade-mésonéphros (AGM)

APECED : Autoimmune polyendocrinopathy-candidiasis-ectodermal dystrophy

APS-1 : Autoimmune polyglandular syndrome type 1

ATO : Artificial thymic organoid

BMP : Bone morphogenetic protein

BTB : Blood-Thymus barrier

CARD : Caspase activation recruitment domain

CAR-T : Chimeric antigenic receptor T cell

CHD : Congenital heart disease

CMH : Complexe majeur d'histocompatibilité

CPM : Cyclopamine

cTEC : Cortical thymic epithelial cell

DC : Dendritic cell

DETC : T épithéliaux dendritiques

DN : Double negative (thymocyte)

DOE : Design optimal d'experiences

EMT : epithelio-mesenchymal transition

DP : Double positive (thymocyte)

ECM : Extra cellular matrix

ESc : Embryonic stem cell

ETP : Early thymic progenitor

FGF : Fibroblast growth factor

FL : Foetal liver

FSH : Follistatin

GFP : Green fluorescent protein

HEC : Hemogenic endothelial cells

HSC : Hematopoietic stem cell

iPSc : Induced pluripotent stem cell

iTEC : iPSc-derived thymic epithelial stem cell

LMPP : progéniteurs multipotents primés lymphoïdes

LTi : cellules inductrices de tissus lymphoïdes

mTEC : Medullary thymic epithelial cell

$mTEC^{hi}$: Medullary thymic epithelial cell, $HLA\text{-}DRA^{hi}$

$mTEC^{lo}$: Medullary thymic epithelial cell, $HLA\text{-}DRA^{lo}$

NKT : Natural killer T cell

nTreg : Natural regulatory T lymphocyte

OFAT : One Factor at the Time

OTFCS2 : Syndrome otofaciocervical de type 2

pCMH : Complexe peptide:CMH

pDC : Plasmacytoid dendritic cell

PPE : Pharyngeal pouch endoderm

PTA : Peripheral tissue antigen

APC : Antigen presenting cell

RA : Retinoic acid

SCID : Severe combined immunodeficiency syndrom

scRNAseq : Single-cell RNA sequencing

SHH : Sonic Hedgehog

SP : Simple-positive (thymocyte)

TAC : TIssue amplifying cell

TCR : T cell receptor

TE : Thymic emigrant

TEC : Thymic epithelial cell

TEP : Thymic epithelial progenitor

TNC : Thymic nurse cell

TSP : Thymus seeding progenitor

UV : Ultra violet (radiation)

WNT : Wingless-int

WT : Wild type

YS : Yolk sack, sac vitellin

Table des figures

INTRODUCTION

Avant-propos

Le système immunitaire protège l'organisme contre les pathogènes étrangers et les cellules tumorales. Cette fonction repose en partie sur la capacité à développer une réponse intense et spécifique à des antigènes : c'est la réponse immunitaire adaptative. Cette réponse dépend d'un système complexe et intégré de cellules et de molécules interagissant étroitement. Un des acteurs clés de ce système sont les lymphocytes T, nommés selon l'organe qui les produit, le thymus (1). Ces lymphocytes T présentent un répertoire de récepteurs diversifiés, capable de reconnaître virtuellement n'importe quel antigène étranger ou tumoral, tout en ignorant ceux produits par les cellules saines de l'organisme. Ils sont tolérants au soi. Cette propriété remarquable découle de mécanismes complexes de signalisation et de communication cellulaire entre de multiples populations d'origine différente. Le concept de différenciation est vital pour la compréhension des mécanismes à l'origine de la tolérance au soi. En effet, ces processus s'inscrivent dans une dimension temporelle. Des cellules progénitrices qui se différencient restreignent leur potence, *i.e* limitent leur capacité à s'orienter en différentes lignées cellulaires. Au terme du processus de différenciation, les cellules deviennent spécialisées et acquièrent leur fonctionnalité : c'est la maturation. Dans un premier temps, cette introduction détaille comment la tolérance au soi émerge de mécanismes complexes de communication cellulaire au sein du thymus. Puis nous présenterons les processus de différenciation des populations cellulaires impliquées, dans leur dimension temporelle et régulationnelle. Enfin, nous détaillerons comment tirer bénéfice de ces connaissances pour développer de nouveaux modèles d'étude de la tolérance au soi, ainsi que des approches thérapeutiques novatrices pour la médecine régénérative.

Chapitre 1 : Le microenvironnement thymique, niche spécialisée pour la différenciation des lymphocytes T

La découverte du rôle vital du thymus dans l'établissement de la réponse immunitaire adaptative est relativement récente. Jusqu'aux années 1960, le thymus est vu comme un organe vestigial, erreur de l'évolution sans fonctionnalité précise et servant de cimetière à lymphocytes. De fait, la thymectomie effectuée sur l'animal adulte n'a pas d'effet sur leur système immunitaire, et les lymphocytes prélevés dans le thymus ne se montrent pas immunocompétents (1). C'est en 1961 que Miller démontre le rôle critique du thymus, en observant que les souris thymectomisées à la naissance sont déficientes en lymphocytes et que leur réponse immunitaire est sévèrement altérée (2). Un nouveau paradigme émerge alors : les lymphocytes T sont originaires du thymus et sont les médiateurs de la réponse adaptative en présentant un répertoire diversifié de récepteurs aux antigènes. Le mécanisme à l'origine de la diversité de ce répertoire est expliqué par Tonegawa en 1978, qui montre comment des recombinaisons aléatoires de l'ADN lors du développement des lymphocytes permettent de générer une grande diversité de récepteurs (3). La fonction principale du thymus est de sélectionner ce répertoire pour qu'il soit diversifié mais non auto-réactif, ce qui engendrerait une auto-immunité généralisée. Ce chapitre décrit comment la fonctionnalité du thymus émerge des interactions complexes entre ses populations cellulaires au sein de leurs microenvironnements spécifiques.

I. Les cellules épithéliales thymiques sont les principaux acteurs de la fonctionnalité du thymus

1. Histologie et morphologie de l'épithélium thymique

Le thymus est un organe bilobé localisé dans la partie antéro-supérieure du médiastin, au-dessus du cœur. Il est délimité par une capsule de matrice entourant deux compartiments histologiques distincts, la zone corticale externe et la zone médullaire interne. La medulla est composée d'un îlot central connecté à de nombreuses foci qui forment une structure branchiale grossièrement subdivisée (4). Elle est séparée du cortex par la jonction cortico-médullaire irriguée par de nombreux capillaires. Les lymphocytes T en cours de développement, les thymocytes, représentent l'écrasante majorité de la cellularité du thymus (5). Ils circulent à travers les niches corticales et médullaires qui instruisent les différentes étapes de leur maturation. Les cellules stromales thymiques sont les principales architectes de ces niches. Parmi celles-ci, les cellules épithéliales thymiques (TEC) jouent un rôle prépondérant. Ces cellules relativement rares comptent pour 0.5% de la cellularité du thymus et forment la structure du stroma thymique (5). L'épithélium thymique a une structure diffuse et apolaire unique, les autres épithéliums de l'organisme s'organisant en couches polarisées et stratifiées, comme les épithéliums intestinaux ou pulmonaires. Les TEC forment une structure en maillage peu dense, "en éponge", maximisant la surface de contact avec les thymocytes. Ces cellules de grande dimension, de l'ordre de 100 microns, peuvent donc interagir simultanément avec un grand nombre de thymocytes (6). Ces interactions physiques intimes sont centrales pour la fonction des TEC comme support de la maturation des thymocytes. Les TEC fournissent aux thymocytes l'ensemble des signaux nécessaires à cette

maturation, sous forme de ligands membranaires ou de facteurs solubles : cytokines, facteurs de croissance ou chimiokines. En cytométrie en flux, on les distingue par leur phénotype $CD45^-$ et $EPCAM^+$.

Les TEC peuvent être subdivisées en deux principales sous-populations selon leur localisation dans le thymus : les TEC corticales, abrégées cTEC et les TEC médullaires, les mTEC (Figure 1). Historiquement, ces deux sous populations ont été distinguées par leur profil d'expression de cytokératines, les cTEC marquant pour KRT8 et KRT18, et les mTECs pour KRT5 et KRT14 (7) (Figure 2). Ces deux populations présentent des phénotypes différents et jouent des rôles distincts dans le contrôle de la maturation des cellules T. La différenciation des thymocytes est un processus graduel nécessitant l'intégration d'une série de signaux fournis par les TEC et organisés spatialement et temporellement. Ainsi, les progéniteurs hématopoïétiques les plus précoces sont produits dans la moelle osseuse et migrent dans le sang jusqu'au thymus. Après y être entrés par la jonction cortico-médullaire, ils migrent dans le cortex par chimiotaxie sous l'effet de signaux sécrétés par les cTEC. Au contact de celles-ci, les thymocytes se restreignent à la lignée T, entrent en expansion et génèrent un récepteur T (TCR) par recombinaison. Le répertoire de TCR est ensuite filtré, d'abord par les cTEC puis par les mTEC, ce qui permet la génération d'un répertoire de T fonctionnels et non auto-réactifs. Chacune de ses étapes de la différentiation T, qui seront présentées en détail plus loin dans ce chapitre, sont finement contrôlées par différentes populations de TEC spécialisées.

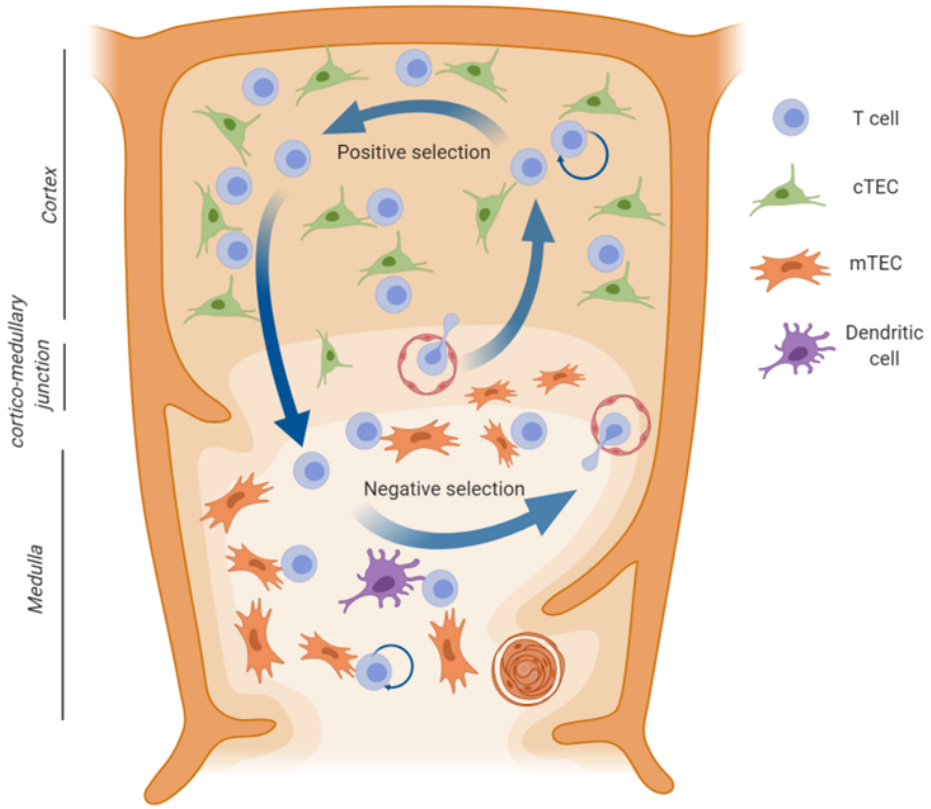

Figure 1: Structure histologique d'un lobule thymique Le thymus est séparé en deux zones, le cortex et la médulla, séparés par la jonction cortico-médullaire, et abritant des cTEC et mTEC. Ces deux populations orchestrent des stades différents de la maturation des thymocytes (adapté de Provin et Giraud, 2022).

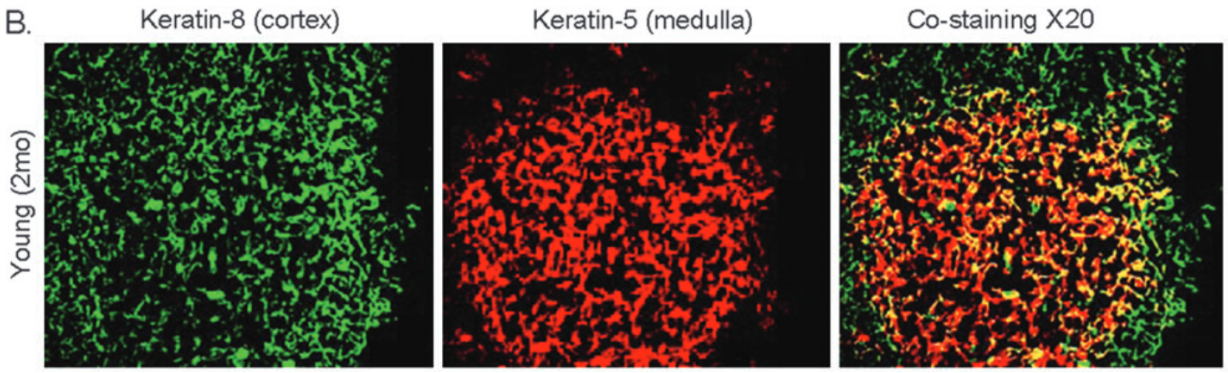

Figure 2 : Séparation cortex-médulla Les cTEC et les mTEC peuvent être différenciées par leur profil d'expression des cytokératines KRT5 et KRT8 (d'après Gui et al, 2007).

2. Les TEC corticales : régulatrices de la thymopoïèse précoce

Les cTEC sont la première population de TEC avec laquelle interagissent les progéniteurs thymiques précoces (ETP). Ceux-ci sont attirés dans le thymus par un gradient de chimiokines sécrétés par les cTEC. CXCL12, CCL19 et CCL25 sont les principales molécules orientant les ETP et induisant leur entrée dans le thymus au niveau de la jonction-cortico médullaire, puis leur migration vers le cortex, où ils entrent physiquement en contact avec les cTEC (8,9). En exprimant à leur surface des ligands de la voie NOTCH, les cTECs favorisent l'engagement des ETP dans la lignée des cellules T (15). Le premier ligand à avoir été mis en évidence est DLL4, un activateur de NOTCH1 et NOTCH4 (10,11). L'expression d'autres molécules activatrices de NOTCH a aussi été caractérisée, comme DLL1, JAG1 et JAG2, ce dernier étant restreint aux cTEC (12). Les cTEC sécrètent aussi des interleukines qui contrôlent la maturation des thymocytes comme IL7 et IL15 (13). Ces facteurs fournissent des signaux de survie, de prolifération et de maturation pour les thymocytes (6,14). D'autres facteurs de croissance sont produits par les cTEC pour induire l'expansion des thymocytes précoces, le principal étant SCF (6).

Ainsi, les trois premières fonctions des cTEC peuvent être résumées en contrôle de la migration, de la prolifération et de la restriction de la potence des thymocytes au destin T (Figure 3).

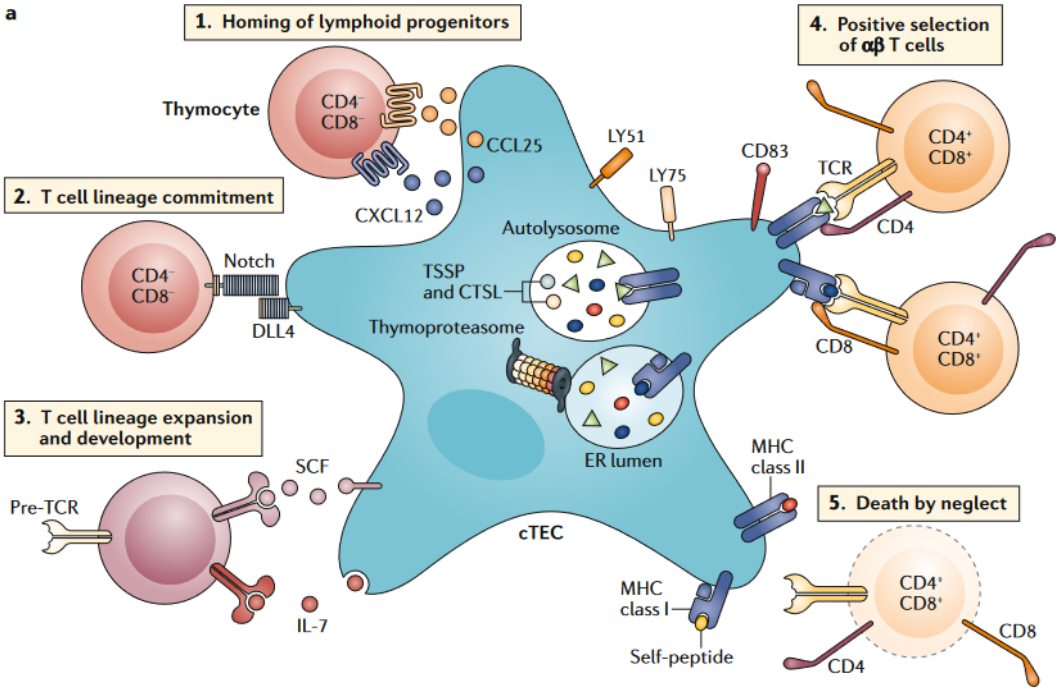

Figure 3 : Synthèse des fonctions des cTEC. Les cTEC sont responsables de la migration des thymocytes précoces dans le cortex, de leur restriction au destin T, promeuvent leur prolifération et sélectionnent les thymocytes dont le TCR est fonctionnel (d'après Kadouri et al., 2019)

Les cTEC sont aussi indispensables au stade suivant de maturation des thymocytes, le réarrangement combinatoire de leur TCR. En effet, une sous population particulière de cTEC, les cellules nourricières thymiques (TNC) fournissent un microenvironnement favorable pour l'étape de sélection positive des thymocytes (15). A ce stade, les thymocytes présentent un répertoire de TCR recombiné aléatoirement, dont de nombreux sont incapables de reconnaître le complexe majeur d'histocompatibilité (CMH) et donc dysfonctionnels. Cette étape de sélection est dite positive, car les cTEC présentent des complexes peptides:CMH aux thymocytes et seuls ceux dont le TCR est fonctionnel reçoivent un signal de survie. Les TNC interagissent de façon très intime avec les thymocytes en les internalisant : une

seule TNC peut ainsi absorber jusqu'à 200 thymocytes (6). Ce rôle est critique pour la thymopoïèse : en l'absence des TNC, le nombre de thymocytes est réduit de 80% (16). Les mécanismes moléculaires de la sélection positive reposent sur le thymoprotéasome. Le protéasome d'une cellule est composé de complexes multiprotéiques lysant les protéines et les dégradant en peptides. Le thymoprotéasome en est une forme particulière exprimée exclusivement par les cTEC. La sous-unité β5, encodée par *PSMB11*, est un constituant du thymoprotéasome spécifique des cTEC. Elle est responsable de la production cytoplasmique d'un ensemble de peptides qui seront assemblés avec le CMHI et présentés à la surface des cTEC. Ces complexes peptide:CMHI ont été montrés avoir une faible affinité pour le TCR et induire la sélection des T CD8 (17). Les cathepsines sont des endopeptidases lysosomales exprimées de manière ubiquitaire. Dans le thymus, les cTEC expriment principalement la cathepsine L (*CTSL*) qui est liée à la production de peptides et leur assemblage avec le CMHII. CTSL est donc cruciale pour la sélection positive des T CD4 (17). La sérine protéase thymus-spécifique TSSP codée par *PRSS16* a aussi été montrée jouer un rôle similaire (18). Ainsi, grâce à leur machinerie cellulaire spécialisée, les cTEC génèrent et présentent des complexes peptides:CMHI et II, sélectionnant les thymocytes portant un TCR capable de reconnaître le CMH. Enfin, le marqueur principal des cTEC est CD205 (*LY75*), un récepteur endocytique capable de capturer des antigènes dans le milieu extracellulaire. Si il est largement utilisé comme marqueur, son rôle fonctionnel est encore flou, la déficience en CD205 n'ayant pas d'effet sur la thymopoïèse (19).

L'hétérogénéité des cTEC est probablement largement sous-estimée. Deux sous-ensembles majeurs de cTECs ont été observés chez la souris qui se

distinguent par une expression différentielle de *Dll4*, *Ccl25*, *Ly6a* et *Cxcl12* (20). Cependant, on ignore encore si ces sous-ensembles de cTEC Dll4^{hi} et Dll4^{lo} ont des rôles fonctionnels distincts, ou représentent différents stades de maturation. De par leur morphologie particulière, les complexes T-cTEC sont en effet probablement éliminés lors des manipulations et sont donc absents des atlas du thymus en cellule unique.

3. les TEC médullaires CCL21^{+} : médiatrices du chimiotactisme des thymocytes

Le compartiment mTEC présente une hétérogénéité encore plus importante, dont l'étude est rendue d'autant plus délicate que nous n'avons pas à disposition chez l'homme de marqueurs membranaires spécifiques. Historiquement, les mTEC étaient classées selon l'intensité de marquage pour les molécules du CMHII comme HLA-DRA et costimulatoires comme CD86. Deux principaux compartiments étaient distingués, les mTEC^{hi} matures et les mTEC^{lo} immatures. Cependant, la population mTEC^{lo} est restée longtemps peu caractérisée.

Les récentes avancées des technologies de séquençage ARN en cellule unique (scRNAseq) et leur application à l'étude du thymus ont permis de décrire peu à peu cette hétérogénéité. Dès 2018 Bornstein *et al.* caractérisent quatres sous-populations de mTEC. Le principal cluster de mTEC^{lo} est identifiable par l'expression de la chimiokine *CCL21* et des intégrines *ITGB4* et *ITGA6*. Ces mTEC-CCL21^{hi} ont une signature transcriptomique proche des cTECs, et seraient localisées au niveau de la jonction cortico-médullaire. Elles joueraient un rôle dans la migration des thymocytes vers la médulla, via le récepteur CCR7. Elles ne montrent pas d'expression d'antigènes du soi, ni des principaux régulateurs de leur

expression. Ces cellules ont longtemps été considérées comme de potentiels progéniteurs des autres mTEC. Les liens progéniteurs-produits des multiples populations de TEC sont encore débattus, et seront explorés plus en détails dans le chapitre suivant.

4. Les mTEC^{hi} : actrices de la sélection négative

La deuxième population de mTEC sont les mTEC^{hi}. Ces cellules expriment des marqueurs épithéliaux spécifiques comme les claudines 3 et 4 (CLDN3-4) et les kératines 5 et 14 (KRT5-14). Caractérisées par une forte expression du CMH-II et des molécules de costimulation CD80 et CD86, ce sont des cellules présentatrices, comme les cTEC. Les mTEC^{hi} possèdent la caractéristique unique d'exprimer quasiment l'ensemble du génome, y compris les protéines exprimées exclusivement dans certains tissus : les antigènes des tissus périphériques (PTA). Cette expression ectopique des antigènes du soi est au cœur de la fonction des mTEC^{hi}. Ce mécanisme repose sur le principal marqueur de la population mTEC^{hi}, le facteur d'activation régulateur de l'auto-immunité (AIRE), qui contrôle l'expression des PTA. En présentant sur leurs CMH en surface les antigènes du soi, les mTEC^{hi} scannent le répertoire des thymocytes et éliminent ceux présentant un TCR auto-réactif : c'est la sélection négative, aussi appelée délétion clonale. C'est la fonction principale des mTEC^{hi}, qui permet la tolérance centrale au soi en éliminant les lymphocytes potentiellement auto-immuns (Figure 4). Cette sélection peut aussi être effectuée par d'autres cellules présentatrices d'antigènes (APC), qui récupèrent les PTA exprimés par les mTEC^{hi}.

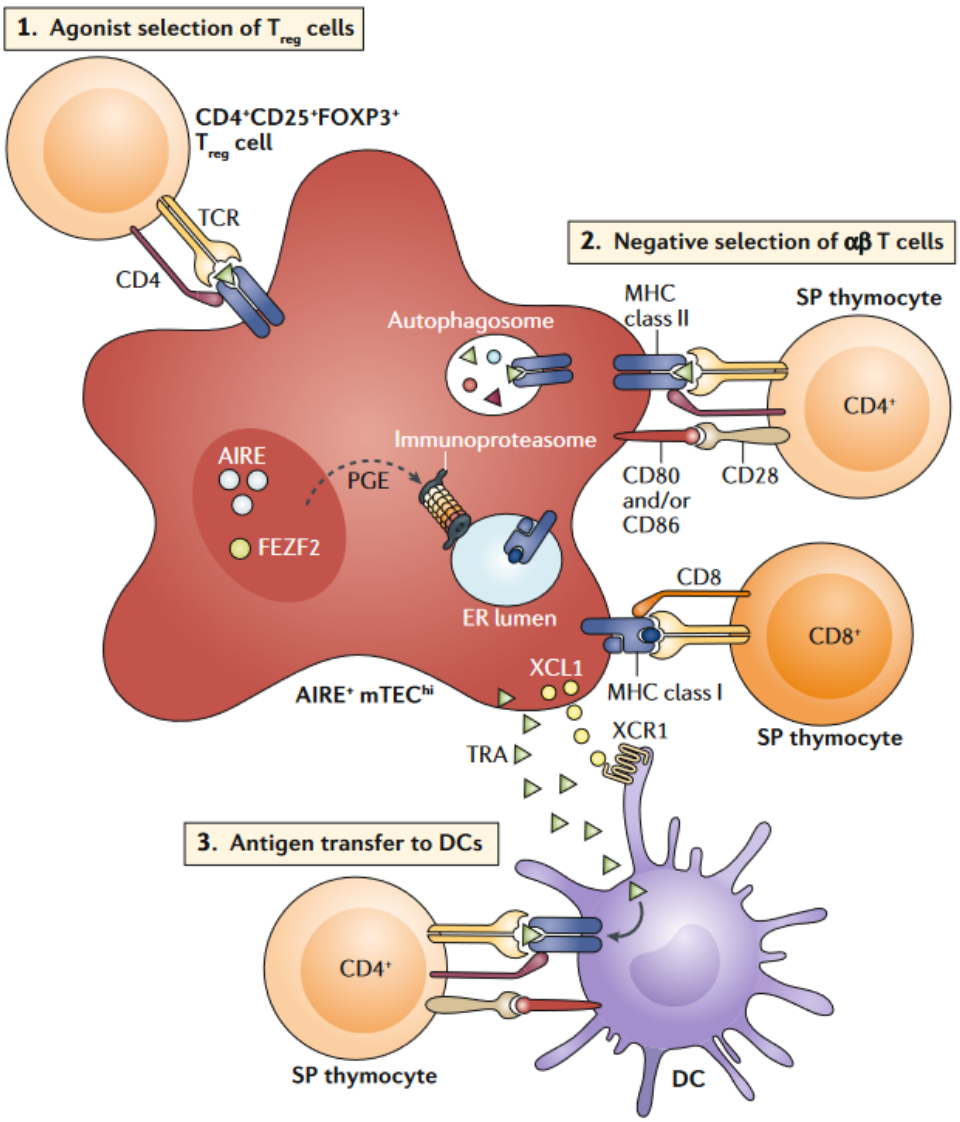

Figure 4 : Synthèse des fonctions des mTEC^{hi}. Les mTEC^{hi} sont les principales médiatrices de la sélection négative. Elles présentent de nombreux antigènes du soi périphériques aux thymocytes et induisent l'apoptose des thymocytes auto-réactifs (d'après Kadouri et al., 2019)

5. Autres sous-populations de mTEC spécialisées

De nombreuses autres populations minoritaires de mTEC ont été récemment identifiées, et leurs origines et fonctions respectives sont encore peu connues. Parmi les sous-populations de $mTEC^{lo}$, un premier niveau d'hétérogénéité à été mis en évidence en identifiant une population en état terminal de différenciation : les mTEC-cornéocytes. Les $mTEC^{hi}$ réduisent l'expression de *AIRE* et des gènes du CMHII puis expriment des marqueurs comme la cytokératine 10 (*KRT10*) et l'involucrine (*IVL*) (21–23). Leur phénotype se rapproche des stades avancés de différenciation des kératinocytes de la peau, les cornéocytes. Ces mTEC-cornéocytes se restreignent à l'expression des PTA dermiques, et ont été montrées être aussi capables de sélectionner les thymocytes (24,25). En plus de leur fonction de sélection, ces cellules jouent un rôle de signalisation distinct en contribuant à maintenir un microenvironnement pro-inflammatoire, favorisant la sélection T (26). En effet, les mTEC-cornéocytes perdent leur noyaux, se kératinisent et forment des kystes, formant une niche spécifique de la médulla, les corpuscules de Hassal.

Une autre sous-population récemment découverte sont les mTEC "tuft", qui présentent des microvilli à leur pôle apical et sont nommés ainsi de par leur ressemblance avec les cellules brosses intestinales. Ces cellules sont caractérisées par l'expression d'interleukines 4 et 25, et modulent la maturation de cellules tueuses naturelles (iNKT) (20,27). Les mTEC-tufts expriment aussi de multiples récepteurs chimiosensoriels et notamment du goût comme *TAS2R* et *TRPM5*, sans qu'aucun lien fonctionnel n'ait pu être y être relié. Enfin, leur fonction principale pourrait être liée à la présentation d'antigènes du soi, ces cellules exprimant les gènes du CMHII et CD74, bien qu'à des niveaux inférieurs aux $mTEC^{hi}$ (20,28).

Les mTEC ciliées expriment des gènes liés à l'assemblage de cils (*SPAG16*, *WDR34*), sont caractérisées par le facteur de transcription *FOXJ1*, et présentent des similitudes avec les cellules épithéliales respiratoires (28,29). Elles forment des kystes dans la medulla et semblent elles aussi capables de sélectionner les thymocytes, la surexpression d'un antigène par cette population étant suffisant pour induire une tolérance spécifique (25).

Enfin, d'autres sous-populations de mTEC ont été récemment caractérisées grâce à l'étude du stroma thymique en scRNAseq, des mTEC au phénotype musculaire (mTEC myoïdes), neuroendocrine (mTEC neuro) ou proches des cellules de Schwann produisant la myéline (mTEC myéline+) (30,31). Si leur caractérisation précise n'a pas encore été réalisée, il a été montré qu'elles expriment aussi des ensembles de PTA et sont liées à la sélection des T (25).

Ainsi, un nouveau paradigme semble sur le point d'émerger sur la nature des mTEC et leur rôle dans la sélection des thymocytes. Le modèle dominant depuis plus de 20 ans statuait qu'une population immature $mTEC^{lo}$ maturait en $mTEC^{hi}$ en surexprimant les gènes du CMHII et *AIRE*, qui induisent une expression aléatoire des PTA (32). De nouveaux éléments semblent indiquer que la réalité est plus complexe, avec plusieurs lignées de mTEC coexistantes et des $mTEC^{hi}$ se compartimentant en plusieurs populations phénotypiquement distinctes et spécialisées dans l'expression et la présentation de plusieurs modules de PTA (Figure 5) (25,33). Nous allons maintenant décrire plus en détails les mécanismes d'action de *AIRE* et les modalités d'expression des PTA dans les $mTEC^{hi}$.

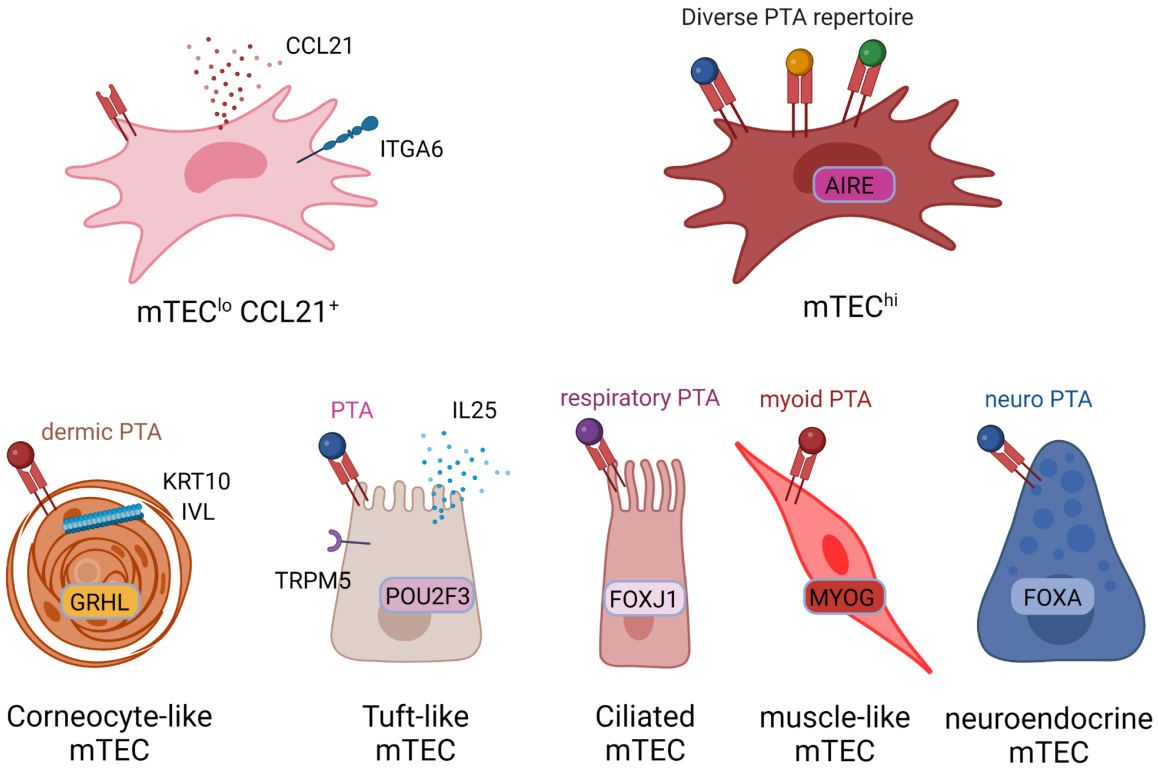

Figure 5 : Hétérogénéité des sous-populations de mTEC. De multiples sous-populations de mTEC ont été identifiées. Au-delà des mTEC^{lo} CCL21^{+} et des mTEC^{hi} AIRE^{+} déjà décrites, de rares sous-populations de mTEC sont caractérisées par l'expression de facteurs de transcription typiques et présentent des modules de PTA spécifiques de certains tissus. Ces populations seraient ainsi des acteurs complémentaires de la sélection négative des thymocytes.

II. L'expression des autoantigènes est principalement régulée par AIRE

1. Expression et mécanisme d'action de AIRE

Les mTEC^{hi} ont la capacité unique d'exprimer jusqu'à 90% du génome, soit 18 000 gènes, à de faibles niveaux d'expression et sans acquérir de fonctionnalité spécialisée. Cette compétence unique repose majoritairement sur *AIRE*. Ce gène joue un rôle crucial illustré par les conséquences graves de sa déficience. En effet,

les porteurs homozygotes d'une version de *AIRE* mutée développent un syndrome auto-immun sévère, le syndrome de polyendocrinopathie de type 1, APS-1 ou APECED (34). AIRE est principalement exprimé dans le thymus, dans la sous-population de $mTEC^{hi}$ HLA-DRA^{hi}, où il a été montré réguler l'expression de 3000 à 4000 PTA AIRE-dépendant (35,36).

AIRE n'est pas un facteur de transcription classique. Aucun motif de liaison commun n'a été identifié en amont des gènes qu'il régule, ni de domaine de liaison direct à l'ADN dans sa séquence. *AIRE* est composé de multiples domaines liés à sa fonctionnalité. Un domaine CARD concentre de nombreuses mutations chez les patients APECED, illustrant son importance. Or ces domaines sont liés à la formation d'oligomères et à la liaison à des séquences oligonucléotidiques (37). Le fait que le marquage *AIRE* apparaisse sous forme ponctuée dans le noyau souligne l'importance de cette polymérisation (38). *AIRE* contient aussi un domaine SAND, potentiellement lié à la fixation de la protéine dans un complexe macromoléculaire plus large (39). Enfin, deux domaines PHD sont situés dans sa partie C-terminale. Ces domaines interagissent avec des marques d'histones H3K4 méthylées spécifiques d'une chromatine fermée au niveau des gènes non exprimés, levant les marques épigénétiques suppressives des gènes ectopiques réprimés (40). Ainsi, *AIRE* peut être classé comme un facteur d'activation non-conventionnel, agissant au sein de complexes macromoléculaires recrutant de nombreux coactivateurs comme CBP, TOP2A, SIRT1 (41,42) et induisant l'expression ectopique des PTA en levant les marques épigénétiques suppressives. Surtout, *AIRE* bloque la pause de la RNAse polymérase II dans les promoteurs des PTA (43,44) et y recrute des facteurs facilitant la transcription (Figure 6) (42). Ce gène est donc crucial pour la fonction du thymus.

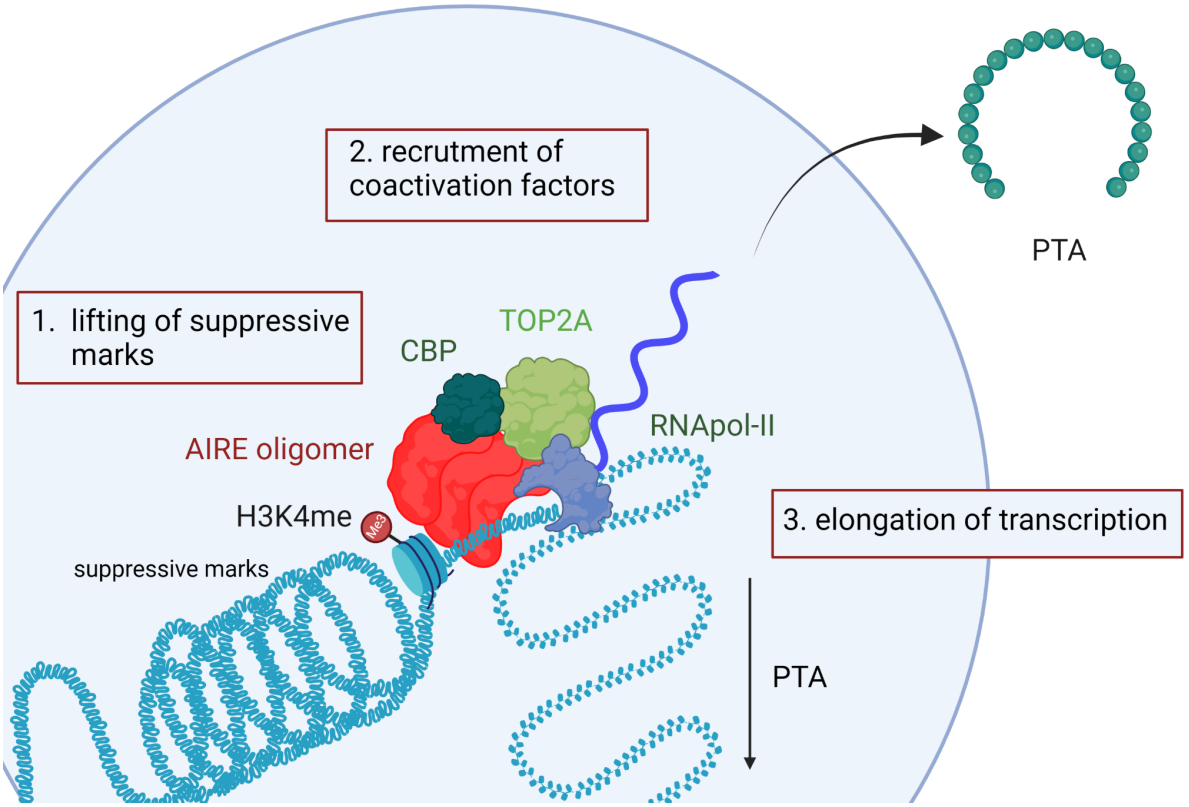

Figure 6 : Mécanismes d'action de AIRE. les oligomères de AIRE localisés dans des corpuscules nucléaires des mTEC^{hi} se fixent sur la chromatine réprimée des loci des PTA. Ils lèvent les marques suppressives et forment des complexes multiprotéiques en recrutant des facteurs de coactivation comme CBP et TOP2A. Ces complexes stimulent la transcription médiée par l'ARNpol-II et favorisent l'élongation de la transcription (inspiré par Abrahamson et Golfarb, 2015)

2. Motifs d'expression des gènes tissus spécifique

Si les mTEC^{hi} expriment collectivement un large répertoire de PTA, les modalités des motifs d'expression entre cellules et pour chaque gène est restée longtemps sans réponse. Quelle proportion du répertoire total les mTEC^{hi} expriment-elles individuellement? L'expression des PTA est-elle totalement aléatoire, ou corrélée en

plusieurs modules de gènes? Ici aussi les avancées en scRNAseq des dernières années ont permis d'apporter de premiers éléments de réponse, en analysant en profondeur et à haute résolution le profil d'expression des PTA cellule par cellule. Ainsi, analyser seulement 200 mTEC matures suffit à détecter jusqu'à 95% des PTA, soulignant que pour être sélectionné négativement un thymocyte n'a à interagir qu'avec un nombre restreint de mTEC^{hi} (35,45). Pourtant, individuellement les PTA *AIRE*-dépendants sont exprimés par seulement 1% des mTEC^{hi} (45). Cependant, les niveaux d'expression des PTA sont relativement élevés dans les mTEC^{hi}, ce qui est cohérent avec la contrainte d'induire une signalisation assez forte pour sélectionner les thymocytes autoréactifs (46,47). Bien que l'expression des PTA semble stochastique, il a été montré qu'elle est en fait ordonnée en plusieurs modules de gènes co-exprimés. La composition de ces modules de gènes semble cependant aléatoire, sans association démontrée avec la localisation chromosomique, des processus biologiques ou des tissus particuliers (28). Cette expression stochastique assure ainsi que les thymocytes interagissent avec l'ensemble du répertoire de PTA sans biais de sélection. Nonobstant ces résultats, un nouveau modèle de l'expression des PTA semble en train d'émerger, notamment à travers la caractérisation par scRNAseq de multiples populations rares de mTEC, décrites précédemment de façon non exhaustive. Bautista et *al.* ont ainsi étudié l'enrichissement en PTA dans ces sous-populations, et montré que certains PTA étaient restreints à certaines populations (30). Un nouveau modèle semble alors prendre forme, dans lequel les mTEC^{hi} *AIRE*$^{+}$ présentent bien un large répertoire d'autoantigènes, stochastique mais ordonné, mais auquel s'additionne des populations de mTEC spécialisées mimant différents tissus et exprimant leurs PTA spécifiques (Figure 7) (33). Des expériences de traçage ont prouvé que ces

populations rares avaient pour origine les mTEC^{hi} *AIRE*$^{+}$ (25,27,48). Bien que le mécanisme précis d'action de *AIRE* reste à identifier, il est possible qu'il induise l'expression de facteurs de transcription tissus-spécifiques, à l'instar de *POU2F3* pour les mTEC tufts ou *FOXJ1* pour les mTEC ciliées (Figure 7) (33). Ces populations rares de mTEC "mimétiques" pourraient avoir été sélectionnées au cours de l'évolution sous la pression de sélection de l'auto-immunité dans des tissus sensibles ou ayant des microenvironnements inflammatoires, comme les épithélia intestinaux, dermiques ou respiratoires. Une caractérisation précise de ces populations, de leurs motifs d'expression de PTA et des validations expérimentales sont encore nécessaires afin d'affiner ce modèle de l'organisation de la sélection négative dans le thymus.

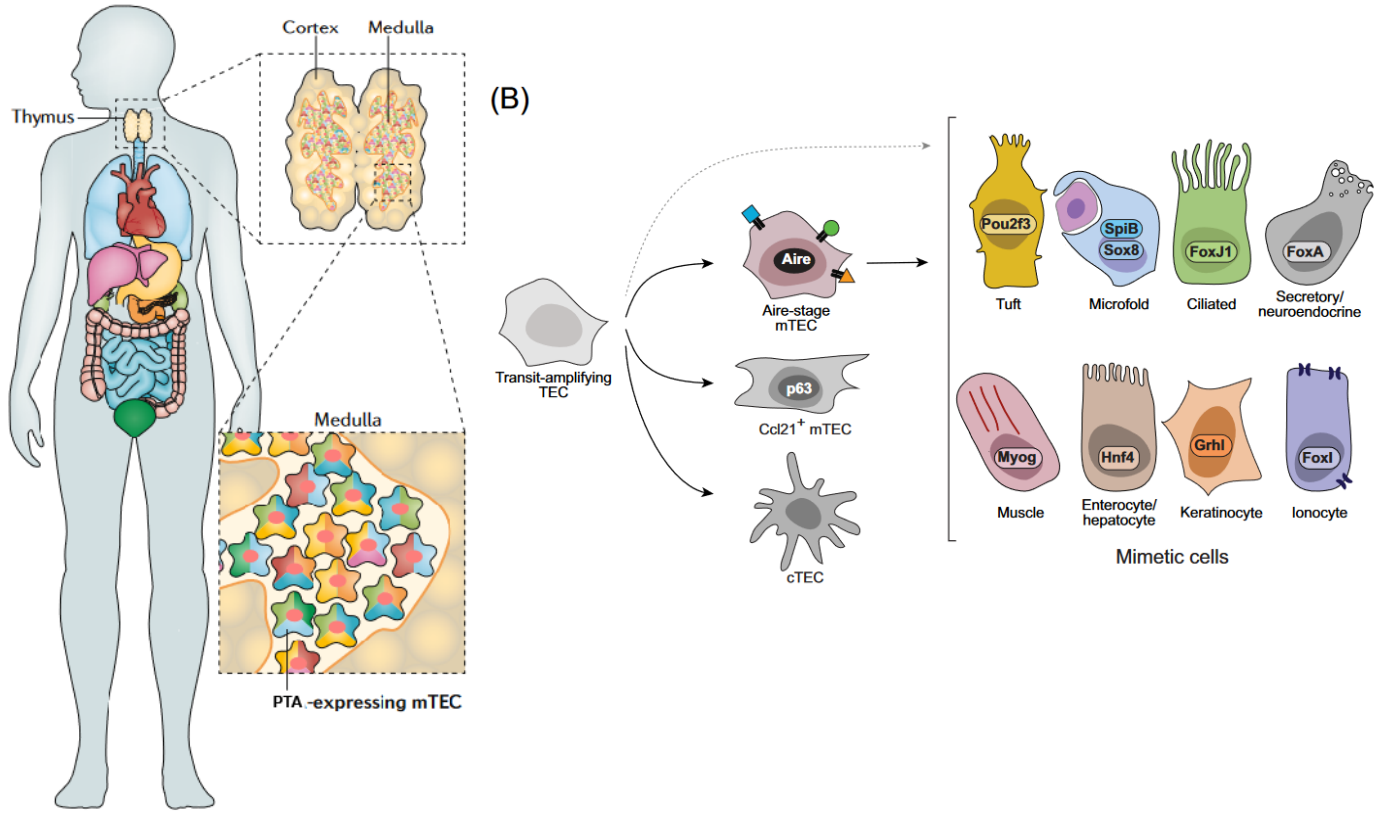

Figure 7 : Modèle actuel de l'expression des PTA dans les mTEC

La medulla héberge des mTEC qui expriment l'ensemble des protéines des tissus périphériques (PTA). La principale population responsable de l'expression des PTA sont les $mTEC^{hi}$ $AIRE^{+}$, qui sont capables de se différencier en mTEC "mimétiques" caractérisées par des facteurs de transcription, des motifs de chromatine et l'expression de modules de PTA spécifiques de tissus périphériques (d'après Michelson et Mathis, 2022 et Kadouri et al., 2019)

III. La thymopoïèse est le processus de différenciation des lymphocytes T

Nous avons décrit la structure du thymus, ses différentes populations de cellules épithéliales et les mécanismes moléculaires uniques leur permettant d'exprimer le soi et de sélectionner les thymocytes en développement. Mais quels mécanismes orchestrent précisément la différenciation de ces derniers ? Quelle est la population progénitrice des T?

1. Origine hématopoïétique des lymphocytes T

Après que le modèle dual des lymphocytes ait émergé en 1966, notamment suite au travaux de Cooper qui identifie les deux grandes populations de lymphocytes, B et T (49) et la compréhension du rôle du thymus comme organe de génération des T par Miller (2), la question de l'origine des lymphocytes T s'est naturellement posée. Deux hypothèses étaient alors étudiées : une origine extrathymique, ou intrathymique par transformation de l'épithélium. La réponse sera apportée par les travaux de Le Douarin *et al.*, qui en utilisant un modèle de xénogreffes cailles-poulet et la

différence de nombre de chromosomes de ces espèces, ont pu identifier l'origine hématopoïétique des T (50). Ainsi, un progéniteur hématopoïétique migre vers le thymus et s'y différencie (51). La caractérisation phénotypique de cette population a longtemps été débattue. Dès 1995, Galy et *al.* ont montré le potentiel multipotent de la population progénitrice de la moelle osseuse $CD34^{+}CD45^{+}$ pour les lignées Natural killer (NK), dendritiques (DC) et lymphoïdes B et T (52). De multiples études se sont depuis succédées pour caractériser le phénotype des différents stades de différenciation des progéniteurs des T, en suivant des marqueurs comme CD7, CD10 ou CD24 (53,54).

Aujourd'hui les différents stades de différenciation des progéniteurs hématopoïétiques ont été caractérisés en détail. La dynamique transcriptionnelle, le régulome, le phénotype et les trajectoires de différenciation ont pu être identifiées par CITE-seq et scRNAseq (31,55–57). La population $CD34^{+}$ de progéniteurs hématopoïétiques ensemençant le thymus (TSP) a ainsi révélée être hétérogène. Une première population, TSP1, CD7 négative mais exprimant *HOXA9*, *CD44*, *CCR9* et *CCR7*, correspond aux progéniteurs canoniques. Une autre population, TSP2, dépourvue d'expression de *HOXA9*, *CCR9* et exprimant *CD7*, *CD44*, *IRF8* et *CD3E* avant même la migration dans le thymus a aussi été identifiée. De manière intéressante, ces deux populations montrent la capacité de migrer vers le thymus et se différencier vers la lignée T. Cependant, cette population TSP2 semble primée vers la lignée dendritique, et contiendrait un progéniteur $CD34^{+}CD123^{+}$ restreint à la lignée DC récemment identifiée (58). Les TSP circulants sont principalement quiescents, mais entrent en prolifération après être entrés dans le thymus et deviennent des progéniteurs de T précoces (ETP). Les ETP perdent l'expression des facteurs de transcription des cellules souches hématopoïétiques comme *MEIS1*

et *HOXA9* et le marqueur CD10, et activent de manière transitoire un programme souche autour des facteurs *HHEX*, *SPI1* et *LYL1*, marquant un potentiel toujours multipotent (55). Surtout, les ETP expriment des récepteurs NOTCH comme CD7, et migrent vers le cortex où ils interagissent avec les ligands présentés par les cTEC. Sous l'effet de cette signalisation les ETP expriment les principaux régulateurs critiques de la lignée T, *GATA3* dans un premier temps, puis *BCL11B*, *TCF7* et *TCF12* : ils deviennent alors unipotents, restreints à la lignée T. Leur immunophénotype évolue, en perdant progressivement CD34, CD44 puis CD62L (*SELL*). Ils deviennent alors des thymocytes doubles négatifs (DN) car n'exprimant pas encore le CD4 ni le CD8.

2. Le stade double-négatif de la thymopoïèse

Dans le cortex, les DN précoces commencent à exprimer les gènes *CD1* et *RAG.* Leur maturation peut être subdivisée en 4 stades en fonction de l'expression de CD44 et CD25. Lors des stades les plus précoces, les DN subissent plusieurs cycles de prolifération médiés par les signaux fournis par les cTEC, via l'IL7 ou SCF. C'est entre le stade DN2 et DN3 que commence le réarrangement du TCR: sous l'effet de *RAG2*, les loci *Tcrb* et *Tcrg* subissent une recombinaison génomique complexe sélectionnant une partie variable (V), de jonction (J), et dans certains cas de diversité (D). La séquence V(D)J aléatoire résultante doit passer ensuite de multiples points de contrôle afin de garantir sa fonctionnalité. La première d'entre elles est la β-sélection au stade DN3. Lors de ce point de contrôle, le pre-TCR composé de chaînes CD3 et d'une chaîne TCRβ, bien qu'incapable de reconnaitre un ligand, émet un faible niveau de signalisation intracellulaire fournissant un signal de survie et levant le bloquage de la différenciation au stade suivant (Figure 8) (59). La levée

de ce blocage lié au protéines E2A dépendrait aussi d'une signalisation NOTCH et CXCR4, dont les ligands sont fournis par les cTEC (60,61).

C'est à ce stade qu'a lieu la divergence entre les lignées Tαβ et Tγδ (62). Les mécanismes précis orientant la divergence de lignée ne sont pas encore bien compris. L'intensité de la signalisation lors de la β-sélection semble impliquée, le signal du TCRγδ étant plus intense (63), possiblement de par sa fixation à un ligand intrathymique (64). Les facteurs de transcription *SOX13*, *EGR1* et *EGR3* ont aussi été montré promouvoir la lignée Tγδ, mais il n'est pas encore prouvé qu'ils soient directement responsable de l'orientation vers cette lignée ou s'ils induisent sa survie et son expansion (65).

Les thymocytes survivants à ces étapes entrent dans une dernière phase d'amplification et commencent à exprimer CD4 et CD8 : ils deviennent alors des thymocytes doubles-positifs (DP) (Figure 8).

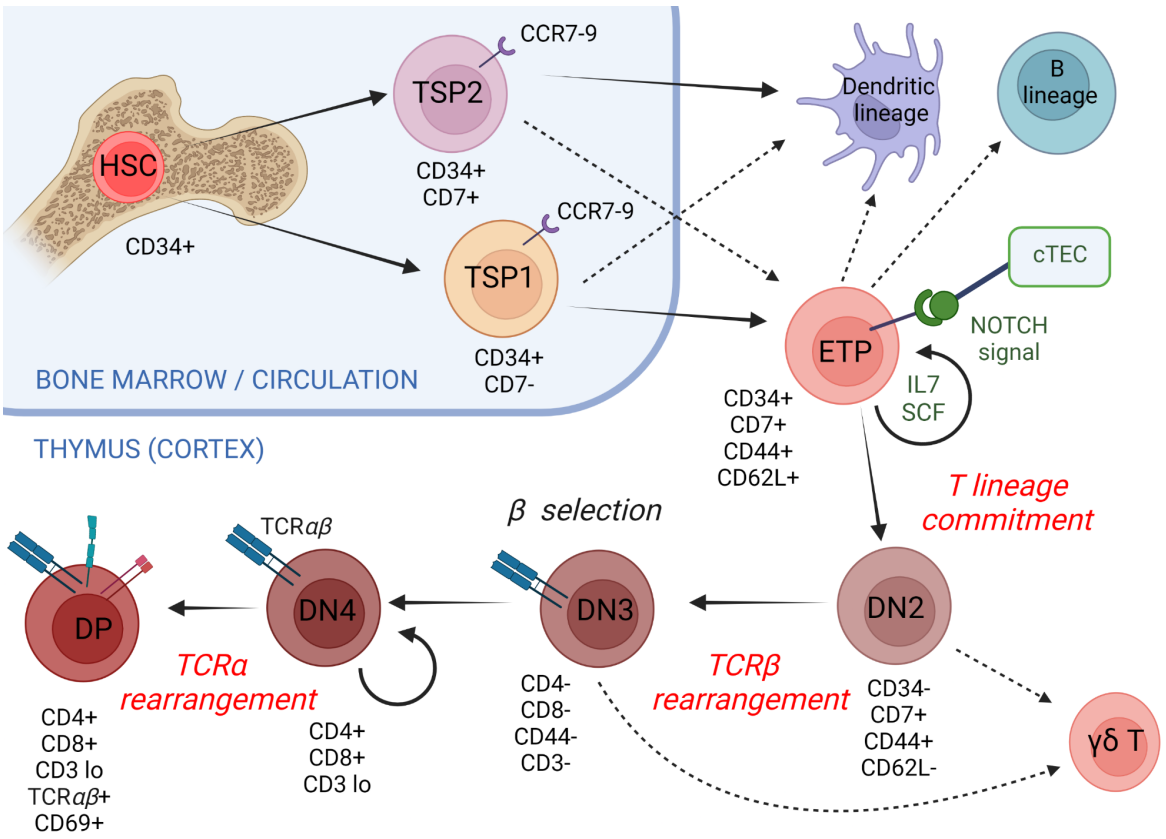

Figure 8 : Régulation et marqueurs clés de la thymopoïèse précoce

Les cellules souches hématopoïétiques (HSC) de la moelle génèrent des progéniteurs multipotents migrants dans le cortex thymique et deviennent des progéniteurs thymiques précoces (ETP) qui se spécifient vers la lignée T. Ils subissent plusieurs stade d'amplification et de réarrangement du TCR et se différencient en thymocytes double-négatifs (DN), puis double-positifs en exprimant CD8 et CD4 (DP).

3. Stade double-positif et sélection positive

Au stade DP les thymocytes commencent à acquérir un phénotype de lymphocyte T mature. Ils ne sont plus sensibles aux signaux cruciaux pour le développement des thymocytes plus précoces, comme l'IL7, en arrêtant d'exprimer son récepteur et en exprimant *SOCS-1*, un inhibiteur de la réponse aux cytokines (66). C'est à ce stade que le dernier niveau de diversité des TCR est généré, via le réarrangement du locus *TCRA,* entraînant la formation de TCRαβ en surface. Or, ce réarrangement

aléatoire produit une majorité de TCR défectueux : soit non-fonctionnels *i.e* incapables de reconnaître des complexes CMH:peptides (pCMH), soit autoréactifs *i.e* réagissant contre un peptide exprimé par l'organisme, et donc entraînant une autoimmunité. Les deux phases de sélection du répertoire sont orchestrées par les cTEC et les mTEC, et ont été évoquées précédemment. Nous décrirons ici en détail les mécanismes moléculaires et la signalisation orientant la différenciation des thymocytes lors de la sélection.

Les thymocytes DP ont une durée de vie courte, de 3 à 4 jours. Ils dépendent en effet de la réception d'un signal de survie qui les "secourt". En l'absence de ce signal de survie, les DP meurent par négligence. Ce signal de secours est fourni par l'interaction du TCR avec les complexes pCMH présentés par les cTEC. Les peptides produits par le thymoprotéasome des cTEC présentent une affinité plus faible avec les TCR que les ligands que les T rencontrent en périphérie, ce qui détermine la sensibilité des futurs T CD8 aux antigènes (67). Les TCR interagissant avec une avidité suffisante avec les pCMH produisent une signalisation qui aboutit à l'expression de molécules antiapoptotiques, sauvant les thymocytes de leur destin de mort par défaut (68,69). La multiplicité des cascades de signalisation actives lors de la sélection positive rend difficile l'isolement du signal précis permettant la survie des thymocytes, et ce malgré les récentes avancées permises par la caractérisation à haute résolution du régulome des DP (70).

En effet, la sélection positive induit aussi l'orientation des DP vers le destin T CD4 "auxiliaire" ou T CD8 "cytotoxique". L'avidité du TCR pour des complexes pCMHI ou pCMHII, médiée respectivement par la coactivation avec CD8 ou CD4, est responsable de la signalisation initiale induisant en aval des programmes transcriptionnels spécifiques. Les facteurs de transcription *THPOK* et *RUNX3* sont

chez la souris les principaux régulateurs du changement de destin vers la lignée T CD4 et T CD8, respectivement (71). De récents résultats semblent indiquer que ce mécanisme est conservé chez l'homme (72). Ces deux gènes, en interagissant avec d'autres régulateurs comme *GATA3* et *STAT5* (73,74), entraînent la baisse de l'expression du CD4 ou CD8 et l'acquisition d'un phénotype T CD8 ou T CD4. Les thymocytes deviennent alors simple-positifs (SP) (Figure 9) .

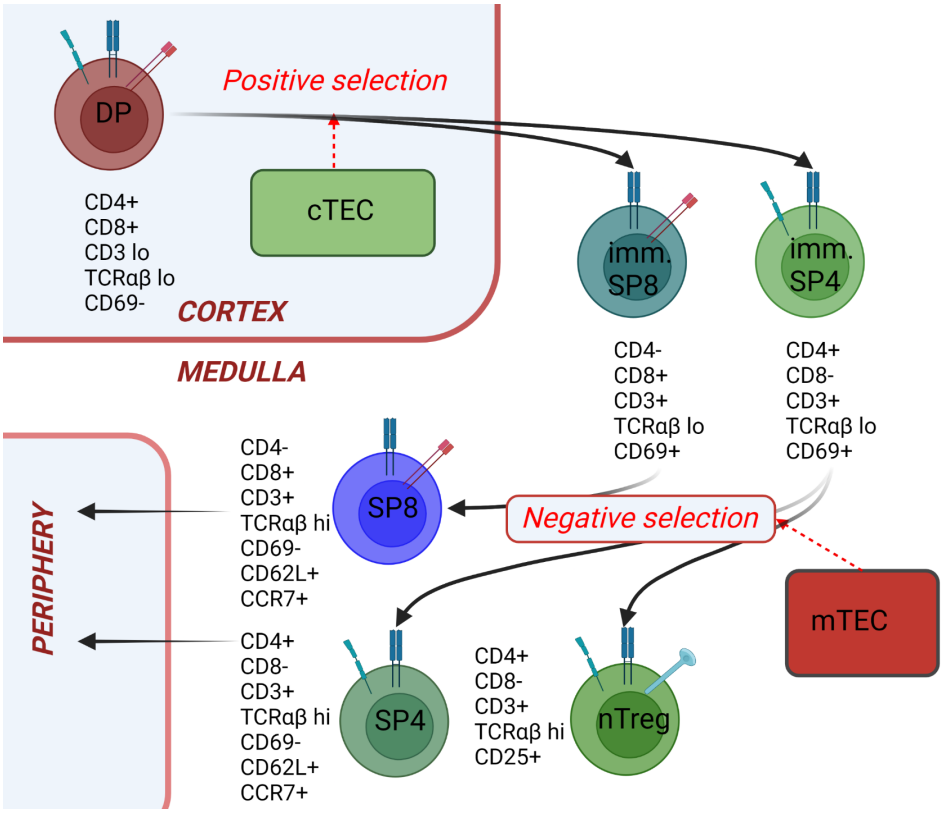

Figure 9 : Régulation et marqueurs clés de la thymopoïèse tardive

Les thymocytes DP sont sélectionnés par les cTEC sur la fonctionnalité de leur TCR, se différencient en thymocytes simples-positifs pour CD4 ou CD8 et migrent dans la médulla. Ils y sont sélectionnés par les mTEC sur leur non-autoréactivité puis maturent en T CD4, T CD8 et nTreg avant de migrer en périphérie.

Enfin, indépendamment du destin des SP, les thymocytes sélectionnés positivement subissent une maturation associée à un retour de l'expression du récepteur à l'IL7 et du récepteur CCR7, ce qui potentialise les thymocytes SP à migrer vers la médulla, sous l'effet d'un gradient de chimiokines sécrété par les mTEC. Il y subiront la phase finale de leur maturation, la sélection négative.

4. Stade simple-positif et sélection négative

Dans la médulla, les thymocytes SP sont exposés au soi par la présentation de PTA, principalement par les mTEC^{hi}. Contrairement à la sélection médiée par les cTEC qui fournit un signal de survie, la sélection négative induit l'apoptose des thymocytes reconnaissant les complexes pCMH (Figure 10). Les mécanismes du signal de mort fourni par les mTEC^{hi} sont encore peu connus. Cependant, l'avidité du TCR pour le pCMH est le principal facteur induisant l'apoptose. En effet, certains thymocytes reconnaissant des PTA avec une faible avidité n'entrent pas en apoptose et sont réorientés vers un destin régulateur. Ils deviennent alors des T régulateurs naturels (nTreg). C'est la sélection agoniste. Les Treg sont des acteurs majeurs de la balance immunitaire dans la périphérie (75). Ils régulent l'homéostasie de la réponse immunitaire, notamment dans les tissus exposés à des antigènes extérieurs ou commensaux, via de nombreux mécanismes de suppression impliquant notamment la sécrétion d' IL-10, IL-35 et de granzyme B (75). Lors de la sélection agoniste, la signalisation TCR entraîne l'expression du récepteur à l'IL-2, *CD25*, qui mène à l'expression de *FOXP3* (76). Ce facteur de transcription est le principal régulateur du programme transcriptionnel Treg.

Lors de leur séjour dans la medulla durant 4 à 5 jours, les SP subissent la dernière étape de leur maturation. Ils transitionnent ainsi d'un phénotype immature

$CD69^{hi}CD62L^{lo}$ à un phénotype mature $CD69^{lo}CD62L^{hi}$ (77,78). Ils deviennent quiescents et plus réfractaires à l'apoptose et acquièrent leur maturité fonctionnelle. Ces T naïfs matures, appelés émigrants thymiques (TE), expriment de hauts niveaux de CCR7, CCR9 et S1P (Figure 9) (78,79). Cette dernière protéine est un récepteur du shingoside-1-phosphate, concentré dans les vaisseaux. Ces récepteurs permettent ainsi la migration par chimiotactisme des TE vers la circulation et la périphérie (77).

Les différentes niches du thymus structurées par les populations de TEC orchestrent donc la différenciation de progéniteurs hématopoïétiques en de multiples populations de lymphocytes T spécialisés, fonctionnels et tolérants au soi (Figure 10).

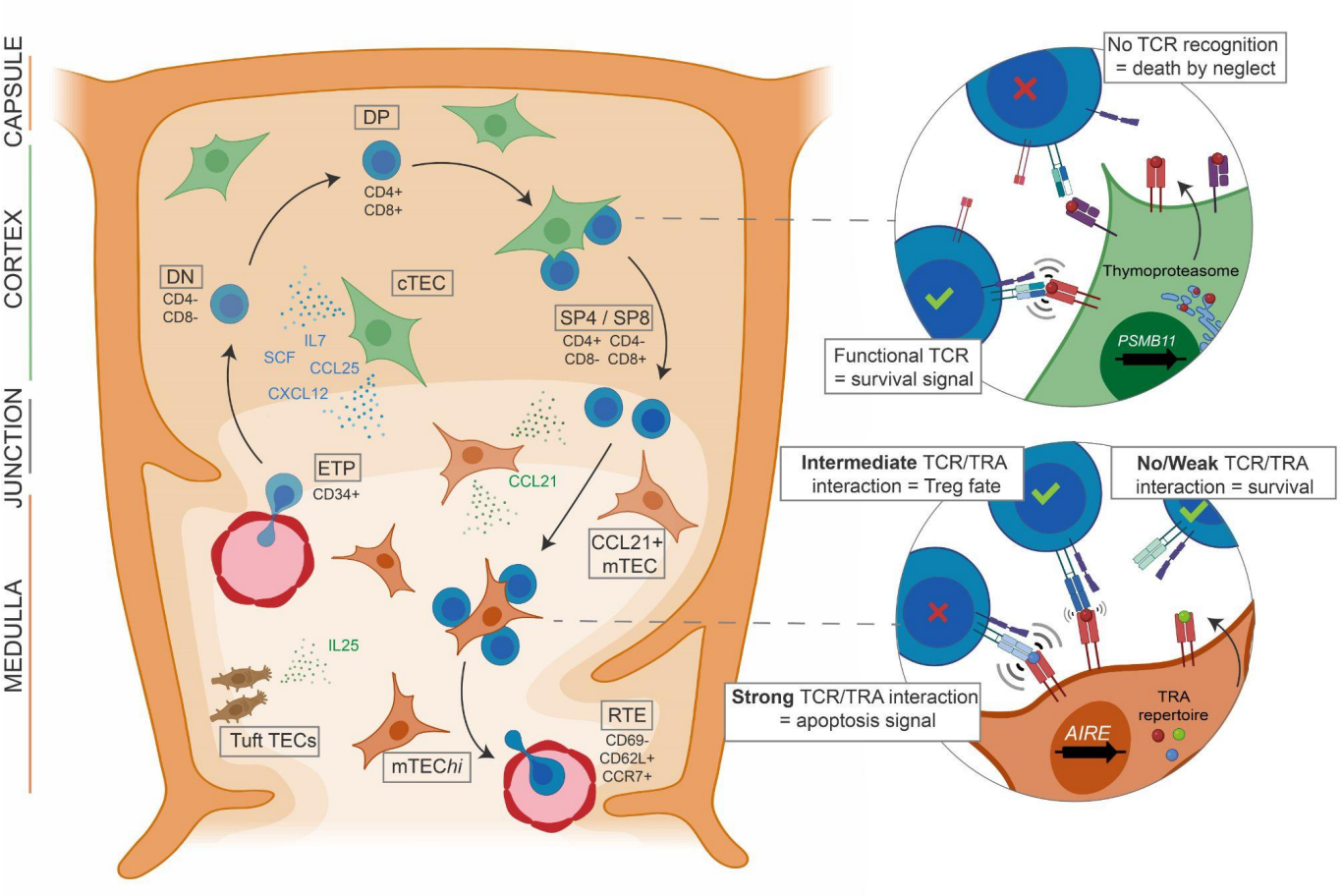

Figure 10 : Synthèse des mécanismes de sélection lors de la thymopoïèse

La signalisation TCR lors de la présentation du thymoprotéasome présenté par les cTEC fournit un signal de survie détournant les thymocytes d'une apoptose par défaut. Leur reconnaissance du CMH-I ou II les conditionne à un destin T $CD8^+$ ou T $CD4^+$. La sélection négative exercée par les mTEC entraîne l'apoptose des thymocytes reconnaissant fortement les antigènes du soi. Une reconnaissance modérée entraîne la différenciation en nTreg. Les thymocytes tolérants maturent et migrent en périphérie. (D'après Provin et Giraud, 2022).

IV. Les autres populations cellulaires du thymus sont impliquées dans la régulation de la thymopoïèse

Si les thymocytes et les TEC sont les deux principales populations cellulaires du thymus et de loin les plus étudiées, l'implication des autres types cellulaires dans la fonctionnalité thymique est de plus en plus considérée. Nous décrirons ici comment les cellules dendritiques, les autres cellules stromales et la matrice extracellulaire (ECM) qu'elles sécrètent sont cruciaux au fonctionnement du thymus.

1. Rôle des cellules dendritiques dans la délétion clonale

Si les principales APC du thymus sont les TEC, celui-ci contient aussi des cellules dendritiques. Comme les TEC sont des cellules relativement rares, comptant pour 0.5% de la cellularité thymique, et elles aussi hétérogènes (80). Les DC thymiques sont composées de DC plasmacytoïdes (pDC) $IL3RA^+CLEC4C^+$, de DC $SIRPA^+CLEC10A^+$ et de DC activées (aCD) $LAMP3^+CCR7^+$ (Figure 11) (31,80,81). La majorité des DC thymiques sont des cellules migratoires qui se développent dans la moelle osseuse, cependant une partie des DC $SIRPA^+CD8^+$ est originaire de la

différenciation intrathymique des ETP (82). Les pDC sont localisées au niveau de la jonction cortico-médullaire, les DC SIRPA^{+} et les aDC sont situées dans la médulla. La forte expression des chimiokines CCL19 et CCL22 par ces dernières indique un rôle potentiel dans l'orientation de la migration des thymocytes DP vers la médulla. Ces aDC sont aussi caractérisées par l'expression de *FOXD4* et *AIRE*, ce qui n'exclut pas la possibilité qu'elles produisent des PTA (31). Les DC expriment de haut niveaux de CMHI et II ainsi que de molécules de costimulation comme CD80 et CD86. Leur capacité à effectuer la sélection négative est depuis longtemps connue (83). Il a été notamment montré que les pDC peuvent collecter des PTA en périphérie et les transporter dans le thymus pour induire la différenciation en Treg (84,85). Cependant, ce mécanisme compte pour une part minoritaire dans l'induction de la tolérance au soi, car il ne compense pas la déficience de *AIRE* chez les patients APECED. La principale source de PTA présentée par les DC reste les mTEC^{hi}. Il a ainsi été montré que les DC s'approvisionnent en PTA par transfert cellulaire auprès des mTEC^{hi} (86). De manière intéressante, les différentes sous-populations de DC interagissent de façon préférentielle avec les différentes sous-populations de mTEC (87). Si les mécanismes de communication cellulaire entre ces populations sont encore à détailler, il est maintenant établi que les DC sont un acteur majeur de la thymopoïèse (Figure 11).

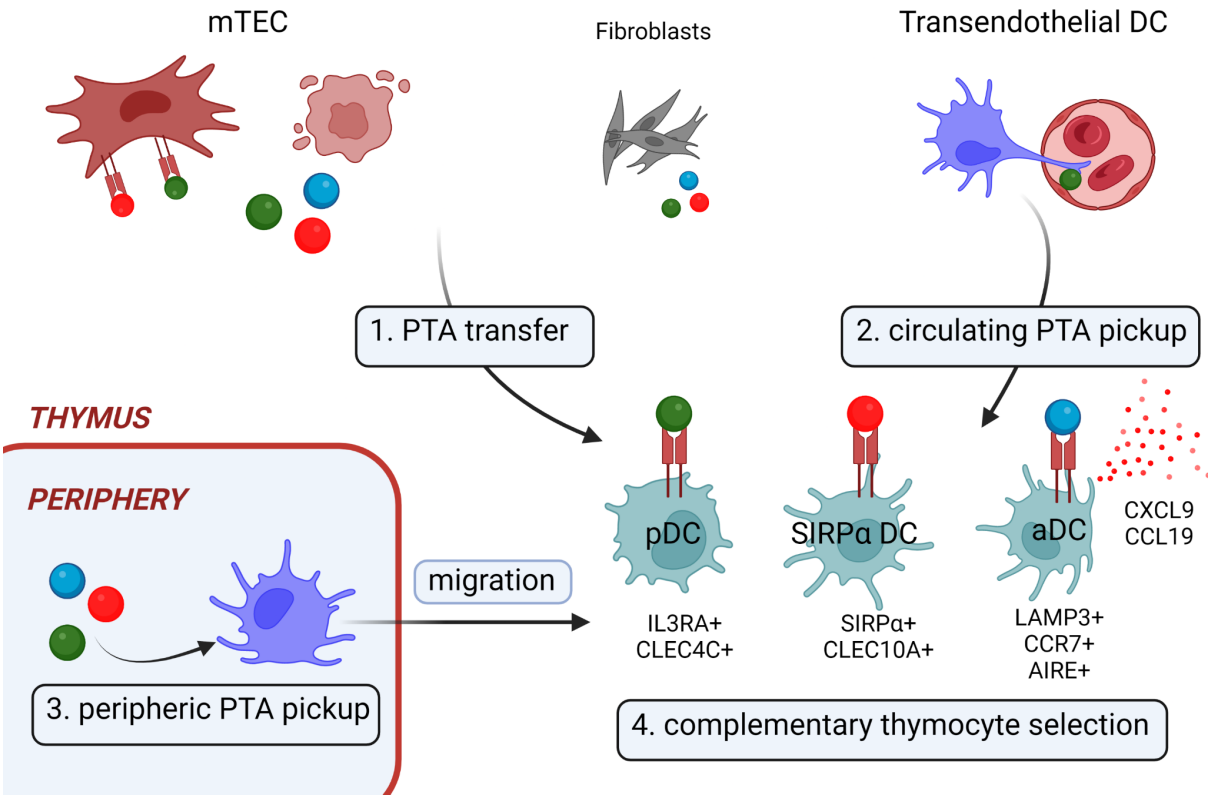

Figure 11 : Fonctionnalité des cellules dendritiques thymiques

Les cellules dendritiques (DC) thymiques forment une population hétérogène provenant de la migration depuis la périphérie et la différenciation intrathymique. Elles récupèrent des PTA périphériques et dans la circulation, ou transférés par les mTEC et les fibroblastes. Les DC sélectionnent les thymocytes en présentant ces PTA *via* le CMHII.

2. Les fibroblastes thymiques, une source complémentaire de PTA

En plus des TEC, deux populations mésenchymales composent le stroma thymique : les fibroblastes et les cellules endothéliales. Historiquement moins étudiées que les TEC, elles ont cependant depuis montré avoir un rôle fonctionnel bien au-delà de la simple organisation du stroma thymique. Comme les TEC, les fibroblastes sont séparés en deux populations, capsulaire et médullaire, phénotypiquement et fonctionnellement distinctes (88). Elles partagent l'expression de gènes typiques des

fibroblastes liés à la sécrétion d'ECM (*COL6A1, LUM, DCN*), des protéases extracellulaires (*HTRA1, MMP2*) et leur inhibiteurs (*SERPING1*) (89). La fonction commune des fibroblastes thymique apparaît ainsi être le renouvellement de la matrice extracellulaire. Les fibroblastes capsulaires sécrètent des ligands de la voie WNT comme WNT2 et WNT5A, et semblent être ainsi des régulateurs de l'homéostasie des cTEC (89). Les fibroblastes médullaires sécrètent des chimiokines CX3CL1 et CXCL14 liées à la migration des DP vers la médulla (90). Le sécrétome des fibroblastes thymiques contient de nombreux modulateurs des voies de signalisation clefs pour les mTEC : BMP4, FGF7-10, IGF1, SFRP2, et pourraient réguler leur développement (Figure 12) (30,31). Enfin, les fibroblastes ont été montrés être une source complémentaire de PTA, sous le contrôle de la voie lymphotoxine β (*LTBR*) (21,91,92). Bloquer spécifiquement LTBR dans les fibroblastes entraîne une auto-immunité spécifique à ces PTA (88,89). Leur faible expression du CMHII suggère que c'est par le mécanisme de transfert d'antigènes à des DC que ces fibroblastes participent à la délétion clonale (93).

Les cellules endothéliales composent la structure vasculaire du thymus. Elles sont caractérisées par l'expression du CD34 et de PECAM1. Les cellules endothéliales sécrètent elles aussi des facteurs régulant les TEC, comme des ligands de WNT et l'Activine A (*INHBA*), ainsi que les thymocytes comme la chimiokine CXCL12 (30). En tant que porte d'entrée et de sortie du thymus, la principale fonction des cellules endothéliales est la régulation de la migration et de l'émigration des thymocytes. Elles présentent à leur surface des molécules comme ICAM-I et VCAM-I permettant l'adhésion des ETP et leur entrée dans le thymus (94). Elles expriment aussi des récepteurs 'leurres' de chimiokines comme ACKR1, qui modulent ainsi les différents gradients dans le thymus (30). La perméabilité de la vasculature thymique est

particulièrement faible : la forte expression de claudine 5 forme une barrière hémato-thymique (BTB) qui compartimente principalement le cortex et la circulation (92), et limite la diffusion de macromolécules dans le thymus (95). La BTB est suspectée d'être une adaptation limitant la sélection des T sur des antigènes circulants lors d'une infection, ce qui limiterait *de facto* l'efficacité de la réponse immunitaire (96).

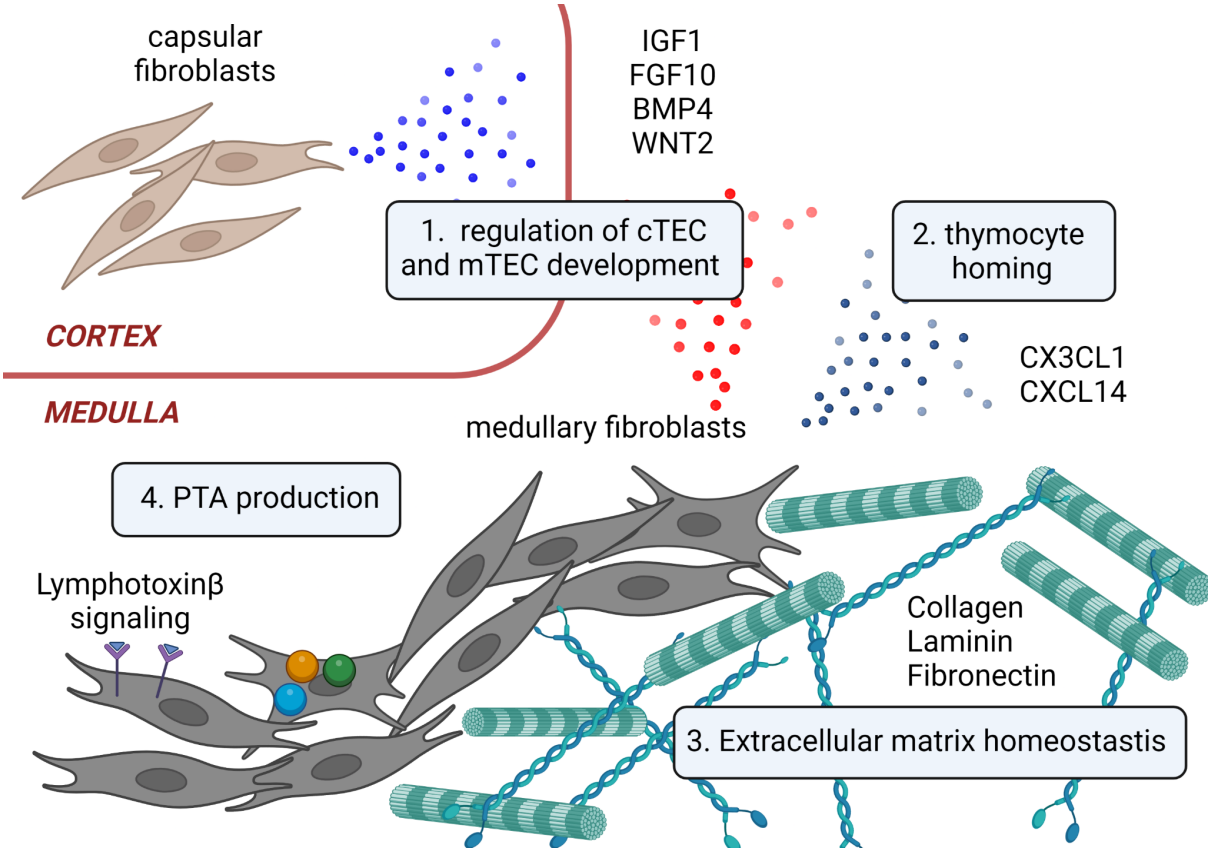

Figure 12 : Fonctionnalité des fibroblastes thymiques

Les fibroblastes dans le cortex et la medulla sécrètent des facteurs de croissance et des chimiokines régulant le développement des TEC et la migration des thymocytes. Leur rôle principal est la sécrétion et la dégradation de la matrice extracellulaire (ECM) thymique. Les fibroblastes médullaires peuvent produire des antigènes du soi (PTA) avec un rôle complémentaire dans la sélection des thymocytes.

3. La matrice extracellulaire, agent structurant de la niche thymique

L'ensemble de ces acteurs cellulaires interagissent dans un microenvironnement structuré par la matrice extracellulaire (ECM). Il est vital d'intégrer l'interaction avec l'ECM dans nos modèles décrivant la fonctionnalité du thymus. En effet, des pathologies comme le syndrome de Down ou des infections à cytomégalovirus sont liées à une altération de l'ECM thymique et une déficience du thymus (97,98). De plus, les TEC perdent leur fonctionnalité *ex vivo* en culture 2D, fonctionnalité qui peut être partiellement restaurée dans des systèmes de cultures en matrice 3D (99–101). L'ECM est composé de structures macromoléculaires en état de "réciprocité dynamique" avec les cellules du thymus (102). Ainsi, l'ECM impacte directement la régulation des programmes transcriptionnels des cellules, qui en retour dégradent où sécrètent des composants de la matrice (103). Cette régulation se fait *via* plusieurs mécanismes : 1. la modulation de la disponibilité des molécules sécrétées par les cellules, facteurs de croissance ou chimiokines 2. une signalisation directe à travers des récepteurs 3. par mécanotransduction.

L'ECM thymique est composée majoritairement de collagène, fibronectine et laminine (98). Ces molécules ont une forte affinité pour de multiples molécules régulatrices, notamment des membres des FGF ou le TGFβ, depuis longtemps connu pour former former des complexes avec l'ECM (104). L'ECM régule aussi plus directement plusieurs processus cellulaires comme la migration et la différenciation, *via* des récepteurs comme les intégrines (30,102,105). Enfin, les propriétés mécaniques de l'ECM, son élasticité et sa plasticité, affectent directement les cellules par mécanotransduction. Les forces auxquelles sont soumises les cellules sont transduites par des molécules réceptrices, situées notamment aux liaisons focales, qui en aval activent des programmes transcriptionnels spécifiques (106).

L’ECM est donc un acteur clé dans la structuration du microenvironnement thymique et la thymopoïèse.

Chapitre 2 : Organogenèse, signalisation, évolution du thymus

Dans le chapitre précédent nous avons décrit en détail comment la fonctionnalité du thymus émerge des interactions entre de multiples populations cellulaires, intégrées dans un microenvironnement spécifique. Nous nous sommes donc concentrés sur l’aspect fonctionnel à un temps *t* de cet organe. Or, il sera vital pour cette thèse de s’inscrire également dans la dimension temporelle. Ce chapitre traitera donc des processus d’organogenèse du thymus et de l’origine embryonnaire de ses différentes populations. Nous décrirons aussi les processus de vieillissement de cet organe, et des mécanismes expliquant son atrophie spectaculaire après la puberté.

I. Développement et morphogenèse du thymus

1. Origine embryonnaire du thymus

Historiquement, les observations anatomiques comparatives et les analyses histologiques des tissus embryonnaires ont été à la base des premières avancées dans notre compréhension de l'organogenèse du thymus. Ces méthodes ont démontré que le thymus dérive des poches pharyngiennes, des structures

embryonnaires transitoires qui apparaissent entre la troisième et la quatrième semaine de développement chez l'homme (107) et au stade E8 chez la souris (108,109). Les poches pharyngiennes sont des invaginations qui se développent à partir du domaine le plus antérieur de l'endoderme du tube digestif primitif (107) et sont un composant de l'appareil pharyngien. Ces structures donnent également naissance aux glandes parathyroïdes, aux amygdales, ainsi qu'aux structures musculosquelettiques de la tête et du cou (Figure 13) (110). Chez les animaux, l'appareil pharyngien est divisé en cinq arcs pharyngiens numérotés de I à VI, le cinquième étant atrophié (111). Les arcs pharyngiens sont divisés en quatre invaginations sur leur face interne recouvertes d'endoderme, les poches pharyngiennes et en invaginations recouvertes d'ectoderme, appelées fentes pharyngiennes, sur leur face externe (112). Chez l'homme, le thymus dérive de la 3éme poche pharyngienne (3PP) (113,114). Cependant, le feuillet embryonnaire duquel provient le thymus est resté longtemps non identifié, et deux modèles ont été proposés (115,116). Le premier modèle théorise une origine unique du primordium thymique à partir de l'endoderme de la 3PP. Le second modèle postule une double origine, les cTEC étant produites à partir de l'ectoderme et les mTEC à partir de l'endoderme de la 3PP, par opposition à l'origine endodermique exclusive du premier modèle. Bien que le modèle de la double origine ait initialement gagné en popularité grâce aux données histologiques obtenues chez la souris (117,118), l'origine endodermique exclusive du primordium thymique a été largement acceptée au début des années 2000, après que des études ont montré que la transplantation ectopique de l'endoderme de la 3PP suffisait à donner naissance à un thymus correctement formé et fonctionnel (50,108).

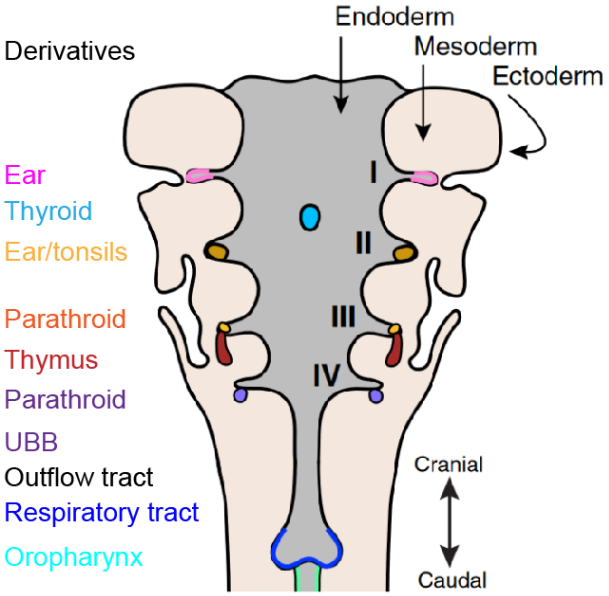

Figure 13 : Les dérivés de l'appareil pharyngien à E10.5 (équivalent semaine 6 chez l'homme, coupe transversale)

Les poches pharyngiennes participent à l'organogenèse de multiples organes antérieurs. La 3éme poche donne naissance au thymus, et en partie aux glandes parathyroïdes. Les poches pharyngiennes les plus postérieures de différencient en tissus participants à la mise en place du pharynx, de l'oesophage et du cœur. (Adapté de Magaletta et al., 2022)

2. Morphogenèse du thymus

Bien que l'organogenèse du thymus chez la souris ait été largement étudiée (115,116), les mécanismes cellulaires et moléculaires qui régissent le développement du thymus humain restent peu connus. Le primordium thymique commence à se former à partir de l'endoderme de la 3PP au cours de la semaine 6 de développement et commence à migrer vers la semaine 8 (119), vraisemblablement sous l'effet de la signalisation du TGFß (120). À la semaine 10, les deux primordia thymiques bilatéraux acquièrent alors leur position définitive dans

le médiastin et fusionnent. L'involution de l'endoderme de la 3PP forme un épithélium stratifié caractérisé par l'expression des claudines 3 et 4, polarisées autour d'un lumen central (121,122). Ces structures rappellent ainsi la morphogenèse d'autres organes présentant un épithélium ramifié, comme le pancréas ou le poumon. Cependant, la structure histologique finale du thymus est radicalement différente. L'épithélium thymique et sa structure spongieuse, en 3D, est très éloignée des épithélia stratifiés des organes ramifiés (123). Cet aspect fondamental de la fonctionnalité thymique permet la maximisation du contact avec les thymocytes et s'explique par le rôle du régulateur maître des TEC, *FOXN1*. Ce gène a été découvert comme étant le responsable du phénotype *nude* décrit dans le modèle de souris mutante éponyme, qui n'ont pas de thymus fonctionnel (124). Chez la souris, *Foxn1* est détecté dans l'endoderme de la 3PP dès E9.5, et atteint un haut niveau d'expression à E11.0 (124,125). Cependant, *Foxn1* n'est pas responsable de l'engagement vers le destin TEC *per se*. En effet, la transplantation ectopique de tissus de la 3PP à E9.0, avant l'apparition de l'expression de *Foxn1*, suffit à générer des thymus fonctionnels (108). Chez les souris nude, le primordium thymique se forme et migre correctement, mais la maturation des TEC et la colonisation par les T est altérée. *Foxn1* est en aval de la cascade de signalisation fixant le destin en l'épithélium thymique et est le principal promoteur de l'activation du programme de maturation des progéniteurs en TEC (108,126–128). De façon intéressante, les thymus des souris déficientes pour *Foxn1* montrent une architecture ramifiée atypique, avec un épithélium stratifié exprimant fortement les Claudines 3 et 4 (*Cldn3-4*), formant de nombreux lumens et développant en une structure ductale proche de celle du pancréas (Figure 14) (129). De plus, une expression ectopique de Foxn1 altère la formation correcte des épithélium ramifiés,

et la formation de lumens (130). Ainsi, *Foxn1* perturbe le programme de morphogenèse tubulaire classique. Enfin, *Foxn1* a été montré réguler directement un ensemble de gènes clés du programme TEC comme *Cxcl12*, *Dll4*, *Ccl25* et les gènes du CMHII (131). Plus récemment, Foxn1 a été montré réguler l'expression d'autres gènes cruciaux des mTEC, comme *Cd80, Cd40, Aire et FgfrII* (131–133). Ainsi, en inhibant la tubulogenèse de l'épithélium thymique et en induisant l'expression du programme TEC, Foxn1 permet l'émergence de la niche thymique (129).

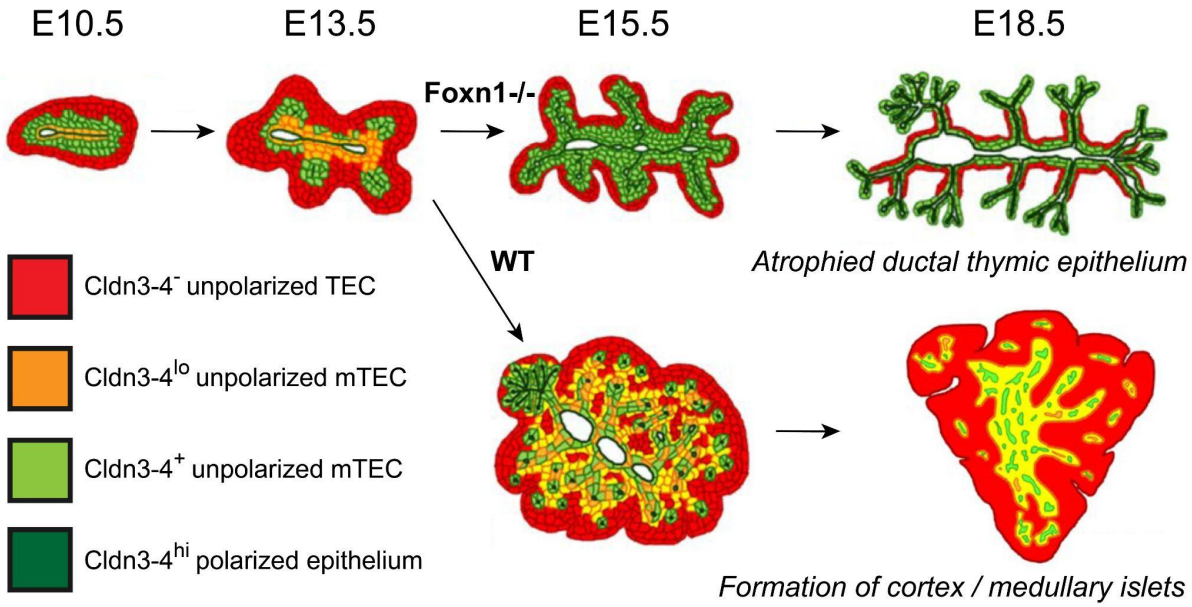

Figure 14 : Rôle de *FOXN1* dans la morphogénèse de l'épithélium thymique
FOXN1 induit un programme de déstructuration de l'épithélium du primordium thymique. En inhibant la morphogenèse tubulaire classique des tissus épithéliaux, *FOXN1* promeut la formation d'un stroma 3D et la formation des îlots médullaires, et donc permet la fonctionnalité thymique (Adapté de Munõz et al., 2019)

3. Colonisation par les cellules progénitrices hématopoïétiques

L'un des phénomènes majeurs structurant l'organogenèse thymique est la colonisation par des cellules hématopoïétiques progénitrices. La caractérisation de ces populations et le détail de leurs liens progéniteurs-produits chez l'homme est depuis longtemps étudiée (134), mais souffre des difficultés notamment éthiques, inhérentes au sujet d'étude.

Des cellules hématopoïétiques $CD45^{+}CD34^{int}CD7^{-}$ peuvent être observées dans le thymus dès la 7ème semaine de développement, et serait majoritairement composée de macrophages impliqués dans le remodelage du primordium thymique (57,119). C'est à partir de la semaine 8 que la première vague de TSP colonise le thymus, et à partir de la semaine 12 les premiers T SP sont générés. La colonisation du thymus par les progéniteurs des cellules T lors du développement présente de fortes différences par rapport à l'adulte. De multiples populations de progéniteurs d'origine distincte colonisent en plusieurs vagues le primordium thymiques organisée temporellement. L'origine la plus précoce de cellules hématopoïétiques dans l'embryon a lieu dans les îlots sanguins du sac vitellin (YS), au jour 19 chez l'homme (57). Ces cellules sanguines primitives sont composées d'érythrocytes, de progéniteurs de macrophages et de mégacaryocytes. Une deuxième série d'hématopoïèse a lieu dans le YS et à partir des cellules endothéliales hémogéniques (HEC) du splanchnopleure para-aortique, et donne naissance à des progéniteurs erythro-myéloïdes et des progéniteurs multipotentes primés lymphoïdes (LMPP) (135). Ces mécanismes sont encore largement inconnus chez l'homme, mais ont lieu chez la souris autour de E10.0. Enfin, la troisième série permet la génération des HSC à partir des HEC dans la zone aorte-gonade-mésonéphros (AGM) entre 32 et 41 jours de développement chez l'homme (56,136). Chez l'adulte,

la niche accueillant ces cellules souches hématopoïétiques est la moelle osseuse, qui apparaît tardivement chez l'embryon, autour de 56 jours de développement. C'est le foie foetal (FL) qui fournit une niche transitoire de prolifération et différenciation des cellules issus des 2éme et 3éme séries, à 28 et 32 jours respectivement (137). A son tour, le foie foetal va être la source de deux vagues de cellules hématopoïétiques progénitrices. La première vague de TSP est caractérisée par l'expression de CD137 et va donner naissance aux T embryonnaires, une population primitive comprenant des T αβ et γδ spécifiques, comme notamment les T épithéliaux dendritiques Vγ5Vδ1^{+} (DETC) (138,139). Chez la souris, cette première vague de colonisation du thymus a lieu à E11.5-E12. Après E16.0, une seconde vague de colonisation par des TSP génère des T matures, mais perd la capacité de générer les les DETC (135,138). Il a donc été supposé que les progéniteurs de ces deux vagues proviennent de deux populations distinctes dans le foie foetal, préalablement orientées vers un destin cellulaire en particulier. Ainsi, l'expression de CD24 est corrélée à la potence vers le destin T de ces LMPP du foie foetal (140).

Enfin, une contribution directe précoce des cellules progénitrices CD137^{+} de l'AGM, sans impliquer une maturation dans la niche hépatique foetale, à été démontrée (56). Ainsi, dès le 33ème jour de développement, ces progéniteurs lymphoïdes contribuent à une lymphopoïèse indépendante des HSC, illustrant l'origine complexe et multiple de la lignée lymphocyte T dans l'embryon.

Les populations de lymphocytes T embryonnaires sont donc distinctes de l'adulte. En plus de la lignée lymphocytaire T, de nombreuses autres cellules lymphoïdes sont impliquées dans l'organogenèse thymique. Citons par exemple les cellules innées lymphoïdes (ILC), qui présentent des similitudes avec les T en termes de fonctionnalité et de développement (141) : aussi appelées cellules inductrices de

tissus lymphoïdes (LTi), elles sont majoritaires dans le thymus précoce à la semaine 8, et régulent la différenciation des TEC et des fibroblastes thymiques en leur fournissant des ligands de la lymphotoxine β (89,135).

La compréhension du système immunitaire humain pendant le développement est très délicate, de par la nature même du sujet de recherche, mais connaît actuellement des avancées remarquables, notamment grâce à la publication d'atlas multi-omiques en cellules uniques dans plusieurs tissus à différents stades du développement embryonnaire et foetal (31,142). Ainsi, l'analyse de près d'un million de cellules, issues de 9 organes à 6 stades de développement publiée récemment par Suo *et al.*, a permis de détailler à une échelle encore inédite les stades précoces du système immunitaire, en intégrant les transcriptomes et les répertoires de des récepteurs B et T, temporellement et spatialement (142). Une des conclusions de cette étude remet en cause le modèle des sites d'hématopoïèse décrit précédemment, et avance que lors du développement l'hématopoïèse a lieu de manière systémique dans l'ensemble des organes périphériques, bien que de manière variées selon les lignées. Ainsi, à l'instar du foie foetal, d'autres organes comme la glande adrénale auraient une fonction hématopoïétique avant de maturer et acquérir leur fonctionnalité adulte.

II. Régulation et signalisation de l'organogenèse thymique

1. Formation de l'axe antéro-postérieur

Puisque la 3PP est une structure du domaine pharyngien, lui même dérivé du domaine le plus antérieur de l'intestin primitif, l'identification des signaux moléculaires qui soutiennent le modelage de l'endoderme définitif est crucial pour la compréhension de l'organogenèse thymique. Chez la souris, la spécification de

l'endoderme définitif est initiée pendant la gastrulation à E6.25. Ensuite, des processus morphogénétiques se produisent et conduisent à la formation de la structure tubulaire de l'intestin vers E8.0 (143). De nombreuses voies de signalisation orchestrent la mise en place de l'axe antéro-postérieur du tube digestif (Figure 15). En effet, la signalisation Bmp-Wnt-Fgf a un effet postériorisant sur le développement de l'endoderme. Ainsi l'inhibition de cette voie de signalisation est nécessaire pour l'acquisition de l'identité de l'intestin primitif antérieur (144–146). De plus, l'inhibition de TGFß/Nodal et la signalisation de l'acide rétinoïque (RA) sont également impliquées dans l'antériorisation de l'endoderme (144).

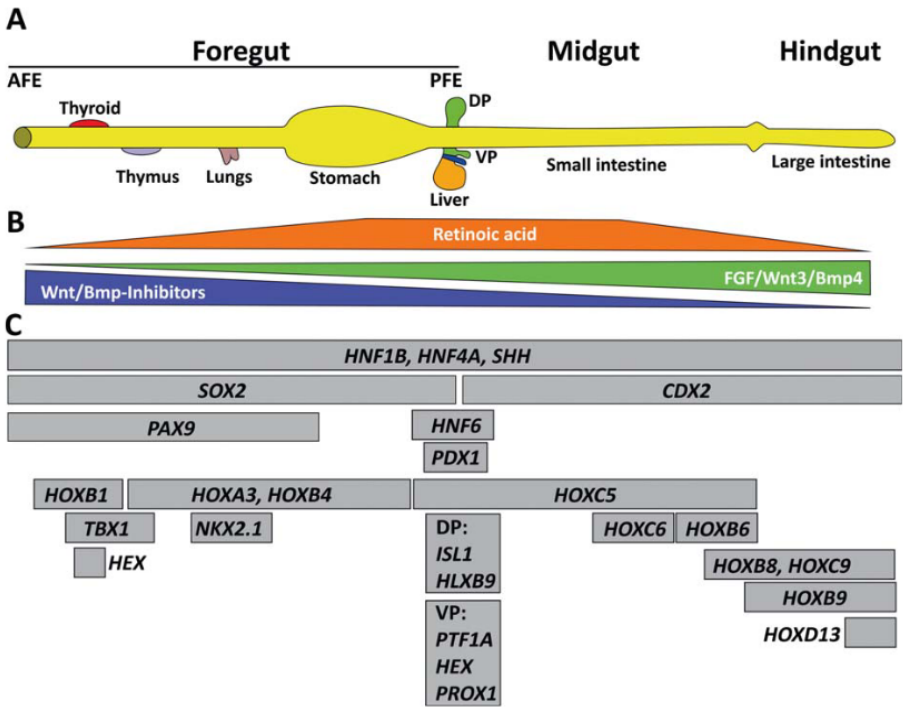

Figure 15 : Carte de la régulation de la formation de l'axe antéro-postérieur
La concentration en acide rétinoïque et des gradients opposés de Wnt-Bmp et leurs antagonistes induisent l'expression de facteurs de transcriptions instruisant le destin cellulaire en spécifiant un axe antéro-postérieur (D'après Davenport et al., 2016)

Récemment, des jeux de données scRNAseq de l'endoderme antérieur ont été générés chez la souris entre E3.5 et E12.5 (143,147–149), incluant le mésoderme de l'intestin primitif antérieur (143) et du domaine pharyngien (149). Ces ressources permettent d'identifier les populations cellulaires impliquées dans le développement précoce du primordium thymique. Ainsi, des ensembles de gènes spécifiques à différents stades du développement pharyngé ont pu être identifiés, tels que *Pax9* et la cascade *Eya1*-*Six1* dans l'endoderme pharyngien à E9.5. Plus généralement, ces études fournissent un modèle de développement de l'endoderme pharyngien à haute résolution. Dans le cas du thymus, une population précoce ventrale de l'endoderme de l'intestin antérieur exprimant *Nkx2-3* et *2-5* à E8.5 se spécifie en endoderme pharyngien exprimant *Bmp4* à E9.5 (143). Les voies clés impliquées à ce stade de différenciation comprennent les signaux *FGF, NOTCH* et RA provenant du mésoderme environnant, ainsi que des ligands BMP autocrines. Parmi les voies non reconnues jusqu'à présent et impliquées dans le développement du tube digestif antérieur, on trouve celles dirigées par HIPPO (148), EGF et NGF (147). À E10.5, la 3PP se forme après activation d'*Eya1* et *Six1*. Cette population cellulaire se différencie ensuite en progéniteurs parathyroïdiens, ultimobranchiaux et en progéniteurs thymiques (TEP) qui exprimant *Foxn1* à E11,5. Ceux-ci se différencient à E12,5 en populations précoces de cTEC et mTEC (149).

Des études comparatives avec des embryons humains ont identifié les mêmes voies et populations, ce qui confirme que l'organogenèse thymique est conservée entre les souris et les humains (119,147). Ces résultats doivent être confirmés *in vivo* par des études appropriées de knock-out ou de traçage de lignée.

2. Régulation de la formation des poches pharyngiennes

De complexes interactions entre les cellules de la crête neurale, le mésenchyme dérivé du mésoderme et l'endoderme de la 3PP contrôle le destin, la migration et l'expansion des populations cellulaires dans le primordium thymique lors de son développement (123). Le principal réseau de régulation génétique est composé des cascades *TBX1-HOXA3-PAX9* et *EYA1-SIX1* qui sont régulées par un ensemble de molécules de signalisation sécrétées par les cellules de la crête neurale et du mésoderme, comme l'acide rétinoïque, les protéines de la famille Wingless-int (WNT), les protéines morphogénétiques osseuses (BMP), les facteurs de croissance des fibroblastes (FGF) et les protéines “sonic hedgehog” (SHH) (Figure 16).

Ces facteurs, qui sont sécrétés par le mésoderme et la crête neurale en plus de l'endoderme, guident le développement du primordium thymique. Le RA est un petit dérivé non peptidique de la vitamine A. Il a été démontré que les gradients de RA régulent la formation des poches postérieure chez plusieurs espèces (150–152). La perturbation du RA pendant le développement entraîne l'absence de formation des poches pharyngiennes postérieures (150,152,153). De plus, il a été démontré que le RA est un acteur clé dans la formation précoce des poches pharyngiennes en régulant l'expression de gènes impliqués dans leur développement, tels que *TBX1*, *HOXA3*, *PAX1* et *PAX9* (131,132,154). Les protéines de la famille WNT, dont WNT4b et WNT5a (155–157), sont exprimées dans les poches pharyngiennes et conduisent à la régulation positive de *FOXN1* en activant la voie canonique WNT/βcaténine (155). Ainsi, la modulation de la signalisation WNT est critique pour la formation du primordium thymique et le maintien de l'épithélium thymique postnatal (156,158,159), et sont exprimés dans les TEC sous la régulation positive de *FOXN1* (133,159). Cependant, une forte signalisation WNT est préjudiciable au

développement thymique (160), ce qui souligne l'importance d'une modulation fine des signaux WNT dans les TEC. Chez la souris, la modulation de la voie Bmp par un gradient Bmp4-Noggin dans les primordia thymiques et parathyroïdiens, est responsable de la séparation correcte de ces tissus et de la formation de la capsule thymique (161,162). Il a été démontré que Bmp4 régulait positivement *Foxn1* et *FgfrIII* directement (163). La signalisation BMP est donc étroitement intégrée aux voies du FGF, elles aussi cruciales pour le développement de la 3PP et du primordium thymique (164,165). En effet, les souris mutantes pour *Fgf8* (166) et *Fgfr2-IIIb*, un récepteur de Fgf7 et Fgf10 (132) montrent un développement du thymus altéré et un arrêt de la maturation des TEC. Cependant, l'inhibition ultérieure du signal FGF par *Spry* est également nécessaire pour la migration du primordium thymique et la prolifération des TEC (167).

Hedgehog joue de multiples rôles régulateurs dans le thymus. Pendant les dernières étapes de la maturation des TEC, SHH a un impact négatif sur la prolifération des TEC mais stimule l'expression de CMHII (168). L'expression de SHH est limitée à l'appareil pharyngien le plus antérieur, à la fois dans l'endoderme et le mésoderme, et joue un rôle dans la spécification des poches pharyngées (169). A E10.5 SHH endosse un rôle dorsalisant, contrastant avec le destin thymique ventral instruit par BMP4. Ces indices, ajoutés au fait que l'expression endodermique de SHH réprime *FOXN1*, indiquent que l'inhibition du signal SHH est nécessaire pour promouvoir un destin thymique plutôt que parathyroïdien (170,171). Globalement, tous ces facteurs sont impliqués dans un réseau de régulation intégré orchestrant la spécification, la maturation et la migration des dérivés des poches pharyngiennes (Figure 16).

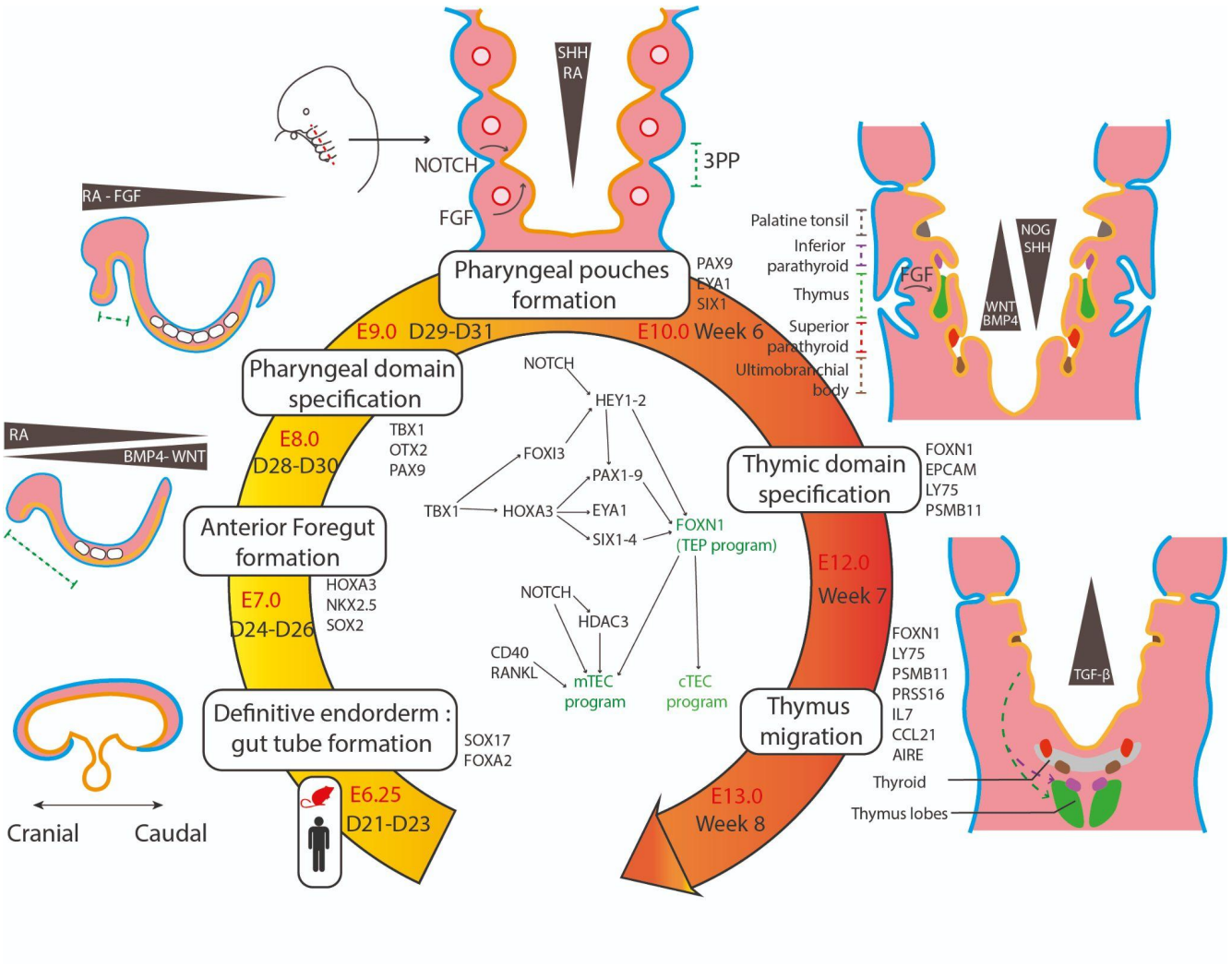

Figure 16 : Réseaux de régulation impliqués dans l'organogenèse du thymus

Le développement embryonnaire du thymus repose sur la régulation intégrée de plusieurs réseaux de gènes avec la signalisation des tissus proches.Une cascade de facteurs de transcriptions *TBX1/HOXA3/EYA1/PAX9* guide l'acquisition de l'identité thymique, induisant l'expression de *FOXN1* et l'exécution du programme transcriptionnel de l'épithélium thymique (d'après Provin et Giraud, 2022)

3. Maturation des progéniteurs de TEC

Les études scRNA-seq du thymus ont contribué à révéler l'existence et l'identité d'une population de progéniteurs des TEC, les TEP (30,48). Les TEP présentent un phénotype cortical caractérisé par l'expression de CD205 et ß5T (14,172). Il a été démontré qu'ils sont la source de mTEC et de cTEC dans les thymus fœtaux et néonataux (32,126,173). Cependant, il y a encore un manque de preuves appuyant

ce modèle chez l'adulte. Après la naissance, le thymus subit une diminution drastique de son activité et de sa cellularité et montre un changement de l'abondance relative des cTEC par rapport aux mTEC en faveur du compartiment mTEC (174,175). Il est supposé que les TEP entrent en quiescence en réponse à la signalisation de BMP4 et de la follistatine (FSH) inhibitrice de l'activine A (30,176,177). Ainsi, le modèle émergent pour l'origine des TEC repose sur les TEP fœtaux bipotents au phénotype cortical qui entrent en quiescence lors du vieillissement et donnent naissance à des populations immatures restreintes en termes de lignage, reconstituant les compartiments médullaires et corticaux des TEC (178). Cependant, des études supplémentaires sont nécessaires pour mieux caractériser ces cellules et les signaux déterminant l'orientation médullaire ou corticale des TEP bipotents.

Des résultats prometteurs ont été obtenus récemment, décrivant notamment le rôle de la modulation de Notch dans cette décision (30,179,180). La signalisation Notch est essentielle pour la spécification des TEP en mTEC, notamment grâce à sa régulation fine par le régulateur épigénétique HDAC3 (181). Ainsi, ces résultats soutiennent le modèle d'une population de TEP bipotents au phénotype cortical subissant une différenciation corticale par défaut, la signalisation Notch favorisant le programme transcriptionnel mTEC. Malgré le paradigme principal d'un compartiment TEC d'origine endodermique exclusive, Chakrabarti *et al.* ont récemment montré qu'une population de progéniteurs hématopoïétiques de la moelle osseuse se transdifférencie en TECs exprimant *Foxn1* dans le thymus (182). Ces progéniteurs hématopoïétiques de la moelle osseuse migreraient de la même manière que les progéniteurs $Cd34^+$, mais se différencieraient en cellules épithéliales exprimant les cytokératines et le régulateur des TEC *Foxn1*. De plus, les cellules $Epcam^+Cd45^+$

pourraient également donner naissance à des fibroblastes thymiques exprimant Fsp1. Ainsi, cette étude identifie une population originaire de la moelle osseuse capable de se transdifférencier en TEC et en fibroblastes pour reconstituer le stroma thymique, ce qui suggère que le développement de la lignée TEC est plus plastique qu'on ne le pensait et peut impliquer diverses populations progénitrices provenant de différentes origines embryonnaires.

4. Maturation des mTEC^{hi} et crosstalk thymique

Les mTEC immatures subissent une dernière phase de différenciation lors de laquelle elles acquièrent leur phénotype mature d'APC et leur expression de *AIRE.* Les mTEC^{hi} ont un taux de renouvellement élevé et une demi-vie courte, de l'ordre de deux semaines, impliquant une maturation constante des progéniteurs de mTEC (183). Wells *et al.* ont récemment identifié une population de cellules d'amplification transitoire (TAC) bipotente et se différenciant en mTEC^{lo} CCL21^{+} et mTEC^{hi} AIRE^{+} (48). Cette population exprimant fortement les gènes du cycle cellulaire a été montré dépendre de signaux de la famille des TNF pour maturer en mTEC^{hi}, notamment de la voie RANK (*TNFSFR11A*). En effet, un blocage utilisant des anticorps anti-RANK, ainsi que des modèles de souris déficientes en RANKL entraîne une altération de la médulla et l'absence de mTEC^{hi} (48,184). Dans le thymus, ces signaux sont apportés par les thymocytes. Les modèles de souris dont la différenciation des thymocytes est bloquée au stade DP présentent une médulla déstructurée et atrophiée (185). Ainsi, non seulement la médulla régule la différenciation des thymocytes, mais ceux-ci régulent aussi la maturation des mTEC. Cette interdépendance de signalisation réciproque pour la maturation de ces deux populations est le "crosstalk" thymique (185–188). Les thymocytes SP CD4^{+}

semblent les principaux acteurs de ce crosstalk, en fournissant aux mTEC les ligands de RANK et CD40 (186,189,190). La voie de la lymphotoxine β a aussi été montré promouvoir la maturation des mTEC, via la présentation de LTα1β2 par les thymocytes SP (21,191,192) (Figure 17).

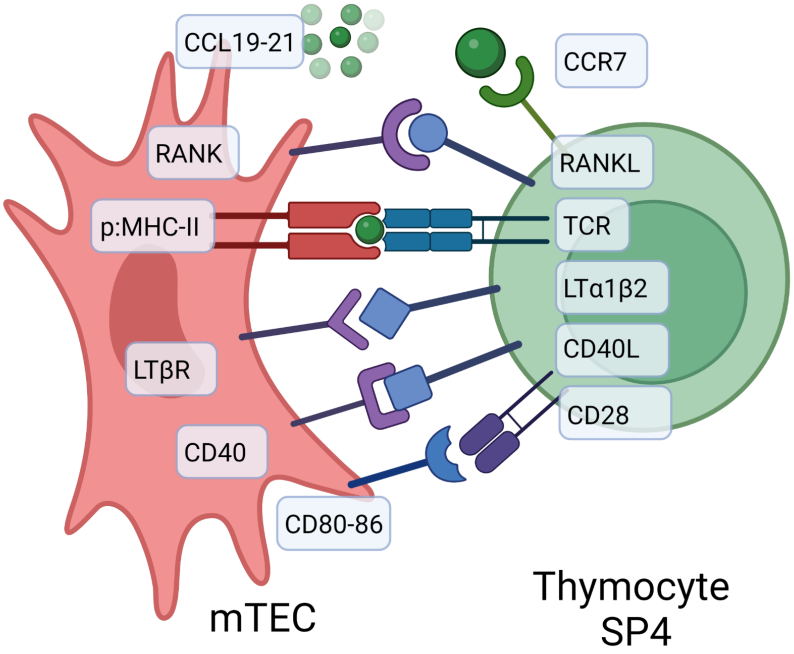

Figure 17 : Signalisation régulant la maturation croisée des mTEC et des thymocytes.
Le crosstalk entre les thymocytes préférentiellement CD4+, et les mTEC promeut l'expression de *AIRE* et la maturation en mTEChi *via* la signalisation RANK/RANKL, CD40/CD40. L'interaction des TCR avec les complexes PTA/CMHII régule aussi positivement la maturation des mTEC et la formation de la medulla. La signalisation LTβR/LTα1β2 et entre les chimiokines CCL19-21 et leur récepteur CCR7 régule aussi la formation de la medulla (adapté de Lopes et al., 2015).

Ainsi, la signalisation croisée entre les thymocytes et les mTEC est un processus central dans l'acquisition d'un phénotype mature de ces cellules, et donc de la mise en place de la fonctionnalité thymique.

III. Evolution post-natale du thymus et involution

1. Involution liée à l'âge et immunosénescence

Paradoxalement le thymus, central pour l'établissement et la maintenance du système immunitaire, est un des organes subissant le plus les effets du vieillissement : son activité se réduit dès la première année chez l'homme. La cellularité des thymocytes diminue en moyenne de 3% par an, le tissu thymique fonctionnel étant progressivement remplacé par du tissu adipeux (193). L'épithélium thymique est particulièrement affecté, avec une chute de la cellularité des TEC et une inversion des proportions cTEC/mTEC : Le nouveau-né présente 90% de cTEC, alors qu'après 25 ans l'épithélium thymique est composé principalement de mTEC, notamment en stade terminal de différenciation (31). Chez les sujets les plus âgés, la génération de nouveaux lymphocytes T est très réduite (194). Ce phénomène d'atrophie, associé à une déstructuration du tissu thymique et notamment la disparition de la séparation cortex-medulla (7), constitue l'involution thymique liée à l'âge (195–197). C'est l'une des causes de la perte de fonctionnalité du système immunitaire liée à l'âge, l'immunosénescence. L'involution du thymus est un phénomène conservé à travers tous les vertébrés, cette caractéristique semblant avoir été sélectionnée et donc apporter un avantage évolutif. Sans qu'il n'y ait pour l'instant de consensus, de multiples hypothèses ont été avancées pour expliquer ce phénomène. C'est lors du développement prénatal et des premières semaines de vie que l'organisme doit constituer un répertoire périphérique de lymphocytes. Ainsi, l'investissement énergétique conséquent lié à une activité de thymopoïèse soutenue y est justifié. En effet, la majorité des thymocytes ne passant pas les étapes de

sélection, la thymopoïèse implique un fort gâchis énergétique (197). De plus, la thymopoïèse implique une importante prolifération cellulaire en milieu inflammatoire, associée à un risque de leucémie (198). Ainsi, la réduction de l'activité du thymus dès la naissance semble être un compromis sélectionné et conservé au cours de l'évolution. Un programme épigénétique conservé reposant sur des histones déméthylases comme Jmjd3 a récemment émergé comme un régulateur clé de la sénescence des TEC (199).

2. Involution lors de la grossesse et régulation par les hormones sexuelles

Au-delà de l'involution liée à l'âge, le thymus subit aussi une involution aiguë et sévère lors de la grossesse. Il perd alors jusqu'à 80% de sa masse, liée à une forte réduction du nombre de TEC (200). Ce mécanisme est lié à la tolérance maternelle pour le fœtus et est corrélée à la fertilité. Après l'accouchement, le thymus entre ensuite dans une phase de régénération spectaculaire caractérisée par une prolifération des TEC et l'intensification de la thymopoïèse. Il a été montré que l'involution lors de la gestation est causée par une répression de *FOXN1*, liée à une dédifférenciation et une perte de fonctionnalité, principalement des cTEC. Lors de la régénération post-partum, *FOXN1* et ses gènes cibles subissent une surexpression transitoire, accompagnée par la prolifération des cTEC et des thymocytes (201).

Les mécanismes et causes précises de ce phénomène sont encore à élucider, bien que les hormones stéroïdes sexuelles apparaissent comme les principaux acteurs de l'involution thymique (202). La testostérone, la progestérone et les oestrogènes ont été montré accélérer l'involution du thymus lors de la puberté, et ciblent principalement les TEC (203).

Ainsi, la sensibilité du thymus à la sénescence semble être liée à la régulation du compartiment TEC par un programme de répression constitutif et conservé évolutionnairement, mais pouvant être modulé au cours de la vie *via* les hormones sexuelles. Enfin, les mécanismes classiques de la sénescence, comme la perte de l'identité épigénétique et le stress oxydatif, affecte aussi le thymus (203,204).

En conclusion, les sujets âgés présentent une perte de fonctionnalité immunitaire, caractérisée par une réponse immunitaire altérée aux pathogènes, une perte de la surveillance immune des tumeurs, et un risque de dysrégulation immunitaire entraînant des pathologies auto-immunes. Dans un contexte de population mondiale vieillissante, l'étude des mécanismes de sénescence des TEC et la mise au point de stratégies de régénération du thymus sont des enjeux de santé publique majeurs.

Chapitre 3 : Les iPSc pour la différenciation thymique et applications potentielles

Après avoir décrit le thymus et son organogenèse dans les deux premiers chapitres, nous aborderons ici les stratégies de régénération de la fonctionnalité thymique. Nous nous concentrerons tout particulièrement sur la génération de tissu thymique à partir de cellules souches pluripotentes induites (iPSc), une stratégie très prometteuse pour le futur de la médecine régénérative. Nous présenterons l'état de l'art, ses limites, les nouvelles approches de culture en 3D, et enfin les perspectives thérapeutiques, notamment appliquées aux pathologies génétiques rares du thymus.

I. Les cellules souches pluripotentes peuvent être différenciées en épithélium thymique

1. Les cellules souches pluripotentes

L'un des phénomènes les plus notables de la biologie est que la plupart des organismes pluricellulaires passent par une phase unicellulaire, le zygote, à partir duquel se forme l'ensemble de l'organisme. Les cellules de l'embryon capables de donner naissance aux cellules des trois feuillets embryonnaires et donc de toute lignée cellulaire de l'organisme adulte sont qualifiées de pluripotentes. Elles sont aussi caractérisées par la capacité de s'auto-amplifier. Ces cellules souches embryonnaires (ESc) ont révolutionné la biologie du développement au début des années 2000, et ont mené à des débouchés en préclinique. Cependant, l'utilisation à grande échelle de ces cellules à été considérablement freinée par les considérations

éthiques liées à leur origine embryonnaire, ainsi qu'à des problèmes de rejet causés par leur allogénicité (205).

Une seconde révolution a eu lieu en 2006 suite aux travaux de Yamanaka, qui montre que des cellules somatiques en différenciation terminale comme des fibroblastes peuvent être reprogrammées vers un état de pluripotence (206). Paradoxalement, la surexpression de seulement quatres gènes, *OCT4 (POU5F1)*, *SOX2*, *C-MYC* et *KLF*, suffit à reprogrammer les cellules somatiques en cellules souches (207,208). Ces cellules présentent les mêmes capacités d'auto-amplification et de pluripotence que les ESc, et ont été nommées cellules souches pluripotentes induites (iPSc). En rendant possible la génération de millions de cellules autologues pour n'importe quel tissu, les iPSc ont soulevé d'énormes espoirs pour la médecine régénérative, allant jusqu'aux essais cliniques (209,210). Les iPSc peuvent aussi être utilisées pour la modélisation de pathologies. Pouvant s'auto amplifier et être différenciées en types cellulaires rares, des iPSc de patients sont une source abondante de matériel et récapitulent le polymorphisme génétique (211). Pour les mêmes raisons, les iPSc se montrent prometteuses comme plateforme de découverte de nouveaux médicaments (210).

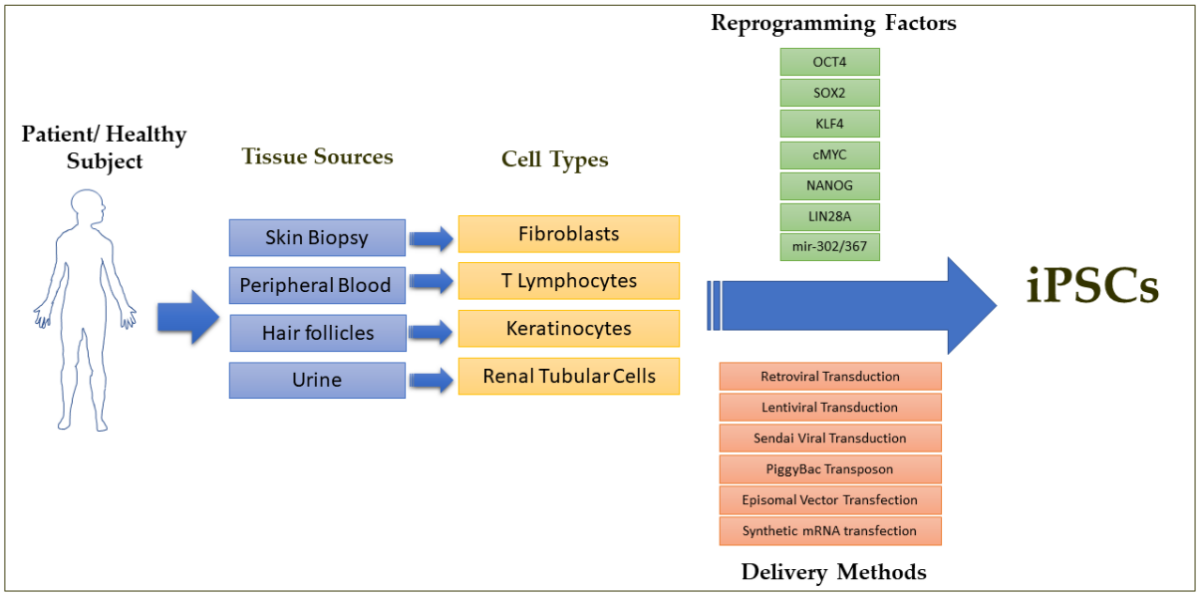

Figure 18 : Stratégies de reprogrammation de cellules souches pluripotentes induites (iPSc)

Les iPSc présentent une multiplicité de tissus et de types cellulaires d'origine, partageant comme caractéristique principale la facilité d'accès. La reprogrammation peut être induite par des cocktails de facteurs différents en utilisant des vecteurs de transfection ou transduction variés (d'après Doss *et al.*).

Cependant, les applications des iPSc pour la médecine régénérative rencontrent encore des limites. La source de cellules somatiques pour la reprogrammation est cruciale : en effet, les iPSc semblent garder une mémoire épigénétique résiduelle, notamment à cause d'une réinitialisation incomplète des marques de méthylation du génome. Ceci biaise alors le potentiel de différenciation vers certains types cellulaires, bien qu'après plusieurs passages cet effet disparaît (212). Le phénotype des TEC étant très proche des kératinocytes, l'utilisation de kératinocytes épidermiques ou des follicules pileux comme source d'iPSc pour la différenciation thymique est pertinent. Cependant, les iPSc dérivées de biopsies dermiques montrent un taux plus élevé de mutations et d'anomalies chromosomiques, probablement à cause de l'exposition aux UV (210). La nécessité de limiter les insertions non voulues, pouvant inactiver des gènes suppresseurs de tumeurs ou au contraire activer des oncogènes, impose un strict contrôle de la méthode de reprogrammation : l'utilisation de plasmides épisomaux ou du virus de Sendai comme vecteurs sont à ce jour considérés comme les méthode de reprogrammation les plus sûres (210). D'autres inquiétudes ont été soulevées à propos de la sécurité des thérapies cellulaires à base d'iPSc, à cause du rôle démontré d'*OCT4* dans la tumorigenèse (123). Le risque de causer la formation de tératomes et de tumeurs malignes doit être soigneusement mesuré. Ainsi, des contrôles qualité stricts sont

nécessaires pendant tout le processus de reprogrammation et de différenciation des iPSc, ainsi qu'une purification stringente des cellules d'intérêt (123).

Enfin, les données sur l'immunogénicité des iPSC sont encore incomplètes. Il a été montré qu'en contexte syngénique, l'immunogénicité des cellules souches transplantées varie selon leur différenciation (213). Les iPSc notamment entraînent la réponse immunitaire la plus marquée. A l'inverse, des résultats cliniques de greffe de cellules épithéliales neurales dérivées d'iPSc ne montrent pas de signes de rejet et sont bien supportées après deux ans (214). Récemment, des techniques d'ingénierie cellulaire ciblant l'inactivation du CMHII et la surexpression de CD47 ont rendu des iPSc hypoimmunogènes, et pouvant être dérivées en cellules transplantables chez des receveurs allogènes sans signes de rejet, et ce en l'absence de traitement immunosuppresseur (215). Ces approches pourraient à terme permettre la constitution de banques d'iPSc ouvrant la porte à l'adoption à grande échelle des thérapies cellulaires à base d'iPSc. Malgré ces contraintes, les succès se sont succédé depuis une dizaine d'années, de multiples tissus ayant été différenciés à partir d'iPSc.

Deux grandes approches ont été développées en parallèle. La première mime l'organogèse, en instruisant la différenciation des iPSc par supplémentation avec des molécules signalisatrices. C'est la différenciation dirigée, qui est aujourd'hui la principale approche pour générer des cellules spécialisées. Une méthode complémentaire est la reprogrammation, en induisant la surexpression d'un ou plusieurs facteurs de transcription dans les iPSc.

Ainsi, des îlots pancréatiques contenant des cellules bêta ont pu être générés à partir d'iPSc, et préviennent le diabète après transplantation chez la souris (216).

Les différenciations cardiaques sont parmi les plus avancées, avec des résultats prometteurs pour la recherche de médicaments (217,218) et en clinique (209).

La génération de tissu hépatique multicellulaire contenant des hépatocytes et des cholangiocytes est aussi prometteuse, montrant *in vivo* une fonctionnalité rudimentaire avec sécrétion d'albumine (219). Enfin, des iPSc ont été différenciées en épithélium branchial pulmonaire correctement vascularisé et ventilé après transplantation, ouvrant des perspectives pour la modélisation et le traitement des maladies respiratoires chroniques (220,221).

Les différenciations en tissu thymique ont aussi connu des progrès considérables que nous allons maintenant détailler.

2. Dix ans de différenciation thymique : succès et limites

Les progrès dans la compréhension de la biologie des TEC et des réseaux de régulation de l'organogenèse thymique ont permis de récentes avancées dans la différenciation thymique d'iPSC (123). Les premiers travaux de Lai et Jin ont démontré la possibilité de générer à partir d'ESc murines des cellules présentant une identité épithéliale thymique (222). Appliquant une approche de différenciation dirigée, ils rapportent la génération de 24% de cellules Epcam^{+} après 10 jours qui expriment les marqueurs d'identité thymique *Foxn1*, *Pax1* et *Pax9*. Cependant ces cellules présentent un phénotype immature. Après transplantation, elles régénèrent des compartiments corticaux et médullaires, confirmant leur nature de progéniteurs bipotents. De manière intéressante, ce thymus reconstitué se montre capable d'attirer des progéniteurs hématopoïétiques et présente une activité de thymopoïèse. Inami *et al.* ont transposé ces avancées aux iPSc humaines (hiPSc) et ont amélioré la maturation des TEP obtenus, démontrant de faibles niveaux d'expression de

marqueurs de fonctionnalité *DLL4*, *DLL1* ainsi que *AIRE* (223). Cependant, la fonctionnalité de ces cellules et la caractérisation des populations obtenues n'ont pas été étudiées. De plus, l'absence de marqueurs membranaires faisant consensus pour l'identification des TEP humaines limite considérablement l'étude des produits de différenciation. Afin de répondre à ces questions, Soh *et al.* ont généré des lignées d'hESc reportrices exprimant une cassette de protéine fluorescente verte (GFP) dans le locus *FOXN1*. De manière intéressante, la différenciation s'est montrée possible après une simple exposition à l'Activine A pendant 4 jours suivi d'une supplémentation en FGF7 à partir du 14ème jour. Ce protocole simplifié a résulté en 27 à 37% de cellules GFP^+ en 35 jours. Cette population exprimait *FOXN1*, *KRT5*, *KRT14* ainsi que les ligands NOTCH *JAG2* et *DLL4*. Cependant, ces cellules n'ont pas démontré de capacité à supporter la thymopoïèse à partir de progéniteurs $CD34^+CD7^+$. La majorité des progrès du domaine proviennent des études de Parent *et al.* et Sun *et al.* publiées en 2013, qui ont optimisé les protocoles de différenciation dirigée en suivant l'expression des marqueurs de chaque stade la différenciation de cellules hESc (Figure 19).

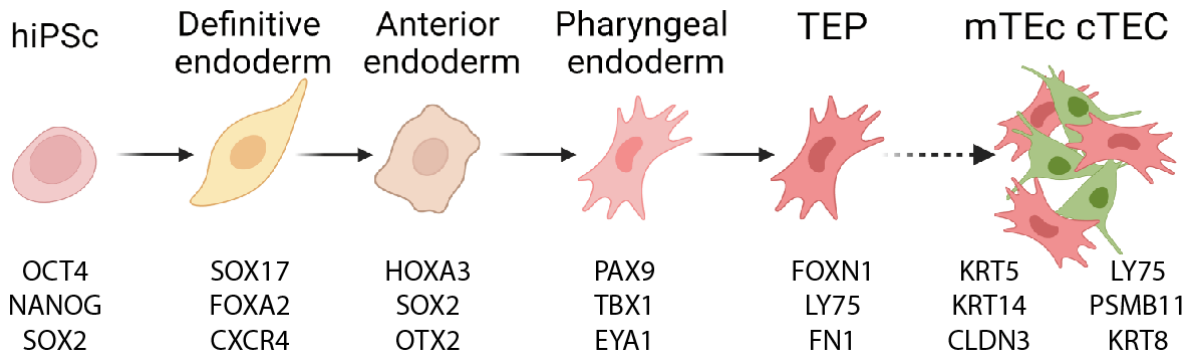

Figure 19 : Itinéraire de différenciation dirigée d'iPSc en TEC
L'approche de différenciation dirigée mime l'organogenèse du thymus en passant par différents stades du développement caractérisés par l'expression de marqueurs clé.

Ces deux études ont démontré l'importance de l'acide rétinoïque pour l'antériorisation de l'endoderme définitif, et de BMP4 et WNT3 pour la différenciation en TEP. De plus, l'inhibition de la voie WNT par IWR1 et de TGFß par LY364947 au jour 5, ainsi que de Hedgehog par la cyclopamine (CPM) du jour 7 au jour 11 ont amélioré les niveaux d'expression de *FOXN1* (224,225). Cependant, l'absence de méthodologie expérimentale non biaisée et la sélection *a priori* des combinaisons de facteurs testées n'a pas permis de mesurer précisément l'effet de chaque molécule sur la différenciation thymique, ce qui implique des résultats sous-optimaux. Néanmoins, ces deux études rapportent une augmentation significative de l'expression des marqueurs de TEP. Cependant, les marqueurs de maturation du TEC n'ont pas été détectés. Les TEP induits ont donc été agrégés et transplantés en modèle murin *nude* afin de poursuivre leur maturation comme décrit précédemment. De façon intéressante, les greffons ont supporté la thymopoïèse et ont reconstitué le compartiment T périphérique. Ces lymphocytes T ont montré un certain niveau de fonctionnalité : un répertoire TCR diversifié, une sécrétion d'IL2 et une prolifération après stimulation et la capacité de rejeter les greffes de peau allogènes. Des Tregs $CD4^+CD25^+FOXP3^+$ ont également été générés. Les mêmes expériences ont été réalisées chez des souris humanisées avec des progéniteurs hématopoïétiques humains. Des résultats similaires ont été obtenus, confirmant ainsi la capacité des greffons thymiques à induire la génération de lymphocytes T humains.

Une autre approche consiste à cibler les facteurs de transcriptions clé du programme TEC. Les premiers indices sont venus de l'étude de Su *et al.*, montrant que la différentiation d'ESc en présence de HOXA3 et FOXN1 recombinants entraînait une augmentation significative du rendement (226). De façon très intéressante, la simple surexpression de *FOXN1* dans des fibroblastes leur permet d'acquérir une identité de TEC, avec des cellules morphologiquement et phénotypiquement similaires (227). Ces cellules expriment des facteurs qui soutiennent le développement des thymocytes tels que DLL4 et CCL25. Ces TECs induites (iTECs) étaient également capables de faire maturer des ETPs en cellules T $CD4^+$ et $CD8^+$, à la fois *in vitro* après 12 jours de coculture et *in vivo* après transplantation chez la souris. Ces cellules T se sont montrées fonctionnelles et sécrètent des interleukines en réponse à une stimulation CD3/CD28. Cette étude illustre la fonction centrale de *FOXN1*, cependant la fiabilité de cette approche de reprogrammation et sa capacité à générer les diverses populations de TEC doit être évaluée et comparée à la différenciation dirigée.

D'autres études ont étudié l'induction d'une tolérance immunitaire *in vivo*, par différenciation dirigée seule (228) ou en conjugaison avec la surexpression de *Foxn1* (229,230). Ainsi, des iPSc murines se différencient en TEP exprimant *Pax9*, *Dll4* et *Foxn1*. Ceux-ci maturent en TEC fonctionnelles après transplantation. Afin de tester la capacité de ces greffes thymiques d'induire une tolérance, des biopsies de peau provenant de la même souche de souris à l'origine des iPSc ont été transplantées chez un receveur d'une autre souche de souris après épuisement immunitaire par irradiation et traitement par anticorps anti-T (229) ou directement chez des souris nude (228). De manière intéressante, les greffes syngéniques présentent une survie

accrue. Ainsi, des iPSc peuvent être différenciées en tissu thymique fonctionnel induisant la tolérance au soi.

Enfin, de récentes études par Ramos *et al.* et Gras-peña *et al.* ont optimisé les protocoles de différenciation, notamment en modulant temporellement la signalisation Hedgehog (231,232). Contrairement à ce qui a été réalisé précédemment (224), ces deux protocoles activent la voie Hedgehog lors de la différenciation en endoderme pharyngien, suivie par son inhibition. Ainsi, une modulation temporelle fine semble être un point clé de la différenciation thymique. De même, l'inhibition puis l'activation de la voie BMP, respectivement du 15ème au 21ème jour, puis à partir du 21ème jour, promeut l'expression de *PAX9* (231). L'ajout de FGF8 pour induire l'antériorisation de l'endoderme définitif au jour 4.5 augmente l'expression de FOXN1 d'un facteur 5 en fin de différenciation. Il est remarquable de noter que ces TEC peuvent être maintenues jusqu'à 30 jours et expriment les marqueurs thymiques *FOXN1, PAX9, EYA1, SIX1* et *AIRE.* Afin d'étudier l'hétérogénéité du produit de différenciation, Ramos *et al.* ont greffé des TEP dérivés d'hiPSc chez la souris et analysé les greffons après 14 à 19 semaines par scRNAseq. La maturation *in vivo* des TEC a été confirmée par des niveaux d'expression élevés de *DLL4* et *HLA-DRA*. De façon intéressante, en utilisant des TEC primaires de thymus post-natal comme contrôle, ces données montrent un clustering commun avec les TEC dérivées d'iPSc, impliquant une proximité des transcriptomes de ces populations. Cependant, la subdivision du cluster TEC a révélé une séparation distincte entre les deux types d'échantillons, les TECs induites étant principalement composés de TEP et de TEC en cours de différenciation, tandis que les cellules des clusters cTEC et mTEC^{hi} plus matures provenaient des échantillons primaires. Ceci implique que même après transplantation *in vivo*, des

freins restent encore à lever pour atteindre une maturation complète des TEC dérivées d'iPSc. Ces données permettent de décrire les mécanismes orientant la différenciation des TEP, notamment le rôle joué par l'Activine A et la voie Notch, révélée par l'expression d'*INHBA* et *DLK1* dans le cluster TEP. D'autres approches en cellule unique multi-omiques seront nécessaires pour comprendre plus en détail les réseaux de régulation pilotant la maturation des TEC et leur différenciation en sous-populations diverses.

Ainsi, la différenciation des TEC à partir de cellules souches pluripotentes a connu une amélioration significative ces dernières années, une amélioration continue des protocoles donnant lieu à des TEC avec un rendement et une pureté accrus (Figure 19). A l'inverse, la maturation en TEC *in vitro* est toujours mal comprise. Des indices sont venus de l'étude du crosstalk thymique avec la découverte que les interactions entre les TEC et les thymocytes sont nécessaires à leur maturation. Il a également été démontré que le crosstalk thymique pouvait être mimé à l'aide de cytokines comme RANKL. Au niveau fonctionnel, ces TECs induites (iTEC) peuvent soutenir la maturation des thymocytes et reconstituer le compartiment des cellules T *in vivo*. Les cellules T en coculture avec les iTEC prolifèrent et sécrètent des cytokines après stimulation. Ils sont également capables d'améliorer le rejet des greffes allogènes de peau, démontrant ainsi leur fonctionnalité. Il est intéressant de noter que les greffons d'iTEC ont induit une tolérance immunitaire aux greffes de peau syngéniques, promouvant ainsi la tolérance au soi.

Bien que tous les protocoles ci-dessus aient réussi à générer des TEP avec une efficacité variable, des obstacles considérables doivent encore être surmontés pour obtenir un organoïde thymique fonctionnel *in vitro*. La compréhension actuelle des

mécanismes gouvernant la différenciation des TEP est encore lacunaire, et la plupart des voies de signalisation modulées dans ces protocoles le sont de manière imprécise. De même, la pureté des produits de différenciation est également un enjeu crucial pour de potentielles applications cliniques. Des stratégies de purification par tri ou par sélection, par exemple par traitement avec des molécules déplétantes des cellules souches comme YM155 (231). De manière contre-intuitive, cette hétérogénéité pourrait avoir un effet positif, par génération de fibroblastes thymiques "nourriciers" sécrétant des facteurs améliorant la différenciation des TEC. De plus, la différenciation en parallèle des mêmes iPSc en lignée hématopoïétique et leur mise en coculture pourrait stimuler la maturation des TEC en mimant le crosstalk thymique.

Enfin, un système de culture à long terme reproduisant fidèlement le microenvironnement thymique in vivo doit encore être développé. Bien que les TEC dérivés d'iPSc puissent être maintenues en culture classique jusqu'à 30 jours (231), un système de culture plus proche de la structure du stroma thymique pourrait améliorer significativement la différenciation et la viabilité des TEC.

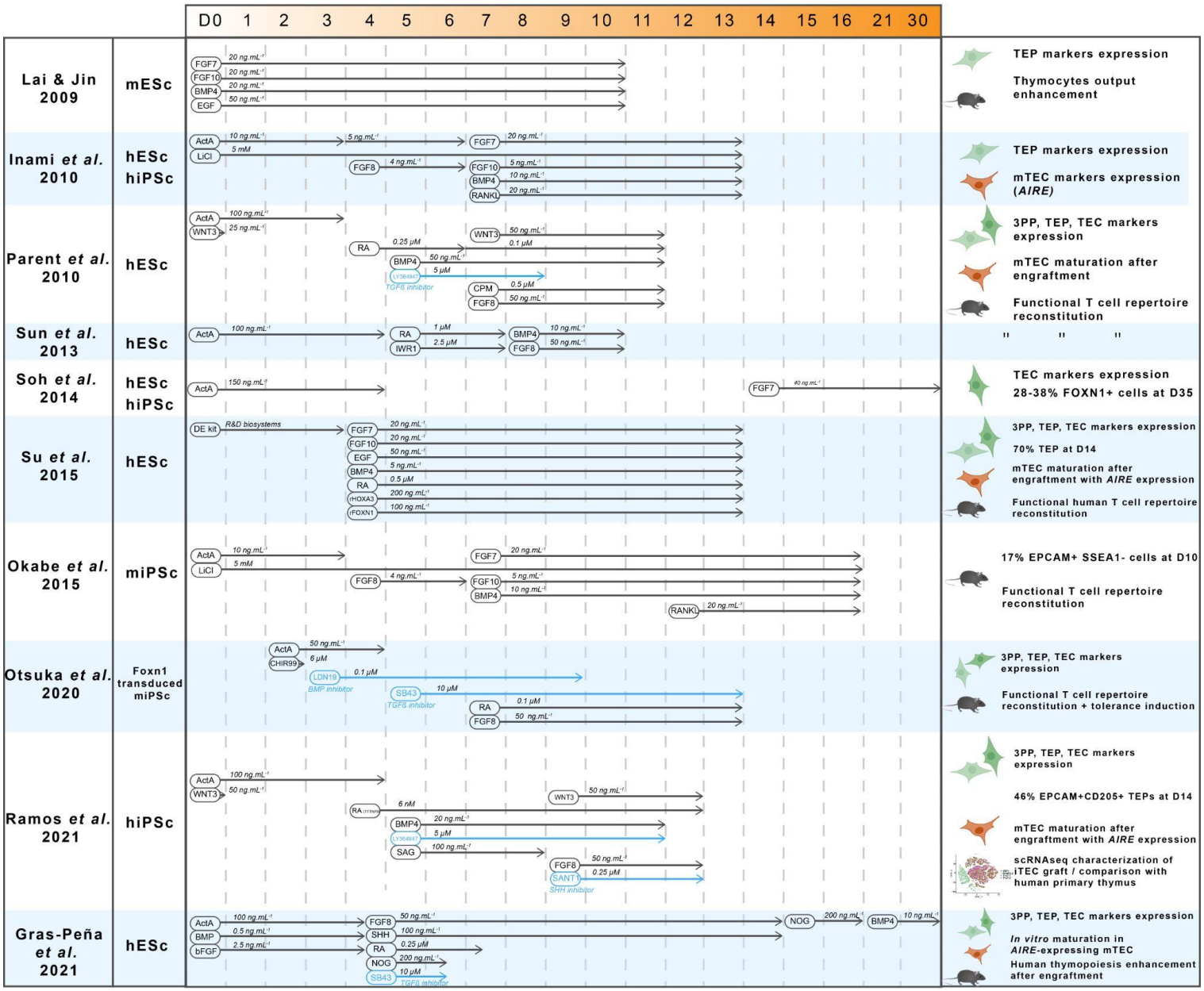

Figure 20 : Synthèse de l'état de l'art des différenciation thymiques à partir de cellules pluripotentes

De multiples protocoles ont été établis depuis 2009. La majorité reposent sur la différenciation dirigée, en modulant les voies de signalisation impliquées dans l'organogenèse du thymus. Ces approches sont limitées, résultant en des cellules immatures nécessitant la transplantation *in vivo* pour acquérir leur fonctionnalité (d'après Provin et Giraud, 2022).

II. Modèles de culture 3D et organoïdes, des avancées prometteuses pour reproduire la fonctionnalité thymique in vitro

1. Culture de TEC dans des hydrogels synthétiques

En culture cellulaire classique, les TEC primaires perdent progressivement l'expression de *FOXN1* et *AIRE* (233) et de leur capacité à exprimer l'ensemble des PTA (99) et donc leur fonctionnalité. Or, il a été montré que la structure 3D est un facteur clé pour le maintien des TEC (234). L'imitation de l'organisation du stroma thymique pourrait donc promouvoir la viabilité et le rendement des iTEC. Cette hypothèse a été explorée par la mise au point de multiples systèmes de culture testés sur des TEC primaires. En coculture avec des fibroblastes dermiques dans un hydrogel de fibrine, des TEC primaires conservent leur phénotype, leur potentiel de prolifération et leur état de maturation (99). De plus, ce système de culture permet la conservation de l'expression des PTA. L'utilisation d'autres polymères comme support de culture a aussi été explorée. Un hydrogel synthétique formé par les peptides EAK16-II/EAKII-H6 (235) a montré induire la formation de cluster de TEC en 3D exprimant *FOXN1* et *EPCAM*. Ces TEC encapsulées ont ensuite été transplantées en modèle de souris nude, et ont reconstitué le compartiment T périphérique. Cependant, les lymphocytes T générés montraient un biais vers la population T CD8, possiblement à cause d'une interaction insuffisante avec les TEC illustrée par l'absence de formation d'une structure cortex-medulla claire (235).

Parmi les autres approches testées, citons une structure de mailles fibreuses fonctionnalisées à la fibronectine (236), des microgels sphériques de gélatine (237) ou un hydrogel de collagène de type I (238). Remarquablement, malgré la diversité

des compositions protéiques de ces matrices, ces systèmes ont tous permis une prolifération, propagation et maintien accru des TEC. Cependant, le modèle de culture de TEC de souris en hydrogel de collagène I ne soutient pas la thymopoïèse (238). Bien que les hydrogels synthétiques soient un outil prometteur pour cultiver les TECs, des recherches plus approfondies et des études d'optimisation sont nécessaires pour imiter avec précision le microenvironnement thymique.

2. Autres approches : matrice primaire et organoides artificiels

Une approche alternative à ces systèmes synthétiques consiste à utiliser directement la matrice du thymus primaire pour bénéficier de la diversité native de ses protéines constitutives tout en conservant sa structure. La décellularisation de lobes thymiques primaires permet ainsi d'obtenir des structures "fantômes" pouvant ensuite être réensemencées (100,101,239). Ces systèmes basés sur la matrice thymique native favorisent la croissance et la maturation des TEC, et de manière remarquable, reforment des compartiments corticaux et médullaires distincts.

La fonctionnalité des thymus ainsi reformés a été démontrée sur modèle murin de greffe de peau, montrant l'induction d'une tolérance spécifique au donneur (101,239). Néanmoins, ces approches sont dépendantes d'une source primaire de matrice thymique et leur application clinique pour la médecine régénérative est difficilement envisageable.

Enfin, outre la différenciation d'iPSc en TEC, des études récentes visant à différencier les lymphocytes T à partir de progéniteurs hématopoïétiques ou d'iPSc ont également mis en évidence l'importance des systèmes de culture 3D la thymopoïèse. Le développement d'organoïdes thymiques artificiels (ATO) (240–242) a connu des progrès considérables ces dernières années. Les ATO sont formés par

réagrégation d'une lignée murine de cellules stromales de moelle osseuse modifiées pour exprimer le ligand de Notch Dll4 avec des cellules souches hématopoïétiques ou des progéniteurs mésodermiques dérivés d'iPSc. Les micromasses cellulaires sont ensuite cultivées en interface air-liquide. Les ATO ensemencés avec des progéniteurs hématopoïétiques murins supportent la thymopoïèse et produisent des cellules CD4 et CD8 matures (241,242). Cependant, ce système a montré être biaisé vers une différenciation CD8 “par défaut”. Fait remarquable, ce système a donné des résultats comparables lorsqu'on a utilisé des progéniteurs mésodermiques dérivés d’ESc et d’iPSc humaines (145). Ainsi, ces organoïdes thymiques artificiels peuvent récapituler la différenciation des cellules T *in vitro*, ce qui montre l'importance de la structure 3D par rapport aux cocultures 2D peu efficaces (243). Cependant, la génération de T CD4 s’est montrée déficiente dans ce système, probablement en raison de l'absence de TEC et de signalisation CMHII. De plus, l’absence de TEC implique l'absence de processus de sélection thymique et donc la génération de nombreux T déficients *i.e* non fonctionnels ou auto-réactifs.

III. Perspectives d’application aux pathologies d’origine génétique affectant le thymus

1. Des pathologies congénitales affectent la fonctionnalité thymique

Les pathologies congénitales affectant le développement et la fonction des TEC conduisent à des états graves d'auto-immunité ou de lymphopénie. Comme décrit précédemment, *AIRE* joue un rôle crucial dans la fonctionnalité des mTEC et leur capacité à présenter le répertoire de PTA, et sa déficience entraîne un syndrome auto-immun, la polyendocrinopathie auto-immune de type 1 (APS-1 ou APECED).

Ce syndrome identifié dans les années 1980 (244) se caractérise notamment par des lésions sévères des tissus périphériques, causées par une activité auto-immune des lymphocytes T non sélectionnés dans le thymus. Les patients reçoivent une combinaison personnalisée de traitements ciblant les symptômes et conduisant à des améliorations cliniques. Cependant, aucune stratégie curative n'est disponible, et les patients atteints d'APECED ont toujours une espérance de vie réduite (245). D'autres pathologies congénitales affectant le thymus ont été identifiées et sont liées à l'haploinsuffisance ou la perte de fonction de plusieurs facteurs clés dans l'organogenèse du thymus. Les plus fréquents cas d'hypoplasie thymique sont liés à des maladies congénitales cardiaques (CHD). Le phénotype clinique des patients atteints de CHD associe de fait l'hypoparathyroïdie et l'hypoplasie thymique, une minorité de patients présentant une athymie et une immunodéficience sévère. La cause la plus fréquente d'athymie congénitale est la microdélétion 22q11.2 affectant 0.25 naissances sur 1000, dont 1.5% développent une athymie : c'est le syndrome de DiGeorges. L'haplodéficience de *TBX1* dont le locus est situé sur la portion chromosomique affectée par cette microdélétion est la cause principale de ce syndrome. Plus rare, le syndrome combiné d'immunodéficience sévère (SCID) est lié à une perte de fonction de *FOXN1,* à l'instar du modèle murin *nude*. Il est associé à une alopécie totale, une dystrophie des ongles et une lymphopénie sévère, avec des taux très faibles de T circulants. Cette pathologie est souvent fatale lors des 2 premières années de vie, à cause de l'extrême sensibilité des patients aux infections (246). Le SCID peut être aussi associé à une déficience de *PAX1* dans le syndrome otofaciocervical de type 2 (OTFCS2). *PAX1* est un régulateur central du développement impliqué dans l'organogenèse des dérivés de l'endorme pharyngien. L'altération du développement du thymus entraîne l'absence de TEC et l'apparition

du SCID. Il est notable de constater que les essais de greffes d'HSC sur ces patients sont restés sans succès, confirmant que la déficience de maturation de lymphocytes T ne provient pas de leurs progéniteurs mais bien d'une altération de la niche thymique.

2. Le thymus, un cas particulier pour la transplantation

La transplantation de tissus thymiques est une piste de traitement de ces pathologies. Chez les patients subissant une chirurgie cardiaque post-natale, la thymectomie partielle est nécessaire à la chirurgie. Les tissus thymiques peuvent être ainsi récupérés et mis en culture pendant 13 à 20 jours afin de dépléter les thymocytes (247), qui entraînent un risque de maladie du greffon contre l'hôte. A cause de toutes ces contraintes, les greffons sont rarement appariés avec l'HLA du receveur. Les échantillons de stroma thymique sont ensuite transplantés dans les quadriceps des receveurs. Les patients atteints du syndrome de DiGeorges ou du SCID ne nécessitent par ailleurs pas de traitement immunosuppresseur, à cause du faible nombre de T circulants qui sont les principales cellules effectrices du rejet de greffe. De manière intéressante, le taux de survie des patients transplantés atteint 75% après deux ans, l'étiologie des patients décédés après transplantation accusant des infections préexistantes (248). Chez les patients transplantés, les HSC migrent de la moelle osseuse au greffon thymique et s'y différencient en lymphocytes T au bout de 2 à 4 mois. Bien que le nombre de lymphocytes T des patients greffés n'atteignent pas les niveaux normaux, ceux-ci présentent un répertoire TCR diversifié et la capacité de proliférer après stimulation. Ceci démontre la capacité des greffes à attirer des ETPs et les différencier en lymphocytes T. Les mécanismes de présentation croisée des PTA décrit précédemment pourraient expliquer ce

paradoxe. Ainsi, des DC du receveur auraient pu migrer dans le greffon et se voir transférer des antigènes du donneur, fourni par les TEC ou les fibroblastes du greffon. Les DC participent alors à la sélection des thymocytes. Une autre hypothèse est qu'une interaction même partielle entre les HLA du donneur et du receveur suffirait à permettre la sélection.

Nonobstant ces résultats prometteurs, les patients greffés développent de multiples complications. En effet, 70% des patients survivants présentaient des symptômes d'auto-immunité (249). L'hypothèse avancée repose sur le fait que le greffon sélectionne principalement les thymocytes sur le répertoire de PTA du donneur, ou que le mésappariement entre les HLA limite cette sélection. En conclusion, bien que faute d'alternatives viables le ratio bénéfice-risque de la greffe de thymus allogène est préférable chez les patients souffrant de malformations congénitales du thymus, cette opération entraîne l'apparition de syndromes auto-immuns chroniques, de sévérité variable, affectant significativement les patients voire causant le décès (246).

3. Perspectives de thérapies de médecine régénératives du thymus

La fonction unique du thymus dans la génération de la tolérance au soi en font un organe difficile à greffer, et une cible de choix pour la médecine régénérative. En effet, la sélection des thymocytes sur le répertoire d'antigènes du soi impose une transplantation autologue. Les avancées considérables réalisées depuis 15 ans sur la reprogrammation en iPSc et leur différenciation en épithélium thymique supportant la thymopoïèse ouvrent la porte à de potentielles applications cliniques dans un futur proche. Ainsi, on peut envisager des approches thérapeutiques visant à régénérer le thymus chez les patients présentant des anomalies congénitales de son

développement entraînant une athymie. Des cellules du patient seraient alors reprogrammées en iPSc et soumises à une édition génique afin de réparer le gène défectueux, à l'aide de vecteurs viraux ou de CRISPR par exemple. Les iPSc seraient ensuite différenciées en épithélium thymique, puis transplantées. Cette approche permettrait la régénération de la fonction thymique, et constituerait une stratégie prometteuse contre l'athymie congénitale. Cette approche est encore limitée par de lourds obstacles : au-delà des problèmes inhérents à l'utilisation des cellules souches déjà évoqués, le contexte de ces pathologies causant une immunodéficience sévère implique une contrainte temporelle forte, de nombreux patients décèdent lors des premiers mois de vie. Or l'ensemble du protocole pourrait nécessiter plusieurs semaines pour produire le greffon thymique. Le succès de cette approche dépendrait donc en partie d'un diagnostic et d'une prise en charge rapide des patients.

Ces récentes percées dans la génération de TEC à partir d'iPSc ouvrent aussi de nouvelles perspectives pour le traitement d'autres pathologies chez l'adulte, comme l'APECED. Le même principe permettrait la correction des mutations de *AIRE et* régénérer des tissus thymiques autologues. La transplantation de ces tissus thymiques artificiels permettrait de restaurer la fonction thymique et de limiter le risque d'auto-immunité (Figure 20). En effet, les tissus transplantés seraient syngéniques et les cellules T générées seraient éduquées sur le répertoire d'auto-antigènes du patient, reconstituant ainsi un système immunitaire tolérant. Cependant, la présence des T autoréactifs en périphérie n'est pas résolue, et des approches d'immunothérapies à base d'anticorps les déplétant spécifiquement doivent être envisagées en complément (250).

Enfin, à plus long terme, un tel système de régénération de tissu thymique *in vitro* pourrait entrer en synergie avec les avancées récentes dans la production de lymphocytes T modifiés, notamment avec un récepteur T chimérique (CAR-T) (251,252). Les protocoles actuels de différentiation d'iPSc en T sont encore considérablement limités, reposant sur des cellules stromales modifiées pour surexprimer des ligands Notch, et incapables de fournir l'ensemble des signaux nécessaires au développement T caractérisant la niche thymique (253). Dans un futur à plus long terme, il serait alors possible d'envisager des approches thérapeutiques de génération de CAR-T *in vitro* dans des organoïdes thymiques dérivés d'iPSc. Ces CAR-T seraient spécifiquement désignés contre une pathologie, par exemple arborant des CAR anti-CD19 pour certaines leucémies ou des CAR-Treg anti-MOG pour la sclérose en plaques (252).

Depuis 15 ans, la compréhension de la biologie du thymus a connu des progrès remarquables. L'arrivée des technologies multi-omiques a permis de détailler à haute résolution les mécanismes gouvernant la thymopoïèse et l'organogenèse thymique. Ces informations ont eu pour effet des avancées notables dans la différentiation d'iPSc en épithélium thymique fonctionnel. Cependant, ces approches sont encore loin d'être matures pour une application clinique.

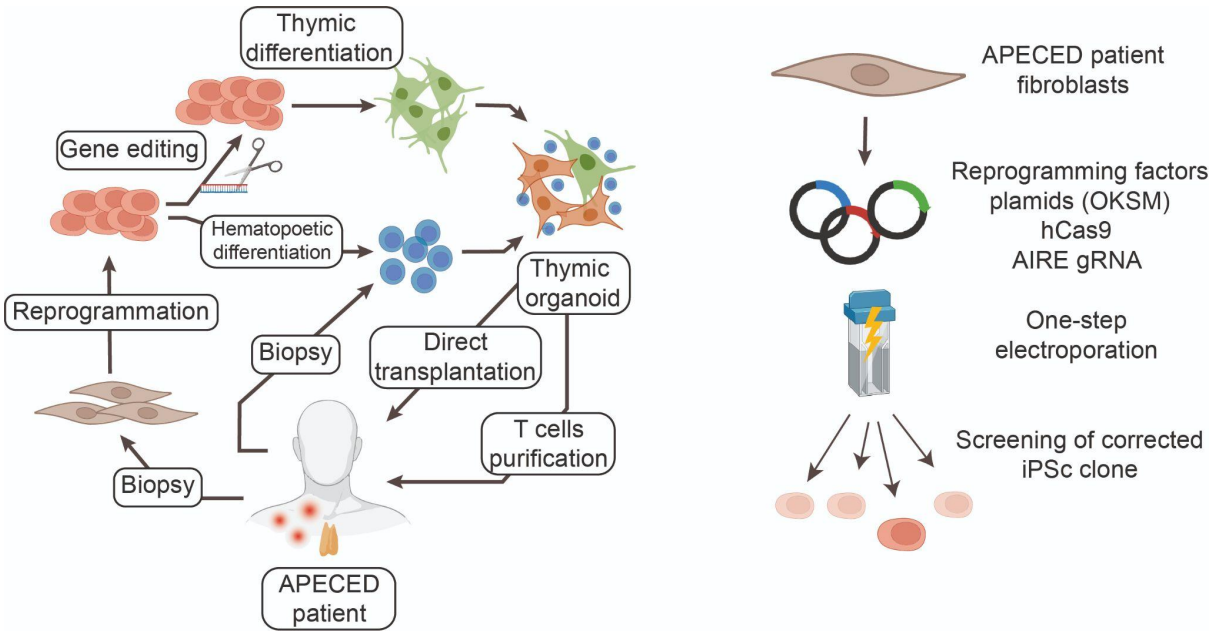

Figure 20 : Application potentielle de différenciation thymique pour la médecine régénérative : cas des patients APECED

La reprogrammation de cellules somatiques et la correction de *AIRE* par édition génique permettrait de générer des iPSc autologues du patient qui seraient ensuite différenciées en tissu thymique. La transplantation directe chez le patient ou l'isolation des lymphocytes T permettrait de régénérer un compartiment lymphocyte T tolérant au soi.

Chapitre 4 : Outils méthodologiques pertinents pour l'analyse des différenciations d'iPSc

I. Le design optimal d'expériences (DOE) : un outil statistique robuste pour l'étude et l'optimisation des différenciations d'iPSc

"To consult the statistician after an experiment is finished is often merely to ask him to conduct a post mortem examination. He can perhaps say what the experiment died of." Cette citation de R.A Fisher illustre l'importance cruciale d'une conception systématique du plan d'expérience tout en amont de la démarche expérimentale. Ceci est d'autant plus vrai pour les expérimentations coûteuses ou avec des échantillons limités. C'est notamment le cas des expérimentations sur les iPSc, notamment des différenciations reposant sur des réactifs chers et durant plusieurs semaines. Ainsi, l'implémentation de méthodes statistiques optimales pour la conception des plans expérimentaux est un point clé pour réaliser efficacement les manipulations.

Or, beaucoup d'études reposent encore sur une conception informelle, 'intuitive' de leurs plans expérimentaux, souvent en étudiant séparément un facteur d'intérêt, la méthode OFAT (One Factor At the Time) (254). Or cette approche sous optimale est limitée lorsque le nombre de facteurs étudiés est important, néglige la prise en compte des interactions possibles entre facteurs comme des synergies et enfin risquent souvent d'atteindre des optimums locaux (Figure 21.A). De plus, l'absence

de construction rigoureuse du plan expérimental peut entraîner la confusion de facteurs : dans ce cas, il est impossible de relier l'effet observé au facteur qui en est responsable. Certaines études proposant des protocoles de différenciation thymiques présentent de telles faiblesses (224,225,231).

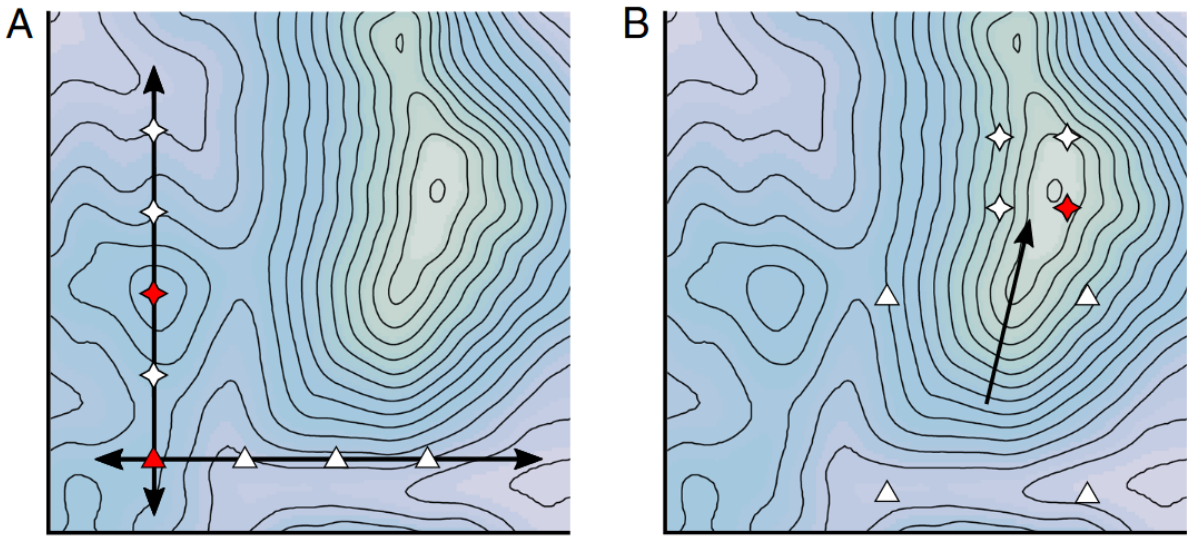

Figure 21 : Bénéfice de l'approche DOE par rapport à une optimisation classique OFAT

Cette figure illustre l'intérêt d'une méthode DOE pour l'optimisation d'un processus par rapport à une méthode classique faisant varier un facteur à la fois (OFAT). Les graphes représentent l'espace expérimental : la surface correspond aux valeurs théoriques de la réponse étudiée en fonction des valeurs de deux facteurs (en abscisse et ordonnée). Dans la méthode OFAT **(A)**, une première série d'expérience (triangles) teste quatre conditions du premier facteur et sélectionne la valeur optimale. Une deuxième série d'expérience (croix) fait de même avec le second facteur, obtenant un résultat sous-optimal. En DOE **(B)**, les facteurs varient simultanément (triangles), ce qui permet de modéliser le gradient de réponse et d'orienter la deuxième série d'expériences (croix), qui permet de localiser précisément l'optimum (tiré de Toms *et al.*).

Une autre approche intuitive pour étudier l'effet de plusieurs facteurs est d'effectuer toutes les combinaisons possibles : il s'agit d'un plan factoriel complet. Si cette approche est la plus puissante en termes d'information, elle est très inefficiente et est limitée à un faible nombre de facteurs. Cette approche a par exemple été utilisée par Soh *et al.* (Figure 1.C) pour leur optimisation de différenciation (255). Cependant, le nombre de manipulations nécessaire est égal à m^k, où k est le nombre de facteurs étudiés sur m modalités, ce qui entraîne une explosion combinatoire rendant impossible l'étude simultanée de nombreux facteurs.

Le design optimal d'expériences (DOE) est une branche des statistiques fondées notamment par Fisher au début du XXème siècle qui permet d'étudier simultanément l'effet de plusieurs variables (facteurs) sur un processus quantifié par une variable réponse, en testant plusieurs valeurs des facteurs (modalités), et ce lors d'un nombre réduits d'expérimentations (les essais). L'analyse des résultats repose sur des statistiques multivariées, par analyse de la variance par ANOVA et MANOVA, voire par une modélisation statistique de la variable réponse par régression linéaire multiple (254,256). Ainsi en DOE la réponse Y est généralement modélisée comme étant une fonction polynomiale de p facteurs X (256):

$$Y = \beta_0 + \sum_{i=1}^{p} \beta_i X_j + \sum_{i=1}^{p} \sum_{j=1}^{p} \beta_{ij} \underset{i \neq j}{X_i X_j} + \sum_{i=1}^{p} \sum_{j=1}^{p} \sum_{k=1}^{p} \beta_{ijk} \underset{i \neq j \neq k}{X_i X_j X_k} + \cdots \quad (1)$$

où β_0 est la réponse moyenne, les β_i sont les effets principaux des facteurs, les β_{ij} les interactions d'ordre 2 entre les facteurs i et j, les β_{ijk} les interactions d'ordre 3, *etc.*

Il est donc possible de sacrifier une partie de la précision de l'estimation de la réponse en confondant les effets de plus haut ordre, afin d'obtenir un plan expérimental nécessitant moins d'essais. Ce compromis entre précision de l'estimation et coût en termes de nombre d'essais est au cœur du principe du DOE.

Concrètement, un plan expérimental se présente comme une table décrivant les *n* combinaisons de facteurs à tester, les essais et les valeurs de leurs modalités, le plus simple étant 2 niveaux, codés + et -, ou par convention +1 et -1 (Figure 22).

Scenario	1	2	3	4	5	6	7	8	9	10	11
1	+	−	+	−	−	−	+	+	+	−	+
2	+	+	−	+	−	−	−	+	+	+	−
3	−	+	+	−	+	−	−	−	+	+	+
4	+	+	+	−	+	+	−	−	−	+	+
5	+	−	+	+	−	−	−	−	−	−	+
6	+	+	−	+	+	+	+	+	−	−	−
7	−	+	+	+	−	+	+	−	+	−	−
8	−	−	+	+	+	−	+	+	−	+	−
9	−	−	−	+	+	+	−	+	+	−	+
10	+	−	−	−	+	+	+	−	+	+	−
11	−	+	−	−	−	+	+	+	−	+	+
12	−	−	−	−	−	−	−	−	−	−	−

Figure 22 : Exemple de plan expérimental factoriel fractionnaire
Cette figure décrit les 12 essais d'un plan de Plackett-Burman à 11 facteurs. Les facteurs varient sur deux modalités, ici codées - et + (d'après Kleijnen *et al.*) (256).

Ainsi un plan factoriel complet présente une forte résolution (dites de résolution V), au prix d'un grand nombre de combinaisons à tester. Au contraire un plan factoriel fractionnaire de résolution IV voire III permet d'étudier simultanément un nombre plus grand de facteurs. Le plan de Plackett-Burman est un exemple de plan fractionnaire adapté au criblage, car il permet de tester un grand nombre de facteurs. Cependant il est limité pour la mesure des interactions entres facteurs, et ne permet pas une optimisation fine des modalités des facteurs. D'autres plans sont adaptés à cet enjeu, comme les plans centraux composites comme le plan de Box-Behnken, qui permet de trouver avec précision un optimum, en faisant varier les

facteurs sur trois niveaux et en modélisant le processus étudié par une surface de réponse (257). De fait, il existe de nombreux plans expérimentaux adaptés à des besoins variés : plans en mélange pour optimiser des proportions, plans à bloc pour corriger des sources de variabilité externe, plans à variables catégoriques si les facteurs ne sont pas quantitatifs (Figure 23)...

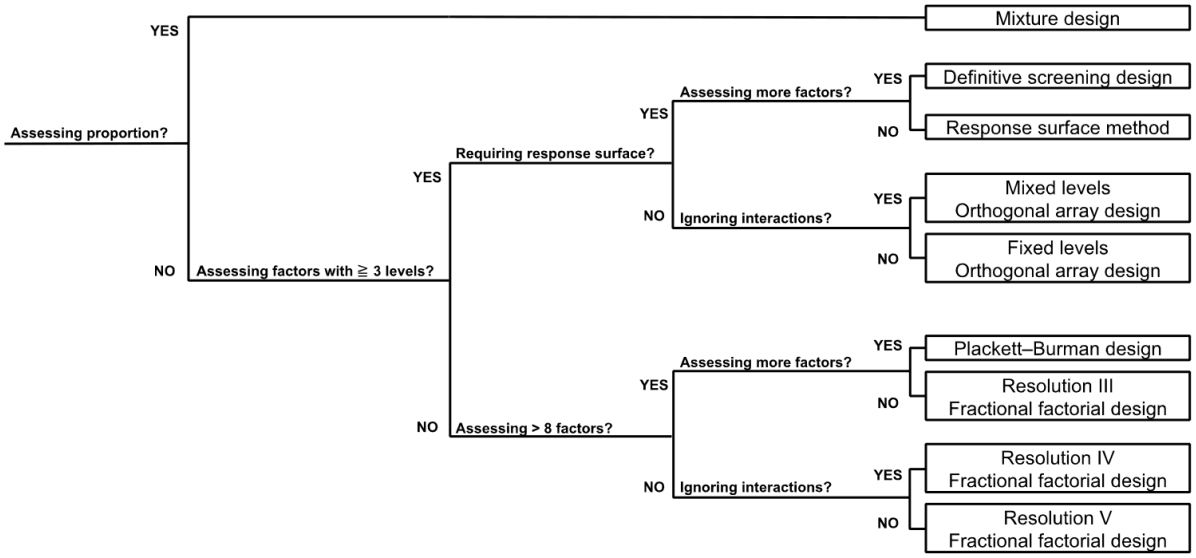

Figure 23 : Arbre décisionnel simplifié pour la sélection de plan expérimental
Le choix du plan expérimental découle d'un compromis entre le nombre de manipulations possibles, la quantité de facteurs à tester et le nombre de leurs modalités. L'assomption que les interactions sont négligeables est aussi cruciale et permet de recourir à des plans de plus basse résolution. (d'après Yasui *et al.*) (257)

Par conséquent, le DOE est avant tout un ensemble de méthodes statistiques flexibles, à utiliser en fonction des besoins afin d'étudier finement des processus biologiques complexes, sujets à une forte variabilité et avec un coût expérimental important.

II. Méthodes de séquençage pour la transcriptomique et analyse bioinformatique

Le processus de différenciation cellulaire est caractérisé entre autres par une régulation génétique précise causée par l'expression de facteurs de transcription régulant l'expression de programmes transcriptionnels permettant l'acquisition de fonctionnalités. Mesurer l'expression d'un grand nombre de gènes par échantillon est donc crucial pour l'étude des différenciations d'iPSc. Des progrès considérables ont été réalisés au cours des dix dernières années et ont permis de réduire dramatiquement les coûts et généraliser l'utilisation des techniques de séquençage (258).

Les méthodes de séquençage peuvent être classifiées selon les technologies utilisées regroupées en deux groupes : générations de fragments courts, longs ou séquençage direct de l'ARN (258). Le séquençage d'expression de gène digitale en 3' (3'-DGEseq) est une technologie récente permettant des hauts débits à faible coût. Son principal avantage est qu'elle repose sur des adapteurs à oligo(dT), amorces spécifiques des queuers poly(A) des transcrits, et non pas sur des amorces aléatoires. Ceci permet une parité fragment-transcrits et évite les biais de quantification des transcrits liés à des différences de taille entre les gènes. Ces spécificités en font une technologie adaptée aux usages reposant sur la quantification des transcrits, comme l'analyse des gènes différentiellement exprimés entre échantillons (258).

Au-delà du séquençage 'bulk' d'une population entière de cellule, qui fournit une expression moyenne des gènes, l'utilisation du séquençage d'ARN en cellule unique (sc-RNAseq) est aujourd'hui répandue. Pour la première fois utilisée en 2009, cette technologie permet d'explorer les transcriptomes de cellules individuelles, révélant

l'hétérogénéité des populations analysées. Différentes techniques, comme le Drop-seq reposant sur l'encapsulation individuelle des cellules, offrent des compromis entre profondeur de séquençage et nombre de cellules (258). Le scRNAseq permet donc l'exploration à une échelle sans précédent du transcriptome d'une population cellulaire, de la signalisation entre populations, des réseaux de régulation (SCENIC) (259) ainsi que des dynamiques de différenciation (RNA Velocity) (260). L'identification des différentes sous-populations repose sur des algorithmes de clustering comme l'algorithme de Louvain ou de Leiden. La nature multidimensionnelle inhérente à ces données implique une réduction de dimension par analyse en composantes principales (ACP) et une projection par UMAP ou tSNE, permettant de les projeter en deux dimensions. L'intégration de multiples jeux de données permet la constitution d'atlas pouvant compter des millions de cellules, originaires de multiples organes au cours du développement. Ainsi, le scRNAseq se positionne comme une technologie indispensable pour l'étude des processus de différenciation et de leur régulation.

OBJECTIFS

L'objectif de cette thèse est de générer à partir d'iPSc humaines un épithélium thymique fonctionnel *in vitro*, *i.e* capable de soutenir le développement de lymphocytes T matures. Dans un premier temps nous avons optimisé le protocole de différenciation dirigée des iPSc en TEP. Nous avons utilisé une approche basée sur le design expérimental pour effectuer un criblage de molécules modulatrices des voies de signalisation impliquées dans l'organogenèse du thymus.

Dans un second temps, nous avons caractérisé le produit de différenciation de notre protocole optimisé. Nous avons ensuite développé un système de culture visant à reproduire fidèlement le micro environnement thymique. Nous avons mis au point un système de coculture en hydrogel 3D permettant la formation d'organoïdes thymiques.

Enfin, nous avons étudié la capacité de ces organoïdes thymiques de supporter la thymopoïèse *in vitro*, en générant des lymphocytes T matures à partir de progéniteurs hématopoïétiques.

RÉSULTATS

Mes travaux de thèse ont résulté d'un article de recherche, encore en rédaction et qui sera soumis sous peu, ainsi que de la publication de deux revues. J'ai aussi participé activement à deux articles dont les sujets rejoignent mon domaine de compétence. Enfin, les protocoles de différenciation thymique d'iPSc et de génération d'organoïdes de thymus mis au point pour ces travaux de thèse ont débouché sur un dépôt de brevet.

Ces résultats seront décrits ci-après de manière synthétique afin de décrire le panorama de la contribution scientifique de ces travaux.

I. Combinatorial experimental design for hiPSc differentiation in thymus epithelium and generation of thymic organoids supporting thymopoeisis *in vitro*

Cet article est mon papier de thèse en premier auteur. Encore en cours de rédaction, nous prévoyons de le soumettre d'ici la fin de l'année. Une série d'expériences est prévue début 2023 afin de disposer du matériel nécessaire pour appliquer les révisions apportées par les correcteurs. Ce papier reprend l'ensemble des problématiques de mes travaux de thèse présentés dans l'introduction. Son principal objectif est de mettre au point un modèle de thymopoïèse *in vitro* en différenciant des iPSc en tissu thymique. Il a donc fallu lever les obstacles freinant le développement d'un tel outil, tels que *1.* mettre au point un protocole de différenciation des iPSc robuste et optimisé, *2.* caractériser précisément le produit de différenciation pour établir le niveau fonctionnel des cellules obtenues, *3.* celles-ci s'étant révélées être des progéniteurs de TEC, développer un système de culture permettant leur maturation et leur survie, *4.* Tester la fonctionnalité, *i.e* la capacité de ces TEC induites à induire la différenciation de lymphocytes T matures.

Nous avons pour cela appliqué un ensemble de méthodes combinant design expérimental, transcriptomique, coculture avec des thymocytes pour reproduire le crosstalk thymique et développement d'un système de culture dans un hydrogel en 3D résultant en la formation d'organoïdes thymiques.

Combinatorial experimental design for hiPSc differentiation in thymus epithelium and generation of thymic organoids supporting thymopoiesis *in vitro*

Nathan Provin[1], Erwan Kervagoret[1], Xavier Saulquin[2], Carole Guillonneau[1], Laurent David[1], Matthieu Giraud[1]

[1] Nantes Université, INSERM, Center for Research in Transplantation and Translational Immunology, UMR 1064, F-44000 Nantes, France.

[2] INSERM, Nantes Angers Center for Research in Integrated Immunology and Cancerology , UMR 1232, Nantes, France.

Abstract

The thymus is a primary lymphoid organ playing a crucial role in immune tolerance. It is the place where the T lymphocytes are generated. Thymocyte maturation and selection is mediated by thymic epithelial cells (TECs). Induced pluripotent stem cells (iPSc) have the unique ability to differentiate into all adult cell lineages and are a promising tool for pathology models and regenerative medicine. Here we address the production of functional iPSc-derived TECs expressing *AIRE* and able to support *in vitro* T cell generation. We set up a protocol for differentiation of thymic epithelial progenitors (TEP) through an unbiased multifactorial method based on optimal experimental design (DOE) and comprehensive transcriptomic profiling of differentiated cells. Modulation of signalling pathways known to regulate embryonic thymus organogenesis resulted in the obtention of TEPs expressing typical thymic markers. We achieved TEP maturation into mature TECs by setting up a coculture with early thymic progenitors (ETPs) in a hydrogel-based 3D system, resulting in the formation of thymic organoids (hTOs). HTOs demonstrate the capacity to induce multilineage maturation into both single-positive CD4 or CD8 T cells, as well as dendritic cells. Generation of iPSc-derived functional TECs and multilineage thymic organoids offers a practical platform for mature T lymphocyte production and paves the road to future cellular therapies for autoimmune diseases.

Introduction

The thymus plays a crucial role in the establishment of central immune self-tolerance. Its main function is the generation of a diverse yet non-autoreactive T lymphocyte repertoire (1). The thymus is subdivided in several lobes structured in two principal niches, a peripheral cortical area surrounding a central medulla. Distinct cellular populations shape specific microenvironnement of these niches. Thymic epithelial cells (TECs) are a crucial actor that regulates the maturation of developing T cells, the thymocytes (2). Two main populations of TECs are identified : the cortical TECs (cTECs) and the medullary TECs (mTECs) that are characterized in human by the KRT8/18 and KRT5/14 cytokeratin expression, respectively, and by the expression of the surface marker CD205 for cTECs (2,3). Recently, single-cell studies have revealed a higher level of heterogeneity for TECs with, notably, the identification of new mTEC subpopulations with various functional roles such as thymocyte homing, commitment, proliferation regulation and selection (3–5). Thymocyte selection is required for the generation of a functional and non-autoreactive T repertoire and is mediated in two steps. Thymocytes originate from a CD34+ circulating hematopoietic early progenitor (ETP) and differentiate in several stages characterized by CD4 and CD8 expression (6–8). Positive selection is mediated by cTEC at the double positive (DP) stage and leads to the selection of thymocytes with a functional T cell receptor (TCR) (3). Negative selection filters out potential autoreactive thymocytes at the single-positive (SP) stage in the medulla (9,10) and is mediated by HLA-DR^{hi} mTECs expressing a great diversity of peripheral tissues antigens (PTAs) under the regulation of *AIRE* (3,11,12). Mature CD4 and CD8 T lymphocytes are called recent thymic emigrants and migrate to the periphery (13).

mTECs and cTECs derive from a common bipotent progenitor with cortical-like phenotype (14,15). Molecular mechanisms regulating TEC fate decision are still elusive, although crucial implication of NOTCH (16,17) and RANK-CD40-LTB signalling (18–20), provided by thymocytes through the thymic crosstalk, have been reported. Regulation of the organogenesis of the thymus has also known remarkable recent progress, notably thanks to the publication of single cell RNA sequencing (scRNAseq) thymic cell atlas at different stages of development (21–23). Thymic epithelial progenitors (TEP) identity is characterized by *FOXN1*, a master regulator inducing expression of the TEC transcriptional program (24–26). TEPs emerge from the third pharyngeal pouch endoderm (3PPE), a transient embryonic structure formed by the involution of the endoderm inside the foregut tube between week 3 and 4 in human (27–29). A gene cascade involving *TBX1*, *PAX9* and *EYA1* has been identified as a crucial regulator of 3PPE formation. 3PPE is derived from the ventral pharyngeal endoderm, itself originating from

the anterior foregut endoderm (AFE) (27,30). Regulation of the fate acquisition in these structures has also shown recent progress at the single-cell level (31–33).

Mimicking thymus organogenesis *in vitro* to generate TECs from embryonic (ESc) and induced pluripotent stem cells (iPSc) has been a long-standing objective over the last decade, using reprogramming and mainly direct differentiation approach (25,34–39). However, the complexity of the regulation of the differentiation process and our limited comprehension of *in vivo* mechanisms hindered the achievement of this goal (40). Indeed, thymic differentiation often yields immature and non-functional cells with a progenitor (TEP) identity and requires grafting *in vivo* to complete the maturation (35–37). Moreover, the available protocols of iPS differentiation into TEPs have not been optimized by unbiased systematic approaches to robustly assess the effects of the supplemented factors at each stage (41–43). Thus, reliable methods for the differentiation of iPSc into functional mature TECs *in vitro* and for their long-term maintenance in a culture system reproducing the thymic niche are yet to be developed. Such sytems would result in the generation of iPSc-derived TECs, opening promising perspectives for regenerative medicine (44). For instance, reprogramming patient cells into iPSc and their correction by gene editing is a promising approach for congenital pathologies of the thymus, such as the severe combined immune deficiency (SCID) and Digeorge syndrome and differentiation of functional TECs would allow restoration of the thymic function. Finally, iPSc-derived TECs could be use to improve *ex vivo* T generation with application against the dramatic loss of thymus function during aging, the thymic involution, linked to weakened immune response in aged patients (34,45). Finally, autoimmune pathologies such as autoimmune polyendocrinopathy-candidiasis-ectodermal dystrophy caused by *AIRE* deficiency, could benefit from such an approach (44). *AIRE* correction in iPSc and TEC differentiation could be used to generate non-autoreactive T lymphocytes for transplantation.

In vitro T Lymphocyte generation has been greatly improved using feeder stromal cells such as OP9-DLL1 or MS5-hDLL4, modified to express NOTCH ligand (46–48). Formation of artificial thymic organoids improved the maturation state of obtained T cells, and partially reproduce thymic function (34,49). Indeed, these setups could only partially reproduce thymic selection, lacking the self-antigen presentation ability assured by mTEC^{hi}.

Here, we used DOE paired with transcriptomics to optimize iPSc thymic differentiation based on recent single cell datasets of thymus organogenesis. We propose a two-weeks protocol that efficiently yields TEPs expressing thymic identity markers. To overcome the difficulty to mature TEPs *ex vivo*, we developed a 3D coculture system with primary thymocytes (ETPs). We set up a fibrin hydrogel air-liquid interface culture that resulted in the formation of human thymic organoids (hTO). hTO could be maintained up to 5 weeks, and showed evidence of TEC

maturation, notably into HLA-DR^{hi} mTECs, with higher *AIRE* expression than cells cultured in monolayer. T-TEC physical interactions were demonstrated, and hTO showed the ability to drive ETP maturation into SP CD4$^+$ and CD8$^+$ T lymphocytes. Further characterization of hTO products by scRNAseq confirmed the mature stage of the generated T lymphocytes and revealed secondary differentiation into dendritic cells (DCs), suggesting that DCs may participate in the T cell selection in hTOs.

Materials and methods

Isolation of human primary early thymocyte progenitors (ETP) and thymic epithelial cells (TEC).

Postnatal human thymic samples were obtained as anonymized, discarded waste from patients undergoing cardiac surgery at Maternité de Nantes, in accordance withFrench CODECOH reglementation under declaration DC-2017-2987. ETPs isolation was performed as described in Lavaert *et al*. (50). Briefly, fresh thymus samples were dissected on the same day in 1 mm^3 fragments in RPMI1640 and dissociated by mechanical pipetting to release thymocytes. A 5 minute incubation in red blood cell lysis solution (Miltenyi, 130-094-183) was performed for erythrocyte depletion. Cells were passed through 70µm meshes and incubated with CD4 and CD8 labeled Dynabeads (Thermofisher, 11031) to deplete most DP and SP thymocytes. ETP-enriched cell suspension was stained for flow cytometry using antibodies referenced in supplementary methods. ETPs were sorted with a FACS ARIA (BD Biosciences) using phenotype CD3$^-$CD4$^-$CD8$^-$CD14$^-$CD19$^-$CD56$^-$CD34$^+$CD7$^+$ and immediately used for reaggregation culture. For TEC isolation, thymic fragments were digested using a 0.5 mg.mL^{-1} collagenaseD (Roche, 11088866001), 1 mg.mL^{-1} dispase (Roche, 04942078001) and 0.5 mg.mL^{-1} DNAseI (Roche, 11284932001) solution in RPMI1640 for 45 minutes at 37°C and dissociated using GentleMACS (Miltenyi, 130-093-235) and C tubes (Miltenyi, 130 093 237). Cell suspension was deposited on a 21% Optiprep (Sigma Aldrich , D1556 250ML) gradient and centrifuged 20 min at 500g for TEC enrichment. Cell suspension was filtered on a 100µm mesh and sorted with phenotype CD45$^-$EPCAM$^+$.

Human induced pluripotent stem cells (hiPSc) culture and differentiation in thymic epithelial progenitors (TEP)

iPSc cell lines were furnished by the Nantes iPSc platform and were maintained on Matrigel (Stem Cell Technologies, 354277) coated 6-well plates in mTESR1 medium (Stem Cell

Technologies). Details on the cell lines used are available in Supplementary figures. iPSc cultures were passaged every 5 to 6 days, using XF passaging solution (Stem Cell Technologies) and were seeded in clumps. In case of anormal colony morphology in cultures, daily cleaning was performed to guarantee optimal iPSc purity. To control cell state variability, iPSc were passaged 4 days before induction of differentiation, then harvested 24 hours before the D0 in single cell suspension using TrypLE (ThermoFisher) with 5 minute incubation at 37°C. Cells were resuspended in mTESR1 medium with 10µM ROCK inhibitor Y27632 (Sigma Aldrich Y0503) and seeded on Matrigel coated 12-well plates at 37.10^3 cells/cm^2. Differentiation was induced at D0 with XVIVO10 medium (Lonza, BE04-380Q) supplemented with 5µM CHIR99 (Miltenyi, 130-106-539) and 100 ng.mL^{-1} ActivinA (BiotechneR&D, 338-AC). Culture medium changes were performed at fixed hours, with quick rinsing by warm PBS to eliminate potential differentiation medium leftovers in wells. D1 and D2 medium contained only 50 ng.mL^{-1} ActivinA. At D3, cells are passaged in single cell as described above and seeded at low density (14.2 to 20.10^3 cells/cm^2 depending on iPSc line) in Matrigel coated 12-well plate with 10 µM Y27 and 50 ng.mL^{-1} ActivinA. Culture medium was changed at D4, D5, D7, D9, D10, D11 and D13 as previously described with supplementation as detailed in Figure 1.

TEP reaggregation with early thymic progenitors (ETP) and thymic organoids (hTO) formation

TEP were harvested at day 13 using TrypLE with a 7 minutes incubation at 37°C and mechanical flushing. TEP were aggregated in low binding 96-well plates (ThermoFisher, 174929), at a 8:1 ratio with fresh ETP sorted as described above. Culture is maintained 24 hours in an XVIVO10-based medium supplemented with 1% Glutamax (Gibco, 35050-38/2165269), 1% non essential amino acids (Gibco, 11140-035), 30 mM L-ascorbic () 0.1µM retinoic acid (Sigma Aldrich, 302-79-4), 50 ng.mL-1 BMP4 (Miltenyi, 130-111-165), RANKL (BiotechneR&D : 6449-TEC), 10 ng.ml-1 FGF8 (BiotechneR&D, 423-F8), FGF10 (Miltenyi, 130-127-858), IGF1 (Miltenyi, 130-093-886), EGF (Miltenyi, 130-097-751), SCF () and 5ng.mL-1 IL7 (), FTL3L (). Cell micromasses must show a typical spheroid morphology with a compact central cell mass surrounded by a crown composed mainly of ETPs. Hydrogels were formed by mixing a 8 mg.mL^{-1} Fibrinogen (Sigma Aldrich, 341578) solution heated at 37°C with 10 U.mL^{-1} Thrombin (Sigma Aldrich,605190) and 26000 U.mL^{-1} Aprotinin (Sigma Aldrich, 616370), and immediately casting it in the superior compartment of 24-well inserts. Between 2-4 spheroids were individually collected using cut 200µL pipette tips pre-coated with anti-adherence solution and seeded delicately on the hydrogels. The same culture medium described above was added in a way to form an air-liquid interface without drowning the hydrogels and changed every three days during the first week. Then retinoic acid, BMP4,

RANKL, FGF8, FGF10, IGF1, and EGF were removed from the culture medium. To harvest the cells, the hydrogels were carefully preleved using cut 1000-µL pipette tips and incubated 15 minutes at 37°C in a 0.5 $mg.mL^{-1}$ Collagenase (Roche, 11088866001) solution in DMEM/F12 . Organoids were subsequently processed with a 10 minutes incubation in TrypLE at 37°C with frequent mechanical disruption by pipetting, then filtered on a 100µm mesh.

RNA-extraction, RT and qPCR

Cell samples were lysed using RLT Lysis buffer (Qiagen, 79216). RNA extraction was performed using RNAeasy mini kit (Qiagen, 74104) and retrotranscription with Superscript III (Thermofisher, 18080093) following manufacturer's guidelines. qPCR was performed with SYBR Green Fast kit (ThermoFisher, 4385612) on a ViiA 7 Real-Time PCR System (ThermoFisher) using the primers listed in supplementary methods. Relative quantification of target gene expression was measured using the delta CT method with *GAPDH* as endogenous control.

DGE–seq bulk RNA sequencing

For 3' Digital gene expression (DGE) bulk RNA sequencing, protocol was performed according to our implementation of previously developed protocols (51). 10 ng total RNA was used for librairie preparation. mRNA were tagged thanks to poly(A) tails-specific adapters, well-specific barcodes and universal molecular identifiers (UMI) with template-switching retrotranscription. cDNAs were pooled, amplified and tagmented by transposon-fragmentation to enrich 3' ends. Sequencing was performed on Illumina® HiSeq 2500 using a Hiseq Rapid SBS Kit. Kits used were Zymo purification kit Researche D4004-1-L, Kit Advantage 2 PCR Enzyme System (Clontech, 639206), QIAquick Gel Extraction, Kit AgencourtAMPure XP magnetic beads, Nextera DNA (FC-121-1031).

DGE–seq data processing and analysis

Reads were kept if passed a quality control test of all 16 bases of the first read reaching quality score of 10. The second reads were aligned to RefSeq human mRNA sequences (hg19) using bwa version 0.7.17. Reads mapping to several transcripts of different genes or containing more than 3 mismatches with the reference sequences were filtered out from the analysis. We generated DGE profiles by counting the number of unique UMIs for each RefSeq genes. Final

processing included filtering out the samples with less than 200 000 total counts and 5000 genes.

DGE–seq data processing and analysis

Read pairs used for analysis matched the following criteria: all 16 bases of the first read had quality scores of at least 10 and the first 6 bases correspond exactly to a designed well-specific barcode. The second reads were aligned to RefSeq human mRNA sequences (hg19) using bwa version 0.7.17. Reads mapping to several transcripts of different genes or containing more than 3 mismatches with the reference sequences were filtered out from the analysis. DGE profiles were generated by counting for each sample the number of unique UMIs associated with each RefSeq genes. DGE-sequenced samples were acquired from five sequencing runs. Sequenced samples with at least 50000 counts and 6000 expressed genes were retained for further analysis. Batch correction and differentially expression (DE) was performed with DEseq2 R package, with threshold of 1 log2 fold change and 0.05 Benjamini Hochberg p-value to classify a gene as differentially expressed vs D0 iPSc controls. Gene Ontology of DE genes modules was performed using ClusterProfiler R package on KEGG database of biological processes. GO network was plotted using REVISEGO and Cytoscape software. Data visualization relied on custom pipelines based on ComplexHeatmap and ggplot2 R package.

scRNAseq data generation

D28 dissociated hTO were sorted on FACS ARIA to purify cell population and remove dead cells and debris. Three samples were labeled by HTO staining and processed with a Chromium Single-Cell 3′ Reagent v2 Kit (10× Genomics, Pleasanton, CA) as per the manufacturer's protocol. Briefly, a small volume of the single-cell suspension was mixed with RT-PCR mix and loaded with partitioning oil and Single Cell 3' Chip. Chip was loaded on Chromium controller (10X Genomics) for single cell generation and barcoding. cDNA were then pooled, pre-amplified and fragmented. Adapters were incorporated and sequenced with Illumina® HiSeq 2500.

scRNAseq data processing and analysis

Primary data analysis was performed on CellRanger. Cell count matrices were exported and secondary analysis was performed on R using Seurat v4 package (52). HTO were demultiplexed and quality control defined by keeping cells with gene number between 2000

and 15000 and less than 0.1 mitochondrial genes proportion. Variable genes identification, data scaling and dimension reduction used functions integrated in Seurat. Dimensionality reduction used UMAP and tSNE embedding on the first 10 dimensions. Clustering used the Louvain algorithm implemented in FindCluster function with a resolution of 0.3. Visualization and marker determination relied on default Seurat functions. For the analysis of public sc datasets of thymus and pharyngeal organogenesis, raw data was downloaded at the accession provided in the data availability section of the relevant papers (21,31,32). Between-sample integration was performed using the integration framework provided by Seurat. Data analysis followed the same pipeline. Park's dataset was downsized by random sampling by a factor of 0.25 to ease data handling. Quality control was set at 500 / 10000 / 10, and 500 / 4000 / 10 for Han's and Magaletta's datasets. Dimension reduction was performed by UMAP on first 10 (Park), 21 (Magaletta) and 25 (Han) dimensions. Clustering was performed with a resolution of 0.75 (Park), 0.5 (Magaletta), 0.6 (Han). Visualization and marker identification was performed as described above. For label transfer of our dataset to the thymus atlas reference dataset, anchor identification, integration and transfer relied on the default Seurat vignette.

Flow cytometry and Immunofluorescence (IF) imaging

Cells were stained with antibodies listed in supplementary according to the manufacturer's guidelines and analyzed on FACS ARIA (BD Biosciences) and Celesta (BD Biosciences). For 2D IF, cells were cultivated on Ibidi 8-well plates (Ibidi, 80806), fixed with 4% PFA for 15 minutes and permeabilized with IF buffer (PBS, 0.2% Triton, 10% inactivated FBS) for 1 hour. Cells were incubated in IF buffer overnight at 4°C with primary antibody and for 2 hours at room temperature for secondary antibodies. Plates were imaged on a confocal SIM microscope. For hTO stainings, the hydrogels were harvested by using a widely cut 1000µL pipette tip pre-coated with anti-adherence solution and carefully deposited in Ibidi 8-well plates in cold PBS. Most of the gel matrix was removed by delicate flushing and several PBS washing, without destructuring the main cellular structures. hTO were fixed with 4% PFA for 20 minutes and permeabilized with IF buffer (PBS, 0.2% Triton, 10% inactivated FBS) for 2 hours. Primary staining was performed in IF buffer for 24h and secondary staining for 4 hours, and imaging on SIM confocal microscope in Z-stack mode.

Statistics and data analysis

Statistical tests were performed on R. Mean comparison significance on qPCR graphs was tested by non-parametric t.tests with a significance p-value threshold of 0.05. DOE

experimental plans were designed using R DOE base package 1.11.6. DOE results were analyzed by factorial ANOVA as detailed in figure legends.

Results

Optimization of directed differentiation protocol using a DOE-based factor screening and bulk transcriptomics

To set up our optimized TEC differentiation protocol, we followed an approach of directed differentiation recapitulating the events of the thymic organogenesis. Recently, the understanding of thymic identity acquisition and its underlying regulation at the cellular and molecular level has greatly improved, thanks to multiple studies using sc-OMICs (31–33,53). Definitive endoderm (DE) anteriorizes into anterior foregut endoderm (AFE), from which emerges the third pouch pharyngeal endoderm (3PPE), a transitory structure that gives rise to the thymic epithelial progenitors (TEP) (Figure 1.A). We thus aimed to recapitulate these events *in vitro* by modulating the main pathways involved in thymic organogenesis, such as BMP, WNT, SHH and FGF.

Exit of pluripotency state and DE induction has been studied extensively (54). The state-of-the art approach, relying on Nodal simulation through ActivinA exposure combined with a 24-hours pulse of WNT through CHIR99, has been applied to induce DE. D5 cells show a peak of *SOX17* expression (Figure Supp 1.A), with most cells co-expressing FOXA2 and SOX17, as observed by immunofluorescence microscopy (Figure Supp 1.B). Therefore, this method correctly induces DE differentiation and was not subject to further optimization.

We then applied optimal design of experiment (DOE) to decipher the effect of differentiation at 3 key timepoints, based on the hypothesis that factor effect was stage-dependent. Thus, modulation of RA, TGb, BMP and WNT pathways on definitive endoderm anteriorization between D5 and D7 was first studied. Then effect FGF8, NOTCH, SHH, BMP and WNT modulation of 3PPE was assessed between D7 and D9. Investigation of BMP, FGF10, EGF, IGF1 and RANKL modulation on TEP fate induction was investigated lastly. These pathways were selected after literature reviewing of previous thymic differentiation studies and thymic organogenesis regulation (40,55–58). A Plackett-Burman combinatorial screening design was performed at each stage (AFE: D5-D7, 3PPE: D7-D11, TEP: D11-D13), testing multiple combinations of factors (Figure Supp 1.C) with two modalities of concentration (Figure 1.B).

Using a low-dimensionality readout, such as measuring the expression of one or a few marker genes, can yield imprecise results due to marker lack of specificity or gene expression

variability. To overcome this weakness and robustly assess factor effects, we performed bulk RNAseq on the DOE samples and compared their transcriptome with recent scRNAseq atlases of pharyngeal development (31,32). We reanalyzed raw data applying uniform manifold approximation and projection (UMAP) to identify thymic precursor cell populations (Figure 1.C, Figure Supp 2) resulting in a transcriptomic map of the thymic differentiation trajectory (31,32). We then scored transcriptome similarity of each of our DOE samples to relevant *in vivo* cell populations at each stage of the trajectory, for each dataset (Figure 1.D), using mean expression of top 100 markers. For better visualization, DOE samples were ordered by increasing score of the targeted cell population : early pharyngeal endoderm at D5-D7 and D7-D11 and mature (late) pharynx/ thymic primordium at D13. in both reference datasets from Han et al. and Magaletta et al., RA supplementation revealed to be crucial for anteriorization of definitive endoderm. However, WNT inhibition is globally detrimental, as shown by IWR1 significance in both datasets (Figure 1.D-E). Moreover, using Han *et al.* data as reference indicated that BMP inhibition by NOGGIN, and with less significance TGFβ inhibition by LY3, promoted anteriorization.

Differentiation into 3PPE is mainly dependent on WNT and NOTCH signals, as inhibition of these pathways with IWR1 and FLI06 significantly reduced scores in both datasets (Figure 1.E). Moreover, WNT activation by CHIR99 greatly promoted pharyngeal induction. Contrary to Parent *et al* study, we observed no effect of Hedgehog inhibition by cyclopamine at this time point. Similarly, BMP4 and FGF8 supplementation showed no significant effect for pharyngeal induction. Such non-significant factors were kept in the protocol if a consensus of half or more of the samples in the top 3 samples, with each reference dataset, were supplemented with them.

Finally, the last stage of the differentiation protocol was shown to be promoted mainly by BMP4. While this third iteration resulted in less significant results, this could originate from the lower number of runs performed, leading to lower statistical power. Interestingly, FOXN1 expression measured by qPCR was revealed to be significantly promoted by IGF1 (Figure Supp 3.C), as well as BMP4 and to a lesser extent FGF10. Particularly, this result showed that IGF1 promotes FOXN1 expression, in accordance with *in vivo* studies (59).

The interest of using a high dimension readout using RNAseq was illustrated by the comparison of qPCR results on a unique marker gene of each stage, which despite being globally coherent, presents several divergences that could have led to classify incorrectly some factors. For instance, D5-D7 IWR1 supplementation induced *HOXA3* expression, as measured by qPCR (Figure Supp 3.A), despite its significant negative effect revealed by the RNAseq. This approach allowed the systematic delineation of the pathways involved in iPSc thymic differentiation (Figure 1.F).

Characterization of the differentiation product demonstrate efficient differentiation into immature TEC

To finely follow the thymic differentiation process at the transcriptome level, we sequenced samples by bulk RNAseq at multiple timepoints across our differentiation protocol. Human primary TECs, sorted on $CD45^{-}EPCAM^{+}$ and originating from pediatric cardiac chirurgy thymic samples, were included to assess the state of maturation of the differentiation product. iPSc samples were included as well as the starting point of the differentiation trajectory.

Differential gene expression was performed on sample transcriptomes, resulting in the isolation of 9 gene modules, enriched at distinct differentiation stages (Figure 2.A). Several known markers of thymic differentiation stages were detected in the differentially expressed genes, such as *SOX17* (DE), *HOXA3* (AFE), *EYA1* (3PPE) or *EPCAM* (TEP).

To determine the biological processes enriched in the 9 gene modules, Gene Ontology (GO) terms were associated using ClusterProfiler. Ordering GO terms by time of differentiation showed a shift from pluripotency state and cell amplification to embryogenesis and organ morphogenesis (Figure 2.B). As expected, GO terms in late differentiation samples and primary TEC controls were associated with lymphocyte interaction and regulation of immune response, indicating the enrichment of our differentiation product in TEC-associated genes. Detailed list of GO terms is available in Figure Supp 4.A. Projection in 2D by PCA illustrated this transcriptome shift from pluripotency to thymic identity along the first principal component (Figure 2.C). The second dimension being associated with T cell genes, probably because of thymocyte contamination in primary TECs controls (Figure Supp 4.B), we observed convergence of sample transcriptomes with primary TECs across differentiation along the first dimension. Heatmap representation of known markers highlighted the distinct stages of the thymic differentiation (Figure 2.D). As anticipated, iPSc samples showed expression of the pluripotency markers *POU5F1* and *NANOG*. DE markers such as *FOXA2* and *SOX17* peaked between D2 and D5. At D7, cells began to express anteriorization markers including *HOXA3* and *MEIS2,* before expressing the third pharyngeal pouch markers *EYA1* and *EYA2*. From D13, TEP markers could be detected in cultures : cortical-associated cytokeratins *KRT8* and *KRT18,* podoplanin (*PDPN*) and fibronectin (*FN1*), as well as low levels of *PAX9* and *FOXN1*. Interestingly, genes associated with TEC functionality as interleukin 7 (*IL7*), *CXCL12* and *CCL21* could be measured in TEPs at this stage. However, markers associated with a more mature TEC phenotype, such as cortical proteasome components encoded by *PSMB11* and *PRSS16*, or genes involved in antigen presentation (*HLA-DRA*, *CD80*, *CD86*), were not expressed in late differentiation cultures and did not reach the expression level measured in primary TECs.

Another round of post-DOE optimization was performed considering recent publications on thymic differentiations highlighting the benefits of FGF8 supplementation for AFE induction (38). We confirmed similar results in our protocol by measuring a significant *FOXN1* expression increase at the end of differentiation in samples exposed to 50 ng/mL FGF8 from day 4 to 6 (Figure 1.G). Similarly, RA supplementation after AFE induction showed no dose-dependent effect (Figure Supp 3.D). We thus selected the lower 0.1 µM dose for this stage of differentiation.

Leveraging these results, we set up an optimal directed differentiation protocol (Figure 1.H). This protocol was benchmarked against two state-of-the-art protocols from Sun *et al.* and Parent *et al.* studies, by measuring thymic identity markers expression at D14 (Figure 1.I). The new protocol yielded cells expressing significantly higher levels of *PAX9* et *FOXN1*. To test if those results came from a protocol overfitting to our iPSc cell line LON71, or a true optimization of the biological phenomenon, we differentiated two other iPSc cell lines (MIPS203 and LON80) and showed no significant differences in *FOXN1* and *PAX9* expression at D14, excepted for the MIPS203 that showed lower *FOXN1* expression (Figure Supp 3.E). Finally, thymic marker expression in the differentiation product was of the same level of magnitude as primary TEC, validating the efficiency of our DOE based approach to optimize iPSc thymic differentiation.

Figure 1 : Combination of DOE and DEGseq results in optimized thymic differentiation from iPSc **(A)** Differentiation itinerary of the thymic epithelium. **(B)** Factor abbreviations, supplementation dosing and timings for the experimental design screening. **(C)** UMAP representation of reference data. Public datasets of pharyngeal and thymic organogenesis from Han *et al.* and Magaletta *et al.* were reanalysed to identify the transcriptomic signature of the thymus organogenesis differentiation trajectory**. (D)** DGEseq results for each DOE experiment ordered by expression score of target clusters in the differentiation trajectory from the public datasets of Fig1.C. Expression score is the mean expression of target cluster markers in each culture sample, i.e factor combination. Statistical significance is measured by ANOVA. Significant factors were selected for the optimized protocol. Non-significant factors levels were fixed using the modality in majority in the union of top 3 samples in both datasets. **(E)** ANOVA main effect plot for each DOE analysis, with Mageletta reference dataset**. (F)** Synthesis of the pathways identified by the DOE analysis: - inhibition, + activation, no sign indicates the pathway was shown to be necessary but was not modulated. **(G)** FGF8 supplementation at D4 improves FOXN1 expression in D14 differentiation product. Relative quantification by qPCR, using GAPDH expression ratio, n = 6. **(H)** Recapitulation table of our optimized protocol**. (I)** qPCR quantification of TEP markers in our optimized protocol at D14 compared with two state-of-the-art protocols. Gene expression is measured as relative quantification of GAPDH, n=6

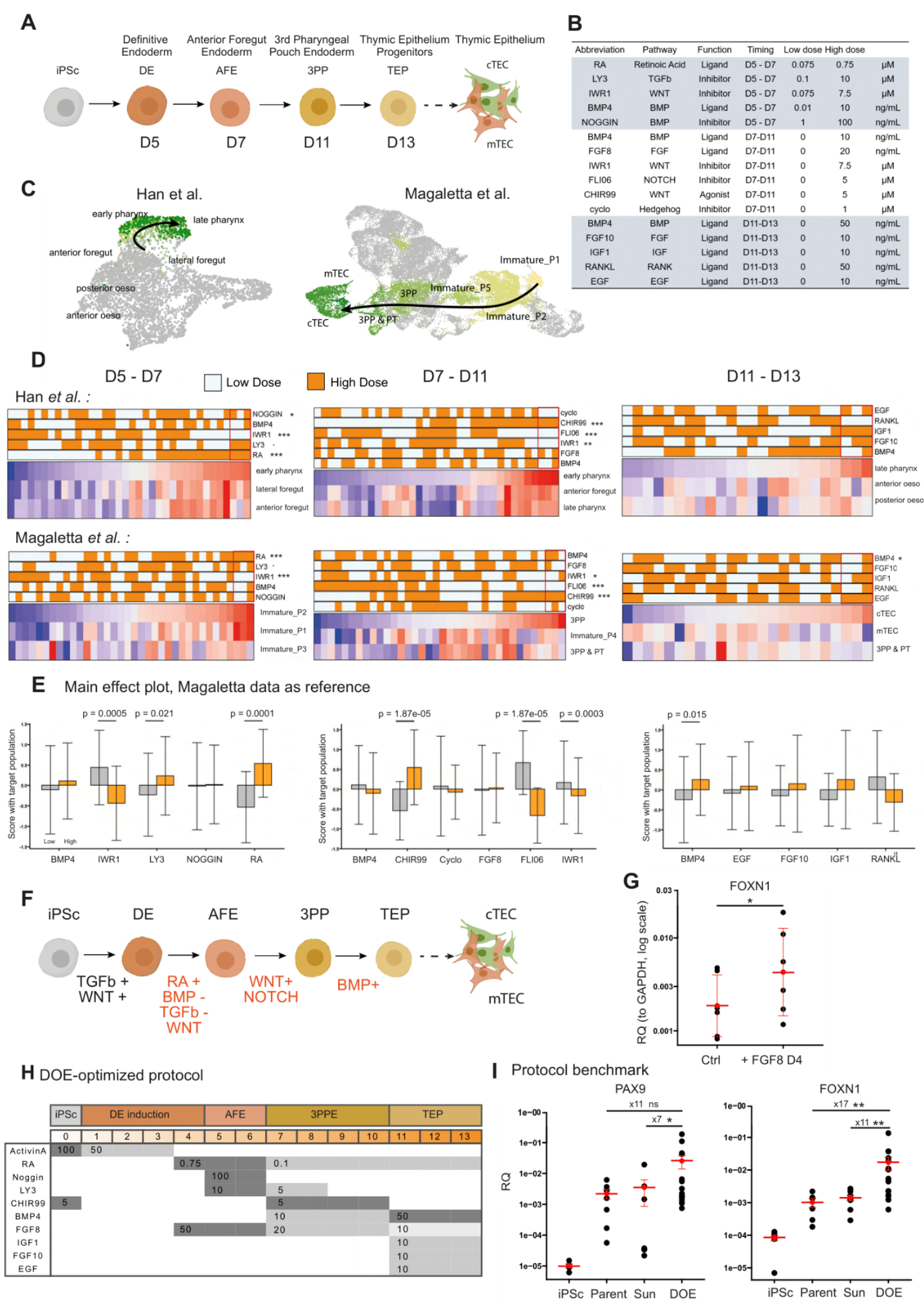

Abbreviation	Pathway	Function	Timing	Low dose	High dose	
RA	Retinoic Acid	Ligand	D5 - D7	0.075	0.75	µM
LY3	TGFb	Inhibitor	D5 - D7	0.1	10	µM
IWR1	WNT	Inhibitor	D5 - D7	0.075	7.5	µM
BMP4	BMP	Ligand	D5 - D7	0.01	10	ng/mL
NOGGIN	BMP	Inhibitor	D5 - D7	1	100	ng/mL
BMP4	BMP	Ligand	D7-D11	0	10	ng/mL
FGF8	FGF	Ligand	D7-D11	0	20	ng/mL
IWR1	WNT	Inhibitor	D7-D11	0	7.5	µM
FLI06	NOTCH	Inhibitor	D7-D11	0	5	µM
CHIR99	WNT	Agonist	D7-D11	0	5	µM
cyclo	Hedgehog	Inhibitor	D7-D11	0	1	µM
BMP4	BMP	Ligand	D11-D13	0	50	ng/mL
FGF10	FGF	Ligand	D11-D13	0	10	ng/mL
IGF1	IGF	Ligand	D11-D13	0	10	ng/mL
RANKL	RANK	Ligand	D11-D13	0	50	ng/mL
EGF	EGF	Ligand	D11-D13	0	10	ng/mL

Protein expression of main thymic markers was validated by immunofluorescence (Figure 3.A). Clear nuclear expression of the transcription factors linked to TEC identity *PAX9* and *FOXN1* was identified in D14 TEP. Interestingly, at this stage all cells display nucleic labelling for these makers, thus revealing a high purity of the differentiated cultures. As TEPs are characterized by cortical features, such as expression of KRT8/18 and CD205 (60), we stained D14 TEPs and observed generalized KRT8 expression associated with a punctuated staining for CD205. Flow cytometry was used to precisely assess the purity of the differentiated TEPs, defined as $EPCAM^{+}CD205^{+}HLA\text{-}DR^{-}$ (Figure 3.B). Cell epithelial identity was demonstrated by high EPCAM expression, with 76% (n=4) of $EPCAM^{+}$ cell population at D10 (Figure 3.C). As expected, CD205 expression was not detected at D10 at the stage of 3PPE, but could be detected at D17, with 23.4% (n=3) of TEPs in the differentiation product. Interestingly, a rare population of cells was positive for HLA-DR, suggesting the emergence of a more mature TEC population. However, the extremely low numbers of positive HLA-DR cells indicated that either this maturation process was in its earliest stage at D17, or that the culture conditions *in vitro* were not suitable for further TEC maturation.

Figure 2 : Transcriptomic characterization of iPSc-derived TEP **(A)** Heatmap representation of differentially expressed genes modules across differentiation. Sample were analysed at several timepoints by DGEseq. Primary human TECs and D0 iPSc were included as controls. **(B)** GO terms enriched in each gene module were identified by ClusterProfiler and organised by shared genes similarity. Network was plotted on Cytoscape by forcing orientation along the day of differentiation, resulting in the graph of significant biological processes enriched for each differentiation stage. **(C)** Differentiation trajectory in PCA-reducted space with iPSc and primary TEC as controls. **(D)** Expression of typical stages markers across differentiation trajectory in DEGseq bulk transcriptomes compared with primary TECs

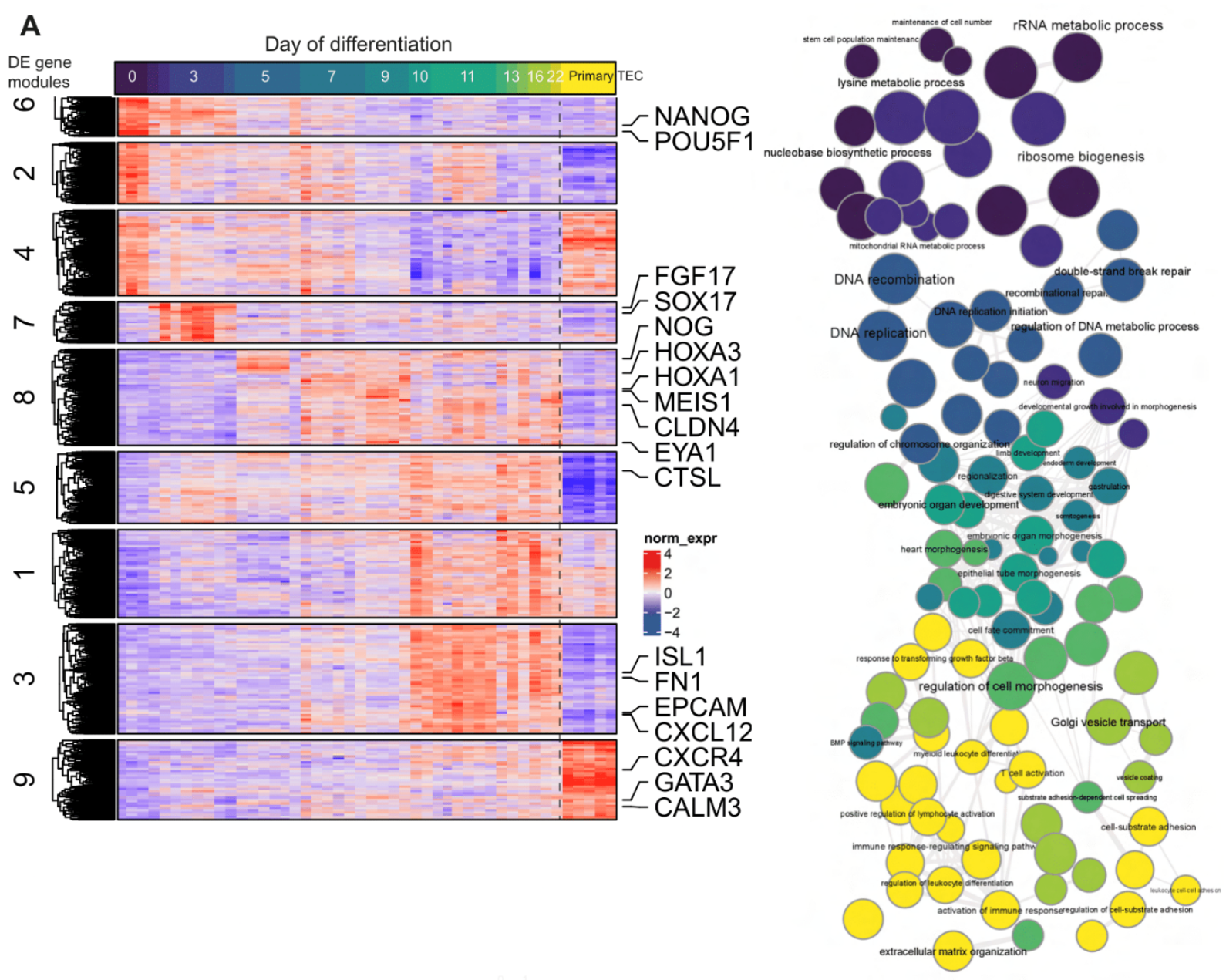
A
Day of differentiation
DE gene modules
0 3 5 7 9 10 11 13 16 22 Primary TEC
6
2
4
7
8
5
1
3
9
NANOG
POU5F1
FGF17
SOX17
NOG
HOXA3
HOXA1
MEIS1
CLDN4
EYA1
CTSL
ISL1
FN1
EPCAM
CXCL12
CXCR4
GATA3
CALM3
norm_expr
4
2
0
−2
−4
maintenance of cell number
stem cell population maintenanc
rRNA metabolic process
lysine metabolic process
nucleobase biosynthetic process
ribosome biogenesis
mitochondrial RNA metabolic process
DNA recombination
double-strand break repair
recombinational repair
DNA replication initiation
DNA replication
regulation of DNA metabolic process
neuron migration
developmental growth involved in morphogenesis
regulation of chromosome organization
limb development
endoderm development
regionalization
gastrulation
digestive system development
embryonic organ development
somitogenesis
embryonic organ morphogenesis
heart morphogenesis
epithelial tube morphogenesis
cell fate commitment
response to transforming growth factor beta
regulation of cell morphogenesis
Golgi vesicle transport
BMP signaling pathway
myeloid leukocyte differentiation
T cell activation
vesicle coating
substrate adhesion-dependent cell spreading
positive regulation of lymphocyte activation
cell-substrate adhesion
immune response-regulating signaling pathway
regulation of leukocyte differentiation
leukocyte cell-cell adhesion
activation of immune response
regulation of cell-substrate adhesion
extracellular matrix organization

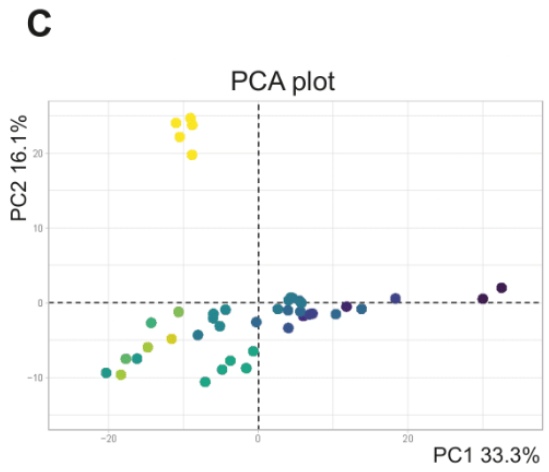
C
PCA plot
PC2 16.1%
PC1 33.3%
20
0
−10
−20
0
20

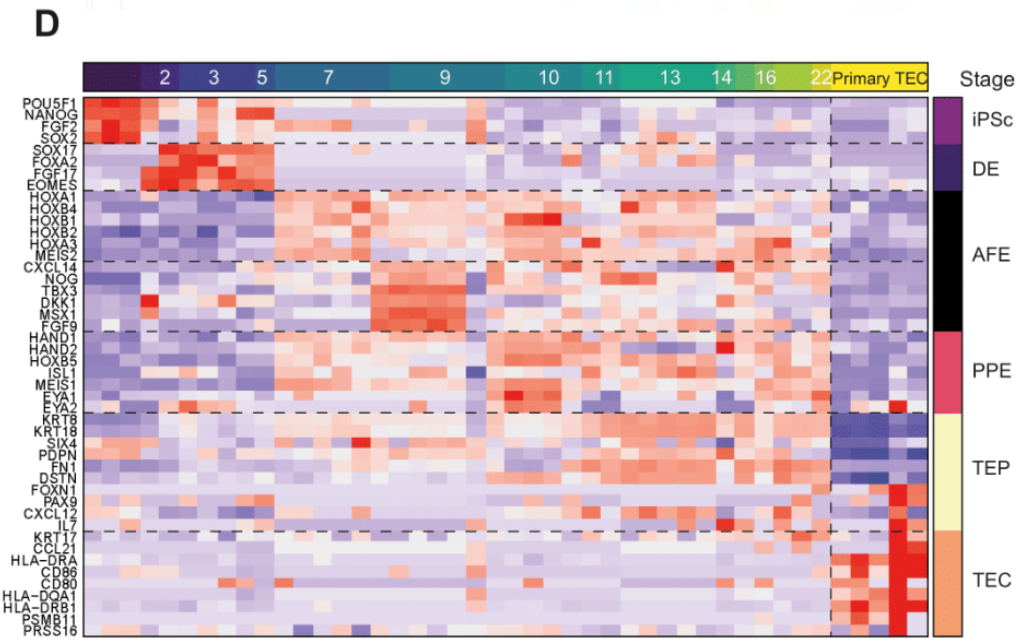
D
2 3 5 7 9 10 11 13 14 16 22 Primary TEC
Stage
iPSc
DE
AFE
PPE
TEP
TEC
POU5F1
NANOG
FGF2
SOX2
SOX17
FOXA2
FGF17
EOMES
HOXA1
HOXB4
HOXB1
HOXB2
HOXA3
MEIS2
CXCL14
NOG
TBX3
DKK1
MSX1
FGF9
HAND1
HAND2
HOXB5
ISL1
MEIS1
EYA1
EYA2
KRT8
KRT18
SIX4
PDPN
FN1
DSTN
FOXN1
PAX9
CXCL12
IL7
KRT17
CCL21
HLA-DRA
CD86
CD80
HLA-DQA1
HLA-DRB1
PSMB11
PRSS16

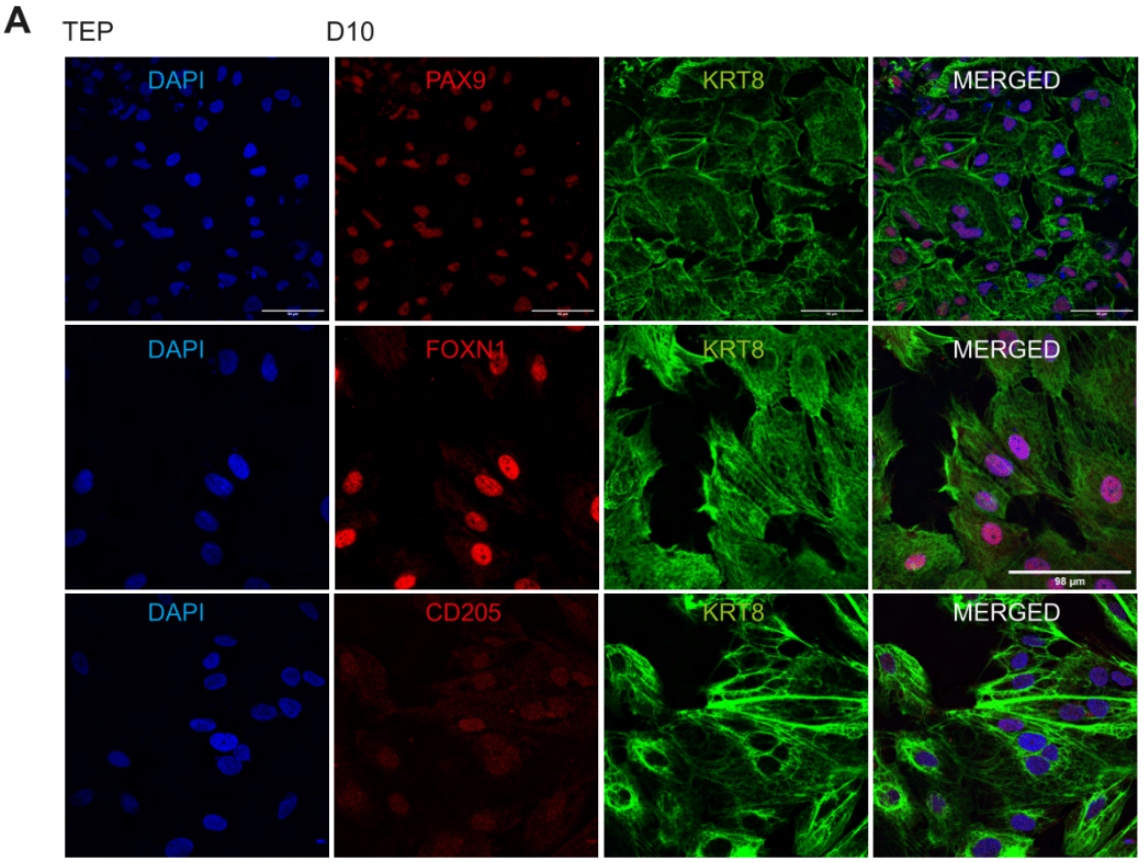
A
TEP
D10
DAPI
PAX9
KRT8
MERGED
DAPI
FOXN1
KRT8
MERGED
98 µm
DAPI
CD205
KRT8
MERGED

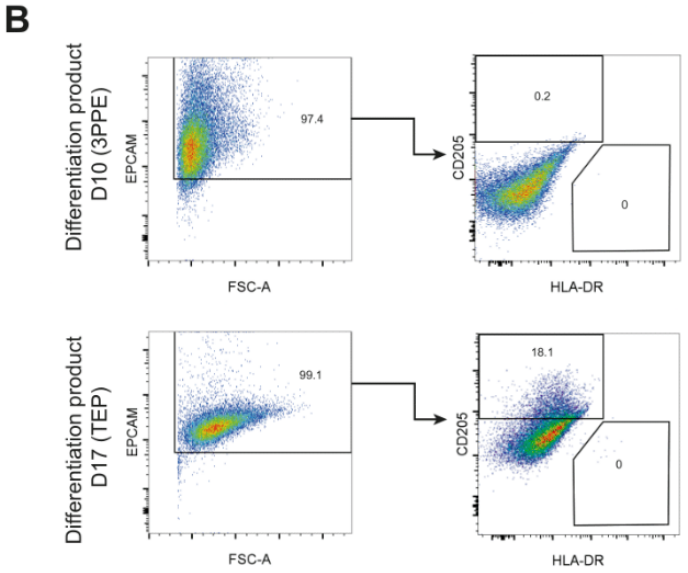
B
Differentiation product D10 (3PPE)
EPCAM
97.4
FSC-A
CD205
0.2
0
HLA-DR
Differentiation product D17 (TEP)
EPCAM
99.1
FSC-A
CD205
18.1
0
HLA-DR

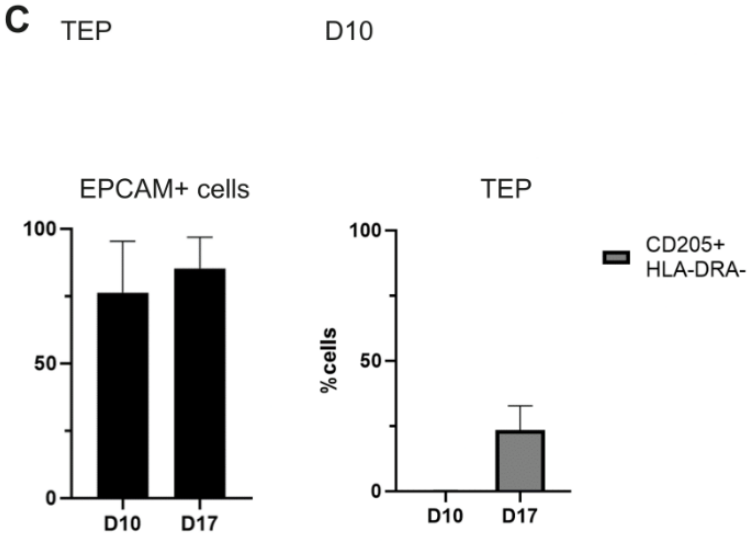
C
TEP
D10
EPCAM+ cells
100
50
0
D10
D17
TEP
100
50
0
% cells
D10
D17
CD205+
HLA-DRA-

Figure 3 : Phenotypic characterization of differentiation product reveals expression of classical TEP markers **(A)** Immunofluorescence imaging of thymic epithelium markers in D14 TEP. Nuclei stained with DAPI. **(B)** Flow cytometry analysis of D10 pharyngeal endoderm and D17 TEP using EPCAM as epithelial marker and CD205+HLA-DRA- for TEP phenotype. **(C)** Quantification of TEP yield in D10 pharyngeal endoderm and D17 TEP.

Early thymocytes (ETP) in cocultures colocalize with TEPs

While the maturation into functional TEC *in vitro* has proved to be challenging, with most studies grafting TEP in mice (35–38), we aimed at inducing TEP maturation fully *in vitro*. Thymocytes have been identified as a crucial source of signalization that regulates thymic medulla formation and maturation, especially for the $mTEC^{hi}$ compartment (61).

Therefore, we investigated the capacity of early thymocytes to promote TEP maturation. Early thymic progenitors (ETP) from human thymus samples were harvested and sorted by flow cytometry using $CD3^-CD4^-CD8^-CD14^-CD19^-CD56^-(Lin)CD34^+CD7^+$ (Figure 4.A). This rare population constitutes multipotent hematopoietic progenitors upstream of the T cell differentiation (7,50). We characterized the sorted cell population by flow cytometry and validated their ETP phenotype (Figure 4.B). Sorted ETP were $CD45^+CD3^-CD34^+$, in majority double negative (DN) for CD4 and CD8, and expressed both CD62L and CD44. A minor $CD44^-$ population could include already committed DN3 thymocytes. ETPs were cocultured with the differentiation product at the TEP stage, at D13. Interestingly, after one week of coculture ETP colocalized with epithelial cells, as illustrated by bright field images (Figure 4.C-D). From a seemingly random repartition shortly after coculture set up, ETPs nearly exclusively located at the surface of the large, differentiated epithelial cells after one week. Given the capacity of TEC to interact with thymocytes and even to incorporate them, forming thymic nurse cells (TNC) complexes, it is possible that this physical interaction is concurrent with cell-cell signalization during thymopoiesis. However, we did not investigate further if thymocytes were incorporated by TECs or only located at their surface. Finally, to assess TEP potential to respond to crosstalk signalization, we investigated expression of genes coding for receptors and regulators of the thymic crosstalk in D14-22 TEPs (Figure 4.E). Interestingly, TEPs expressed TRAF and REL family genes, regulators of the NF-kappa-B signalization, as well as LTB receptor, and could be thus receptive to signals presented by thymocytes.

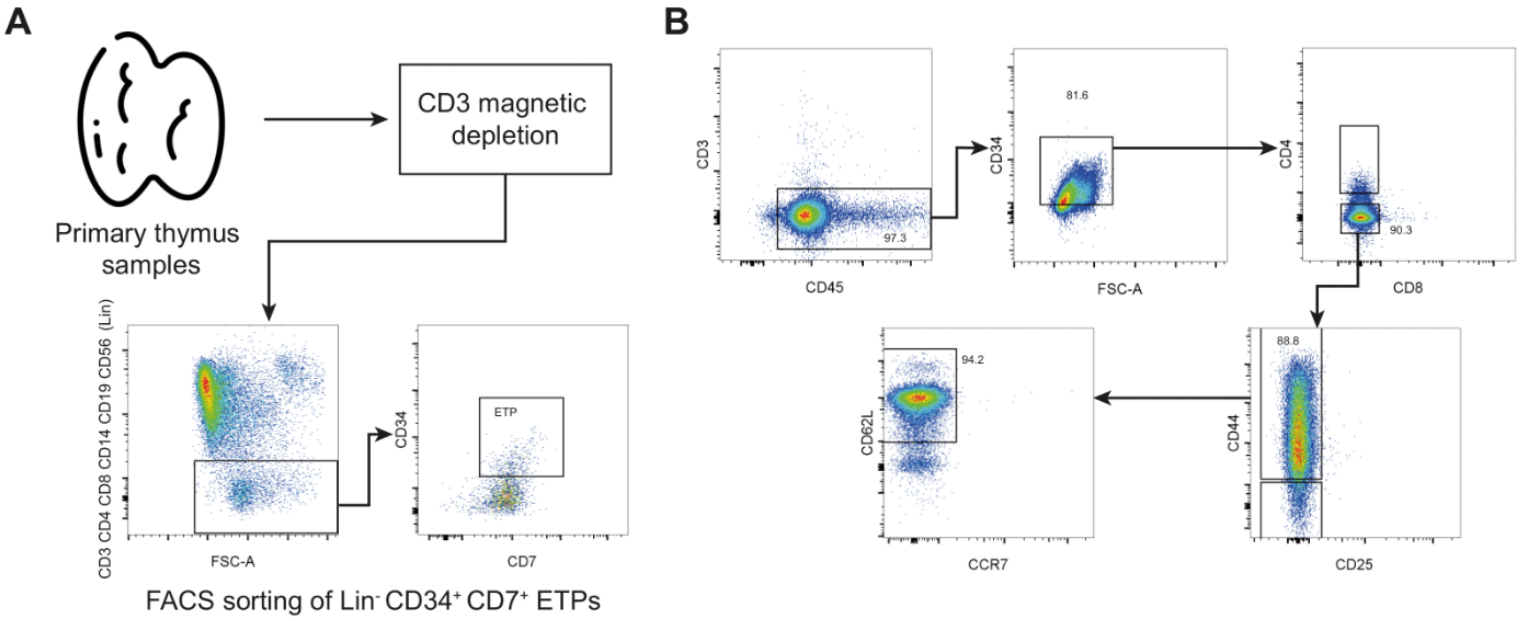
A
Primary thymus samples
CD3 magnetic depletion
CD3 CD4 CD8 CD14 CD19 CD56 (Lin)
FSC-A
CD34
CD7
ETP
FACS sorting of Lin⁻ CD34⁺ CD7⁺ ETPs
B
CD3
CD45
97.3
CD34
81.6
FSC-A
CD4
CD8
90.3
CD62L
CCR7
94.2
CD44
CD25
88.8

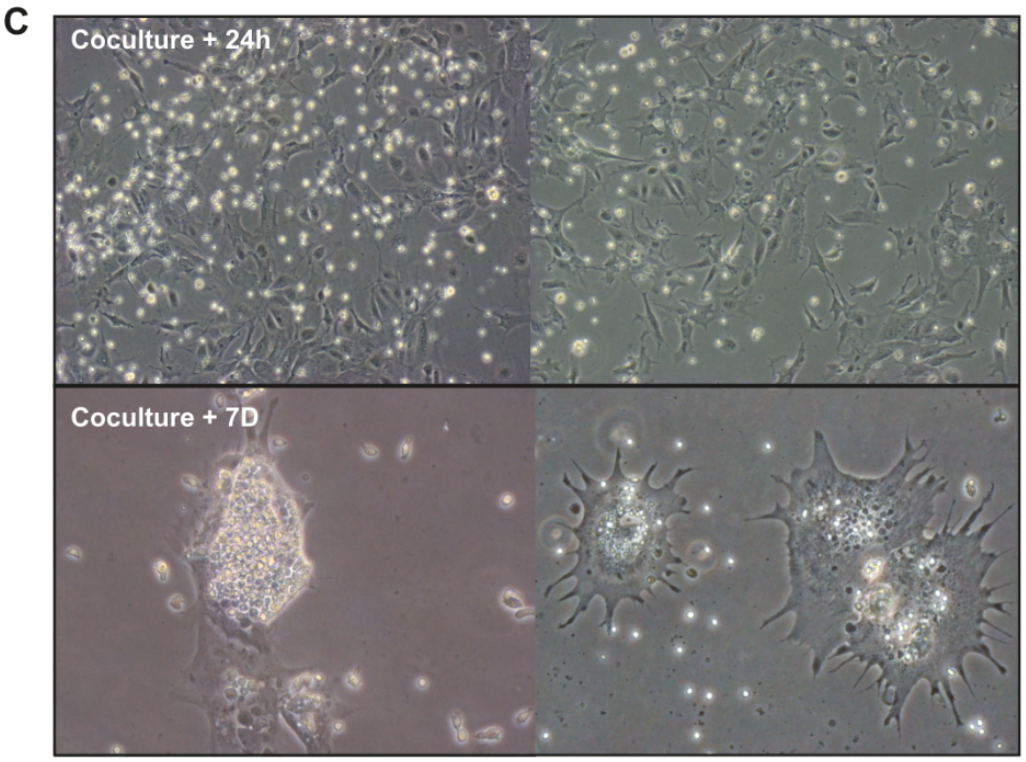
C
Coculture + 24h
Coculture + 7D

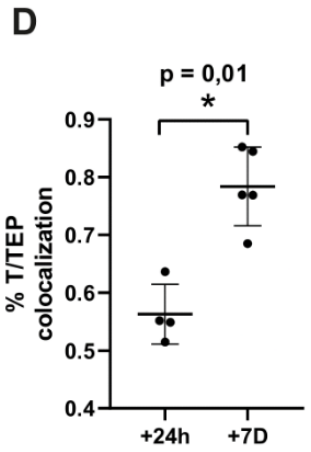
D
p = 0,01
*
% T/TEP colocalization
0.9
0.8
0.7
0.6
0.5
0.4
+24h
+7D

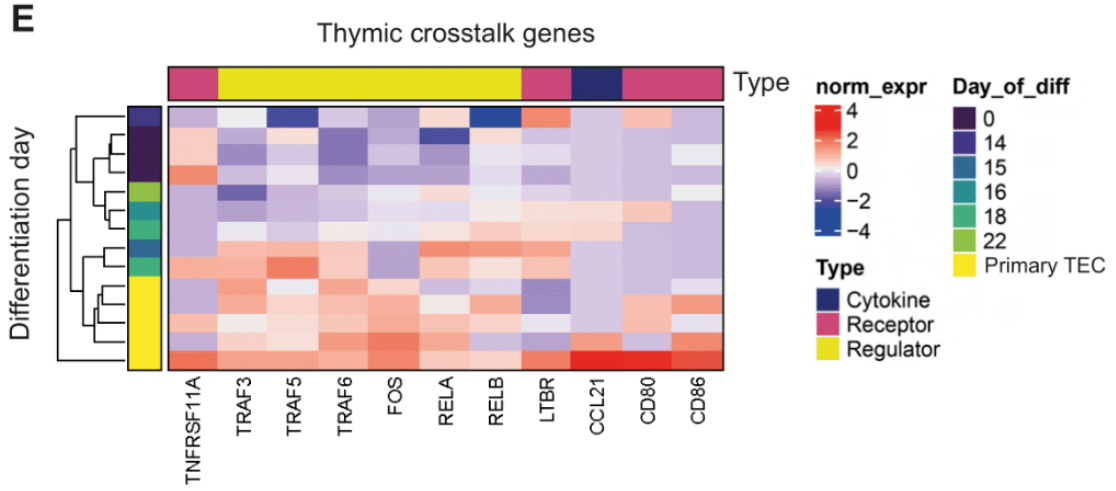
E
Thymic crosstalk genes
Type
Differentiation day
TNFRSF11A
TRAF3
TRAF5
TRAF6
FOS
RELA
RELB
LTBR
CCL21
CD80
CD86
norm_expr
4
2
0
−2
−4
Type
Cytokine
Receptor
Regulator
Day_of_diff
0
14
15
16
18
22
Primary TEC

Figure 4 : Early thymocytes (ETP) in cocultures colocalize with TEPs **(A)** Sorting of human primary early thymic progenitors (ETP) characterized as CD3-CD4-CD8-CD14-CD19-CD56-(Lin)CD34+CD7+ by flow cytometry after enrichment by magnetic depletion of CD3+ thymocytes. **(B)** FACS characterization of freshly sorted ETP show high purity of CD45+CD3-CD34+ ETP progenitors, expressing CD44 and CD62L **(C)** Bright field optical microscopy images of TEP coculture with ETP after 24h and 1 week of coculture. ETP coculture induces morphological changes in TEPs and **(D)** show significant colocalization. **(E)** Transcriptomic data of D14-D22 TEP show expression of genes involved in thymic crosstalk, with D0 iPSc and primary TECs as controls.

Coculture with ETP promotes maturation into HLA-DR expressing mTEC

TEP differentiation into mature mTEC would translate in the loss of their cortical-like phenotype and the acquisition of HLA-DR, as a marker of their APC functionality. Flow cytometry was used to assess the effect of coculture with ETP on TEP maturation and showed induction of a $EPCAM^{+}CD205^{-}HLA\text{-}DR^{+}$ population displaying a mature mTEC phenotype (Figurer 5.A). Thus, thymocyte-TEP interaction in coculture is associated with a higher degree of maturation of the $mTEC^{hi}$ population. Further characterization was performed by IF and confirmed induction of a medullary phenotype as early as D17, with coexpression of the mTEC-associated KRT5 and KRT14 (Figure 5.B). Claudin 3, another mTEC marker (Figure Supp 5.D), was detected with typical focal point staining. HLA-DR expression was confirmed in these CLDN3-expressing cells, as well as in costaining with FOXN1, thus indicating ETP coculture ability to induce a more mature mTEC phenotype.

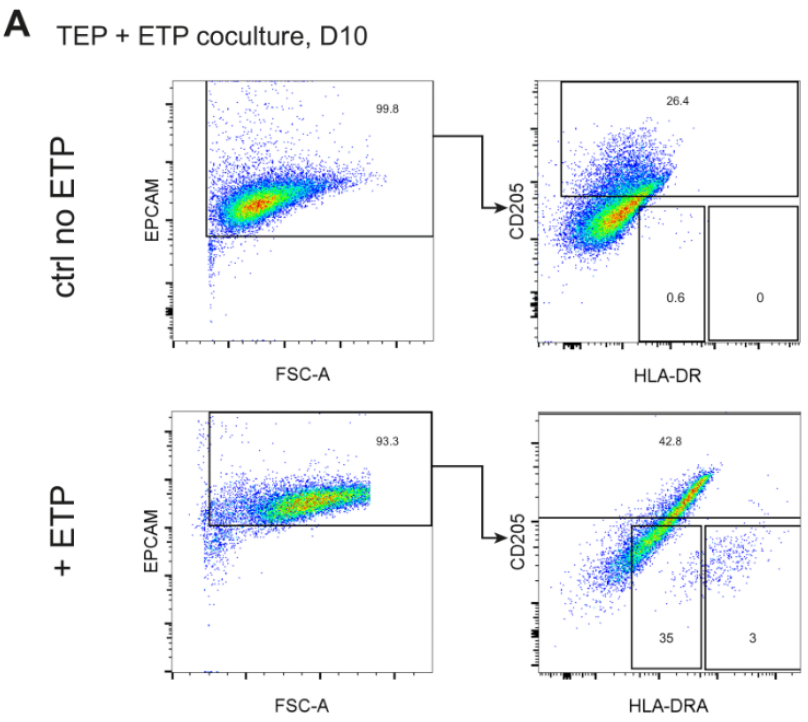
A
TEP + ETP coculture, D10
ctrl no ETP
+ ETP
EPCAM
FSC-A
CD205
HLA-DR
HLA-DRA
99.8
26.4
0.6
0
93.3
42.8
35
3

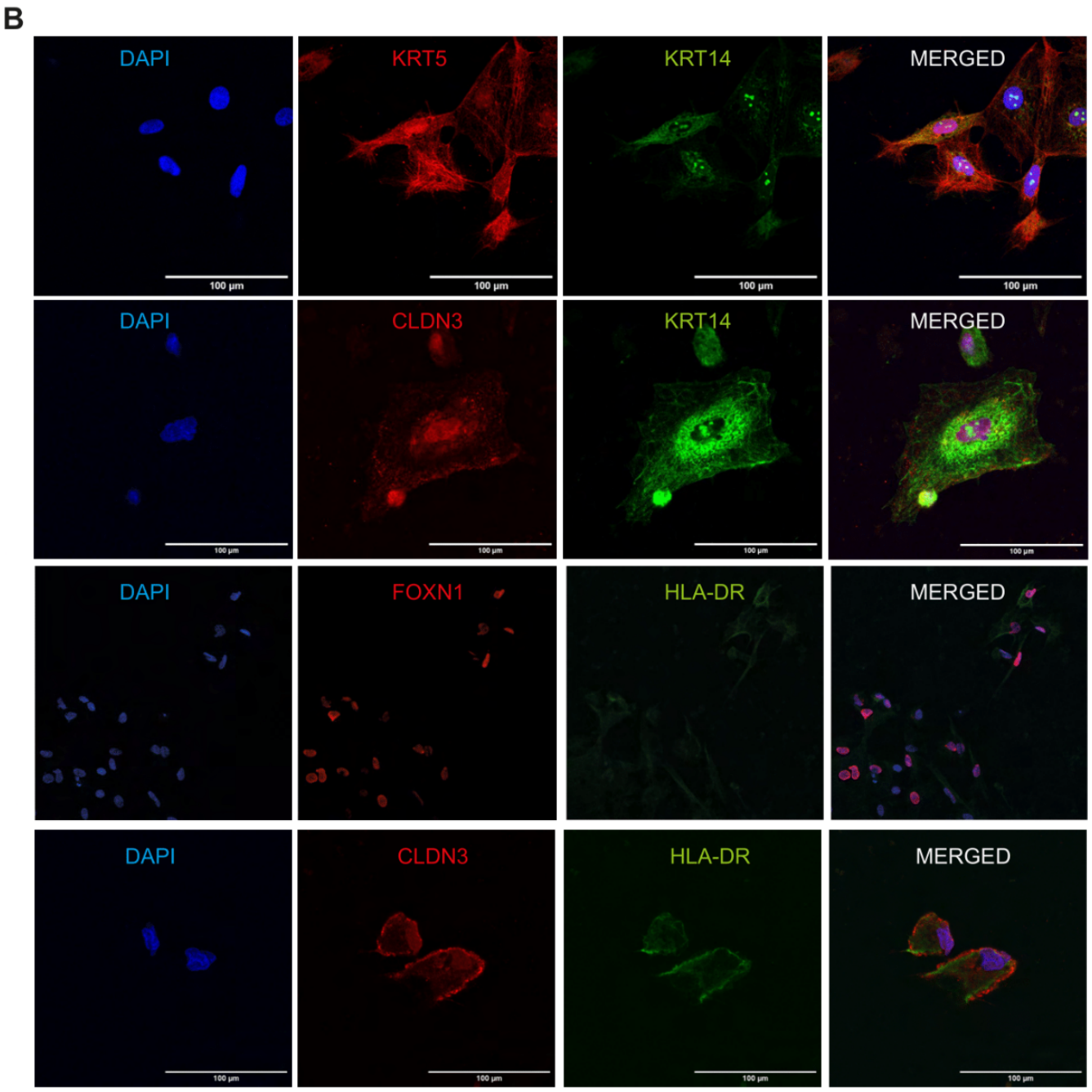
B
DAPI
KRT5
KRT14
MERGED
CLDN3
FOXN1
HLA-DR
100 µm

Figure 5 : TEP coculture with ETP induces TEP maturation into HLA-DR^{hi} TECs **(A)** Flow cytometry of TEPs at D10 of coculture with ETPs show maturation into CD205^{-}HLA-DRA^{hi} mTECs **(B)** Immunofluorscence by confocal microscopy in D17 TEPs colcultured with ETP show expression of mTEC markers with CLDN3, KRT5/KRT14 coexpression, and HLA-DR staining. Nuclei stained with DAPI.

An 3D thymic organoid system further induce mTEC maturation

Classical culture in monolayer is known to be unsuitable for TEC maintenance, leading to a quick loss of TEC functional markers (62). Considerable progress has been made recently, with development of 3D culture systems in hydrogels and the set-up of artificial thymic organoids (47,63–65). We developed a human thymic organoid (hTO) coculture system by reaggregating human primary ETPs with our differentiation product at D13 and seeding the cell mass in a fibrin hydrogel (Figure 6.A). Organoids were cultured in air-liquid interfaces on cell inserts, in the same XVIVO10 base culture medium, as other tested media such as DMEM did not supported comparable cell growth (data not shown). We supplemented this medium as previously described (47,62): cytokines stimulating TEC and T growth and maturation such as RANKL and IL7, SCF and FTL3L were added. After 24 hours, organoids showed a spheroid shape with a crown-like structure of thymocytes (Figure 6.B). Organoids showed signs of growth from D4 after seeding, with total size increase and formation of cellular projections in the hydrogel. hTO could be maintained several weeks in the 3D culture system and reached 5 mm size. At D11 organoids morphology evolves from a spheroid to a complex structure with multiple projections colonizing the gel. Interestingly, thymocytes were concentrated around the cellular projections as illustrated in Figure 6B. Confocal microscopy was performed on D23 organoids to resolve their 3D structure, using KRT5 and CD45 to highlight the thymic epithelium and hematopoietic compartments respectively (Figure 6.C). Epithelial nature of the cellular projections in the organoids was confirmed by KRT5 staining, also implying medullary TEC differentiation. Moreover, physical interaction between CD45^{+} thymocytes and KRT5^{+} mTECs in the organoids could be observed, with colocalization of CD45^{+} cells at the surface of the epithelial structures. Interestingly, z-slices more distant from the organoid in the gel volume contained dispersed thymocytes as well, highlighting their ability to freely circulate in the gel, originally devoid of cells during its casting (Figure 6.C, bottom left). This property was confirmed for mTECs too, with migration far from the initial seeded micromass (Figure 6.C, bottom right). To test the effect of culture in the 3D organoid system against classical 2D monolayer on mTEC marker expression, we quantified *FOXN1*, *KRT5* and *AIRE* expression by qPCR. Independently from the effect of coculture with ETP, cells maintained in the 3D organoid system showed significantly higher expression levels of these TEC and mTEC

markers (Figure 6 F). Remarkably, *AIRE* expression was higher in organoids, thus revealing the pertinence of 3D organoid culture for mTEC maturation. Finally, we investigated by flow cytometry the cellular composition in D28 organoids, and identified 4 main populations : the TEC compartment ($EPCAM^{+}CD45^{-}$), the T cells ($EPCAM^{-}CD45^{+}$) compartment, and two uncharacterized $EPCAM^{-}CD45^{-}$ and $EPCAM^{lo}CD45^{+}$ populations (Figure6.D). Further analysis of the $EPCAM^{hi}$ TEC compartment with CD205 and HLA-DR revealed two populations distinguished by their HLA-DR expression. The $CD205^{-}$HLA-DR^{hi} population is coherent with a mature mTEC phenotype. Strikingly, coculture with ETP in 2D as control did not yield such an amount of HLA-DR^{hi} mTECs, showing mainly a $CD205^{+}$HLA-DR^{lo} population, comforting the fact that HLA-DR^{hi} mTECs are particularly sensitive to 3D structure for their maintenance or for the induction of their maturation (Figure 64.E-F). Moreover, hTO also comprise a $CD205^{+}$HLA-DR^{lo} compartment that could represent cTECs or maturating TEPs,

The non-epithelial and non-hematopoietic compartment could correspond to fibroblasts originating from a side-product in the differentiation, or TEC transdifferentiation to a mesenchymal signature (63). We detected expression of fibroblast-associated genes in the transcriptome of our organoids, such as *DCN, COL1A1* and *LUM* (Figure Supp 5.A). Interestingly, given the recent advances on thymic fibroblast role *in vivo* (66–68), this minor stromal population may result in unexpected positive outcomes for the maintenance and maturation of TECs in our hTOs, for instance by secreting growth factors regulating TECs.

Figure 6: TEP coculture with ETPs induces TEP maturation into HLA-DR^{hi} TECs **(A)** Reaggregation of D13 TEP differentiated from iPSc with primary human ETP forms human Thymic Organoids (hTO) cultured in a 3D fibrin hydrogel in air-liquid interface supplemented with RANKL, IL7 and FTL3L. **(B)** Bright field images of ATO at 24h, 4 days and 11 days after reaggregation. **(C)** 3D immunofluorescence confocal imaging of the medullary epithelial compartment (KRT5) and hematopoietic compartment (CD45) in D23 ATO show physical colocalization. **(D)** Flow cytometry analysis of D23 organoids, gating on TEC ($EPCAM^{hi}CD45^{-}$). TEC compartment can be subdivided in TEP ($CD205^{+}$HLA-DRA^{-}), $mTEC^{lo}$ ($CD205^{-}$HLA-DRA^{-}), $mTEC^{hi}$ ($CD205^{-}$HLA-DRA^{hi}). **(E)** Quantification of the TEP and $mTEC^{hi}$ populations as total cell proportion by flow cytometry at D28 between organoids (3D) and 2D coculture. hTO system shows significantly higher proportion of mTEC **(F)** qPCR quantification of TEC (FOXN1) and mTEC (KRT5, AIRE) marker expression in D23 TEP-ETP coculture in classical monolayer culture (2D) and in hTO system (3D). Relative quantification to GAPDH, n=6

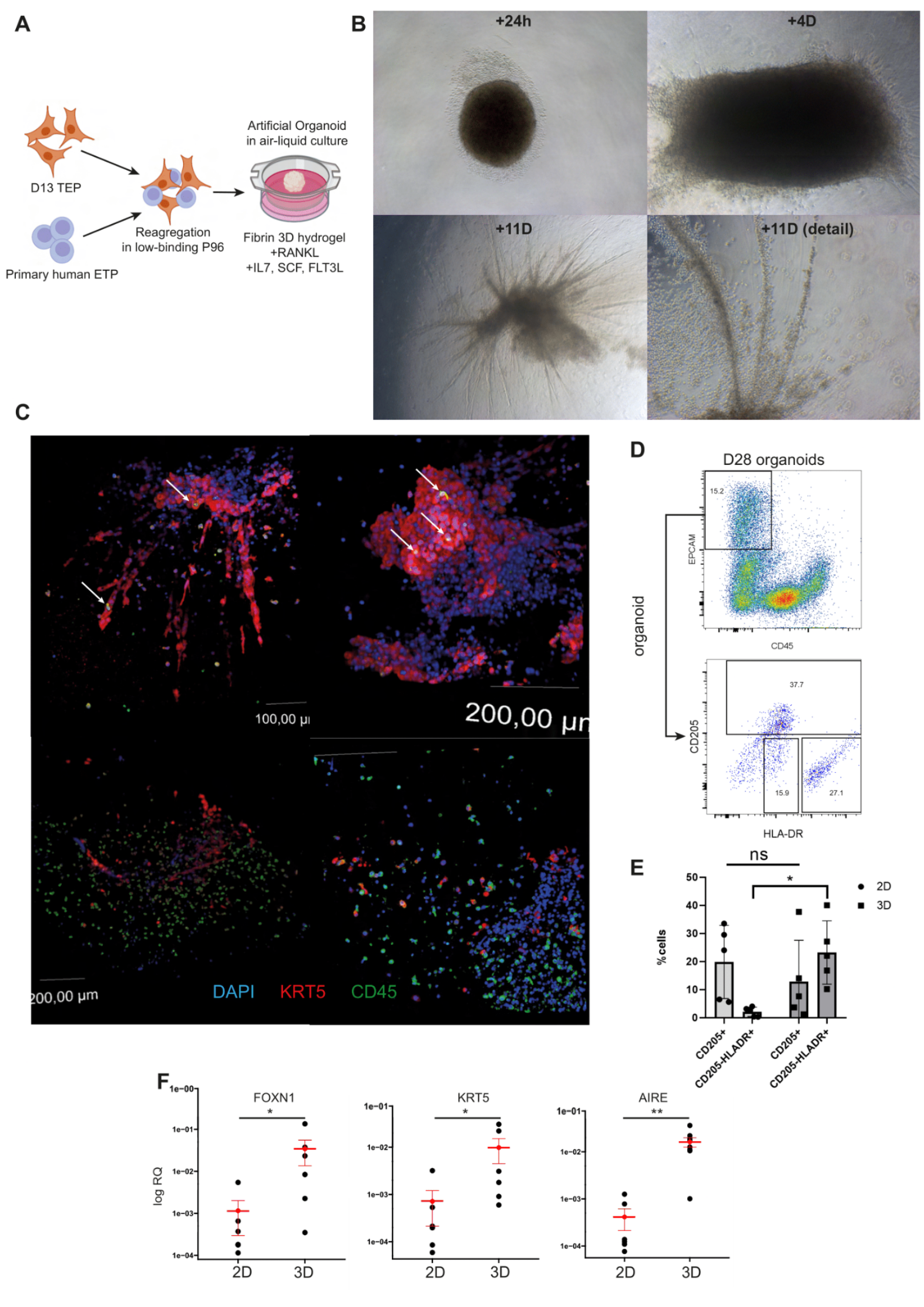
A
D13 TEP
Primary human ETP
Reagregation
in low-binding P96
Artificial Organoid
in air-liquid culture
Fibrin 3D hydrogel
+RANKL
+IL7, SCF, FLT3L
B
+24h
+4D
+11D
+11D (detail)
C
100,00 µm
200,00 µm
200,00 µm
DAPI
KRT5
CD45
D
D28 organoids
organoid
EPCAM
CD45
15.2
CD205
HLA-DR
37.7
15.9
27.1
E
ns
*
2D
3D
% cells
CD205+
CD205-HLADR+
CD205+
CD205-HLADR+
F
FOXN1
KRT5
AIRE
log RQ
*
*
**
2D
3D

hTOs support thymopoeisis and maturate into SP CD4+ and CD8+ T lymphocytes with thymic emigrants (TE) phenotypes

To investigate the capacity of hTOs to differentiate ETPs into mature SP T cells, hTOs were dissociated and analysed by flow cytometry . Soft mechanical dissociation yielded mostly non-adherent hematopoietic cells, as revealed by the majority of CD45 expression in the hTO product. Expression of CD34 was absent, confirming the loss of the hematopoietic progenitor identity and thus ETP differentiation (Figure Supp 5.B). CD3 expression confirmed the commitment to a T cell fate. The proportion of CD3 expressing cells increased with time, reaching 60% at W5 (n=1) (Figure 7.A-B). TCR expression was analyzed by flow cytometry to decipher αβ vs γδ T lineage orientation in hTO (Figure 7.C). Both αβ and γδ populations were detected in $CD3^+$ thymocytes. αβ lineage was nonetheless predominant compared with rare γδ thymocytes, contrary to recent results using a similar system (69). Most of the $CD3^+$ cells are $CD4^-CD8^-$ DN thymocytes, however hTO includes $CD4^+CD8^+$ DP, $CD4^+CD8^-$ SP4 and $CD4^-CD8^+$ SP8, albeit in lesser proportions (Figure 7.D). Thymocyte maturation may be biased to the CD8 fate, illustrated by the dominance of $CD8^+$ T cells. However, lesser SP CD4+ populations were detected, illustrating a MHC-II dependent selection inside hTOs.Interestingly, we observed high experimental variability of the frequencies of $CD4^+$ and $CD8^+$ (Figure 7.E). Differences of abundance in MHC-I and II expressing TEC populations in hTOs could these explain thymocyte differentiation biases. The state of maturation of the SP thymocyte was assessed with expression of the markers CCR7, CD62L and CD69. Minor populations of SP thymocytes in the hTO displayed mature $CCR7^+CD62L^+CD69^-$ phenotypes. This demonstrated hTO capacity to drive thymopoiesis, especially considering that control ETPs cultivated alone showed high mortality (Figure Supp 5.C).

Figure 7 : hTO induce ETP maturation into SP CD4+ and CD8+ T lymphocytes with thymic emigrants (TE) phenotypes **(A)** Flow cytometry analysis of the cinetic of thymopoeisis in hTOs shows accumulation of CD3+ T cells, with extensive increase after week 3 of coculture (*n = 1 to 7*) **(B). (C)** Frequency of CD4+ and CD8+ T cells shows variability between experiments, revealed by FACS of hTOs at the same timepoint (D35) **(D)** Flow cytometry shows expression of both alpha beta and gamma delta TCRs in W3 hTOs.**(E)** Flow cytometry of the hematopoietic fraction of W3 hTO confirms loss of CD34, clear CD3 expression and presence of CD8+ SP T cells and less abundant CD4+ SP T cells. A subset of SP populations shows a mature phenotype $CD62L^+CCR7^+CD69^-$ typical of thymic emigrants.

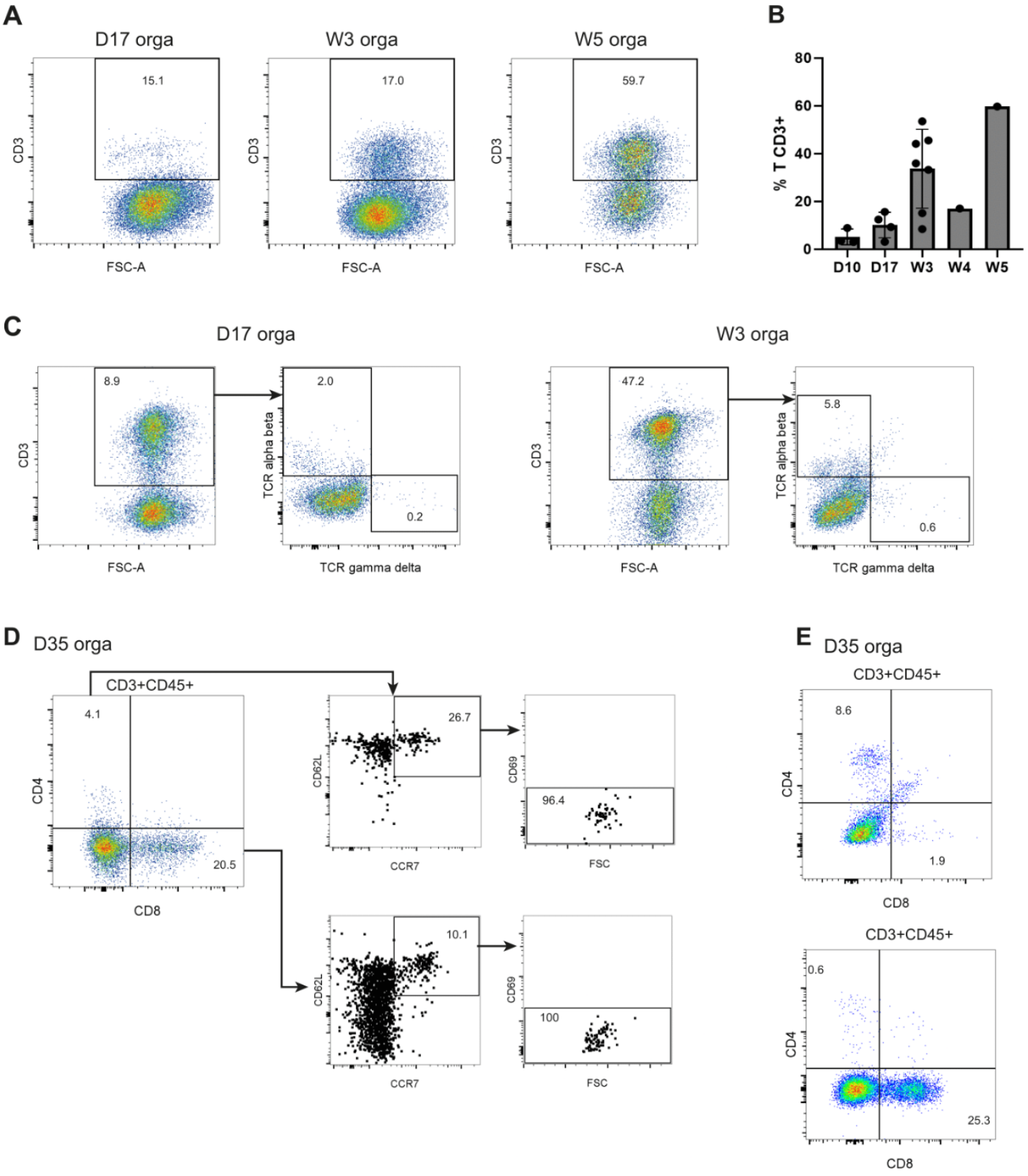
A
D17 orga
W3 orga
W5 orga
15.1
17.0
59.7
CD3
FSC-A
B
% T CD3+
80
60
40
20
0
D10
D17
W3
W4
W5
C
D17 orga
W3 orga
8.9
2.0
0.2
47.2
5.8
0.6
TCR alpha beta
TCR gamma delta
D
D35 orga
CD3+CD45+
4.1
20.5
CD4
CD8
26.7
10.1
CD62L
CCR7
96.4
100
CD69
FSC
E
D35 orga
CD3+CD45+
8.6
1.9
0.6
25.3

Single cell RNA sequencing (scRNAseq) of hTOs demonstrates multilineage differentiation of dendritic cells and mature T lymphocytes

To characterize in more details the CD45+EPCAMlo compartment in our hTOs, transcriptome sequencing was performed by SMART-seq on the purified population (Figure 8.A). Gene ontology analysis of differentially expressed genes showed enrichment of terms linked to antigen processing and presentation by the MHCII complex, as well as to interaction with lymphocytes (Figure 8.B). Finally, DE genes in this CD45+EPCAMlo population comprised many dendritic cells (DC) markers (Figure 8.C) : using the Thymus single cell atlas from Park et al. (21), we identified markers of the 3 thymic DCs populations, SIRPA+ DCs, plasmacytoid DCs (pDC) and activated DCs (aDCs), and showed high expression of these markers in the CD45+EPCAMlo population. No specific marker signature was identified, potentially hinting presence of distinct DCs subsets in our population.

To further explore the heterogeneity of this population and characterize thymocyte state of maturation in the hTOs, scRNAseq was performed on dissociated D28 hTO. Most harvested cells were shown to be $CD45^+$ cells, probably because of differences of cell adherence leading to loss of the stromal hTO compartment during manipulations. Three clusters were identified as illustrated by UMAP projection, two of them of hematopoietic identity and a minor one of epithelial/stromal identity (Figure 8.D). Differential gene expression isolated *KRT8*, *KRT18*, *FN1* and *PDPN* as markers of this last cluster, coherent with a TEP signature. Identification of key markers for each hematopoietic cluster allowed identification of the dendritic cell population (*PLEK*, *LY86*, *HLA-DRA*) and SP T cells (*CD3E*, *CD7*, *TCF7*) (Figure 8.E). The T cell clusters are separated in a actively proliferating minor cluster, and a main quiescent one (Figure Supp. 6). To finely label clusters and identify their *in vivo* counterparts, we projected our dataset as query to the reference thymic atlas from Park *et al.* (21). Label transfer revealed high prediction scores for the two main DC populations in Park's study and for SP mature thymocytes (Figure 6.C). Thus, hTO supports multilineage hematopoietic differentiation. As expected, single cell transcriptomic data confirmed the maturation state of the generated T cells, with expression of maturation markers such as *CCR7*, *CD27* or *IL2RA* (CD25) (Figure Supp 8.E,Figure Supp 6). To confirm that the DC population originated from ETPs and not from iPSc-derived differentiation product, scSPLIT was executed on hTO data. Thus, each cell single nucleotide polymorphism (SNP) profile was compared and regrouped by their individual of origin, the ETP donor or the donor from which iPSc were derived. As expected, results showed cell appurtenance to two individuals, with one restricted to the stromal cluster and the

other to the hematopoietic compartment (Figure 8.D). Therefore, both DC and T populations generated in the hTO originated from the ETP, revealing hTO ability to support multilineage hematopoietic differentiation.

Figure 8 : single cell RNA sequencing (scRNAseq) of hTOs demonstrates multilineage differentiation of dendritic cells and mature T lymphocytes **(A)** The $CD45^{hi}EPCAM^{lo}$ population in D28 hTOs was sorted by flow cytometry and their transcriptome sequenced by SMART-seq **(B)** GO terms in differentially expressed genes of $CD45^{hi}EPCAM^{lo}$ samples show enrichment of biological processes linked to antigen processing and presentation **(C)** Park et al. Thymic human cell atlas was reanalyzed and markers of the 3 main populations of thymic dendritic cells were identified. These markers are significantly upregulated in the $CD45^{hi}EPCAM^{lo}$ population transcriptomes, confirming their identification as dendritic cell. iPSc and differentiated TEPs were included as controls **(D)** D28 hTO hematopoietic compartment was further analyzed by scRNAseq. UMAP projection reveals 3 main cell clusters. Cell origin, either from iPSc differentiation product or ETP maturation product, was assessed by comparing SNP profiles using scSPLIT, identifying the 2 individuals of origin and confirming that the DC and T population derive from a common progenitor. Cluster cell identity was determined by the expression of differentially expressed markers **(E)** CD3 and CD7 identify T lymphocytes, LY86 and PLEK the dendritic cell (DC) population and KRT8-18 a rare stomal population **(F)** To confirm cell cluster identification, data were projected on the thymus atlas dataset from Park et al. using Seurat default integration on a reference data. **(G)** Our query data show prediction for SP T lymphocytes and DC clusters on the reference dataset.

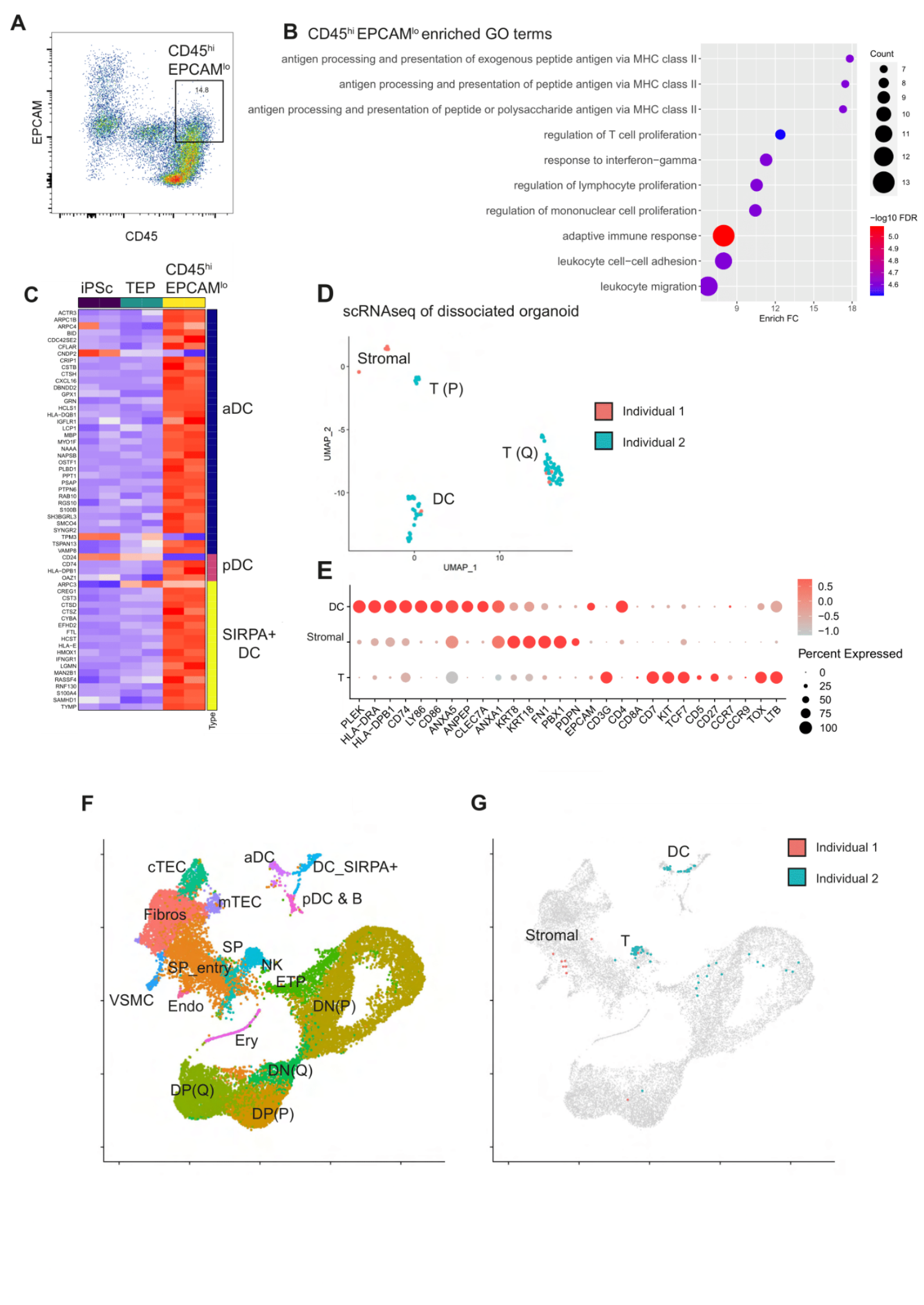
A
CD45hi EPCAMlo
14.8
EPCAM
CD45
B CD45hi EPCAMlo enriched GO terms
antigen processing and presentation of exogenous peptide antigen via MHC class II
antigen processing and presentation of peptide antigen via MHC class II
antigen processing and presentation of peptide or polysaccharide antigen via MHC class II
regulation of T cell proliferation
response to interferon−gamma
regulation of lymphocyte proliferation
regulation of mononuclear cell proliferation
adaptive immune response
leukocyte cell−cell adhesion
leukocyte migration
9
12
15
18
Enrich FC
Count
7
8
9
10
11
12
13
−log10 FDR
5.0
4.9
4.8
4.7
4.6
C
iPSc
TEP
CD45hi EPCAMlo
aDC
pDC
SIRPA+ DC
Type
D
scRNAseq of dissociated organoid
Stromal
T (P)
T (Q)
DC
Individual 1
Individual 2
UMAP_2
UMAP_1
E
DC
Stromal
T
PLEK
HLA−DRA
HLA−DPB1
CD74
LY86
CD86
ANXA5
ANPEP
CLEC7A
ANXA1
KRT8
KRT18
FN1
PBX1
PDPN
EPCAM
CD3G
CD4
CD8A
CD7
KIT
TCF7
CD5
CD27
CCR7
CCR9
TOX
LTB
0.5
0.0
−0.5
−1.0
Percent Expressed
0
25
50
75
100
F
cTEC
aDC
DC_SIRPA+
mTEC
pDC & B
Fibros
SP
SP_entry
NK
ETP
VSMC
Endo
DN(P)
Ery
DN(Q)
DP(Q)
DP(P)
G
DC
Individual 1
Individual 2
Stromal
T

Discussion

This work provides a new protocol for *directed* differentiation of iPSc into TEP and their further maturation into functional thymic tissue supporting full thymopoiesis *in vitro*. Our original approach relies on the combination of an experimental design-based optimization of differentiation factor and the setup of a 3D organoid model leveraging thymocyte crosstalk in a three-dimensional hydrogel structure.

Previous proposed thymic differentiation protocols were built by testing only a few distinct combinations of factors, often iteratively, and without a robust statistical approach (35–39,70). If this methodology can improve differentiation efficiency, it could nonetheless lead to suboptimal results or even confounding factor effects. A DOE-based optimization approach allows for less bias, by simultaneously testing multiple factor combinations. Moreover, readout quality is crucial for the optimization. Instead of relying only on expression of a few markers, we leveraged bulk RNAseq and public scRNAseq data from thymic and pharyngeal organogenesis to classify the efficiency of the differentiation. This multidimensional readout allowed us to measure the effect of each differentiation factor on our sample transcriptomes and to select those with highest similarity to *in vivo* developing pharyngeal populations. Although public data used as reference were mice, thymus organogenesis was found to be mostly conserved with humans (53). Moreover, the positive results of the optimization advocate for the pertinence of the approach. Because we used only one iPSc line for DOE optimization, there was a risk of overfitting the protocol to this specific line. However, we show that our protocol can differentiate two more iPSc cell lines thymic tissue, demonstrating its robustness.

In addition to previously identified regulators of AFE and 3PPE induction, such as RA and WNT, we identified for the first time a positive effect of IGF1 and FGF10 supplementation in TEP differentiation. On the contrary, this study contradicts previous works using BMP4 for AFE induction (35,37), showing no significant BMP4 effect and even the benefits of its inhibition by NOGGIN. Hedgehog inhibition showed no significant effect in our data as well. However, recent studies indicate that a fine temporal modulation of SHH promotes thymic development (37,38), thus suggesting testing SHH activation or inhibition at other timepoints. Finally, this work suggests that systematic robust experimental design is an adapted tool for iPSc differentiation study, because of their inherent variability, temporal susceptibility, multifactorial aspect and required workload. Broader DOE designs, testing more factors with more informative readouts such as single-cell-OMICS could be powerful tools to decipher the gene regulation during cell differentiation. In addition, we reported high variability both inter- and intra-experiments, with variable differentiation yield. iPSc state during D-1 seeding could be an

important source of variation. Reactive variability such as Matrigel is another potential source that must be carefully controlled. Thus, rigorous standardization and quality approach is required for reliable iPSc thymic differentiation.

Characterization of the differentiation product showed expression of TEP markers both at the RNA and protein level. However, weak expression of TEC markers demonstrates their immaturity, concordant with previous results where TEP grafting *in vivo* is required for the acquisition of functionality (35,36). However, development of an accessible and practical platform for thymopoiesis study and compatibility with future clinical applications imply an integral *in vitro* culture. A crucial contribution of this work is the setup of a 3D coculture system to mature TEP into HLA-DR^{hi} mTECs. Thymic crosstalk has been shown to be crucial for mTEC maturation and medulla structuration, through signalling provided by thymocytes and involving RANK-LTB-CD40 pathways. Then, classical 2D culture has been shown to be detrimental to primary TEC functionality, while 3D culture promoted maintenance and maturation of primary TECs (62). Therefore, we adapted previous works (47,62) to develop a fibrin-based hydrogel, seeded by ETP-TEP reaggregates. This resulted in the formation of human thymic organoids (hTO) growing at the air-liquid interface in 3D hydrogels. We observed that both coculture with ETP and 3D hydrogel culture promotes mTEC maturation. Induction of *AIRE* expression conjugated with maturation of an HLA-DR^{hi} population in hTO suggest presence of functional mTECs able to select thymocytes. This result is supported by IF showing mostly medullary differentiation. Or, *in vivo* thymopoiesis rely on the successive circulation through cortical and medullary niches. Thus, a proper cortico-medullary segregation in hTO must be pursued. Modulating matrix physical properties or avoiding the destructurating TEP reaggregation stage could be promising approaches to reach this goal.

Although we did not report direct proof of thymic selection occurring in hTOs, we observe generation from ETPs of SP T lymphocytes with mature phenotypes CD62L^{+}CCR7^{+}CD69^{-}. Because acquisition of those markers and survival signal is TEC-dependent on TECs, this demonstrates indirectly the hTO ability to perform thymic selection. We reported a bias in T cell fate commitment to the CD8^{+} lineage, that could be explained by an insufficient interaction with MHCII^{hi} cells in the HTO. However, presence of rare CD4^{+} SP T lymphocytes demonstrate that, while minor, selection of DP thymocytes into the CD4^{+} fate still occurs in hTOs. Interestingly, TCR type analysis by flow cytometry shows both αβ and γδ T cells, confirming the correct ability of hTO to support thymopoiesis, contrary to studies showing anormal exclusive γδ T generation (69). Interestingly, deeper analysis of the hematopoietic compartment of hTOs by scRNAseq revealed the presence of dendritic cells (DC). This population can be linked to the EPCAM^{lo}CD45^{+} unidentified population in hTO flow cytometry data. Given the recent studies revealing the crucial role of intrathymic DCs for thymocyte complementary selection, this unexpected population could participate in thymopoiesis in

hTOs, for instance in promoting commitment to the CD4+ SP fate. Finally, enrichment of fibroblast genes in hTO transcriptomes could indicate a transdifferentiation of TEC to mesenchymal identity. Fibroblasts as well have been recently revealed to be involved in thymic microenvironment homeostasis, and even be involved in thymocyte selection (66). Therefore, presence of a fibroblastic stromal population, probably associated to the $CD45^{-}EPCAM^{-}$ compartment in hTO, could contribute to hTO functionality.

This work thus provides insights on the regulation of iPSc thymic differentiation and advocates for the application of robust statistical tools to this subject. It provides an iPSc-derived human thymic organoid model, developed integrally *in vitro*. This multilineage organoid includes TEC, thymic fibroblasts, DC and T cells, and demonstrates thymic functionality, *i.e* ability to generate mature SP T lymphocytes. Thus, it provides crucial resources for the modelisation of thymopoiesis *in vitro.* Utilization of iPSc opens promising long-term perspectives for regenerative medicine and cellular therapies applied to pathologies affecting the thymus and *in vitro* generation of engineered T lymphocytes.

References

1. Miller JFAP. The function of the thymus and its impact on modern medicine. Science. 2020 Jul 31;369(6503):eaba2429.

2. Abramson J, Anderson G. Thymic Epithelial Cells. Annu Rev Immunol. 2017 Apr 26;35:85–118.

3. Kadouri N, Nevo S, Goldfarb Y, Abramson J. Thymic epithelial cell heterogeneity: TEC by TEC. Nat Rev Immunol [Internet]. 2019 Dec 5 [cited 2020 Feb 18]; Available from: http://www.nature.com/articles/s41577-019-0238-0

4. Bautista JL, Cramer NT, Miller CN, Chavez J, Berrios DI, Byrnes LE, et al. Single-cell transcriptional profiling of human thymic stroma uncovers novel cellular heterogeneity in the thymic medulla. Nat Commun. 2021 Feb 17;12(1):1096.

5. Bornstein C, Nevo S, Giladi A, Kadouri N, Pouzolles M, Gerbe F, et al. Single-cell mapping of the thymic stroma identifies IL-25-producing tuft epithelial cells. Nature. 2018 Jul;559(7715):622–6.

6. Carpenter AC, Bosselut R. Decision checkpoints in the thymus. Nat Immunol. 2010 Aug;11(8):666–73.

7. Deng Y, Chen H, Zeng Y, Wang K, Zhang H, Hu H. Leaving no one behind: tracing every human thymocyte by single-cell RNA-sequencing. Semin Immunopathol. 2021 Feb;43(1):29–43.

8. Chopp LB, Gopalan V, Ciucci T, Ruchinskas A, Rae Z, Lagarde M, et al. An Integrated Epigenomic and Transcriptomic Map of Mouse and Human αβ T Cell Development. Immunity. 2020 Dec 15;53(6):1182-1201.e8.

9. Klein L, Klugmann M, Nave KA, Tuohy VK, Kyewski B. Shaping of the autoreactive T-cell repertoire by a splice variant of self protein expressed in thymic epithelial cells. Nat Med. 2000 Jan;6(1):56–61.

10. Klein L, Kyewski B, Allen PM, Hogquist KA. Positive and negative selection of the T cell repertoire: what thymocytes see and don't see. Nat Rev Immunol. 2014 Jun;14(6):377–91.

11. Anderson MS, Venanzi ES, Klein L, Chen Z, Berzins SP, Turley SJ, et al. Projection of an immunological self shadow within the thymus by the aire protein. Science. 2002 Nov 15;298(5597):1395–401.

12. Cumano A, Berthault C, Ramond C, Petit M, Golub R, Bandeira A, et al. New Molecular Insights into Immune Cell Development. Annu Rev Immunol. 2019;37(1):497–519.

13. Cosway EJ, James KD, Lucas B, Anderson G, White AJ. The thymus medulla and its control of αβT cell development. Semin Immunopathol. 2021 Feb 1;43(1):15–27.

14. Alves NL, Takahama Y, Ohigashi I, Ribeiro AR, Baik S, Anderson G, et al. Serial progression of cortical and medullary thymic epithelial microenvironments. Eur J Immunol. 2014 Jan;44(1):16–22.

15. Baik S, Jenkinson EJ, Lane PJL, Anderson G, Jenkinson WE. Generation of both cortical and Aire+ medullary thymic epithelial compartments from CD205+ progenitors. Eur J Immunol. 2013;43(3):589–94.

16. Li J, Gordon J, Chen ELY, Xiao S, Wu L, Zúñiga-Pflücker JC, et al. NOTCH1 signaling establishes the medullary thymic epithelial cell progenitor pool during mouse fetal development. Dev Camb Engl. 2020 Jun 22;147(12):dev178988.

17. Liu D, Kousa AI, O'Neill KE, Rouse P, Popis M, Farley AM, et al. Canonical Notch signaling controls the early thymic epithelial progenitor cell state and emergence of the medullary epithelial lineage in fetal thymus development. Dev Camb Engl. 2020 Jun 22;147(12):dev178582.

18. Irla M. RANK Signaling in the Differentiation and Regeneration of Thymic Epithelial Cells. Front Immunol [Internet]. 2021 [cited 2022 Feb 25];11. Available from: https://www.frontiersin.org/article/10.3389/fimmu.2020.623265

19. Irla M, Hugues S, Gill J, Nitta T, Hikosaka Y, Williams IR, et al. Autoantigen-Specific Interactions with CD4+ Thymocytes Control Mature Medullary Thymic Epithelial Cell Cellularity. Immunity. 2008 Sep 19;29(3):451–63.

20. Lopes N, Boucherit N, Santamaria JC, Provin N, Charaix J, Ferrier P, et al. Thymocytes trigger self-antigen-controlling pathways in immature medullary thymic epithelial stages. eLife. 2022 Feb 21;11:e69982.

21. Park JE, Botting RA, Domínguez Conde C, Popescu DM, Lavaert M, Kunz DJ, et al. A cell atlas of human thymic development defines T cell repertoire formation. Science. 2020 Feb 21;367(6480):eaay3224.

22. Gao H, Cao M, Deng K, Yang Y, Song J, Ni M, et al. The Lineage Differentiation and Dynamic Heterogeneity of Thymic Epithelial Cells During Thymus Organogenesis. Front Immunol. 2022 Jan 1;13:805451.

23. Zeng Y, Liu C, Gong Y, Bai Z, Hou S, He J, et al. Single-Cell RNA Sequencing Resolves Spatiotemporal Development of Pre-thymic Lymphoid Progenitors and Thymus Organogenesis in Human Embryos. Immunity. 2019 Nov 19;51(5):930-948.e6.

24. Blackburn CC, Augustine CL, Li R, Harvey RP, Malin MA, Boyd RL, et al. The nu gene acts cell-autonomously and is required for differentiation of thymic epithelial progenitors. Proc Natl Acad Sci. 1996 Jun 11;93(12):5742–6.

25. Bredenkamp N, Ulyanchenko S, O'Neill KE, Manley NR, Vaidya HJ, Blackburn CC. An organized and functional thymus generated from FOXN1-reprogrammed fibroblasts. Nat Cell Biol. 2014 Sep;16(9):902–8.

26. Nowell CS, Bredenkamp N, Tetélin S, Jin X, Tischner C, Vaidya H, et al. Foxn1 regulates lineage progression in cortical and medullary thymic epithelial cells but is dispensable for medullary sublineage divergence. PLoS Genet. 2011 Nov;7(11):e1002348.

27. Farley AM, Morris LX, Vroegindeweij E, Depreter MLG, Vaidya H, Stenhouse FH, et al. Dynamics of thymus organogenesis and colonization in early human development. Development. 2013 May 1;140(9):2015–26.

28. Gordon J, Bennett AR, Blackburn CC, Manley NR. Gcm2 and Foxn1 mark early parathyroid- and thymus-specific domains in the developing third pharyngeal pouch. Mech Dev. 2001 May;103(1–2):141–3.

29. Gordon J, Manley NR. Mechanisms of thymus organogenesis and morphogenesis. Development. 2011 Sep 15;138(18):3865–78.

30. Figueiredo M, Zilhão R, Neves H. Thymus Inception: Molecular Network in the Early Stages of Thymus Organogenesis. Int J Mol Sci. 2020 Jan;21(16):5765.

31. Han L, Chaturvedi P, Kishimoto K, Koike H, Nasr T, Iwasawa K, et al. Single cell transcriptomics identifies a signaling network coordinating endoderm and mesoderm diversification during foregut organogenesis. Nat Commun. 2020 Dec;11(1):4158.

32. Magaletta ME, Lobo M, Kernfeld EM, Aliee H, Huey JD, Parsons TJ, et al. Integration of single-cell transcriptomes and chromatin landscapes reveals regulatory programs driving pharyngeal organ development. Nat Commun. 2022 Jan 24;13(1):457.

33. Nowotschin S, Setty M, Kuo YY, Liu V, Garg V, Sharma R, et al. The emergent landscape of the mouse gut endoderm at single-cell resolution. Nature. 2019 May;569(7756):361–7.

34. Chhatta A, Mikkers HMM, Staal FJT. Strategies for thymus regeneration and generating thymic organoids. J Immunol Regen Med. 2021 Nov 1;14:100052.

35. Parent AV, Russ HA, Khan IS, LaFlam TN, Metzger TC, Anderson MS, et al. Generation of Functional Thymic Epithelium from Human Embryonic Stem Cells that Supports Host T Cell Development. Cell Stem Cell [Internet]. 2013 Aug 1 [cited 2019 Jun 18];13(2). Available from: https://www.ncbi.nlm.nih.gov/pmc/articles/PMC3869399/

36. Sun X, Xu J, Lu H, Liu W, Miao Z, Sui X, et al. Directed Differentiation of Human Embryonic Stem Cells into Thymic Epithelial Progenitor-like Cells Reconstitutes the Thymic Microenvironment In Vivo. Cell Stem Cell. 2013 Aug;13(2):230–6.

37. Ramos SA, Morton JJ, Yadav P, Reed B, Alizadeh SI, Shilleh AH, et al. Generation of functional human thymic cells from induced pluripotent stem cells. J Allergy Clin Immunol. 2021 Jul;S0091674921011416.

38. Gras-Peña R, Danzl NM, Khosravi-Maharlooei M, Campbell SR, Ruiz AE, Parks CA, et al. Human stem cell-derived thymic epithelial cells enhance human T-cell development in a xenogeneic thymus. J Allergy Clin Immunol [Internet]. 2021 Oct 21 [cited 2022 Jan 5];0(0). Available from: https://www.jacionline.org/article/S0091-6749(21)01624-9/fulltext

39. Soh CL, Giudice A, Jenny RA, Elliott DA, Hatzistavrou T, Micallef SJ, et al. FOXN1GFP/w Reporter hESCs Enable Identification of Integrin-β4, HLA-DR, and EpCAM as Markers of Human PSC-Derived FOXN1+ Thymic Epithelial Progenitors. Stem Cell Rep. 2014 May 22;2(6):925–37.

40. Provin N, Giraud M. Differentiation of Pluripotent Stem Cells Into Thymic Epithelial Cells and Generation of Thymic Organoids: Applications for Therapeutic Strategies Against APECED. Front Immunol. 2022 Jun 29;13:930963.

41. Callaghan NI, Durland LJ, Ireland RG, Santerre JP, Simmons CA, Davenport Huyer L. Harnessing conserved signaling and metabolic pathways to enhance the maturation of functional engineered tissues. Npj Regen Med. 2022 Sep 3;7(1):1–25.

42. Toms D, Deardon R, Ungrin M. Climbing the mountain: experimental design for the efficient optimization of stem cell bioprocessing. J Biol Eng [Internet]. 2017 Dec 4 [cited 2020 Oct 19];11. Available from: https://www.ncbi.nlm.nih.gov/pmc/articles/PMC5712411/

43. Yasui R, Sekine K, Taniguchi H. Clever Experimental Designs: Shortcuts for Better iPSC Differentiation. Cells. 2021 Dec;10(12):3540.

44. Besnard M, Padonou F, Provin N, Giraud M, Guillonneau C. AIRE deficiency, from preclinical models to human APECED disease. Dis Model Mech [Internet]. 2021 Feb 5 [cited 2021 Nov 5];14(2). Available from: https://doi.org/10.1242/dmm.046359

45. Chaudhry MS, Velardi E, Dudakov JA, van den Brink MRM. Thymus: the next (re)generation. Immunol Rev. 2016 May;271(1):56–71.

46. Bosticardo M, Pala F, Calzoni E, Delmonte OM, Dobbs K, Gardner CL, et al. Artificial thymic organoids represent a reliable tool to study T-cell differentiation in patients with severe T-cell lymphopenia. Blood Adv. 2020 Jun 17;4(12):2611–6.

47. Montel-Hagen A, Sun V, Casero D, Tsai S, Zampieri A, Jackson N, et al. In Vitro Recapitulation of Murine Thymopoiesis from Single Hematopoietic Stem Cells. Cell Rep. 2020 Oct 27;33(4):108320.

48. Seet CS, He C, Bethune MT, Li S, Chick B, Gschweng EH, et al. Generation of mature T cells from human hematopoietic stem and progenitor cells in artificial thymic organoids. Nat Methods. 2017 May;14(5):521–30.

49. Iriguchi S, Yasui Y, Kawai Y, Arima S, Kunitomo M, Sato T, et al. A clinically applicable and scalable method to regenerate T-cells from iPSCs for off-the-shelf T-cell immunotherapy. Nat Commun. 2021 Jan 18;12(1):430.

50. Lavaert M, Liang KL, Vandamme N, Park JE, Roels J, Kowalczyk MS, et al. Integrated scRNA-Seq Identifies Human Postnatal Thymus Seeding Progenitors and Regulatory Dynamics of Differentiating Immature Thymocytes. Immunity. 2020 Jun 16;52(6):1088-1104.e6.

51. Kilens S, Meistermann D, Moreno D, Chariau C, Gaignerie A, Reignier A, et al. Parallel derivation of isogenic human primed and naive induced pluripotent stem cells. Nat Commun. 2018 Jan 24;9(1):360.

52. Hao Y, Hao S, Andersen-Nissen E, Mauck WM, Zheng S, Butler A, et al. Integrated analysis of multimodal single-cell data. Cell. 2021 Jun 24;184(13):3573-3587.e29.

53. Li LC, Wang X, Xu ZR, Wang YC, Feng Y, Yang L, et al. Single-cell patterning and axis characterization in the murine and human definitive endoderm. Cell Res. 2021 Mar;31(3):326–44.

54. D'Amour KA, Agulnick AD, Eliazer S, Kelly OG, Kroon E, Baetge EE. Efficient differentiation of human embryonic stem cells to definitive endoderm. Nat Biotechnol. 2005 Dec;23(12):1534–41.

55. Davenport C, Diekmann U, Budde I, Detering N, Naujok O. Anterior–Posterior Patterning of Definitive Endoderm Generated from Human Embryonic Stem Cells Depends on the Differential Signaling of Retinoic Acid, Wnt-, and BMP-Signaling. STEM CELLS. 2016;34(11):2635–47.

56. Balciunaite G, Keller MP, Balciunaite E, Piali L, Zuklys S, Mathieu YD, et al. Wnt glycoproteins regulate the expression of FoxN1, the gene defective in nude mice. Nat Immunol. 2002 Nov;3(11):1102–8.

57. Barbarulo A, Lau CI, Mengrelis K, Ross S, Solanki A, Saldaña JI, et al. Hedgehog Signalling in the Embryonic Mouse Thymus. J Dev Biol. 2016 Jul 16;4(3):22.

58. Bleul CC, Boehm T. BMP Signaling Is Required for Normal Thymus Development. J Immunol. 2005 Oct 15;175(8):5213–21.

59. Chu YW, Schmitz S, Choudhury B, Telford W, Kapoor V, Garfield S, et al. Exogenous insulin-like growth factor 1 enhances thymopoiesis predominantly through thymic epithelial cell expansion. Blood. 2008 Oct 1;112(7):2836–46.

60. Nusser A, Sagar, Swann JB, Krauth B, Diekhoff D, Calderon L, et al. Developmental dynamics of two bipotent thymic epithelial progenitor types. Nature. 2022 May 25;1–7.

61. Lopes N, Sergé A, Ferrier P, Irla M. Thymic Crosstalk Coordinates Medulla Organization and T-Cell Tolerance Induction. Front Immunol [Internet]. 2015 [cited 2022 Sep 2];6. Available from: https://www.frontiersin.org/articles/10.3389/fimmu.2015.00365

62. Pinto S, Schmidt K, Egle S, Stark HJ, Boukamp P, Kyewski B. An organotypic coculture model supporting proliferation and differentiation of medullary thymic epithelial cells and promiscuous gene expression. J Immunol. 2013 Feb 1;190(3):1085–93.

63. Campinoti S, Gjinovci A, Ragazzini R, Zanieri L, Ariza-McNaughton L, Catucci M, et al. Reconstitution of a functional human thymus by postnatal stromal progenitor cells and natural whole-organ scaffolds. Nat Commun. 2020 Dec;11(1):6372.

64. Hun M, Barsanti M, Wong K, Ramshaw J, Werkmeister J, Chidgey AP. Native thymic extracellular matrix improves in vivo thymic organoid T cell output, and drives in vitro thymic epithelial cell differentiation. Biomaterials. 2017 Feb;118:1–15.

65. Fan Y, Tajima A, Goh SK, Geng X, Gualtierotti G, Grupillo M, et al. Bioengineering Thymus Organoids to Restore Thymic Function and Induce Donor-Specific Immune Tolerance to Allografts. Mol Ther. 2015 Jul 1;23(7):1262–77.

66. Nitta T, Ota A, Iguchi T, Muro R, Takayanagi H. The fibroblast: An emerging key player in thymic T cell selection. Immunol Rev. 2021;302(1):68–85.

67. Nitta T, Takayanagi H. Non-Epithelial Thymic Stromal Cells: Unsung Heroes in Thymus Organogenesis and T Cell Development. Front Immunol [Internet]. 2021 [cited 2021 May 10];11. Available from: https://www.frontiersin.org/articles/10.3389/fimmu.2020.620894/full

68. Nitta T, Tsutsumi M, Nitta S, Muro R, Suzuki EC, Nakano K, et al. Fibroblasts as a source of self-antigens for central immune tolerance. Nat Immunol. 2020 Oct;21(10):1172–80.

69. Hosaka N, Kanda S, Shimono T, Nishiyama T. Induction of γδT cells from HSC-enriched BMCs co-cultured with iPSC-derived thymic epithelial cells. J Cell Mol Med [Internet]. [cited 2021 Nov 5];n/a(n/a). Available from: https://onlinelibrary.wiley.com/doi/abs/10.1111/jcmm.16993

70. Inami Y, Yoshikai T, Ito S, Nishio N, Suzuki H, Sakurai H, et al. Differentiation of induced pluripotent stem cells to thymic epithelial cells by phenotype. Immunol Cell Biol. 2011 Feb;89(2):314–21.

II. Differentiation of Pluripotent Stem Cells Into Thymic Epithelial Cells and Generation of Thymic Organoids: Applications for Therapeutic Strategies Against APECED

Cette revue que nous avons publiée en juin 2022 (123) fournit un travail de synthèse de l'état de l'art sur les différenciation thymiques d'iPSc, les principales limitations du domaine et les futures perspectives, notamment thérapeutiques, en se concentrant comme exemple sur la pathologie monogénique APECED.

Les paragraphes de mon introduction décrivant l'organogenèse du thymus, les protocoles de différenciation d'iPSc et la culture 3D reprennent ces travaux récents et complets, en les amendant des avancées les plus récentes.

Cette revue permet donc de situer les grands enjeux du domaine, enjeux auxquels mon article de recherche propose un début de réponse.

ANNEXE 1 : Differentiation of Pluripotent Stem Cells Into Thymic Epithelial Cells and Generation of Thymic Organoids: Applications for Therapeutic Strategies Against APECED

III. Thymocytes trigger self-antigen controlling pathways in immature medullary thymic epithelial stages

J'ai collaboré à cet article de recherche du Dr. Noëlla Lopes et l'équipe du Dr. Magali Irla du Centre d'Immunologie de Marseille-Luminy en tant que co-second auteur, en réalisant un travail de bioinformatique d'analyse de données et de visualisation.
Cet article décrit les mécanismes par lesquels le crosstalk thymique régule les populations de mTEC (188). Si la signalisation croisée entre thymocytes et $mTEC^{hi}$ a été étudiée en détail, la capacité des thymocytes à réguler d'autres populations de mTEC, dont celles récemment identifiées par scRNAseq était encore floue. Les populations cellulaires concernées, les voies de signalisation impliquées et les facteurs de transcriptions régulés n'avaient pas été décrits.
Ainsi, Lopes *et al*. ont utilisé 3 lignées murines dont la présentation d'antigènes du soi est spécifiquement perturbée avec les thymocytes $CD4^+$. Combinée à du RNAseq haut débit, cette approche a permis d'identifier que les thymocytes autoréactif CD4+ régulent les sous-populations de mTEC en induisant l'expression de différents facteurs de transcriptions, cytokines et molécules d'adhésion.
Mon apport dans cette étude a concerné l'analyse bioinformatique des données de séquençage, et notamment leur comparaison avec des jeux de données scRNAseq publics chez la souris (20,28,48). J'ai ainsi téléchargé les données brutes, et programmé un pipeline d'analyse sous R, reposant sur le package Seurat (261). J'ai ensuite analysé l'expression des gènes différentiellement exprimés entre les différentes lignées mutées de souris, afin d'isoler les gènes cibles du crosstalk induit par les thymocytes $CD4^+$, dans ces jeux de données en cellule unique. Les résultats ont ensuite été présentés sous forme de Heatmap, permettant ainsi une visualisation

rapide des gènes cibles du crosstalk dans les différentes sous-populations de mTEC.

ANNEXE 2 : Thymocytes trigger self-antigen controlling pathways in immature medullary thymic epithelial stages

IV. Aire-dependent transcripts escape Raver2-induced splice-event inclusion in the thymic epithelium

Cet article du Dr. Francine Padonou étudie les événements d'épissage alternatifs dans les mTEC^{hi}. En effet, les mTEC^{hi} ont la capacité d'exprimer de multiples isoformes des PTA, reproduisant la diversité issue d'un épissage différent en périphérie. Or le contrôle moléculaire de ce mécanisme, et notamment son lien avec la régulation induite par *Aire, a été* peu décrit. Le séquençage de mTEC^{hi} de souris WT et *Aire*-KO a montré que paradoxalement, les gènes dépendants de *AIRE* présentent des niveaux d'épissage faibles, contrairement aux gènes *Aire*-indépendants. L'identification de facteurs candidats et leur transduction dans des mTEC^{hi} cultivées en 3D a permis d'isoler *Raver2* comme facteur principal d'épissage alternatif des gènes *Aire*-indépendants, reposant sur un contrôle épigénétique médié par la marque d'histone H3K36me3.
J'ai apporté à ce projet une contribution expérimentale, notamment pour la culture de mTEC^{hi} murines primaires sur hydrogel de fibrine pour la transduction. Ce modèle est basé sur les travaux de Pinto *et al.* (99) et a été précurseur pour le modèle de culture d'organoïde thymique que j'ai développé ensuite pour les différenciations

thymiques d'iPSc. J'ai ainsi effectué les expérimentations d'isolation des mTEC^{hi} primaire à partir de thymus de souris, leur enrichissement et isolation par cytométrie en flux puis leur culture en hydrogel pendant 5 jours. Enfin, les gels ont été dissociés et les différentes populations de mTEC triées par cytométrie en flux. J'ai aussi participé à la rédaction de figures et aux expérimentations complémentaires requises par les correcteurs.

ANNEXE 3 : Aire-dependent transcripts escape Raver2-induced splice-event inclusion in the thymic epithelium

V. AIRE deficiency, from preclinical models to human APECED disease

Cette revue a été écrite par notre équipe et présente l'état de l'art des modèles précliniques de la pathologie APECED. Après avoir décrit l'étiologie et la symptomatologie de cette maladie auto-immune, cette revue décrit les modèles *in vivo* de souris et de rat ainsi que leurs avantages et défauts respectifs. Elle expose ensuite les modèles *ex vivo*, comme les cocultures de cellules thymiques primaires sur gel 3D, les différenciation thymiques d'iPSc et la formation d'organoïdes de thymus. Ma contribution à cette revue a concerné cette partie de la modélisation *ex vivo* de l'APECED.

ANNEXE 4 : AIRE deficiency, from preclinical models to human APECED disease

VI. Brevet : Process for obtaining functional Lymphocytes cells

Déposant : Nantes Université et Institut National de la Santé Et de la Recherche Médicale

Inventeur : PROVIN Nathan et GIRAUD Matthieu

V/Réf : DV 4813 / N/Réf : BR 130620

Le développement d'un modèle permettant la thymopoïèse *in vivo* pourrait permettre la génération de lymphocytes T modifiés, potentiellement prometteurs pour des applications en thérapie cellulaire. Ces résultats ont donc été suivis d'un dépôt de brevet visant à les protéger et potentiellement permettre un transfert de technologie à l'industrie.

DISCUSSION ET PERSPECTIVES

Le thymus est un organe crucial pour l'établissement d'un système immunitaire fonctionnel et tolérant au soi. Nous avons décrit dans l'introduction comment cette fonctionnalité émerge des interactions entre les populations du thymus, et comment celles-ci sont générées. Nous avons aussi détaillé l'état de l'art sur la génération de tissu thymique à partir d'iPSc et ses limitations.

Ce travail de thèse permet de lever quelques unes de ses limites. Nous avons optimisé le protocole en mesurant en parallèle l'effet de nombreux modulateurs de la différenciation. Nous avons ainsi obtenu des TEP et avons ensuite développé un système de coculture en 3D qui induit leur maturation en TEC. Les organoïdes thymiques ainsi obtenus permettent de maturer *in vitro* des progéniteurs hématopoïétiques en lymphocytes T CD4 et CD8, ainsi qu'en cellules dendritiques. Ce résultat est très intéressant car jusqu'ici la plupart des différenciations thymiques proposées se trouvaient bloquées au stade TEP et nécessitaient la transplantation *in vivo* pour maturer. Or, dans une optique de plateforme de production de lymphocytes T, cette approche n'est pas compatible avec les contraintes d'une application clinique. Nous apportons donc une solution supportant la production de lymphocytes T entièrement *in vitro.*

I. Le Design optimal d'expériences, un outil puissant pour le criblage et l'optimisation des protocoles de différenciation

Notre approche de mise au point du protocole est radicalement différente de ce qui a été jusque-là proposé. Au lieu de sélectionner *a priori* quelques facteurs de différenciation et d'en tester une poignée de combinaisons, parfois en les incrémentant selon les intuitions des expérimentateurs, nous avons dès le début basé notre méthodologie sur le design optimal d'expériences (DOE) (254). Ce type d'approche gagnerait à être appliqué systématiquement aux recherches utilisant les iPSc, notamment à cause de la variabilité conséquente des expérimentations sur celle-ci (257). En effet, un premier niveau de variabilité difficile à contrôler réside dans les différences entre lignées d'iPSc. Un second dans la variabilité de l'état des cellules lors du lancement de la différenciation. Le nombre de passages, l'état de cycle cellulaire et le niveau de confluence ont montré empiriquement influer sur la qualité des différenciations. Pour contrôler ces deux facteurs, nous avons donc introduit une standardisation stricte des cultures d'iPSc et amplifié 3 lignées d'iPSc que nous avons banquées.

Enfin, les dernières contraintes sont soulevées par la nature même du processus de différenciation, qui implique de multiples voies de signalisation activées ou inhibées et interagissant entre elles. Ces voies de signalisation ne sont pas indépendantes entre elles, et peuvent présenter des synergies ou des antagonismes (143). De plus, les effets des facteurs montrent une dépendance temporelle : une même molécule peut montrer des effets différents en fonction du stade de différenciation des cellules (143,144).

Ainsi, une approche de DOE est pertinente face à de telles contraintes. L'objectif est de maximiser la quantité d'information en testant simultanément le plus de facteurs de transcription, avec le moins de cultures possibles. Le coût des différenciations étant élevé en termes de temps et de réactifs, nous nous sommes limités au plus à 36 cultures par expérimentation. Le design de Plackett-Burman répond à ces critères. Il s'agit d'un design de criblage permettant de mesurer les effets principaux d'un grand nombre de facteurs, et ce en un minimum de cultures. Il a pour inconvénient d'avoir une faible résolution, et permet seulement de mesurer les effets principaux et d'approximer les interactions de premier ordre par régression linéaire multiple et sélection de modèle.

Cette méthodologie s'est montrée efficace pour optimiser la différenciation thymique. Nous avons ainsi identifié des combinaisons de molécules à 3 stades de différenciation permettant de mimer l'organogenèse du thymus. Il serait pertinent d'approfondir l'étude en testant d'autres voies de signalisation. Par exemple, il a été montré que les voies NGF et HIPPO seraient impliquées dans la différenciation des TEC (148). De même, plusieurs modulateurs de chaque voie gagneraient à être testés, inhibiteurs comme agonistes. Si pendant longtemps des protéines recombinantes ont été utilisées, aujourd'hui de nombreuses petites molécules pharmaceutiques sont disponibles pour moduler finement la signalisation cellulaire. Modifier le design expérimental pour en augmenter la résolution serait ainsi bénéficiaire : un plan central composite, comme un design de Box Behnken, permet de modéliser finement l'effet de la concentration de multiples facteurs, ainsi que leurs interactions, *via* une analyse de surface de réponse. En contrepartie, ce type de design nécessite beaucoup plus de cultures. De même, notre plan expérimental a été réalisé en trois manipulations indépendantes pour optimiser chacun des trois

stades de différenciation, et ce sur une seule lignée cellulaire. Il serait plus efficace d'ajouter ces facteurs "temps" et "lignée" dans un seul plan expérimental. Notre étude a démontré la pertinence de ce type d'approche, qui gagnerait à être mise à l'échelle, en passant de la centaine de combinaisons testée à des milliers ou dizaines de milliers. Un tel nombre de cultures implique de modifier le système de culture en passant par exemple en plaque 96 et avec plusieurs expérimentateurs. Les effets inter-plaques et inter-expérimentateurs devront être contrôlés, par exemple en incluant un design en blocs.

Le choix de la variable réponse à mesurer est un point crucial du DOE. Nous avons dans un premier temps mesuré par qPCR l'expression de gènes marqueurs des 3 stades de la différenciation optimisés, *HOXA3*, *PAX9* et *FOXN1*. Cette méthode offre une réponse rapide et économique, mais avec un faible débit car elle ne permet de mesurer que quelques gènes. De plus, si *FOXN1* est bien spécifique, *HOXA3* et *PAX9* peuvent être exprimés par d'autres types cellulaires que les dérivés ciblés. Nous avons donc ensuite mesuré l'ensemble du transcriptome de chaque culture par DGEseq, ce qui permet de lier l'effet de chaque facteur à l'expression de milliers de gènes. La comparaison avec des données transcriptomique publiques de l'organogenèse du thymus permet une mesure robuste et non biaisée de l'effet des facteurs testés sur la différenciation. Nous avons ainsi réanalysé les données brutes des articles de Han *et al.* et Magaletta *et al.* pour identifier la trajectoire des populations à l'origine du thymus, et isoler les signatures transcriptomiques de ces populations (143,149). Nous avons ensuite comparé l'enrichissement de ces listes de gènes dans nos différentes cultures, *via* leur expression médiane. Nous avons sélectionné les modalités des facteurs associés significativement à une augmentation de l'enrichissement, mesurée par ANOVA. Pour les facteurs non

significatifs, non avons sélectionné la modalité consensus dans les 3 cultures les mieux différenciées.

Une des limites dans cette approche est qu'elle suppose la conservation inter-espèces, les jeux de données étant issus d'embryons de souris. Cependant, cette hypothèse ne semble pas être restrictive, plusieurs études comparatives montrant une conservation de plusieurs mécanismes de l'organogenèse pharyngienne (147). A l'avenir, nous disposerons de jeux de données de l'embryogenèse humaine avec une résolution temporelle et un nombre de cellules suffisant pour y appliquer notre méthodologie. Enfin, la baisse des coûts des technologies multi-omiques en cellules uniques laisse envisager dans un futur proche une optimisation des différenciation par DOE reposant sur ces technologies. Il serait alors possible d'étudier l'effet de centaines de molécules sur l'ensemble du transcriptome et de l'épigénome le long de la différenciation, et ce à la résolution de la cellule unique. Couplée à des algorithmes reconstituant les trajectoires (Velocyto) (260) et le régulome (SCENIC) (259), ces approches promettent une augmentation radicale de notre compréhension des différenciations d'iPSc.

II. Mise au point et limitations du système de culture pour la différenciation

Notre protocole de différenciation en TEP repose sur de la culture 2D sur tapis de Matrigel. Ce système de culture découle de l'origine iPSc des cellules différenciées. Le Matrigel leur fournit une matrice d'accroche et des facteurs de croissance cruciaux à leur maintenance. Cependant, le Matrigel étant un produit dérivé de matrice purifiée de sarcome murin, son utilisation introduit une source de variabilité supplémentaire pour la différenciation. Il est de plus incompatible avec une

application en clinique. Le protocole de culture que nous avons utilisé est largement libre de produits xénogéniques, notre milieu de base étant synthétique. Remplacer le matrigel par une matrice compatible et les cytokines par des molécules pharmaceutiques sera donc requis pour passer en clinique. Bien que le Matrigel utilisé étant déplété en facteurs de croissance, il est probable qu'il reste un niveau résiduel exposé aux iPSc lors de la différenciation. Cette source de facteurs pourraient affecter notre protocole de différenciation et introduire une source de variabilité entre lots.

Un autre point clé du protocole est la fréquence de changement du milieu. En effet, nous avons observé une variabilité intra-expérimentale, entre les différents puits d'une même différenciation. Nous pensons qu'une sécrétion autocrine de facteurs de différenciation variable entre les puits s'additionnerait à la supplémentation exogène et induirait des variations de l'efficacité de différenciation entre réplicats. Cette hypothèse est appuyée par la mise en évidence d'une expression de plusieurs molécules orientant la différenciation dans nos cultures comme BMP4 et Activine A. La capacité des iPSc à moduler leur propre différenciation par signalisation autocrine est bien décrite (262,263). Cette source de variation semble difficile à contrôler, le milieu de culture étant changé en moyenne toutes les 48h dans notre protocole. Une fréquence de changement plus rapide du milieu, comme 12h, pourrait permettre de limiter l'effet des molécules sécrétées par les cultures. Cependant, des études quantifiant précisément ce phénomène sont encore nécessaires afin de contrôler précisément la différenciation. De plus, ceci expliquerait l'absence d'effet de certains facteurs testés dans notre approche de criblage, les différences de concentration introduites étant masquées par le niveau de sécrétion propre des cultures, comme pour le BMP4. Si les systèmes de culture classique ne semblent pas permettre de

contrôler cet effet, les avancées récentes sur la mise au point de systèmes de culture en microfluidique ouvrent des perspectives prometteuses sur le contrôle précis des conditions expérimentales en direct, en plus de permettre une automatisation et un débit radicalement améliorés (264).

Les premiers jours de différenciation de notre protocole reposent sur une induction en endoderme définitif (DE). Cette différenciation est bien étudiée et l'état de l'art montre un consensus sur les voies de signalisation à cibler, avec un pulse de WNT et une supplémentation en Activine A pour activer NODAL identifié dès 2005 par D'Amour et al (145,265,266). Nous n'avons donc pas cherché à optimiser cette étape du protocole, ayant de plus mesuré une surexpression des marqueurs du DE *SOX17* et *FOXA2,* et la coexpression de ces facteurs de transcription dans les cellules au J5 de la différenciation, ce qui confirme l'induction du DE. Cette étape est effectuée en culture 2D, cependant il serait pertinent d'étudier une approche de différenciation directement en 3D, qui pourrait améliorer significativement l'efficacité du protocole. En effet, au stade ultérieur de l'endoderme de la 3PP, le repli de l'épithélium et l'involution de la poche sont des moments cruciaux de la formation du primordium thymique, et il est probablement difficile de mimer ces mécanismes en culture monocouche 2D. Ainsi, différencier en 3D dès le stade DE est une piste prometteuse pour l'amélioration du protocole de différenciation thymique.

III. Améliorations et innovations apportées par notre approche

Lors d'expériences préliminaires sur ce projet, nous avons répliqué les protocoles des deux articles de 2013, de Parent *et al.* et Sun *et al.* Bien que nous avons réussi à montrer par qPCR une expression des marqueurs d'identité thymique *PAX9* et *FOXN1*, les niveaux d'expression faibles (avec des Ct supérieur à 35), la forte variabilité entre les expérimentations et une mortalité cellulaire importante, notamment pour le protocole de Parent, nous on poussé à chercher à optimiser ces approches. Ceci soulève par ailleurs le problème de la reproductibilité des résultats entre laboratoires. Notre approche a permis d'augmenter significativement l'expression de *FOXN1* et *PAX9*, indiquant une meilleure efficacité de différenciation. De plus, notre protocole s'est montré être capable de différencier 3 lignées d'iPSc, ce qui démontre la robustesse des résultats obtenus et prouve que l'approche de design expérimental n'a pas sur-optimisé le protocole à la seule lignée testée. Il est intéressant de comparer les résultats de notre phase d'optimisation avec les conclusions de Sun et Parent. Ainsi, contrairement à ce qui a été avancé par Sun *et al.*, inhiber WNT au J5 *via* l'ajout d'IWR1 se montre détrimentaire à l'induction en endoderme pharyngien antérieur. Ceci semble aussi entrer en contradiction avec nos connaissances sur la détermination de l'axe antéro-postérieur, l'inhibition de WNT et BMP promouvant l'antériorisation de l'endoderme. Ainsi, des doses plus faibles d'IWR1 que celles testées pourraient se montrer efficaces. Un autre point divergent concerne la supplémentation en BMP4 à J5 de Parent *et al*. Nous avons démontré qu'au contraire, c'est l'inhibition de cette voie *via* NOGGIN qui promeut l'antériorisation. Une confusion des facteurs dans l'étude de Parent, avec un effet bénéfique de BMP4 après J7 surpassant son effet négatif au J5, peut expliquer ce

résultat et démontre l'importance d'un design expérimental non biaisé. Enfin, nous avons montré que l'inhibition de Hedgehog par la cyclopamine au J7 est associée à des niveaux d'expression des marqueurs de l'endoderme pharyngien plus faibles. Ce résultat entre aussi en contradiction avec l'étude de Parent. De plus, la signalisation Hedgehog a été montrée être cruciale à la formation des poches pharyngiennes, comme présenté en introduction. L'étude plus récente de Ramos *et al.* (232) est cohérente avec nos conclusions et active même Hedgehog pendant 48h avant de l'inhiber plus tardivement, à partir du J9. Il semblerait donc qu'une modulation temporelle fine de Hedgehog instruise la différenciation en endoderme pharyngien. Enfin, d'autres voies de signalisation impliquées dans le développement du thymus ont pu être inférées à partir des jeux de données scRNAseq. Nous prévoyons donc de tester des modulateurs de ces voies avec de nouveaux designs expérimentaux. Citons par exemple la voie des facteurs de croissance nerveux (NGF) ou HIPPO, connue pour réguler l'expansion et la prolifération des cellules souches en cours de différenciation (267).

Un aspect novateur apporté par notre étude concerne la mise au point d'un système de culture d'organoïde thymique. Nous avons démontré que la coculture avec des thymocytes et la structure tridimensionnelle sont cruciaux pour la maturation du produit de différenciation en TEC et l'acquisition de fonctionnalité. L'état de l'art ayant montré l'intérêt de la culture en 3D pour les TEC primaires, nous avons formulé l'hypothèse qu'un tel système serait bénéfique à la maturation de nos TEP dérivés d'iPSc. Nous avons donc testé différents systèmes de culture. Dans un premier temps, nous avons utilisé du Matrigel dilué au 1⁄2 pour encapsuler les TEP et les ETP réagrégés, formant ainsi des sphéroïdes de 3 à 4 mm de diamètre, mis en suspension dans le milieu. Cependant, nous avons observé une limitation

considérable de la croissance cellulaire dans ce modèle. Il est possible que la concentration de l'hydrogel soit trop importante, ou que l'immersion dans le milieu de culture limite les échanges gazeux, auxquels les TEC sont particulièrement sensibles (232). Nous avons donc choisi d'utiliser un modèle mis au point par Pinto *et al* : une solution de fibrinogène est polymérisée par de la thrombine dans des inserts (99), formant un hydrogel ensuite ensemencé avec les micromasses des TEP et ETP réagrégés. Un tel hydrogel s'est montré plus permissif pour la croissance cellulaire, les micromasses formant des projections colonisant l'hydrogel, et en quelques semaines produisant des organoïdes mesurant jusqu'à 5 mm. De plus, ce modèle d'hydrogel permet la migration des thymocytes à travers la matrice. Nous avons en effet observé par imagerie que les thymocytes circulaient librement dans l'hydrogel. Enfin, les hydrogels étant coulés sur inserts, il est possible de cultiver les organoïdes en interface air-liquide, ce qui a été montré être crucial à la culture des TEC (268). Ces caractéristiques expliquent notre choix de modèle de culture 3D, bien que ce modèle nécessite encore d'être optimisé. La difficulté de dissocier les organoïdes entraîne un faible rendement lors de la récolte des cellules, ce qui pénalise les analyses en aval. Nous avons obtenu les meilleurs résultats avec une digestion à base de collagénase et trypsine conjuguée à une dissociation mécanique manuelle, un traitement agressif résultant en une mortalité cellulaire non négligeable. Enfin, ce modèle d'hydrogel ne permet pas la reconstitution de compartiments corticaux et médullaires bien définis. Or, cette structuration est cruciale pour la fonctionnalité du thymus. Nous cherchons donc à mieux comprendre le rôle de l'ECM dans la maturation des TEP, et l'instruction de leur différenciation corticale ou médullaire. Dans cette optique, nous cherchons à produire des matrices thymiques primaires décellularisées afin de les réensemencer avec notre produit de

différenciation. Nous avons adapté le protocole d'Asnaghi *et al.* aux mêmes prélèvements de thymus humains utilisés comme source d'ETP. Après décellularisation par choc osmotique, les matrices sont congelées à -80°C puis séchées par sublimation. Une étape de crosslinking permet de fixer les matrices et d'assurer leur stabilité. Nous avons adapté ce protocole et généré des lots d'ECM, prêtes à être ensemencées. Ces recherches sont en cours et devront permettre à terme d'améliorer notre modèle d'organoïde thymique dérivé d'iPSc.

Les mTEC^{hi} ont une demi-vie courte, de l'ordre de 2 semaines, et sont donc en constant renouvellement. La thymopoïèse est un processus de différenciation long, les premiers T SP nécessitant plusieurs semaines de différenciation. La question se pose donc du renouvellement du compartiment mTEC^{hi} dans les organoïdes. En effet, la synchronisation des cellules pendant la différenciation rend peu probable la conservation d'une population progénitrice. Développer un modèle d'organoïdes hétérogènes contenant plusieurs niches et permettant de conserver une population de progéniteurs quiescente sera nécessaire pour maintenir la thymopoïèse à long terme.

IV. Les organoïdes thymiques présentent une hétérogénéité stromale

La caractérisation fine de l'hétérogénéité des populations cellulaires de notre modèle d'organoïde est un enjeu clé pour décrire les mécanismes de communication impliqués. Nous avons observé dans leur transcriptome l'expression de groupes de gènes enrichis dans des populations de fibroblastes. Ces gènes sont associés à la sécrétion et la régulation de la matrice extracellulaire, comme *LUM, VIM* et *COL1A1*.

Bien que les TEC puissent exprimer à faible niveau ces gènes, il est plus probable que ces transcrits proviennent de populations soit mal différenciées, c'est à dire ayant dévié de la trajectoire de différenciation thymique, soit issues d'une transdifférenciation, c'est à dire de TEP ou de TEC qui perdent leur identité épithéliale pour se différencier en fibroblastes. En effet, il a été montré que les TEC présentent une plasticité remarquable et on la capacité d'exprimer un programme transcriptionnel mésenchymal, marqué par l'expression de CD90 (*THY1)*, un marqueur classique des fibroblastes du thymus (269). Il a été montré que les cellules épithéliales de plusieurs organes, comme le rein, peuvent entrer en transition épithélio-mésenchymateuse (EMT) lorsqu'elles sont exposées à une situation de stress ou un microenvironnement inflammatoire (269). Bien que notre modèle d'organoïde cherche à mimer au plus proche le microenvironnement du thymus *in vivo,* il est probable que, de par la nature même de la culture *in vitro*, les cellules dans les systèmes organoides soient exposé à des signaux de stress, qui induirait une perte de leur identité épithéliale en entrant en EMT. Nous pouvons observer dans les organoïdes par cytométrie en flux une population $EPCAM^{-}CD45^{-}$, bien distincte du compartiment T, mais confondue avec les TEC. Ceci semble donc appuyer la possibilité d'une transition d'une partie des TEC en fibroblastes. De plus, nous avons analysé par scRNAseq des TEC dérivées d'iPSc par notre protocole, dans nos organoïdes ainsi qu'en culture 2D. Les clusters de cellules présentant une signature transcriptomique de fibroblastes sont enrichis dans les échantillons en culture 2D. Ainsi, le modèle de culture organoïde semble protéger, au moins partiellement, les TEC de cette perte de fonctionnalité. Ceci est cohérent avec les récentes études démontrant l'importance de la culture 3D pour maintenir la fonctionnalité des TEC primaires (99). Paradoxalement, il est possible d'envisager

que la génération d'une population restreinte de fibroblastes dans le modèle d'organoide thymique puissent positivement affecter la régulation du microenvironnement. *In vivo,* l'importance des fibroblastes du thymus est de plus en plus étudiée, et a été démontré réguler la différenciation des TEC, la migration des thymocytes, et la production de PTA (89). Nous observons dans nos données scRNAseq l'expression de nombreuses molécules régulatrices de la différenciation TEC : ainsi des clusters présentent une signature de fibroblastes expriment BMP4, FGF7 et l'activine A. Ces cellules régulent affectent probablement la maturation des TEC dans notre modèle organoïde, et sa capacité à supporter la thymopoïèse. Nous avons ainsi mis au point un modèle d'organoïde multicellulaire, composé de populations hématopoïétiques, épithéliales thymiques et fibroblastiques.

V. Le modèle d'organoïde thymique pour la modélisation de la thymopoïèse *in vitro*

Une des innovations majeures apportée par ces travaux est la mise au point d'une plateforme permettant de générer *in vitro* des lymphocytes T par coculture avec des cellules épithéliales thymiques. En effet, la différenciation *ex vivo* de lymphocytes T est décrite depuis des années, notamment suite aux développement de modèles de coculture avec des cellules stromales surexprimant des ligands NOTCH, commes les OP9 (270). Cependant, l'absence de TEC dans ces systèmes et donc de sélection positive et négative est la cause de nombreux défaut de différenciation, notamment un biais de différenciation en T CD8 et des répertoires peu diversifiés (241). La faible expression du CMHII est avancée pour expliquer ce défaut de

maturation en T CD4. Notre modèle d'organoïdes thymiques supporte la différenciation de progéniteurs ETP en lymphocytes T matures. La sélection des ETP se justifie par leur nature de progéniteurs multipotents précoces, non engagés dans la lignée T et par la possibilité d'en obtenir en quantité à partir des prélèvements humains thymiques. Nous avons contrôlé par cytométrie en flux le phénotype des ETP triés et confirmé une population hématopoïétique pure $CD45^{+}$, majoritairement $CD34^{+}CD7^{+}CD3^{-}CD44^{+}$, ce qui confirme leur phénotype ETP. De manière intéressante, une sous-population $CD44^{-}$ pourrait correspondre à des thymocytes DN déjà engagés en lignée T et réarrangeant leur TCR. Cette population est cependant minoritaire, à hauteur de 10% des cellules triées. Ainsi, nous formons les organoïdes en mettant en coculture les TEP dérivés d'iPSc et une population d'ETP purifiés. Les prochaines perspectives seront de reproduire ces résultats avec d'autres sources d'HSC. La population de TSP, plus précoce que les ETP, pourrait être purifiée à partir de cellules sanguines et démontrer que la capacité du modèle organoïde à différencier des progéniteurs extrathymiques. Notre objectif final est de différencier des HSC différenciées à partir des mêmes iPSc que celles générant les TEP. Les protocoles de différenciation d'iPSc vers la lignée lymphoïde ont connu des progrès remarquables ces dernières années (243,252,253). Nous pouvons donc envisager d'effectuer en parallèle la différenciation en épithélium thymique et en HSC, puis de réagréger les deux populations pour former les organoïdes thymiques. Une telle approche devrait significativement améliorer le modèle, les deux populations de cellules étant syngéniques. De par l'importance cruciale de la signalisation médiée par les CMH lors de la thymopoïèse, la complémentarité des allèles HLA entre les TEC et les thymocytes est un point clé dans notre modèle d'organoïde. L'état de l'art ayant montré une interaction correcte entre des donneurs

non complémentaires, voire même une cross-réactivité interespèces entre l'homme et la souris (224,225), nous ne nous sommes pas restreints à des cocultures entre cellules de donneurs aux HLA compatibles. Différencier des HSC et des TEP à partir des mêmes iPSc permettrait de résoudre ce point en s'assurant de la compatibilité HLA, ce qui pourrait potentiellement améliorer notre modèle d'organoide thymique, et modéliser plus finement la thymopoïèse *in vitro.*

VI. Futures perspectives et identification d'une différenciation des ETP en cellules dendritiques potentiellement impliquées dans la sélection

Notre organoïde supporte le réarrangement au stade DN, la beta sélection et la sélection positive fournissant les signaux de survie jusqu'au stade SP.

La présence de T avec un phénotype d'émigrants thymique au phénotype $CD69^{-}CD62L^{hi}CCR7^{+}$ et l'expression de *AIRE* et du CMHII dans les organoïdes semble impliquer une activité de sélection négative. Nous n'avons cependant pas mis en évidence la mesurer directement. Certaines caspases sont activées spécifiquement lors de l'apoptose induite par la délétion clonale (271). La détection par cytométrie en flux de caspase-3 active dans les thymocytes de nos organoïdes serait donc une preuve directe de leur sélection.

Au-delà de la maturation en T CD4 et CD8, les thymocytes SP sélectionnés négativement peuvent aussi maturer en nTreg. Des résultats récents (232,241) semblent indiquer que cette maturation puisse avoir lieu *in vitro.* En effet, l'orientation vers le destin Treg est causée par une interaction faible avec les complexes CMHII:PTA présentés par les mTEC. La présence de TEC et d'expression de *AIRE* dans notre modèle organoïde permettrait donc la

différenciation de nTreg, qui pourrait être mise en évidence par cytométrie en flux par la détection d'une population $CD4^+CD25^+FOXP3^+$. La validation de la capacité à produire des nTreg ouvre des perspectives intéressantes, pour l'étude des mécanismes régulant cette différenciation ou comme support pour une production optimisée de nTreg. Cependant, la fonctionnalité tolérogène de ces cellules doit encore être confirmée *in vivo*. A plus long terme, ces travaux pourraient permettre des avancées pour les thérapies cellulaires ciblant la modulation de la tolérance immunitaire, avec des applications potentielles pour certaines pathologies auto-immunes ou la transplantation.

Les ETP ayant un potentiel multipotent, nous avons cherché à identifier d'autres populations hématopoïétiques hors lignée T dans nos organoïdes. Nous n'avons pas détecté de lymphocytes B ni de cellules tueuses naturelles (NK) dans les données scRNAseq de nos organoïdes. Ceci semble confirmer une induction correcte vers le destin T. Cependant, nous avons observé une population de cellules dendritiques, caractérisées par l'expression de *LY86* et *CLEC7A*. Parmi les sous-populations de DC thymiques, cette population est plus proche des DC SIRPa, avec une forte expression des marqueurs SIRPA, IL3RA et CLEC10A. Cette population présente un phénotype $CD45^+EPCAM^{lo}$ facilement identifiable en cytométrie en flux dans les organoïdes. La morphologie de cette population, proche des thymocytes ($CD45^+EPCAM^-$) et ne montrant pas de distinction claire, laisse supposer une origine commune à partir des ETP. Cette hypothèse est cohérente avec les connaissances actuelles sur la différenciation intra thymique de cellules dendritiques (55), notamment à partir d'une population de TSP biaisée vers ce destin cellulaire, comme décrit précédemment. Pour tester cette hypothèse, nous avons utilisé scSPLIT, un algorithme d'identification des signatures du polymorphisme SNP dans les transcrits

de chaque cellule de notre jeu de données scRNAseq. Nous avons ainsi pu identifier pour chaque population de cellules des organoïdes leur individu d'origine, soit le donneur des cellules reprogrammées en iPSc, soit le donneur du thymus dont les ETP sont originaires. L'ensemble des T et des DC des organoïdes proviennent du même individu, ce qui confirme une origine commune, et exclut la possibilité que les DC des organoïdes soient des contaminants issus d'une mauvaise différenciation des iPSc. Ainsi, les ETP sont aussi capables de se différencier en DC dans notre modèle organoïde. Ceci avait été observé dans un modèle d'organoïdes à base de cellules stromales surexprimant les ligands NOTCH (241). De manière intéressante, cette étude rapporte elle aussi une différenciation en T CD4, contrairement à la majorité des maturations de T *in vitro*, le plus souvent biaisées vers les T CD8. Il est donc possible que cette population minoritaire de DC, *via* leur forte expression du CMHII, promeuve la sélection négative et la maturation en T CD4. Cette hypothèse est aussi conforme avec la mise en évidence récente du transfert d'antigènes du soi des mTEC aux DC dans le thymus et leur rôle fonctionnel dans la délétion clonale. Une validation expérimentale sera nécessaire afin de confirmer le rôle fonctionnel des DC dans le modèle organoïde.

La confirmation de la fonctionnalité de notre modèle *in vivo* est un point crucial sur lequel nous travaillons actuellement. La transplantation dans un modèle de souris athymiques *nude* testera sa capacité à régénérer un compartiment T circulant et fonctionnel, par exemple capable de rejeter une greffe de peau. Ce modèle induisant cependant une cross-réactivité inter-espèces, il sera à terme nécessaire de mettre au point des modèles de souris entièrement humanisées. Ainsi, transplanter notre modèle d'organoïdes thymiques dans une souche de souris NSG, possiblement transplantées préalablement avec des progéniteurs CD34+ humains, ouvrira la

porte à une modélisation plus fine des mécanismes régulés par les lymphocytes T *in vivo.*

VII. Perspectives à long terme pour la modélisation de pathologies des TEC ou l'utilisation clinique pour la thérapie cellulaire.

Le modèle d'organoïde thymique que nous avons développé ouvre des perspectives très intéressantes pour la modélisation des pathologies affectant les TEC, comme APECED. L'avantage des iPSc est qu'elles permettent de reproduire les mutations à l'origine de ces pathologies. Ainsi, la reprogrammation de cellules somatiques de patients APECED générerait des iPSc portant la mutation de *AIRE.* Des iPSc ainsi reprogrammées ne montrent pas de défauts de prolifération ou d'apoptose et expriment les marqueurs classiques de pluripotence (272), malgré un rôle potentiel de *AIRE* dans la régulation de la pluripotence. Ainsi les iPSc dérivées de patients APECED pourraient être différenciées en TEC selon notre protocole. Il serait alors possible de reproduire *in vitro* des organoïdes thymiques mimant la pathologie APECED, ce qui fournirait un modèle d'étude précieux pour approfondir notre connaissance de cette pathologie. Enfin à plus long terme, l'objectif est de corriger le défaut de *AIRE* à l'aide d'outils d'édition génique comme CRISPR-Cas9 dans les iPSc issus des patients APECED. Celles-ci permettront de régénérer des organoïdes thymiques dont la fonctionnalité serait restaurée. A terme, transplanter ces tissus autologues chez le patient APECED regénérerait, du moins partiellement, un répertoire de lymphocytes T tolérants. Cette approche nécessite de dépléter au préalable les T autoréactifs déjà en circulation, par exemple par immunothérapies à base d'anticorps (250).

De même, notre modèle d'organoïdes thymiques pourrait ouvrir des portes pour la génération de lymphocytes T *in vitro* pour la thérapie cellulaire. Cet enjeu concentre des efforts de recherche importants, bien que la génération de T fonctionnels à partir d'iPSc est limitée par la difficulté à reproduire la niche thymique *ex vivo.* Nous pouvons ainsi envisager à long terme le développement d'approche d'immunothérapies personnalisées reposant sur des T générés *in vitro* dans des organoïdes thymiques. Cependant les coûts et les délais conséquents des reprogrammations d'iPSc restreindront probablement cette approche à quelques cas particuliers. Ainsi, il serait plus probable de générer à partir de multiples lignées d'iPSc des lymphocytes T modifiés, présentant par exemple un phénotype hypoimmunogène et des CAR ciblant des antigènes spécifiques, afin de constituer des banques permettant des thérapie cellulaires off-the-shelf et adaptées à un large spectre de pathologies (251–253).

Pour conclure, nos travaux ont permis d'approfondir la connaissance des processus de différenciation des TEC. Nous avons développé un protocole optimisé pour la génération de TEC à partir d'iPSc humaines, en utilisant les outils statistiques robustes du design expérimental. Notre approche de différenciation dirigée mime l'organogenèse *in vitro* et permet de produire des TEP. En exploitant les connaissances sur la communication croisée entre TEC et thymocytes, ainsi que sur l'importance de la structure 3D du stroma thymique, nous avons mis au point un système de coculuture dans un hydrogel en 3D permettant la maturation en TEC. Nous avons ainsi généré des organoïdes thymiques humains, supportant la thymopoïèse *in vitro* et générant des lymphocytes T matures.

RÉFÉRENCES

1. Miller JFAP. The function of the thymus and its impact on modern medicine. Science. 2020 Jul 31;369(6503):eaba2429.

2. Miller JFAP. Etiology and Pathogenesis of Mouse Leukemia. In: Haddow A, Weinhouse S, editors. Advances in Cancer Research . Academic Press; 1962 . p. 291–368.

3. Brack C, Hirama M, Lenhard-Schuller R, Tonegawa S. A complete immunoglobulin gene is created by somatic recombination. Cell. 1978 Sep 1;15(1):1–14.

4. Irla M, Guenot J, Sealy G, Reith W, Imhof BA, Sergé A. Three-dimensional visualization of the mouse thymus organization in health and immunodeficiency. J Immunol Baltim Md 1950. 2013 Jan 15;190(2):586–96.

5. Sakata M, Ohigashi I, Takahama Y. Cellularity of Thymic Epithelial Cells in the Postnatal Mouse. J Immunol. 2018 Feb 15;200(4):1382–8.

6. Kadouri N, Nevo S, Goldfarb Y, Abramson J. Thymic epithelial cell heterogeneity: TEC by TEC. Nat Rev Immunol . 2019 Dec 5

7. Gui J, Zhu X, Dohkan J, Cheng L, Barnes PF, Su DM. The aged thymus shows normal recruitment of lymphohematopoietic progenitors but has defects in thymic epithelial cells. Int Immunol. 2007 Oct;19(10):1201–11.

8. Plotkin J, Prockop SE, Lepique A, Petrie HT. Critical role for CXCR4 signaling in progenitor localization and T cell differentiation in the postnatal thymus. J Immunol Baltim Md 1950. 2003 Nov 1;171(9):4521–7.

9. Jenkinson WE, Rossi SW, Parnell SM, Agace WW, Takahama Y, Jenkinson EJ, et al. Chemokine receptor expression defines heterogeneity in the earliest thymic migrants. Eur J Immunol. 2007 Aug;37(8):2090–6.

10. Koch U, Fiorini E, Benedito R, Besseyrias V, Schuster-Gossler K, Pierres M, et al. Delta-like 4 is the essential, nonredundant ligand for Notch1 during thymic T cell lineage commitment. J Exp Med. 2008 Oct 27;205(11):2515–23.

11. Hozumi K, Mailhos C, Negishi N, Hirano K ichi, Yahata T, Ando K, et al. Delta-like 4 is indispensable in thymic environment specific for T cell development. J Exp Med. 2008 Oct 27;205(11):2507–13.

12. García-León MJ, Fuentes P, de la Pompa JL, Toribio ML. Dynamic regulation of NOTCH1 activation and Notch ligand expression in human thymus development. Development. 2018 Aug 13;145(16):dev165597.

13. Alves NL, Goff ORL, Huntington ND, Sousa AP, Ribeiro VSG, Bordack A, et al. Characterization of the thymic IL-7 niche in vivo. Proc Natl Acad Sci. 2009 Feb

3;106(5):1512–7.

14. Alves NL, Takahama Y, Ohigashi I, Ribeiro AR, Baik S, Anderson G, et al. Serial progression of cortical and medullary thymic epithelial microenvironments. Eur J Immunol. 2014 Jan;44(1):16–22.

15. Nakagawa Y, Ohigashi I, Nitta T, Sakata M, Tanaka K, Murata S, et al. Thymic nurse cells provide microenvironment for secondary T cell receptor rearrangement in cortical thymocytes. Proc Natl Acad Sci. 2012 Dec 11;109(50):20572–7.

16. Guyden JC, Pezzano M. Thymic nurse cells: a microenvironment for thymocyte development and selection. Int Rev Cytol. 2003;223:1–37
.
17. Ohigashi I, Matsuda-Lennikov M, Takahama Y. Peptides for T cell selection in the thymus. Peptides. 2021 Dec 1;146:170671.

18. Gommeaux J, Grégoire C, Nguessan P, Richelme M, Malissen M, Guerder S, et al. Thymus-specific serine protease regulates positive selection of a subset of CD4+ thymocytes. Eur J Immunol. 2009 Apr;39(4):956–64.

19. Jenkinson WE, Nakamura K, White AJ, Jenkinson EJ, Anderson G. Normal T Cell Selection Occurs in CD205-Deficient Thymic Microenvironments. PLOS ONE. 2012 Dec 31;7(12):e53416.

20. Bornstein C, Nevo S, Giladi A, Kadouri N, Pouzolles M, Gerbe F, et al. Single-cell mapping of the thymic stroma identifies IL-25-producing tuft epithelial cells. Nature. 2018 Jul;559(7715):622–6.

21. White AJ, Nakamura K, Jenkinson WE, Saini M, Sinclair C, Seddon B, et al. Lymphotoxin signals from positively selected thymocytes regulate the terminal differentiation of medullary thymic epithelial cells. J Immunol Baltim Md 1950. 2010 Oct 15;185(8):4769–76.

22. Metzger TC, Khan IS, Gardner JM, Mouchess ML, Johannes KP, Krawisz AK, et al. Lineage tracing and cell ablation identify a post-Aire-expressing thymic epithelial cell population. Cell Rep. 2013 Oct 17;5(1):166–79.

23. Nishikawa Y, Nishijima H, Matsumoto M, Morimoto J, Hirota F, Takahashi S, et al. Temporal Lineage Tracing of Aire-Expressing Cells Reveals a Requirement for Aire in Their Maturation Program. J Immunol. 2014 Mar 15;192(6):2585–92
.
24. Wang X, Laan M, Bichele R, Kisand K, Scott HS, Peterson P. Post-Aire Maturation of Thymic Medullary Epithelial Cells Involves Selective Expression of Keratinocyte-Specific Autoantigens. Front Immunol . 2012 Mar 5

25. Michelson DA, Hase K, Kaisho T, Benoist C, Mathis D. Thymic epithelial cells co-opt lineage-defining transcription factors to eliminate autoreactive T cells. Cell. 2022 Jul 7;185(14):2542-2558.e18.

26. Laan M, Salumets A, Klein A, Reintamm K, Bichele R, Peterson H, et al. Post-Aire Medullary Thymic Epithelial Cells and Hassall's Corpuscles as Inducers of Tonic Pro-Inflammatory Microenvironment. Front Immunol . 2021

27. Miller CN, Proekt I, von Moltke J, Wells KL, Rajpurkar AR, Wang H, et al. Thymic tuft cells promote an IL-4-enriched medulla and shape thymocyte development. Nature. 2018 Jul;559(7715):627–31.

28. Dhalla F, Baran-Gale J, Maio S, Chappell L, Hollander GA, Ponting CP. Biologically indeterminate yet ordered promiscuous gene expression in single medullary thymic epithelial cells. EMBO J. 2020 Jan 2;39(1):e101828.

29. Dooley J, Erickson M, Farr AG. An Organized Medullary Epithelial Structure in the Normal Thymus Expresses Molecules of Respiratory Epithelium and Resembles the Epithelial Thymic Rudiment of Nude Mice. J Immunol. 2005 Oct 1;175(7):4331–7.

30. Bautista JL, Cramer NT, Miller CN, Chavez J, Berrios DI, Byrnes LE, et al. Single-cell transcriptional profiling of human thymic stroma uncovers novel cellular heterogeneity in the thymic medulla. Nat Commun. 2021 Feb 17;12(1):1096.

31. Park JE, Botting RA, Domínguez Conde C, Popescu DM, Lavaert M, Kunz DJ, et al. A cell atlas of human thymic development defines T cell repertoire formation. Science. 2020 Feb 21;367(6480):eaay3224.

32. Abramson J, Anderson G. Thymic Epithelial Cells. Annu Rev Immunol. 2017 Apr 26;35:85–118.

33. Michelson DA, Mathis D. Thymic mimetic cells: tolerogenic masqueraders. Trends Immunol . 2022 Aug 22

34. Aaltonen J, Björses P, Perheentupa J, Horelli–Kuitunen N, Palotie A, Peltonen L, et al. An autoimmune disease, APECED, caused by mutations in a novel gene featuring two PHD-type zinc-finger domains. Nat Genet. 1997 Dec;17(4):399–403.

35. Meredith M, Zemmour D, Mathis D, Benoist C. Aire controls gene expression in the thymic epithelium with ordered stochasticity. Nat Immunol. 2015 Sep;16(9):942–9.

36. Chan AY, Anderson MS. Central tolerance to self revealed by the autoimmune regulator. Ann N Y Acad Sci. 2015 Nov;1356:80–9.

37. Purohit S, Kumar PG, Laloraya M, She JX. Mapping DNA-binding domains of the autoimmune regulator protein. Biochem Biophys Res Commun. 2005 Feb 18;327(3):939–44.

38. Hobbs RP, DePianto DJ, Jacob JT, Han MC, Chung BM, Batazzi AS, et al. Keratin-dependent regulation of Aire and gene expression in skin tumor keratinocytes. Nat Genet. 2015 Aug;47(8):933–8.

39. Carles CC, Fletcher JC. Missing links between histones and RNA Pol II arising from SAND? Epigenetics. 2010 Jul 1;5(5):381–5.

40. Mathis D, Benoist C. Aire. Annu Rev Immunol. 2009;27(1):287–312.

41. Savkur RS, Burris TP. The coactivator LXXLL nuclear receptor recognition motif. J Pept Res Off J Am Pept Soc. 2004 Mar;63(3):207–12.

42. Abramson J, Giraud M, Benoist C, Mathis D. Aire's Partners in the Molecular Control of Immunological Tolerance. Cell. 2010 Jan 8;140(1):123–35.

43. Giraud M, Yoshida H, Abramson J, Rahl PB, Young RA, Mathis D, et al. Aire unleashes stalled RNA polymerase to induce ectopic gene expression in thymic epithelial cells. Proc Natl Acad Sci U S A. 2012 Jan 10;109(2):535–40.

44. Giraud M, Jmari N, Du L, Carallis F, Nieland TJF, Perez-Campo FM, et al. An RNAi screen for Aire cofactors reveals a role for Hnrnpl in polymerase release and

Aire-activated ectopic transcription. Proc Natl Acad Sci U S A. 2014 Jan 28;111(4):1491–6.

45. Sansom SN, Shikama-Dorn N, Zhanybekova S, Nusspaumer G, Macaulay IC, Deadman ME, et al. Population and single-cell genomics reveal the Aire dependency, relief from Polycomb silencing, and distribution of self-antigen expression in thymic epithelia. Genome Res. 2014 Dec;24(12):1918–31.

46. Derbinski J, Pinto S, Rösch S, Hexel K, Kyewski B. Promiscuous gene expression patterns in single medullary thymic epithelial cells argue for a stochastic mechanism. Proc Natl Acad Sci. 2008 Jan 15;105(2):657–62.

47. Brennecke P, Reyes A, Pinto S, Rattay K, Nguyen M, Küchler R, et al. Single-cell transcriptome analysis reveals coordinated ectopic gene-expression patterns in medullary thymic epithelial cells. Nat Immunol. 2015 Sep;16(9):933–41.

48. Wells KL, Miller CN, Gschwind AR, Wei W, Phipps JD, Anderson MS, et al. Combined transient ablation and single cell RNA sequencing reveals the development of medullary thymic epithelial cells . Immunology; 2020 Jun

49. Cooper MD, Peterson RDA, South MA, Good RA. THE FUNCTIONS OF THE THYMUS SYSTEM AND THE BURSA SYSTEM IN THE CHICKEN. J Exp Med. 1966 Jan 1;123(1):75–102.

50. Le Douarin NM, Jotereau FV. Tracing of cells of the avian thymus through embryonic life in interspecific chimeras. J Exp Med. 1975 Jul 1;142(1):17–40.

51. Moore M a. S, Owen JJT. EXPERIMENTAL STUDIES ON THE DEVELOPMENT OF THE THYMUS. J Exp Med. 1967 Oct 1;126(4):715–26.

52. Galy A, Travis M, Cen D, Chen B. Human T, B, natural killer, and dendritic cells arise from a common bone marrow progenitor cell subset. Immunity. 1995 Oct 1;3(4):459–73.

53. Hao QL, George AA, Zhu J, Barsky L, Zielinska E, Wang X, et al. Human intrathymic lineage commitment is marked by differential CD7 expression: identification of CD7− lympho-myeloid thymic progenitors. Blood. 2008 Feb 1;111(3):1318–26.

54. Six EM, Bonhomme D, Monteiro M, Beldjord K, Jurkowska M, Cordier-Garcia C, et al. A human postnatal lymphoid progenitor capable of circulating and seeding the thymus. J Exp Med. 2007 Dec 24;204(13):3085–93.

55. Lavaert M, Liang KL, Vandamme N, Park JE, Roels J, Kowalczyk MS, et al. Integrated scRNA-Seq Identifies Human Postnatal Thymus Seeding Progenitors and Regulatory Dynamics of Differentiating Immature Thymocytes. Immunity. 2020 Jun 16;52(6):1088-1104.e6.

56. Zeng Y, Liu C, Gong Y, Bai Z, Hou S, He J, et al. Single-Cell RNA Sequencing Resolves Spatiotemporal Development of Pre-thymic Lymphoid Progenitors and Thymus Organogenesis in Human Embryos. Immunity. 2019 Nov 19;51(5):930-948.e6.

57. Liu C, Lan Y, Liu B, Zhang H, Hu H. T Cell Development: Old Tales Retold By Single-Cell RNA Sequencing. Trends Immunol. 2021 Feb 1;42(2):165–75.

58. Martín-Gayo E, González-García S, García-León MJ, Murcia-Ceballos A, Alcain J, García-Peydró M, et al. Spatially restricted JAG1-Notch signaling in human thymus provides suitable DC developmental niches. J Exp Med. 2017 Nov 6;214(11):3361–79.

59. Carpenter AC, Bosselut R. Decision checkpoints in the thymus. Nat Immunol. 2010 Aug;11(8):666–73.

60. Trampont PC, Tosello-Trampont AC, Shen Y, Duley AK, Sutherland AE, Bender TP, et al. CXCR4 acts as a costimulator during thymic β-selection. Nat Immunol. 2010 Feb;11(2):162–70.

61. Maillard I, Tu L, Sambandam A, Yashiro-Ohtani Y, Millholland J, Keeshan K, et al. The requirement for Notch signaling at the β-selection checkpoint in vivo is absolute and independent of the pre–T cell receptor. J Exp Med. 2006 Oct 2;203(10):2239–45.

62. Kreslavsky T, Garbe AI, Krueger A, von Boehmer H. T cell receptor–instructed αβ versus γδ lineage commitment revealed by single-cell analysis. J Exp Med. 2008 May 12;205(5):1173–86.

63. Hayes SM, Li L, Love PE. TCR Signal Strength Influences αβ/γδ Lineage Fate. Immunity. 2005 May 1;22(5):583–93.

64. Haks MC, Lefebvre JM, Lauritsen JPH, Carleton M, Rhodes M, Miyazaki T, et al. Attenuation of γδTCR Signaling Efficiently Diverts Thymocytes to the αβ Lineage. Immunity. 2005 May 1;22(5):595–606.

65. Taghon T, Rothenberg EV. Molecular mechanisms that control mouse and human TCR-αβ and TCR-γδ T cell development. Semin Immunopathol. 2008 Dec 1;30(4):383–98.

66. Chong MMW, Cornish AL, Darwiche R, Stanley EG, Purton JF, Godfrey DI, et al. Suppressor of Cytokine Signaling-1 Is a Critical Regulator of Interleukin-7-Dependent CD8+ T Cell Differentiation. Immunity. 2003 Apr 1;18(4):475–87.

67. Sasaki K, Takada K, Ohte Y, Kondo H, Sorimachi H, Tanaka K, et al. Thymoproteasomes produce unique peptide motifs for positive selection of CD8+ T cells. Nat Commun. 2015 Jun 23;6(1):7484.

68. Zhang N, Hartig H, Dzhagalov I, Draper D, He YW. The role of apoptosis in the development and function of T lymphocytes. Cell Res. 2005 Oct;15(10):749–69.

69. Dzhagalov I, Dunkle A, He YW. The Anti-Apoptotic Bcl-2 Family Member Mcl-1 Promotes T Lymphocyte Survival at Multiple Stages. J Immunol. 2008 Jul 1;181(1):521–8.

70. Li Y, Li K, Zhu L, Li B, Zong D, Cai P, et al. Development of double-positive thymocytes at single-cell resolution. Genome Med. 2021 Mar 26;13(1):49.

71. Liu X, Taylor BJ, Sun G, Bosselut R. Analyzing Expression of Perforin, Runx3, and Thpok Genes during Positive Selection Reveals Activation of CD8-Differentiation Programs by MHC II-Signaled Thymocytes. J Immunol. 2005 Oct 1;175(7):4465–74.

72. Chopp LB, Gopalan V, Ciucci T, Ruchinskas A, Rae Z, Lagarde M, et al. An Integrated Epigenomic and Transcriptomic Map of Mouse and Human αβ T Cell Development. Immunity. 2020 Dec 15;53(6):1182-1201.e8.

73. Wang L, Wildt KF, Zhu J, Zhang X, Feigenbaum L, Tessarollo L, et al. Distinct functions for the transcription factors GATA-3 and ThPOK during intrathymic differentiation of CD4+ T cells. Nat Immunol. 2008 Oct;9(10):1122–30.

74. Park JH, Adoro S, Guinter T, Erman B, Alag AS, Catalfamo M, et al. Signaling by

intrathymic cytokines, not T cell antigen receptors, specifies CD8 lineage choice and promotes the differentiation of cytotoxic-lineage T cells. Nat Immunol. 2010 Mar;11(3):257–64.

75. Josefowicz SZ, Lu LF, Rudensky AY. Regulatory T cells: mechanisms of differentiation and function. Annu Rev Immunol. 2012;30:531–64.

76. Morgana F, Opstelten R, Slot MC, Scott AM, Lier RAW van, Blom B, et al. Single-Cell Transcriptomics Reveals Discrete Steps in Regulatory T Cell Development in the Human Thymus. J Immunol. 2022 Jan 15;208(2):384–95

.
77. Love PE, Bhandoola A. Signal integration and crosstalk during thymocyte migration and emigration. Nat Rev Immunol. 2011 Jul;11(7):469–77.
78. Xu X, Zhang S, Li P, Lu J, Xuan Q, Ge Q. Maturation and Emigration of Single-Positive Thymocytes. Clin Dev Immunol. 2013 Sep 29;2013:e282870.

79. Allende ML, Dreier JL, Mandala S, Proia RL. Expression of the sphingosine 1-phosphate receptor, S1P1, on T-cells controls thymic emigration. J Biol Chem. 2004 Apr 9;279(15):15396–401.

80. Wu L, Shortman K. Heterogeneity of thymic dendritic cells. Semin Immunol. 2005 Aug;17(4):304–12.

81. Wang H, Zúñiga-Pflücker JC. Thymic Microenvironment: Interactions Between Innate Immune Cells and Developing Thymocytes. Front Immunol . 2022

82. Wu L, Vremec D, Ardavin C, Winkel K, Süss G, Georgiou H, et al. Mouse thymus dendritic cells: kinetics of development and changes in surface markers during maturation. Eur J Immunol. 1995 Feb;25(2):418–25.

83. Bonasio R, Scimone ML, Schaerli P, Grabie N, Lichtman AH, von Andrian UH. Clonal deletion of thymocytes by circulating dendritic cells homing to the thymus. Nat Immunol. 2006 Oct;7(10):1092–100.

84. Proietto AI, van Dommelen S, Zhou P, Rizzitelli A, D'Amico A, Steptoe RJ, et al. Dendritic cells in the thymus contribute to T-regulatory cell induction. Proc Natl Acad Sci U S A. 2008 Dec 16;105(50):19869–74.

85. Vollmann EH, Rattay K, Barreiro O, Thiriot A, Fuhlbrigge RA, Vrbanac V, et al. Specialized transendothelial dendritic cells mediate thymic T-cell selection against blood-borne macromolecules. Nat Commun. 2021 Oct 28;12(1):6230.

86. Kroger CJ, Spidale NA, Wang B, Tisch R. Thymic Dendritic Cell Subsets Display Distinct Efficiencies and Mechanisms of Intercellular MHC Transfer. J Immunol Baltim Md 1950. 2017 Jan 1;198(1):249–56.

87. Vobořil M, Březina J, Brabec T, Dobeš J, Ballek O, Dobešová M, et al. A model of preferential pairing between epithelial and dendritic cells in thymic antigen transfer. Zúñiga-Pflücker JC, Taniguchi T, Zúñiga-Pflücker JC, editors. eLife. 2022 Jan 31;11:e71578.

88. Nitta T, Tsutsumi M, Nitta S, Muro R, Suzuki EC, Nakano K, et al. Fibroblasts as a source of self-antigens for central immune tolerance. Nat Immunol. 2020 Oct;21(10):1172–80.

89. Nitta T, Ota A, Iguchi T, Muro R, Takayanagi H. The fibroblast: An emerging key player in thymic T cell selection. Immunol Rev. 2021;302(1):68–85.

90. Sitnik KM, Wendland K, Weishaupt H, Uronen-Hansson H, White AJ, Anderson G, et al. Context-Dependent Development of Lymphoid Stroma from Adult CD34(+) Adventitial Progenitors. Cell Rep. 2016 Mar 15;14(10):2375–88.

91. Nitta T, Murata S, Ueno T, Tanaka K, Takahama Y. Chapter 3 Thymic Microenvironments for T-Cell Repertoire Formation. In: Advances in Immunology . Academic Press; 2008

92. Nitta T, Takayanagi H. Non-Epithelial Thymic Stromal Cells: Unsung Heroes in Thymus Organogenesis and T Cell Development. Front Immunol . 2021

93. Perry JSA, Lio CWJ, Kau AL, Nutsch K, Yang Z, Gordon JI, et al. Distinct Contributions of Aire and Antigen-Presenting-Cell Subsets to the Generation of Self-Tolerance in the Thymus. Immunity. 2014 Sep 18;41(3):414–26.

94. Rossi FMV, Corbel SY, Merzaban JS, Carlow DA, Gossens K, Duenas J, et al. Recruitment of adult thymic progenitors is regulated by P-selectin and its ligand PSGL-1. Nat Immunol. 2005 Jun;6(6):626–34.

95. Mentlein R, Kendall MD. The brain and thymus have much in common: a functional analysis of their microenvironments. Immunol Today. 2000 Mar;21(3):133–40.

96. Savino W. The Thymus Is a Common Target Organ in Infectious Diseases. PLoS Pathog. 2006 Jun;2(6):e62.

97. Savino W. The thymic microenvironment in infectious diseases. Mem Inst Oswaldo Cruz. 1990 Sep;85:255–60.

98. Lins MP. Thymic Extracellular Matrix in the Thymopoiesis: Just a Supporting? BioTech. 2022 Sep;11(3):27.

99. Pinto S, Schmidt K, Egle S, Stark HJ, Boukamp P, Kyewski B. An organotypic coculture model supporting proliferation and differentiation of medullary thymic epithelial cells and promiscuous gene expression. J Immunol. 2013 Feb 1;190(3):1085–93.

100. Hun M, Barsanti M, Wong K, Ramshaw J, Werkmeister J, Chidgey AP. Native thymic extracellular matrix improves in vivo thymic organoid T cell output, and drives in vitro thymic epithelial cell differentiation. Biomaterials. 2017 Feb;118:1–15.

101. Asnaghi MA, Barthlott T, Gullotta F, Strusi V, Amovilli A, Hafen K, et al. Thymus Extracellular Matrix-Derived Scaffolds Support Graft-Resident Thymopoiesis and Long-Term In Vitro Culture of Adult Thymic Epithelial Cells. Adv Funct Mater. :2010747.

102. Sharma H, Moroni L. Recent Advancements in Regenerative Approaches for Thymus Rejuvenation. Adv Sci. 2021;8(14):2100543.

103. Bissell MJ, Aggeler J. Dynamic reciprocity: how do extracellular matrix and hormones direct gene expression? Prog Clin Biol Res. 1987;249:251–62.

104. Flaumenhaft R, Rifkin DB. Extracellular matrix regulation of growth factor and protease activity. Curr Opin Cell Biol. 1991 Oct 1;3(5):817–23.

105. Crisa L, Cirulli V, Ellisman MH, Ishii JK, Elices MJ, Salomon DR. Cell adhesion and migration are regulated at distinct stages of thymic T cell development: the roles of fibronectin, VLA4, and VLA5. J Exp Med. 1996 Jul 1;184(1):215–28.

106. Alenghat FJ, Ingber DE. Mechanotransduction: All Signals Point to Cytoskeleton,

Matrix, and Integrins. Sci STKE. 2002 Feb 12;2002(119):pe6–pe6.

107. Graham A, Richardson J. Developmental and evolutionary origins of the pharyngeal apparatus. EvoDevo. 2012 Oct 1;3(1):24.

108. Gordon J, Wilson VA, Blair NF, Sheridan J, Farley A, Wilson L, et al. Functional evidence for a single endodermal origin for the thymic epithelium. Nat Immunol. 2004 May;5(5):546–53.

109. Gordon J, Manley NR. Mechanisms of thymus organogenesis and morphogenesis. Development. 2011 Sep 15;138(18):3865–78.

110. Frisdal A, Trainor PA. Development and evolution of the pharyngeal apparatus. WIREs Dev Biol. 2014;3(6):403–18.

111. Sperber GH, Sperber GHS Geoffrey D Guttmann, Steven M. Craniofacial Development (Book for Windows & Macintosh). PMPH-USA; 2001. 236 p.

112. Grevellec A, Tucker AS. The pharyngeal pouches and clefts: Development, evolution, structure and derivatives. Semin Cell Dev Biol. 2010 May;21(3):325–32.

113. Norris EH. The morphogenesis and histogenesis of the thymus gland in man: in which the origin of the Hassall's corpuscles of the human thymus is discovered. 1938.

114. Van Dyke JH. On the origin of accessory thymus tissue, thymus IV: The occurrence in man. Anat Rec. 1941;79(2):179–209.

115. Blackburn CC, Manley NR. Developing a new paradigm for thymus organogenesis. Nat Rev Immunol. 2004 Apr;4(4):278–89.

116. Manley NR, Condie BG. Transcriptional Regulation of Thymus Organogenesis and Thymic Epithelial Cell Differentiation. In: Liston A, editor. Progress in Molecular Biology and Translational Science . Academic Press; 2010

117. Cordier AC, Haumont SM. Development of thymus, parathyroids, and ultimo-branchial bodies in NMRI and nude mice. Am J Anat. 1980;157(3):227–63.

118. Cordier AC, Heremans JF. Nude Mouse Embryo: Ectodermal Nature of the Primordial Thymic Defect. Scand J Immunol. 1975;4(2):193–6.

119. Farley AM, Morris LX, Vroegindeweij E, Depreter MLG, Vaidya H, Stenhouse FH, et al. Dynamics of thymus organogenesis and colonization in early human development. Development. 2013 May 1;140(9):2015–26.

120. Jurberg AD, Vasconcelos-Fontes L, Cotta-de-Almeida V. A Tale from TGF-β Superfamily for Thymus Ontogeny and Function. Front Immunol . 2015

121. Hamazaki Y. Adult thymic epithelial cell (TEC) progenitors and TEC stem cells: Models and mechanisms for TEC development and maintenance. Eur J Immunol. 2015;45(11):2985–93.

122. Muñoz JJ, Zapata AG. Epithelial Development Based on a Branching Morphogenesis Program: The Special Condition of Thymic Epithelium . Histology. IntechOpen; 2018

123. Provin N, Giraud M. Differentiation of Pluripotent Stem Cells Into Thymic Epithelial Cells and Generation of Thymic Organoids: Applications for Therapeutic Strategies Against APECED. Front Immunol. 2022 Jun 29;13:930963.

124. Nehls M, Pfeifer D, Schorpp M, Hedrich H, Boehm T. New member of the winged-helix protein family disrupted in mouse and rat nude mutations. Nature. 1994 Nov;372(6501):103–7.

125. Gordon J, Bennett AR, Blackburn CC, Manley NR. Gcm2 and Foxn1 mark early parathyroid- and thymus-specific domains in the developing third pharyngeal pouch. Mech Dev. 2001 May;103(1–2):141–3.

126. Bleul CC, Corbeaux T, Reuter A, Fisch P, Mönting JS, Boehm T. Formation of a functional thymus initiated by a postnatal epithelial progenitor cell. Nature. 2006 Jun;441(7096):992–6.

127. Blackburn CC, Augustine CL, Li R, Harvey RP, Malin MA, Boyd RL, et al. The nu gene acts cell-autonomously and is required for differentiation of thymic epithelial progenitors. Proc Natl Acad Sci. 1996 Jun 11;93(12):5742–6.

128. Nehls M, Kyewski B, Messerle M, Waldschütz R, Schüddekopf K, Smith AJH, et al. Two Genetically Separable Steps in the Differentiation of Thymic Epithelium. Science. 1996 May 10;272(5263):886–9.

129. Muñoz JJ, Cejalvo T, Tobajas E, Fanlo L, Cortés A, Zapata AG. 3D immunofluorescence analysis of early thymic morphogenesis and medulla development. Histol Histopathol. 2015 May;30(5):589–99.

130. Prowse DM, Lee D, Weiner L, Jiang N, Magro CM, Baden HP, et al. Ectopic expression of the nude gene induces hyperproliferation and defects in differentiation: implications for the self-renewal of cutaneous epithelia. Dev Biol. 1999 Aug 1;212(1):54–67.

131. Nowell CS, Bredenkamp N, Tetélin S, Jin X, Tischner C, Vaidya H, et al. Foxn1 regulates lineage progression in cortical and medullary thymic epithelial cells but is dispensable for medullary sublineage divergence. PLoS Genet. 2011 Nov;7(11):e1002348.

132. Revest JM, Suniara RK, Kerr K, Owen JJT, Dickson C. Development of the Thymus Requires Signaling Through the Fibroblast Growth Factor Receptor R2-IIIb. J Immunol. 2001 Aug 15;167(4):1954–61.

133. Bredenkamp N, Nowell CS, Blackburn CC. Regeneration of the aged thymus by a single transcription factor. Development. 2014 Apr 15;141(8):1627–37.

134. Galy A, Verma S, Bárcena A, Spits H. Precursors of CD3+CD4+CD8+ cells in the human thymus are defined by expression of CD34. Delineation of early events in human thymic development. J Exp Med. 1993 Aug 1;178(2):391–401.

135. Deng Y, Chen H, Zeng Y, Wang K, Zhang H, Hu H. Leaving no one behind: tracing every human thymocyte by single-cell RNA-sequencing. Semin Immunopathol. 2021 Feb;43(1):29–43.

136. Hou S, Li Z, Zheng X, Gao Y, Dong J, Ni Y, et al. Embryonic endothelial evolution towards first hematopoietic stem cells revealed by single-cell transcriptomic and functional analyses. Cell Res. 2020 May;30(5):376–92.

137. Tavian M, Hallais MF, Péault B. Emergence of intraembryonic hematopoietic precursors in the pre-liver human embryo. Dev Camb Engl. 1999 Feb;126(4):793–803.

138. Ramond C, Berthault C, Burlen-Defranoux O, de Sousa AP, Guy-Grand D, Vieira P, et

al. Two waves of distinct hematopoietic progenitor cells colonize the fetal thymus. Nat Immunol. 2014 Jan;15(1):27–35.

139. Park JE, Jardine L, Gottgens B, Teichmann SA, Haniffa M. Prenatal development of human immunity. Science. 2020 May 8;368(6491):600–3.

140. Cumano A, Berthault C, Ramond C, Petit M, Golub R, Bandeira A, et al. New Molecular Insights into Immune Cell Development. Annu Rev Immunol. 2019;37(1):497–519.

141. Allan DS, Kirkham CL, Aguilar OA, Qu LC, Chen P, Fine JH, et al. An in vitro model of innate lymphoid cell function and differentiation. Mucosal Immunol. 2015 Mar;8(2):340–51.

142. Suo C, Dann E, Goh I, Jardine L, Kleshchevnikov V, Park JE, et al. Mapping the developing human immune system across organs. Science. 2022 May 12;376(6597):eabo0510.

143. Han L, Chaturvedi P, Kishimoto K, Koike H, Nasr T, Iwasawa K, et al. Single cell transcriptomics identifies a signaling network coordinating endoderm and mesoderm diversification during foregut organogenesis. Nat Commun. 2020 Dec;11(1):4158.

144. Davenport C, Diekmann U, Budde I, Detering N, Naujok O. Anterior–Posterior Patterning of Definitive Endoderm Generated from Human Embryonic Stem Cells Depends on the Differential Signaling of Retinoic Acid, Wnt-, and BMP-Signaling. STEM CELLS. 2016;34(11):2635–47.

145. Green MD, Chen A, Nostro MC, d'Souza SL, Schaniel C, Lemischka IR, et al. Generation of anterior foregut endoderm from human embryonic and induced pluripotent stem cells. Nat Biotechnol. 2011 Mar;29(3):267–72.

146. Kearns NA, Genga RMJ, Ziller M, Kapinas K, Peters H, Brehm MA, et al. Generation of organized anterior foregut epithelia from pluripotent stem cells using small molecules. Stem Cell Res. 2013 Nov 1;11(3):1003–12.

147. Li LC, Wang X, Xu ZR, Wang YC, Feng Y, Yang L, et al. Single-cell patterning and axis characterization in the murine and human definitive endoderm. Cell Res. 2021 Mar;31(3):326–44.

148. Nowotschin S, Setty M, Kuo YY, Liu V, Garg V, Sharma R, et al. The emergent landscape of the mouse gut endoderm at single-cell resolution. Nature. 2019 May;569(7756):361–7.

149. Magaletta ME, Lobo M, Kernfeld EM, Aliee H, Huey JD, Parsons TJ, et al. Integration of single-cell transcriptomes and chromatin landscapes reveals regulatory programs driving pharyngeal organ development. Nat Commun. 2022 Jan 24;13(1):457.

150. Wendling O, Dennefeld C, Chambon P, Mark M. Retinoid signaling is essential for patterning the endoderm of the third and fourth pharyngeal arches. Dev Camb Engl. 2000 Apr;127(8):1553–62.

151. Kopinke D, Sasine J, Swift J, Stephens WZ, Piotrowski T. Retinoic acid is required for endodermal pouch morphogenesis and not for pharyngeal endoderm specification. Dev Dyn. 2006;235(10):2695–709.

152. Quinlan R, Gale E, Maden M, Graham A. Deficits in the posterior pharyngeal endoderm in the absence of retinoids. Dev Dyn. 2002;225(1):54–60.

153. Niederreither K, Vermot J, Roux IL, Schuhbaur B, Chambon P, Dollé P. The regional pattern of retinoic acid synthesis by RALDH2 is essential for the development of posterior pharyngeal arches and the enteric nervous system. Development. 2003 Jun 1;130(11):2525–34.

154. Rhinn M, Dollé P. Retinoic acid signalling during development. Development. 2012 Mar 1;139(5):843–58.

155. Balciunaite G, Keller MP, Balciunaite E, Piali L, Zuklys S, Mathieu YD, et al. Wnt glycoproteins regulate the expression of FoxN1, the gene defective in nude mice. Nat Immunol. 2002 Nov;3(11):1102–8.

156. Osada M, Jardine L, Misir R, Andl T, Millar SE, Pezzano M. DKK1 Mediated Inhibition of Wnt Signaling in Postnatal Mice Leads to Loss of TEC Progenitors and Thymic Degeneration. PLOS ONE. 2010 Feb 8;5(2):e9062.

157. Jin S, O J, Stellabotte F, Choe CP. Foxi1 promotes late-stage pharyngeal pouch morphogenesis through ectodermal Wnt4a activation. Dev Biol. 2018 Sep 1;441(1):12–8.

158. Osada M, Ito E, Fermin HA, Vazquez-Cintron E, Venkatesh T, Friedel RH, et al. The Wnt Signaling Antagonist Kremen1 is Required for Development of Thymic Architecture. Clin Dev Immunol. 2006;13(2–4):299–319.

159. Brunk F, Augustin I, Meister M, Boutros M, Kyewski B. Thymic Epithelial Cells Are a Nonredundant Source of Wnt Ligands for Thymus Development. J Immunol. 2015 Dec 1;195(11):5261–71.

160. Swann JB, Happe C, Boehm T. Elevated levels of Wnt signaling disrupt thymus morphogenesis and function. Sci Rep. 2017 Apr 11;7(1):785.

161. Gordon J, Manley NR. Tissue-specific requirements for BMP signaling during thymus and parathyroid morphogenesis. Dev Biol. 2006 Jul 1;295(1):455.

162. Patel SR, Gordon J, Mahbub F, Blackburn CC, Manley NR. Bmp4 and Noggin expression during early thymus and parathyroid organogenesis. Gene Expr Patterns. 2006 Oct 2;6(8):794–9.

163. Tsai PT, Lee RA, Wu H. BMP4 acts upstream of FGF in modulating thymic stroma and regulating thymopoiesis. Blood. 2003 Dec 1;102(12):3947–53.

164. Lovely CB, Swartz ME, McCarthy N, Norrie JL, Eberhart JK. Bmp signaling mediates endoderm pouch morphogenesis by regulating Fgf signaling in zebrafish. Development. 2016 Jun 1;143(11):2000–11.

165. Macatee TL, Hammond BP, Arenkiel BR, Francis L, Frank DU, Moon AM. Ablation of specific expression domains reveals discrete functions of ectoderm- and endoderm-derived FGF8 during cardiovascular and pharyngeal development. Development. 2003 Dec 22;130(25):6361–74.

166. Abu-Issa R, Smyth G, Smoak I, Yamamura K ichi, Meyers EN. Fgf8 is required for pharyngeal arch and cardiovascular development in the mouse. Development. 2002 Oct 1;129(19):4613–25.

167. Gardiner JR, Jackson AL, Gordon J, Lickert H, Manley NR, Basson MA. Localised inhibition of FGF signalling in the third pharyngeal pouch is required for normal thymus and parathyroid organogenesis. Development. 2012 Sep 15;139(18):3456–66.

168. Saldaña JI, Solanki A, Lau CI, Sahni H, Ross S, Furmanski AL, et al. Sonic Hedgehog regulates thymic epithelial cell differentiation. J Autoimmun. 2016 Apr;68:86–97.

169. Moore-Scott BA, Manley NR. Differential expression of Sonic hedgehog along the anterior–posterior axis regulates patterning of pharyngeal pouch endoderm and pharyngeal endoderm-derived organs. Dev Biol. 2005 Feb 15;278(2):323–35.

170. Bain VE, Gordon J, O'Neil JD, Ramos I, Richie ER, Manley NR. Tissue-specific roles for sonic hedgehog signaling in establishing thymus and parathyroid organ fate. Dev Camb Engl. 2016 Nov 1;143(21):4027–37.

171. Garg V, Yamagishi C, Hu T, Kathiriya IS, Yamagishi H, Srivastava D. Tbx1, a DiGeorge Syndrome Candidate Gene, Is Regulated by Sonic Hedgehog during Pharyngeal Arch Development. Dev Biol. 2001 Jul 1;235(1):62–73.

172. Alawam AS, Anderson G, Lucas B. Generation and Regeneration of Thymic Epithelial Cells. Front Immunol . 2020

173. Rossi SW, Jenkinson WE, Anderson G, Jenkinson EJ. Clonal analysis reveals a common progenitor for thymic cortical and medullary epithelium. Nature. 2006 Jun 22;441(7096):988–91.

174. Chen L, Xiao S, Manley NR. Foxn1 is required to maintain the postnatal thymic microenvironment in a dosage-sensitive manner. Blood. 2009 Jan 15;113(3):567–74.

175. O'Neill KE, Bredenkamp N, Tischner C, Vaidya HJ, Stenhouse FH, Peddie CD, et al. Foxn1 Is Dynamically Regulated in Thymic Epithelial Cells during Embryogenesis and at the Onset of Thymic Involution. PloS One. 2016 Jan 1;11(3):e0151666.

176. Lepletier et al. Interplay between follistatin, activin A and Bmp4 signaling regulates postnatal thymic epithelial progenitor cell differentiation during aging.

177. Barsanti M, Lim JMC, Hun ML, Lister N, Wong K, Hammett MV, et al. A novel Foxn1eGFP/+ mouse model identifies Bmp4-induced maintenance of Foxn1 expression and thymic epithelial progenitor populations. Eur J Immunol. 2017;47(2):291–304.

178. Nusser A, Sagar, Swann JB, Krauth B, Diekhoff D, Calderon L, et al. Developmental dynamics of two bipotent thymic epithelial progenitor types. Nature. 2022 Jun;606(7912):165–71.

179. Liu D, Kousa AI, O'Neill KE, Rouse P, Popis M, Farley AM, et al. Canonical Notch signaling controls the early thymic epithelial progenitor cell state and emergence of the medullary epithelial lineage in fetal thymus development. Dev Camb Engl. 2020 Jun 22;147(12):dev178582.

180. Li J, Gordon J, Chen ELY, Xiao S, Wu L, Zúñiga-Pflücker JC, et al. NOTCH1 signaling establishes the medullary thymic epithelial cell progenitor pool during mouse fetal development. Dev Camb Engl. 2020 Jun 22;147(12):dev178988.

181. Goldfarb Y, Kadouri N, Levi B, Sela A, Herzig Y, Cohen RN, et al. HDAC3 is a master regulator of mTEC development. Cell Rep. 2016 Apr 19;15(3):651–65.

182. Chakrabarti S, Hoque M, Jamil NZ, Singh VJ, Pollacksmith D, Meer N, et al. Bone Marrow-Derived Cells Contribute to the Maintenance of Thymic Stroma including TECs. J Immunol Res. 2022 Apr 29;2022:e6061746.

183. Gray D, Abramson J, Benoist C, Mathis D. Proliferative arrest and rapid turnover of thymic epithelial cells expressing Aire. J Exp Med. 2007 Oct 29;204(11):2521–8.

184. Akiyama T, Shimo Y, Yanai H, Qin J, Ohshima D, Maruyama Y, et al. The tumor necrosis factor family receptors RANK and CD40 cooperatively establish the thymic medullary microenvironment and self-tolerance. Immunity. 2008 Sep 19;29(3):423–37.

185. van Ewijk W, Shores EW, Singer A. Crosstalk in the mouse thymus. Immunol Today. 1994 May;15(5):214–7.

186. Lopes N, Sergé A, Ferrier P, Irla M. Thymic Crosstalk Coordinates Medulla Organization and T-Cell Tolerance Induction. Front Immunol . 2015 Jul 20

187. Irla M. RANK Signaling in the Differentiation and Regeneration of Thymic Epithelial Cells. Front Immunol . 2021

188. Lopes N, Boucherit N, Santamaria JC, Provin N, Charaix J, Ferrier P, et al. Thymocytes trigger self-antigen-controlling pathways in immature medullary thymic epithelial stages. eLife. 2022 Feb 21;11:e69982.

189. Irla M, Hollander G, Reith W. Control of central self-tolerance induction by autoreactive CD4+ thymocytes. Trends Immunol. 2010 Feb;31(2):71–9.

190. Irla M, Guerri L, Guenot J, Sergé A, Lantz O, Liston A, et al. Antigen recognition by autoreactive $CD4^+$ thymocytes drives homeostasis of the thymic medulla. PloS One. 2012;7(12):e52591.

191. Seach N, Ueno T, Fletcher AL, Lowen T, Mattesich M, Engwerda CR, et al. The lymphotoxin pathway regulates Aire-independent expression of ectopic genes and chemokines in thymic stromal cells. J Immunol Baltim Md 1950. 2008 Apr 15;180(8):5384–92.

192. Lkhagvasuren E, Sakata M, Ohigashi I, Takahama Y. Lymphotoxin β Receptor Regulates the Development of CCL21-Expressing Subset of Postnatal Medullary Thymic Epithelial Cells. J Immunol. 2013 May 15;190(10):5110–7.

193. Steinmann GG, Klaus B, Müller-Hermelink HK. The involution of the ageing human thymic epithelium is independent of puberty. A morphometric study. Scand J Immunol. 1985 Nov;22(5):563–75.

194. George AJ, Ritter MA. Thymic involution with ageing: obsolescence or good housekeeping? Immunol Today. 1996 Jun;17(6):267–72.

195. Pawelec G, Akbar A, Caruso C, Solana R, Grubeck-Loebenstein B, Wikby A. Human immunosenescence: is it infectious? Immunol Rev. 2005;205(1):257–68.

196. Aw D, Silva AB, Palmer DB. Immunosenescence: emerging challenges for an ageing population. Immunology. 2007;120(4):435–46.

197. Shanley DP, Aw D, Manley NR, Palmer DB. An evolutionary perspective on the mechanisms of immunosenescence. Trends Immunol. 2009 Jul 1;30(7):374–81.

198. Dorshkind K, Montecino-Rodriguez E, Signer RAJ. The ageing immune system: is it ever too old to become young again? Nat Rev Immunol. 2009 Jan;9(1):57–62.

199. Hu C, Zhang K, Jiang F, Wang H, Shao Q. Epigenetic modifications in thymic epithelial

cells: an evolutionary perspective for thymus atrophy. Clin Epigenetics. 2021 Nov 24;13(1):210.
200. Laan M, Haljasorg U, Kisand K, Salumets A, Peterson P. Pregnancy-induced thymic involution is associated with suppression of chemokines essential for T-lymphoid progenitor homing. Eur J Immunol. 2016 Aug;46(8):2008–17.

201. Dumont-Lagacé M, Daouda T, Depoërs L, Zumer J, Benslimane Y, Brochu S, et al. Qualitative Changes in Cortical Thymic Epithelial Cells Drive Postpartum Thymic Regeneration. Front Immunol . 2020

202. Olsen NJ, Watson MB, Henderson GS, Kovacs WJ. Androgen deprivation induces phenotypic and functional changes in the thymus of adult male mice. Endocrinology. 1991 Nov;129(5):2471–6.

203. Chaudhry MS, Velardi E, Dudakov JA, van den Brink MRM. Thymus: the next (re)generation. Immunol Rev. 2016 May;271(1):56–71.

204. Venables T, Griffith AV, DeAraujo A, Petrie HT. Dynamic changes in epithelial cell morphology control thymic organ size during atrophy and regeneration. Nat Commun. 2019 Sep 27;10(1):4402.

205. Aach J, Lunshof J, Iyer E, Church GM. Addressing the ethical issues raised by synthetic human entities with embryo-like features. eLife. 2017 Mar 21;6:e20674.

206. Takahashi K, Yamanaka S. Induction of Pluripotent Stem Cells from Mouse Embryonic and Adult Fibroblast Cultures by Defined Factors. Cell. 2006 Aug;126(4):663–76.

207. Nakagawa M, Koyanagi M, Tanabe K, Takahashi K, Ichisaka T, Aoi T, et al. Generation of induced pluripotent stem cells without Myc from mouse and human fibroblasts. Nat Biotechnol. 2008 Jan;26(1):101–6.

208. Loh YH, Agarwal S, Park IH, Urbach A, Huo H, Heffner GC, et al. Generation of induced pluripotent stem cells from human blood. Blood. 2009 May 28;113(22):5476–9.

209. Cyranoski D. “Reprogrammed” stem cells approved to mend human hearts for the first time. Nature. 2018 May 1;557(7706):619–619.

210. Doss MX, Sachinidis A. Current Challenges of iPSC-Based Disease Modeling and Therapeutic Implications. Cells. 2019 May;8(5):403.

211. Gunaseeli I, Doss MX, Antzelevitch C, Hescheler J, Sachinidis A. Induced Pluripotent Stem Cells as a Model for Accelerated Patient- and Disease-specific Drug Discovery. Curr Med Chem. 2010 Mar 1;17(8):759–66.

212. Kim K, Doi A, Wen B, Ng K, Zhao R, Cahan P, et al. Epigenetic memory in induced pluripotent stem cells. Nature. 2010 Sep;467(7313):285–90.

213. Zhao T, Zhang Z ning, Westenskow PD, Todorova D, Hu Z, Lin T, et al. Humanized Mice Reveal Differential Immunogenicity of Cells Derived from Autologous Induced Pluripotent Stem Cells. Cell Stem Cell. 2015 Sep 3;17(3):353–9.
214. Mandai M, Watanabe A, Kurimoto Y, Hirami Y, Morinaga C, Daimon T, et al. Autologous Induced Stem-Cell–Derived Retinal Cells for Macular Degeneration. N Engl J Med. 2017 Mar 16;376(11):1038–46.

215. Deuse T, Hu X, Gravina A, Wang D, Tediashvili G, De C, et al. Hypoimmunogenic derivatives of induced pluripotent stem cells evade immune rejection in fully immunocompetent allogeneic recipients. Nat Biotechnol. 2019 Mar;37(3):252–8.

216. Maxwell KG, Millman JR. Applications of iPSC-derived beta cells from patients with diabetes. Cell Rep Med. 2021 Apr 20;2(4):100238.

217. Giacomelli E, Meraviglia V, Campostrini G, Cochrane A, Cao X, van Helden RWJ, et al. Human-iPSC-Derived Cardiac Stromal Cells Enhance Maturation in 3D Cardiac Microtissues and Reveal Non-cardiomyocyte Contributions to Heart Disease. Cell Stem Cell. 2020 Jun 4;26(6):862-879.e11.

218. Hnatiuk AP, Briganti F, Staudt DW, Mercola M. Human iPSC modeling of heart disease for drug development. Cell Chem Biol. 2021 Mar 18;28(3):271–82.

219. Olgasi C, Cucci A, Follenzi A. iPSC-Derived Liver Organoids: A Journey from Drug Screening, to Disease Modeling, Arriving to Regenerative Medicine. Int J Mol Sci. 2020 Jan;21(17):6215.

220. Gilpin SE, Ren X, Okamoto T, Guyette JP, Mou H, Rajagopal J, et al. Enhanced Lung Epithelial Specification of Human Induced Pluripotent Stem Cells on Decellularized Lung Matrix. Ann Thorac Surg. 2014 Nov 1;98(5):1721–9.

221. Ahmed E, Sansac C, Assou S, Gras D, Petit A, Vachier I, et al. Lung development, regeneration and plasticity: From disease physiopathology to drug design using induced pluripotent stem cells. Pharmacol Ther. 2018 Mar 1;183:58–77.

222. Lai L, Jin J. Generation of Thymic Epithelial Cell Progenitors by Mouse Embryonic Stem Cells. Stem Cells. 2009;N/A-N/A.

223. Inami Y, Yoshikai T, Ito S, Nishio N, Suzuki H, Sakurai H, et al. Differentiation of induced pluripotent stem cells to thymic epithelial cells by phenotype. Immunol Cell Biol. 2011 Feb;89(2):314–21.

224. Parent AV, Russ HA, Khan IS, LaFlam TN, Metzger TC, Anderson MS, et al. Generation of Functional Thymic Epithelium from Human Embryonic Stem Cells that Supports Host T Cell Development. Cell Stem Cell . 2013 Aug 1

225. Sun X, Xu J, Lu H, Liu W, Miao Z, Sui X, et al. Directed Differentiation of Human Embryonic Stem Cells into Thymic Epithelial Progenitor-like Cells Reconstitutes the Thymic Microenvironment In Vivo. Cell Stem Cell. 2013 Aug;13(2):230–6.

226. Su M, Hu R, Jin J, Yan Y, Song Y, Sullivan R, et al. Efficient in vitro generation of functional thymic epithelial progenitors from human embryonic stem cells. Sci Rep. 2015 Jun 5;5(1):1–8.

227. Bredenkamp N, Ulyanchenko S, O'Neill KE, Manley NR, Vaidya HJ, Blackburn CC. An organized and functional thymus generated from FOXN1-reprogrammed fibroblasts. Nat Cell Biol. 2014 Sep;16(9):902–8.

228. Okabe M, Ito S, Nishio N, Tanaka Y, Isobe KI. Thymic Epithelial Cells Induced from Pluripotent Stem Cells by a Three-Dimensional Spheroid Culture System Regenerates Functional T Cells in Nude Mice. Cell Reprogramming. 2015 Oct 1;17(5):368–75.

229. Otsuka R, Wada H, Tsuji H, Sasaki A, Murata T, Itoh M, et al. Efficient generation of thymic epithelium from induced pluripotent stem cells that prolongs allograft survival. Sci Rep. 2020 Jan 14;10(1):1–8.

230. Chhatta AR, Cordes M, Hanegraaf MAJ, Vloemans S, Cupedo T, Cornelissen JJ, et al. De novo generation of a functional human thymus from induced pluripotent stem cells.

J Allergy Clin Immunol. 2019 Nov 1;144(5):1416-1419.e7.

231. Gras-Peña R, Danzl NM, Khosravi-Maharlooei M, Campbell SR, Ruiz AE, Parks CA, et al. Human stem cell-derived thymic epithelial cells enhance human T-cell development in a xenogeneic thymus. J Allergy Clin Immunol . 2021 Oct 21

232. Ramos SA, Morton JJ, Yadav P, Reed B, Alizadeh SI, Shilleh AH, et al. Generation of functional human thymic cells from induced pluripotent stem cells. J Allergy Clin Immunol. 2021 Jul;S0091674921011416.

233. Kont V, Laan M, Kisand K, Merits A, Scott HS, Peterson P. Modulation of Aire regulates the expression of tissue-restricted antigens. Mol Immunol. 2008 Jan;45(1):25–33.

234. Silva CS, Reis RL, Martins A, Neves NM. Recapitulation of Thymic Function by Tissue Engineering Strategies. Adv Healthc Mater. n/a(n/a):2100773.

235. Tajima A, Liu W, Pradhan I, Bertera S, Lakomy RA, Rudert WA, et al. Promoting 3-D Aggregation of FACS Purified Thymic Epithelial Cells with EAK 16-II/EAKIIH6 Self-assembling Hydrogel. J Vis Exp. 2016 Jun 27;(112):54062.

236. Silva CS, Pinto RD, Amorim S, Pires RA, Correia-Neves M, Reis RL, et al. Fibronectin-Functionalized Fibrous Meshes as a Substrate to Support Cultures of Thymic Epithelial Cells. Biomacromolecules. 2020 Dec 14;21(12):4771–80.

237. Suraiya AB, Hun ML, Truong VX, Forsythe JS, Chidgey AP. Gelatin-Based 3D Microgels for In Vitro T Lineage Cell Generation. ACS Biomater Sci Eng. 2020 Apr 13;6(4):2198–208.

238. Bortolomai I, Sandri M, Draghici E, Fontana E, Campodoni E, Marcovecchio GE, et al. Gene Modification and Three-Dimensional Scaffolds as Novel Tools to Allow the Use of Postnatal Thymic Epithelial Cells for Thymus Regeneration Approaches. STEM CELLS Transl Med. 2019;8(10):1107–22.

239. Fan Y, Tajima A, Goh SK, Geng X, Gualtierotti G, Grupillo M, et al. Bioengineering Thymus Organoids to Restore Thymic Function and Induce Donor-Specific Immune Tolerance to Allografts. Mol Ther. 2015 Jul;23(7):1262–77.

240. Seet CS, He C, Bethune MT, Li S, Chick B, Gschweng EH, et al. Generation of mature T cells from human hematopoietic stem and progenitor cells in artificial thymic organoids. Nat Methods. 2017 May;14(5):521–30.

241. Montel-Hagen A, Sun V, Casero D, Tsai S, Zampieri A, Jackson N, et al. In Vitro Recapitulation of Murine Thymopoiesis from Single Hematopoietic Stem Cells. Cell Rep. 2020 Oct 27;33(4):108320.

242. Montel-Hagen A, Seet CS, Li S, Chick B, Zhu Y, Chang P, et al. Organoid-Induced Differentiation of Conventional T Cells from Human Pluripotent Stem Cells. Cell Stem Cell. 2019 Mar 7;24(3):376-389.e8.

243. Kennedy M, Awong G, Sturgeon CM, Ditadi A, LaMotte-Mohs R, Zúñiga-Pflücker JC, et al. T Lymphocyte Potential Marks the Emergence of Definitive Hematopoietic Progenitors in Human Pluripotent Stem Cell Differentiation Cultures. Cell Rep. 2012 Dec 27;2(6):1722–35.

244. Perheentupa J. Autoimmune Polyendocrinopathy-Candidiasis-Ectodermal Dystrophy. J Clin Endocrinol Metab. 2006 Aug 1;91(8):2843–50.

245. Besnard M, Padonou F, Provin N, Giraud M, Guillonneau C. AIRE deficiency, from preclinical models to human APECED disease. Dis Model Mech . 2021 Feb 5

246. Kreins AY, Bonfanti P, Davies EG. Current and Future Therapeutic Approaches for Thymic Stromal Cell Defects. Front Immunol. 2021 Mar 18;12:655354.

247. Markert ML, Kostyu DD, Ward FE, McLaughlin TM, Watson TJ, Buckley RH, et al. Successful formation of a chimeric human thymus allograft following transplantation of cultured postnatal human thymus. J Immunol. 1997 Jan 15;158(2):998–1005.

248. Markert ML, Devlin BH, McCarthy EA. Thymus Transplantation. Clin Immunol Orlando Fla. 2010 May;135(2):236–46.

249. Davies EG, Cheung M, Gilmour K, Maimaris J, Curry J, Furmanski A, et al. Thymus transplantation for complete DiGeorge syndrome: European experience. J Allergy Clin Immunol. 2017 Dec;140(6):1660-1670.e16.

250. Besnard M, Sérazin C, Ossart J, Moreau A, Vimond N, Flippe L, et al. Anti-CD45RC antibody immunotherapy prevents and treats experimental autoimmune polyendocrinopathy–candidiasis–ectodermal dystrophy syndrome. J Clin Invest . 2022 Apr 1

251. Ueda T, Kaneko S. In Vitro Differentiation of T Cell: From CAR-Modified T-iPSC. Methods Mol Biol Clifton NJ. 2019;2048:85–91.

252. Wang Z, McWilliams-Koeppen HP, Reza H, Ostberg JR, Chen W, Wang X, et al. 3D-organoid culture supports differentiation of human CAR+ iPSCs into highly functional CAR T cells. Cell Stem Cell. 2022 Apr 7;29(4):515-527.e8.

253. Iriguchi S, Yasui Y, Kawai Y, Arima S, Kunitomo M, Sato T, et al. A clinically applicable and scalable method to regenerate T-cells from iPSCs for off-the-shelf T-cell immunotherapy. Nat Commun. 2021 Jan 18;12(1):430.

254. Toms D, Deardon R, Ungrin M. Climbing the mountain: experimental design for the efficient optimization of stem cell bioprocessing. J Biol Eng . 2017 Dec 4

255. Soh CL, Giudice A, Jenny RA, Elliott DA, Hatzistavrou T, Micallef SJ, et al. FOXN1GFP/w Reporter hESCs Enable Identification of Integrin-β4, HLA-DR, and EpCAM as Markers of Human PSC-Derived FOXN1+ Thymic Epithelial Progenitors. Stem Cell Rep. 2014 May 22;2(6):925–37.

256. Kleijnen JPC. An overview of the design and analysis of simulation experiments for sensitivity analysis. Eur J Oper Res. 2005 Jul 16;164(2):287–300.

257. Yasui R, Sekine K, Taniguchi H. Clever Experimental Designs: Shortcuts for Better iPSC Differentiation. Cells. 2021 Dec;10(12):3540.

258. Stark R, Grzelak M, Hadfield J. RNA sequencing: the teenage years. Nat Rev Genet. 2019 Nov;20(11):631–56.

259. Aibar S, González-Blas CB, Moerman T, Huynh-Thu VA, Imrichova H, Hulselmans G, et al. SCENIC: single-cell regulatory network inference and clustering. Nat Methods. 2017 Nov;14(11):1083–6.

260. La Manno G, Soldatov R, Zeisel A, Braun E, Hochgerner H, Petukhov V, et al. RNA velocity of single cells. Nature. 2018 Aug;560(7719):494–8.

261. Hao Y, Hao S, Andersen-Nissen E, Mauck WM, Zheng S, Butler A, et al. Integrated

analysis of multimodal single-cell data. Cell. 2021 Jun 24;184(13):3573-3587.e29.

262. Ackermann M, Haake K, Kempf H, Kaschutnig P, Weiss AC, Nguyen AHH, et al. A 3D iPSC-differentiation model identifies interleukin-3 as a regulator of early human hematopoietic specification. Haematologica. 2020 Apr 23;106(5):1354–67.

263. An C, Feng G, Zhang J, Cao S, Wang Y, Wang N, et al. Overcoming Autocrine FGF Signaling-Induced Heterogeneity in Naive Human ESCs Enables Modeling of Random X Chromosome Inactivation. Cell Stem Cell. 2020 Sep 3;27(3):482-497.e4.

264. Coluccio ML, Perozziello G, Malara N, Parrotta E, Zhang P, Gentile F, et al. Microfluidic platforms for cell cultures and investigations. Microelectron Eng. 2019 Mar 1;208:14–28.

265. D'Amour KA, Agulnick AD, Eliazer S, Kelly OG, Kroon E, Baetge EE. Efficient differentiation of human embryonic stem cells to definitive endoderm. Nat Biotechnol. 2005 Dec;23(12):1534–41.

266. Ikonomou L, Kotton DN. Derivation of Endodermal Progenitors From Pluripotent Stem Cells. J Cell Physiol. 2015;230(2):246–58.

267. Zhao B, Tumaneng K, Guan KL. The Hippo pathway in organ size control, tissue regeneration and stem cell self-renewal. Nat Cell Biol. 2011 Aug;13(8):877–83.

268. Han J, Zúñiga-Pflücker JC. High-Oxygen Submersion Fetal Thymus Organ Cultures Enable FOXN1-Dependent and -Independent Support of T Lymphopoiesis. Front Immunol . 2021

269. Sun S, Li JY, Nim HT, Piers A, Ramialison M, Porrello ER, et al. CD90 Marks a Mesenchymal Program in Human Thymic Epithelial Cells In Vitro and In Vivo. Front Immunol. 2022 Mar 16;13:846281.

270. Vodyanik MA, Bork JA, Thomson JA, Slukvin II. Human embryonic stem cell–derived CD34+ cells: efficient production in the coculture with OP9 stromal cells and analysis of lymphohematopoietic potential. Blood. 2005 Jan 15;105(2):617–26.

271. Jiang D, Zheng L, Lenardo MJ. Caspases in T-cell receptor-induced thymocyte apoptosis. Cell Death Differ. 1999 May;6(5):402–11.

272. Karvonen E, Krohn KJE, Ranki A, Hau A. Generation and Characterization of iPS Cells Derived from APECED Patients for Gene Correction. Front Endocrinol. 2022;13:794327.

De temps en temps
Les nuages nous reposent
De tant regarder la lune.

Matsuo Basho (松尾 芭蕉), 1644 - 1694

ANNEXES

ANNEXE 1 : Differentiation of Pluripotent Stem Cells Into Thymic Epithelial Cells and Generation of Thymic Organoids: Applications for Therapeutic Strategies Against APECED

ANNEXE 2 : Thymocytes trigger self-antigen controlling pathways in immature medullary thymic epithelial stages

ANNEXE 3 : Aire-dependent transcripts escape Raver2-induced splice-event inclusion in the thymic epithelium

ANNEXE 4 : AIRE deficiency, from preclinical models to human APECED disease

frontiers | Frontiers in Immunology

REVIEW
published: 29 June 2022
doi: 10.3389/fimmu.2022.930963

Differentiation of Pluripotent Stem Cells Into Thymic Epithelial Cells and Generation of Thymic Organoids: Applications for Therapeutic Strategies Against APECED

*Nathan Provin and Matthieu Giraud**

Nantes Université, INSERM, Center for Research in Transplantation and Translational Immunology, UMR 1064, Nantes, France

OPEN ACCESS

Edited by:
Rachid Tazi Ahnini, The University of Sheffield, United Kingdom

Reviewed by:
Agustin G. Zapata, Complutense University of Madrid, Spain
Ann Chidgey, Monash University, Australia
Rachel Thomas, Alcon Research, LLC, United States

***Correspondence:**
Matthieu Giraud, matthieu.giraud@inserm.fr

Specialty section:
This article was submitted to Autoimmune and Autoinflammatory Disorders, a section of the journal Frontiers in Immunology

Received: *28 April 2022*
Accepted: *26 May 2022*
Published: *29 June 2022*

Citation:
Provin N and Giraud M (2022) Differentiation of Pluripotent Stem Cells Into Thymic Epithelial Cells and Generation of Thymic Organoids: Applications for Therapeutic Strategies Against APECED. Front. Immunol. 13:930963. doi: 10.3389/fimmu.2022.930963

The thymus is a primary lymphoid organ essential for the induction of central immune tolerance. Maturing T cells undergo several steps of expansion and selection mediated by thymic epithelial cells (TECs). In APECED and other congenital pathologies, a deficiency in genes that regulate TEC development or their ability to select non auto-reactive thymocytes results in a defective immune balance, and consequently in a general autoimmune syndrome. Restoration of thymic function is thus crucial for the emergence of curative treatments. The last decade has seen remarkable progress in both gene editing and pluripotent stem cell differentiation, with the emergence of CRISPR-based gene correction, the trivialization of reprogramming of somatic cells to induced pluripotent stem cells (iPSc) and their subsequent differentiation into multiple cellular fates. The combination of these two approaches has paved the way to the generation of genetically corrected thymic organoids and their use to control thymic genetic pathologies affecting self-tolerance. Here we review the recent advances in differentiation of iPSc into TECs and the ability of the latter to support a proper and efficient maturation of thymocytes into functional and non-autoreactive T cells. A special focus is given on thymus organogenesis and pathway modulation during iPSc differentiation, on the impact of the 2/3D structure on the generated TECs, and on perspectives for therapeutic strategies in APECED based on patient-derived iPSc corrected for *AIRE* gene mutations.

Keywords: thymus, IPSC, thymic epithelial cells (TEC), differentiation, APECED, tolerance

Abbreviations: AIRE, autoimmune regulator; APECED, polyendocrinopathy candidiasis ectodermal dystrophy syndrome; ATO, artificial thymic organoid; DN, double negative CD4-CD8- thymocyte; DP, double positive CD4+CD8+ thymocyte; ESc, embryonic stem cells; ETP, early thymic progenitor; iPSc, induced pluripotent stem cells; mTEChi, MHC-II high medullary thymic epithelial cell; nTreg, natural regulatory T cell; RA, retinoic acid; RTE, recent thymic emigrant; SCID, severe combined immunodeficiency; TCR, T cell receptor; TEC, thymic epithelial cells; TEP, thymic epithelial progenitor; TRA, tissue restricted autoantigen; 3PP, third pharyngeal pouch.

INTRODUCTION

Immune tolerance is primarily set in the thymus with the generation of non-autoreactive T cells originated from the maturation of thymocytes through intimate interactions with specialized sets of thymic epithelial cells (TECs). These complex interactions enable the selection of maturing thymocytes for the functionality and non autoreactivity of their T cell receptors (TCR). The step of negative selection, which is responsible for the induction of thymocyte self-tolerance, is mediated by TECs that reside in the thymic medulla and express the autoimmune regulator (AIRE) (1). Loss-of-function mutations in the *AIRE* gene result in the rare autoimmune polyendocrinopathy candidiasis ectodermal dystrophy syndrome (APECED), a life-threatening autoimmune disease characterized by severe autoimmune lesions in peripheral tissues (2). The direct cause of this syndrome is the impairment of negative selection due to AIRE deficiency, resulting in the escape of autoreactive T cells into the periphery. Current treatments of APECED are only symptomatic including the administration of immunosuppressants, antifungal drugs with a constant monitoring of candidiasis infection, and hormone replacement. Although these therapeutics have improved the course of APECED, they don't address the root cause of the disease, leaving the patients at risk of premature death (3). Induced pluripotent stem cells (iPSc) are a promising tool for the development of new cellular and genetic therapies for APECED. These cells are reprogrammed somatic cells obtained by the induced expression of four genes (*OCT4*/*POU5F1*, *KLF4*, *SOX2*, *MYC*) (4). The remarkable proliferation potential of iPSc and their ability to differentiate into various cell fates (5–7) have paved the way to promising therapeutic strategies aiming to restore tissue functions, notably in rare genetic diseases. Several iPSc-derived cell therapies against various pathologies such as cancer, autoimmune disorders or Parkinson's disease are currently being evaluated by clinical trials (8–10). However, some concerns have been raised regarding the overall safety of stem-cell based therapies, since reprogramming of somatic cells can lead to enhanced mutation susceptibility and selection of deleterious mutations originally present in a minority of somatic cells. In addition, with the implication of *OCT4* in tumorigenesis, the risk of inducing teratoma and malignant tumor formation is to be seriously considered (11). Thus, stringent quality controls of the generated iPSc and their differentiated products, as well as the fine purification of the populations of interest are crucial (12). This review covers the recent developments of iPSc differentiation into TECs, the different approaches used to mimic thymic embryological development and how it can provide new strategies for therapeutic application against APECED.

THYMUS FUNCTION: T CELL MATURATION AND SELECTION

In the thymus, maturing T cells undergo several steps of expansion and selection mediated by TECs that account for 0.5% of the thymic cellularity in the adult thymus (13) (**Figure 1**). TECs form the backbone of the stromal compartment and interact with a large number of thymocytes (14). They have been historically separated into cortical TECs (cTECs) and medullary TECs (mTECs) located in the outermost and the core areas of the thymic lobules, respectively. These two populations exhibit different phenotypes and play distinct roles in the control of T cell maturation. cTECs drive the commitment of the early thymic progenitors (ETPs) to the T cell lineage by providing Notch ligands such as Dll4 (15). They also control ETP homing and expansion through the secretion of chemokines and growth factors such as Ccl25, Cxcl12, Scf and Il-7 (16). At the later double-positive (DP) stage, thymocytes with TCR that are able to recognize peptide:major histocompatibility complex (MHC) receive survival signals from cTECs and are thereby positively selected (**Figure 1**). The peptides presented by cTECs are generated by a unique proteasome comprising the cortical marker ß5t encoded by the *Psmb11* gene (15, 17). After the positive selection, thymocytes undergo a step of negative selection aiming to deplete those with a TCR having a high avidity for self-antigen peptides. This step is mediated by mTECs that attract single-positive (SP) thymocytes through the secretion of chemokines like Ccl21 (18). The negative selection is enabled by the unique ability of mTECs to express 90% of the genome (19–21), including the expression of a broad repertoire of tissue-restricted antigen (TRA) genes under the regulation of transcriptional activators such as FEZF2, CHD4 and especially AIRE (22–24). The non-conventional activation factor Aire controls the expression of a large fraction of these TRAs (25, 26) and is specifically expressed in the mature subpopulation of mTECs showing high levels of the major histocompatibility class II (MHCII) molecule (mTEChi) and a high turnover. Importantly, the last decade has seen many aspects of the Aire-driven regulation of TRA expression being uncovered (26, 27). In mice, the expression of TRA genes follows a stochastic order: they are co-expressed in modules randomly present in individual mTEChi spread out in the thymic medulla. This pattern of expression enables a complete screening of the TRA repertoire by the thymocytes passing through the medulla. The intensity of the interactions between TRA peptide:MHCII complexes at the surface of mTEChi and the TCR is determinant for the fate of thymocytes (1). Thus, thymocytes with a strong self-reactive TCR will undergo apoptosis, while those harboring a self-reactive TCR with an intermediate strength will be directed into the natural T regulator (nTreg) lineage which plays a major role in peripheral immune tolerance (28) (**Figure 1**). At their final stage of maturation, the thymocytes will enter the periphery through the cortico-medullary junction vasculature, as recent thymic emigrants (RTEs) characterized by their expression levels of CD69, CD62L (*SELL*), Qa2 and CCR7 (29, 30) (**Figure 1**).

TEC HETEROGENEITY AND MATURATION

From the homing of hematopoietic progenitors to the thymus to the escape of RTEs into the periphery, the maturation of T cells mostly relies on intimate interactions between thymocytes and TECs. These interactions are crucial for the maturation of TECs

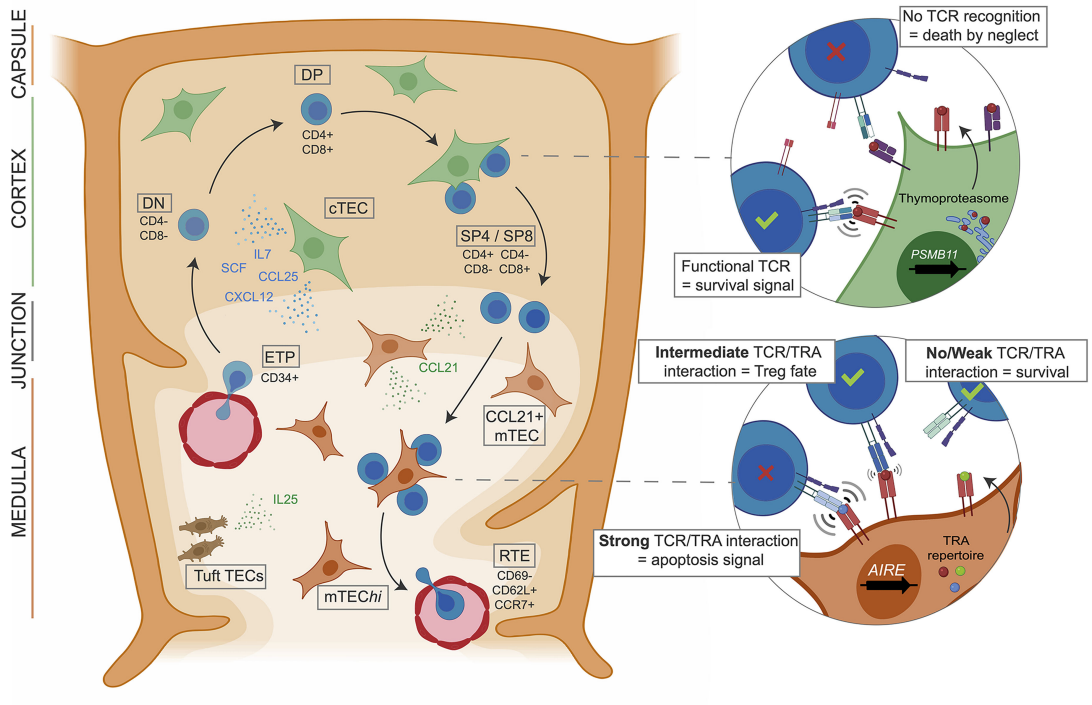

FIGURE 1 | cTEC and mTEC orchestrate thymocyte maturation and selection. Early thymic progenitors (ETP) originating from the bone marrow enter the thymus and are attracted to the cortical region by chimiokines expressed by cTECs, also inducing growth and T lineage commitment by contact with NOTCH ligands. After TCR rearrangement CD4/CD8 DP thymocytes enter positive selection of the functional TCRs mediated by cTEC expressing the thymoproteasome. Resulting SP T cells are attracted to the medulla where thymocytes with auto-reactive TCRs are negatively selected by mature mTECs presenting the self-antigen repertoire under AIRE regulation. Thus, T cells with functional TCRs, able to recognize foreign antigens but tolerant to the self, are generated by the thymus.

through a process referred to as thymic crosstalk (31–34). Indeed, TECs need to receive signals such as those mediated by Rankl and Cd40l to mature and survive (35). In recent years, advances in high-throughput single-cell (sc)RNA sequencing (scRNA-seq) have pushed further our understanding of TEC heterogeneity beyond the typical dichotomy between cTEC and mTEC in mice (16, 21, 36) and humans (37–39). Hence, new TEC populations were identified, notably populations composed of atypical tuft cells sharing similarities with intestinal tuft cells (16), myoid-like epithelial cells or neuroendocrine epithelial cells (37). While these populations are well characterized at the transcriptomic level, their functional role in the thymic microenvironment and their potential effect on thymocyte development remain elusive.

scRNA-seq studies of TEC heterogeneity in individuals of different ages also contributed to reveal the existence and identity of a TEC progenitor (TEP) population (36, 38). TEPs exhibit a cortical phenotype characterized by the expression of CD205 and ß5T (encoded by the *LY75* and *PSMB11* genes, respectively) (40–42). They were shown to be the source of mTECs and cTECs in fetal and neonatal thymuses (14, 43, 44). However, there is still a lack of evidence supporting this model in adults. After birth the thymus undergoes involution with a drastic decrease of its activity and cellularity, and shows a shift of the relative cTEC vs mTEC abundance in favor of the mTEC compartment (45, 46). In addition, it is assumed that TEPs enter quiescence in response to BMP4 and Activin A inhibitor follistatin (FSH) signaling (37, 47, 48). Thus, the emerging model for the origin of TECs relies on bipotent cTEC-like fetal TEPs entering quiescence upon aging and giving rise to lineage-restricted immature populations for the replenishment of medullary and cortical TEC compartments. However, additional studies based on single-cell fate-mapping need to be carried out to precisely understand the relationship between TECs and their progenitors upon aging. Another question left unanswered is the nature of signals underlying the medullary or cortical orientation of bipotent TEPs.

Promising results have been obtained over the last years, notably describing the role of Notch modulation in this fate decision (37, 49, 50). Indeed, Notch signaling has been shown to be essential for the mTEC specification of TEPs, notably through its fine-tuned regulation by the chromatin regulator HDAC3 (51). Thus, these findings support a model of a cTEC-like bipotent TEP population undergoing a default cortical differentiation, with Notch signalization promoting the mTEC transcriptional program. Despite the main paradigm of a TEC compartment of exclusive endoderm origin, Chakrabarti et al. recently showed that a population of bone-marrow hematopoietic progenitors transdifferentiate in true *Foxn1*-expressing TECs in the thymus (52). These hematopoietic bone

marrow progenitors would migrate in the same manner as Cd34 + thymus seeding progenitors but would further differentiate into epithelial cells expressing cytokeratins and the master regulator of TEC development Foxn1. Moreover, Cd45+ Epcam+ cell could also give rise to Fsp1-expressing thymic fibroblasts. Thus, this fate mapping study identify a bone-marrow originating population able to transdifferentiate into TECs and fibroblasts to replenish the thymic stroma, suggesting that the TEC lineage development is more plastic than previously thought and may involve various progenitor populations originating from different embryological layers. However, proper characterization studies using high-throughput omics are still needed to precisely describe this newly identified cell population.

We mainly focus here on the role of TECs in thymocyte selection given the origin of APECED. However, other cell populations in the thymus have been shown to participate to this process. Indeed, dendritic cells (DC) have also the ability to induce clonal deletion and Treg generation (53–55). Different processes involving multiple DC subpopulations have been described. Briefly, migrating DCs can transport peripheral antigens to the thymus, negatively select thymocytes and induce Tregs (56, 57). Transendothelial DCs located in thymic vasculature capture blood circulating antigens and use them for selection (58, 59). Another source of antigens for DCs directly come from the thymic stroma through a mechanism of intercellular antigen transfer from the TECs (60, 61). Lymphotoxin β receptor (LTβR) expressed by mTECs has been shown to be central in this interaction by controlling the frequency and composition of intrathymic DC populations (62). DCs could also process self-antigens produced by thymic fibroblasts as a complementary source of self-antigens (63). Often neglected, thymic fibroblasts are now revealed as a crucial actor of the thymic microenvironment, with distinct subpopulations involved in functions as diverse as self-antigen production and regulation of both TEC and T cell maturation (63–65). Finally, these alternative sources of autoantigens or presenting cells are supported by studies in which disrupted thymuses with low TEC cellularity and morphological anomalies have no effect on mature T cell population frequency nor on the repertoire diversity (66).

THYMUS ORGANOGENESIS

The first advances in the understanding of thymus organogenesis relied on comparative anatomical observations and histology studies of fetal tissues. These approaches revealed that the thymus is derived from the pharyngeal pouches that are transitory embryonic structures appearing between the third and fourth week of development in humans (67) and from E8 in mice (68, 69) (**Figure 2**). The pharyngeal pouches are invaginations originating from the most anterior foregut endoderm (67, 70, 71). It was shown in human fetuses that the thymus mostly derived from the third pharyngeal pouch (3PP) (72, 73). However, the embryological layer of origin of the thymus has long (74, 75) been uncertain. In the early 2000s, the single endodermal origin was demonstrated after ectopic transplantation experiments of pharyngeal endoderm proving that it is sufficient to give rise to a fully formed and functional thymus (68, 76).

Although thymus organogenesis has been well described in mice (74, 75) the precise cellular and molecular mechanisms governing human thymus development are still elusive. In humans, the thymus forms from the 3PP endoderm at week 7 of development and initiates migration at 8.5 week (77). Involution of the 3PP endoderm results in a stratified epithelium of Cldn3/4-expressing cells polarized around a central lumen (78, 79) showing an early morphogenesis similar to other organs with epithelia organized in branching ducts, such as lung or pancreas. However, the definitive histological structure of the thymus is radically different, with formation of a 3D network of TECs that is far from the stratified epithelium constituting a branching architecture. This key aspect of thymic functionality, allowing the maximization of contacts between thymocytes and TECs, is mainly explained by the expression of the main TEC marker, Foxn1. This gene was first identified as the nude gene, originally described in the eponym hairless mice mutants exhibiting an absence of functional thymus (80). In mice, *Foxn1* expression is detected in the 3PP endoderm as early as E9.5 and reaches high levels at E11 (80, 81). However, *Foxn1* is not directly responsible for the commitment to thymic epithelial cell fate, since ectopically transplanted E9 3PP tissues, which do not express *Foxn1* yet, are still able to generate fully developed thymuses (68). Nude mice show normal thymic primordium formation and migration but impaired maturation of the TEC compartment and consequently of T cell colonization (82). Thus, *Foxn1* may be downstream of a regulatory network driving the commitment to thymic epithelial progenitors but would play a central role in the differentiation of TEPs into TECs (44, 68, 80, 83). Thymus rudiments from *Foxn1* deficient mice shows an atypical branching structure, with formation of multiple lumens giving rise to a fully develop ductal system similar to the pancreas. In addition, ectopic expression of Foxn1 results in impaired epithelium formation and absence of lumen (84), showing Foxn1 ability to disrupt the classical tubular morphogenesis program. Finally, Foxn1 has been shown to be necessary for the expression of a full set of factors that control TEC transcriptional programs, such as *Cxcl12*, *Ccl25*, *Dll4* and MHCII genes (85). More recently, *Foxn1* has also been shown to control the expression of *Cd40*, *Cd80*, *Aire* and *FgfrII* that are crucial for TEC differentiation, amplification and function (85–87). Thus, by inhibiting tubulogenesis of the thymic epithelium and inducing expression of key genes of the TEC program, Foxn1 allows the structuration of the thymic environment and TEC generation (88).

Molecular Regulatory Networks in 3PP and Thymus Organogenesis

A complex interplay between the neural crest cells, the mesoderm-derived mesenchyme and the 3PP endoderm controls the fate, migration and expansion of cell populations

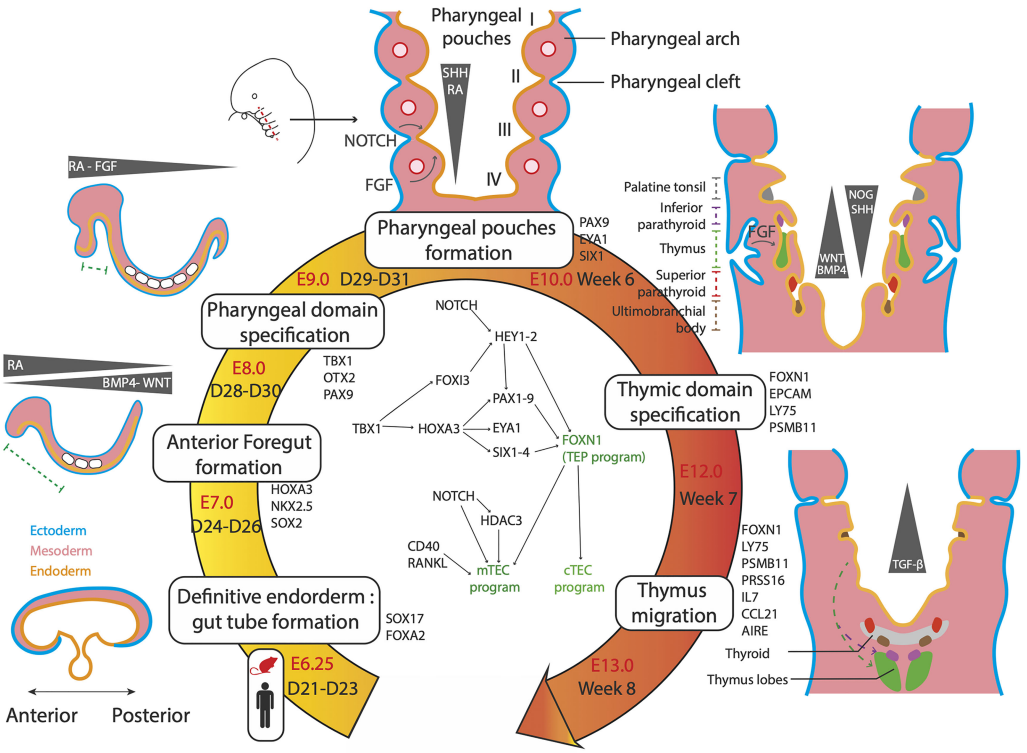

FIGURE 2 | Genetic and molecular networks regulating the thymus organogenesis. The thymus is a definitive endoderm derivative. The main steps of organogenesis of the pharyngeal apparatus and thymus formation are described, with time scales in mouse and human, key markers genes and signalling molecules. First, gradients of cytokines and small molecules pattern the endoderm, resulting in an anterior domain between D24-D26 in human. Further patterning results in formation of the pharyngeal domain and its segmentation in pharyngeal arches at 6 weeks. The 3PP forms under singling involving retinoic acid (RA), Hedgehog (SHH), NOTCH and fibroblast growth factors (FGF). 3PP gives rise to the thymic primordium expressing FOXN1 by week 7. By week 8, the thymic primordium migrates under TGFβ signaling to its final position and TEC mature in cTEC and mTEC.

in the developing thymus. The main genetic regulatory network is composed of the *TBX1-HOXA3-PAX9* and *EYA1-SIX1* cascades that are regulated by a set of signaling molecules secreted by the neural crest and mesoderm cells, such as retinoic acid (RA), proteins of the Wingless-int (WNT) family, bone morphogenetic proteins (BMP), fibroblast growth factors (FGF) and sonic hedgehog (SHH) proteins (**Figure 2**).

These factors, which are secreted by the mesoderm core and the neural crests in addition to the endoderm, guide the development of the thymic primordium. RA is a small non-peptidic vitamin A derivative that plays a key role throughout the embryonic development (89, 90). Gradients of RA have been shown to regulate the posterior pouch formation in several species (91–93). Disrupting RA activity during the development results in the absence of formation of posterior pharyngeal pouches (91, 93, 94). Moreover, RA was shown to be a key player in the early formation of pharyngeal pouches by regulating the expression of genes of central importance in their development, such as *TBX1*, *HOXA3*, *PAX1* and *PAX9* (85, 87, 89, 90, 95) (**Figure 2**). Proteins of the WNT family, including WNT4b and WNT5a (96–98), are expressed in the pharyngeal pouches and lead to the upregulation of *FOXN1* by activating the canonical WNT/beta catenin pathway (96). Thus, modulation of the WNT signaling is critical to the formation of the thymic primordium and the maintenance of the thymic postnatal epithelium (97, 99, 100). Several studies have shown that genes of the WNT family are down-regulated in aged involuted thymuses (101–103) and are expressed in TECs under FOXN1 positive regulation (86, 100). However, a strong WNT signaling is detrimental to the thymic development (104) highlighting the importance of a proper modulation of WNT signals in TEC physiology. In mice, modulation of the Bmp pathway through a Bmp4-Noggin gradient in the thymic and parathyroid primordia, is responsible for a correct organ separation and thymic capsule formation (105, 106). Bmp4 has been shown to directly upregulate *Foxn1* and *FgfrIII* (107). BMP signaling is thus closely integrated into FGF pathways that have been shown to play a crucial role in 3PP and thymic development (108, 109). Indeed, mutant mice for *Fgf8* (110) and *Fgfr2-IIIb*, a receptor of Fgf7 and Fgf10 (87) show an impaired thymus development and arrest of TEC maturation. In zebrafish, the secretion of FGF8 in closeby mesoderm directs 3PP formation. However, later FGF

signal inhibition through Spry is also necessary for thymic primordium migration and TEC proliferation (111). Similarly to the above molecules, Hedgehog plays multiple regulatory roles in the thymus. During the later steps of TEC maturation, SHH negatively impacts TEC proliferation but stimulates MHCII expression (112). SHH expression is restricted to the anteriormost pharyngeal apparatus, both in the endoderm and mesoderm, and plays a role in pharyngeal pouch patterning (113). At E10.5 SHH endorses a dorsalizing role, contrasting with the ventral thymic fate instructed by BMP4. These clues, added to the fact that SHH endodermal expression represses *FOXN1*, indicate that SHH signal inhibition is necessary to promote a thymic over parathyroid fate (114, 115). Overall, all these factors are involved in an integrated regulatory network orchestrating the specification, maturation and migration of the pharyngeal pouch derivatives.

Axis Patterning of the Definitive Endoderm and Emergence of the Foregut

Since the 3PP is a structure of the pharyngeal domain that is the anterior-most segment of the foregut endoderm, the identification of the molecular signals that sustain definitive endoderm patterning is a prerequisite for the control of the first steps of iPSc differentiation towards TECs. In mice, definitive endoderm specification is initiated during the gastrulation at E6.25, after which morphogenetic processes occur leading to the formation of the tubular gut structure by E8.0 (116) (**Figure 2**). Most of the pathways involved in pharyngeal pouch formation have also been shown to orchestrate the antero-posterior patterning of the gut tube. Indeed, it is now well established that the Bmp-Wnt-Fgf signaling has a posteriorizing effect on endoderm development and that its inhibition is required for the acquisition of foregut identity (117–119). In addition, the TGFß/Nodal inhibition and the RA signaling are also involved in the anteriorization of the endoderm (117). Recently, scRNA-seq datasets of foregut endoderm have been generated in mice between E3.5 and E12.5 (116, 120–122), including foregut mesoderm (116) and pharyngeal endoderm (122) lineages, thereby constituting atlases of endodermal and mesodermal cell populations involved in pharyngeal development. Hence, sets of genes specific to different stages of pharyngeal development could be identified, such as *Pax9* and the *Eya1-Six1* cascade for pharyngeal endoderm at E9.5 (**Figure 2**). More generally, these studies provide a model of pharyngeal endoderm development of unprecedented precision. In the case of the thymus, an early ventral foregut endoderm population expressing *Nkx2-3* and 2-5 at E8.5 gives rise to the ventral pharynx expressing *Bmp4* at E9.5 (116). It appeared that the key pathways involved at this stage of differentiation include FGF, NOTCH and RA signals arising from the surrounding mesoderm, as well as BMP autocrine ligands. Among the previously unrecognized pathways involved in anterior foregut development are those driven by HIPPO (121), EGF and NGF (120). At E10.5, the 3PP undergoes its formation upon activation of *Eya1* and *Six1*. This cell population further differentiates into progenitors of parathyroid, ultimobranchial bodies and TEPs that begin to express *Foxn1* at E11.5 and eventually give rise to early cTEC and mTEC populations at E12.5 (122).

Comfortingly, the same populations and signaling pathways are found in comparative studies with human embryos, validating that foregut endoderm organogenesis is conserved between mice and humans (77, 120). Finally, these studies provide key insights into which signaling pathways need to be modulated to direct differentiation of pluripotent human cells into TECs, even if most of the results presented above need to be confirmed by proper *in vivo* knock-out or lineage tracing studies.

DIFFERENTIATION OF PLURIPOTENT STEM CELLS INTO THE THYMIC LINEAGE

Thanks to the growing understanding of signals driving the formation of the thymus, considerable progress has been made in the differentiation of pluripotent stem cells into the thymic epithelial lineage. We hereby review the different approaches, their achievements and limitations. A pioneer work was carried out by Lai & Jin, who successfully differentiated mouse embryonic stem cells (mESc) into cells showing a TEP phenotype (123) (**Figure 3**). Using a combination of FGFs, EGF and BMP4, they obtained a 24% proportion of EPCAM-positive cells after 10 days in a monolayer culture system. Despite this low proportion, EPCAM+ cells showed the expression of the TEP markers *Pax1*, *Pax9* and *Foxn1*. These induced TEPs were able to successfully reconstitute a cortical and medullary compartment 6 weeks after engraftment under the kidney capsule, confirming their nature of bipotent progenitors. This regenerated thymus contained TCRαß+ CD3+ thymocytes expressing CD4 and CD8 in similar proportions than in native thymus.

Further advances were made by Inami et al. one year later (124). Using human iPSc and by adding RANK ligand (RANKL) to an optimized cytokine cocktail at day 12, they not only reproduce the differentiation into TEP with protein expression of their markers *Pax1*, *Krt5*, and Notch ligands DLL4 and DLL1, but for the first time they detected low levels of *AIRE* expression indicating further maturation of TEPs into mature mTECs. However, the functionality of this mTEC-enriched differentiated population was not addressed in this study, nor its heterogeneity which is an important parameter to control since a significant proportion of unwanted cell lineages are expected to arise from this differentiation and hinder inter-experimental reproducibility. In addition, the poor understanding of late TEC development and the lack of specific markers were major obstacles for a thorough analysis of the differentiated cells. To identify a combination of cell surface markers that are specific to TEPs, Soh et al. designed hESc reporter lines with a GFP cassette inserted into the exon 2 of the *FOXN1* gene locus (125). Surprisingly, the differentiation of these hESc was successfully performed using a simple protocol consisting of exposure to Activin A for the first 4 days and supplementation of FGF7 from day 14 in embryoid bodies (**Figure 3**). Depending on the cell line, this protocol resulted in

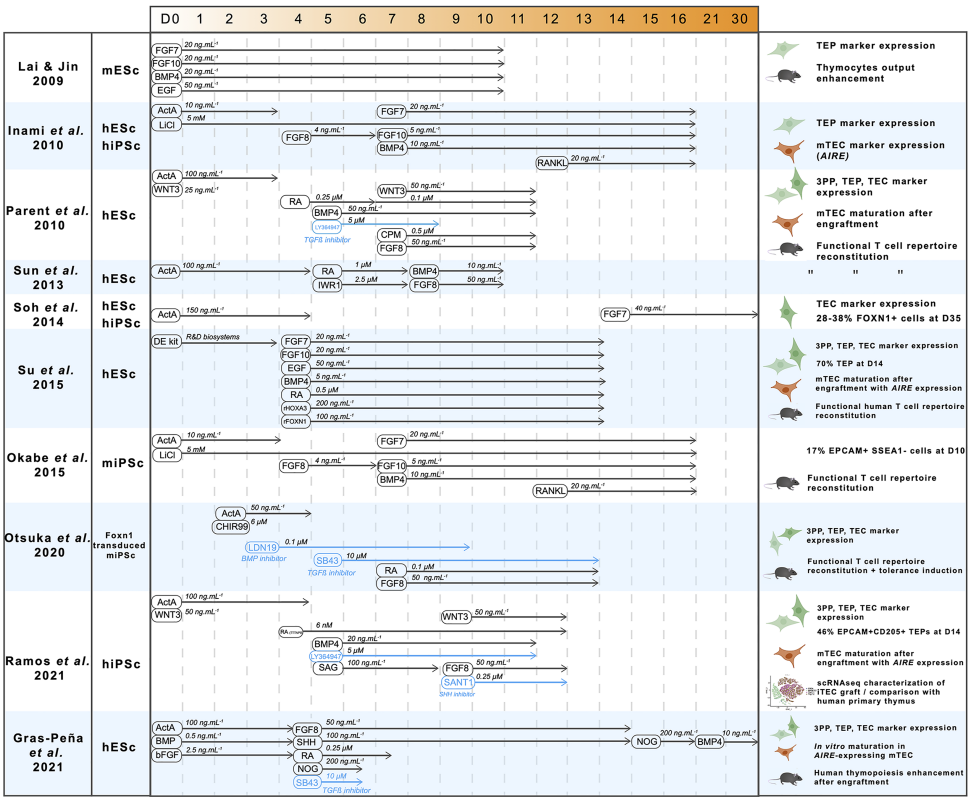

FIGURE 3 | A synthesis of pluripotent stem cells thymic differentiation strategies. A decade of advances in thymic differentiation resulted in perfected protocols allowing production of mature mTEC by mimicking the thymic organogenesis *in vitro*. For each reference, cell type used, pathway-modulating molecules timings and concentrations are indicated, as well as results in terms of nature of the obtained cells and their ability to induce T cell maturation. ActivinA (ActA), Fibroblast growth factors 7,8,10 (FGF7-8-10), Bone Morphogenetic Protein 4 (BMP4), LiCl (Lithium Chloride), Retinoic acid (RA), Cyclopamine (CPM, hedgehog inhibitor), Sonic Hedgehog (SHH), LY364947 (TGFβ inhibitor), SB43 (TGFβ inhibitor), Wingless family member 3 (WNT3), IWR1 (WNT inhibitor), Epidermal Growth Factor (EGF), CHIR99 (WNT3 agonist), LDN19 (BMP inhibitor), Noggin (NOG), SANT1 (Hedgehog inhibitor), Smoothened Agonist (SAG, Hedgehog agonist).

a strong proportion of GFP-positive cells (27-37%) after 35 days. Consistent with engagement in the thymic epithelial lineage, this GFP+ population was positive for TEC-specific markers such as KRT5, KRT14 and Notch ligands JAG2 and DLL4. However, characterization of the differentiated cells has not been performed further, leaving unanswered their maturation stage as well as their cortical and medullary identity. In addition, these cells were not able to support thymopoiesis since coculture with CD34+CD7+ proT cells failed to result in thymocyte differentiation.

Most of the progress made on the differentiation of pluripotent stem cells into TECs came from the studies of Parent et al. and Sun et al. that sought to optimize the differentiation protocol by monitoring the expression of markers of the intermediate foregut and pharyngeal pouch endoderm stages after cultivating hESc with different combinations of factors (126, 127) (**Figure 3**). These two studies showed that RA is needed for anteriorization of definitive endoderm, as well as BMP4 and WNT3 for acquisition of TEP identity. In addition, inhibition of WNT by IWR1, of TGFß by LY364947 at day 5, and Hedgehog by Cyclopamin (CPM) from day 7 to day 11 was shown to be required to increase FOXN1 expression. However, absence of unbiased experimental design did not allow an unambiguous and accurate identification of the effect of each factor on thymic differentiation, likely resulting in suboptimal results. Both protocols resulted in a significant upregulation of markers of thymic identity. However, no markers of TEC maturation were detectable. The induced TEPs were reaggregated and transplanted into nude mice to maturate further as described by Lai & Jin. The graft matured and was able to support thymopoiesis and reconstitute peripheral blood T cell compartments (127). Spectratype analysis of the TCR repertoire showed increased TCR Vß rearrangement diversity in mice engrafted with hESc-derived TEPs compared with controls (127). CD4+CD25+FOXP3+ Treg were also detected in engrafted mice (127). Importantly, the T cells generated in engrafted nude mice were functional showing IL2 secretion and proliferation after stimulation. They were also able to reject skin grafts. Since this model relies on cross-species reactivity, the same experiments were carried out in humanized mice with human hematopoietic progenitors. Similar results were obtained, therefore confirming the ability of thymic grafts to induce human T cell generation.

Additional approaches based on different strategies than directed differentiation, showed that the key factor FOXN1 was

sufficient to induce TEC differentiation. First clues came from the study of Su et al., showing that culturing hESc with recombinant HOXA3 and FOXN1 resulted in significantly increased TEP yield (128). Additional evidence came from the reprogramming of fibroblasts by *FOXN1* over-expression (86) showing that it is sufficient to drive differentiation towards the thymic epithelium fate with large, polygonal cells resembling TECs and expressing factors that sustain thymocyte development such as DLL4 and CCL25. These induced TECs (iTECs) were also able to mature ETPs into CD4+ and CD8+ SP T cells, both *in vitro* after 12 days of coculture and *in vivo* after engraftment in mice. In these mice, T cell functionality was confirmed with increased IL2 secretion in response to CD3/CD28 stimulation. These findings revealed that TECs can be generated from fibroblasts through the sole overexpression of *FOXN1* thus highlighting a key role of this transcription factor in driving the TEC fate program. Together with the advancement of the delineation of the regulatory cascade inducing thymic fate, these results confirm that FOXN1 is necessary and sufficient for the induction of the TEC program, even if it does not induce thymic fate by itself. However, the reliability of the reprogramming approach to reconstitute the TEC compartment with its full heterogeneity needs to be evaluated and compared to the directed differentiation of iPSc that mimics thymus organogenesis. Several other studies have replicated these results, through directed differentiation alone (129) or in conjugation with *Foxn1* overexpression (130, 131) and raised the question of induction of immune tolerance. As expected, *Foxn1* overexpression in mouse iPSc significatively enhances the differentiation into TEPs, resulting in cells that express TEP markers *Pax9*, *Dll4* and *Foxn1* (129, 130) and undergo a proper TEC maturation after engraftment in mice. The effect of these iPSc-derived thymic grafts on immune tolerance has been studied by grafting skin biopsies from the same donor mouse strain from which the iPSc were generated in a recipient of another mouse strain after immune depletion by irradiation and anti-T antibody treatment (130) or directly in nude mice (129). Interestingly, recipient mice with a B6-derived thymic graft showed increased B6 skin graft survival. However, the cellular mechanisms leading to the induction of self-tolerance after iPSc-derived thymic graft needed to be more thoroughly examined.

More recently, comprehensive studies came out and pushed this topic further. Indeed, Ramos et al. and Gras-peña et al. optimized the differentiation protocols, notably by modulating temporal Hedgehog signaling (132, 133) (**Figure 3**). Interestingly, both protocols include Hedgehog activation during the step of pharyngeal endoderm induction, contrary to what was done in a previous report (126). Hence, the fine temporal modulation of the Hedgehog-specific pathways may be key to trigger a proper differentiation towards pharyngeal endoderm. Other examples of temporal modulations are also observed with the inhibition of BMP through Noggin between day 15 to day 21 followed by a more classical activation of BMP4 from day 21, resulting in a significant 10-fold increase of *PAX9* expression (133). Another key insight from this study was the addition of FGF8b during endoderm anteriorization at day 4.5 which results in a 5-fold increase of *FOXN1* expression. Remarkably, TECs derived from hESc following this protocol could be maintained for up to 30 days in classical 2D culture and they expressed the thymic markers *FOXN1*, *PAX9*, *EYA1*, *SIX1* and *AIRE* at similar levels than in the human fetal thymus. Another crucial aim is the characterization of the induced TECs at the single-cell level. After a directed differentiation protocol yielding 46% of TEPs (EPCAM+ CD205+) at day 14, Ramos et al. reaggregated the cells and perform their engraftment in nude mice. After 14 to 19 weeks, the thymic grafts were analyzed by bulk and scRNA-seq. Confirmation of further maturation in TECs was provided by high levels of expression of *HLA-DRA* and *DLL4*. Remarkably, the scRNA-seq data of these grafts showed a common clustering of TECs derived from iPSc with primary TECs from postnatal thymuses. However, subclustering of the TEC population revealed a distinct separation between the two types of samples, with induced TECs mainly composed of TEPs and differentiating TECs, while cells from the more mature cTEC and mTEChi clusters were originating from the primary samples.

These data shed a new light on the mechanisms leading to TEP differentiation, notably in pointing out the roles of Activin A and the Notch pathway detected by the expression of *INHBA* and *DLK1* in the TEP cluster. This direct differentiation protocol allows precise differentiation of iPSc into TEPs that mature into functional TECs *in vivo* with a transcriptomic profile close to primary TECs. Further application of scRNA-seq techniques to TEC differentiation could lead to a deeper understanding of the mechanisms driving the generation of the diverse TEC populations and leverage this new knowledge to differentiate specific TEC subpopulations.

Together, TEC differentiation from pluripotent stem cells has shown significant improvement in recent years with a continuous improvement of the protocols giving rise to TEPs, with greater yield and purity. Conversely, less progress was achieved in the approaches aiming to obtain mature TECs from TEPs. Regarding this stage of maturation, important clues came from the study of the thymic crosstalk with the finding that the interactions between TECs and developing thymocytes are necessary to the maturation of TECs. It was also shown that the thymic crosstalk could be mimicked *in vitro* using cytokines including but not restricted to RANKL. At a functional level, these induced TECs (iTEC) can support the maturation of thymocytes and reconstitute the T cell compartment *in vivo*. T cells cocultured with iTEC proliferate and secrete cytokines after stimulation. They are also able to improve skin graft rejection, thus showing evidence of functionality. Interestingly, nTreg can also be generated by iTEC grafts and induce immune tolerance to syngeneic skin grafts.

Although all the above protocols succeeded in generating TEPs with various efficiency, considerable obstacles still need to be addressed to obtain a functional thymic organoid *in vitro*. This highlights the fact that our current level of control over thymic iPSc differentiation is still incomplete and that most of the modulated pathways in these protocols may not be necessary nor sufficient.

Heterogeneity of the directed differentiation products is also a crucial stake for clinical applications since undifferentiated iPSc can lead to teratoma formation after transplantation. Purification strategies and treatment by selective anti-iPSc molecules such as YM155 (133) are promising approaches to mitigate this risk. This differentiation heterogeneity could also counter-intuitively positively affect the generation of iPSc-derived TECs. As described above, multiple cell types collaborate for thymic functionality. Thus, a differentiation strategy yielding not only isolated TECs but also thymic fibroblast or even T progenitors and dendritic cells would improve TEC differentiation.

Finally, a long-term culture system accurately reproducing *in vivo* thymic microenvironment still needs to be developed. Although TECs derived from iPSc can be maintained in classical 2D culture for up to 30 days (133), a culture system closer to the 3D sponge-like structure of the thymic stroma could significantly improve TEC differentiation and viability.

3D CULTURE AND ORGANOIDS

In classical 2D culture, primary TECs show a progressive loss of *AIRE* and *FOXN1* expression (134) and of their ability to express the full set of TRA genes (135). Since the 3D structure is an important factor for TEC maintenance (136), recapitulating such an organization in culture systems for thymic differentiation could improve yields and viability of iTECs. Several 3D models have been developed and tested on primary TECs. One of them relies on the coculture of mTECs with dermal fibroblasts embedded in a fibrin hydrogel, allowing proliferation, phenotype conservation, and further maturation of these cells (135). In comparison to simpler 2D culture systems, this organotypic 3D culture allows mTECs to keep their primary ability to express TRA genes. Other synthetic hydrogels have been developed to reconstitute the thymic microenvironment, such as a self-assembling synthetic hydrogel formed by EAK16-II/EAKII-H6 peptides (137). This gel was shown to induce the organization of primary TECs in 3D clusters and maintain the expression of *FOXN1* and *EPCAM*. After transplantation in nude mice, these hydrogel-embedded TECs supported the generation of T cell populations that were able to induce self-tolerance, as assessed by mixed leukocyte reactions. However, no cortico-medullary TEC segregation was observed in the reconstituted thymus, and the generated T cells were considerably biased toward CD8+ SP T cells. Additional systems were also generated to support the 3D culture of TECs, such as those based on fibronectin functionalized fibrous meshes (138), gelatin spheric microgels (139) or type I collagen hydrogel (140). Despite the various protein compositions of their matrices, these systems supported an enhanced proliferation, spreading and maintenance of the main TEC populations. However, the collagen hydrogel seeded with mice TEC did not seem to support thymopoiesis *in vivo* (140). Although synthetic hydrogels are a promising tool to culture TECs, more thorough research and optimization are needed to accurately mimic the thymic microenvironment.

An alternative approach to these synthetic systems is to directly use the primary thymus matrix to benefit from the

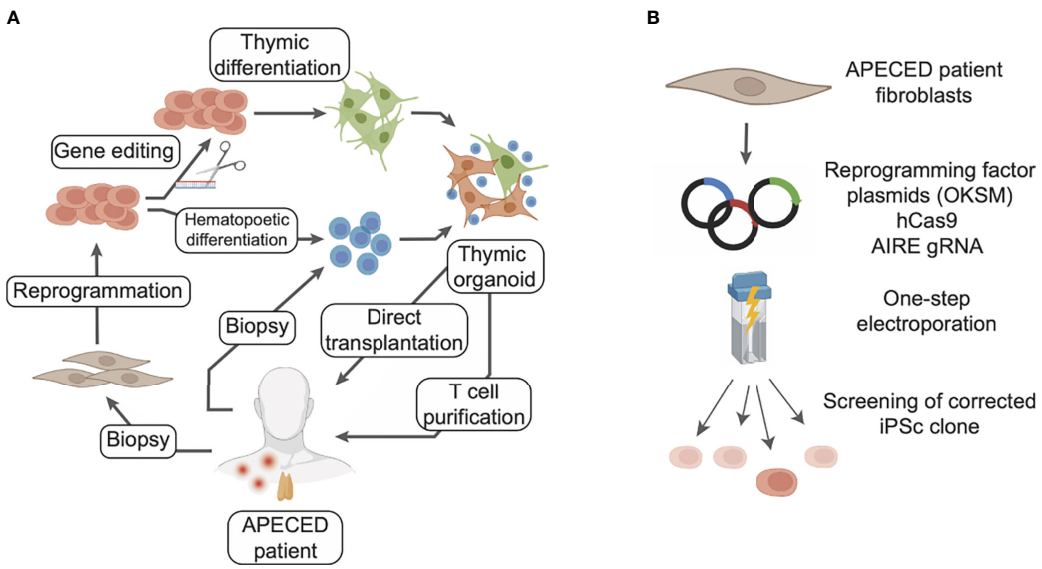

FIGURE 4 | Potential cellular therapy strategies for treating APECED with induced TECs to restore thymic functionality. **(A)** Fibroblasts from the patient can be reprogrammed to iPSc and the defective gene corrected with gene editing tools. Differentiation of these iPSc into thymic epithelial cells, in combination with T cell progenitors differentiated from the same iPSc or directly purified from patient blood, would allow generation of artificial thymic organoids. These organoids could be either directly transplanted or used to generate competent T cells *ex vivo* to reconstitute the patient immune system. In this scenario T cell progenitors could be purified from patient blood or differentiated from patient iPSc. **(B)** Gene editing of a deficient gene from a patient can rely on CRISPR/Cas9 and be combined with reprogramming steps for the obtention of iPSc.

native diversity of its constituting proteins and 3D structure. Decellularization of primary thymic lobes results in scaffolds that conserve the microstructure and the protein composition of the thymic microenvironment (141–143). These scaffolds support TEC growth and differentiation with the conservation of FOXN1 expression and the reformation of distinct medullary and cortical compartments. Moreover, after engraftment, the reconstituted thymuses can support the generation of functional T cells that can induce donor-specific tolerance in a skin graft model (141, 143). However, these approaches are dependent on a primary source of mouse or human thymuses, thus hindering clinical use.

Lastly, beside TEC differentiation, recent studies aiming to obtain functional T cells from hematopoietic progenitors or iPSc have also highlighted the importance of 3D culture systems to leverage obstacles in order to generate TEC organoids. Development of artificial thymic organoids (ATO) (144–146) has been achieved through reaggregation of a bone marrow stromal cell line engineered to express the Notch ligand Dll4 with either hematopoietic stem cells or mesodermal progenitors derived from iPSc. The cocultured cells formed a 3D structure cultured in an air-liquid interface. Using bone marrow stem cells from mice of three different backgrounds, the ATO system was able to consistently reproduce thymopoiesis, and generate mature single-positive CD4 and CD8 cells (145, 146). Remarkably, this system resulted in comparable results when using mesodermal progenitors derived from hESc and human iPSc (145). Thus, thymic organoids can recapitulate T cell differentiation *in vitro*, therefore showing the importance of 3D structure in comparison to less efficient 2D cocultures (147). However, CD4 single-positive T cell frequency was lower than expected, probably because of the absence of TECs in this system, resulting in an impaired MHCII signaling. Another crucial drawback is the conservation of numerous clones naturally eliminated in the thymus, illustrating the absence of negative selection in the ATOs.

CLINICAL APPLICATIONS TO APECED AND PERSPECTIVES

Congenital pathologies affecting TEC development and function lead to severe conditions of autoimmunity or lymphopenia. APECED is caused by loss-of-function mutations in the *AIRE* gene resulting in a general autoimmune syndrome. Patients receive a personalized combination of treatments targeting the symptoms and leading to clinical improvements. However, no curative strategy is available yet, and APECED patients still risk premature death. Remarkably, the recent breakthroughs in TEC generation from iPSc lead to new perspectives for treatment of APECED (**Figure 4A**). Reprogramming patient cells and correcting the *AIRE* mutations through gene editing techniques would produce iPSc that could be used to regenerate 3D thymic tissues. Transplantation of these autologous engineered thymic tissues would restore thymic function and limit the risk of autoimmunity. Indeed, the transplanted tissues would be syngeneic and T cells generated would be educated to the patient's autoantigen repertoire, reconstituting its immune system (**Figure 4A**).

Reprogramming of somatic cells from APECED patients has been shown feasible despite the role that AIRE plays in the regulation of ESc pluripotency and in their self-renewal (148, 149). Indeed iPSc have recently been generated from APECED patient cells (150), showing that the *AIRE* R257X mutation does not impair cell reprogramming, iPSc proliferation and pluripotency. In this study, PBMCs from 2 female APECED patients were transduced by a Sendai virus vector, yielding 10 iPSc clones in which the *AIRE* mutation was confirmed. These iPSc show similar proliferation and expression of pluripotency markers than iPSc with functional *AIRE*, therefore validating the use of iPSc-based approaches in APECED. If *AIRE* has not been reportedly corrected in iPSc, this approach has been demonstrated in several models of monogenic pathologies, affecting diverse organs such as retina, kidney and liver (151–153). In these studies, the mutated genes *RPGR*, *IFT140* and *LDLR* causing Retinitis pigmentosa, nephronophthisis and homozygous familial hypercholesterolemia, respectively, were corrected in iPSc from patient cells. The corrected iPSc were then differentiated into retinal organoids, kidney organoids or hepatocyte-like cells, all of them showing a rescued phenotype and functionality (151–153). The CRISPR/Cas9 system was used for gene edition in these 3 studies, delivering plasmids and Cas9 to the iPSc by electroporation (152, 153), or in a one-step protocol during reprogramming (151). In the latter, patient dermal fibroblasts are electroporated by two pulses at 1,400 V for 20 ms with a cocktail of plasmids coding for the reprogramming factors, a guide RNA for the target gene, its corrected sequence, and a spCas9-gem. This specific Cas9 variants have been developed for gene editing iPSc (154). Thus, given those converging clues, using CRISPR/Cas9 to edit *AIRE* in iPSc derived from APECED patients could be a valid curative strategy (**Figure 4B**).

Beyond APECED, other pathologies affecting the thymus are also caused by genetic defects. DiGeorges syndrome is caused by a microdeletion of the TBX1-containing chromosome region 22q11.2, nude SCID by mutations in the FOXN1 gene and Otofaciocervical Syndrome type 2 in the PAX1 gene (155). These conditions lead to partial or total athymia and life-threatening lymphopenia. Curative treatments of these diseases could also rely on transplantation of autologous engineered thymic tissues to restore thymic function while limiting the risk of autoimmunity. Nonetheless, a crucial limitation is the long lapse of time needed to reprogram iPSc and to differentiate them into functional thymic tissue. Applied to APECED, early diagnosis would be crucial, since this approach cannot cure the damage already caused by autoimmunity, even though promising immunotherapies are emerging to treat autoimmune manifestations (156). For pathologies causing lymphopenia, early diagnosis would also be vital to limit the risk of potentially lethal infections during the time needed to generate the engineered thymic tissues. To envision the use of such therapies, additional challenges would need to be met with the need to develop clinical-grade differentiation protocols not relying on any xenogenous reactives and based on well-accepted synthetic hydrogels for 3D culture. Finally, the risk of transplanting iSPc-

derived TECs should be carefully assessed to limit teratoma formation, with purification of differentiated cells and anti-pluripotency treatment.

Because of the complex interactions between cell populations in the thymus, the crucial importance of its 3D organization and the still-improving understanding of TEC biology, generation of *in vitro* culture systems closely reproducing the thymus is a major challenge. In recent years, great advances have been made in the understanding of thymus organogenesis, the generation of TECs from pluripotent stem cells and 3D culture systems. These complementary progress will very likely result in preclinical applications for the treatment of pathologies affecting T cell development in the thymus.

AUTHOR CONTRIBUTIONS

NP and MG designed/outlined the manuscript; NP wrote the manuscript and MG edited the manuscript.

FUNDING

NP was supported by "la fondation d'entreprise ProGreffe" and by the EJP-Rare Disease JTC2019 program TARID project (ANR-19-RAR4-0011-05) to MG.

REFERENCES

1. Kadouri N, Nevo S, Goldfarb Y, Abramson J. Thymic Epithelial Cell Heterogeneity: TEC by TEC. *Nat Rev Immunol* (2019) 20:239–253. doi: 10.1038/s41577-019-0238-0
2. Perheentupa J. Autoimmune Polyendocrinopathy-Candidiasis-Ectodermal Dystrophy. *J Clin Endocrinol Metab* (2006) 91(8):2843–50. doi: 10.1210/jc.2005-2611
3. Borchers J, Pukkala E, Mäkitie O, Laakso S. Patients With APECED Have Increased Early Mortality Due to Endocrine Causes, Malignancies and Infections. *J Clin Endocrinol Metab* (2020) 105(6):dgaa140. doi: 10.1210/clinem/dgaa140
4. Takahashi K, Yamanaka S. Induction of Pluripotent Stem Cells From Mouse Embryonic and Adult Fibroblast Cultures by Defined Factors. *Cell* (2006) 126(4):663–76. doi: 10.1016/j.cell.2006.07.024
5. Yoshida Y, Yamanaka S. Induced Pluripotent Stem Cells 10 Years Later. *Circ Res* (2017) 120(12):1958–68. doi: 10.1161/CIRCRESAHA.117.311080
6. Tukker AM, Wijnolts FMJ, de Groot A, Westerink RHS. Human iPSC-Derived Neuronal Models for *In Vitro* Neurotoxicity Assessment. *NeuroToxicology* (2018) 67:215–25. doi: 10.1016/j.neuro.2018.06.007
7. Kondo Y, Toyoda T, Inagaki N, Osafune K. iPSC Technology-Based Regenerative Therapy for Diabetes. *J Diabetes Investig* (2018) 9(2):234–43. doi: 10.1111/jdi.12702
8. Fate Therapeutics Announces FDA Clearance of Landmark IND for FT500 iPSC-Derived, Off-The-Shelf NK Cell Cancer Immunotherapy. *Fate Therapeutics Inc* (2021).
9. Parmar M, Grealish S, Henchcliffe C. The Future of Stem Cell Therapies for Parkinson Disease. *Nat Rev Neurosci* (2020) 21(2):103–15. doi: 10.1038/s41583-019-0257-7
10. Kumar A, Das JK, Peng HY, Wang L, Ren Y, Xiong X, et al. Chapter 14 - Current Development in iPSC-Based Therapy for Autoimmune Diseases. In: Advances in Stem Cell Biology, A Birbrair, editor. *Recent Advances in iPSCs for Therapy*. Academic Press (2021) , 3:315–338. Available at: https://www.sciencedirect.com/science/article/pii/B9780128222294000012.
11. Pan GJ, Chang ZY, Schöler HR, Pei D. Stem Cell Pluripotency and Transcription Factor Oct4. *Cell Res* (2002) 12(5):321–9. doi: 10.1038/sj.cr.7290134
12. Desgres M, Menasché P. Clinical Translation of Pluripotent Stem Cell Therapies: Challenges and Considerations. *Cell Stem Cell* (2019) 25 (5):594–606. doi: 10.1016/j.stem.2019.10.001
13. Sakata M, Ohigashi I, Takahama Y. Cellularity of Thymic Epithelial Cells in the Postnatal Mouse. *J Immunol* (2018) 200(4):1382–8. doi: 10.4049/jimmunol.1701235
14. Abramson J, Anderson G. Thymic Epithelial Cells. *Annu Rev Immunol* (2017) 35:85–118. doi: 10.1146/annurev-immunol-051116-052320
15. Ohigashi I, Zuklys S, Sakata M, Mayer CE, Zhanybekova S, Murata S, et al. Aire-Expressing Thymic Medullary Epithelial Cells Originate From β5t-Expressing Progenitor Cells. *Proc Natl Acad Sci* (2013) 110(24):9885–90. doi: 10.1073/pnas.1301799110
16. Bornstein C, Nevo S, Giladi A, Kadouri N, Pouzolles M, Gerbe F, et al. Single-Cell Mapping of the Thymic Stroma Identifies IL-25-Producing Tuft Epithelial Cells. *Nature* (2018) 559(7715):622–6. doi: 10.1038/s41586-018-0346-1
17. Apavaloaei A, Brochu S, Dong M, Rouette A, Hardy MP, Villafano G, et al. PSMB11 Orchestrates the Development of CD4 and CD8 Thymocytes *via* Regulation of Gene Expression in Cortical Thymic Epithelial Cells. *J Immunol* (2019) 202(3):966–78. doi: 10.4049/jimmunol.1801288
18. Kozai M, Kubo Y, Katakai T, Kondo H, Kiyonari H, Schaeuble K, et al. Essential Role of CCL21 in Establishment of Central Self-Tolerance in T Cells. *J Exp Med* (2017) 214(7):1925–35. doi: 10.1084/jem.20161864
19. Sansom SN, Shikama-Dorn N, Zhanybekova S, Nusspaumer G, Macaulay IC, Deadman ME, et al. Population and Single-Cell Genomics Reveal the Aire Dependency, Relief From Polycomb Silencing, and Distribution of Self-Antigen Expression in Thymic Epithelia. *Genome Res* (2014) 24(12):1918–31. doi: 10.1101/gr.171645.113
20. Danan-Gotthold M, Guyon C, Giraud M, Levanon EY, Abramson J. Extensive RNA Editing and Splicing Increase Immune Self-Representation Diversity in Medullary Thymic Epithelial Cells. *Genome Biol* (2016) 17 (1):219. doi: 10.1186/s13059-016-1079-9
21. Dhalla F, Baran-Gale J, Maio S, Chappell L, Hollander GA, Ponting CP. Biologically Indeterminate Yet Ordered Promiscuous Gene Expression in Single Medullary Thymic Epithelial Cells. *EMBO J* (2020) 39(1):e101828. doi: 10.15252/embj.2019101828
22. Takaba H, Morishita Y, Tomofuji Y, Danks L, Nitta T, Komatsu N, et al. Fezf2 Orchestrates a Thymic Program of Self-Antigen Expression for Immune Tolerance. *Cell* (2015) 163(4):975–87. doi: 10.1016/j.cell.2015.10.013
23. Tomofuji Y, Takaba H, Suzuki HI, Benlaribi R, Martinez CDP, Abe Y, et al. Chd4 Choreographs Self-Antigen Expression for Central Immune Tolerance. *Nat Immunol* (2020) 21(8):892–901. doi: 10.1038/s41590-020-0717-2
24. Björses P, Halonen M, Palvimo JJ, Kolmer M, Aaltonen J, Ellonen P, et al. Mutations in the AIRE Gene: Effects on Subcellular Location and Transactivation Function of the Autoimmune Polyendocrinopathy-Candidiasis–Ectodermal Dystrophy Protein. *Am J Hum Genet* (2000) 66 (2):378–92. doi: 10.1086/302765
25. Anderson MS, Venanzi ES, Klein L, Chen Z, Berzins SP, Turley SJ, et al. Projection of an Immunological Self Shadow Within the Thymus by the Aire Protein. *Science* (2002) 298(5597):1395–401. doi: 10.1126/science.1075958
26. Giraud M, Yoshida H, Abramson J, Rahl PB, Young RA, Mathis D, et al. Aire Unleashes Stalled RNA Polymerase to Induce Ectopic Gene Expression in Thymic Epithelial Cells. *Proc Natl Acad Sci U S A* (2012) 109(2):535–40. doi: 10.1073/pnas.1119351109
27. Giraud M, Jmari N, Du L, Carallis F, Nieland TJF, Perez-Campo FM, et al. An RNAi Screen for Aire Cofactors Reveals a Role for Hnrnpl in Polymerase Release and Aire-Activated Ectopic Transcription. *Proc Natl Acad Sci U S A* (2014) 111(4):1491–6. doi: 10.1073/pnas.1323535111
28. Li MO, Rudensky AY. T Cell Receptor Signaling in the Control of Regulatory T Cell Differentiation and Function. *Nat Rev Immunol* (2016) 16(4):220–33. doi: 10.1038/nri.2016.26

29. Cowan JE, Parnell SM, Nakamura K, Caamano JH, Lane PJL, Jenkinson EJ, et al. The Thymic Medulla is Required for Foxp3+ Regulatory But Not Conventional CD4+ Thymocyte Development. *J Exp Med* (2013) 210 (4):675–81. doi: 10.1084/jem.20122070
30. Teh CE, Daley SR, Enders A, Goodnow CC. T-Cell Regulation by Casitas B-Lineage Lymphoma (Cblb) is a Critical Failsafe Against Autoimmune Disease Due to Autoimmune Regulator (Aire) Deficiency. *Proc Natl Acad Sci U S A* (2010) 107(33):14709–14. doi: 10.1073/pnas.1009209107
31. Holländer GA, Wang B, Nichogiannopoulou A, Platenburg PP, van Ewijk W, Burakoff SJ, et al. Developmental Control Point in Induction of Thymic Cortex Regulated by a Subpopulation of Prothymocytes. *Nature* (1995) 373 (6512):350–3. doi: 10.1038/373350a0
32. Irla M, Guerri L, Guenot J, Sergé A, Lantz O, Liston A, et al. Antigen Recognition by Autoreactive $CD4^+$ Thymocytes Drives Homeostasis of the Thymic Medulla. *PloS One* (2012) 7(12):e52591. doi: 10.1371/journal.pone.0052591
33. Irla M, Hugues S, Gill J, Nitta T, Hikosaka Y, Williams IR, et al. Autoantigen-Specific Interactions With CD4+ Thymocytes Control Mature Medullary Thymic Epithelial Cell Cellularity. *Immunity* (2008) 29(3):451–63. doi: 10.1016/j.immuni.2008.08.007
34. Lopes N, Sergé A, Ferrier P, Irla M. Thymic Crosstalk Coordinates Medulla Organization and T-Cell Tolerance Induction. *Front Immunol* (2015) 6:365/abstract. doi: 10.3389/fimmu.2015.00365/abstract
35. Irla M. RANK Signaling in the Differentiation and Regeneration of Thymic Epithelial Cells. *Front Immunol* (2021) 11:623265. doi: 10.3389/fimmu.2020.623265
36. Wells KL, Miller CN, Gschwind AR, Wei W, Phipps JD, Anderson MS, et al. Combined Transient Ablation and Single-Cell RNA-Sequencing Reveals the Development of Medullary Thymic Epithelial Cells. *Elife* (2020) 9:e60188. doi: 10.7554/elife.60188
37. Bautista JL, Cramer NT, Miller CN, Chavez J, Berrios DI, Byrnes LE, et al. Single-Cell Transcriptional Profiling of Human Thymic Stroma Uncovers Novel Cellular Heterogeneity in the Thymic Medulla. *Nat Commun* (2021) 12(1):1096. doi: 10.1038/s41467-021-21346-6
38. Park JE, Botting RA, Domínguez Conde C, Popescu DM, Lavaert M, Kunz DJ, et al. A Cell Atlas of Human Thymic Development Defines T Cell Repertoire Formation. *Science* (2020) 367(6480):eaay3224. doi: 10.1126/science.aay3224
39. Zeng Y, Liu C, Gong Y, Bai Z, Hou S, He J, et al. Single-Cell RNA Sequencing Resolves Spatiotemporal Development of Pre-Thymic Lymphoid Progenitors and Thymus Organogenesis in Human Embryos. *Immunity* (2019) 51(5):930–948.e6. doi: 10.1016/j.immuni.2019.09.008
40. Alawam AS, Anderson G, Lucas B. Generation and Regeneration of Thymic Epithelial Cells. *Front Immunol* (2020) 11:858. doi: 10.3389/fimmu.2020.00858
41. Baik S, Jenkinson EJ, Lane PJL, Anderson G, Jenkinson WE. Generation of Both Cortical and Aire+ Medullary Thymic Epithelial Compartments From CD205+ Progenitors. *Eur J Immunol* (2013) 43(3):589–94. doi: 10.1002/eji.201243209
42. Alves NL, Takahama Y, Ohigashi I, Ribeiro AR, Baik S, Anderson G, et al. Serial Progression of Cortical and Medullary Thymic Epithelial Microenvironments. *Eur J Immunol* (2014) 44(1):16–22. doi: 10.1002/eji.201344110
43. Rossi SW, Jenkinson WE, Anderson G, Jenkinson EJ. Clonal Analysis Reveals a Common Progenitor for Thymic Cortical and Medullary Epithelium. *Nature* (2006) 441(7096):988–91. doi: 10.1038/nature04813
44. Bleul CC, Corbeaux T, Reuter A, Fisch P, Mönting JS, Boehm T. Formation of a Functional Thymus Initiated by a Postnatal Epithelial Progenitor Cell. *Nature* (2006) 441(7096):992–6. doi: 10.1038/nature04850
45. Chen L, Xiao S, Manley NR. Foxn1 is Required to Maintain the Postnatal Thymic Microenvironment in a Dosage-Sensitive Manner. *Blood* (2009) 113 (3):567–74. doi: 10.1182/blood-2008-05-156265
46. O'Neill KE, Bredenkamp N, Tischner C, Vaidya HJ, Stenhouse FH, Peddie CD, et al. Foxn1 Is Dynamically Regulated in Thymic Epithelial Cells During Embryogenesis and at the Onset of Thymic Involution. *PloS One* (2016) 11 (3):e0151666. doi: 10.1371/journal.pone.0151666
47. Lepletier A, Hun ML, Hammett MV, Wong K, Naeem H, Hedger M, et al. nterplay Between Follistatin, Activin A, and BMP4 Signaling Regulates Postnatal Thymic Epithelial Progenitor Cell Differentiation During Aging. *Cell Rep* (2019) 27(13):3887–901. doi: 10.1016/j.celrep.2019.05.045
48. Barsanti M, Lim JMC, Hun ML, Lister N, Wong K, Hammett MV, et al. A Novel Foxn1eGFP/+ Mouse Model Identifies Bmp4-Induced Maintenance of Foxn1 Expression and Thymic Epithelial Progenitor Populations. *Eur J Immunol* (2017) 47(2):291–304. doi: 10.1002/eji.201646553
49. Liu D, Kousa AI, O'Neill KE, Rouse P, Popis M, Farley AM, et al. Canonical Notch Signaling Controls the Early Thymic Epithelial Progenitor Cell State and Emergence of the Medullary Epithelial Lineage in Fetal Thymus Development. *Dev Camb Engl* (2020) 147(12):dev178582. doi: 10.1242/dev.178582
50. Li J, Gordon J, Chen ELY, Xiao S, Wu L, Zúñiga-Pflücker JC, et al. NOTCH1 Signaling Establishes the Medullary Thymic Epithelial Cell Progenitor Pool During Mouse Fetal Development. *Dev Camb Engl* (2020) 147(12): dev178988. doi: 10.1242/dev.178988
51. Goldfarb Y, Kadouri N, Levi B, Sela A, Herzig Y, Cohen RN, et al. HDAC3 is a Master Regulator of mTEC Development. *Cell Rep* (2016) 15(3):651–65. doi: 10.1016/j.celrep.2016.03.048
52. Chakrabarti S, Hoque M, Jamil NZ, Singh VJ, Pollacksmith D, Meer N, et al. Bone Marrow-Derived Cells Contribute to the Maintenance of Thymic Stroma Including TECs. *J Immunol Res* (2022) 2022:e6061746. doi: 10.1155/2022/6061746
53. Vobořil M, Brabec T, Dobeš J, Šplíchalová I, Březina J, Čepková A, et al. Toll-Like Receptor Signaling in Thymic Epithelium Controls Monocyte-Derived Dendritic Cell Recruitment and Treg Generation. *Nat Commun* (2020) 11 (1):2361. doi: 10.1038/s41467-020-16081-3
54. Wang H, Zúñiga-Pflücker JC. Thymic Microenvironment: Interactions Between Innate Immune Cells and Developing Thymocytes. *Front Immunol* (2022) 13:885280. doi: 10.3389/fimmu.2022.885280
55. Hasegawa H, Matsumoto T. Mechanisms of Tolerance Induction by Dendritic Cells *In Vivo*. *Front Immunol* (2018) 9:350. doi: 10.3389/fimmu.2018.00350
56. Proietto AI, van Dommelen S, Zhou P, Rizzitelli A, D'Amico A, Steptoe RJ, et al. Dendritic Cells in the Thymus Contribute to T-Regulatory Cell Induction. *Proc Natl Acad Sci U S A* (2008) 105(50):19869–74. doi: 10.1073/pnas.0810268105
57. Bonasio R, Scimone ML, Schaerli P, Grabie N, Lichtman AH, von Andrian UH. Clonal Deletion of Thymocytes by Circulating Dendritic Cells Homing to the Thymus. *Nat Immunol* (2006) 7(10):1092–100. doi: 10.1038/ni1385
58. Vollmann EH, Rattay K, Barreiro O, Thiriot A, Fuhlbrigge RA, Vrbanac V, et al. Specialized Transendothelial Dendritic Cells Mediate Thymic T-Cell Selection Against Blood-Borne Macromolecules. *Nat Commun* (2021) 12 (1):6230. doi: 10.1038/s41467-021-26446-x
59. Zegarra-Ruiz DF, Kim DV, Norwood K, Kim M, Wu WJH, Saldana-Morales FB, et al. Thymic Development of Gut-Microbiota-Specific T Cells. *Nature* (2021) 594(7863):413–7. doi: 10.1038/s41586-021-03531-1
60. Kroger CJ, Spidale NA, Wang B, Tisch R. Thymic Dendritic Cell Subsets Display Distinct Efficiencies and Mechanisms of Intercellular MHC Transfer. *J Immunol Baltim Md* (2017) 198(1):249–56. doi: 10.4049/jimmunol.1601516
61. Koble C, Kyewski B. The Thymic Medulla: A Unique Microenvironment for Intercellular Self-Antigen Transfer. *J Exp Med* (2009) 206(7):1505–13. doi: 10.1084/jem.20082449
62. Cosway EJ, Lucas B, James KD, Parnell SM, Carvalho-Gaspar M, White AJ, et al. Redefining Thymus Medulla Specialization for Central Tolerance. *J Exp Med* (2017) 214(11):3183–95. doi: 10.1084/jem.20171000
63. Nitta T, Tsutsumi M, Nitta S, Muro R, Suzuki EC, Nakano K, et al. Fibroblasts as a Source of Self-Antigens for Central Immune Tolerance. *Nat Immunol* (2020) 21(10):1172–80. doi: 10.1038/s41590-020-0756-8
64. Nitta T, Ota A, Iguchi T, Muro R, Takayanagi H. The Fibroblast: An Emerging Key Player in Thymic T Cell Selection. *Immunol Rev* (2021) 302 (1):68–85. doi: 10.1111/imr.12985
65. Nitta T, Takayanagi H. Non-Epithelial Thymic Stromal Cells: Unsung Heroes in Thymus Organogenesis and T Cell Development. *Front Immunol* (2021) 11:620894/full. doi: 10.3389/fimmu.2020.620894/full
66. Muñoz JJ, García-Ceca J, Montero-Herradón S, Sánchez del Collado B, Alfaro D, Zapata A. Can a Proper T-Cell Development Occur in an Altered

Thymic Epithelium? Lessons From EphB-Deficient Thymi. *Front Endocrinol* (2018) 9:135. doi: 10.3389/fendo.2018.00135
67. Graham A, Richardson J. Developmental and Evolutionary Origins of the Pharyngeal Apparatus. *EvoDevo* (2012) 3(1):24. doi: 10.1186/2041-9139-3-24
68. Gordon J, Wilson VA, Blair NF, Sheridan J, Farley A, Wilson L, et al. Functional Evidence for a Single Endodermal Origin for the Thymic Epithelium. *Nat Immunol* (2004) 5(5):546–53. doi: 10.1038/ni1064
69. Gordon J, Manley NR. Mechanisms of Thymus Organogenesis and Morphogenesis. *Development* (2011) 138(18):3865–78. doi: 10.1242/dev.059998
70. Sperber GH, Guttmann SGHSGD, Steven M. *Craniofacial Development (Book for Windows & Macintosh)*. Craniofacial Development PMPH-USA (2001) 220 p.
71. Frisdal A, Trainor PA. Development and Evolution of the Pharyngeal Apparatus. *WIREs Dev Biol* (2014) 3(6):403–18. doi: 10.1002/wdev.147
72. Norris EH. The Morphogenesis and Histogenesis of the Thymus Gland in Man: In Which the Origin of the Hassall's Corpuscles of the Human Thymus is Discovered. *Contrib Embryol* (1938) 27(166):191–208.
73. Van Dyke JH. On the Origin of Accessory Thymus Tissue, Thymus IV: The Occurrence in Man. *Anat Rec* (1941) 79(2):179–209. doi: 10.1002/ar.1090790204
74. Blackburn CC, Manley NR. Developing a New Paradigm for Thymus Organogenesis. *Nat Rev Immunol* (2004) 4(4):278–89. doi: 10.1038/nri1331
75. Manley NR, Condie BG. Transcriptional Regulation of Thymus Organogenesis and Thymic Epithelial Cell Differentiation. In: A Liston, editor. *Progress in Molecular Biology and Translational Science*. Academic Press (2010) 92:103–120. Available at: http://www.sciencedirect.com/science/article/pii/S187711731092005X.
76. Le Douarin NM, Jotereau FV. Tracing of Cells of the Avian Thymus Through Embryonic Life in Interspecific Chimeras. *J Exp Med* (1975) 142 (1):17–40. doi: 10.1084/jem.142.1.17
77. Farley AM, Morris LX, Vroegindeweij E, Depreter MLG, Vaidya H, Stenhouse FH, et al. Dynamics of Thymus Organogenesis and Colonization in Early Human Development. *Development* (2013) 140 (9):2015–26. doi: 10.1242/dev.087320
78. Hamazaki Y. Adult Thymic Epithelial Cell (TEC) Progenitors and TEC Stem Cells: Models and Mechanisms for TEC Development and Maintenance. *Eur J Immunol* (2015) 45(11):2985–93. doi: 10.1002/eji.201545844
79. Muñoz JJ, Zapata AG. Epithelial Development Based on a Branching Morphogenesis Program: The Special Condition of Thymic Epithelium In: Heinbockel T and Shields VD, editors. *Histology [Internet]*. London: IntechOpen [cited 2022 Jun 09]. (2018). doi: 10.5772/intechopen.81193
80. Nehls M, Pfeifer D, Schorpp M, Hedrich H, Boehm T. New Member of the Winged-Helix Protein Family Disrupted in Mouse and Rat Nude Mutations. *Nature* (1994) 372(6501):103–7. doi: 10.1038/372103a0
81. Gordon J, Bennett AR, Blackburn CC, Manley NR. Gcm2 and Foxn1 Mark Early Parathyroid- and Thymus-Specific Domains in the Developing Third Pharyngeal Pouch. *Mech Dev* (2001) 103(1–2):141–3. doi: 10.1016/S0925-4773(01)00333-1
82. Blackburn CC, Augustine CL, Li R, Harvey RP, Malin MA, Boyd RL, et al. The Nu Gene Acts Cell-Autonomously and is Required for Differentiation of Thymic Epithelial Progenitors. *Proc Natl Acad Sci* (1996) 93(12):5742–6. doi: 10.1073/pnas.93.12.5742
83. Nehls M, Kyewski B, Messerle M, Waldschütz R, Schüddekopf K, Smith AJH, et al. Two Genetically Separable Steps in the Differentiation of Thymic Epithelium. *Science* (1996) 272(5263):886–9. doi: 10.1126/science.272.5263.886
84. Prowse DM, Lee D, Weiner L, Jiang N, Magro CM, Baden HP, et al. Ectopic Expression of the Nude Gene Induces Hyperproliferation and Defects in Differentiation: Implications for the Self-Renewal of Cutaneous Epithelia. *Dev Biol* (1999) 212(1):54–67. doi: 10.1006/dbio.1999.9328
85. Nowell CS, Bredenkamp N, Tetélin S, Jin X, Tischner C, Vaidya H, et al. Foxn1 Regulates Lineage Progression in Cortical and Medullary Thymic Epithelial Cells But is Dispensable for Medullary Sublineage Divergence. *PloS Genet* (2011) 7(11):e1002348. doi: 10.1371/journal.pgen.1002348
86. Bredenkamp N, Nowell CS, Blackburn CC. Regeneration of the Aged Thymus by a Single Transcription Factor. *Development* (2014) 141 (8):1627–37. doi: 10.1242/dev.103614
87. Revest JM, Suniara RK, Kerr K, Owen JJT, Dickson C. Development of the Thymus Requires Signaling Through the Fibroblast Growth Factor Receptor R2-IIIb. *J Immunol* (2001) 167(4):1954–61. doi: 10.4049/jimmunol.167.4.1954
88. Muñoz JJ, Cejalvo T, Tobajas E, Fanlo L, Cortés A, Zapata AG. 3D Immunofluorescence Analysis of Early Thymic Morphogenesis and Medulla Development. *Histol Histopathol* (2015) 30(5):589–99. doi: 10.14670/HH-30.589
89. Rhinn M, Dollé P. Retinoic Acid Signalling During Development. *Development* (2012) 139(5):843–58. doi: 10.1242/dev.065938
90. Graham A, Okabe M, Quinlan R. The Role of the Endoderm in the Development and Evolution of the Pharyngeal Arches. *J Anat* (2005) 207 (5):479–87. doi: 10.1111/j.1469-7580.2005.00472.x
91. Wendling O, Dennefeld C, Chambon P, Mark M. Retinoid Signaling is Essential for Patterning the Endoderm of the Third and Fourth Pharyngeal Arches. *Dev Camb Engl* (2000) 127(8):1553–62. doi: 10.1242/dev.127.8.1553
92. Kopinke D, Sasine J, Swift J, Stephens WZ, Piotrowski T. Retinoic Acid is Required for Endodermal Pouch Morphogenesis and Not for Pharyngeal Endoderm Specification. *Dev Dyn* (2006) 235(10):2695–709. doi: 10.1002/dvdy.20905
93. Quinlan R, Gale E, Maden M, Graham A. Deficits in the Posterior Pharyngeal Endoderm in the Absence of Retinoids. *Dev Dyn* (2002) 225 (1):54–60. doi: 10.1002/dvdy.10137
94. Niederreither K, Vermot J, Roux IL, Schuhbaur B, Chambon P, Dollé P. The Regional Pattern of Retinoic Acid Synthesis by RALDH2 is Essential for the Development of Posterior Pharyngeal Arches and the Enteric Nervous System. *Development* (2003) 130(11):2525–34. doi: 10.1242/dev.00463
95. Arnold JS, Werling U, Braunstein EM, Liao J, Nowotschin S, Edelmann W, et al. Inactivation of Tbx1 in the Pharyngeal Endoderm Results in 22q11ds Malformations. *Development* (2006) 133(5):977–87. doi: 10.1242/dev.02264
96. Balciunaite G, Keller MP, Balciunaite E, Piali L, Zuklys S, Mathieu YD, et al. Wnt Glycoproteins Regulate the Expression of FoxN1, the Gene Defective in Nude Mice. *Nat Immunol* (2002) 3(11):1102–8. doi: 10.1038/ni850
97. Osada M, Jardine L, Misir R, Andl T, Millar SE, Pezzano M. DKK1 Mediated Inhibition of Wnt Signaling in Postnatal Mice Leads to Loss of TEC Progenitors and Thymic Degeneration. *PloS One* (2010) 5(2):e9062. doi: 10.1371/journal.pone.0009062
98. Jin S OJ, Stellabotte F, Choe CP. Foxi1 Promotes Late-Stage Pharyngeal Pouch Morphogenesis Through Ectodermal Wnt4a Activation. *Dev Biol* (2018) 441(1):12–8. doi: 10.1016/j.ydbio.2018.06.011
99. Osada M, Ito E, Fermin HA, Vazquez-Cintron E, Venkatesh T, Friedel RH, et al. The Wnt Signaling Antagonist Kremen1 is Required for Development of Thymic Architecture. *Clin Dev Immunol* (2006) 13(2–4):299–319. doi: 10.1080/17402520600935097
100. Brunk F, Augustin I, Meister M, Boutros M, Kyewski B. Thymic Epithelial Cells Are a Nonredundant Source of Wnt Ligands for Thymus Development. *J Immunol* (2015) 195(11):5261–71. doi: 10.4049/jimmunol.1501265
101. Wei T, Zhang N, Guo Z, Chi F, Song Y, Zhu X. Wnt4 Signaling is Associated With the Decrease of Proliferation and Increase of Apoptosis During Age-Related Thymic Involution. *Mol Med Rep* (2015) 12(5):7568–76. doi: 10.3892/mmr.2015.4343
102. Griffith AV, Fallahi M, Venables T, Petrie HT. Persistent Degenerative Changes in Thymic Organ Function Revealed by an Inducible Model of Organ Regrowth. *Aging Cell* (2012) 11(1):169–77. doi: 10.1111/j.1474-9726.2011.00773.x
103. Kvell K, Varecza Z, Bartis D, Hesse S, Parnell S, Anderson G, et al. Wnt4 and LAP2alpha as Pacemakers of Thymic Epithelial Senescence. *PloS One* (2010) 5(5):e10701. doi: 10.1371/journal.pone.0010701
104. Swann JB, Happe C, Boehm T. Elevated Levels of Wnt Signaling Disrupt Thymus Morphogenesis and Function. *Sci Rep* (2017) 7(1):785. doi: 10.1038/s41598-017-00842-0
105. Gordon J, Manley NR. Tissue-Specific Requirements for BMP Signaling During Thymus and Parathyroid Morphogenesis. *Dev Biol* (2006) 295 (1):455. doi: 10.1016/j.ydbio.2006.04.402
106. Patel SR, Gordon J, Mahbub F, Blackburn CC, Manley NR. Bmp4 and Noggin Expression During Early Thymus and Parathyroid Organogenesis. *Gene Expr Patterns* (2006) 6(8):794–9. doi: 10.1016/j.modgep.2006.01.011

107. Tsai PT, Lee RA, Wu H. BMP4 Acts Upstream of FGF in Modulating Thymic Stroma and Regulating Thymopoiesis. *Blood* (2003) 102(12):3947–53. doi: 10.1182/blood-2003-05-1657
108. Lovely CB, Swartz ME, McCarthy N, Norrie JL, Eberhart JK. Bmp Signaling Mediates Endoderm Pouch Morphogenesis by Regulating Fgf Signaling in Zebrafish. *Development* (2016) 143(11):2000–11. doi: 10.1242/dev.129379
109. Macatee TL, Hammond BP, Arenkiel BR, Francis L, Frank DU, Moon AM. Ablation of Specific Expression Domains Reveals Discrete Functions of Ectoderm- and Endoderm-Derived FGF8 During Cardiovascular and Pharyngeal Development. *Development* (2003) 130(25):6361–74. doi: 10.1242/dev.00850
110. Abu-Issa R, Smyth G, Smoak I, Meyers EN. Fgf8 is Required for Pharyngeal Arch and Cardiovascular Development in the Mouse. *Development* (2002) 129(19):4613–25. doi: 10.1242/dev.129.19.4613
111. Gardiner JR, Jackson AL, Gordon J, Lickert H, Manley NR, Basson MA. Localised Inhibition of FGF Signalling in the Third Pharyngeal Pouch is Required for Normal Thymus and Parathyroid Organogenesis. *Development* (2012) 139(18):3456–66. doi: 10.1242/dev.079400
112. Saldaña JI, Solanki A, Lau CI, Sahni H, Ross S, Furmanski AL, et al. Sonic Hedgehog Regulates Thymic Epithelial Cell Differentiation. *J Autoimmun* (2016) 68:86–97. doi: 10.1016/j.jaut.2015.12.004
113. Moore-Scott BA, Manley NR. Differential Expression of Sonic Hedgehog Along the Anterior–Posterior Axis Regulates Patterning of Pharyngeal Pouch Endoderm and Pharyngeal Endoderm-Derived Organs. *Dev Biol* (2005) 278(2):323–35. doi: 10.1016/j.ydbio.2004.10.027
114. Bain VE, Gordon J, O'Neil JD, Ramos I, Richie ER, Manley NR. Tissue-Specific Roles for Sonic Hedgehog Signaling in Establishing Thymus and Parathyroid Organ Fate. *Dev Camb Engl* (2016) 143(21):4027–37. doi: 10.1242/dev.141903
115. Garg V, Yamagishi C, Hu T, Kathiriya IS, Yamagishi H, Srivastava D. Tbx1, a DiGeorge Syndrome Candidate Gene, Is Regulated by Sonic Hedgehog During Pharyngeal Arch Development. *Dev Biol* (2001) 235(1):62–73. doi: 10.1006/dbio.2001.0283
116. Han L, Chaturvedi P, Kishimoto K, Koike H, Nasr T, Iwasawa K, et al. Single Cell Transcriptomics Identifies a Signaling Network Coordinating Endoderm and Mesoderm Diversification During Foregut Organogenesis. *Nat Commun* (2020) 11(1):4158. doi: 10.1038/s41467-020-17968-x
117. Davenport C, Diekmann U, Budde I, Detering N, Naujok O. Anterior–Posterior Patterning of Definitive Endoderm Generated From Human Embryonic Stem Cells Depends on the Differential Signaling of Retinoic Acid, Wnt-, and BMP-Signaling. *Stem Cells* (2016) 34(11):2635–47. doi: 10.1002/stem.2428
118. Green MD, Chen A, Nostro MC, d'Souza SL, Schaniel C, Lemischka IR, et al. Generation of Anterior Foregut Endoderm From Human Embryonic and Induced Pluripotent Stem Cells. *Nat Biotechnol* (2011) 29(3):267–72. doi: 10.1038/nbt.1788
119. Kearns NA, Genga RMJ, Ziller M, Kapinas K, Peters H, Brehm MA, et al. Generation of Organized Anterior Foregut Epithelia From Pluripotent Stem Cells Using Small Molecules. *Stem Cell Res* (2013) 11(3):1003–12. doi: 10.1016/j.scr.2013.06.007
120. Li LC, Wang X, Xu ZR, Wang YC, Feng Y, Yang L, et al. Single-Cell Patterning and Axis Characterization in the Murine and Human Definitive Endoderm. *Cell Res* (2021) 31(3):326–44. doi: 10.1038/s41422-020-00426-0
121. Nowotschin S, Setty M, Kuo YY, Liu V, Garg V, Sharma R, et al. The Emergent Landscape of the Mouse Gut Endoderm at Single-Cell Resolution. *Nature* (2019) 569(7756):361–7. doi: 10.1038/s41586-019-1127-1
122. Magaletta ME, Lobo M, Kernfeld EM, Aliee H, Huey JD, Parsons TJ, et al. Integration of Single-Cell Transcriptomes and Chromatin Landscapes Reveals Regulatory Programs Driving Pharyngeal Organ Development. *Nat Commun* (2022) 13(1):457. doi: 10.1038/s41467-022-28067-4
123. Lai L, Jin J. Generation of Thymic Epithelial Cell Progenitors by Mouse Embryonic Stem Cells. *Stem Cells* (2009) 27:3012–3020. doi: 10.1002/stem.238
124. Inami Y, Yoshikai T, Ito S, Nishio N, Suzuki H, Sakurai H, et al. Differentiation of Induced Pluripotent Stem Cells to Thymic Epithelial Cells by Phenotype. *Immunol Cell Biol* (2011) 89(2):314–21. doi: 10.1038/icb.2010.96
125. Soh CL, Giudice A, Jenny RA, Elliott DA, Hatzistavrou T, Micallef SJ, et al. FOXN1GFP/w Reporter hESCs Enable Identification of Integrin-β4, HLA-DR, and EpCAM as Markers of Human PSC-Derived FOXN1+ Thymic Epithelial Progenitors. *Stem Cell Rep* (2014) 2(6):925–37. doi: 10.1016/j.stemcr.2014.04.009
126. Parent AV, Russ HA, Khan IS, LaFlam TN, Metzger TC, Anderson MS, et al. Generation of Functional Thymic Epithelium From Human Embryonic Stem Cells That Supports Host T Cell Development. *Cell Stem Cell* (2013) 13(2):219–229. doi: 10.1016/j.stem.2013.04.004
127. Sun X, Xu J, Lu H, Liu W, Miao Z, Sui X, et al. Directed Differentiation of Human Embryonic Stem Cells Into Thymic Epithelial Progenitor-Like Cells Reconstitutes the Thymic Microenvironment *In Vivo*. *Cell Stem Cell* (2013) 13(2):230–6. doi: 10.1016/j.stem.2013.06.014
128. Su M, Hu R, Jin J, Yan Y, Song Y, Sullivan R, et al. Efficient *In Vitro* Generation of Functional Thymic Epithelial Progenitors From Human Embryonic Stem Cells. *Sci Rep* (2015) 5(1):1–8. doi: 10.1038/srep09882
129. Okabe M, Ito S, Nishio N, Tanaka Y, Isobe KI. Thymic Epithelial Cells Induced From Pluripotent Stem Cells by a Three-Dimensional Spheroid Culture System Regenerates Functional T Cells in Nude Mice. *Cell Reprogramming* (2015) 17(5):368–75. doi: 10.1089/cell.2015.0006
130. Otsuka R, Wada H, Tsuji H, Sasaki A, Murata T, Itoh M, et al. Efficient Generation of Thymic Epithelium From Induced Pluripotent Stem Cells That Prolongs Allograft Survival. *Sci Rep* (2020) 10(1):1–8. doi: 10.1038/s41598-019-57088-1
131. Chhatta AR, Cordes M, Hanegraaf MAJ, Vloemans S, Cupedo T, Cornelissen JJ, et al. *De Novo* Generation of a Functional Human Thymus From Induced Pluripotent Stem Cells. *J Allergy Clin Immunol* (2019) 144(5):1416–1419.e7. doi: 10.1016/j.jaci.2019.05.042
132. Ramos SA, Morton JJ, Yadav P, Reed B, Alizadeh SI, Shilleh AH, et al. Generation of Functional Human Thymic Cells From Induced Pluripotent Stem Cells. *J Allergy Clin Immunol* (2022) 149:767–781.e6. doi: 10.1016/j.jaci.2021.07.021
133. Gras-Peña R, Danzl NM, Khosravi-Maharlooei M, Campbell SR, Ruiz AE, Parks CA, et al. Human Stem Cell-Derived Thymic Epithelial Cells Enhance Human T-Cell Development in a Xenogeneic Thymus. *J Allergy Clin Immunol* (2022) 149:1755–1771. doi: 10.1016/j.jaci.2021.09.038
134. Kont V, Laan M, Kisand K, Merits A, Scott HS, Peterson P. Modulation of Aire Regulates the Expression of Tissue-Restricted Antigens. *Mol Immunol* (2008) 45(1):25–33. doi: 10.1016/j.molimm.2007.05.014
135. Pinto S, Schmidt K, Egle S, Stark HJ, Boukamp P, Kyewski B. An Organotypic Coculture Model Supporting Proliferation and Differentiation of Medullary Thymic Epithelial Cells and Promiscuous Gene Expression. *J Immunol* (2013) 190(3):1085–93. doi: 10.4049/jimmunol.1201843
136. Silva CS, Reis RL, Martins A, Neves NM. Recapitulation of Thymic Function by Tissue Engineering Strategies. *Adv Healthc Mater* 10:2100773. doi: 10.1002/adhm.202100773
137. Tajima A, Liu W, Pradhan I, Bertera S, Lakomy RA, Rudert WA, et al. Promoting 3-D Aggregation of FACS Purified Thymic Epithelial Cells With EAK 16-II/EAKIIH6 Self-Assembling Hydrogel. *J Vis Exp* (2016) 112):54062. doi: 10.3791/54062
138. Silva CS, Pinto RD, Amorim S, Pires RA, Correia-Neves M, Reis RL, et al. Fibronectin-Functionalized Fibrous Meshes as a Substrate to Support Cultures of Thymic Epithelial Cells. *Biomacromolecules* (2020) 21 (12):4771–80. doi: 10.1021/acs.biomac.0c00933
139. Suraiya AB, Hun ML, Truong VX, Forsythe JS, Chidgey AP. Gelatin-Based 3d Microgels for *In Vitro* T Lineage Cell Generation. *ACS Biomater Sci Eng* (2020) 6(4):2198–208. doi: 10.1021/acsbiomaterials.9b01610
140. Bortolomai I, Sandri M, Draghici E, Fontana E, Campodoni E, Marcovecchio GE, et al. Gene Modification and Three-Dimensional Scaffolds as Novel Tools to Allow the Use of Postnatal Thymic Epithelial Cells for Thymus Regeneration Approaches. *Stem Cells Transl Med* (2019) 8(10):1107–22. doi: 10.1002/sctm.18-0218
141. Asnaghi MA, Barthlott T, Gullotta F, Strusi V, Amovilli A, Hafen K, et al. Thymus Extracellular Matrix-Derived Scaffolds Support Graft-Resident Thymopoiesis and Long-Term *In Vitro* Culture of Adult Thymic Epithelial Cells. *Adv Funct Mater* (2021) 31:2010747. doi: 10.1002/adfm.202010747
142. Hun M, Barsanti M, Wong K, Ramshaw J, Werkmeister J, Chidgey AP. Native Thymic Extracellular Matrix Improves *In Vivo* Thymic Organoid T Cell Output, and Drives *In Vitro* Thymic Epithelial Cell Differentiation. *Biomaterials* (2017) 118:1–15. doi: 10.1016/j.biomaterials.2016.11.054

143. Fan Y, Tajima A, Goh SK, Geng X, Gualtierotti G, Grupillo M, et al. Bioengineering Thymus Organoids to Restore Thymic Function and Induce Donor-Specific Immune Tolerance to Allografts. *Mol Ther* (2015) 23(7):1262–77. doi: 10.1038/mt.2015.77
144. Seet CS, He C, Bethune MT, Li S, Chick B, Gschweng EH, et al. Generation of Mature T Cells From Human Hematopoietic Stem and Progenitor Cells in Artificial Thymic Organoids. *Nat Methods* (2017) 14(5):521–30. doi: 10.1038/nmeth.4237
145. Montel-Hagen A, Sun V, Casero D, Tsai S, Zampieri A, Jackson N, et al. *In Vitro* Recapitulation of Murine Thymopoiesis From Single Hematopoietic Stem Cells. *Cell Rep* (2020) 33(4):108320. doi: 10.1016/j.celrep.2020.108320
146. Montel-Hagen A, Seet CS, Li S, Chick B, Zhu Y, Chang P, et al. Organoid-Induced Differentiation of Conventional T Cells From Human Pluripotent Stem Cells. *Cell Stem Cell* (2019) 24(3):376–389.e8. doi: 10.1016/j.stem.2018.12.011
147. Kennedy M, Awong G, Sturgeon CM, Ditadi A, LaMotte-Mohs R, Zúñiga-Pflücker JC, et al. T Lymphocyte Potential Marks the Emergence of Definitive Hematopoietic Progenitors in Human Pluripotent Stem Cell Differentiation Cultures. *Cell Rep* (2012) 2(6):1722–35. doi: 10.1016/j.celrep.2012.11.003
148. Bin G, Jiarong Z, Shihao W, Xiuli S, Cheng X, Liangbiao C, et al. Aire Promotes the Self-Renewal of Embryonic Stem Cells Through Lin28. *Stem Cells Dev* (2012) 21(15):2878–90. doi: 10.1089/scd.2012.0097
149. Gu B, Zhang J, Chen Q, Tao B, Wang W, Zhou Y, et al. Aire Regulates the Expression of Differentiation-Associated Genes and Self-Renewal of Embryonic Stem Cells. *Biochem Biophys Res Commun* (2010) 394(2):418–23. doi: 10.1016/j.bbrc.2010.03.042
150. Karvonen E, Krohn KJE, Ranki A, Hau A. Generation and Characterization of iPS Cells Derived From APECED Patients for Gene Correction. *Front Endocrinol* (2022) 13:794327. doi: 10.3389/fendo.2022.794327
151. Forbes TA, Howden SE, Lawlor K, Phipson B, Maksimovic J, Hale L, et al. Patient-iPSC-Derived Kidney Organoids Show Functional Validation of a Ciliopathic Renal Phenotype and Reveal Underlying Pathogenetic Mechanisms. *Am J Hum Genet* (2018) 102(5):816–31. doi: 10.1016/j.ajhg.2018.03.014
152. Deng WL, Gao ML, Lei XL, Lv JN, Zhao H, He KW, et al. Gene Correction Reverses Ciliopathy and Photoreceptor Loss in iPSC-Derived Retinal Organoids From Retinitis Pigmentosa Patients. *Stem Cell Rep* (2018) 10 (4):1267–81. doi: 10.1016/j.stemcr.2018.02.003
153. Okada H, Nakanishi C, Yoshida S, Shimojima M, Yokawa J, Mori M, et al. Function and Immunogenicity of Gene-Corrected iPSC-Derived Hepatocyte-Like Cells in Restoring Low Density Lipoprotein Uptake in Homozygous Familial Hypercholesterolemia. *Sci Rep* (2019) 9(1):4695. doi: 10.1038/s41598-019-41056-w
154. Howden SE, McColl B, Glaser A, Vadolas J, Petrou S, Little MH, et al. A Cas9 Variant for Efficient Generation of Indel-Free Knockin or Gene-Corrected Human Pluripotent Stem Cells. *Stem Cell Rep* (2016) 7(3):508–17. doi: 10.1016/j.stemcr.2016.07.001
155. Kreins AY, Bonfanti P, Davies EG. Current and Future Therapeutic Approaches for Thymic Stromal Cell Defects. *Front Immunol* (2021) 12:655354. doi: 10.3389/fimmu.2021.655354
156. Besnard M, Sérazin C, Ossart J, Moreau A, Vimond N, Flippe L, et al. Anti-CD45RC Antibody Immunotherapy Prevents and Treats Experimental Autoimmune Polyendocrinopathy–Candidiasis–Ectodermal Dystrophy Syndrome. *J Clin Invest* (2022) 132:e156507. doi: 10.1172/JCI156507

Conflict of Interest: The authors declare that the research was conducted in the absence of any commercial or financial relationships that could be construed as a potential conflict of interest.

Publisher's Note: All claims expressed in this article are solely those of the authors and do not necessarily represent those of their affiliated organizations, or those of the publisher, the editors and the reviewers. Any product that may be evaluated in this article, or claim that may be made by its manufacturer, is not guaranteed or endorsed by the publisher.

Copyright © 2022 Provin and Giraud. This is an open-access article distributed under the terms of the Creative Commons Attribution License (CC BY). The use, distribution or reproduction in other forums is permitted, provided the original author(s) and the copyright owner(s) are credited and that the original publication in this journal is cited, in accordance with accepted academic practice. No use, distribution or reproduction is permitted which does not comply with these terms.

RESEARCH ARTICLE

Thymocytes trigger self-antigen-controlling pathways in immature medullary thymic epithelial stages

Noella Lopes[1], Nicolas Boucherit[1†], Jérémy C Santamaria[1†], Nathan Provin[2†], Jonathan Charaix[1], Pierre Ferrier[1], Matthieu Giraud[2], Magali Irla[1*]

[1]Aix-Marseille University, CNRS, INSERM, Centre d'Immunologie de Marseille-Luminy, Marseille, France; [2]Nantes Université, INSERM, Center for Research in Transplantation and Translational Immunology, UMR 1064, Nantes, France

Abstract Interactions of developing T cells with Aire$^+$ medullary thymic epithelial cells expressing high levels of MHCII molecules (mTEC^{hi}) are critical for the induction of central tolerance in the thymus. In turn, thymocytes regulate the cellularity of Aire$^+$ mTEC^{hi}. However, it remains unknown whether thymocytes control the precursors of Aire$^+$ mTEC^{hi} that are contained in mTEC^{lo} cells or other mTEC^{lo} subsets that have recently been delineated by single-cell transcriptomic analyses. Here, using three distinct transgenic mouse models, in which antigen presentation between mTECs and CD4$^+$ thymocytes is perturbed, we show by high-throughput RNA-seq that self-reactive CD4$^+$ thymocytes induce key transcriptional regulators in mTEC^{lo} and control the composition of mTEC^{lo} subsets, including Aire$^+$ mTEC^{hi} precursors, post-Aire and tuft-like mTECs. Furthermore, these interactions upregulate the expression of tissue-restricted self-antigens, cytokines, chemokines, and adhesion molecules important for T-cell development. This gene activation program induced in mTEC^{lo} is combined with a global increase of the active H3K4me3 histone mark. Finally, we demonstrate that these self-reactive interactions between CD4$^+$ thymocytes and mTECs critically prevent multiorgan autoimmunity. Our genome-wide study thus reveals that self-reactive CD4$^+$ thymocytes control multiple unsuspected facets from immature stages of mTECs, which determines their heterogeneity.

***For correspondence:** Magali.Irla@inserm.fr

†These authors contributed equally to this work

Competing interest: The authors declare that no competing interests exist.

Funding: See page 26

Preprinted: 29 November 2020
Received: 03 May 2021
Accepted: 14 January 2022
Published: 21 February 2022

Reviewing Editor: Sarah Russell, Peter MacCallum Cancer Centre, Australia

© Copyright Lopes *et al*. This article is distributed under the terms of the Creative Commons Attribution License, which permits unrestricted use and redistribution provided that the original author and source are credited.

Editor's evaluation

This manuscript is of interest to readers in the field of immunology and especially in the induction of immune tolerance in the thymus. The work uses several mouse models to substantially broaden the current understanding of MHCII/TCR-mediated cell-cell crosstalk in the thymus and suggests a novel mechanism that contributes to the generation of functional and self-tolerant T-cells.

Introduction

The thymic medulla ensures the generation of a self-tolerant T-cell repertoire (***Klein et al., 2014***; ***Lopes et al., 2015***). By their unique ability to express tissue-restricted self-antigens (TRAs) (***Derbinski et al., 2001***; ***Sansom et al., 2014***), medullary thymic epithelial cells (mTECs) promote the development of Foxp3$^+$ regulatory T cells and the deletion by apoptosis of self-reactive thymocytes capable of inducing autoimmunity (***Klein et al., 2019***). The expression of TRAs that mirrors body's self-antigens is controlled by Aire (*Autoimmune regulator*) and Fezf2 (*Fez family zinc finger 2*) transcription factors (***Anderson et al., 2002***; ***Takaba et al., 2015***). Aire-dependent TRAs are generally characterized by a repressive chromatin state enriched in the trimethylation of lysine-27 of histone H3 (H3K27me3)

histone mark (**Handel et al., 2018**; **Org et al., 2009**; **Sansom et al., 2014**). In accordance with their essential role in regulating the expression of TRAs, *Aire*$^{-/-}$ and *Fezf2*$^{-/-}$ mice show defective clonal deletion of autoreactive thymocytes and develop signs of autoimmunity in several peripheral tissues (**Anderson et al., 2002**; **Takaba et al., 2015**).

Based on the level of the co-expressed MHC class II and CD80 molecules, mTECs were initially subdivided into mTEC^{lo} (MHCII^{lo}CD80^{lo}) and mTEC^{hi} (MHCII^{hi}CD80^{hi}) (**Gray et al., 2006**). The relationship between these two subsets has been established with reaggregate thymus organ cultures in which mTEC^{lo} give rise to mature Aire^{+} mTEC^{hi} (**Gäbler et al., 2007**; **Gray et al., 2007**). Although mTEC^{hi} express a highly diverse array of TRAs under Aire's action that releases stalled RNA polymerase and modulates chromatin accessibility, mTEC^{lo} already express a substantial amount of TRAs (**Derbinski et al., 2005**; **Giraud et al., 2012**; **Koh et al., 2018**; **Kyewski and Klein, 2006**; **Sansom et al., 2014**). Recent single-cell transcriptomic analyses indicate that the heterogeneity of mTECs, especially in the mTEC^{lo} compartment, is more complex than previously thought (**Irla, 2020**; **Kadouri et al., 2020**). mTEC^{lo} with low or no expression of CD80 have been shown to be divided into three main subsets: CCL21^{+} mTECs, implicated in the attraction of positively selected thymocytes in the medulla (**Lkhagvasuren et al., 2013**), involucrin^{+}TPA^{hi} post-Aire mTECs corresponding to the ultimate mTEC differentiation stage (**Metzger et al., 2013**; **Michel et al., 2017**; **Nishikawa et al., 2010**), and the newly reported tuft-like mTECs that show properties of gut chemosensory epithelial tuft cells expressing the doublecortin-like kinase 1 (DCLK1) marker (**Bornstein et al., 2018**; **Miller et al., 2018**). Based on single-cell transcriptomic analyses, mTECs were then classified into four major groups encompassing mTEC I:CCL21^{+} mTECs, mTEC II:Aire^{+} mTECs, mTEC III:post-Aire mTECs, and mTEC IV:tuft-like mTECs (**Bornstein et al., 2018**). Furthermore, mTEC^{lo} with intermediate levels of CD80 and MHCII lie into mTEC single-cell clusters that are defined as proliferating and maturational, expressing Fezf2 and preceding the Aire^{+} mTEC^{hi} stage (**Baran-Gale et al., 2020**; **Dhalla et al., 2020**). These transit-amplifying cells were recently referred as to as TAC-TECs (**Wells et al., 2020**).

In the postnatal thymus, while mTECs control the selection of thymocytes, conversely CD4^{+} thymocytes control the cellularity of Aire^{+} mTEC^{hi} by activating RANK and CD40-induced NF-κb signaling pathways (**Akiyama et al., 2008**; **Hikosaka et al., 2008**; **Irla, 2020**; **Irla et al., 2008**). These bidirectional interactions between mTECs and thymocytes are commonly referred to as thymic crosstalk (**Lopes et al., 2015**; **van Ewijk et al., 1994**). However, it remains unknown whether CD4^{+} thymocytes act exclusively on mature Aire^{+} mTEC^{hi} or upstream on their TAC-TEC precursors contained in mTEC^{lo} and whether the development of the newly identified Fezf2^{+}, post-Aire, and tuft-like subsets is regulated or not by CD4^{+} thymocytes.

In this study, using high-throughput RNA-sequencing (RNA-seq), we show that self-reactive CD4^{+} thymocytes induce in mTEC^{lo} pivotal transcriptional regulators for their differentiation and function. Accordingly, self-reactive CD4^{+} thymocytes control the composition of the mTEC^{lo} compartment, that is the precursors of Aire^{+} mTEC^{hi}, post-Aire cells, and tuft-like mTECs. Our data also reveal that self-reactive CD4^{+} thymocytes upregulate in mTEC^{lo} the expression of TRAs, chemokines, cytokines, and adhesion molecules involved in T-cell development. This gene activation program correlates with increased levels of the active trimethylation of lysine-4 of histone 3 (H3K4me3) mark, including the loci of Fezf2-dependent and Aire/Fezf2-independent TRAs, indicative of an epigenetic regulation for their expression. Finally, we demonstrate that disrupted MHCII/TCR interactions between mTECs and CD4^{+} thymocytes lead to the generation of mature T cells containing self-specificities capable of inducing multiorgan autoimmunity. Altogether, our genome-wide study reveals that self-reactive CD4^{+} thymocytes control the developmental transcriptional programs of mTEC^{lo}, which conditions their differentiation and function as inducers of T-cell tolerance.

Results

CD4^{+} thymocytes induce key transcriptional programs in mTEC^{lo} cells

Several NF-κb members are involved in Aire^{+} mTEC^{hi} development (**Burkly et al., 1995**; **Lomada et al., 2007**; **Riemann et al., 2017**; **Shen et al., 2019**; **Zhang et al., 2006**). However, it remains unclear whether the NF-κb or other signaling pathways are activated by CD4^{+} thymocytes specifically in mTEC^{lo} cells. To investigate the effects of CD4^{+} thymocytes in mTEC^{lo}, we used mice deficient in CD4^{+} thymocytes (ΔCD4 mice) because they lack the promoter IV of the class II transactivator

(*Ciita*) gene that controls MHCII expression in cortical TECs (cTECs) (**Waldburger et al., 2003**). We first analyzed by flow cytometry the total and phosphorylated forms of IKKα, p65, and RelB NF-κb members and p38 and Erk1/2 MAPK proteins in mTEC^{lo} from ΔCD4 mice according to the gating strategy shown in **Figure 1—figure supplement 1A**. Interestingly, the phosphorylation level of IKKα and p38 MAPK was substantially reduced in ΔCD4 mice (**Figure 1A and B**, **Figure 1—figure supplement 2**), indicating that CD4$^+$ thymocytes may have an impact in mTEC^{lo} by activating the IKKα intermediate of the nonclassical NF-κB pathway and the p38 MAPK pathway.

To gain insights into the effects of CD4$^+$ thymocytes in mTEC^{lo}, we analyzed by high-throughput RNA-seq the gene expression profiles of mTEC^{lo} purified from WT and ΔCD4 mice (**Figure 1—figure supplement 1B**). We found that CD4$^+$ thymocytes upregulated 989 genes (fold change [FC] >2) reaching significance for 248 of them (Cuffdiff p<0.05) (**Figure 1C**). 957 genes were also downregulated (FC < 0.5) with 178 genes reaching significance (Cuffdiff p<0.05). We analyzed whether the genes significantly up- or downregulated by CD4$^+$ thymocytes corresponded to TRAs, as defined by an expression restricted to 1–5 of peripheral tissues (**Sansom et al., 2014**). Interestingly, the genes upregulated by CD4$^+$ thymocytes exhibited approximately fourfold more of TRAs over non-TRAs (**Figure 1D**, left panel). The comparison of the proportion of TRAs among the upregulated genes with those of the genome revealed a strong statistical TRA overrepresentation ($p=5.2 \times 10^{-10}$) (**Figure 1D**, right panel). Most of the TRAs upregulated by CD4$^+$ thymocytes were sensitive to the action of Aire (Aire-dependent TRAs) or controlled by Aire and Fezf2-independent mechanisms (Aire/Fezf2-independent TRAs) (**Figure 1E**, **Supplementary file 1**). The upregulation of some of these TRAs by CD4$^+$ thymocytes was confirmed by qPCR in mTEC^{lo} purified from ΔCD4 mice (**Figure 1F**). The same results were observed with mTEC^{lo} purified from MHCII$^{-/-}$ mice, also lacking CD4$^+$ thymocytes, excluding any potential indirect effect of CIITA in the phenotype observed in ΔCD4 mice (**Figure 1—figure supplement 3A**).

Remarkably, among the non-TRAs upregulated by CD4$^+$ thymocytes in mTEC^{lo}, 37 corresponded to 50 mTEC-specific transcription factors that are induced by the histone deacetylase 3 (HDAC3) (**Goldfarb et al., 2016**; **Figure 1G**). Some of them, such as the interferon regulatory factor 4 (*Irf4*), *Irf7,* and the Ets transcription factor member, *Spib,* are known to regulate mTEC differentiation and function (**Akiyama et al., 2014**; **Haljasorg et al., 2017**; **Otero et al., 2013**). We also identified other transcription factors such as *Nfkb2*, *Trp53,* and *Relb* implicated in mTEC differentiation (**Riemann et al., 2017**; **Rodrigues et al., 2017**; **Zhang et al., 2006**). Finally, we found that CD4$^+$ thymocytes upregulate in mTEC^{lo} the expression of some cytokines and cell adhesion molecules such as integrins and cadherins (**Figure 1H**, **Figure 1—figure supplement 3B**). Given that mTEC^{lo} are heterogeneous (**Irla, 2020**; **Kadouri et al., 2020**), we then analyzed whether the cytokines and adhesion molecules, which are upregulated by CD4$^+$ thymocytes, are specific to a particular subset of mTEC^{lo}. To this end, we reanalyzed single-cell RNA-seq data performed on total CD45$^-$EpCAM$^+$ TECs (**Wells et al., 2020**). Single cells were projected into a UMAP reduced-dimensional space and, using the 15 first principal components, six clusters were obtained, as in **Wells et al., 2020** (**Figure 1—figure supplement 4A**). Well-established markers were used to distinguish the different TEC subsets such as *Psmb11* and *Prss16* for cTECs, *Ccl21a* and *Krt5* for CCL21$^+$ mTECs (also called mTEC I), *Stmn1, Ska1, Fezf2* and *Aire* for TAC-TECs, *Aire* and *Fezf2* for Aire$^+$ mTECs (also called mTEC II), *Pigr* and *Cldn3* for post-Aire mTECs (also called mTEC III), and *Avil* and *Pou2f3* for tuft-like mTECs (also called mTEC IV) (**Figure 1—figure supplement 4B**). In contrast to CCL21$^+$ mTECs, some genes upregulated by CD4$^+$ thymocytes were expressed by tuft-like mTECs (**Figure 1I**). Interestingly, many genes encoding for cytokines and cell adhesion molecules were associated with Aire$^+$ mTECs and post-Aire cells with some of them already expressed in TAC-TECs, suggesting that CD4$^+$ thymocytes may act upstream of Aire$^+$ mTEC^{hi}. These results thus provide the first evidence that CD4$^+$ thymocytes are able to induce in mTEC^{lo} essential transcriptional regulators for mTEC differentiation and function as well as TRAs, adhesion molecules, and cytokines.

CD4$^+$ thymocytes regulate maturational programs in mTEC^{lo} through MHCII/TCR interactions

We next investigated by which mechanism CD4$^+$ thymocytes regulate the transcriptional programs of mTEC^{lo}. Given that MHCII/TCR interactions with mTECs are critical for CD4$^+$ T-cell selection (**Klein et al., 2019**), we hypothesized that these interactions could play an important role in initiating

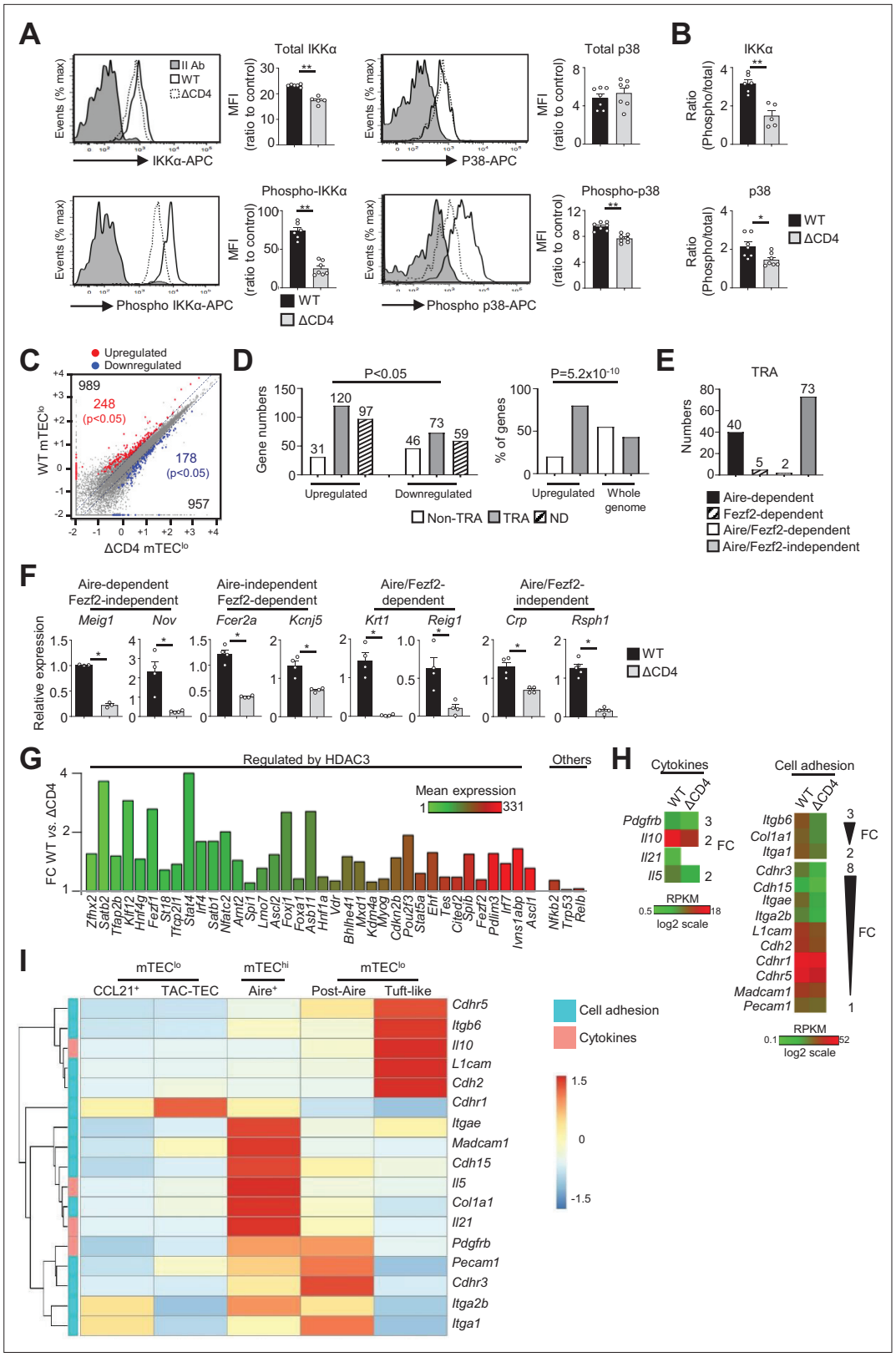

Figure 1. The transcriptional profile and IKKα and p38 MAPK signaling pathways are impaired in mTEC^{lo} of ΔCD4 mice. (**A, B**) Total IKKα, p38 MAPK, phospho-IKKα(Ser180)/IKKβ(Ser181), and p38 MAPK (Thr180/Tyr182) (**A**) and the ratio of phospho/total proteins (**B**) analyzed by flow cytometry in mTEC^{lo} from WT and ΔCD4 mice. Data are representative of two independent experiments (n = 3–4 mice per group and experiment). (**C**) Scatter

Figure 1 continued on next page

Figure 1 continued

plot of gene expression levels (fragments per kilobase of transcript per million mapped reads [FPKM]) of mTEC^{lo} from WT versus ΔCD4 mice. Genes with fold difference ≥2 and p-adj<0.05 were considered as upregulated or downregulated genes (red and blue dots, respectively). RNA-seq was performed on two independent biological replicates with mTEC^{lo} derived from 3 to 5 mice. (**D**) Numbers of tissue-restricted self-antigens (TRAs) and non-TRAs in genes up- and downregulated (left panel) and the proportion of upregulated TRAs compared to those in the all genome (right panel). ND, not determined. (**E**) Numbers of induced Aire-dependent, Fezf2-dependent, Aire/Fezf2-dependent, and Aire/Fezf2-independent TRAs. (**F**) The expression of Aire-dependent (*Meig1, Nov*), Fezf2-dependent (*Fcer2a, Kcnj5*), Aire/Fezf2-dependent (*Krt1, Reig1*), and Aire/Fezf2-independent (*Crp, Rsph1*) TRAs measured by qPCR in WT (n = 3–4) and ΔCD4 (n = 3–4) mTEC^{lo}. (**G**) Expression fold change in HDAC3-induced transcriptional regulators and other transcription factors significantly upregulated in WT versus ΔCD4 mTEC^{lo}. The color code represents gene expression level. (**H**) Heatmaps of genes encoding for cell adhesion molecules and cytokines that were significantly downregulated in mTEC^{lo} from ΔCD4 mice. (**I**) Hierarchical clustering and heatmap of mean expression of these cell adhesion molecules and cytokines in mTEC subsets identified by scRNA-seq. Error bars show mean ± SEM, *p<0.05, **p<0.01 using two-tailed Mann–Whitney test for (**A**), (**B**) and (**F**) and chi-squared test for (**D**).

The online version of this article includes the following figure supplement(s) for figure 1:

Figure supplement 1. Gating strategy used to purify mTEC^{lo} cells.

Figure supplement 2. Normal total and phosphorylated p65, RelB, and Erk1/2 proteins in mTEC^{lo} from ΔCD4 mice.

Figure supplement 3. Impaired TRA expression in mTEC^{lo} from MHCII$^{-/-}$ mice.

Figure supplement 4. Identification of thymic epithelial cell (TEC) subsets by single-cell RNA-seq.

transcriptional programs that govern the functional and developmental properties of mTEC^{lo}. To this end, we used a unique transgenic mouse model in which MHCII expression is selectively abrogated in mTECs (mTEC$^{\Delta MHCII}$ mice) (***Irla et al., 2008***). In contrast to their WT counterparts, we found that $OVA_{323-339}$-loaded mTECs from mTEC$^{\Delta MHCII}$ mice were ineffective at activating OTII-specific CD4$^+$ T cells, demonstrating that the capacity of antigen presentation of mTECs to CD4$^+$ T cells is impaired in these mice (***Figure 2A***).

The comparison of the gene expression profiles of mTEC^{lo} purified from WT and mTEC$^{\Delta MHCII}$ mice (***Figure 1—figure supplement 1B***) revealed that MHCII/TCR interactions with CD4$^+$ thymocytes resulted in the upregulation of 1300 genes (FC > 2), 449 of them reaching statistical significance (Cuffdiff p<0.05). 846 genes were also downregulated (FC < 0.5) with 340 reaching significance (Cuffdiff p<0.05) (***Figure 2B***). Similarly to the comparison of WT versus ΔCD4 mice (***Figure 1D***), the genes significantly upregulated by MHCII/TCR interactions in mTEC^{lo} corresponded preferentially to TRAs ($p=4.5 \times 10^{-13}$) that are mainly Aire-dependent and Aire/Fezf2-independent (***Figure 2C–E***, ***Supplementary file 2***). In line with the recent discovery of *Aire* expression in mTECs expressing intermediate levels of CD80 identified in the proliferating and maturational stage mTEC single-cell clusters (***Dhalla et al., 2020***), we found a strong correlation ($p=2 \times 10^{-16}$) between gene upregulation induced by MHCII/TCR interactions and the responsiveness of genes to Aire's action obtained from the comparison between WT and *Aire*$^{-/-}$ mTEC^{hi} (***Figure 2F***). These data are in agreement with the identification of a list of activation factors including *Aire* among the non-TRA genes induced by MHCII/TCR interactions with CD4$^+$ thymocytes in mTEC^{lo} (***Figure 2G***). mTEC^{lo} from mTEC$^{\Delta MHCII}$ mice expressed ~4.5-fold less *Aire* than WT mTEC^{lo}, with substantial levels of 15.8 and 73.7 fragments per kilobase of transcript per million mapped reads (FPKM), respectively. For comparison, *Aire* expression level in WT mTEC^{hi} was 448.9 FPKM. mTEC^{lo} from mTEC$^{\Delta MHCII}$ mice also expressed ~1.5-fold less *Fezf2* than WT mTEC^{lo} (90.2 versus 134.5 FPKM, respectively). This reduction in *Aire* and *Fezf2* expression in mTEC$^{\Delta MHCII}$ mice was also confirmed by qPCR (***Figure 2H***). These results highlight the importance of MHCII/TCR interactions with CD4$^+$ thymocytes in upregulating *Aire* and *Fezf2* mRNAs and some of their associated TRAs in mTEC^{lo}. Interestingly, 17 HDAC3-regulated transcription factors as well as *Nfkb2*, *Trp53,* and *Relb* transcription factors were induced by MHCII/TCR interactions with CD4$^+$ thymocytes (***Figure 2I***). Moreover, the expression of several cytokines, chemokines, and cell adhesion molecules was also upregulated (***Figure 2J***, ***Figure 2—figure supplement 1A***). Using single-cell RNA-seq data (***Figure 1—figure supplement 4***), we found that these genes were poorly associated with CCL21$^+$ and tuft-like mTEC^{lo} (***Figure 2K***). Consistently with the altered cellularity of Aire$^+$ mTECs in mTEC$^{\Delta MHCII}$

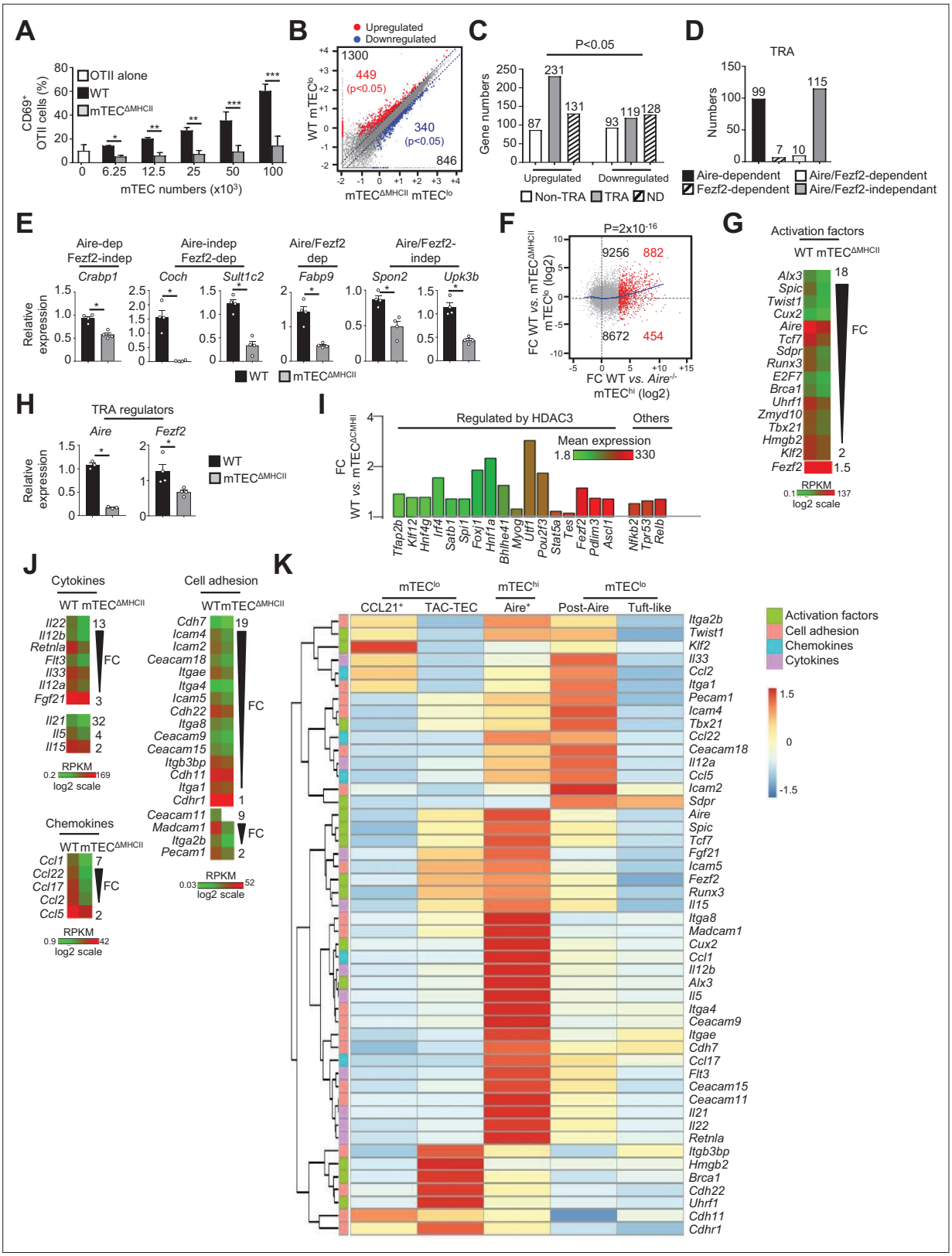

Figure 2. The transcriptional and functional properties of mTEC^{lo} are impaired in mTEC$^{\Delta MHCII}$ mice. (**A**) Percentages of CD69^{+} OTII CD4^{+} T cells cultured or not with variable numbers of OVA$_{323-339}$-loaded WT or mTEC$^{\Delta MHCII}$ mTECs derived from two independent experiments (n = 2–3 mice per group and experiment). (**B**) Scatter plot of gene expression levels (fragments per kilobase of transcript per million mapped reads [FPKM]) of mTEC^{lo} from WT versus mTEC$^{\Delta MHCII}$ mice. Genes with fold difference ≥2 and p-adj<0.05 were considered as upregulated or downregulated genes (red and blue dots,

Figure 2 continued on next page

Figure 2 continued

respectively). RNA-seq was performed on two independent biological replicates with mTEC^{lo} derived from 3 to 5 mice. (**C**) Numbers of tissue-restricted self-antigens (TRAs) and non-TRAs in genes up- and downregulated in mTEC^{lo} from WT versus mTEC$^{\Delta MHCII}$ mice. ND, not determined. (**D**) Numbers of induced TRAs regulated or not by Aire and/or Fezf2. (**E**) Aire-dependent (*Crabp1*), Fezf2-dependent (*Coch, Sult1c2*), Aire/Fezf2-dependent (*Fabp9*), and Aire/Fezf2-independent (*Spon2, Upk3b*) TRAs were measured by qPCR in mTEC^{lo} from WT (n = 4) and mTEC$^{\Delta MHCII}$ (n = 4) mice. (**F**) Scatter plot of gene expression variation in mTEC^{lo} from WT versus mTEC$^{\Delta MHCII}$ mice and in mTEC^{hi} from WT versus *Aire*$^{-/-}$ mice. The loess fitted curve is shown in blue and the induced Aire-dependent genes (fold change [FC] > 5) in red. (**G**) Heatmap of significantly downregulated activation factors in mTEC^{lo} from mTEC$^{\Delta MHCII}$ mice. (**H**) *Aire* and *Fezf2* mRNAs were measured by qPCR in mTEC^{lo} from WT (n = 3–4) and mTEC$^{\Delta MHCII}$ (n = 4) mice. (**I**) FC in the expression of HDAC3-induced transcriptional regulators and other transcription factors significantly upregulated in WT versus mTEC$^{\Delta MHCII}$ mice. The color code represents gene expression level. (**J**) Heatmap of significantly downregulated cytokines, chemokines, and cell adhesion molecules in mTEC^{lo} from mTEC$^{\Delta MHCII}$ mice. (**K**) Hierarchical clustering and heatmap of mean expression of these activation factors, cell adhesion molecules, chemokines, and cytokines in mTEC subsets identified by scRNA-seq. Error bars show mean ± SEM, *p<0.05, **p<0.01, ***p<0.001 using two-tailed Mann–Whitney test for (**A**), (**E**) and (**H**) and chi-squared test for (**C**) and (**F**).

The online version of this article includes the following figure supplement(s) for figure 2:

Figure supplement 1. Altered expression of some cytokines, cell adhesion molecules, and chemokines in mTEC^{lo} from mTEC$^{\Delta MHCII}$ mice.

mice (***Irla et al., 2008***), some of these genes were associated with post-Aire cells. Strikingly, many genes upregulated by CD4$^+$ thymocytes in mTEC^{lo} were highly expressed by Aire$^+$ mTECs. Interestingly, several of these genes were already expressed by TAC-TECs, including *Aire* and *Fezf2*, strongly suggesting that an enhanced transcriptional activity promoted by MHCII/TCR interactions with CD4$^+$ thymocytes accompanies the transition from TAC-TECs to Aire$^+$ mTECs. Altogether, these data show that CD4$^+$ thymocytes, through MHCII/TCR interactions, control the functional properties of mTEC^{lo} and activate key transcriptional programs governing their differentiation and function.

TCR/MHCII interactions with CD4$^+$ thymocytes regulate the development of Fezf2$^+$ pre-Aire, post-Aire, and tuft-like mTEC subsets

Since key transcription factors implicated in mTEC differentiation were upregulated in mTEC^{lo} by MHCII/TCR-mediated interactions with CD4$^+$ thymocytes (***Figures 1G and 2I***), we next analyzed the composition for the newly identified mTEC subsets in ΔCD4 and mTEC$^{\Delta MHCII}$ mice. In agreement with our previous study (***Irla et al., 2008***), we first observed a substantial reduction in the frequencies and numbers of mTEC^{hi} in both mice (***Figure 3A***). Furthermore, numbers of mTEC^{lo} were also substantially reduced. Consequently, ΔCD4 and mTEC$^{\Delta MHCII}$ mice have a globally reduced cellularity in total mTECs. An Aire/Fezf2 co-staining both by histology and flow cytometry then revealed a substantial reduction in Aire$^-$Fezf2$^+$ and Aire$^+$Fezf2$^+$ cells (***Figure 3B and C***). We further analyzed by flow cytometry Aire and Fezf2 expression specifically in mTEC^{lo} and mTEC^{hi}, according to the gating strategy shown in ***Figure 1—figure supplement 1A***. In agreement with the detection of *Aire* in the proliferating and maturational single-cell clusters in mTEC^{lo} (***Baran-Gale et al., 2020***; ***Dhalla et al., 2020***; ***Wells et al., 2020***), we found that Aire protein was expressed in a small fraction of mTEC^{lo} compared to mTEC^{hi} in WT, ΔCD4, and mTEC$^{\Delta MHCII}$ mice (***Figure 3C***). Aire$^-$Fezf2$^+$ and Aire$^+$Fezf2$^+$ mTECs were reduced in mTEC^{lo} of ΔCD4 and mTEC$^{\Delta MHCII}$ mice with a more marked effect in mTEC^{hi}. This decrease was not due to impaired proliferation since normal frequencies of Ki-67$^+$ proliferating cells were observed in ΔCD4 and mTEC$^{\Delta MHCII}$ mice (***Figure 3—figure supplement 1***). Furthermore, numbers of involucrin$^+$TPA$^+$Aire$^-$ post-Aire cells were reduced in the medulla of ΔCD4 and mTEC$^{\Delta MHCII}$ mice (***Figure 3—figure supplement 2A***), consistently with the decrease of Aire$^+$ mTEC^{hi} (***Figure 3B and C***). In contrast, the frequencies of CCL21$^+$ cells among mTEC^{lo} were not altered in ΔCD4 and mTEC$^{\Delta MHCII}$ mice (***Figure 3D***). This is in line with the observation that few genes upregulated by TCR/MHCII interactions with CD4$^+$ thymocytes were associated with CCL21$^+$ mTECs (***Figures 1I and 2K***). We also analyzed tuft-like mTECs since the expression of the transcription factor *Pou2f3*, known to control the development of this cell type (***Bornstein et al., 2018***; ***Miller et al., 2018***), was decreased in mTEC^{lo} of ΔCD4 and mTEC$^{\Delta MHCII}$ mice (***Figures 1G and 2I***). We found that numbers of tuft-like mTECs identified by flow cytometry using the DCLK1 marker were reduced in both mice (***Figure 3E***, ***Figure 3—figure supplement 2B***), indicating that their development is promoted by MHCII/TCR interactions with CD4$^+$ thymocytes. Importantly, Aire$^-$Fezf2$^+$ and Aire$^+$Fezf2$^+$ mTEC^{lo} and mTEC^{hi} as well as CCL21$^+$ and DCLK1$^+$ tuft-like mTEC^{lo} were similarly reduced in MHCII$^{-/-}$ mice, further confirming that CD4$^+$ thymocytes control the cellularity of these novel mTEC subsets (***Figure 3—figure supplement 3***).

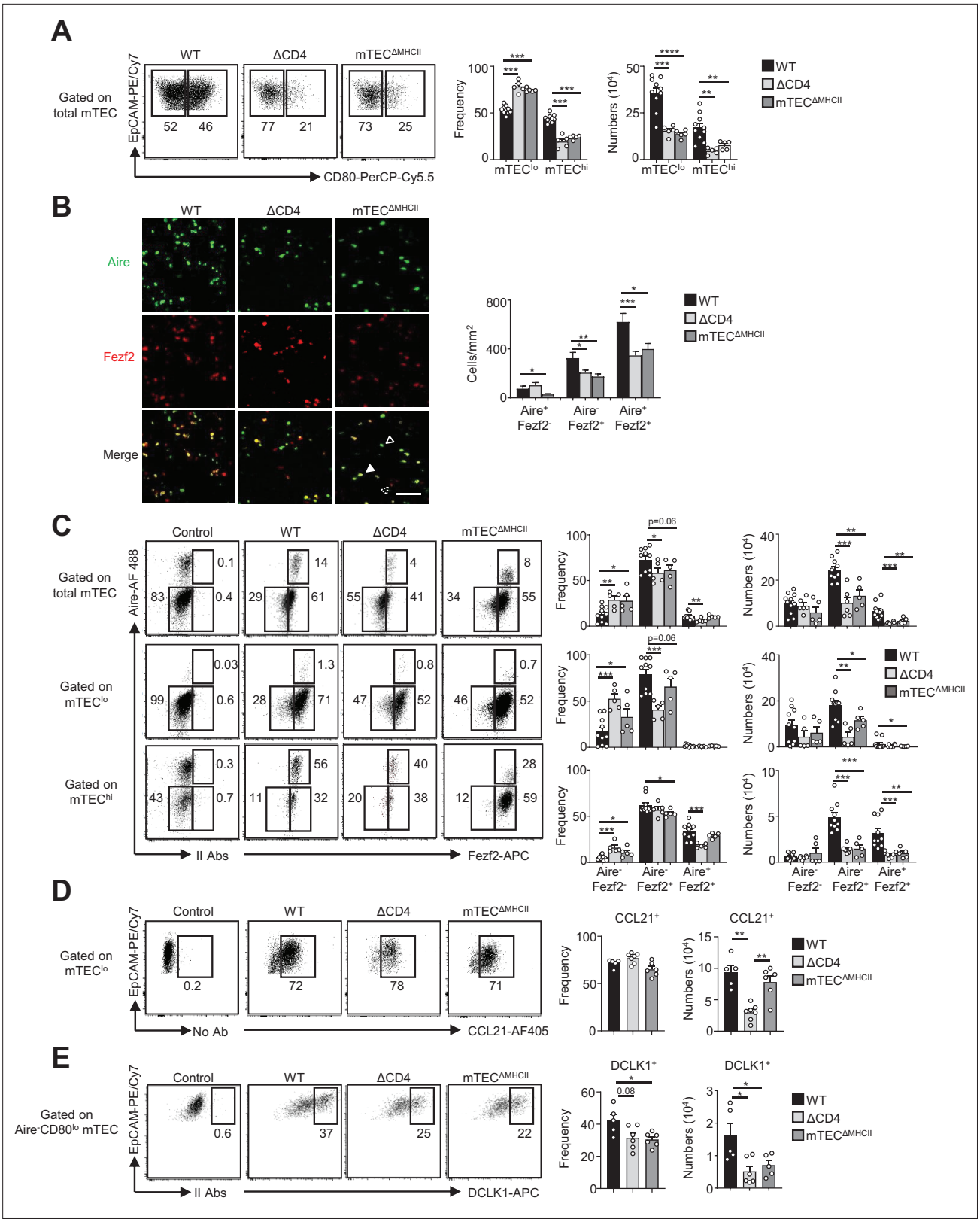

Figure 3. The composition in medullary thymic epithelial cell (mTEC) subsets is altered in ΔCD4 and mTEC$^{\Delta MHCII}$ mice. (**A**) Flow cytometry profiles, frequencies, and numbers of mTEC^{lo} and mTEC^{hi} in WT, ΔCD4, and mTEC$^{\Delta MHCII}$ mice. Data are representative of 2–3 independent experiments (n = 2–5 mice per group and experiment). (**B**) Confocal images of thymic sections from WT, ΔCD4, and mTEC$^{\Delta MHCII}$ mice stained for Aire (green) and Fezf2 (red). 12 and 20 sections derived from two WT, two ΔCD4, and two mTEC$^{\Delta MHCII}$ mice were quantified. Scale bar, 50 μm. Unfilled, dashed and

Figure 3 continued on next page

Figure 3 continued

solid arrowheads indicate Aire^{+}Fezf2^{-}, Aire^{-}Fezf2^{+}, and Aire^{+}Fezf2^{+} cells, respectively. The histogram shows the density of Aire^{+}Fezf2^{-}, Aire^{-}Fezf2^{+}, and Aire^{+}Fezf2^{+} cells. (**C–E**) Flow cytometry profiles, frequencies, and numbers of Aire^{-}Fezf2^{-}, Aire^{-}Fezf2^{+}, and Aire^{+}Fezf2^{+} cells in total mTECs, mTEC^{lo}, and mTEC^{hi} (**C**), of CCL21^{+} cells in mTEC^{lo} (**D**) and of DCKL1^{+} cells in Aire^{-} mTEC^{lo} (**E**) from WT, ΔCD4, and mTEC$^{\Delta MHCII}$ mice. II Abs: secondary antibodies. Data are representative of 2–3 independent experiments (n = 2–5 mice per group and experiment). Error bars show mean ± SEM, *p<0.05, **p<0.01, ***p<0.001, ****p<0.0001 using unpaired Student's *t*-test for (**B**) and two-tailed Mann–Whitney test for (**A**) and (**C**-**E**).

The online version of this article includes the following figure supplement(s) for figure 3:

Figure supplement 1. Normal proliferation of Aire^{-}Fezf2^{+} and Aire $^{+}$Fezf2^{+} medullary thymic epithelial cell (mTECs) in ΔCD4 and mTEC$^{\Delta MHCII}$ mice.

Figure supplement 2. Reduced post-Aire medullary thymic epithelial cells (mTECs) in ΔCD4 and mTEC$^{\Delta MHCII}$ mice.

Figure supplement 3. Analysis of medullary thymic epithelial cell (mTEC) subsets in MHCII$^{-/-}$ mice.

Altogether, these data reveal that MHCII/TCR-mediated interactions with CD4^{+} thymocytes have a broad impact on mTEC composition by controlling the cellularity of not only Aire^{+}Fezf2^{+} mTECs but also Fezf2^{+} pre-Aire^{+} mTECs, post-Aire, and tuft-like cells.

Highly self-reactive CD4^{+} thymocytes activate maturational programs in mTEC^{lo}

We next assessed the impact of highly self-reactive interactions with CD4^{+} thymocytes in mTEC^{lo} using OTII-*Rag2*$^{-/-}$ and RipmOVAxOTII-*Rag2*$^{-/-}$ transgenic mice. Both models possess CD4^{+} thymocytes expressing an MHCII-restricted TCR specific for the chicken ovalbumin (OVA). The Rip-mOVA line expresses a membrane-bound OVA form specifically in mTECs, and consequently high-affinity interactions between OVA-expressing mTECs and OTII CD4^{+} thymocytes are only possible in RipmOVAxOTII-*Rag2*$^{-/-}$ mice (***Kurts et al., 1996***). In contrast to total Erk1/2 MAPK, p38 MAPK, IKKα, and p65, the nonclassical NF-kB subunit RelB was increased in mTEC^{lo} at mRNA and protein levels in RipmOVAxOTII-*Rag2*$^{-/-}$ compared to OTII-*Rag2*$^{-/-}$ mice (***Figure 4A and B***, ***Figure 4—figure supplement 1***). By reanalyzing single-cell RNA-seq data on mTEC^{lo} subsets, we found that in contrast to CCL21^{+} and tuft-like mTECs *Relb* is highly expressed by TAC-TECs and post-Aire cells, arguing again in favor that self-reactive CD4^{+} thymocytes act from the TAC-TEC stage to induce their differentiation into Aire^{+} cells and then into post-Aire cells (***Figure 4—figure supplement 2A***). The level of RelB phosphorylation was also higher in RipmOVAxOTII-*Rag2*$^{-/-}$ than OTII-*Rag2*$^{-/-}$ mice (***Figure 4B***), suggesting that self-reactive CD4^{+} thymocytes may activate the nonclassical NF-κB pathway in mTEC^{lo}.

To define the genome-wide effects of highly self-reactive CD4^{+} thymocytes in mTEC^{lo}, we compared the gene expression profiles of mTEC^{lo} from RipmOVAxOTII-*Rag2*$^{-/-}$ versus OTII-*Rag2*$^{-/-}$ mice (***Figure 1—figure supplement 1B***) and found an upregulation of 1438 genes (FC > 2) reaching statistical significance for 522 of them (Cuffdiff p<0.05). 620 genes were also downregulated (FC < 0.5) with 136 reaching significance (Cuffdiff p<0.05) (***Figure 4C***). The genes upregulated exhibited an approximately fourfold more of TRA over non-TRA genes ($p=4.7 \times 10^{-23}$), which corresponded mainly to Aire-dependent and Aire/Fezf2-independent TRAs (***Figure 4D–F***, ***Supplementary file 3***). Similarly to the WT versus mTEC$^{\Delta MHCII}$ comparison, we found a strong correlation ($p=6.2 \times 10^{-7}$) between the genes upregulated by self-reactive CD4^{+} thymocytes and the responsiveness of genes to Aire's action obtained from the comparison between WT and *Aire*$^{-/-}$ mTEC^{hi} (***Figure 4G***). These results support an impact of antigen-specific interactions in the expression of TRAs in mTEC^{lo}, notably on Aire-dependent TRAs. Importantly, these results are in agreement with the induction of a list of activation factors including *Aire* and *Fezf2* among the non-TRA genes (***Figure 4H***). Similarly to the comparisons of the WT versus ΔCD4 or mTEC$^{\Delta MHCII}$ mice, numerous HDAC3-induced regulators as well as *Sirt1*, *Nfkb2*, *Relb*, and *Trp53* transcription factors were upregulated in mTEC^{lo} of RipmOVAxOTII-*Rag2*$^{-/-}$ mice compared to OTII-*Rag2*$^{-/-}$ mice (***Figure 4I***). Interestingly, 21 out of 30 top targets of the Foxn1 transcription factor, implicated in TEC differentiation and growth (***Žuklys et al., 2016***), as well as cytokines, chemokines, and cell adhesion molecules, were also upregulated (***Figure 4J***, K ***Figure 4—figure supplement 2B***). We found that few of these genes were associated with CCL21^{+} and tuft-like mTECs (***Figure 4L***). In contrast, many genes encoding for activation factors, cytokines, chemokines, and cell adhesion molecules were associated with Aire^{+} and post-Aire mTECs, consistently with the fact that antigen-specific interactions with CD4^{+} thymocytes control the cellularity of Aire^{+} mTECs. Moreover, most of these genes, including *Aire* and *Fezf2*, were already expressed by

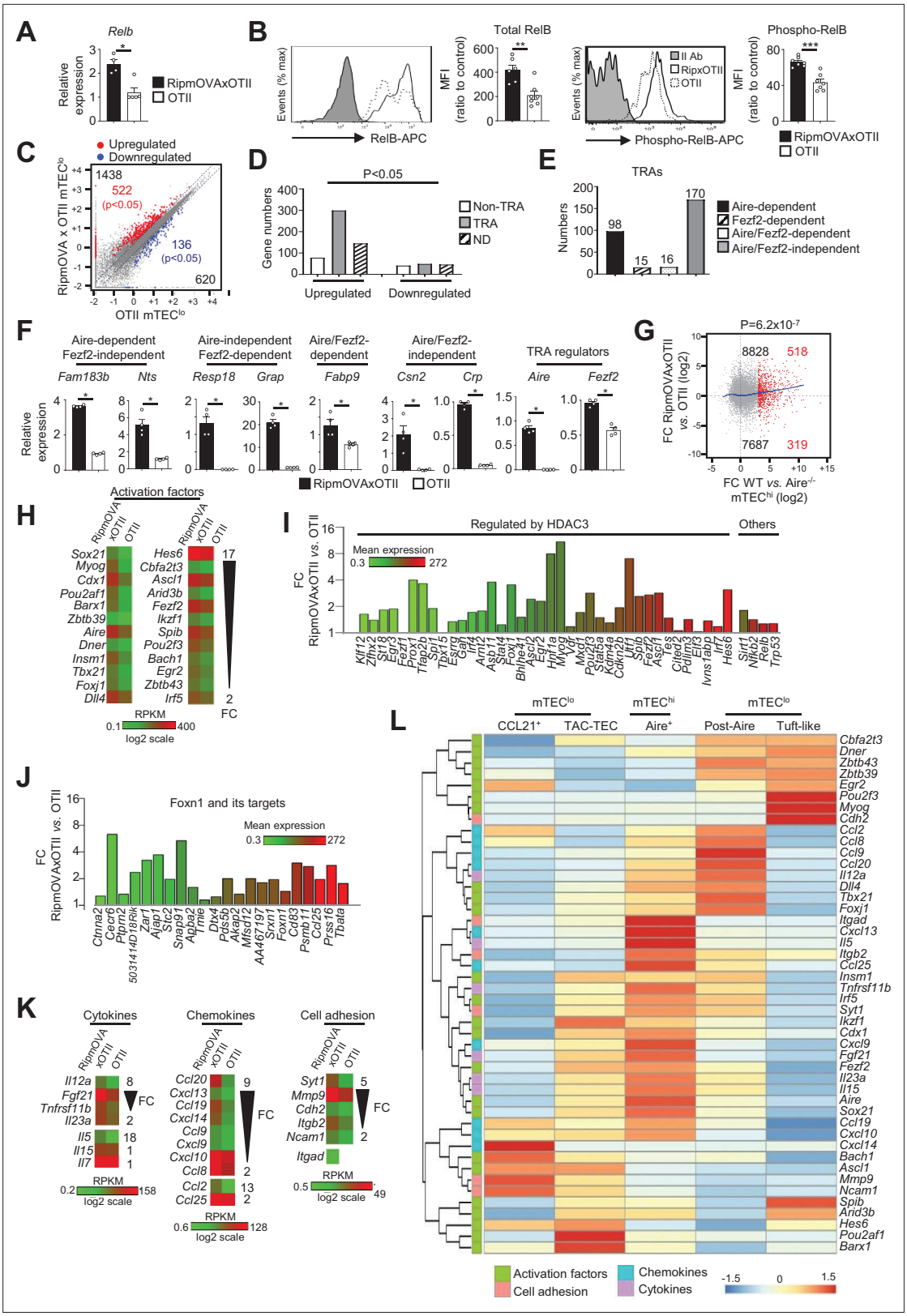

Figure 4. Highly self-reactive CD4+ thymocytes control the transcriptional and functional properties of mTEC^{lo}. (**A**) *Relb* mRNA was measured by qPCR in mTEC^{lo} from RipmOVAxOTII-*Rag2*$^{-/-}$ (n = 4) and OTII-*Rag2*$^{-/-}$ (n = 5) mice. (**B**) Total and phospho-RelB (Ser552) were analyzed by flow cytometry in mTEC^{lo} from RipmOVAxOTII-*Rag2*$^{-/-}$ and OTII-*Rag2*$^{-/-}$ mice. Data are representative of two independent experiments (n = 3–4 mice per group and experiment). (**C**) Scatter plot of gene expression levels (fragments per kilobase of transcript per million mapped reads [FPKM]) in mTEC^{lo} from

Figure 4 continued on next page

Figure 4 continued

RipmOVAxOTII-*Rag2*$^{-/-}$ versus OTII-*Rag2*$^{-/-}$ mice. Genes with fold difference ≥2 and p-adj<0.05 were considered as upregulated or downregulated genes (red and blue dots, respectively). RNA-seq was performed on two independent biological replicates with mTEC^{lo} derived from 5 to 8 mice. (**D**) Numbers of tissue-restricted self-antigens (TRAs) and non-TRAs in genes up- and downregulated in mTEC^{lo} from RipmOVAxOTII-*Rag2*$^{-/-}$ versus OTII-*Rag2*$^{-/-}$ mice. ND, not determined. (**E**) Numbers of induced Aire-dependent, Fezf2-dependent, Aire/Fezf2-dependent, and Aire/Fezf2-independent TRAs. (**F**) Aire-dependent (*Fam183b, Nts*), Fezf2-dependent (*Resp18, Grap*), Aire/Fezf2-dependent (*Fabp9*), Aire/Fezf2-independent (*Csn2, Crp*) TRAs, *Aire* and *Fezf2* mRNAs were measured by qPCR in mTEC^{lo} from RipmOVAxOTII-*Rag2*$^{-/-}$ (n = 4) and OTII-*Rag2*$^{-/-}$ (n = 4) mice. (**G**) Scatter plot of gene expression variation in mTEC^{lo} from RipmOVAxOTII-*Rag2*$^{-/-}$ versus OTII-*Rag2*$^{-/-}$ mice and in mTEC^{hi} from WT versus *Aire*$^{-/-}$ mice. The loess fitted curve is shown in blue and induced Aire-dependent genes (fold change [FC] > 5) in red. (**H**) Heatmap of significantly upregulated activation factors in mTEC^{lo} from RipmOVAxOTII-*Rag2*$^{-/-}$ compared to OTII-*Rag2*$^{-/-}$ mice. (**I, J**) Expression FC in HDAC3-induced transcriptional regulators and other transcription factors (**I**) and in Foxn1 targets (**J**) in mTEC^{lo} from RipmOVAxOTII-*Rag2*$^{-/-}$ versus OTII-*Rag2*$^{-/-}$ mice. The color code represents gene expression level. (**K**) Heatmap of significantly upregulated cytokines, chemokines, and cell adhesion molecules in mTEC^{lo} from RipmOVAxOTII-*Rag2*$^{-/-}$ mice. (**L**) Hierarchical clustering and heatmap of mean expression of these activation factors, cell adhesion molecules, chemokines, and cytokines in mTEC subsets identified by scRNA-seq. Error bars show mean ± SEM, *p<0.05, **p<0.01, ***p<0.001 using two-tailed Mann–Whitney test for (**A**), (**B**) and (**F**) and chi-squared test for (**D**) and (**G**).

The online version of this article includes the following figure supplement(s) for figure 4:

Figure supplement 1. Similar levels of total and phosphorylated p65, Erk1/2, p38, and IKKα proteins in mTEC^{lo} from RipmOVAxOTII-*Rag2*$^{-/-}$ and OTII-*Rag2*$^{-/-}$ mice.

Figure supplement 2. Expression of *Relb*, cytokines, chemokines, and cell adhesion molecules that was altered in mTEC^{lo} from RipmOVAxOTII-*Rag2*$^{-/-}$ and OTII-*Rag2*$^{-/-}$ mice.

TAC-TECs, further highlighting that CD4^{+} thymocytes act upstream of Aire^{+} mTEC^{hi}. Altogether, these data reveal that highly self-reactive CD4^{+} thymocytes control in mTEC^{lo} not only key transcription factors driven by their differentiation but also key molecules for T-cell development and selection such as TRAs, cytokines, chemokines, and adhesion molecules.

Highly self-reactive CD4^{+} thymocytes control mTEC subset composition from a progenitor stage

Given that highly self-reactive CD4^{+} thymocytes induce key transcription factors in mTEC^{lo} (***Figure 4H and I***), we examined their respective impact on mTEC subset development. Strikingly, numbers of total TECs and mTECs were higher in RipmOVAxOTII-*Rag2*$^{-/-}$ than in OTII-*Rag2*$^{-/-}$ mice (***Figure 5A and B***). We analyzed four TEC subsets based on MHCII and UEA-1 levels, as previously described (***Lopes et al., 2017***; ***Wong et al., 2014***; ***Figure 5C***). In contrast to cTEC^{hi} (MHCII^{hi}UEA-1^{lo}), numbers of TEC^{lo} (MHCII^{lo}UEA-1^{lo}), mTEC^{lo} (MHCII^{lo}UEA-1^{+}), and mTEC^{hi} (MHCII^{hi}UEA-1^{+}) were higher in RipmOVAxOTII-*Rag2*$^{-/-}$ than in OTII-*Rag2*$^{-/-}$ mice. Consistently, numbers of mTEC^{lo} and mTEC^{hi} identified based on the level of CD80 expression were also higher in RipmOVAxOTII-*Rag2*$^{-/-}$ mice (***Figure 5—figure supplement 1***). Interestingly, numbers of α6-integrin^{hi}Sca-1^{hi} thymic epithelial progenitor (TEPC)-enriched cells in the TEC^{lo} subset were also increased (***Figure 5D***), indicating that self-reactive CD4^{+} thymocytes control TEC development from a progenitor stage. Of note, this strategy of TEC identification was not possible in ΔCD4 and mTEC$^{\Delta MHCII}$ mice since MHCII expression is abrogated in TECs of these mice (***Irla et al., 2008***).

A higher density of Aire^{+}Fezf2^{-}, Aire^{-}Fezf2^{+}, and Aire^{+}Fezf2^{+} cells was observed in medullary regions of RipmOVAxOTII-*Rag2*$^{-/-}$ mice by immunohistochemistry (***Figure 5E***). Furthermore, numbers of Aire^{-}Fezf2^{-} mTEC^{lo} analyzed by flow cytometry were also higher in RipmOVAxOTII-*Rag2*$^{-/-}$ mice, confirming that self-reactive CD4^{+} thymocytes control mTEC differentiation from an early stage (***Figure 5F***). Numbers of Aire^{-}Fezf2^{+} and Aire^{+}Fezf2^{+} mTEC^{lo} and mTEC^{hi} were also markedly increased in these mice, although similar frequencies of proliferating Ki-67^{+} cells were observed (***Figure 5—figure supplement 2***). In agreement with increased Aire^{+} mTECs, involucrin^{+}TPA^{+}Aire^{-} post-Aire cells were enhanced (***Figure 5—figure supplement 3***). Furthermore, numbers of CCL21^{+} and DCLK1^{+} tuft-like cells in mTEC^{lo} were also increased in RipmOVAxOTII-*Rag2*$^{-/-}$ mice compared to OTII-*Rag2*$^{-/-}$ mice (***Figure 5G and H***). These observations are consistent with our previous findings that antigen-specific interactions between mTECs and CD4^{+} thymocytes induce medulla development (***Irla et al., 2012***). Altogether, these results demonstrate that highly self-reactive CD4^{+} thymocytes regulate mTECs from an early to a late developmental stage and thus mTEC composition.

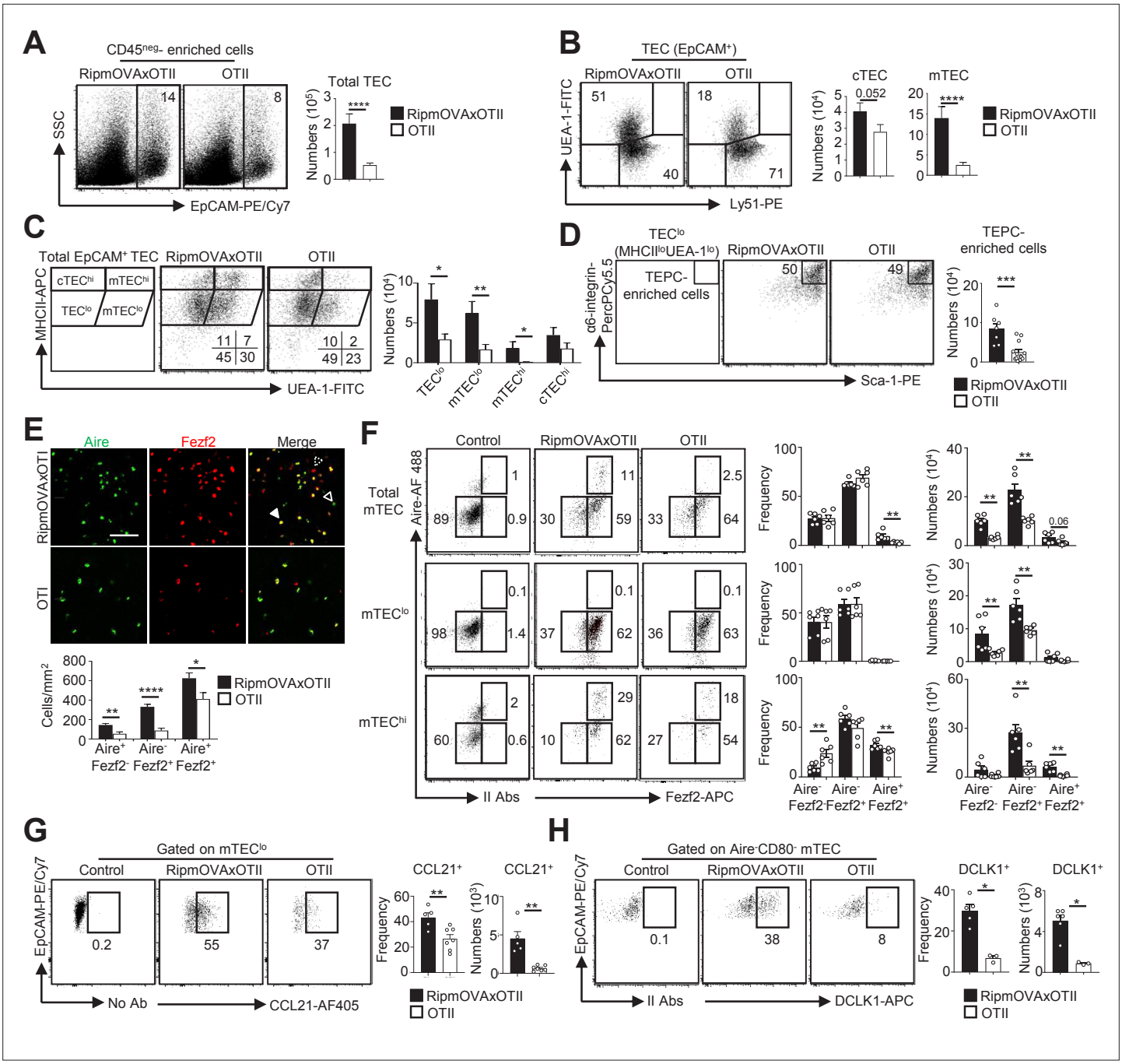

Figure 5. Highly self-reactive CD4$^+$ thymocytes control medullary thymic epithelial cell (mTEC) development from an early progenitor stage. (**A–D**) Flow cytometry profiles and numbers of total thymic epithelial cells (TECs) (EpCAM$^+$) (**A**), cortical thymic epithelial cell (cTECs) (UEA-1$^-$Ly51^{hi}), mTECs (UEA-1$^+$Ly51^{lo}) (**B**), TEC^{lo} (MHCII^{lo}UEA-1^{lo}), cTEC^{hi} (MHCII^{hi}UEA-1^{lo}), mTEC^{lo} (MHCII^{lo}UEA-1^{hi}), and mTEC^{hi} (MHCII^{hi}UEA-1^{hi}) (**C**), α6-integrin^{hi}Sca-1^{hi} TEPC-enriched cells in TEC^{lo} (**D**) in CD45^{neg}-enriched cells from RipmOVAxOTII-*Rag2*$^{-/-}$ and OTII-*Rag2*$^{-/-}$ mice. Data are representative of four experiments (n = 3 mice per group and experiment). (**E**) Confocal images of thymic sections from RipmOVAxOTII-*Rag2*$^{-/-}$ and OTII-*Rag2*$^{-/-}$ mice stained for Aire (green) and Fezf2 (red). 11 and 22 sections derived from two RipmOVAxOTII-*Rag2*$^{-/-}$ and OTII-*Rag2*$^{-/-}$ mice were quantified, respectively. Scale bar, 50 µm. Unfilled, dashed and solid arrowheads indicate Aire$^+$Fezf2^{lo}, Aire$^-$Fezf2$^+$, and Aire$^+$Fezf2$^+$ cells, respectively. The histogram shows the density of Aire$^+$Fezf2^{lo}, Aire$^-$Fezf2$^+$, and Aire$^+$Fezf2$^+$ cells. (**F–H**) Flow cytometry profiles, frequencies, and numbers of Aire$^-$Fezf2$^-$, Aire$^-$Fezf2$^+$, and Aire$^+$Fezf2$^+$ cells in total mTECs, mTEC^{lo}, and mTEC^{hi} (**F**), of CCL21$^+$ cells in mTEC^{lo} (**G**) and of DCKL1$^+$ cells in Aire$^-$ mTECs (**H**) from RipmOVAxOTII-*Rag2*$^{-/-}$ and OTII-*Rag2*$^{-/-}$ mice. II Abs: secondary antibodies. Data are representative of two independent experiments (n = 3–4 mice per group and experiment). Error bars show mean ± SEM, *p<0.05, **p<0.01, ***p<0.001, ****p<0.0001 using unpaired Student's *t*-test for (**A–E**) and two-tailed Mann–Whitney test for (**F–H**).

The online version of this article includes the following figure supplement(s) for figure 5:

Figure 5 continued on next page

Figure 5 continued

Figure supplement 1. mTEC^{lo} and mTEC^{hi} cells are increased in RipmOVAxOTII-*Rag2*$^{-/-}$ compared to OTII-*Rag2*$^{-/-}$ mice.

Figure supplement 2. The proliferation of Aire^{-}Fezf2^{+} and Aire^{+}Fezf2^{+} medullary thymic epithelial cells (mTECs) is similar in RipmOVAxOTII-*Rag2*$^{-/-}$ and OTII-*Rag2*$^{-/-}$ mice.

Figure supplement 3. Post-Aire medullary thymic epithelial cells (mTECs) are increased in RipmOVAxOTII-*Rag2*$^{-/-}$ compared to OTII-*Rag2*$^{-/-}$ mice.

Self-reactive CD4^{+} thymocytes enhance the level of active H3K4me3 mark in mTEC^{lo}

Since histone modifications constitute important regulatory mechanisms that control the open and closed states of mTEC chromatin (***Ucar and Rattay, 2015***), we investigated whether self-reactive CD4^{+} thymocytes induce histone modifications in mTECs. We first analyzed in WT mTEC^{lo} the repressive H3K27me3 and the active H3K4me3 marks using chromatin immunoprecipitation (ChIP) followed by high-throughput sequencing (ChIP-seq). As expected, metagene analyses showed that Aire-dependent TRAs had higher levels of H3K27me3 in their genes than in all genes of the genome, confirming that they are in a repressive state (***Figure 6A***). In contrast, Fezf2-dependent TRAs had a significant enrichment of H3K4me3 in their transcriptional start site (TSS) (***Figure 6B***). Similarly, Aire/Fezf2-independent TRAs were associated with low levels of H3K27me3 in their genes and high levels of H3K4me3 in their TSS. Thus, in contrast to Aire-dependent TRAs that are associated with the repressive H3K27me3 histone mark, Fezf2-dependent and Aire/Fezf2-independent TRAs are associated with the active H3K4me3 mark, indicating that these distinct TRAs are subjected to a specific epigenetic regulation.

We next assessed whether highly self-reactive CD4^{+} thymocytes control the H3K27me3 and H3K4me3 chromatin landscape in mTEC^{lo}. In contrast to H3K27me3, we found an increased global level of H3K4me3 in RipmOVAxOTII-*Rag2*$^{-/-}$ compared to OTII-*Rag2*$^{-/-}$ mice by flow cytometry (***Figure 6C***). We further analyzed by nano-ChIP-seq whether self-reactive CD4^{+} thymocytes regulate in mTEC^{lo} the level of these two histone marks in Aire-dependent, Fezf2-dependent, and Aire/Fezf2-independent TRA genes. H3K27me3 levels in Aire-dependent TRA genes were comparable in mTEC^{lo} from RipmOVAxOTII-*Rag2*$^{-/-}$ and OTII-*Rag2*$^{-/-}$ mice (***Figure 6D***, left panel). Although lower, H3K27me3 levels in Fezf2-dependent and Aire/Fezf2-independent TRAs as well as in all genes were similar in both mice, indicating that the interactions with self-reactive CD4^{+} thymocytes do not regulate this repressive mark in TRA genes (***Figure 6D***, left panel). In contrast, H3K4me3 global level was increased in the TSS of all TRAs in RipmOVAxOTII-*Rag2*$^{-/-}$ compared to OTII-*Rag2*$^{-/-}$ mice as well as in all genes (***Figure 6D***, right panel). For representation, whereas the Aire/Fezf2-independent TRA, E2F transcription factor 2 (*E2f2*) induced by these interactions, was barely devoid of H3K27me3 in both mice, it was marked by H3K4me3 in its TSS specifically in RipmOVAxOTII-*Rag2*$^{-/-}$ mice (***Figure 6E***). These results thus show that self-reactive CD4^{+} thymocytes enhance the global level of the active H3K4me3 histone mark in mTEC^{lo} and in particular in the TSS of Fezf2-dependent and Aire/Fezf2-independent TRAs, indicative of an epigenetic regulation for their expression.

MHCII/TCR interactions between mTECs and CD4^{+} thymocytes prevent the development of autoimmunity

We next evaluated the impact of mTEC-CD4^{+} thymocyte interactions on the generation of self-tolerant T cells by taking advantage that CD4^{+} and CD8^{+} T cells develop in mTEC$^{\Delta MHCII}$ mice, in which MHCII/TCR interactions between mTECs and CD4^{+} thymocytes are abrogated. Interestingly, since TRAs induced by MHCII/TCR interactions showed a diverse peripheral tissue distribution in mTEC^{lo} (***Figure 7A***, ***Supplementary file 4***), we analyzed the TCRVβ usage in mTEC$^{\Delta MHCII}$ mice by flow cytometry. TCRVβ usage was more altered in CD69^{-} mature CD4^{+} thymocytes than in CD8^{+} thymocytes (***Figure 7B***). Some TCRVβ were also altered in splenic CD4^{+} and CD8^{+} T cells. To determine whether these T cells contained self-reactive specificities, we adoptively transferred splenocytes from mTEC$^{\Delta MHCII}$ or WT mice into lymphopenic *Rag2*$^{-/-}$ recipients (***Figure 7C***). Mice that received splenocytes derived from mTEC$^{\Delta MHCII}$ mice lost significantly more weight than mice transferred with WT splenocytes (***Figure 7D***). They also exhibited splenomegaly with increased follicle areas and T-cell numbers showing a CD62L^{lo}CD44^{hi} effector and CD62L^{hi}CD44^{hi} central memory phenotype (***Figure 7E–G***). Immune infiltrates in lungs and salivary glands were observed by histology and flow cytometry in 75

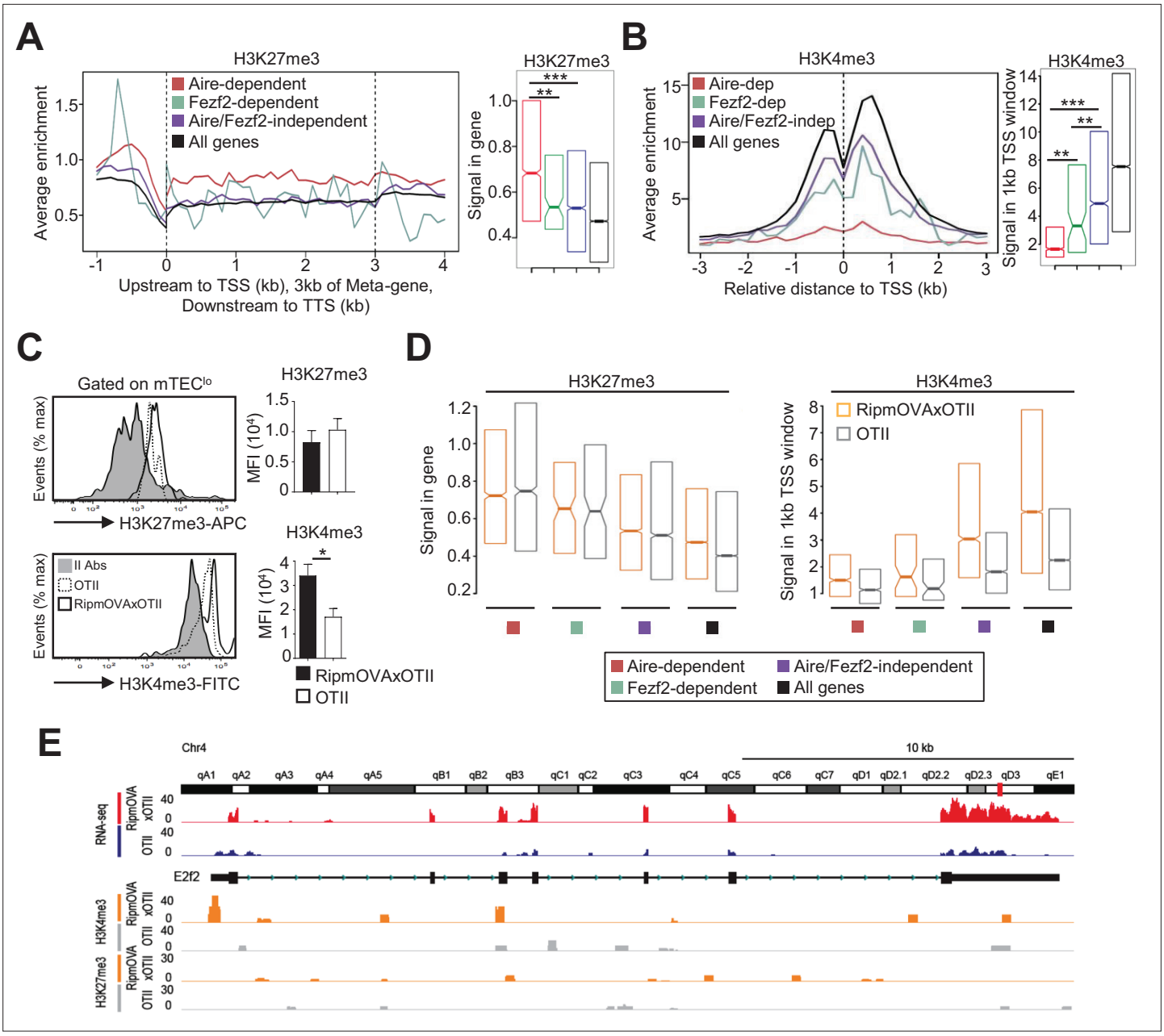

Figure 6. H3K27me3 and H3K4me3 landscape in tissue-restricted self-antigen (TRA) genes of mTEC^{lo} from WT, RipmOVAxOTII-*Rag2*$^{-/-}$, and OTII-*Rag2*$^{-/-}$ mice. (**A, B**) Metagene profiles of the average normalized enrichment of H3K27me3 (**A**) and H3K4me3 (**B**) against input for Aire-dependent, Fezf2-dependent, and Aire/Fezf2-independent TRAs as well as for all genes of WT mTEC^{lo}. Boxplots represent the median enrichment, the 95% CI of the median (notches), and the 75th and 25th percentiles of H3K27me3 and H3K4me3. (**C**) H3K27me3 and H3K4me3 levels were analyzed by flow cytometry in mTEC^{lo} from RipmOVAxOTII-*Rag2*$^{-/-}$ (n = 4) and OTII-*Rag2*$^{-/-}$ (n = 5) mice. Histograms show the MFI. (**D**) Boxplots represent the median enrichment of H3K27me3 and H3K4me3 of Aire-dependent, Fezf2-dependent, and Aire/Fezf2-independent TRAs and in all genes of mTEC^{lo} from RipmOVAxOTII-*Rag2*$^{-/-}$ and OTII-*Rag2*$^{-/-}$ mice. (**E**) Expression (RNA-seq) and H3K27me3 and H3K4me3 chromatin state (ChIP-seq) of the Aire/Fezf2-independent TRA, *E2f2*, in mTEC^{lo} from RipmOVAxOTII-*Rag2*$^{-/-}$ and OTII-*Rag2*$^{-/-}$ mice. *p<0.05, **p<10^{-3}, ***p<10^{-7}, using the Mann–Whitney test for (**A**) and (**B**) and unpaired Student's *t*-test for (**C**).

and 41% of mice, respectively (***Figure 7H and I***). These two tissues contained increased numbers of central memory as well as CD44^{+}CD69^{+} and CD44^{+}CD69^{-} activated CD4^{+} and CD8^{+} T cells (***Figure 7J***). T-cell infiltrates were also observed in other tissues such as kidney, liver, and colon in agreement with the defective TRA expression associated with these tissues (***Figure 7A and K***). Altogether, these data show that in the absence of MHCII/TCR interactions between mTECs and CD4^{+} thymocytes, T cells

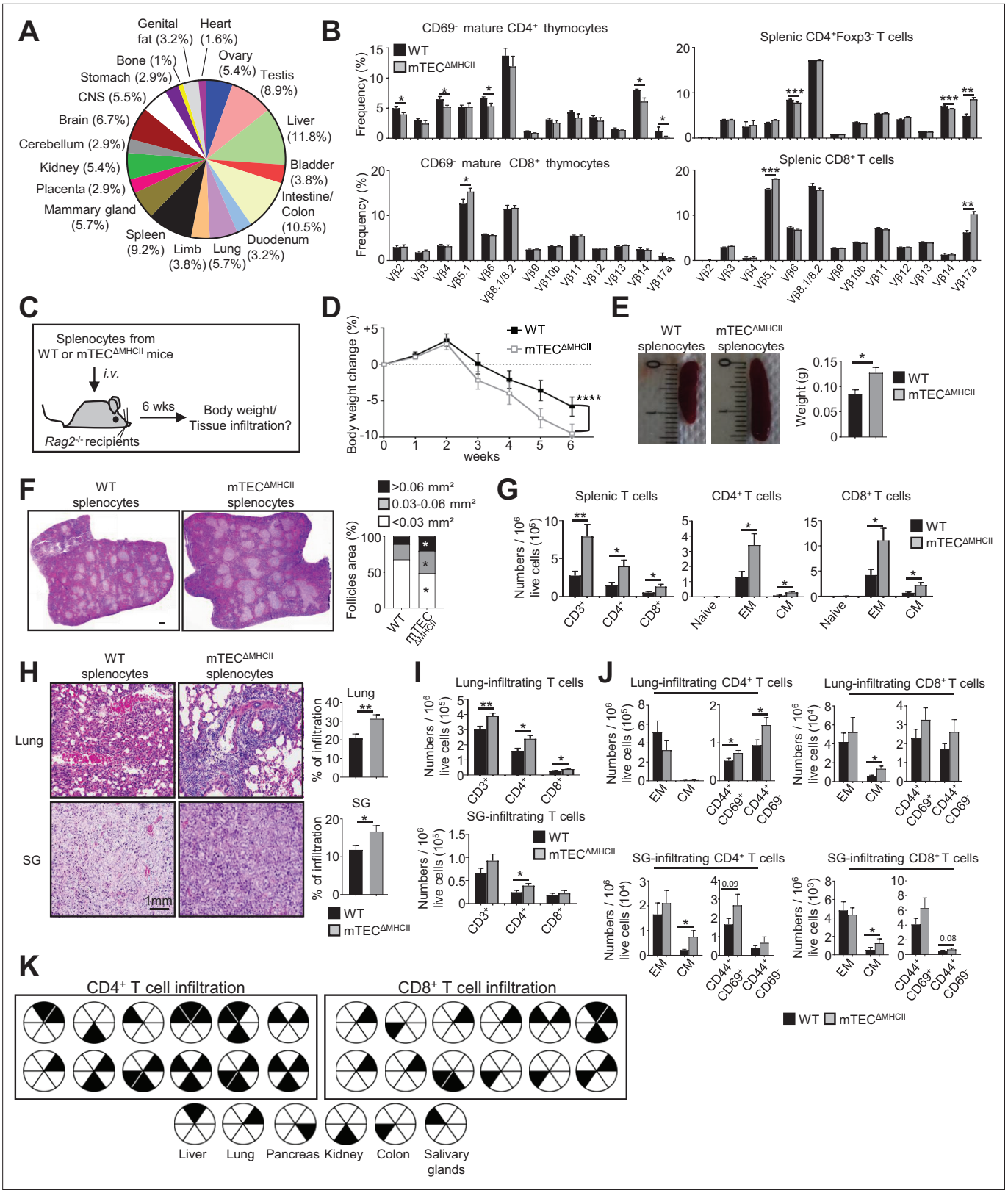

Figure 7. The adoptive transfer of T cells from mTEC$^{\Delta MHCII}$ mice into *Rag2*$^{-/-}$ recipients induces autoimmunity. (**A**) Tissue-restricted self-antigens (TRAs) underexpressed in mTEC^{lo} from mTEC$^{\Delta MHCII}$ mice were assigned to their peripheral expression. (**B**) TCRVβ usage by CD69^{-} mature CD4^{+} and CD8^{+} thymocytes (left panel) and CD4^{+}Foxp3^{-} and CD8^{+} splenic T cells (right panel) from WT and mTEC$^{\Delta MHCII}$ mice. (**C**) Body weight of *Rag2*$^{-/-}$ recipients transferred with splenic T cells from WT or mTEC$^{\Delta MHCII}$ was monitored during 6 weeks, and tissue infiltration was examined. (**D**) Weight loss relative

Figure 7 continued on next page

Figure 7 continued

to the initial weight. (**E, F**) Representative spleen pictures and their weights (**E**) and hematoxylin/eosin counterstained splenic sections (**F**). Scale bar, 1 mm. The histogram shows follicle areas. (**G**) Numbers of splenic $CD3^+$, $CD4^+$, and $CD8^+$ T cells and of naive ($CD44^{lo}CD62L^{hi}$), effector memory (EM; $CD44^{hi}CD62L^{lo}$) and central memory (CM; $CD44^{hi}CD62L^{hi}$) phenotype. (**H**) Lung and salivary gland (SG) immune infiltrates detected by hematoxylin/eosin counterstaining. Scale bar, 1 mm. (**I, J**) Numbers of T cells (**I**) and of naive, effector and central memory phenotype as well as $CD44^+CD69^+$ and $CD44^+CD69^-$ T cells (**J**) in lungs and SG. (**K**) Schematic of T-cell infiltrates in mice transferred with $mTEC^{\Delta MHCII}$ T cells relative to those transferred with WT T cells. Each circle and black triangles represent an individual mouse and T-cell infiltration in a specific tissue, respectively. Data are representative of two independent experiments (n = 5–7 mice per group and experiment). Error bars show mean ± SEM, ****p<0.0001 using two-way ANOVA for (**D**) and unpaired Student's *t*-test for (**B**) and (**E**-**J**). *p<0.05, **p<0.01, ***p<0.001.

The online version of this article includes the following figure supplement(s) for figure 7:

Figure supplement 1. $CD4^+$ thymocytes through MHCII/TCR-mediated interactions control transcriptional programs of $mTEC^{lo}$ that drive their differentiation and function.

contained self-reactive specificities and thus that these interactions are critical to the establishment of T-cell tolerance.

Discussion

Since mTECs play a crucial role in immunological tolerance by their exclusive expression of TRAs, it is essential to deepen our knowledge of the mechanisms that sustain their differentiation. Here using three distinct transgenic models, we found that self-reactive $CD4^+$ thymocytes control the developmental transcriptional programs from the $mTEC^{lo}$ stage, including TAC-TECs that precede $Aire^+$ mTECs. $CD4^+$ thymocytes increase in $mTEC^{lo}$ the phosphorylation of p38 MAPK and IKKα, the latter implicated in mTEC development (***Lomada et al., 2007***; ***Shen et al., 2019***). Moreover, self-reactive $CD4^+$ thymocytes increase RelB phosphorylation level. Interestingly, this nonclassical NF-κB subunit is crucial for mTEC differentiation and Aire-dependent and -independent TRA expression (***Riemann et al., 2017***). These data thus suggest that $CD4^+$ thymocytes activate intracellular pathways from the $mTEC^{lo}$ stage, although alterations in $mTEC^{lo}$ subset composition could also contribute to the differences observed. Nevertheless, the substantial and homogeneous reduction in the levels of phospho-IKKα, -p38, and -RelB argues instead for impaired activation of IKKα, p38, and RelB signaling in the absence of self-reactive $CD4^+$ thymocytes. Analysis of the $mTEC^{lo}$ transcriptional landscape by high-throughput RNA-seq revealed that self-reactive $CD4^+$ thymocytes upregulate *Nfkb2* (p52), known to form an heterocomplex with RelB in the nucleus upon activation (***Irla et al., 2010***). p52 is important for mTEC development, Aire, and TRA expression (***Zhang et al., 2006***; ***Zhu et al., 2006***). Consequently, ΔCD4, $mTEC^{\Delta MHCII}$, and OTII-$Rag2^{-/-}$ mice in which MHCII/TCR interactions between mTECs and $CD4^+$ thymocytes are disrupted have altered *Relb* and *Nfkb2* expression, and reduced $Aire^+$ mTEC numbers and Aire-dependent TRA representation. Our results are in agreement with the fact that RANK-induced NF-κB signaling is activated by membrane-bound RANKL and not soluble RANKL and thereby in the context of physical interactions between mTECs and $CD4^+$ thymocytes (***Asano et al., 2019***).

These interactions also upregulate *Trp53* (p53) that controls the mTEC niche (***Rodrigues et al., 2017***) and *Irf4* and *Irf7* transcription factors that regulate key chemokines implicated in thymocyte medullary localization and mTEC differentiation (***Haljasorg et al., 2017***; ***Otero et al., 2013***). Furthermore, the deacetylase Sirtuin-1 (*Sirt1*), which regulates Aire activity (***Chuprin et al., 2015***), and *Spib*, which limits mTEC differentiation (***Akiyama et al., 2014***), were also upregulated. Self-reactive $CD4^+$ thymocytes thus induce key transcription factors that both positively and negatively control mTEC differentiation. Remarkably, our three different transgenic models revealed that $CD4^+$ thymocytes induce HDAC3-dependent mTEC-specific transcription factors (***Goldfarb et al., 2016***). Among them, *Pou2f3* is involved in tuft-like mTEC development (***Bornstein et al., 2018***; ***Miller et al., 2018***), which is consistent with our results showing that self-reactive $CD4^+$ thymocytes control the cellularity of these cells. Our data thus identify that $CD4^+$ thymocytes control the expression of master transcriptional regulators of mTEC differentiation and function.

In line with these data, we found that self-reactive $CD4^+$ thymocytes regulate TEC development from a progenitor stage since they increase numbers of TEPC-enriched cells that express non-negligible MHCII levels. Interestingly, we provide the first evidence that self-reactive $CD4^+$ thymocytes

control the cellularity of Fezf2^{+} mTECs. Accordingly, the expression of Fezf2 and its respective TRAs was enhanced by CD4^{+} thymocytes. Moreover, self-reactive CD4^{+} thymocytes regulate the cellularity of CCL21^{+}, post-Aire, and tuft-like cells in mTEC^{lo}. These results are in full agreement with our previous findings that self-reactive thymocytes drive medulla expansion and increase the overall cellularity of the mTEC compartment (***Irla et al., 2012***). Because the heterogeneous composition in mTEC^{lo} could influence the expression of the upregulated genes by self-reactive CD4^{+} thymocytes, we reanalyzed single-cell RNA-seq data in order to define their respective expression pattern in mTEC subsets. In accordance with the moderately altered frequencies of CCL21^{+} cells among mTEC^{lo} observed by flow cytometry, few genes upregulated by self-reactive CD4^{+} thymocytes were associated with this mTEC subset. In contrast, we found that antigen-specific interactions with CD4^{+} thymocytes strongly upregulate genes associated with TAC-TECs, Aire^{+} mTECs, and post-Aire cells. These findings indicate that self-reactive CD4^{+} thymocytes act from the precursors of Aire^{+} mTEC^{hi} (i.e., in TAC-TECs) to the post-Aire stage. It is interesting to note that although strongly altered the development of mTEC^{hi} is not completely abrogated in the absence of CD4^{+} thymocytes or MHCII/TCR-mediated interactions with CD4^{+} thymocytes. This could be explained by the fact that invariant NKT have been proposed to participate in mTEC differentiation by expressing RANKL (***White et al., 2014***). Overall, our results thus reveal that antigen-specific interactions with CD4^{+} thymocytes have an unsuspected broad impact on mTEC composition by driving their development from an early progenitor to a late post-Aire stage.

Interestingly, high-throughput RNA-seq showed that MHCII/TCR interactions with CD4^{+} thymocytes upregulate the expression of chemokines in mTEC^{lo}. Among them, CCL19 (CCR7 ligand) is implicated in the medullary localization of thymocytes and the emigration of newly generated T cells (***Ueno et al., 2004***); and CCL22 (CCR4 ligand) implicated in medullary entry and thymocyte/dendritic cell interactions (***Hu et al., 2015***). Self-reactive CD4^{+} thymocytes also enhance CCL2 (CCR2 ligand) and CCL20 (CCR6 ligand) that promote the entry of peripheral dendritic cells and Foxp3^{+} regulatory T cells into the thymus (***Baba et al., 2009***; ***Cédile et al., 2014***; ***Cowan et al., 2018***; ***Lopes et al., 2018***; ***Borelli and Irla, 2021***). mTEC-CD4^{+} thymocyte interactions thus induce key chemokines that regulate the trafficking of thymocytes and dendritic cells that participate in tolerance induction. Moreover, cytokines such as *Il15* and *Fgf21* implicated in invariant NKT development and TEC protection against senescence, as well as adhesion molecules involved in mTEC-thymocyte interactions, were also induced (***Pezzi et al., 2016***; ***White et al., 2014***; ***Youm et al., 2016***). Altogether, our data show that self-reactive CD4^{+} thymocytes regulate functional properties of mTECs by inducing chemokines, cytokines, and adhesion molecules that are critical for T-cell development.

The expression of TRAs is regulated by Aire and to a lesser extent by Fezf2 (***Anderson et al., 2002***; ***Takaba et al., 2015***). In agreement with other studies (***Gray et al., 2007***; ***Takaba et al., 2015***), we found Fezf2 in both mTEC^{lo} and mTEC^{hi}, whereas Aire protein is mainly expressed in mTEC^{hi}. Nevertheless and in line with recent single-cell transcriptomic analyses (***Baran-Gale et al., 2020***; ***Dhalla et al., 2020***; ***Wells et al., 2020***), we detected Aire by flow cytometry, qPCR, and RNA-seq in a small subset (~1.5%) of mTEC^{lo}. CD4^{+} thymocyte interactions upregulate *Aire* and *Fezf2* and some of their respective TRAs in these cells. Interestingly, in contrast to Aire-dependent TRAs that are characterized by high levels of H3K27me3 (***Handel et al., 2018***; ***Sansom et al., 2014***), we found that Fezf2-dependent TRAs show high levels of H3K4me3. This highlights that Aire and Fezf2 use distinct epigenetic modes in regulating TRA expression. Remarkably, these interactions also induce in mTEC^{lo} numerous Aire/Fezf2-independent TRAs, whose regulation remains unknown. Similarly to Fezf2-dependent TRAs, they had high levels of H3K4me3 in their TSS, suggesting that Aire/Fezf2-independent TRAs are not subjected to the same regulatory transcriptional mechanisms than Aire-dependent TRAs. Our results are consistent with a previous study indicating that the Aire-independent TRA, *Gad1*, shows active epigenetic marks (***Tykocinski et al., 2010***). Remarkably, self-reactive CD4^{+} thymocytes increase H3K4me3 level in the TSS of all TRA categories, thus providing a novel epigenetic mechanistic insight into how they regulate the mTEC gene expression profile. In line with TRA regulation and the development of distinct mTEC subsets, the repertoire of mature T cells contains autoreactive cells when MHCII/TCR interactions were abrogated between mTECs and CD4^{+} thymocytes. Accordingly, the adoptive transfer of splenocytes from mTEC$^{\Delta MHCII}$ mice is capable of inducing signs of autoimmunity, illustrating the fact that mTEC-CD4^{+} thymocyte interactions are critical for the generation of a self-tolerant T-cell repertoire. Future investigations based on TCR sequencing analysis are expected to define to which extent the TCR repertoire is altered in mTEC$^{\Delta MHCII}$ mice.

In summary, our genome-wide scale study reveals that self-reactive CD4$^+$ thymocytes activate transcriptional programs from the TAC-TEC stage that sustains the differentiation into Aire$^+$Fezf2$^+$ and post-Aire mTECs (***Figure 7—figure supplement 1***). These interactions also upregulate the expression of TRAs, cytokines, chemokines, and adhesion molecules that are all implicated in mTEC function. Thus, CD4$^+$ thymocytes control several unsuspected aspects of mTEC^{lo} required for the establishment of T-cell tolerance.

Materials and methods

Key resources table

Reagent type (species) or resource	Designation	Source or reference	Identifiers	Additional information
Genetic reagent (*Mus musculus*)	C57BL/6J background	Charles River	RRID:IMSR_JAX:000664	
Genetic reagent (*M. musculus*)	*Ciita*^{tm2Wrth}/*Ciita*^{tm2Wrth}	***LeibundGut-Landmann et al., 2004***	RRID:MGI:3052466	C57BL/6 background, ΔCD4 mice
Genetic reagent (*M. musculus*)	H2$^{dlAb1\text{-}Ea}$/H2$^{dlAb1\text{-}Ea}$	***Madsen et al., 1999***	RRID:MGI:4436873	C57BL/6 background, MHCII$^{-/-}$ mice
Genetic reagent (*M. musculus*)	K14x*Ciita*$^{III+IV-/-}$	***Irla et al., 2008***		C57BL/6 background, mTEC$^{\Delta MHCII}$ mice
Genetic reagent (*M. musculus*)	Tg(TcraTcrb)425Cbn	***Barnden et al., 1998***	RRID:MGI:3762632	C57BL/6 background, OTII mice
Genetic reagent (*M. musculus*)	Tg(Ins2-TFRC/OVA)296Wehi	***Kurts et al., 1996***	RRID:MGI:3623748	C57BL/6 background, Rip-mOVA mice
Genetic reagent (*M. musculus*)	*Rag2*^{tm1Fwa}/*Rag2*^{tm1Fwa}	***Shinkai et al., 1992***	RRID:MGI:2174910	C57BL/6 background, *Rag2*$^{-/-}$ mice
Antibody	Anti-IKKα (rabbit polyclonal)	Cell Signaling Technology	Cat# 2682; RRID:AB_331626	FACS (1:500)
Antibody	Anti-phospho IKKα (Ser180)/ IKKβ(Ser181) (rabbit polyclonal)	Cell Signaling Technology	Cat# 2681S; RRID:AB_331624	FACS (1:500)
Antibody	Anti-p38 MAPK (rabbit polyclonal)	Cell Signaling Technology	Cat# 9212; RRID:AB_330713	FACS (1:500)
Antibody	Anti-phospho p38 MAPK (Thr180/ Tyr182) (rabbit polyclonal)	Cell Signaling Technology	Cat# 9211S; RRID:AB_331641	FACS (1:500)
Antibody	Anti-Erk1/2 (rabbit polyclonal)	Cell Signaling Technology	Cat# 9102; RRID:AB_330744	FACS (1:500)
Antibody	Anti-phospho Erk1/2 (Thr202/Tyr204) (rabbit polyclonal)	Cell Signaling Technology	Cat# 9101S; RRID:AB_331646	FACS (1:500)
Antibody	Anti-NF- κ B p65 (clone D14E12, rabbit monoclonal)	Cell Signaling Technology	Cat# 8242S; RRID:AB_10859369	FACS (1:500)
Antibody	Phospho-NF- κ B p65 (Ser536) (clone 93H1, rabbit monoclonal)	Cell Signaling Technology	Cat# 3033S; RRID:AB_331284	FACS (1:3000)
Antibody	Anti-RelB (clone C-19, rabbit polyclonal)	Santa Cruz Biotechnology	Cat# sc-226; RRID:AB_632341	FACS (1:200)
Antibody	Anti-phospho RelB (ser552) (clone D41B9, rabbit monoclonal)	Cell Signaling Technology	Cat# 5025S; RRID:AB_10622001	FACS (1:1000)
Antibody	Anti-DCLK1 (clone D2U3L, rabbit monoclonal)	Cell Signaling Technology	Cat# 62257; RRID:AB_2799622	FACS (1:200)
Antibody	Anti-H3K4me3 (rabbit polyclonal)	Abcam	Cat# ab8580; RRID:AB_306649	FACS (1:1000) ChIP-seq (2 µg:25 µg chromatin)
Antibody	Anti-H3K27me3 (clone C36B11, rabbit monoclonal)	Cell Signaling Technology	Cat# 9733; RRID:AB_2616029	FACS (1:1000) ChIP-seq (1:50)

Continued on next page

Continued

Reagent type (species) or resource	Designation	Source or reference	Identifiers	Additional information
Antibody	PE-Cy7 anti-CD326 (EpCAM) (clone G8.8, rat monoclonal)	eBioscience	Cat# 25-5791-80; RRID:AB_1724047	FACS (1:3000)
Antibody	Alexa Fluor 488 anti-Aire (clone 5H12, rat monoclonal)	eBioscience	Cat# 53-5934-82; RRID:AB_10854132	FACS, IF (1:200)
Antibody	PE anti-Ly51 (clone BP-1, mouse monoclonal)	BD Biosciences	Cat# 553735; RRID:AB_395018	FACS (1:3000)
Antibody	PerCP-Cy5.5 anti-CD80 (clone 16-10A1, Armenian hamster monoclonal)	BioLegend	Cat# 104722; RRID:AB_2291392	FACS (1:200)
Antibody	eFluor 450 anti-Ki-67 (clone SolA15, rat monoclonal)	eBioscience	Cat# 48-5698-82; RRID:AB_11149124	FACS (1:200)
Antibody	Anti-Fezf2 (clone F441, rabbit polyclonal)	IBL Tecan	Cat# JP18997; RRID:AB_2341444	FACS, IF (1:200)
Antibody	Anti-Involucrin (clone Poly19244, rabbit polyclonal)	BioLegend	Cat# 924401; RRID:AB_2565452	IF (1:100)
Antibody	PE anti-Ly-6A/E (Sca-1) (clone D7, rat monoclonal)	BD Biosciences	Cat# 553108; RRID:AB_394629	FACS (1:600)
Antibody	Biotin anti-CD49f (α6-integrin) (clone GoH3, rat monoclonal)	BioLegend	Cat# 313604; RRID:AB_345298	FACS (1:200)
Antibody	Alexa Fluor 647 anti-I-Ab (MHCII) (clone AF6-120.1, mouse monoclonal)	BioLegend	Cat# 116412; RRID:AB_493141	FACS (1:200)
Antibody	Brilliant Violet 421 anti-CD4 (clone RM4-5, rat monoclonal)	BioLegend	Cat# 100544; RRID:AB_11219790	FACS (1:200)
Antibody	PerCP-Cy5.5 anti-CD4 (clone RM4-5, rat monoclonal)	BD Biosciences	Cat# 550954; RRID:AB_393977	FACS (1:200)
Antibody	Pacific Blue anti-CD8α (clone 53-6.7, rat monoclonal)	BD Biosciences	Cat# 558106; RRID:AB_397029	FACS (1:200)
Antibody	PE/Cy7 anti-CD8α (clone 53-6.7, rat monoclonal)	BioLegend	Cat# 100722; RRID:AB_312761	FACS (1:600)
Antibody	Alexa Fluor 488 anti-CD44 (clone IM7, rat monoclonal)	BioLegend	Cat# 103016; RRID:AB_493679	FACS (1:200)
Antibody	PE anti-CD69 (clone H1.2F3, rat monoclonal)	BioLegend	Cat# 104508; RRID:AB_313111	FACS (1:400)
Antibody	PE anti-CD62L (clone MEL-14, rat monoclonal)	BD Biosciences	Cat# 553151; RRID:AB_394666	FACS (1:300)
Antibody	PerCP-Cy5.5 anti-CD3ε (clone 17A2, rat monoclonal)	BD Biosciences	Cat# 560527; RRID:AB_1727463	FACS (1:200)
Antibody	Alexa Fluor 405 anti-CCL21 (clone 59106, rat monoclonal)	R&D Systems	Cat# IC457V	FACS (1:100)
Antibody	CD45 MicroBeads, mouse (clone 30F11.1, rat monoclonal)	Miltenyi	Cat# 130052301; RRID:AB_2877061	
Antibody	Cy5 anti-rabbit IgG (goat polyclonal)	Invitrogen	Cat# A10523; RRID:AB_2534032	FACS (1:500)
Antibody	Cyanine 3 anti-rabbit IgG (goat polyclonal)	Invitrogen	Cat# A10520; RRID:AB_2534029	IF (1:500)
Antibody	FITC anti-TCR Vβ2 (clone B20.6, rat monoclonal)	BD Biosciences	Cat# 557004; RRID:AB_647180	FACS (20 µl per 10^6 cells)
Antibody	FITC anti-TCR Vβ3 (clone KJ25, Armenian hamster monoclonal)	BD Biosciences	Cat# 557004; RRID:AB_647180	FACS (20 µl per 10^6 cells)

Continued on next page

Continued

Reagent type (species) or resource	Designation	Source or reference	Identifiers	Additional information
Antibody	FITC anti-TCR Vβ4 (clone KT4, rat monoclonal)	BD Biosciences	Cat# 557004; RRID:AB_647180	FACS (20 µl per 10^6 cells)
Antibody	FITC anti-TCR Vβ5.1, 5.2 (clone MR9-4, mouse monoclonal)	BD Biosciences	Cat# 553189; RRID:AB_394697	FACS (1:100)
Antibody	FITC anti-TCR Vβ6 (clone RR4-7, rat monoclonal)	BD Biosciences	Cat# 557004; RRID:AB_647180	FACS (20 µl per 10^6 cells)
Antibody	PE anti-TCR Vβ8.1, 8.2 (clone MR5-2, mouse monoclonal)	BioLegend	Cat# 140103; RRID:AB_10641144	FACS (1:300)
Antibody	FITC anti-TCR Vβ9 (clone MR10-2, mouse monoclonal)	BD Biosciences	Cat# 557004; RRID:AB_647180	FACS (20 µl per 10^6 cells)
Antibody	PE anti-TCR Vβ10b (clone B21.5, rat monoclonal)	BD Biosciences	Cat# 553285; RRID:AB_394757	FACS (1:300)
Antibody	Biotin anti-TCR Vβ11 (clone RR3-15, rat monoclonal)	BD Biosciences	Cat# 553196; RRID:AB_394702	FACS (1:300)
Antibody	FITC anti-TCR Vβ12 (clone MR11-1, mouse monoclonal)	BD Biosciences	Cat# 557004; RRID:AB_647180	FACS (20 µl per 10^6 cells)
Antibody	FITC anti-TCR Vβ13 (clone MR12-3, mouse monoclonal)	BD Biosciences	Cat# 557004; RRID:AB_647180	FACS (20 µl per 10^6 cells)
Antibody	FITC anti-TCR Vβ14 (clone 14-2, rat monoclonal)	BD Biosciences	Cat# 557004; RRID:AB_647180	FACS (20 µl per 10^6 cells)
Antibody	FITC anti-TCR Vβ17a (clone KJ23, rat monoclonal)	BD Biosciences	Cat# 557004; RRID:AB_647180	FACS (20 µl per 10^6 cells)
Antibody	$CD4^+$ T cell isolation kit, mouse	Miltenyi Biotec	Cat# 130-104-454	
Peptide, recombinant protein	PerCP-Cy5.5 Streptavidin	BioLegend	Cat# 405214; RRID:AB_2716577	FACS (1:400)
Peptide, recombinant protein	Alexa Fluor 488 Streptavidin	Invitrogen	Cat# S11223	IF (1:1000)
Peptide, recombinant protein	Ovalbumin (323–339)	PolyPeptide	Cat# SC1303	5 µM
Chemical compound, drug	Liberase TM	Roche	Cat# 05401127001	50 µg/ml
Chemical compound, drug	DNase I	Roche	Cat# 10104159001	100 µg/ml
Chemical compound, drug	TRIzol	Thermo Fisher Scientific	Cat# 15596018	
Software, algorithm	GraphPad Prism	GraphPad Software	RRID:SCR_002798	
Software, algorithm	FlowJo	FlowJo	https://www.flowjo.com/ RRID:SCR_008520	
Software, algorithm	Fiji/ImageJ software	Fiji-ImageJ	https://imagej.nih.gov/ij/ RRID:SCR_003070	
Software, algorithm	7500 Real-Time PCR Software	Thermo Fisher	https://www.thermofisher.com/us/en/home/technical-resources/software-downloads/applied-biosystems-7500-real-time-pcr-system.html RRID:SCR_014596	
Software, algorithm	Pheatmap 0.2	https://github.com/raivokolde/pheatmap (***Kolde, 2018***)	RRID:SCR_016418	
Software, algorithm	Seurat	***Hao et al., 2021***	RRID:SCR_016341	

Continued on next page

Continued

Reagent type (species) or resource	Designation	Source or reference	Identifiers	Additional information
Sequence-based reagent	Actin-FW	Sigma-Aldrich	PCR primers	CAGAAGGAGATTACTGCTCTGGCT
Sequence-based reagent	Actin-RV	Sigma-Aldrich	PCR primers	GGAGCCACCGATCCACACA
Sequence-based reagent	Aire-FW	Sigma-Aldrich	PCR primers	GCATAGCATCCTGGACGGCTTCC
Sequence-based reagent	Aire-RV	Sigma-Aldrich	PCR primers	CTGGGCTGGAGACGCTCTTTGAG
Sequence-based reagent	Ccl19-FW	Sigma-Aldrich	PCR primers	GCTAATGATGCGGAAGACTG
Sequence-based reagent	Ccl19-RV	Sigma-Aldrich	PCR primers	ACTCACATCGACTCTCTAGG
Sequence-based reagent	Ccl2-FW	Sigma-Aldrich	PCR primers	TGGAGCATCCACGTGTTG
Sequence-based reagent	Ccl2-RV	Sigma-Aldrich	PCR primers	ACTCATTGGGATCATCTTGCT
Sequence-based reagent	Ccl22-FW	Sigma-Aldrich	PCR primers	CTGATGCAGGTCCCTATGGT
Sequence-based reagent	Ccl22-RV	Sigma-Aldrich	PCR primers	GGAGTAGCTTCTTCACCCAG
Sequence-based reagent	Ccl25-FW	Sigma-Aldrich	PCR primers	GCCTGGTTGCCTGTTTTGTT
Sequence-based reagent	Ccl25-RV	Sigma-Aldrich	PCR primers	ACCCAGGCAGCAGTCTTCAA
Sequence-based reagent	Cdh2-FW	Sigma-Aldrich	PCR primers	AGCGCAGTCTTACCGAAGG
Sequence-based reagent	Cdh2-RV	Sigma-Aldrich	PCR primers	TCGCTGCTTTCATACTGAACTTT
Sequence-based reagent	Coch-FW	Sigma-Aldrich	PCR primers	GTGCAGCAAAACCTGCTACAA
Sequence-based reagent	Coch -RV	Sigma-Aldrich	PCR primers	AGCTAGGACGTTCTCTTTGGT
Sequence-based reagent	Crabp1-FW	Sigma-Aldrich	PCR primers	CAGCAGCGAGAATTTCGACGA
Sequence-based reagent	Crabp1-RV	Sigma-Aldrich	PCR primers	CGCACAGTAGTGGATGTCTTGA
Sequence-based reagent	Crp-FW	Sigma-Aldrich	PCR primers	CATAGCCATGGAGAAGCTAC
Sequence-based reagent	Crp-RV	Sigma-Aldrich	PCR primers	CAGTGGCTTCTTTGACTCTG
Sequence-based reagent	Csn2-FW	Sigma-Aldrich	PCR primers	CTCCACTAAAGGACTTGACAG
Sequence-based reagent	Csn2-RV	Sigma-Aldrich	PCR primers	ACCTTCTGAAGTTTCTGCTC
Sequence-based reagent	Fabp9-FW	Sigma-Aldrich	PCR primers	CACTGCAGACAACCGAAAAG
Sequence-based reagent	Fabp9-RV	Sigma-Aldrich	PCR primers	TCTGTTTGCCAAGCCATTTT
Sequence-based reagent	Fam183b-FW	Sigma-Aldrich	PCR primers	CGTGTGGGGCAGATGAAGAAT

Continued on next page

Continued

Reagent type (species) or resource	Designation	Source or reference	Identifiers	Additional information
Sequence-based reagent	Fam183b-RV	Sigma-Aldrich	PCR primers	GGTGAATGAGGTTCAGGAACTTG
Sequence-based reagent	Fcer2a-FW	Sigma-Aldrich	PCR primers	CCAGGAGGATCTAAGGAACGC
Sequence-based reagent	Fcer2a-RV	Sigma-Aldrich	PCR primers	TCGTCTTGGAGTCTGTTCAGG
Sequence-based reagent	Fezf2-FW	Sigma-Aldrich	PCR primers	CAGCACTCTCTGCAGACACAA
Sequence-based reagent	Fezf2-RV	Sigma-Aldrich	PCR primers	TGCCGCACTGGTTACACTTA
Sequence-based reagent	Grap-FW	Sigma-Aldrich	PCR primers	GATCAGGGAGAGTGAGAGTTCC
Sequence-based reagent	Grap-RV	Sigma-Aldrich	PCR primers	CAGCTCGTTGAGGGAGTTGA
Sequence-based reagent	Icam2-FW	Sigma-Aldrich	PCR primers	ATCAACTGCAGCACCAACTG
Sequence-based reagent	Icam2-RV	Sigma-Aldrich	PCR primers	ACTTGAGCTGGAGGCTGGTA
Sequence-based reagent	Il15-FW	Sigma-Aldrich	PCR primers	AGCAGATAACCAGCCTACAGGA
Sequence-based reagent	Il15-RV	Sigma-Aldrich	PCR primers	TGTTGAAGATGAGCTGGCTATGG
Sequence-based reagent	Il21-FW	Sigma-Aldrich	PCR primers	CGCCTCCTGATTAGACTTCG
Sequence-based reagent	Il21-RV	Sigma-Aldrich	PCR primers	TGGAGCTGATAGAAGTTCAGGA
Sequence-based reagent	Il5-FW	Sigma-Aldrich	PCR primers	CCGCCAAAAAGAGAAGTGTGGCGA
Sequence-based reagent	Il5-RV	Sigma-Aldrich	PCR primers	GCCTCAGCCTTCCATTGCCCA
Sequence-based reagent	Il7-FW	Sigma-Aldrich	PCR primers	GGGTCCTGGGAGTGATTATGG
Sequence-based reagent	Il7-RV	Sigma-Aldrich	PCR primers	CGGGAGGTGGGTGTAGTCAT
Sequence-based reagent	Itgad-FW	Sigma-Aldrich	PCR primers	CGAAAGGGTTCAGACTTTGC
Sequence-based reagent	Itgad-RV	Sigma-Aldrich	PCR primers	ACACCTCCACGGATAGAAGTC
Sequence-based reagent	Itgb6-FW	Sigma-Aldrich	PCR primers	GCTGGTCTGCCTGTTTCTGC
Sequence-based reagent	Itgb6-RV	Sigma-Aldrich	PCR primers	TGAGCAGCTTTCTGCACCAC
Sequence-based reagent	Kcnj5-FW	Sigma-Aldrich	PCR primers	AAAACCTTAGCGGCTTTGTATCT
Sequence-based reagent	Kcnj5-RV	Sigma-Aldrich	PCR primers	AAGGCATTAACAATCGAGCCC
Sequence-based reagent	Krt1-FW	Sigma-Aldrich	PCR primers	TGGGAGATTTTCAGGAGGAGG
Sequence-based reagent	Krt1-RV	Sigma-Aldrich	PCR primers	GCCACACTCTTGGAGATGCTC

Continued on next page

Continued

Reagent type (species) or resource	Designation	Source or reference	Identifiers	Additional information
Sequence-based reagent	Meig1-FW	Sigma-Aldrich	PCR primers	CTTCAGCGGAGGGACAATAC
Sequence-based reagent	Meig1-RV	Sigma-Aldrich	PCR primers	CAAGGTTTCAAGGTGGGTGT
Sequence-based reagent	Nov-FW	Sigma-Aldrich	PCR primers	AGACCCCAACAACCAGACTG
Sequence-based reagent	Nov-RV	Sigma-Aldrich	PCR primers	CGGTAAATGACCCCATCGAAC
Sequence-based reagent	Nts-FW	Sigma-Aldrich	PCR primers	GCAAGTCCTCCGTCTTGGAAA
Sequence-based reagent	Nts-RV	Sigma-Aldrich	PCR primers	TGCCAACAAGGTCGTCATCAT
Sequence-based reagent	Reig1-FW	Sigma-Aldrich	PCR primers	ATGGCTAGGAACGCCTACTTC
Sequence-based reagent	Reig1-RV	Sigma-Aldrich	PCR primers	CCCAAGTTAAACGGTCTTCAGT
Sequence-based reagent	Resp18-FW	Sigma-Aldrich	PCR primers	CCAGCCAAGATGCAGAGTTCGTTAAAG
Sequence-based reagent	Resp18-RV	Sigma-Aldrich	PCR primers	TCAGTCAGCAACAAGGTTGAGGCCCAC
Sequence-based reagent	Rsph1-FW	Sigma-Aldrich	PCR primers	ACGGGGACACATATGAAGGA
Sequence-based reagent	Rsph1-RV	Sigma-Aldrich	PCR primers	GGCCGTGCTTTTTATTTTTG
Sequence-based reagent	Spon2-FW	Sigma-Aldrich	PCR primers	ATGGAAAACGTGAGTCTTGCC
Sequence-based reagent	Spon2-RV	Sigma-Aldrich	PCR primers	TGATGCTGTATCTAGCCAGAGG
Sequence-based reagent	Sult1c2-FW	Sigma-Aldrich	PCR primers	ATGGCCTTGACCCCAGAAC
Sequence-based reagent	Sult1c2-RV	Sigma-Aldrich	PCR primers	TCGAAGGTCTGAATCTGCCTC
Sequence-based reagent	Upk3b-FW	Sigma-Aldrich	PCR primers	CATCTGGCTAGTGGTGGCTTT
Sequence-based reagent	Upk3b-RV	Sigma-Aldrich	PCR primers	GGTAATGTCATATAGTGGCCGTC
Other	Biotinylated Lotus Tetragonolobus Lectin (LTL)	Vector Laboratories	Cat# B-1325; RRID:AB_2336558	IF (1:500)
Other	FITC Ulex Europaeus Agglutinin I (UEA I)	Vector Laboratories	Cat# FL-1061; RRID:AB_2336767	FACS (1:600)
Other	SuperScript II Reverse Transcriptase	Thermo Fisher	Cat# 18064022	
Other	SYBR Premix Ex Taq master mix	Takara	Cat# RR390A	
Other	miRNeasy Micro Kit	QIAGEN	Cat# 217084	
Other	TruSeq ChIP Library Preparation Kit	Illumina	Cat# IP-202-2012	

Mice

C57BL/6 WT mice were purchased from Charles River. *Ciita*$^{III+IV-/-}$ (ΔCD4) (***LeibundGut-Landmann et al., 2004***), MHCII$^{-/-}$ (***Madsen et al., 1999***), K14x*Ciita*$^{III\ -/-}$ (mTEC$^{\Delta MHCII}$) (***Irla et al., 2008***), OTII (***Barnden et al., 1998***), RipmOVAxOTII (***Kurts et al., 1996***), and *Rag2*$^{-/-}$ (***Shinkai et al., 1992***) mice were on C57BL/6J background. OTII and RipmOVAxOTII were backcrossed on *Rag2*$^{-/-}$ background. All mice were maintained under specific pathogen-free conditions at an ambient temperature of 22°C at

the animal facilities of the CIML (Marseille, France). Standard food and water were given ad libitum. Males and females were used at the age of 5–6 weeks. All experiments were done in accordance with national and European laws for laboratory animal welfare (EEC Council Directive 2010/63/UE), and were approved by the Marseille Ethical Committee for Animal Experimentation (Comité National de Réflexion Ethique sur l'Expérimentation Animale no. 14).

mTEC purification

mTECs were isolated by enzymatic digestion with 50 µg/ml of Liberase TM (Roche) and 100 µg/ml of DNase I (Roche) in HBSS medium, as previously described (***Lopes et al., 2017***). $CD45^+$ hematopoietic cells were depleted using anti-CD45 magnetic beads by autoMACS with the depleteS program (Miltenyi Biotec). Total mTECs ($EpCAM^+UEA\text{-}1^+Ly51^{lo}$), $mTEC^{lo}$ ($EpCAM^+UEA\text{-}1^+Ly51^{lo}CD80^{lo/int}$), and $mTEC^{hi}$ ($EpCAM^+UEA\text{-}1^+Ly51^{lo}CD80^{hi}$) were sorted with a FACSAriaIII cell sorter (BD). The purity of sorted $mTEC^{lo}$ was >98%. Flow cytometry gating strategies are shown in ***Figure 1—figure supplement 1***.

mTEC antigen presentation assays

Variable numbers of mTECs from WT and $mTEC^{\Delta MHCII}$ mice loaded or not with $OVA_{323\text{-}339}$ (5 µM, PolyPeptide group) were co-cultured with 10^5 OTII $CD4^+$ T cells (purified with a $CD4^+$ T cell isolation kit, Miltenyi Biotec) in RPMI medium (Thermo Fisher) supplemented with 10% FCS (Sigma-Aldrich), L-glutamine (2 mM, Thermo Fisher), sodium pyruvate (1 mM, Thermo Fisher), 2-mercaptoethanol (2×10^{-5} M, Thermo Fisher), penicillin (100 IU/ml, Thermo Fisher), and streptomycin (100 µg/ml, Thermo Fisher). The activation of OTII $CD4^+$ T cells was assessed 18 hr later by flow cytometry based on the upregulation of the CD69 marker.

Flow cytometry

TECs, thymocytes, and splenic T cells were analyzed by flow cytometry (FACSCanto II, BD) with standard procedures. Cells were incubated for 15 min at 4°C with Fc-block (anti-CD16/CD32, 2.4G2, BD Biosciences) before staining. Antibodies are listed in the Key resources table. For intracellular staining with anti-Foxp3, anti-Ki-67, anti-p38 MAPK, anti-phospho p38 MAPK (Thr180/Tyr182), anti-IKKα, anti-phospho IKKα(Ser180)/IKKβ(Ser181), anti-Erk1/2 MAPK, anti-phospho Erk1/2 MAPK (Thr202/Tyr204), anti-p65, anti-phospho p65(ser536), anti-RelB, anti-phospho RelB(ser552), and anti-DCLK1 antibodies, cells were fixed, permeabilized, and stained with the Foxp3 staining kit according to the manufacturer's instructions (eBioscience). Intracellular staining with anti-Aire, anti-Fezf2, anti-CCL21, anti-H3K4me3, and anti-H3K27me3 antibodies was performed with Fixation/Permeabilization Solution Kit (BD). Secondary antibodies (II Abs) were used to set positive staining gates. Flow cytometry analysis was performed with a FACSCanto II (BD), and data were analyzed using FlowJo software (BD).

Quantitative RT-PCR

Total RNA was prepared with TRIzol (Invitrogen). cDNAs was synthesized with oligo(dT) using Superscript II reverse transcriptase (Invitrogen). qPCR was performed with the ABI 7500 fast real-time PCR system (Applied Biosystems) and SYBR Premix Ex Taq master mix (Takara). Primers are listed in the Key resources table.

In vivo transfer of splenocytes into *Rag2*$^{-/-}$ recipients

3.10^6 splenocytes purified from the spleen of WT and $mTEC^{\Delta MHCII}$ mice of 8 weeks of age were intravenously injected into *Rag2*$^{-/-}$ female recipients. $CD3^+$, $CD4^+$, and $CD8^+$ T-cell infiltrates were analyzed 6 weeks after transfer by histology and flow cytometry in different peripheral tissues.

Histology

Tissues were fixed in 10% buffered formalin (Sigma) and embedded in paraffin blocks. 4-µm-thick sections were stained with hematoxylin-eosin (Thermo Fisher) and analyzed by light microscopy (Nikon Statif eclipse Ci-L). For immunofluorescence experiments, frozen thymic sections were stained as previously described (***Sergé et al., 2015***) with Alexa Fluor 488 or Alexa Fluor 647-conjugated anti-Aire (5H12; eBioscience), biotinylated anti-TPA (LTL; Vector Laboratories), rabbit anti-Fezf2 (F441; IBL Tecan), and rabbit anti-involucrin (BioLegend) antibodies. Rabbit anti-Fezf2 and rabbit anti-involucrin

were revealed with Cy3-conjugated anti-rabbit IgG (Invitrogen), and biotinylated anti-TPA was revealed with Alexa Fluor 488-conjugated streptavidin (Invitrogen). Sections were mounted with Mowiol (Calbiochem). Immunofluorescence confocal microscopy was performed with a LSM780 Leica SP5X confocal microscope. Images were analyzed with ImageJ software.

RNA-seq experiments

Total RNA purified from mTEC^{lo} (***Figure 1—figure supplement 1***) was extracted with miRNeasy Micro Kit (QIAGEN), and RNA quality was assessed on an Agilent 2100 BioAnalyzer (Agilent Technologies). RNA Integrity Number values over 8 were obtained. RNA-seq libraries were generated using the SMART-Seq-v4-Ultra Low Input RNA Kit (Clontech) combined to the Nextera library preparation kit (Illumina) following the manufacturer's instructions. Libraries were sequenced with the Illumina NextSeq 500 machine to generate datasets of single-end 75 bp reads. Two independent biological replicates were used per each condition. RNA-seq data have been deposited with Gene Expression Omnibus (GEO) under the accession number GSE144650.

RNA-seq analysis

The sequencing reads were mapped to the *Mus musculus* (mm10) reference genome using the TopHat 2 (version 2.0.12) aligner (***Kim et al., 2013***). The reads mapping to the annotated genes (igenome UCSC mm10 GTF: https://support.illumina.com/sequencing/sequencing_software/igenome.html) were counted, normalized, and compared using Cuffdiff2 (version 2.2.1; ***Trapnell et al., 2013***) between two conditions. Cuffdiff2 generated expression levels as FPKM, FCs, and p-values to assess the statistical significance of the FPKM difference of each gene between the tested two conditions. Genes showing a significant variation in gene expression between WT and ΔCD4, or WT and mTEC$^{\Delta MHCII}$, or RIPmOVAxOTII-*Rag2*$^{-/-}$ and OTII-*Rag2*$^{-/-}$ mice (p-value≤0.05, FC difference ≥ 2 or ≤ 0.5) were considered as up- or downregulated. The TRA and non-TRA gene assignments were obtained from ***Sansom et al., 2014***. In this report, the identification of the specificity of expression for each gene in the genome was carried out by analyzing the microarray expression profiles of a large number of different mouse tissues. Aire-dependent, Fezf2-dependent, Aire/Fezf2-dependent, and Aire/Fezf2-independent TRAs were identified using *Aire*$^{-/-}$ mTEC^{hi} RNA-seq datasets and *Fezf2*$^{-/-}$ total mTEC microarray datasets, obtained from the NCBI GEO database (GSE87133 and GSE69105, respectively).

Correlation between the variation of gene expression in mTEC^{lo} from WT versus mTEC$^{\Delta MHCII}$ or RIPmOVAxOTII-*Rag2*$^{-/-}$ versus OTII-*Rag2*$^{-/-}$ mice, and of the same genes in mTEC^{hi} from WT versus *Aire*$^{-/-}$ mice was performed doing a locally regression (loess) with the R software (http://www.r-project.org/). Differential gene expression in WT versus *Aire*$^{-/-}$ mTEC^{hi} was obtained by processing using TopHat2 and Cuffdiff2, the sequencing reads corresponding to WT (***Chuprin et al., 2015***) and *Aire*$^{-/-}$ (***Danan-Gotthold et al., 2016***) mTEC^{hi} RNA-seq datasets, which were obtained from the NCBI GEO database (GSE68190 and GSE87133, respectively). HDAC3-dependent mTEC-specific transcription factors regulated by mTEC-thymocyte crosstalk were identified by comparing the top 50 transcriptional regulators that are induced by HDAC3 (***Goldfarb et al., 2016***) with genes upregulated in the different mouse models. TRAs differentially expressed between mTEC^{lo} from WT and mTEC$^{\Delta MHCII}$ mice were classified according to their tissue distribution using the mouse ENCODE transcriptome database (***Yue, 2014***). Only tissues that showed the highest expression were taken into account.

Single-cell RNA-seq analysis

Single-cell RNA-seq count matrix from ***Wells et al., 2020*** (accession number GSE137699) was reanalyzed with the Seurat package (***Hao et al., 2021***). QC analysis was performed by filtering out cells with a number of feature counts under 200 or over 4000, and a proportion of mitochondrial counts over 4%. Sample integration was performed as described in the Seurat vignette. After PCA for dimension reduction, 15 first dimensions were conserved. Cells were clustered and visualized with UMAP. Cluster annotation was performed by identifying sets of specific markers to each cluster using a differential expression test (FindMarkers function, test = 'roc'). Heatmaps were generated using the pheatmap R package.

Nano-ChIP-seq experiments

Nano-ChIP-seq was performed as previously described (***Adli and Bernstein, 2011***) on 5.10^4 purified mTEC^{lo} (***Figure 1—figure supplement 1***). ChIP-seq libraries were prepared with TruSeq ChIP Sample Preparation Kit (Illumina), and 2 × 75 bp paired-end reads were sequenced on an Illumina HiSeq. ChIP-seq data have been deposited with GEO under the accession number GSE144680.

ChIP-seq analysis

Reads were aligned on the mouse genome (mm10) using Bowtie 2 and default parameters (***Langmead and Salzberg, 2012***). Properly paired alignments were selected using Samtools view with the 0x2flag (-f option). Nonuniquely mapped reads-pairs were filtered out by removing reads with the 'XS' tag set by Bowtie 2. Normalized bedgraphs for ChIP and input samples were generated using MACS2 (***Zhang et al., 2008***) with the callpeak command in BAMPE mode with the --SPMR option. For the diffused H3K27me3 histone mark, the -broad option was used. ChIP enrichment was calculated parsing the ChIP and input normalized bedgraphs with MACS2 and the bdgcmp command (-m FE option). The obtained bedgraphs were converted to wig using the bedGraphToWig.pl script with the --step 10 parameter. MACS2-generated peak calling files were converted to BED files using the cut -f 1-6 command. The obtained Wig and BED files were parsed by CEAS (***Shin et al., 2009***) to generate metagene profile plots corresponding to the average enrichment of H3K4me3 in 3 kb TSS windows or H3K27me3 at gene loci. H3K4me3 and H3K27me3 CEAS-dumped files were parsed to compute ratios of ChIP/input in 1 kb TSS windows and gene loci, respectively. Statistical significance between ChIP enrichment data was tested using the nonparametric Mann–Whitney test. Data were visualized using the Integrative Genomics Viewer (IGV) (***Robinson et al., 2011***).

Statistics

Data are presented as means ± standard error of mean (SEM). Statistical analysis was performed with GraphPad Prism 7.03 software by using ANOVA, chi-square, unpaired Student's *t*-test, or Mann–Whitney test. ****p<0.0001, ***p<0.001, **p<0.01, *p<0.05. Normal distribution of the data was assessed using d'Agostino–Pearson omnibus normality test.

Acknowledgements

We thank Pr. Arnauld Sergé (LAI, Marseille, France) for critical reading of the manuscript, Pr. Walter Reith (University of Geneva, Switzerland) for providing *Ciita*$^{III+IV-/-}$ and K14x*Ciita*$^{III\ -/-}$ mice, and Dr. Bruno Lucas (Institut Cochin, Paris, France) for providing MHCII$^{-/-}$ mice. We also thank Cloé Zamit and Alexia Borelli (CIML, Marseille, France) for help with mouse genotyping and Lionel Chasson (CIML, Marseille, France) for help with paraffin-embedded tissues. We acknowledge the flow cytometry, the imaging core (ImagImm) and animal facility platforms at CIML for excellent technical support. NL and JC were supported by a PhD fellowship from Aix-Marseille University and the Ministère de l'Enseignement Supérieur et de la Recherche, respectively.

Additional information

Funding

Funder	Grant reference number	Author
H2020 Marie Skłodowska-Curie Actions	CIG_SIGnEPI4Tol_618541	Magali Irla
Agence Nationale de la Recherche	2011-CHEX-001-R12004KK	Matthieu Giraud
Agence Nationale de la Recherche	ANR-19-CE18-0021-01 RANKLthym	Magali Irla

The funders had no role in study design, data collection and interpretation, or the decision to submit the work for publication.

Author contributions

Noella Lopes, Formal analysis, Investigation, Methodology, Validation, Writing – original draft; Nicolas Boucherit, Methodology, Validation; Jérémy C Santamaria, Data curation, Formal analysis, Validation; Nathan Provin, Conceptualization, Data curation, Formal analysis, Visualization; Jonathan Charaix, Matthieu Giraud, Data curation, Formal analysis, Methodology, Software, Validation, Writing - review and editing; Pierre Ferrier, Conceptualization, Funding acquisition, Methodology, Supervision, Writing – original draft, Writing - review and editing; Magali Irla, Conceptualization, Data curation, Formal analysis, Funding acquisition, Methodology, Supervision, Visualization, Writing – original draft, Writing - review and editing

Author ORCIDs

Noella Lopes http://orcid.org/0000-0002-6296-8426
Jérémy C Santamaria http://orcid.org/0000-0001-7613-3668
Matthieu Giraud http://orcid.org/0000-0002-1208-9677
Magali Irla http://orcid.org/0000-0001-8803-9708

Ethics

All mice were housed, bred and manipulated under specific pathogen-free conditions at the animal facilities of the CIML (Marseille, France). All experiments were done in accordance with national and European laws for laboratory animal welfare (EEC Council Directive 2010/63/UE), and were approved by the Marseille Ethical Committee for Animal Experimentation (Comité National de Réflexion Ethique sur l'Expérimentation Animale no. 14; Permit Number: 02373.03).

Decision letter and Author response

Decision letter https://doi.org/10.7554/eLife.69982.sa1
Author response https://doi.org/10.7554/eLife.69982.sa2

Additional files

Supplementary files

- Supplementary file 1. List of tissue-restricted self-antigens (TRAs) differentially expressed in mTEC^{lo} from WT and ΔCD4 mice.
- Supplementary file 2. List of tissue-restricted self-antigens (TRAs) differentially expressed in mTEC^{lo} from WT and mTEC$^{\Delta MHCII}$ mice.
- Supplementary file 3. List of tissue-restricted self-antigens (TRAs) differentially expressed in mTEC^{lo} from OTII-*Rag2*$^{-/-}$ and RipmOVAxOTII-*Rag2*$^{-/-}$ mice.
- Supplementary file 4. Main target organs and fold change associated with the expression of tissue-restricted self-antigens (TRAs) differentially expressed in mTEC^{lo} from WT and mTEC$^{\Delta MHCII}$ mice.
- Transparent reporting form

Data availability

RNA-seq data have been deposited in GEO under the accession number GSE144650. ChIP-seq data have been deposited in GEO under the accession number GSE144680.

The following datasets were generated:

Author(s)	Year	Dataset title	Dataset URL	Database and Identifier
Irla M, Giraud M	2020	mTEClo/int RNAseq profiling in three mouse models of impaired mTEC/Tcell crosstalk	https://www.ncbi.nlm.nih.gov/geo/query/acc.cgi?acc=GSE144650	NCBI Gene Expression Omnibus, GSE144650

The following previously published datasets were used:

Author(s)	Year	Dataset title	Dataset URL	Database and Identifier
Wells KL	2020	ingle cell sequencing defines a branched progenitor population of stable medullary thymic epithelial cells	https://www.ncbi.nlm.nih.gov/geo/query/acc.cgi?acc=GSE137699	NCBI Gene Expression Omnibus, GSE137699
Abramson J, Giraud M	2016	Aire-KO MEChi RNAseq profiling	https://www.ncbi.nlm.nih.gov/geo/query/acc.cgi?acc=GSE87133	NCBI Gene Expression Omnibus, GSE87133
Abramson J, Giraud M	2015	Sirt1 is essential for Aire-mediated induction of central immunological tolerance	https://www.ncbi.nlm.nih.gov/geo/query/acc.cgi?acc=GSE68190	NCBI Gene Expression Omnibus, GSE68190

References

Adli M, Bernstein BE. 2011. Whole-genome chromatin profiling from limited numbers of cells using nano-ChIP-seq. *Nature Protocols* **6**:1656–1668. DOI: https://doi.org/10.1038/nprot.2011.402, PMID: 21959244

Akiyama T, Shimo Y, Yanai H, Qin J, Ohshima D, Maruyama Y, Asaumi Y, Kitazawa J, Takayanagi H, Penninger JM, Matsumoto M, Nitta T, Takahama Y, Inoue J-I. 2008. The tumor necrosis factor family receptors RANK and CD40 cooperatively establish the thymic medullary microenvironment and self-tolerance. *Immunity* **29**:423–437. DOI: https://doi.org/10.1016/j.immuni.2008.06.015, PMID: 18799149

Akiyama N, Shinzawa M, Miyauchi M, Yanai H, Tateishi R, Shimo Y, Ohshima D, Matsuo K, Sasaki I, Hoshino K, Wu G, Yagi S, Inoue J, Kaisho T, Akiyama T. 2014. Limitation of immune tolerance-inducing thymic epithelial cell development by Spi-B-mediated negative feedback regulation. *The Journal of Experimental Medicine* **211**:2425–2438. DOI: https://doi.org/10.1084/jem.20141207, PMID: 25385757

Anderson MS, Venanzi ES, Klein L, Chen Z, Berzins SP, Turley SJ, von Boehmer H, Bronson R, Dierich A, Benoist C, Mathis D. 2002. Projection of an immunological self shadow within the thymus by the aire protein. *Science* **298**:1395–1401. DOI: https://doi.org/10.1126/science.1075958, PMID: 12376594

Asano T, Okamoto K, Nakai Y, Tsutsumi M, Muro R, Suematsu A, Hashimoto K, Okamura T, Ehata S, Nitta T, Takayanagi H. 2019. Soluble RANKL is physiologically dispensable but accelerates tumour metastasis to bone. *Nature Metabolism* **1**:868–875. DOI: https://doi.org/10.1038/s42255-019-0104-1, PMID: 32694743

Baba T, Nakamoto Y, Mukaida N. 2009. Crucial contribution of thymic Sirp alpha+ conventional dendritic cells to central tolerance against blood-borne antigens in a CCR2-dependent manner. *Journal of Immunology* **183**:3053–3063. DOI: https://doi.org/10.4049/jimmunol.0900438, PMID: 19675159

Baran-Gale J, Morgan MD, Maio S, Dhalla F, Calvo-Asensio I, Deadman ME, Handel AE, Maynard A, Chen S, Green F, Sit RV, Neff NF, Darmanis S, Tan W, May AP, Marioni JC, Ponting CP, Holländer GA. 2020. Ageing compromises mouse thymus function and remodels epithelial cell differentiation. *eLife* **9**:e56221. DOI: https://doi.org/10.7554/eLife.56221, PMID: 32840480

Barnden MJ, Allison J, Heath WR, Carbone FR. 1998. Defective TCR expression in transgenic mice constructed using cDNA-based alpha- and beta-chain genes under the control of heterologous regulatory elements. *Immunology and Cell Biology* **76**:34–40. DOI: https://doi.org/10.1046/j.1440-1711.1998.00709.x, PMID: 9553774

Borelli A, Irla M. 2021. Lymphotoxin: from the physiology to the regeneration of the thymic function. *Cell Death and Differentiation* **28**:2305–2314. DOI: https://doi.org/10.1038/s41418-021-00834-8, PMID: 34290396

Bornstein C, Nevo S, Giladi A, Kadouri N, Pouzolles M, Gerbe F, David E, Machado A, Chuprin A, Tóth B, Goldberg O, Itzkovitz S, Taylor N, Jay P, Zimmermann VS, Abramson J, Amit I. 2018. Single-cell mapping of the thymic stroma identifies IL-25-producing tuft epithelial cells. *Nature* **559**:622–626. DOI: https://doi.org/10.1038/s41586-018-0346-1, PMID: 30022162

Burkly L, Hession C, Ogata L, Reilly C, Marconi LA, Olson D, Tizard R, Cate R, Lo D. 1995. Expression of relB is required for the development of thymic medulla and dendritic cells. *Nature* **373**:531–536. DOI: https://doi.org/10.1038/373531a0, PMID: 7845467

Cédile O, Løbner M, Toft-Hansen H, Frank I, Wlodarczyk A, Irla M, Owens T. 2014. Thymic CCL2 influences induction of T-cell tolerance. *Journal of Autoimmunity* **55**:73–85. DOI: https://doi.org/10.1016/j.jaut.2014.07.004, PMID: 25129504

Chuprin A, Avin A, Goldfarb Y, Herzig Y, Levi B, Jacob A, Sela A, Katz S, Grossman M, Guyon C, Rathaus M, Cohen HY, Sagi I, Giraud M, McBurney MW, Husebye ES, Abramson J. 2015. The deacetylase Sirt1 is an essential regulator of Aire-mediated induction of central immunological tolerance. *Nature Immunology* **16**:737–745. DOI: https://doi.org/10.1038/ni.3194, PMID: 26006015

Cowan JE, Baik S, McCarthy NI, Parnell SM, White AJ, Jenkinson WE, Anderson G. 2018. Aire controls the recirculation of murine Foxp3$^+$ regulatory T-cells back to the thymus. *European Journal of Immunology* **48**:844–854. DOI: https://doi.org/10.1002/eji.201747375, PMID: 29285761

Danan-Gotthold M, Guyon C, Giraud M, Levanon EY, Abramson J. 2016. Extensive RNA editing and splicing increase immune self-representation diversity in medullary thymic epithelial cells. *Genome Biology* **17**:219. DOI: https://doi.org/10.1186/s13059-016-1079-9

Derbinski J., Schulte A, Kyewski B, Klein L. 2001. Promiscuous gene expression in medullary thymic epithelial cells mirrors the peripheral self. *Nature Immunology* **2**:1032–1039. DOI: https://doi.org/10.1038/ni723, PMID: 11600886

Derbinski Jens, Gäbler J, Brors B, Tierling S, Jonnakuty S, Hergenhahn M, Peltonen L, Walter J, Kyewski B. 2005. Promiscuous gene expression in thymic epithelial cells is regulated at multiple levels. *The Journal of Experimental Medicine* **202**:33–45. DOI: https://doi.org/10.1084/jem.20050471, PMID: 15983066

Dhalla F, Baran-Gale J, Maio S, Chappell L, Holländer GA, Ponting CP. 2020. Biologically indeterminate yet ordered promiscuous gene expression in single medullary thymic epithelial cells. *The EMBO Journal* **39**:e101828. DOI: https://doi.org/10.15252/embj.2019101828, PMID: 31657037

Gäbler J, Arnold J, Kyewski B. 2007. Promiscuous gene expression and the developmental dynamics of medullary thymic epithelial cells. *European Journal of Immunology* **37**:3363–3372. DOI: https://doi.org/10.1002/eji.200737131, PMID: 18000951

Giraud M, Yoshida H, Abramson J, Rahl PB, Young RA, Mathis D, Benoist C. 2012. Aire unleashes stalled RNA polymerase to induce ectopic gene expression in thymic epithelial cells. *PNAS* **109**:535–540. DOI: https://doi.org/10.1073/pnas.1119351109, PMID: 22203960

Goldfarb Y, Kadouri N, Levi B, Sela A, Herzig Y, Cohen RN, Hollenberg AN, Abramson J. 2016. HDAC3 Is a Master Regulator of mTEC Development. *Cell Reports* **15**:651–665. DOI: https://doi.org/10.1016/j.celrep.2016.03.048, PMID: 27068467

Gray DHD, Seach N, Ueno T, Milton MK, Liston A, Lew AM, Goodnow CC, Boyd RL. 2006. Developmental kinetics, turnover, and stimulatory capacity of thymic epithelial cells. *Blood* **108**:3777–3785. DOI: https://doi.org/10.1182/blood-2006-02-004531, PMID: 16896157

Gray D, Abramson J, Benoist C, Mathis D. 2007. Proliferative arrest and rapid turnover of thymic epithelial cells expressing Aire. *The Journal of Experimental Medicine* **204**:2521–2528. DOI: https://doi.org/10.1084/jem.20070795, PMID: 17908938

Haljasorg U, Dooley J, Laan M, Kisand K, Bichele R, Liston A, Peterson P. 2017. Irf4 Expression in Thymic Epithelium Is Critical for Thymic Regulatory T Cell Homeostasis. *Journal of Immunology* **198**:1952–1960. DOI: https://doi.org/10.4049/jimmunol.1601698, PMID: 28108558

Handel AE, Shikama-Dorn N, Zhanybekova S, Maio S, Graedel AN, Zuklys S, Ponting CP, Holländer GA. 2018. Comprehensively Profiling the Chromatin Architecture of Tissue Restricted Antigen Expression in Thymic Epithelial Cells Over Development. *Frontiers in Immunology* **9**:2120. DOI: https://doi.org/10.3389/fimmu.2018.02120, PMID: 30283453

Hao Y, Hao S, Andersen-Nissen E, Mauck WM, Zheng S, Butler A, Lee MJ, Wilk AJ, Darby C, Zager M, Hoffman P, Stoeckius M, Papalexi E, Mimitou EP, Jain J, Srivastava A, Stuart T, Fleming LM, Yeung B, Rogers AJ, et al. 2021. Integrated analysis of multimodal single-cell data. *Cell* **184**:3573–3587. DOI: https://doi.org/10.1016/j.cell.2021.04.048, PMID: 34062119

Hikosaka Y, Nitta T, Ohigashi I, Yano K, Ishimaru N, Hayashi Y, Matsumoto M, Matsuo K, Penninger JM, Takayanagi H, Yokota Y, Yamada H, Yoshikai Y, Inoue J-I, Akiyama T, Takahama Y. 2008. The cytokine RANKL produced by positively selected thymocytes fosters medullary thymic epithelial cells that express autoimmune regulator. *Immunity* **29**:438–450. DOI: https://doi.org/10.1016/j.immuni.2008.06.018, PMID: 18799150

Hu Z, Lancaster JN, Sasiponganan C, Ehrlich LIR. 2015. CCR4 promotes medullary entry and thymocyte-dendritic cell interactions required for central tolerance. *The Journal of Experimental Medicine* **212**:1947–1965. DOI: https://doi.org/10.1084/jem.20150178, PMID: 26417005

Irla M, Hugues S, Gill J, Nitta T, Hikosaka Y, Williams IR, Hubert FX, Scott HS, Takahama Y, Holländer GA, Reith W. 2008. Autoantigen-specific interactions with CD4+ thymocytes control mature medullary thymic epithelial cell cellularity. *Immunity* **29**:451–463. DOI: https://doi.org/10.1016/j.immuni.2008.08.007, PMID: 18799151

Irla M, Hollander G, Reith W. 2010. Control of central self-tolerance induction by autoreactive CD4+ thymocytes. *Trends in Immunology* **31**:71–79. DOI: https://doi.org/10.1016/j.it.2009.11.002, PMID: 20004147

Irla M, Guerri L, Guenot J, Sergé A, Lantz O, Liston A, Imhof BA, Palmer E, Reith W. 2012. Antigen recognition by autoreactive CD4+ thymocytes drives homeostasis of the thymic medulla. *PLOS ONE* **7**:e52591. DOI: https://doi.org/10.1371/journal.pone.0052591, PMID: 23300712

Irla M. 2020. RANK Signaling in the Differentiation and Regeneration of Thymic Epithelial Cells. *Frontiers in Immunology* **11**:623265. DOI: https://doi.org/10.3389/fimmu.2020.623265

Kadouri N, Nevo S, Goldfarb Y, Abramson J. 2020. Thymic epithelial cell heterogeneity: TEC by TEC. *Nature Reviews. Immunology* **20**:239–253. DOI: https://doi.org/10.1038/s41577-019-0238-0, PMID: 31804611

Kim D, Pertea G, Trapnell C, Pimentel H, Kelley R, Salzberg SL. 2013. TopHat2: accurate alignment of transcriptomes in the presence of insertions, deletions and gene fusions. *Genome Biology* **14**:R36. DOI: https://doi.org/10.1186/gb-2013-14-4-r36, PMID: 23618408

Klein L, Kyewski B, Allen PM, Hogquist KA. 2014. Positive and negative selection of the T cell repertoire: what thymocytes see (and don't see). *Nature Reviews. Immunology* **14**:377–391. DOI: https://doi.org/10.1038/nri3667, PMID: 24830344

Klein L, Robey EA, Hsieh CS. 2019. Central CD4+ T cell tolerance: deletion versus regulatory T cell differentiation. *Nature Reviews. Immunology* **19**:7–18. DOI: https://doi.org/10.1038/s41577-018-0083-6, PMID: 30420705

Koh AS, Miller EL, Buenrostro JD, Moskowitz DM, Wang J, Greenleaf WJ, Chang HY, Crabtree GR. 2018. Rapid chromatin repression by Aire provides precise control of immune tolerance. *Nature Immunology* **19**:162–172. DOI: https://doi.org/10.1038/s41590-017-0032-8, PMID: 29335648

Kolde R. 2018. pheatmap. b333453. GitHub. https://github.com/raivokolde/pheatmap

Kurts C, Heath WR, Carbone FR, Allison J, Miller JF, Kosaka H. 1996. Constitutive class I-restricted exogenous presentation of self antigens in vivo. *The Journal of Experimental Medicine* **184**:923–930. DOI: https://doi.org/10.1084/jem.184.3.923, PMID: 9064352

Kyewski B, Klein L. 2006. A central role for central tolerance. *Annual Review of Immunology* **24**:571–606. DOI: https://doi.org/10.1146/annurev.immunol.23.021704.115601, PMID: 16551260

Langmead B, Salzberg SL. 2012. Fast gapped-read alignment with Bowtie 2. *Nature Methods* **9**:357–359. DOI: https://doi.org/10.1038/nmeth.1923, PMID: 22388286

LeibundGut-Landmann S, Waldburger J-M, Reis e Sousa C, Acha-Orbea H, Reith W. 2004. MHC class II expression is differentially regulated in plasmacytoid and conventional dendritic cells. *Nature Immunology* **5**:899–908. DOI: https://doi.org/10.1038/ni1109, PMID: 15322541

Lkhagvasuren E, Sakata M, Ohigashi I, Takahama Y. 2013. Lymphotoxin β receptor regulates the development of CCL21-expressing subset of postnatal medullary thymic epithelial cells. *Journal of Immunology* **190**:5110–5117. DOI: https://doi.org/10.4049/jimmunol.1203203, PMID: 23585674

Lomada D, Liu B, Coghlan L, Hu Y, Richie ER. 2007. Thymus medulla formation and central tolerance are restored in IKKalpha-/- mice that express an IKKalpha transgene in keratin 5+ thymic epithelial cells. *Journal of Immunology* **178**:829–837. DOI: https://doi.org/10.4049/jimmunol.178.2.829, PMID: 17202344

Lopes N, Serge A, Ferrier P, Irla M. 2015. Thymic Crosstalk Coordinates Medulla Organization and T-Cell Tolerance Induction. *Frontiers in Immunology* **6**:365. DOI: https://doi.org/10.3389/fimmu.2015.00365

Lopes N, Vachon H, Marie J, Irla M. 2017. Administration of RANKL boosts thymic regeneration upon bone marrow transplantation. *EMBO Molecular Medicine* **9**:835–851. DOI: https://doi.org/10.15252/emmm.201607176, PMID: 28455312

Lopes N, Charaix J, Cedile O, Serge A, Irla M. 2018. Lymphotoxin alpha fine-tunes T cell clonal deletion by regulating thymic entry of antigen-presenting cells. *Nature Communications* **9**:1262. DOI: https://doi.org/10.1038/s41467-018-03619-9

Madsen L, Labrecque N, Engberg J, Dierich A, Svejgaard A, Benoist C, Mathis D, Fugger L. 1999. Mice lacking all conventional MHC class II genes. *PNAS* **96**:10338–10343. DOI: https://doi.org/10.1073/pnas.96.18.10338, PMID: 10468609

Metzger TC, Khan IS, Gardner JM, Mouchess ML, Johannes KP, Krawisz AK, Skrzypczynska KM, Anderson MS. 2013. Lineage tracing and cell ablation identify a post-Aire-expressing thymic epithelial cell population. *Cell Reports* **5**:166–179. DOI: https://doi.org/10.1016/j.celrep.2013.08.038, PMID: 24095736

Michel C, Miller CN, Küchler R, Brors B, Anderson MS, Kyewski B, Pinto S. 2017. Revisiting the Road Map of Medullary Thymic Epithelial Cell Differentiation. *Journal of Immunology* **199**:3488–3503. DOI: https://doi.org/10.4049/jimmunol.1700203, PMID: 28993517

Miller CN, Proekt I, von Moltke J, Wells KL, Rajpurkar AR, Wang H, Rattay K, Khan IS, Metzger TC, Pollack JL, Fries AC, Lwin WW, Wigton EJ, Parent AV, Kyewski B, Erle DJ, Hogquist KA, Steinmetz LM, Locksley RM, Anderson MS. 2018. Thymic tuft cells promote an IL-4-enriched medulla and shape thymocyte development. *Nature* **559**:627–631. DOI: https://doi.org/10.1038/s41586-018-0345-2, PMID: 30022164

Nishikawa Y, Hirota F, Yano M, Kitajima H, Miyazaki J, Kawamoto H, Mouri Y, Matsumoto M. 2010. Biphasic Aire expression in early embryos and in medullary thymic epithelial cells before end-stage terminal differentiation. *The Journal of Experimental Medicine* **207**:963–971. DOI: https://doi.org/10.1084/jem.20092144

Org T, Rebane A, Kisand K, Laan M, Haljasorg U, Andreson R, Peterson P. 2009. AIRE activated tissue specific genes have histone modifications associated with inactive chromatin. *Human Molecular Genetics* **18**:4699–4710. DOI: https://doi.org/10.1093/hmg/ddp433, PMID: 19744957

Otero DC, Baker DP, David M. 2013. IRF7-Dependent IFN-beta Production in Response to RANKL Promotes Medullary Thymic Epithelial Cell Development. *Journal of Immunology* **10**:1203086. DOI: https://doi.org/10.4049/jimmunol.1203086

Pezzi N, Assis AF, Cotrim-Sousa LC, Lopes GS, Mosella MS, Lima DS, Bombonato-Prado KF, Passos GA. 2016. Aire knockdown in medullary thymic epithelial cells affects Aire protein, deregulates cell adhesion genes and decreases thymocyte interaction. *Molecular Immunology* **77**:157–173. DOI: https://doi.org/10.1016/j.molimm.2016.08.003, PMID: 27505711

Riemann M, Andreas N, Fedoseeva M, Meier E, Weih D, Freytag H, Schmidt-Ullrich R, Klein U, Wang ZQ, Weih F. 2017. Central immune tolerance depends on crosstalk between the classical and alternative NF-κB pathways in medullary thymic epithelial cells. *Journal of Autoimmunity* **81**:56–67. DOI: https://doi.org/10.1016/j.jaut.2017.03.007, PMID: 28385374

Robinson JT, Thorvaldsdóttir H, Winckler W, Guttman M, Lander ES, Getz G, Mesirov JP. 2011. Integrative genomics viewer. *Nature Biotechnology* **29**:24–26. DOI: https://doi.org/10.1038/nbt.1754, PMID: 21221095

Rodrigues PM, Ribeiro AR, Perrod C, Landry JJM, Araújo L, Pereira-Castro I, Benes V, Moreira A, Xavier-Ferreira H, Meireles C, Alves NL. 2017. Thymic epithelial cells require p53 to support their long-term function in thymopoiesis in mice. *Blood* **130**:478–488. DOI: https://doi.org/10.1182/blood-2016-12-758961, PMID: 28559356

Sansom SN, Shikama-Dorn N, Zhanybekova S, Nusspaumer G, Macaulay IC, Deadman ME, Heger A, Ponting CP, Holländer GA. 2014. Population and single-cell genomics reveal the Aire dependency, relief from Polycomb silencing, and distribution of self-antigen expression in thymic epithelia. *Genome Research* **24**:1918–1931. DOI: https://doi.org/10.1101/gr.171645.113, PMID: 25224068

Sergé A, Bailly A-L, Aurrand-Lions M, Imhof BA, Irla M. 2015. For3D: Full organ reconstruction in 3D, an automatized tool for deciphering the complexity of lymphoid organs. *Journal of Immunological Methods* **424**:32–42. DOI: https://doi.org/10.1016/j.jim.2015.04.019, PMID: 25956038

Shen H, Ji Y, Xiong Y, Kim H, Zhong X, Jin MG, Shah YM, Omary MB, Liu Y, Qi L, Rui L. 2019. Medullary thymic epithelial NF-kB-inducing kinase (NIK)/IKKα pathway shapes autoimmunity and liver and lung homeostasis in mice. *PNAS* **116**:19090–19097. DOI: https://doi.org/10.1073/pnas.1901056116, PMID: 31481626

Shin H, Liu T, Manrai AK, Liu XS. 2009. CEAS: cis-regulatory element annotation system. *Bioinformatics* **25**:2605–2606. DOI: https://doi.org/10.1093/bioinformatics/btp479, PMID: 19689956

Shinkai Y, Rathbun G, Lam KP, Oltz EM, Stewart V, Mendelsohn M, Charron J, Datta M, Young F, Stall AM. 1992. RAG-2-deficient mice lack mature lymphocytes owing to inability to initiate V(D)J rearrangement. *Cell* **68**:855–867. DOI: https://doi.org/10.1016/0092-8674(92)90029-c, PMID: 1547487

Takaba H, Morishita Y, Tomofuji Y, Danks L, Nitta T, Komatsu N, Kodama T, Takayanagi H. 2015. Fezf2 Orchestrates a Thymic Program of Self-Antigen Expression for Immune Tolerance. *Cell* **163**:975–987. DOI: https://doi.org/10.1016/j.cell.2015.10.013, PMID: 26544942

Trapnell C, Hendrickson DG, Sauvageau M, Goff L, Rinn JL, Pachter L. 2013. Differential analysis of gene regulation at transcript resolution with RNA-seq. *Nature Biotechnology* **31**:46–53. DOI: https://doi.org/10.1038/nbt.2450, PMID: 23222703

Tykocinski LO, Sinemus A, Rezavandy E, Weiland Y, Baddeley D, Cremer C, Sonntag S, Willecke K, Derbinski J, Kyewski B. 2010. Epigenetic regulation of promiscuous gene expression in thymic medullary epithelial cells. *PNAS* **107**:19426–19431. DOI: https://doi.org/10.1073/pnas.1009265107, PMID: 20966351

Ucar O, Rattay K. 2015. Promiscuous Gene Expression in the Thymus: A Matter of Epigenetics, miRNA, and More? *Frontiers in Immunology* **6**:93. DOI: https://doi.org/10.3389/fimmu.2015.00093, PMID: 25784915

Ueno T, Saito F, Gray DHD, Kuse S, Hieshima K, Nakano H, Kakiuchi T, Lipp M, Boyd RL, Takahama Y. 2004. CCR7 signals are essential for cortex-medulla migration of developing thymocytes. *The Journal of Experimental Medicine* **200**:493–505. DOI: https://doi.org/10.1084/jem.20040643, PMID: 15302902

van Ewijk W, Shores EW, Singer A. 1994. Crosstalk in the mouse thymus. *Immunology Today* **15**:214–217. DOI: https://doi.org/10.1016/0167-5699(94)90246-1, PMID: 8024681

Waldburger JM, Rossi S, Hollander GA, Rodewald HR, Reith W, Acha-Orbea H. 2003. Promoter IV of the class II transactivator gene is essential for positive selection of CD4+ T cells. *Blood* **101**:3550–3559. DOI: https://doi.org/10.1182/blood-2002-06-1855, PMID: 12506036

Wells KL, Miller CN, Gschwind AR, Wei W, Phipps JD, Anderson MS, Steinmetz LM. 2020. Combined transient ablation and single-cell RNA-sequencing reveals the development of medullary thymic epithelial cells. *eLife* **9**:e60188. DOI: https://doi.org/10.7554/eLife.60188, PMID: 33226342

White AJ, Jenkinson WE, Cowan JE, Parnell SM, Bacon A, Jones ND, Jenkinson EJ, Anderson G. 2014. An essential role for medullary thymic epithelial cells during the intrathymic development of invariant NKT cells. *Journal of Immunology* **192**:2659–2666. DOI: https://doi.org/10.4049/jimmunol.1303057, PMID: 24510964

Wong K, Lister NL, Barsanti M, Lim JMC, Hammett MV, Khong DM, Siatskas C, Gray DHD, Boyd RL, Chidgey AP. 2014. Multilineage potential and self-renewal define an epithelial progenitor cell population in the adult thymus. *Cell Reports* **8**:1198–1209. DOI: https://doi.org/10.1016/j.celrep.2014.07.029, PMID: 25131206

Youm YH, Horvath TL, Mangelsdorf DJ, Kliewer SA, Dixit VD. 2016. Prolongevity hormone FGF21 protects against immune senescence by delaying age-related thymic involution. *PNAS* **113**:1026–1031. DOI: https://doi.org/10.1073/pnas.1514511113, PMID: 26755598

Yue F. 2014. A comparative encyclopedia of DNA elements in the mouse genome. *Nature* **515**:355–364. DOI: https://doi.org/10.1038/nature13992

Zhang B, Wang Z, Ding J, Peterson P, Gunning WT, Ding HF. 2006. NF-kappaB2 is required for the control of autoimmunity by regulating the development of medullary thymic epithelial cells. *The Journal of Biological Chemistry* **281**:38617–38624. DOI: https://doi.org/10.1074/jbc.M606705200, PMID: 17046818

Zhang Y, Liu T, Meyer CA, Eeckhoute J, Johnson DS, Bernstein BE, Nusbaum C, Myers RM, Brown M, Li W, Liu XS. 2008. Model-based analysis of ChIP-Seq (MACS). *Genome Biology* **9**:R137. DOI: https://doi.org/10.1186/gb-2008-9-9-r137, PMID: 18798982

Zhu M, Chin RK, Christiansen PA, Lo JC, Liu X, Ware C, Siebenlist U, Fu YX. 2006. NF-kappaB2 is required for the establishment of central tolerance through an Aire-dependent pathway. *The Journal of Clinical Investigation* **116**:2964–2971. DOI: https://doi.org/10.1172/JCI28326, PMID: 17039258

Žuklys S, Handel A, Zhanybekova S, Govani F, Keller M, Maio S, Mayer CE, Teh HY, Hafen K, Gallone G, Barthlott T, Ponting CP, Holländer GA. 2016. Foxn1 regulates key target genes essential for T cell development in postnatal thymic epithelial cells. *Nature Immunology* **17**:1206–1215. DOI: https://doi.org/10.1038/ni.3537, PMID: 27548434

Article

TRANSPARENT PROCESS

EMBO reports

Aire-dependent transcripts escape Raver2-induced splice-event inclusion in the thymic epithelium

Francine Padonou[1,2], Virginie Gonzalez[2], Nathan Provin[1], Sümeyye Yayilkan[1], Nada Jmari[2], Julia Maslovskaja[3], Kai Kisand[3], Pärt Peterson[3], Magali Irla[4] & Matthieu Giraud[1,2,*]

Abstract

Aire allows medullary thymic epithelial cells (mTECs) to express and present a large number of self-antigens for central tolerance. Although mTECs express a high diversity of self-antigen splice isoforms, the extent and regulation of alternative splicing events (ASEs) in their transcripts, notably in those induced by Aire, is unknown. In contrast to Aire-neutral genes, we find that transcripts of Aire-sensitive genes show only a low number of ASEs in mTECs, with about a quarter present in peripheral tissues excluded from the thymus. We identify Raver2, as a splicing-related factor overexpressed in mTECs and dependent on H3K36me3 marks, that promotes ASEs in transcripts of Aire-neutral genes, leaving Aire-sensitive ones unaffected. H3K36me3 profiling reveals its depletion at Aire-sensitive genes and supports a mechanism that is preceding Aire expression leading to transcripts of Aire-sensitive genes with low ASEs that escape Raver2-induced alternative splicing. The lack of ASEs in Aire-induced transcripts would result in an incomplete Aire-dependent negative selection of autoreactive T cells, thus highlighting the need of complementary tolerance mechanisms to prevent activation of these cells in the periphery.

Keywords Aire; alternative splicing; central tolerance; Raver2; thymic epithelial cells

Subject Categories Chromatin, Transcription & Genomics; Immunology; RNA Biology

DOI 10.15252/embr.202153576 | Received 6 July 2021 | Revised 14 December 2021 | Accepted 21 December 2021 | Published online 17 January 2022

EMBO Reports (2022) 23: e53576

Introduction

Tolerance against self-tissues is an essential feature of the immune system. It is established in the thymus following the presentation of self-antigen peptides to developing T cells. T cells recognizing their cognate antigen either undergo negative selection by apoptosis, preventing the release of autoreactive T cells, or develop into regulatory T cells (Tregs) able to suppress potential autoreactive T cells in the periphery (Goodnow *et al*, 2005; Cowan *et al*, 2013; Klein *et al*, 2014). The subset of medullary thymic epithelial cells characterized by high levels of major histocompatibility complex class II (MHC II) molecules (mTEChi) is essential to the presentation of self-antigens to developing T cells. Indeed, mTEChi have the unique ability to load, onto MHC II molecules, antigenic peptides originated from a wide array of endogenously expressed self-antigens (Sansom *et al*, 2014; Danan-Gotthold *et al*, 2016), including those controlled by the autoimmune regulator (Aire) and restricted to specific peripheral tissues (Derbinski *et al*, 2001; Sansom *et al*, 2014). In mice, invalidation of the *Aire* gene results in a drop of Aire-sensitive gene expression in mTEChi, and the presence of autoantibodies and immune infiltrates directed at multiple peripheral tissues due to impaired negative selection of autoreactive T cells and their harmful activation in the periphery (Anderson *et al*, 2002). Mutations in the human *AIRE* gene also cause the multi-organ devastating autoimmune disorder named Autoimmune Polyendocrine Syndrome type 1 (APS1) (Nagamine *et al*, 1997; Peterson *et al*, 2004).

The breadth of the repertoire of self-peptides presented by mTEChi does not only rely on the expression of a high number of self-antigen genes but also on the high diversity of their transcript isoforms whose translation produces multiple protein variants as a result of high rates of alternative splicing (Keane *et al*, 2015; Danan-Gotthold *et al*, 2016). Hence, a variety of alternative splicing events (ASEs) are expected to be spliced-in in mTEChi and the resulting processed peptides presented to developing T cells, thereby ensuring the efficient elimination of T cells capable to elicit autoreactive responses against peptides derived from these ASEs in the periphery. Although the expression of a wide range of transcript isoforms has been unambiguously established in mTEChi, the impact and the regulation mechanisms of alternative splicing on the genes controlled by Aire remain to be determined. Notably, it is unknown whether they encode a high transcript-isoform diversity similarly to total mTEChi, or whether the ASEs included in their transcripts equal the diversity of spliced-in ASEs detected for the same genes in their tissues of expression.

We therefore investigated the pattern of ASE inclusion for transcripts of Aire-sensitive genes in WT and *Aire*-KO mTEChi, as well as in peripheral tissues. Comparison of ASE inclusion for transcripts

1 Nantes Université, INSERM, Center for Research in Transplantation and Translational Immunology, UMR 1064, Nantes, France
2 Institut Cochin, INSERM, CNRS, Paris Université, Paris, France
3 Molecular Pathology Research Group, University of Tartu, Tartu, Estonia
4 Aix-Marseille Université, CNRS, INSERM, CIML, Centre d'Immunologie de Marseille-Luminy, Marseille, France
*Corresponding author. Tel: +33 02 40 08 47 23; E-mail: matthieu.giraud@inserm.fr

© 2022 The Authors

14693178, 2022, 3, Downloaded from https://www.embopress.org/doi/10.15252/embr.202153576 by Université De Nantes, Wiley Online Library on [25/10/2022]. See the Terms and Conditions (https://onlinelibrary.wiley.com/terms-and-conditions) on Wiley Online Library for rules of use; OA articles are governed by the applicable Creative Commons License

of Aire-sensitive versus neutral genes in mTEChi revealed an unexpected conservation of alternative splicing regulation between Aire-positive and Aire-negative subsets. Differences in the pattern of ASE inclusion with peripheral tissues provided clues on the relative importance of the role of negative selection, in comparison to peripheral mechanisms, for the establishment and maintenance of immunological tolerance against Aire-dependent self-antigens. Finally, we identified an epigenetic mechanism, involving the splicing-related factor Raver2 that sustains the regulation of alternative splicing in mTECs and explains the patterns of ASE inclusion for transcripts of Aire-sensitive and neutral genes in these cells.

Results

Aire-sensitive genes encode a low diversity of transcript isoforms in mTEChi

To characterize the alternative splicing complexity of Aire-sensitive genes in mTEChi sorted following the outline strategy (Appendix Fig S1 and S2), we determined the diversity of Aire-induced transcript isoforms that result from alternative splicing through the calculation of the median splicing entropy of these genes (Ritchie *et al*, 2008). For a given gene, splicing entropy was calculated using the levels of transcript-isoform expression obtained by assignment of paired-end sequencing reads to the RefSeq mRNA isoform annotations (Fig 1A). The more diverse the transcript isoforms, the greater the associated splicing entropy. Since a sufficient number of mapped junction-spanning reads is necessary for accurate characterization of transcript isoforms, we looked for the minimum expression value below which transcript isoform diversity could not be reliably captured in our mTEChi RNA-seq data. For that purpose, we binned the genes based on expression and calculated their median splicing entropy (Fig 1B). We found stable values of splicing entropy for genes with expression levels over 1 FPKM and highly degraded values for genes showing lower expression levels. This prevented the detection of minor transcript isoforms and therefore prompted us to exclude weakly expressed genes for subsequent splicing analyses. Next, we selected the Aire-sensitive genes characterized by a twofold expression increase in WT versus *Aire*-KO mTEChi (Fig 1C) and found that

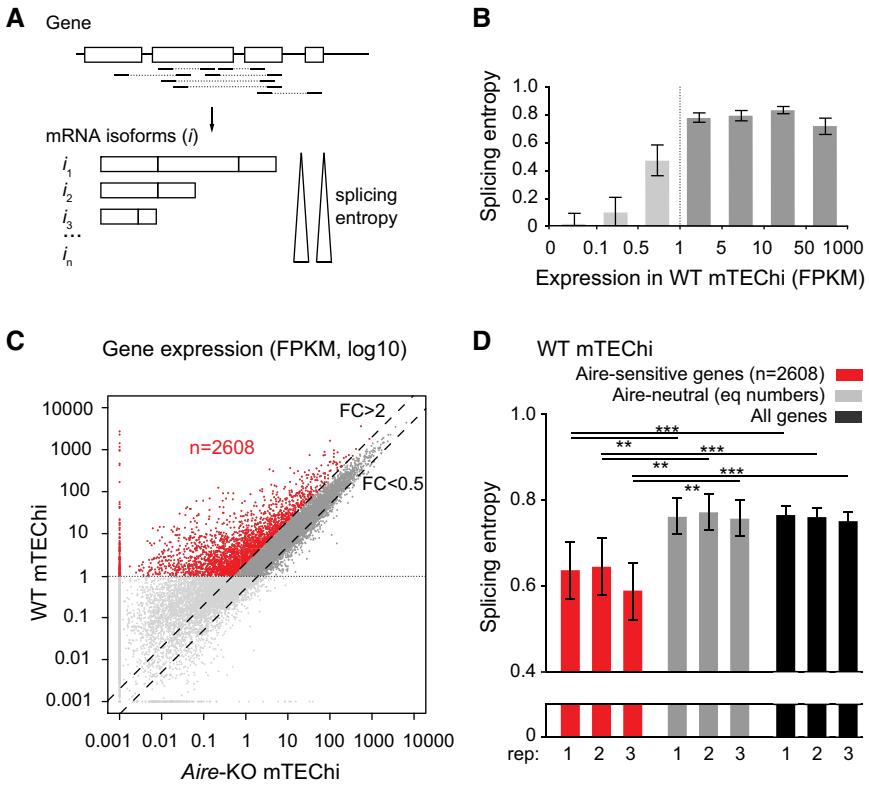

Figure 1. Low splicing entropy of Aire-sensitive genes in mTEChi.

A Schematic representation of a hypothetical gene with mapped paired-end sequencing reads identifying transcript isoforms. The isoform diversity of this gene is evaluated by calculation of its splicing entropy.

B Median splicing entropy of genes binned according to their expression levels. FPKM of 1 corresponds to the threshold over which the transcript isoform diversity can be accurately characterized in our RNA-seq dataset. (three mTEChi biological replicates [combined]; error bars show the 95% confidence interval of the medians).

C Identification of Aire-sensitive genes upregulated by Aire in WT versus *Aire*-KO mTEChi (FC > 2) and matching the threshold of 1 FPKM in WT mTEChi (red dots, $n = 2{,}608$). Aire-neutral genes ($0.5 < FC < 2$) with expression levels over 1 FPKM in WT mTEChi are represented by dark gray dots between the dashed lines. ($n = 3$ WT and three *Aire*-KO mTEChi biological replicates).

D Median splicing entropy of Aire-sensitive genes, Aire-neutral genes (equal numbers), and all genes in each of the three mTEChi biological replicates (rep). Error bars show the 95% confidence interval of the medians. $^{**}P < 10^{-3}$, $^{***}P < 10^{-4}$ (Wilcoxon test, $n = 2{,}608$, performed in each of the three biological replicates).

© 2022 The Authors

14693178, 2022, 3, Downloaded from https://www.embopress.org/doi/10.15252/embr.202153576 by Université De Nantes, Wiley Online Library on [25/10/2022]. See the Terms and Conditions (https://onlinelibrary.wiley.com/terms-and-conditions) on Wiley Online Library for rules of use; OA articles are governed by the applicable Creative Commons License

14693178, 2022, 3, Downloaded from https://www.embopress.org/doi/10.15252/embr.202153576 by Université De Nantes, Wiley Online Library on [25/10/2022]. See the Terms and Conditions (https://onlinelibrary.wiley.com/terms-and-conditions) on Wiley Online Library for rules of use; OA articles are governed by the applicable Creative Commons License

their median splicing entropy was significantly lower than those of Aire-neutral genes and of all genes taken together (Fig 1D). This finding thus revealed that Aire-sensitive genes encode a lower diversity of transcript isoforms in mTEChi, denoting lower rates of alternative splicing at these genes.

Aire-induced transcripts show low ASE inclusion in mTEChi

We next sought to determine whether the low diversity of transcript isoforms induced by Aire was sustained by a biased inclusion of ASE. To this end, we first identified all ASEs from the RefSeq mRNA annotation database in parsing its content using rMATS and considered the types of ASEs whose inclusion is susceptible to add amino acid content to the encoded protein isoforms without removing some, that is, skipped exon (SE), alternative 5′ splicing site (5SS), alternative 3′ splicing site (3SS), and intron retention (IR) events. We then computed their percent splicing inclusion (PSI), that is, the relative expression of transcript isoforms spliced in versus spliced in or out for each ASE (Fig 2A). Comparison of PSI values for Aire-sensitive versus neutral genes in mTEChi revealed a significant imbalance toward lower values (< 0.1), therefore showing a reduced inclusion of ASEs in the transcripts induced by Aire(Aire-sensitive: PSI < 0.1 [$n = 163$], PSI > 0.1 [$n = 265$]; Aire-neutral: PSI < 0.1 [$n = 93$], PSI > 0.1 [$n = 332$]; Chisq = 3.6×10^{-7}; Fig 2 B). We then calculated, for Aire-sensitive and neutral genes, the levels of ASE inclusion imbalance, that is, the number ratio of ASEs showing some level of active inclusion (PSI > 0.1) to ASEs showing no or background inclusion (PSI < 0.1), and found similar reduced levels for Aire-sensitive genes across three replicates (Fig 2C, Left). Comparison of the levels of ASE inclusion imbalance for Aire-neutral genes between mTEChi and peripheral tissues for which we collected RNA-seq datasets (Li *et al*, 2017) revealed higher levels in mTEChi, which is in line with reports showing higher rates of alternative splicing in mTEChi (Keane *et al*, 2015; Danan-Gotthold *et al*, 2016). In addition, the breadth of the reduction of ASE inclusion between transcripts of Aire-neutral and Aire-sensitive genes in mTEChi is striking since it is much wider than the reduction observed for Aire-neutral genes between mTEChi and each peripheral tissue (Fig 2C, Right). Since alternative splicing was reported to be influenced by gene expression in some systems (Kornblihtt *et al*, 2013), we calculated the median expression level of neutral genes in each mTEChi replicate and peripheral tissues. We found no significant correlation with the levels of ASE inclusion imbalance, therefore ruling out gene expression as a primary factor responsible for variation of ASE inclusion in our tested samples (Appendix Fig S3).

Next, we calculated in mTEChi, the inclusion imbalance of the different types of considered ASEs, and found decreased levels for each type of ASE, with SE, 5SS, and IR events reaching statistical significance (Fig 2D).

Finally, to address whether the transcripts induced by Aire also show reduced inclusion of ASEs in human mTEChi, we isolated mTEChi from human thymic tissues obtained during pediatric cardiac surgery and performed RNA-seq experiments. We identified the minimum expression values over which transcript isoforms could be accurately characterized in these samples, as shown by the example of two individuals (Fig EV1A). We then identified all ASEs from human RefSeq mRNA annotations and selected human Aire-sensitive and neutral ortholog genes for which we calculated the PSI values of their associated ASEs. Comparison of ASE inclusion imbalance for the Aire-sensitive and neutral genes in one male (indiv 1) and four female (indiv 2–5) human individuals showed a marked reduction for Aire-sensitive genes similar to what we found in mice, therefore revealing conservation of ASE inclusion in mTEChi between mice and humans (Fig EV1B).

Together, these findings revealed that the transcripts induced by Aire in mTEChi show conserved low ASEs in contrast to those that are neutral to Aire.

Low ASE inclusion in transcripts of Aire-sensitive genes is a general feature of TECs

To discriminate whether the reduced inclusion of ASEs in the transcripts induced by Aire was directly associated with the Aire's induction of gene expression or was also observed in the absence of Aire, we selected the genes with twofold increased expression in WT versus *Aire*-KO mTEChi and with levels of expression over 1 FPKM in both WT and *Aire*-KO mTEChi (Fig 3 A). We noted that meeting the threshold of 1 FPKM in *Aire*-KO mTEChi shrank the selection of Aire-sensitive genes since most of Aire-sensitive genes are inactive or expressed at very low level in the absence of Aire.

We calculated the PSI values of ASEs of the selected Aire-sensitive and neutral genes and compared their distributions in WT and *Aire*-KO mTEChi using three-dimensional representations (Fig 3 B). We observed similar PSI values for Aire-sensitive genes in WT and *Aire*-KO mTEChi, as well as for Aire-neutral genes. We then calculated the values of ASE inclusion imbalance and identified similar low levels for Aire-sensitive genes in mTEChi from WT and *Aire*-KO mice, showing that the reduced inclusion of ASEs in the transcripts of Aire-sensitive genes was independent of Aire expression (Fig 3C).

Figure 2. Low levels of ASE inclusion imbalance for Aire-sensitive genes in mTEChi.

A Schematic representation exemplifying the characterization of two transcript isoforms defined by a spliced in (*i*1) and a spliced out (*i*2) ASE, respectively, as well as, of an additional isoform (*i*3) unrelated to the ASE. The PSI value of the ASE is calculated using the specific expression of the transcript isoforms having the ASE spliced in or out.

B Distribution of ASEs according to their PSI values for Aire-sensitive (Left) and neutral genes (Right) in mTEChi. ASEs with PSI < 0.1 are considered as excluded, whereas ASEs with PSI > 0.1 as present, with some level of active inclusion.

C Levels of ASE inclusion imbalance for Aire-sensitive and neutral genes (equal numbers) in each of the three mTEChi biological replicates (rep; Left) and for Aire-neutral genes in peripheral tissues (unique samples; Right).

D Inclusion imbalance of each type of ASE in each of the three mTEChi biological replicates (rep).

Data information: In (C, D) *** $P < 10^{-4}$, ** $P < 10^{-3}$, * $P < 0.05$ (chi-squared test).

© 2022 The Authors

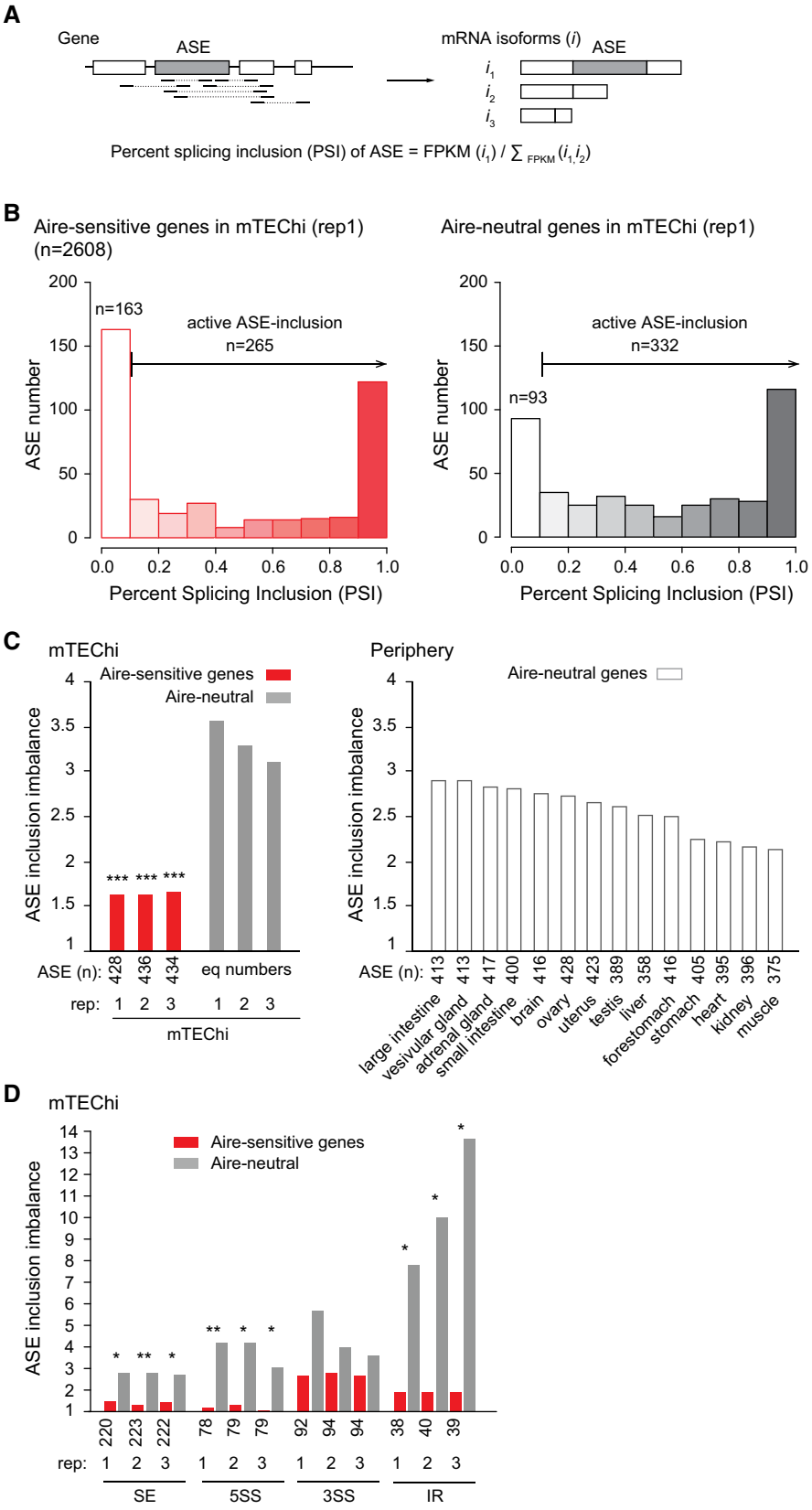

Figure 2.

© 2022 The Authors

14693178, 2022, 3, Downloaded from https://www.embopress.org/doi/10.15252/embr.202153576 by Université De Nantes, Wiley Online Library on [25/10/2022]. See the Terms and Conditions (https://onlinelibrary.wiley.com/terms-and-conditions) on Wiley Online Library for rules of use; OA articles are governed by the applicable Creative Commons License

Since mTEChi correspond to a stage of differentiation derived from precursor cells in mTEClo that lack Aire expression (Gäbler *et al*, 2007; Hamazaki *et al*, 2007; Dhalla *et al*, 2020), we asked whether the low ASE inclusion in transcripts of Aire-sensitive genes could be a feature already present in mTEClo. To this end, we selected the genes with expression values over 1 FPKM in mTEChi and mTEClo for calculation of PSI values of their associated ASEs (Fig 3D). As for the WT versus *Aire*-KO mTEChi comparison, we observed similar PSI values for Aire-sensitive genes in mTEChi and mTEClo, as well as for Aire-neutral genes (Fig 3E). Finally, calculation of the values of ASE inclusion imbalance revealed similar low levels for Aire-sensitive genes in mTEChi and mTEClo (Fig 3F). This finding thus shows that the low number of ASEs in the transcripts of Aire-sensitive genes in mTEChi is also a feature of mTEClo.

Next, we sought to definitively confirm this observation in analyzing an independent RNA-seq dataset of mTEChi/lo sorted as CD45$^-$EpCAM$^+$UEA1$^+$Ly51$^-$CD80^{high}MHCII^{high}/CD80^{low}MHCII^{low} (St-Pierre *et al*, 2015). We first showed that the level of expression

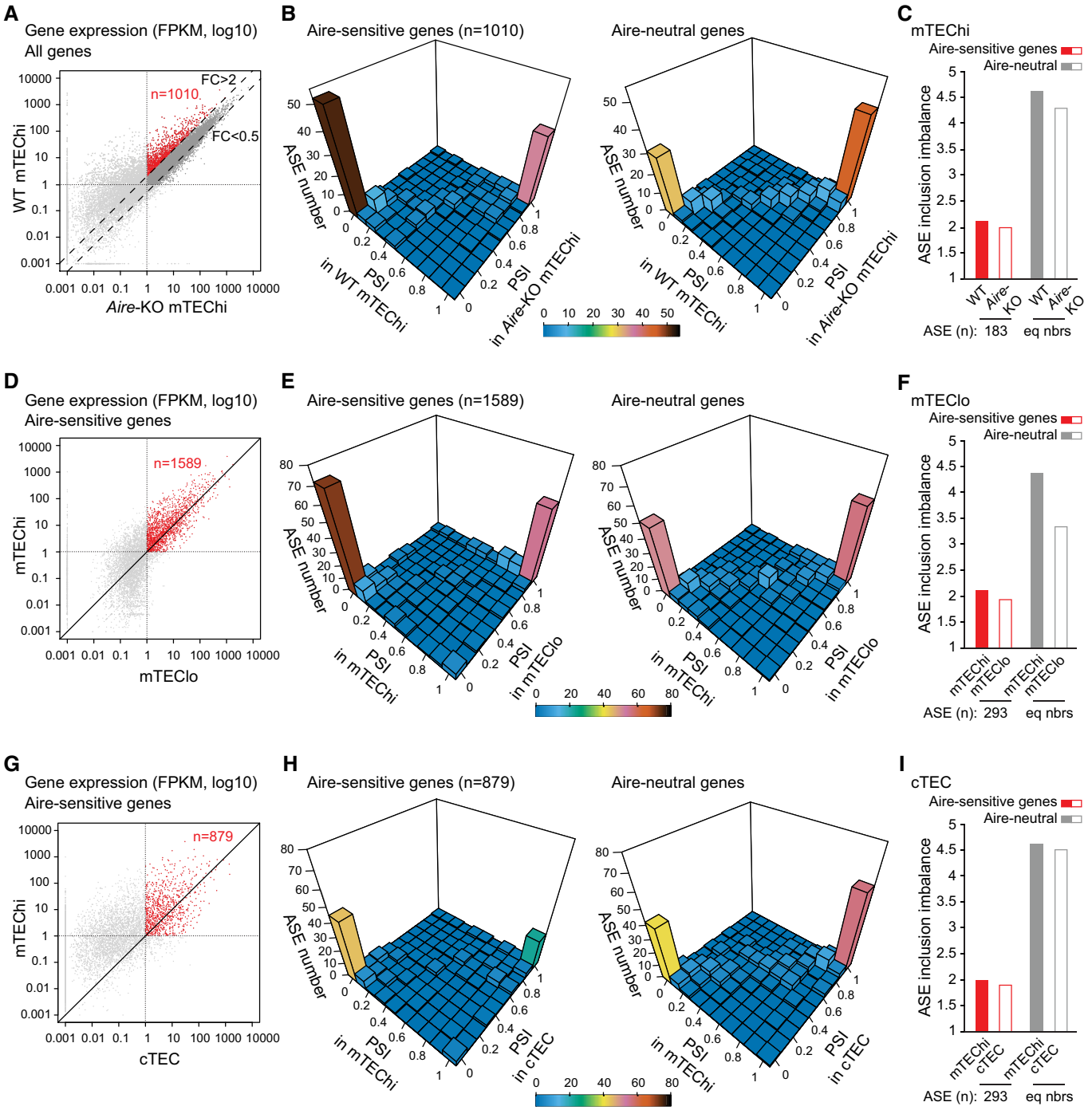

Figure 3.

14693178, 2022, 3, Downloaded from https://www.embopress.org/doi/10.15252/embr.202153576 by Université De Nantes, Wiley Online Library on [25/10/2022]. See the Terms and Conditions (https://onlinelibrary.wiley.com/terms-and-conditions) on Wiley Online Library for rules of use; OA articles are governed by the applicable Creative Commons License

Figure 3. Low levels of ASE inclusion imbalance for Aire-sensitive genes in Aire-negative TECs.

A Identification of Aire-sensitive genes upregulated by Aire in WT versus *Aire*-KO mTEChi (FC > 2) and matching the threshold of 1 FPKM in WT and *Aire*-KO mTEChi (red dots, $n = 1{,}010$). (three WT and three *Aire*-KO mTEChi biological replicates).

B 3D representation of the distribution of ASEs of Aire-sensitive (Left) and neutral genes (Right) according to their PSI values calculated from three WT (combined) and three *Aire*-KO mTEChi replicates (combined).

C Levels of ASE inclusion imbalance for Aire-sensitive and neutral genes (equal numbers) based on PSI values calculated from three WT (combined) and three *Aire*-KO mTEChi replicates (combined).

D Differential gene expression of Aire-sensitive genes between mTEChi and mTEClo. Red dots show the Aire-sensitive genes with FPKM > 1 in mTEChi and mTEClo ($n = 1{,}589$). (three mTEChi biological replicates and one mTEClo dataset).

E 3D representation of the distribution of ASEs of Aire-sensitive (Left) and neutral genes (Right) according to their PSI values calculated from three mTEChi replicates (combined) and one mTEClo dataset.

F Levels of ASE inclusion imbalance for Aire-sensitive and neutral genes (equal numbers) based on PSI values calculated from three mTEChi replicates (combined) and one mTEClo dataset.

G Differential gene expression of Aire-sensitive genes between mTEChi and cTEC. Red dots show the Aire-sensitive genes with FPKM > 1 in mTEChi and cTEC ($n = 879$). (three mTEChi and three cTEC biological replicates).

H 3D representation of the distribution of ASEs of Aire-sensitive (Left) and neutral genes (Right) according to their PSI values calculated from three mTEChi replicates (combined) and three cTEC replicates (combined).

I Levels of ASE inclusion imbalance for Aire-sensitive and neutral genes (equal numbers) based on PSI values calculated from three mTEChi replicates (combined) and three cTEC replicates (combined).

of the markers used to sort these cells and of a set of genes specific to mTEChi and mTEClo were identical or very close to those measured in our mTEChi and mTEClo data (Appendix Fig S4A and B). Then, we analyzed the extent of ASE inclusion in the independent mTEChi/lo dataset and confirmed similar low levels of ASE inclusion imbalance for Aire-sensitive genes in mTEChi and mTEClo (Appendix Fig S4C–E).

To evaluate the levels of ASE inclusion in cTECs, we analyzed RNA-seq data of cTECs that were also generated in (St-Pierre *et al*, 2015) and showed that the low ASE inclusion in transcripts of Aire-sensitive genes was also a feature of cTECs (Fig 3G–I), suggesting that it could stem from a common thymic epithelial progenitor.

Together these findings revealed that the low inclusion of ASEs in the transcripts of Aire-sensitive genes is a general feature of TECs, independent of Aire expression and conserved upon maturation of mTEClo into mTEChi.

Transcripts of Aire-sensitive genes show enhanced ASE inclusion in those tissues where they are expressed

Since transcripts of Aire-sensitive genes are subject to low ASE inclusion in mTEChi, we asked whether they could exhibit a stronger inclusion when their expression is driven by tissue-specific transcriptional mechanisms in the periphery. To address this question, we selected for each tissue in our dataset, the Aire-sensitive genes showing a specific or selective expression by using the Specificity Measurement (SPM) method (Pan *et al*, 2013) as in Guyon *et al* (2020), and determined the levels of ASE inclusion imbalance. Comparison with mTEChi revealed overall stronger ASE inclusion in peripheral tissues (Fig 4A), indicating that ASE inclusion for transcripts of Aire-sensitive genes is differentially regulated in the periphery. We further identified for each ASE, its PSI values in mTEChi and in the peripheral tissue(s) of specific/selective expression of its corresponding Aire-sensitive gene (Fig EV2A). We selected the ASEs with PSI values < 0.1 in mTEChi and > 0.1 in the periphery, as exemplified in (Figs EV2A–C), and found that nearly a quarter of ASEs present in the tissues of specific Aire-sensitive gene expression, were excluded in mTEChi (Fig 4B, Left). This exclusion of ASEs in mTEChi would therefore increase the risk of release of autoreactive T cells. Conversely, a significantly lower percentage of ASEs present in mTEChi were excluded in the tissues of specific Aire-sensitive gene expression (Fig 4B, Right). We noted that among the latter ASEs, only a minority (about 2%) showed a full inclusion in mTEChi (PSI > 0.9 in mTEChi and < 0.1 in the periphery; Fig EV2A), indicating that only few autoreactive T cells specific for the antigenic epitopes generated upon the exclusion of these ASEs, would leave the thymus and contribute to the risk for autoimmunity.

We next compared for Aire-sensitive and neutral genes the proportion of ASEs excluded in mTEChi among those expressed in peripheral tissues and found significantly lower proportions for neutral genes (Fig 4C). Since Aire-neutral genes can be expressed in multiple tissues, increasing their likelihood of undergoing ASE inclusion, we sought to determine for their transcripts, the proportion of exclusion in mTEChi of their ASEs present in the periphery, considering all tissues together. Hence, we considered all 1–14 permutations of the 14 tissues in our dataset and calculated for each set of permutations of the same number of tissues, the mean proportion of ASEs exclusively excluded in mTEChi (Fig 4D). We observed that the proportion of exclusion tended to reach, with the increasing number of considered tissues, the proportion of exclusion detected for Aire-sensitive genes in mTEChi (Fig 4D and B, Left).

Together these findings revealed that transcripts of Aire-sensitive genes show stronger ASE inclusion in their tissues of expression than in mTEChi and that an important proportion of these ASEs expressed in the periphery are excluded from mTEChi, similarly to the ASEs of Aire-neutral genes.

Aire-sensitive genes escape Raver2-dependent promotion of ASE inclusion in mTECs

To get insights into the molecular mechanisms that underlie the differential inclusion of ASEs between Aire-sensitive and neutral genes in mTEChi, we searched for the preferential or deprived gene expression of a full set of RNA-binding proteins including factors known to influence RNA splicing, in mTEChi versus peripheral tissues. We identified a handful of RNA-binding proteins showing statistically significant differential expression in mTEChi, including a single factor reported to modulate alternative splicing, namely

© 2022 The Authors

14693178, 2022, 3, Downloaded from https://www.embopress.org/doi/10.15252/embr.202153576 by Université De Nantes, Wiley Online Library on [25/10/2022]. See the Terms and Conditions (https://onlinelibrary.wiley.com/terms-and-conditions) on Wiley Online Library for rules of use; OA articles are governed by the applicable Creative Commons License

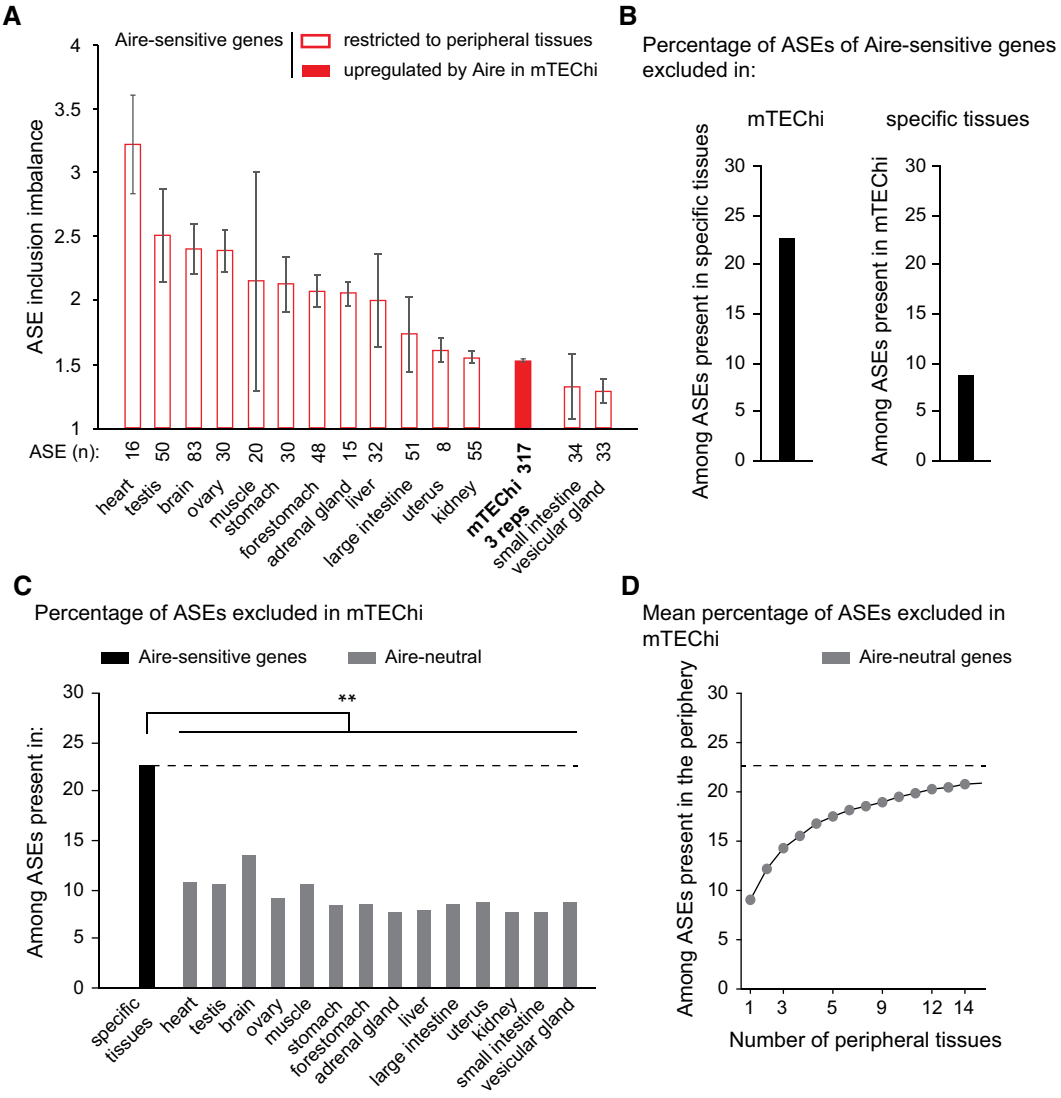

Figure 4. Higher levels of ASE inclusion imbalance for Aire-sensitive genes in their tissues of expression.

A Levels of ASE inclusion imbalance for Aire-sensitive genes in their tissues of expression. Open red bars are for particular peripheral tissues, whereas the solid red bar is for mTEChi. The ASE inclusion imbalance is calculated for each of the three mTEChi biological replicates on an identical set of ASEs ($n = 3$, error bars show mean $\pm$ STD).

B Percentage of ASEs of Aire-sensitive genes that are excluded in mTEChi among ASEs showing some level of inclusion in the tissues of specific expression (Left). The percentage of ASEs excluded in specific tissues among ASEs present in mTEChi is shown (Right).

C, D Percentage of ASE exclusion for Aire-neutral genes in mTEChi among ASEs present in each peripheral tissue (C) or (D) in all 1–14 permutations of the 14 peripheral tissues in our database, as a mean percentage. The dashed line represents the percentage of ASE exclusion shown in (B, Left) and (C), $^{**}P < 10^{-3}$ (pnorm (cumulative distribution function) to the normal distribution defined by the mean and STD of ASE exclusion percentages in the 14 peripheral tissues).

Raver2 (Bartoletti-Stella *et al*, 2015) (Fig 5A and Appendix Fig S5). We further showed that *Raver2* expression is over-represented in mTEChi, mTEClo, or cTECs (Fig 5B). Then, to determine whether the higher expression of *Raver2* is specific to the thymic epithelium or shared with epithelia from other tissues, we collected public RNA-seq datasets of epithelia isolated from a variety of peripheral tissues (ENCODE Project Consortium, 2012; St-Pierre *et al*, 2013; Tan *et al*, 2020; Marincola Smith *et al*, 2021; Pal *et al*, 2021; Wiles *et al*, 2021) and calculated in each sample the expression of *Raver2*. This comparison revealed a preferential expression of *Raver2* in the thymic epithelium supporting an important role for Raver2 in the thymus (Fig EV3).

To determine whether Raver2 was able to exert an effect on Aire-sensitive or neutral genes, we first sought to correlate its expression to variation of ASE inclusion imbalance across individual mTEChi. To this end, we collected full-length single-cell RNA-seq data enabling splicing analyses that were generated in mTEChi (Handel *et al*, 2018). We calculated, for each cell, the PSI values of ASEs of Aire-sensitive and neutral genes, as well as their levels of ASE inclusion imbalance. Note that the comparison of the distribution of the

© 2022 The Authors

14693178, 2022, 3, Downloaded from https://www.embopress.org/doi/10.15252/embr.202153576 by Université De Nantes, Wiley Online Library on [25/10/2022]. See the Terms and Conditions (https://onlinelibrary.wiley.com/terms-and-conditions) on Wiley Online Library for rules of use; OA articles are governed by the applicable Creative Commons License

levels of ASE inclusion imbalance across the individual mTEChi and between Aire-sensitive and neutral genes showed significantly lower levels for Aire-sensitive genes (Appendix Fig S6A), therefore confirming, at the single-cell level, the difference that we identified at the cell population level in (Figs 2C and EV1B). The absence of Aire effect on the low inclusion of ASEs in transcripts of Aire-sensitive genes was confirmed by the lack of significant correlation between the levels of ASE inclusion imbalance and those of *Aire* expression across the individual mTEChi (Appendix Fig S6B). We then identified which cells expressed *Raver2* (threshold > 1 FPKM; Fig 5C,

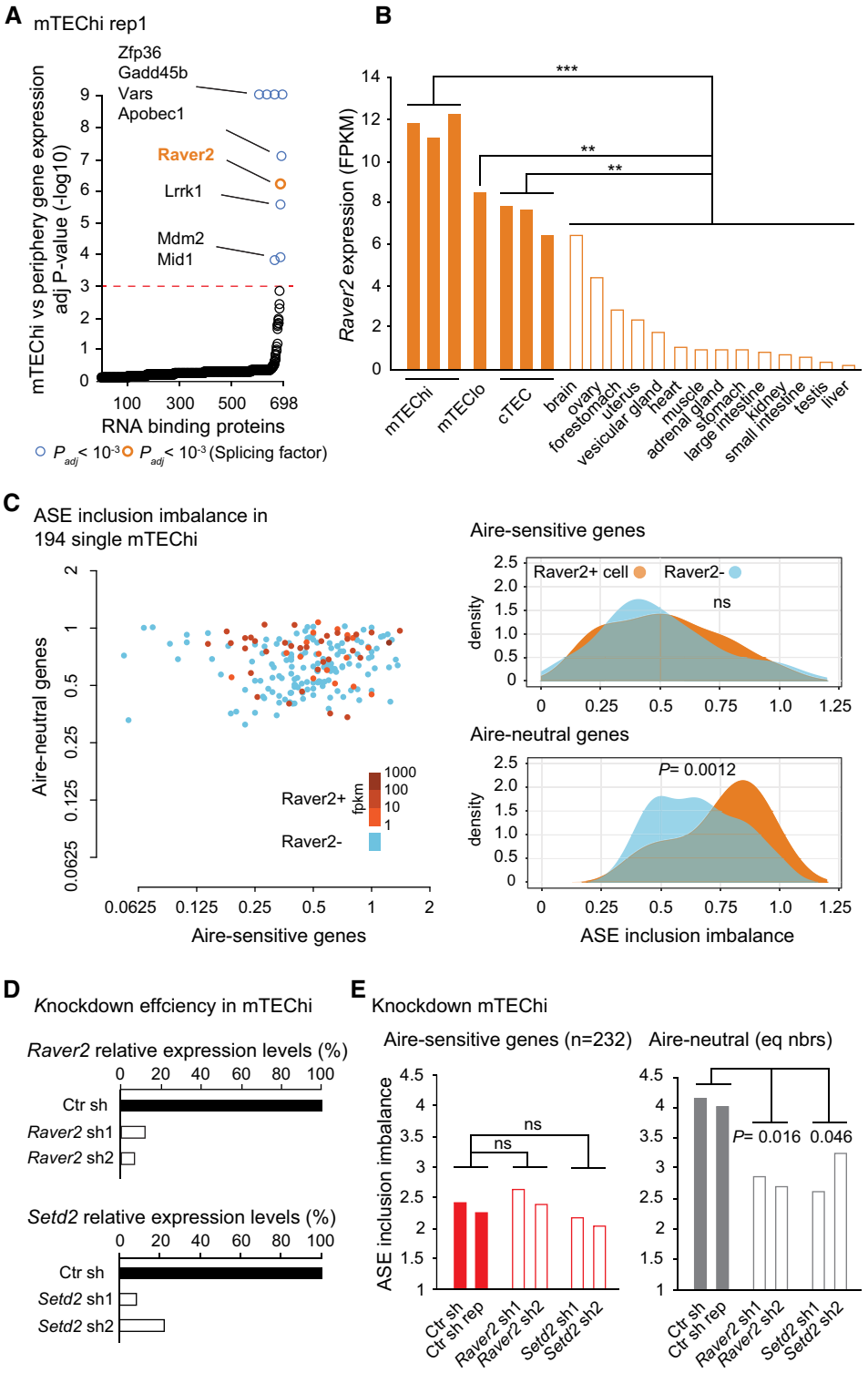

Figure 5.

© 2022 The Authors

14693178, 2022, 3, Downloaded from https://www.embopress.org/doi/10.15252/embr.202153576 by Université De Nantes, Wiley Online Library on [25/10/2022]. See the Terms and Conditions (https://onlinelibrary.wiley.com/terms-and-conditions) on Wiley Online Library for rules of use; OA articles are governed by the applicable Creative Commons License

Figure 5. Effect of Raver2 and Setd2 on the level of ASE inclusion imbalance for Aire-sensitive and neutral genes in mTECs.

A Differential expression of genes coding for RNA-binding proteins in mTEChi vs peripheral tissues. For each gene, the expression in mTEChi is compared to the normal distribution estimated based on the levels of expression in the periphery. The red dashed line represents the threshold for statistical significance (Benjamini–Hochberg adjusted $P < 0.001$). RNA-binding proteins showing significant differential gene expression are represented by colored circles, in orange if the RNA-binding proteins have been reported to be involved in splicing, in blue otherwise.

B *Raver2* expression levels in mTEChi, mTEClo, cTEC, and across peripheral tissues (open bars). Significance of Raver2 over-representation in mTEChi, in mTEClo and in cTEC versus the peripheral tissues is shown. *** $P < 10^{-7}$, ** $P < 10^{-3}$ (pnorm (cumulative distribution function) to the normal distribution defined by the mean and STD of *Raver2* expression in the 14 peripheral tissues).

C Levels of ASE inclusion imbalance (Left) and their distributions (Right) are shown for Aire-neutral and Aire-sensitive genes in 194 single mTEChi. Blue is for cells negative for Raver2, whereas orange shades are for Raver2-positive cells. Statistical significance assessed by a Student's test.

D Relative expression levels of *Raver2* (Top) and *Setd2* (Bottom) in mTEChi infected by lentiviruses containing *Raver2*, *Setd2*, or the Ctr (LacZ) shRNAs.

E Levels of ASE inclusion for transcripts of Aire-sensitive and neutral genes (equal numbers) in mTEChi infected by lentiviruses targeting *Raver2*, *Setd2* (open bars), or the Ctr (LacZ; solid bars). Statistical significance of cumulative sh1 and sh2 assessed by a chi-squared test (two Ctr and two sh-treated biological replicates).

Left) and compared the distribution of the levels of ASE inclusion imbalance between the Raver2-positive and Raver2-negative cells. In contrast to Aire-sensitive genes, we observed a significant association between the presence of Raver2 and the high levels of ASE inclusion imbalance for Aire-neutral genes, strongly suggesting that Raver2 promotes the inclusion of ASEs specifically in transcripts of Aire-neutral genes (Fig 5C, Right).

Then, to evaluate the specific impact of Raver2 on ASE inclusion in mTECs, we used a 3D organotypic culture system adapted from Ref Pinto *et al* (2013) in which we seed medullary- and MHCII-enriched TECs (mTEChi: ~ 62%; mTEClo: ~ 7%; Appendix Fig S7), and retrieve, after 5 days in culture, pure mTECs showing a relative increase of mTEClo (mTEChi: ~ 70%; mTEClo: ~ 25%; Appendix Fig S8A). This shift toward mTEClo is dramatically enhanced in the absence of the addition of RankL, suggesting that it is caused by an increased mTEChi mortality and/or de-differentiation (Appendix Fig S8B). In addition, we observe a strong expression of *Aire* and *Ins2* (prototypic self-antigen gene controlled by Aire) in the seeded and retrieved cells, with higher levels (2-fold) at the beginning of the culture (Appendix Fig S9). This observation is consistent with the transitory nature of *Aire* expression and the fact that it does not seem to be balanced out by new Aire-expressing mTEChi arising from the differentiation/maturation of cells from the mTEClo pool. Right after the seeding of mTECs onto the 3D system, we performed infection with concentrated lentiviruses encoding shRNAs targeting *Raver2* (shRNA 1 or 2) or the control LacZ, cloned into a vector expressing GFP as a marker of transduction (Fig EV4). Three days later, we cell-sorted GFP^+ mTECs and quantified *Raver2* expression level. We found a strong knockdown efficiency for each of the two *Raver2* shRNAs with 10–20% remaining expression in comparison to control knockdown samples (Fig 5D, Top). To ensure that the newly transcribed isoforms, resulting from potential alternative splicing alterations promoted by *Raver2* knockdown, stabilize and accumulate to be accurately detected, we isolated GFP^+ mTECs 5 days after infection. RNA-seq experiments on these cells revealed a significant reduction of the levels of ASE inclusion imbalance for Aire-neutral genes (Fig 5E, Right), whereas no effect was detected on Aire-sensitive genes (Fig 5E, Left). This finding demonstrated that Raver2 promotes the inclusion of ASEs in transcripts of Aire-neutral genes and that those of Aire-sensitive genes escape its effect.

Raver2 is a heterogeneous nuclear ribonucleoprotein (Hnrnp) that has been reported to bind to the polypyrimidine track-binding protein (Ptb) (Kleinhenz *et al*, 2005; Henneberg *et al*, 2010) which regulates alternative splicing at regions enriched in H3K36me3 through interaction with H3K36me3 adaptor proteins (Luco *et al*, 2010, 2011). To evaluate the effect of H3K36 methylation on ASE inclusion in mTECs, we performed knockdown of Setd2 that is recognized as the only enzyme able to methylate H3K36 into H3K36me3 in somatic cells (Husmann & Gozani, 2019). We first validated the efficient knockdown of two shRNAs targeting *Setd2* (Fig 5D, Bottom) and then performed RNA-seq experiments to determine the levels of ASE inclusion imbalance in the knockdown samples. As for *Raver2*, *Setd2* knockdown resulted in a significant reduction of ASE inclusion for the transcripts of Aire-neutral genes, whereas no effect was detected for those of Aire-sensitive genes (Fig 5E).

Together these findings showed that Aire-sensitive genes escape Raver2's effect promoting ASE inclusion in mTECs and suggested that the effect on Aire-neutral genes require H3K36me3 as an anchor for this factor.

Aire-sensitive genes are devoid of H3K36me3 and H3K36me3-associated ASE inclusion in mTEClo

Since the low ASE inclusion in the transcripts induced by Aire in mTEChi is already present in mTEClo (Fig 3D–F), we sought to determine whether a potential escape of Raver2's effect due to a lack of H3K36me3 could apply for such a mechanism in these cells. We looked for H3K36me3 enrichment by ChIP-seq experiments and found very low levels of H3K36me3 at Aire-sensitive genes in comparison to all genes (Figs 6A and EV5A). We then selected the genes with expression values over 1 FPKM and the presence of H3K36me3 marks within the last third of their gene bodies and compared the levels of ASE inclusion imbalance to those of the counterpart genes lacking H3K36me3 (Fig 6B). We observed a significant increase of ASE inclusion in transcripts of genes harboring H3K36me3 marks, very likely reflecting the functional link that we detected between increased H3K36me3 and stronger ASE inclusion in mTECs (Fig 5E, Right). Thus, these findings supported the assumption that the low ASE inclusion observed for transcripts of Aire-sensitive genes in mTEClo was due, at least in part, to the lack of H3K36me3 deposition and the subsequent impairment of Raver2 recruitment.

However, since H3K36me3 is involved in transcription (Vojnic *et al*, 2006; de Almeida & Carmo-Fonseca, 2012), we asked whether the lack of H3K36me3 at Aire-sensitive genes was specific to these genes or associated with their low expression. To address this question, we selected a set of Aire-neutral genes with expression levels

© 2022 The Authors

14693178, 2022, 3, Downloaded from https://www.embopress.org/doi/10.15252/embr.202153576 by Université De Nantes, Wiley Online Library on [25/10/2022]. See the Terms and Conditions (https://onlinelibrary.wiley.com/terms-and-conditions) on Wiley Online Library for rules of use; OA articles are governed by the applicable Creative Commons License

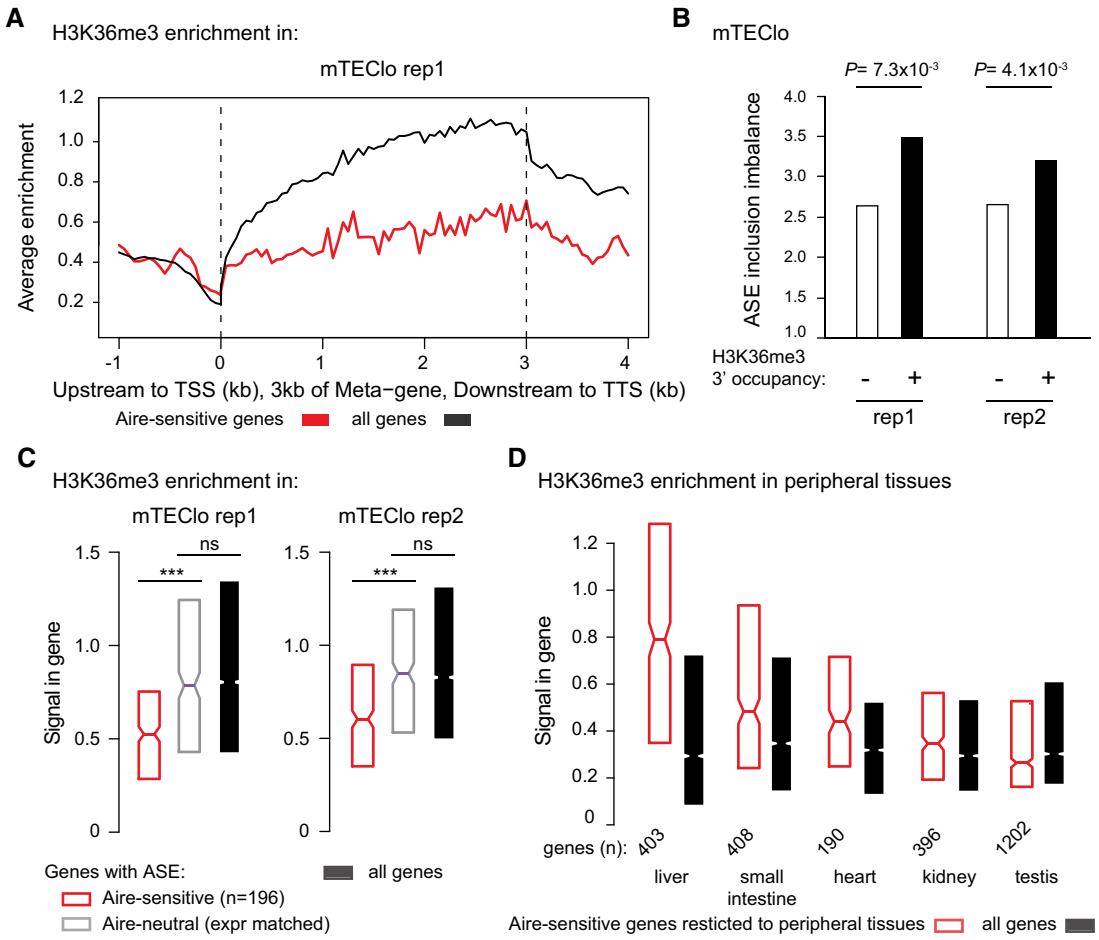

Figure 6. Aire-sensitive genes show low levels of H3K36me3 correlated with low levels of ASE inclusion imbalance in mTEClo.

A Metagene profiles of the average normalized enrichment of H3K36me3 for Aire-sensitive genes (red) and all genes (black) in mTEClo.

B Levels of ASE inclusion imbalance for genes with and without H3K36me3 in the last third of their gene bodies, in each biological replicate (rep1 and 2). The statistical significance is assessed by a chi-squared test performed in each of the two replicates.

C Median enrichment of H3K36me3 for Aire-sensitive genes and neutral genes (expression matched), as well as all genes in each biological replicate. *** $P < 10^{-13}$ (Wilcoxon test).

D Median enrichment of H3K36me3 for Aire-sensitive genes in their tissues of expression and for all genes.

Data information: In (C) and (D), notches represent the 95% confidence interval of the medians, and the limits of the upper and lower boxes the 75th and 25th percentile of H3K36me3 enrichment, respectively.

matching those of Aire-sensitive genes and measured their enrichment for H3K36me3. We found significantly lower levels of H3K36me3 at Aire-sensitive genes, therefore showing that the lack of H3K36me3 was specific to these genes and unrelated to their low expression (Fig 6C). In addition, a comparison of the levels of ASE inclusion imbalance for the same Aire-sensitive and expression-matched neutral genes showed a clear reduction of the former (Fig EV5B), confirming that the weak ASE inclusion for transcripts of Aire-sensitive genes is not a reflection of their low expression levels.

Finally, to address whether the lack of H3K36me3 deposition at Aire-sensitive genes was a differential feature between mTEClo and peripheral tissues, we collected H3K36me3 ChIP-seq data generated from mouse tissues, as part of the ENCODE project (ENCODE Project Consortium *et al*, 2007). For each tissue, we measured the enrichment of H3K36me3 at all genes and found that Aire-sensitive genes with a specific or selective expression showed similar to higher levels of H3K36me3 in comparison to all genes (Figs 6D and EV5C). This finding is consistent with the observation that Aire-sensitive genes exhibit enhanced ASE inclusion, globally, in the periphery, but showed a poor correlation with ASE inclusion in each individual tested tissue (Fig 4A), indicating that H3K36me3 may be permissive to tissue-specific mechanisms of alternative splicing without orchestrating a coordinated tissue-independent pattern of the latter.

Discussion

In our present study, we demonstrated that, while mTEChi express a wide range of self-antigen splice isoforms, Aire-upregulated transcripts exhibit a low diversity and a weak inclusion of ASEs. We

© 2022 The Authors

14693178, 2022, 3, Downloaded from https://www.embopress.org/doi/10.15252/embr.202153576 by Université De Nantes, Wiley Online Library on [25/10/2022]. See the Terms and Conditions (https://onlinelibrary.wiley.com/terms-and-conditions) on Wiley Online Library for rules of use; OA articles are governed by the applicable Creative Commons License

showed that this low ASE inclusion was independent of Aire's action on gene expression and resulted from a mechanism that was sustained by the specific depletion of H3K36me3. The linked mechanism between the decrease of H3K36me3 and the reduction of ASE inclusion that we propose was consistent with the report showing that alternative exons, subjected to exclusion or partial inclusion, have lower H3K36me3 signals than constitutive exons in *Caenorhabditis elegans* (Kolasinska-Zwierz *et al*, 2009). In addition, a recent report showed that high inclusion levels of skipped exon (SE) ASEs correlate with the strong enrichment of H3K36me3 in the exon flanking regions in mice (Hu *et al*, 2020).

Unlike Aire-sensitive genes, we showed that the genes neutral to the effect of Aire in mTECs were characterized by an enrichment of H3K36me3 and a strong enhancement of ASE inclusion. Identification of Raver2 as a splicing-related factor overrepresented in mTECs and able to promote ASE inclusion led us to propose a mechanism by which ASE inclusion for Aire-neutral genes is driven by the coordinated action of Raver2 and the splicing factor Ptb that is specifically recruited at H3K36me3-rich regions. This mechanism was supported by the observation that Ptb is not only able to repress alternatively spliced exons (Wagner & Garcia-Blanco, 2002) but also enhances the inclusion of a large number of ASEs, as shown by the effect of *Ptb* knockdown on ASE inclusion at the genomic scale (Luco *et al*, 2010). In addition, Raver2 was characterized as a potent modulator of the splicing activity of Ptb (Bartoletti-Stella *et al*, 2015), therefore opening the possibility that Raver2 may function through interaction with Ptb to enhance ASE inclusion for transcripts of genes with H3K36me3 enrichment. The role of Raver2 in mTECs is further strengthened by the higher expression of *Ptb* in mTEChi (105 FPKM) and mTEClo (91 FPKM) than in peripheral tissues (median expression: 31 FPKM).

Hence, through depletion of H3K36me3, the self-antigen genes controlled by Aire likely escape the effect of Raver2/Ptb and thereby generate transcripts with fewer ASEs. This weak ASE inclusion indicated that the Aire-induced transcripts do not include all the ASEs that are spliced-in in the periphery. Lack of presentation of Aire-dependent antigenic peptides corresponding to ASEs absent from mTEChi, is likely to result in a number of autoreactive T cells leaving the thymus and potentially able to elicit autoimmune reactions. The formal identification and characterization of such autoreactive T cells by the use of MHC tetramers carrying peptides from thymus-excluded ASEs of Aire-dependent genes will be necessary to evaluate the direct impact of the described weak ASE inclusion on central tolerance. In addition, thanks to the progress of the Knockout Mouse Project (https://www.mmrrc.org) with the recent availability of *Raver2* KO cryopreserved embryos, the effect of the deletion of *Raver2* on the diversity of autoreactive T cells will be assessable, as well as on the susceptibility to autoimmunity in the next future.

The negative selection triggered by Aire may then be not as comprehensive as originally thought and complementary peripheral mechanisms would be likely necessary to maintain tolerance. As a possible mechanism, Tregs selected against peptides derived from constitutive exons of Aire-sensitive genes in mTEChi would suppress the autoimmune responses triggered against immunogenic ASE-derived peptides. This is in line with previous studies showing the importance of Aire-induced self-antigen expression in the selection and development of suppressive Tregs (Aschenbrenner *et al*, 2007; Pomié *et al*, 2011; Malchow *et al*, 2013). In humans, the study of APS1 patients revealed a role for AIRE in the development of Tregs (Ryan *et al*, 2005; Kekäläinen *et al*, 2007), as well as in the enforcement of immune tolerance by directing differentiation of autoreactive T cells into the Treg lineage (Malchow *et al*, 2016). This latter mechanism would thus provide the possibility for autoreactive T cells directed against immunogenic ASE-derived peptides, to convert into Tregs, therefore preventing potential autoimmune reactions and favoring Treg-associated suppressive responses.

Our study also revealed that the proportion of ASEs selectively excluded in mTEChi is similar between Aire-sensitive and neutral genes. This indicated that the lack of H3K36me3 at Aire-sensitive genes, and therefore the absence of Raver2 recruitment, would result in a certain degree of autoreactivity that Tregs may control similarly to autoreactive reactions against immunogenic peptides derived from ASEs of Aire-neutral genes. Hence, the weak ASE inclusion for Aire-sensitive genes in mTECs may be sufficient to impose, with the support of Tregs, immune tolerance against the full set of Aire-dependent self-antigens. If Aire-mediated immunological tolerance was entirely under the control of the sole mTEChi-dependent negative selection, which happens not to be the case, the full set of ASEs of Aire-sensitive genes would be present in mTEChi with the full diversity of tissue-specific splicing mechanisms activated. Such a broaden activation would certainly conflict with the proper function and physiology of mTEChi and represent a tremendous energetic cost, most probably unreachable.

Materials and Methods

Mice

Aire-deficient (C57BL/6) mice, previously obtained by D. Mathis and C. Benoist (Harvard Medical School, Boston, MA), were bred and maintained at Cochin Institute. Wild-type B6 mice were purchased from Charles River laboratory. Animal housing and experiments were conducted in specific-pathogen-free conditions according to the protocols and guidelines of the French Veterinary Department under procedures approved by the Paris-Descartes Ethical Committee for Animal Experimentation (decision CEEA34.MG.021.11).

Isolation of medullary thymic epithelial cells

Thymi of 4- to 6-week-old mice were trimmed of fat, cut into pieces, and digested by mechanic coercion to release thymocytes. Enzymatic digestion was first performed with collagenase D (1 mg/ml; Roche) and DNase I (1 mg/ml; Sigma) for 30 min at 37°C, then with Collagenase/Dispase (2 mg/ml; Roche) and DNase I (2 mg/ml) at 37°C up to the obtention a single-cell fraction. The cells were then filtered through a 70-μm cell strainer and resuspended in PBS containing 1% FBS and 5 mM of EDTA. mTECs were then isolated from the obtained cell fraction using the following methods:

Isolation of mTEChi and mTEClo

Thymic stromal cells from pools of 4 thymi were enriched by CD45 depletion of thymocytes using magnetic CD45 MicroBeads (Miltenyi Biotec) and the magnetic cell sorter (autoMACS, Miltenyi Biotec).

© 2022 The Authors

14693178, 2022, 3, Downloaded from https://www.embopress.org/doi/10.15252/embr.202153576 by Université De Nantes, Wiley Online Library on [25/10/2022]. See the Terms and Conditions (https://onlinelibrary.wiley.com/terms-and-conditions) on Wiley Online Library for rules of use; OA articles are governed by the applicable Creative Commons License

The depleted cell fraction was then stained for 20 min at 4°C with a cocktail of fluorophore-labeled antibodies CD45-PerCPCy5.5 (1:50; Biolegend, ref: 103131), Ly51-PE (1:800; Biolegend, ref: 108307) and I-A/E-APC (MHCII; 1:1,200; eBioscience, ref: 17–5321) for sorting of mTEChi/lo ($CD45^{-}Ly51^{-}I\text{-}A/E^{high/low}$) on a FACSAria III instrument (BD Bioscience), as previously described (Giraud *et al*, 2014; Guyon *et al*, 2020). The phenotypic validation of the isolated mTEChi and mTEClo was performed using the additional antibodies EpCAM-PE-Dazzle 549 (1:200; Biolegend, ref: 118235), CD80-PE-Cy7 (1:200; Biolegend, ref: 104733), and the lectin UEA-1-FITC (1:200; Thermo Fisher, L32476).

Isolation of total mTECs for 3D organotypic culture

As above, a CD45 depletion of thymocytes using magnetic beads was first performed. The depleted cell fraction was then stained for 20 min at 4°C with the CD45-PerCPCy5.5 antibody (1:50; Biolegend) and the EpCAM-FITC antibody (G8.8 clone; 1:500; Biolegend, ref: 118207) for FACS sorting of $CD45^{-}EpCAM^{+}$ cells. The sorted fraction was sequentially stained for 20 min at 4°C with the Ly51-PE antibody (1:800; Biolegend) and depleted of Ly51-positive cells using anti-PE Microbeads (Miltenyi Biotec), then stained with the I-A/E-APC antibody (MHCII; 1:1,200; eBioscience) and positively selected for I-A/E-positive cells using anti-APC Microbeads (Biolegend). The obtained final cell fraction consisted of total mTECs ($CD45^{-}EpCAM^{+}Ly51^{-}I\text{-}A/E^{+}$).

shRNA-containing lentivirus production

pLKO.1 plasmids bearing the shRNA sequences (sh1: TRCN0000181363 and sh2: TRCN0000242035 for *Raver2*; sh1: TRCN0000238533 and sh2: TRCN0000238536 for *Setd2*; Ctr sh: TRCN0000072240 for LacZ; Sigma) were subcloned into the lentiviral pLKO.3G vector containing an eGFP cassette (Addgene #14748), by transferring the BamHI-NdeI restriction fragments containing the shRNAs. Lentiviruses were produced into HEK293T cells by using the calcium phosphate co-transfection method for each specific subcloned lentiviral pLKO.3G vector with the packaging plasmids gag/pol (Addgene #14887) and VSV-G (Addgene #14888). HEK293T were grown in Dulbecco's modified Eagles medium (DMEM) with high glucose (4,500 mg/l), supplemented with 10% fetal bovine serum (FBS), pen/strep antibiotics. HEK293T cells were transfected at 70–80% confluence in two T175 flasks. The transfection solution was prepared with 500 µl of 1 M $CaCl_2$ (Sigma), the lentiviral vector (32 µg), the packaging plasmids (VSV-G: 16 µg, gag/pol: 24 µg), and DNAse-free water (Invitrogen) for a final volume of 2 ml. Then, 2 ml of HEPES-buffered saline pH 7.0 (2× for transfection; VWR) was added dropwise to the previous mixture, under constant agitation. The obtained solution was kept at room temperature for 15 min and subsequently equally transferred to the HEK293T flasks. The next day, the medium was changed. 48 h after transfection, the culture medium containing the lentiviral particles was collected and ultracentrifuged at 113,000 *g* for 90 min at 4°C using a Beckman SW28 ultracentrifuge rotor (Beckman Coulter) for the obtention of concentrated virus, that was resuspended in cold PBS 1X. Viral titration was performed in HEK293 cells. For individual evaluation of shRNAs, mTECs were transduced at a multiplicity of infection of 10.

3D organotypic culture of primary mTECs

Preparation of the fibrin gel

The 3D organotypic co-culture system described in (Pinto *et al*, 2013) was set up using a ~ 1.2-mm-thick viscose-coated nonwoven fibrous fabric: Jettex 2005/45 (Orsa) that was placed as a scaffold into 12-well filter inserts (polyester capillary membrane with 3 µm pores; Dutscher). A semi-solid fibrin gel inoculated in the insert that serves as support for the culture system was prepared seeding human dermal fibroblasts (200,000) re-suspended in a fibrin gel made of fibrinogen (Merck-Millipore), thrombin (Merck-Millipore), and aprotinin (Euromedex) which prevents precocious fibrinolysis by serine proteases secreted by fibroblasts. Human dermal fibroblasts were generated from explant cultures of de-epidermized dermis as described (Boehnke *et al*, 2007) and grown up to passage 4 in DMEM/F-12 (Thermo Fisher) complemented with 10% FBS and pen/strep antibiotics. The fibrin gel polymerized at 37°C for 1 h or 2, forming a smooth upper surface for the culture of primary mTECs. A pre-culture of 5 days is required for the fibroblast activation and is set up by the submersion of the polymerized gel in medium 1 containing DMEM/F-12, 10% FBS, pen/strep antibiotics, L-ascorbic acid (50 µg/ml; Sigma), and TGF-β (1 ng/ml; R&D Systems). The medium 1 was changed every day. On the day of mTEC seeding, medium 1 was replaced by medium 2 containing DMEM high glucose + DMEM/F12 1:1 (v/v) with 10% FBS, pen/strep antibiotics, cholera toxin (10^{-10} M; Sigma), hydrocortisone (0.4 µg/µl; Sigma), L-ascorbic acid (50 µg/ml), aprotinin (500 U/ml), and RankL (80 ng/ml; R&D Systems).

mTEC seeding and lentiviral infection

Freshly isolated mTECs were seeded at the top of the fibroblast-containing fibrin gel with the addition of 10 µl of concentrated shRNA-bearing lentiviruses that we produced against *Raver2*, *Setd2,* and the Ctr (LacZ). The next day, medium 2 was replaced by medium 3 that is similar to medium 2 but containing reduced amount of aprotinin (250 U/ml) and increased amount of RankL (100 ng/ml). The RankL supplemented in mediums 2 and 3 helped maintain mTEChi maturity.

Isolation of knockdown mTECs

Three days after infection, a first part of the 3D organotypic co-culture was terminated by cutting out half of the fibrin gel to evaluate the *Raver2* and *Setd2* knockdown efficiencies by RT–qPCR. Two days later, the other half of the fibrin gel was processed to evaluate the impact of *Raver2* and *Setd2* knockdown on ASE inclusion of Aire-sensitive and neutral genes by RNA-seq. Using small dissecting scissors, the fibrin gel portions were cut into small pieces to be properly digested in an enzymatic solution of Collagenase/Dispase (0.5 mg/ml; Roche) and DNase I (0.5 mg/ml) at 37°C for 15 min for the obtention a single-cell fraction. After three rounds of centrifugation and clean-up in PBS containing 1% FBS and 5 mM of EDTA, the single-cell fraction was stained for 20 min at 4°C with the I-A/E-APC (MHCII) antibody (1:1,200; eBioscience) and for 5 min at 4°C with the DAPI viability dye solution (1 µg/ml; Sigma) to identify dead cells. We then sorted by flow cytometry $DAPI^{-}I\text{-}A/E^{+}GFP^{+}$ cells corresponding to viable lentivirus-infected mTECs.

© 2022 The Authors

14693178, 2022, 3, Downloaded from https://www.embopress.org/doi/10.15252/embr.202153576 by Université De Nantes, Wiley Online Library on [25/10/2022]. See the Terms and Conditions (https://onlinelibrary.wiley.com/terms-and-conditions) on Wiley Online Library for rules of use; OA articles are governed by the applicable Creative Commons License

shRNA knockdown efficiency

RNA extraction from knockdown mTECs cultured in the 3D organotypic system was performed using the Single Cell RNA Purification Kit (Norgen Biotek). First-strand cDNA was synthesized using SuperScript IV VILO Master Mix (Thermo Fisher). cDNA was used for subsequent PCR amplification using the viia7 Real-time PCR system (Thermo Fisher) and the Fast SYBR Green Master Mix (Thermo Fisher). Knockdown efficiency was assessed by comparing the level of expression of *Raver2* (forward primer: AACCAGAAGACACCGCAGAG; reverse: TCTCCCAAGAGTGAAGTCTGATT) and *Setd2* (forward primer: CAGCATGCAGATGTAGAAGTCA; reverse: TCCAGGACAAAGGTGTTCG) between the knockdown and control samples using *Gapdh* (forward primer: GGCAAATTCAACGGCACAGT; reverse: AGATGGTGATGGGCTTCCC) for normalization.

RNA-seq of medullary epithelial cells

Total RNA of knockdown mTECs cultured in the 3D organotypic system was extracted using the Single Cell RNA Purification Kit (Norgen Biotek). Total RNA of mTEChi isolated from WT or *Aire*-KO mice was extracted with TRIzol (Thermo Fisher) and used to generate the third replicate of two independent paired-end RNA-seq datasets that we previously generated and deposited in the GEO database (GSE140683). We used mTEClo paired-end RNA-seq data that we previously generated (GSE140815). Single-cell full-length and paired-end (2 × 125 bp) RNA-seq data of mTEChi were obtained from the GEO database (GSE114713). For mTECs in the 3D organotypic system, polyA-selected transcriptome libraries were constructed using the SMART-seq v4 Ultra Low Input RNA Kit (Takara) combined to the Nextera XT DNA Library Preparation Kit (Illumina) and sequenced on the Illumina NextSeq 500 machine as paired-end data (2 × 150 bp). Sequences were deposited in the GEO database as GSE177063. For WT and *Aire*-KO mTEChi, polyA-selected transcriptome libraries were constructed using the TruSeq Stranded mRNA Library Prep (Illumina) and sequenced on the Illumina HiSeq 2000 machine as paired-end data (2 × 100 bp). Sequences were deposited in the GEO database as GSE177062. All paired-end reads of the different datasets were homogenized to 2 × 100 bp by read-trimming and mapped to the mm10 genome using the TopHat 2 program (Trapnell *et al*, 2009) with default parameters. Levels of gene and transcript isoform expression were determined using the cufflinks 2 program (Trapnell *et al*, 2010) that assembles all reads on the RefSeq transcript annotations and estimates their abundances. We also used cuffdiff 2 (Trapnell *et al*, 2013) to compute differential gene expression between WT and *Aire*-KO mTEChi and between mTEChi and mTEClo.

Human medullary epithelial cell isolation and RNA-seq

The thymi from cardiac surgery pediatric patients (the ethical permission #170/T-I from Ethics Review Committee on Human Research of the University of Tartu) were minced in 1× PBS to release the thymocytes and then treated four times with collagenase/dispase (1:200) and DNaseI (1:1,000) digestion, and the cell fractions were further dissociated with gentleMACS treatment. All fractions were combined and filtered through the 100 μm Falcon cell strainer. The cells were collected by centrifugation, washed, and transferred to Optiprep density gradient. The upper cell layer was combined into one tube, washed, and counted resulting in 0.4–6.5 × 10^8 thymic cells. The cell fraction was then depleted with human CD45 beads (100 μl beads per 2 × 10^8 cells; Miltenyi Biotec) using autoMACS. After the CD45 depletion, the cells were sorted with BD FACSAria for mTEC MHC^{hi} (CD45$^-$ CDR2$^-$ EpCAM$^+$ HLA-DR^{hi}) directly into TRIzol (Thermo Fisher) solution, RNA was isolated with miRNAeasy Mini Kit (Qiagen) with DNase treatment. The RNA quality was assessed with TapeStation (Agilent D1000) before the processing with SMART-Seq v4 Ultra Low Input RNA Kit for Sequencing, and the library preparation with Illumina Nextera XT DNA Library Preparation Kit. The paired-end sequencing (2 × 150 bp) was performed on the Illumina NextSeq500. Sequences were deposited in the GEO database as GSE176445. The reads were homogenized to 2 × 100bp by read-trimming and mapped to the hg38 genome with TopHat 2. Levels of gene and transcript isoform expression were determined using cufflinks 2 and expression data as well as GTF files were used for ASE analysis.

H3K36me3 ChIP-seq. experiment and analysis

Nano-ChIP-seq on H3K36me3 was performed as previously described (Adli & Bernstein, 2011) on 50,000 isolated mTEClo. ChIP-seq libraries were prepared with the TruSeq ChIP Sample Preparation Kit (Illumina) and 2 × 75 bp paired-end reads were sequenced on an Illumina HiSeq 2000 machine. Sequences were deposited in the GEO database as GSE176371. Alignment to the mm10 genome was done using Bowtie 2 (Langmead *et al*, 2009). Duplicate alignments were removed using Samtools (Li *et al*, 2009) and the command line: "samtools view -S -hf 0x2 alignments.sam | grep -v "XS:i:" | foo.py > filtered.alignments.sam" the foo.py script been available online: "https://www.biostars.org/p/95929/". Peak calling for a sample (in comparison to the inputs) was done using MACS2 callpeak (Zhang *et al*, 2008) and the options -f BAMPE, --SPMR and –broad. Enrichment to the inputs was calculated using MACS2 bdgcmp and the option -m FE. For multi-tissue comparison, H3K36me3 ChIP-seq data generated by the Bing Ren's lab (http://renlab.sdsc.edu/), as part of the ENCODE project (ENCODE Project Consortium *et al*, 2007), were obtained from the GEO database: GSE31039 for heart, kidney, liver, small intestine, and testis of adult (8-week-old) mice. These data were available as signal (bigWig) and peak (bed) files processed on the mm9 genome following ENCODE standards. Finally, we used the CEAS distribution (Shin *et al*, 2009) on mTEClo and tissue data to calculate the average H3K36me3 enrichment within gene bodies and their upstream and downstream regions.

Splicing entropy calculation

The splicing entropy of a specific gene is a measure of diversity of the transcript isoforms that result from alternative splicing for this gene (Ritchie *et al*, 2008). The higher the number of transcript isoforms, the higher the splicing entropy. For a particular gene, the expression values of its transcript isoforms, computed by cufflinks, are used to calculate the splicing entropy:

$$\text{Splicing entropy} = \sum_{i=1}^{n} P_i \log_2(P_i)$$

n is the number of isoforms and Pi is the proportion that each isoform (i) contributes to the overall expression of the gene. We

© 2022 The Authors

14693178, 2022, 3, Downloaded from https://www.embopress.org/doi/10.15252/embr.202153576 by Université De Nantes, Wiley Online Library on [25/10/2022]. See the Terms and Conditions (https://onlinelibrary.wiley.com/terms-and-conditions) on Wiley Online Library for rules of use; OA articles are governed by the applicable Creative Commons License

calculated the splicing entropy of each gene in our samples of interest and used the median splicing entropy for sample-to-sample comparison.

ASE inclusion analysis

We used the rMATS program (Multivariate Analysis of Transcript Splicing) (Shen *et al*, 2014) to identify all ASEs from the mm10 or hg19 RefSeq mRNA annotations database, including skipped exon (SE), alternative 5′ splicing site (5SS), alternative 3′ splicing site (3SS) or intron retention (IR). For a particular ASE, we computed the percent splicing inclusion (PSI), that is, the relative expression of transcript isoforms spliced in versus spliced in or out, using the R-script that we developed (https://github.com/TeamGiraud/TEC_splicing_2021):

$$\text{Percent splicing inclusion} = \frac{\sum_{i=1}^{n_{\text{spliced-in}}} \text{FPKM}(i)}{\sum_{j=1}^{m_{\text{spliced-in/-out}}} \text{FPKM}(j)}$$

$n_{\text{spliced-in}}$ is the number of isoforms with the ASE spliced in. $m_{\text{spliced-in/-out}}$ is the number of isoforms with the ASE spliced in or spliced out. To compare the PSI values between different set of genes and/or samples, we determined the splicing inclusion imbalance by dividing the number of ASEs showing some level of active inclusion (PSI > 0.1) by the number of excluded ASEs, that is, showing no or background inclusion (PSI < 0.1).

Multi-tissue comparison analysis

Whole tissue level

We considered 14 homogeneously sequenced RNA-seq datasets (paired-end) of mouse peripheral tissues (Brain, Liver, Kidney, Adrenal Gland, Heart, Ovary, Testis, Stomach, Forestomach, Small intestine, Large Intestine, Muscle, Uterus, Vesicular Gland) generated by (Li *et al*, 2017) and obtained from the NCBI BioProject database (PRJNA375882). The reads were mapped to the mouse reference genome (mm10) with TopHat 2, using default parameters. Expression levels of transcript isoforms were calculated using Cufflinks. We determined the tissue specificity (one tissue of restricted expression) or selectivity (two-to-three tissues of restricted expression) of Aire-sensitive genes, by using the specificity measurement (SPM) and the contribution measurement (CTM) methods (Pan *et al*, 2013), as described in Guyon *et al* (2020). For each considered gene, the SPM and CTM values were evaluated based on the level of gene expression in each tissue. A gene was considered tissue-specific for a particular tissue if its SPM value in the tissue was > 0.9. A gene was considered tissue-selective (2 or 3 tissue), if its SPM values were > 0.3 in those tissues and its CTM value for the corresponding tissue > 0.9. If the previous conditions were not met, the gene was left unassigned.

Epithelial cell level

To compare gene expression between TECs and epithelial cells from different mouse peripheral tissues, we collected public RNA-seq datasets of epithelial cells isolated from skin (St-Pierre *et al*, 2013) (GEO database: GSE44945); brain, caecum, large and small intestine, heart, kidney, lever, lung, lymph node, spleen (Krausgruber *et al*, 2020) (GSE134659); neural tube (ENCODE Project Consortium, 2012) (GSE78315); mammary glands (Pal *et al*, 2021) (GSE164307); olfactory system (Tan *et al*, 2020) (GSE146043); esophagus (Wiles *et al*, 2021) (GSE154129), and colon (Marincola Smith *et al*, 2021) (GSE100082). The reads were mapped to the mouse reference genome (mm10) with TopHat 2, using default parameters. Expression levels of transcript isoforms were calculated using Cufflinks.

Data availability

RNA-seq data for WT and *Aire*-KO mTEChi, human mTEChi, and knockdown mouse mTECs can be accessed in GEO (https://www.ncbi.nlm.nih.gov/geo/) with accession codes GSE177062 (http://www.ncbi.nlm.nih.gov/geo/query/acc.cgi?acc=GSE177062), GSE176445 (http://www.ncbi.nlm.nih.gov/geo/query/acc.cgi?acc=GSE176445), and GSE177063 (http://www.ncbi.nlm.nih.gov/geo/query/acc.cgi?acc=GSE177063). H3K36me3 ChIP-seq data are available with the accession code GSE176371 (http://www.ncbi.nlm.nih.gov/geo/query/acc.cgi?acc=GSE176371). We have provided the documented R code that we developed for ASE inclusion analysis as a Git repository available from GitHub (https://github.com/TeamGiraud/TEC_splicing_2021).

Expanded View for this article is available online.

Acknowledgements

We thank Drs. D. Mathis and C. Benoist (Harvard Medical School) for *Aire*-KO (B6) mice. This work was supported by the Agence Nationale de la Recherche (ANR) 2011-CHEX-001-R12004KK to M.G., IHU-Cesti funded by the «Investissements d'Avenir» ANR-10-IBHU-005 as well as by Nantes Metropole and Region Pays de la Loire to M.G., and EJP-Rare Disease JTC2019 program TARID project (EJPRD19-208) funded by the ANR (ANR-19-RAR4-0011-5) to M.G., by Estonian Ministry of Social Affairs to P.P. The work was also supported by the University of Tartu Center of Translational Genomics (SP1GVARENG) and the Estonian Research Council grant PRG377 to P.P. and the Marie Curie Actions (Career Integration Grants, CIG_SIGnEPI4Tol_618541) to M.I. We would like to thank the members of the 'Genomic'IC' core facility head by Franck Letourneur at Cochin Institute, Paris, France, for RNA-seq data production, as well as Ms. Maire Pihlap for her excellent technical assistance in preparing sequencing samples, Dr Mario Saare for his help in analyzing human mTEC data and Nicolas Richard for his help with the single-cell analysis. F.P. was supported by the Labex IGO (project «Investissements d'Avenir» ANR- 11-LABX-0016-01) and the RFI Bioregate grant (ThymIPS) from la Region Pays de la Loire to M.G. N.P. was supported by "la fondation d'entreprise ProGreffe". S.Y. was supported by the ANR (ANR-19-RAR4-0011-5) to M.G. and la Region Pays de la Loire.

Author contributions

Francine Padonou: Software; Formal analysis; Investigation; Visualization; Methodology; Writing - original draft; Writing - review & editing. **Virginie Gonzalez:** Investigation. **Nathan Provin:** Formal analysis; Investigation; Visualization. **Sümeyye Yayilkan:** Formal analysis; Investigation; Visualization. **Nada Jmari:** Investigation. **Julia Maslovskaja:** Investigation. **Kai Kisand:** Investigation. **Pärt Peterson:** Resources; Writing - review & editing. **Magali Irla:** Conceptualization; Resources; Methodology; Writing - review & editing. **Matthieu Giraud:** Conceptualization; Software; Formal analysis; Supervision; Funding acquisition; Visualization; Methodology; Writing - original draft; Project administration; Writing - review & editing.

© 2022 The Authors

14693178, 2022, 3, Downloaded from https://www.embopress.org/doi/10.15252/embr.202153576 by Université De Nantes, Wiley Online Library on [25/10/2022]. See the Terms and Conditions (https://onlinelibrary.wiley.com/terms-and-conditions) on Wiley Online Library for rules of use; OA articles are governed by the applicable Creative Commons License

In addition to the CRediT author contributions listed above, the contributions in detail are:

FP and MG designed the study and wrote the manuscript; FP and VG performed most of the experimental work; NP, SY, NJ, JM, and KK performed experiments. FP, NP, SY, and MG performed bioinformatics analyses; PP and MI provided key material, datasets and edited the manuscript.

Disclosure statement and competing interests

The authors declare that they have no conflict of interest.

References

Adli M, Bernstein BE (2011) Whole-genome chromatin profiling from limited numbers of cells using nano-ChIP-seq. *Nat Protoc* 6: 1656–1668

de Almeida SF, Carmo-Fonseca M (2012) Design principles of interconnections between chromatin and pre-mRNA splicing. *Trends Biochem Sci* 37: 248–253

Anderson MS, Venanzi ES, Klein L, Chen Z, Berzins SP, Turley SJ, von Boehmer H, Bronson R, Dierich A, Benoist C *et al* (2002) Projection of an immunological self shadow within the thymus by the Aire protein. *Science* 298: 1395–1401

Aschenbrenner K, D'Cruz LM, Vollmann EH, Hinterberger M, Emmerich J, Swee LK, Rolink A, Klein L (2007) Selection of Foxp3+ regulatory T cells specific for self antigen expressed and presented by Aire+ medullary thymic epithelial cells. *Nat Immunol* 8: 351–358

Bartoletti-Stella A, Gasparini L, Giacomini C, Corrado P, Terlizzi R, Giorgio E, Magini P, Seri M, Baruzzi A, Parchi P *et al* (2015) Messenger RNA processing is altered in autosomal dominant leukodystrophy. *Hum Mol Genet* 24: 2746–2756

Boehnke K, Mirancea N, Pavesio A, Fusenig NE, Boukamp P, Stark H-J (2007) Effects of fibroblasts and microenvironment on epidermal regeneration and tissue function in long-term skin equivalents. *Eur J Cell Biol* 86: 731–746

Cowan JE, Parnell SM, Nakamura K, Caamano JH, Lane PJL, Jenkinson EJ, Jenkinson WE, Anderson G (2013) The thymic medulla is required for Foxp3+ regulatory but not conventional CD4+ thymocyte development. *J Exp Med* 210: 675–681

Danan-Gotthold M, Guyon C, Giraud M, Levanon EY, Abramson J (2016) Extensive RNA editing and splicing increase immune self-representation diversity in medullary thymic epithelial cells. *Genome Biol* 17: 219

Derbinski J, Schulte A, Kyewski B, Klein L (2001) Promiscuous gene expression in medullary thymic epithelial cells mirrors the peripheral self. *Nat Immunol* 2: 1032–1039

Dhalla F, Baran-Gale J, Maio S, Chappell L, Holländer GA, Ponting CP (2020) Biologically indeterminate yet ordered promiscuous gene expression in single medullary thymic epithelial cells. *EMBO J* 39: e101828

ENCODE Project Consortium, Birney E, Stamatoyannopoulos JA, Dutta A, Guigo R, Gingeras TR, Margulies EH, Weng Z, Snyder M, Dermitzakis ET *et al* (2007) Identification and analysis of functional elements in 1% of the human genome by the ENCODE pilot project. *Nature* 447: 799–816

ENCODE Project Consortium (2012) An integrated encyclopedia of DNA elements in the human genome. *Nature* 489: 57–74

Gäbler J, Arnold J, Kyewski B (2007) Promiscuous gene expression and the developmental dynamics of medullary thymic epithelial cells. *Eur J Immunol* 37: 3363–3372

Giraud M, Jmari N, Du L, Carallis F, Nieland TJF, Perez-Campo FM, Bensaude O, Root DE, Hacohen N, Mathis D *et al* (2014) An RNAi screen for Aire cofactors reveals a role for Hnrnpl in polymerase release and Aire-activated ectopic transcription. *Proc Natl Acad Sci USA* 111: 1491–1496

Goodnow CC, Sprent J, de St F, Groth B, Vinuesa CG (2005) Cellular and genetic mechanisms of self tolerance and autoimmunity. *Nature* 435: 590–597

Guyon C, Jmari N, Padonou F, Li Y-C, Ucar O, Fujikado N, Coulpier F, Blanchet C, Root DE, Giraud M (2020) Aire-dependent genes undergo Clp1-mediated 3'UTR shortening associated with higher transcript stability in the thymus. *Elife* 9: e52985

Hamazaki Y, Fujita H, Kobayashi T, Choi Y, Scott HS, Matsumoto M, Minato N (2007) Medullary thymic epithelial cells expressing Aire represent a unique lineage derived from cells expressing claudin. *Nat Immunol* 8: 304–311

Handel AE, Shikama-Dorn N, Zhanybekova S, Maio S, Graedel AN, Zuklys S, Ponting CP, Holländer GA (2018) Comprehensively profiling the chromatin architecture of tissue restricted antigen expression in thymic epithelial cells over development. *Front Immunol* 9: 2120

Henneberg B, Swiniarski S, Becke S, Illenberger S (2010) A conserved peptide motif in Raver2 mediates its interaction with the polypyrimidine tract-binding protein. *Exp Cell Res* 316: 966–979

Hu Q, Greene CS, Heller EA (2020) Specific histone modifications associate with alternative exon selection during mammalian development. *Nucleic Acids Res* 48: 4709–4724

Husmann D, Gozani O (2019) Histone lysine methyltransferases in biology and disease. *Nat Struct Mol Biol* 26: 880–889

Keane P, Ceredig R, Seoighe C (2015) Promiscuous mRNA splicing under the control of AIRE in medullary thymic epithelial cells. *Bioinformatics* 31: 986–990

Kekäläinen E, Tuovinen H, Joensuu J, Gylling M, Franssila R, Pöntynen N, Talvensaari K, Perheentupa J, Miettinen A, Arstila TP (2007) A defect of regulatory T cells in patients with autoimmune polyendocrinopathy-candidiasis-ectodermal dystrophy. *J Immunol* 178: 1208–1215

Klein L, Kyewski B, Allen PM, Hogquist KA (2014) Positive and negative selection of the T cell repertoire: what thymocytes see (and don't see). *Nat Rev Immunol* 14: 377–391

Kleinhenz B, Fabienke M, Swiniarski S, Wittenmayer N, Kirsch J, Jockusch BM, Arnold HH, Illenberger S (2005) Raver2, a new member of the hnRNP family. *FEBS Lett* 579: 4254–4258

Kolasinska-Zwierz P, Down T, Latorre I, Liu T, Liu XS, Ahringer J (2009) Differential chromatin marking of introns and expressed exons by H3K36me3. *Nat Genet* 41: 376–381

Kornblihtt AR, Schor IE, Allo M, Dujardin G, Petrillo E, Muñoz MJ (2013) Alternative splicing: a pivotal step between eukaryotic transcription and translation. *Nat Rev Mol Cell Biol* 14: 153–165

Krausgruber T, Fortelny N, Fife-Gernedl V, Senekowitsch M, Schuster LC, Lercher A, Nemc A, Schmidl C, Rendeiro AF, Bergthaler A *et al* (2020) Structural cells are key regulators of organ-specific immune responses. *Nature* 583: 296–302

Langmead B, Trapnell C, Pop M, Salzberg SL (2009) Ultrafast and memory-efficient alignment of short DNA sequences to the human genome. *Genome Biol* 10: R25

Li H, Handsaker B, Wysoker A, Fennell T, Ruan J, Homer N, Marth G, Abecasis G, Durbin R; Durbin R1000 Genome Project Data Processing Subgroup (2009) The sequence alignment/Map format and SAMtools. *Bioinformatics* 25: 2078–2079

Li B, Qing T, Zhu J, Wen Z, Yu Y, Fukumura R, Zheng Y, Gondo Y, Shi L (2017) A comprehensive mouse transcriptomic BodyMap across 17 tissues by RNA-seq. *Sci Rep* 7: 4200

© 2022 The Authors

14693178, 2022, 3, Downloaded from https://www.embopress.org/doi/10.15252/embr.202153576 by Université De Nantes, Wiley Online Library on [25/10/2022]. See the Terms and Conditions (https://onlinelibrary.wiley.com/terms-and-conditions) on Wiley Online Library for rules of use; OA articles are governed by the applicable Creative Commons License

Luco RF, Pan Q, Tominaga K, Blencowe BJ, Pereira-Smith OM, Misteli T (2010) Regulation of alternative splicing by histone modifications. *Science* 327: 996–1000

Luco RF, Allo M, Schor IE, Kornblihtt AR, Misteli T (2011) Epigenetics in alternative pre-mRNA splicing. *Cell* 144: 16–26

Malchow S, Leventhal DS, Nishi S, Fischer BI, Shen L, Paner GP, Amit AS, Kang C, Geddes JE, Allison JP *et al* (2013) Aire-dependent thymic development of tumor-associated regulatory T cells. *Science* 339: 1219–1224

Malchow S, Leventhal DS, Lee V, Nishi S, Socci ND, Savage PA (2016) Aire enforces immune tolerance by directing autoreactive T cells into the regulatory T cell lineage. *Immunity* 44: 1102–1113

Marincola Smith P, Choksi YA, Markham NO, Hanna DN, Zi J, Weaver CJ, Hamaamen JA, Lewis KB, Yang J, Liu QI *et al* (2021) Colon epithelial cell TGFβ signaling modulates the expression of tight junction proteins and barrier function in mice. *Am J Physiol Gastrointest Liver Physiol* 320: G936–G957

Nagamine K, Peterson P, Scott HS, Kudoh J, Minoshima S, Heino M, Krohn KJ, Lalioti MD, Mullis PE, Antonarakis SE *et al* (1997) Positional cloning of the APECED gene. *Nat Genet* 17: 393–398

Pal B, Chen Y, Milevskiy MJG, Vaillant F, Prokopuk L, Dawson CA, Capaldo BD, Song X, Jackling F, Timpson P *et al* (2021) Single cell transcriptome atlas of mouse mammary epithelial cells across development. *Breast Cancer Res* 23: 69

Pan J-B, Hu S-C, Shi D, Cai M-C, Li Y-B, Zou Q, Ji Z-L (2013) PaGenBase: a pattern gene database for the global and dynamic understanding of gene function. *PLoS One* 8: e80747

Peterson P, Pitkänen J, Sillanpää N, Krohn K (2004) Autoimmune polyendocrinopathy candidiasis ectodermal dystrophy (APECED): a model disease to study molecular aspects of endocrine autoimmunity. *Clin Exp Immunol* 135: 348–357

Pinto S, Schmidt K, Egle S, Stark H-J, Boukamp P, Kyewski B (2013) An organotypic coculture model supporting proliferation and differentiation of medullary thymic epithelial cells and promiscuous gene expression. *J Immunol* 190: 1085–1093

Pomié C, Vicente R, Vuddamalay Y, Lundgren BA, van der Hoek M, Enault G, Kagan J, Fazilleau N, Scott HS, Romagnoli P *et al* (2011) Autoimmune regulator (AIRE)-deficient CD8+CD28low regulatory T lymphocytes fail to control experimental colitis. *Proc Natl Acad Sci USA* 108: 12437–12442

Ritchie W, Granjeaud S, Puthier D, Gautheret D (2008) Entropy measures quantify global splicing disorders in cancer. *PLoS Comput Biol* 4: e1000011

Ryan KR, Lawson CA, Lorenzi AR, Arkwright PD, Isaacs JD, Lilic D (2005) CD4+CD25+ T-regulatory cells are decreased in patients with autoimmune polyendocrinopathy candidiasis ectodermal dystrophy. *J Allergy Clin Immunol* 116: 1158–1159

Sansom SN, Shikama-Dorn N, Zhanybekova S, Nusspaumer G, Macaulay IC, Deadman ME, Heger A, Ponting CP, Hollander GA (2014) Population and single-cell genomics reveal the Aire dependency, relief from Polycomb silencing, and distribution of self-antigen expression in thymic epithelia. *Genome Res* 24: 1918–1931

Shen S, Park JW, Lu Z-X, Lin L, Henry MD, Wu YN, Zhou Q, Xing Y (2014) rMATS: robust and flexible detection of differential alternative splicing from replicate RNA-Seq data. *Proc Natl Acad Sci USA* 111: E5593–E5601

Shin H, Liu T, Manrai AK, Liu XS (2009) CEAS: cis-regulatory element annotation system. *Bioinformatics* 25: 2605–2606

St-Pierre C, Brochu S, Vanegas JR, Dumont-Lagacé M, Lemieux S, Perreault C (2013) Transcriptome sequencing of neonatal thymic epithelial cells. *Sci Rep* 3: 1860–1910

St-Pierre C, Trofimov A, Brochu S, Lemieux S, Perreault C (2015) Differential features of AIRE-induced and AIRE-independent promiscuous gene expression in thymic epithelial cells. *J Immunol* 195: 498–506

Tan K, Jones SH, Lake BB, Dumdie JN, Shum EY, Zhang L, Chen S, Sohni A, Pandya S, Gallo RL *et al* (2020) The role of the NMD factor UPF3B in olfactory sensory neurons. *Elife* 9: e57525

Trapnell C, Pachter L, Salzberg SL (2009) TopHat: discovering splice junctions with RNA-Seq. *Bioinformatics* 25: 1105–1111

Trapnell C, Williams BA, Pertea G, Mortazavi A, Kwan G, van Baren MJ, Salzberg SL, Wold BJ, Pachter L (2010) Transcript assembly and quantification by RNA-Seq reveals unannotated transcripts and isoform switching during cell differentiation. *Nat Biotechnol* 28: 511–515

Trapnell C, Hendrickson DG, Sauvageau M, Goff L, Rinn JL, Pachter L (2013) Differential analysis of gene regulation at transcript resolution with RNA-seq. *Nat Biotechnol* 31: 46–53

Vojnic E, Simon B, Strahl BD, Sattler M, Cramer P (2006) Structure and carboxyl-terminal domain (CTD) binding of the Set2 SRI domain that couples histone H3 Lys36 methylation to transcription. *J Biol Chem* 281: 13–15

Wagner EJ, Garcia-Blanco MA (2002) RNAi-mediated PTB depletion leads to enhanced exon definition. *Mol Cell* 10: 943–949

Wiles KN, Alioto CM, Hodge NB, Clevenger MH, Tsikretsis LE, Lin FTJ, Tétreault M-P (2021) IκB Kinase-β regulates neutrophil recruitment through activation of STAT3 signaling in the esophagus. *Cell Mol Gastroenterol Hepatol* 12: 1743–1759

Zhang Y, Liu T, Meyer CA, Eeckhoute J, Johnson DS, Bernstein BE, Nusbaum C, Myers RM, Brown M, Li W *et al* (2008) Model-based analysis of ChIP-Seq (MACS). *Genome Biol* 9: R137–R139

© 2022 The Authors

14693178, 2022, 3, Downloaded from https://www.embopress.org/doi/10.15252/embr.202153576 by Université De Nantes, Wiley Online Library on [25/10/2022]. See the Terms and Conditions (https://onlinelibrary.wiley.com/terms-and-conditions) on Wiley Online Library for rules of use; OA articles are governed by the applicable Creative Commons License

© 2021. Published by The Company of Biologists Ltd | Disease Models & Mechanisms (2021) 14, dmm046359. doi:10.1242/dmm.046359

REVIEW

AIRE deficiency, from preclinical models to human APECED disease

Marine Besnard[1,*], Francine Padonou[1,*], Nathan Provin[1], Matthieu Giraud[1,‡] and Carole Guillonneau[1,‡]

ABSTRACT

Autoimmune polyendocrinopathy candidiasis ectodermal dystrophy (APECED) is a rare life-threatening autoimmune disease that attacks multiple organs and has its onset in childhood. It is an inherited condition caused by a variety of mutations in the autoimmune regulator (*AIRE)* gene that encodes a protein whose function has been uncovered by the generation and study of *Aire*-KO mice. These provided invaluable insights into the link between *AIRE* expression in medullary thymic epithelial cells (mTECs), and the broad spectrum of self-antigens that these cells express and present to the developing thymocytes. However, these murine models poorly recapitulate all phenotypic aspects of human APECED. Unlike *Aire*-KO mice, the recently generated *Aire*-KO rat model presents visual features, organ lymphocytic infiltrations and production of autoantibodies that resemble those observed in APECED patients, making the rat model a main research asset. In addition, *ex vivo* models of AIRE-dependent self-antigen expression in primary mTECs have been successfully set up. Thymus organoids based on pluripotent stem cell-derived TECs from APECED patients are also emerging, and constitute a promising tool to engineer *AIRE*-corrected mTECs and restore the generation of regulatory T cells. Eventually, these new models will undoubtedly lead to main advances in the identification and assessment of specific and efficient new therapeutic strategies aiming to restore immunological tolerance in APECED patients.

KEY WORDS: AIRE, mTEC, APECED, APS-1, Organoid, Knockout model

Introduction

Preclinical research using experimental animal models of diseases is pivotal to advance the understanding of mechanisms involved in these diseases and to successfully translate bench research to the clinic. The selection of the model and its accuracy remain critical since the success rate of drugs reaching clinical development remains low. Worldwide, there are 7000 rare diseases recognized, affecting more than 350 million people, but only <10% of these diseases have an approved drug treatment (Villalón-García et al., 2020). Clinical trials to evaluate therapeutic candidates for rare diseases are challenging as, by definition, only small groups of patient population are affected.

The autoimmune polyendocrinopathy candidiasis ectodermal dystrophy (APECED; also known as autoimmune polyglandular syndrome type I, APS I) is one of these rare human autoimmune diseases (Perheentupa, 1980). APECED is an autosomal-recessive disorder caused by a mutation in the autoimmune regulator (*AIRE*) gene that is expressed in the thymus and whose protein product, AIRE, is essential for central immune tolerance (Villasenor et al., 2005). AIRE is involved in the expression of tissue-restricted antigens (TRAs), i.e. tissue constituents that are not ubiquitously expressed. These antigens are essential for negative selection as they contribute to the projection of the complete self repertoire at the local site of negative selection and, thus, enable the elimination of all autoreactive T cells. The APECED disease, thus, involves autoreactive T cells that escape deletion, as well as autoantibodies, and leads to premature death in young adults. To date, there is no cure to prevent or treat the APECED syndrome (Kisand and Peterson, 2011).

To better understand the human APECED pathology, AIRE-deficient mouse models have been generated since the identification of causative gene; they have been essential to study and get a better understanding of the APECED disease (Hubert et al., 2009; Mathis and Benoist, 2009). However, flaws remain, since these models only recapitulate limited aspects of human ACEPED pathology and its clinical features and, to the best of our knowledge, these mouse models have not been used to translate therapeutic drug candidates to the clinic.

In this Review, we aim to describe the latest advances in the different APECED models, including a rat model generated by our lab and used to study the disease. Moreover, we discuss new approaches, such as *ex vivo* models and organoids generated from embryonic or induced pluripotent stem cells, to better understand, challenge and assess immunotherapies.

Human APECED: clinical features and genetic causes

The first documented case of APECED syndrome was reported in 1929 by Thorpe and Handley, describing of a four-and-a-half-year-old girl suffering from chronic tetany (see Glossary, Box 1), hypoparathyroidism, chronic oral mycelial infection and cornea ulceration (Thorpe, 1929). However, the term APECED is more descriptive of the syndrome and appeared only in 1980 (Perheentupa, 1980). One characteristic of this potentially fatal disease is the incidence of several severe auto-immune lesions within peripheral tissues – not all of which are present in affected individuals – resulting from the central immune tolerance defect. In the past, patients were only diagnosed with APECED if presenting with at least two symptoms of the so-called Whitaker's triad, comprising chronic mucocutaneous candidiasis (CMC), hypoparathyroidism (HP) and adrenal insufficiency (Addison disease, AD) (Box 1) – all three of which are considered to be hallmarks of this disease (Esselborn et al., 1956; Neufeld et al., 1980). More recently, the spectrum of APECED symptoms has been expanded to include ≤30 related manifestations. Amongst others, they include type 1 diabetes (T1D), hypergonadotropic hypogonadism, ovarian failure, hepatitis,

[1]Université de Nantes, Inserm, CNRS, Centre de Recherche en Transplantation et Immunologie, UMR 1064, ITUN, F-44000 Nantes, France.
*These authors contributed equally to this work

‡Authors for correspondence (carole.guillonneau@univ-nantes.fr, matthieu.giraud@univ-nantes.fr)

C.G., 0000-0002-7195-0631

This is an Open Access article distributed under the terms of the Creative Commons Attribution License (https://creativecommons.org/licenses/by/4.0), which permits unrestricted use, distribution and reproduction in any medium provided that the original work is properly attributed.

Disease Models & Mechanisms (2021) 14, dmm046359. doi:10.1242/dmm.046359

Box 1. Glossary

- **Addison disease (AD), also known as primary adrenal insufficiency and hypocortisolism:** an endocrine pathology affecting adrenal glands, resulting in a deficit in steroid hormone synthesis. Symptoms include weight loss, abdominal pain and weakness.
- **Alopecia:** complete or partial loss of hair that can happen on the scalp, i.e. in patches (alopecia areata) or the entire head (alopecia totalis), or over the whole body (alopecia universalis).
- **Aromatic L-amino acid decarboxylase (AADC, officially known as DCC):** an enzyme that catalyzes several different decarboxylation reactions in the biosynthesis of various neurotransmitters and neuromodulators.
- **Chronic mucocutaneous candidiasis (CMC):** chronic *Candida* spp. infection of the mucosa, nails and skin that persists, owing to an immune disorder linked to a T cell defect.
- **Chronic tetany:** a condition characterized by spasms, cramps and overactive neurological reflexes as a result of low calcium blood levels that are often the consequence of hypoparathyroidism (see below).
- **Enamel hypoplasia:** a developmental defect that weakens the surface of teeth, due to defective formation of the hard protective layer covering the outside of the tooth.
- **Epithelial cell adherence molecule (EpCAM):** a common surface marker protein of epithelial cells.
- **Glutamate decarboxylase (GAD):** an enzyme that catalyzes the decarboxylation of glutamate to GABA, the main inhibitory neurotransmitter.
- **Gonadic failure:** a disorder in which testes or ovaries fail to produce either sex hormones or gametes, resulting in fertility issues.
- **Hypergonadotropic hypogonadism (HH), also known as primary or peripheral gonadal hypogonadism:** the defective response of gonads to hormones, caused by problems with the pituitary gland or hypothalamus. It is the result of decreased testosterone or estradiol production, respectively, in males or females, inducing a delay in sexual development and diminished reproductive functions.
- **Hypoparathyroidism (HP):** failure of the parathyroid gland to efficiently produce the parathyroid hormone, *in fine* leading to low blood calcium levels.
- **Immunological tolerance:** capacity of the immune system to recognize the body's own components and not react to them, which is vital for the protection against autoimmune diseases. The tolerance process takes place in the thymus, whose main function is to control thymocyte development, and to discriminate between self- and non-self antigens.
- **Induced pluripotent stem cells (iPSCs):** somatic cells reprogrammed back to an embryonic-like pluripotent state.
- **Keratoconjunctivis:** simultaneous inflammation of the cornea and conjunctiva.
- **Medullary thymic epithelial cells (mTECs):** a population of TECs located in the medulla of the thymus. mTECs express and present a large number of self-antigens to the developing T cell to ensure their education and prevent autoimmune reactions.
- **Protein-disulfide isomerase pancreas specific (PDIp, officially known as PDIA2):** a member of the protein disulfide isomerase (PDI) family, acting as a molecular chaperone that catalyzes the formation of disulfide bonds in secretory proteins.
- **Pernicious anemia:** decrease of red blood cell due to B12 vitamin malabsorption in the intestines.
- **Regulatory T cells (Tregs):** a subpopulation of T cells that help prevent autoimmune manifestations by regulating the activity of immune cells. They control the immune response to and self- and non-self antigens.
- **T cell receptor (TCR) repertoire:** describes the T cell diversity within the immune system of an individual in a physiopathological context and it represents the repertoire of antigens encountered by the TCR.
- **Tissue-restricted antigens (TRAs):** tissue constituents that are not ubiquitously expressed.
- **Type 1 diabetes (T1D):** an autoimmune disorder that affects pancreatic Langerhans islet cells and results in very little to no insulin production.
- **Vitiligo:** a progressive autoimmune disorder affecting the skin that manifests as patchy loss of pigmentation.

keratoconjunctivis, pernicious anemia, malabsorption, alopecia, vitiligo, urtical eruption and enamel hypoplasia (Fig. 1; Box 1) (Ferre et al., 2016; Orlova et al., 2017). APECED patients usually harbor between five and 20 symptoms that, preferentially, appear during childhood; however, some develop with age and without any predictability of severity or diversity (Ahonen et al., 1990; Constantine and Lionakis, 2019; Ferre et al., 2016; Perheentupa, 2006). In many cases, the development of symptoms is preceded by production of specific autoantibodies – another characteristic of the APECED syndrome (Ekwall et al., 1998). Indeed, patients produce a wide array of autoantibodies, some of which correlate with the presence of organ-specific autoimmune manifestations. For example, antibodies directed against cobalamin binding intrinsic factor (CBLIF, also known as GIF), glutamate decarboxylase (GAD; Box 1) and GA-binding protein transcription factor subunit beta 2 (GABPB2) are associated with the development of pernicious anemia, vitiligo and autoimmune hepatitis, respectively (Fishman et al., 2017). However, in contrast to the progressive development of symptoms with age, the antigen repertoire targeted by autoantibodies does not expand. This implies that autoantibodies alone cannot fully explain the accumulation of the APECED-associated autoimmune manifestations (Fishman et al., 2017). Autoantibodies that were found in APECED patients to target cytokines, such as interleukin (IL)-17 and IL-22, have been linked to CMC, whereas autoantibodies targeting type I interferon (type I IFNs) negatively correlate with the incidence of T1D; the latter might, therefore, be of therapeutic interest (Meyer et al., 2016). Anti-IFNω antibodies are highly specific of this pathology, as they are only found in patients diagnosed with a thymoma or with APECED (Burbelo et al., 2010). Moreover, they usually appear before the onset of other clinical manifestations and can be found in all APECED patients. For these reasons, anti-IFNω antibodies are now used as a diagnostic tool for APECED syndrome (Kisand et al., 2008). This discovery fundamentally improved the diagnosis of APECED as, until then, only two diagnostic criteria had been available – the presence of the classic association of symptoms, i.e. those from Whitaker's triad or an *AIRE* mutation. Indeed, the clinical picture has evolved with the discovery of new manifestations and the documentation of prevalent symptoms from Whitaker's triad has declined (Perheentupa, 2002). In addition, since APECED is mostly inherited recessively, scrutiny of the *AIRE* gene by sequence analysis is only done when relatives of the patient are affected or when specific symptoms have developed. However, recent studies have shown that APECED can also be inherited in a dominant manner through mono-allelic missense mutations in the first plant homeodomain (PHD1) zinc finger of AIRE, which then suppress wild-type AIRE in a dominant-negative manner (Cetani et al., 2001; Oftedal et al., 2015). Prevalence of APECED remains relatively low, with an average incidence of

Disease Models & Mechanisms (2021) 14, dmm046359. doi:10.1242/dmm.046359

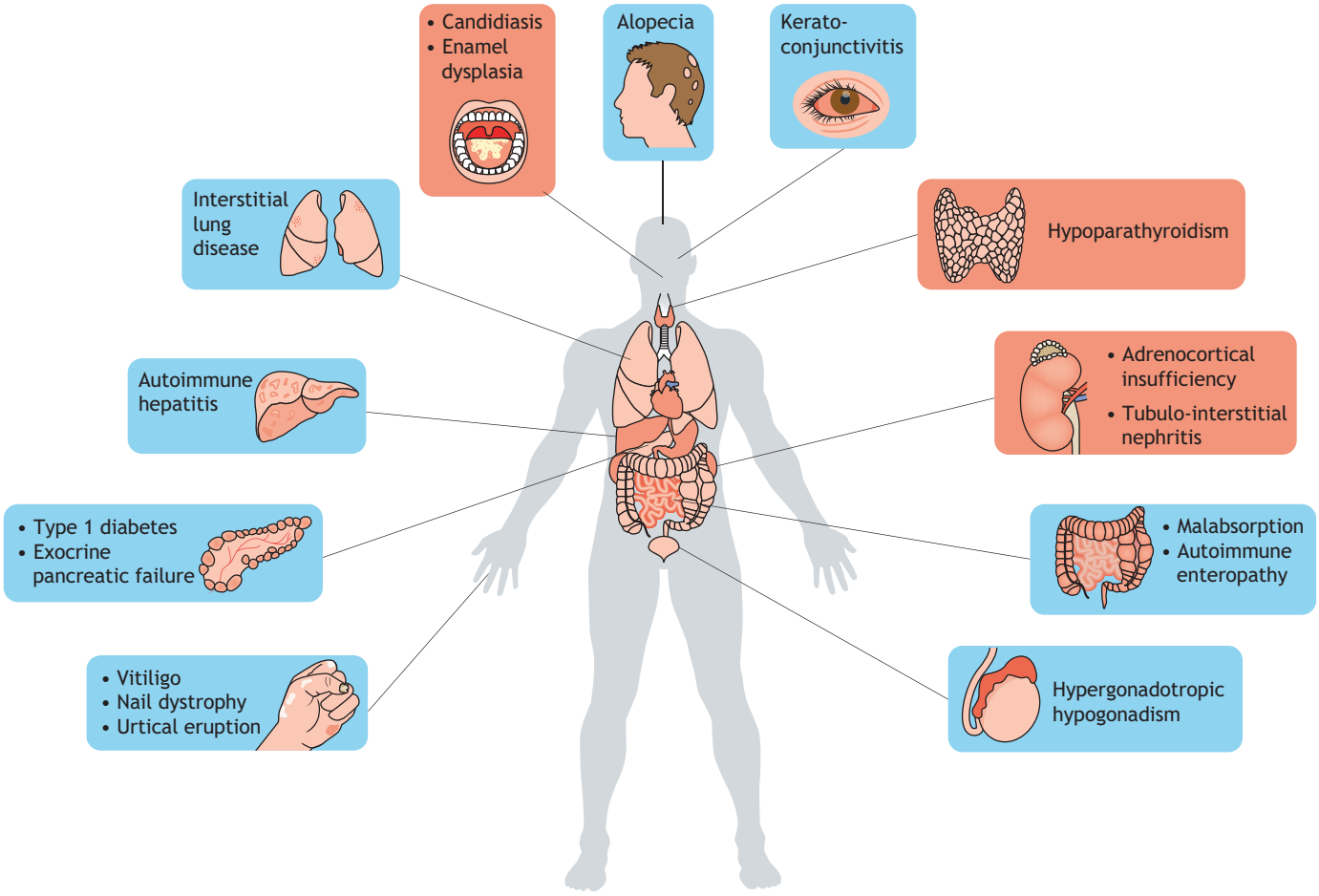

Fig. 1. Common symptoms of APECED. Representation of different manifestations usually observed in APECED patients, including the historical Whitaker's triad (candidiasis, hypoparathyroidism and adrenocortical insufficiency; red) and the symptoms that have been linked to APECED syndrome only recently (blue).

1:90,000–1:200,000 in most European countries (Ferre et al., 2016). However, this strongly increases within an isolated population, such as the Finnish (1:25,000) and Sardinian (1:14,000) or within that of Iranian Jews (1:9000), probably due to a historic founder-mutation effect, specifically the Arg257X, Arg139X and Tyr85Cys mutations (with X representing any amino acid), respectively (Ahonen et al., 1990; Rosatelli et al., 1998; Zlotogora and Shapiro, 1992).

AIRE mutations and APECED

To date, 145 *AIRE* mutations, including numerous mutant alleles, have been associated with APECED, from single-nucleotide mutations to large deletions across the gene's entire coding sequence. Although missense mutations of the gene seem to cluster preferentially in the exons that encode the CARD and PHD1 domains, there seems to be no such pattern for insertions or deletions (indels). Most *AIRE* mutations that are not indels occur in the CARD domain; however, the most prevalent mutation, p.R257*, is located in the SAND domain (Stolarski et al., 2006; Trebušak Podkrajšek et al., 2005). It was initially believed that all *AIRE* mutations lead to the autosomal recessive inheritance of APECED; but, recent studies identified dominant *AIRE* mutations in the SAND and PHD1 domains that induce a non-classic form of APECED. This form features very few, if not unique, milder autoimmune manifestations (Ahonen et al., 1990; Cetani et al., 2001; Oftedal et al., 2015), and its discovery suggests that dominant *AIRE* mutations play a previously unrecognized role in the induction of common organ-specific autoimmune disorders (Oftedal et al., 2015).

AIRE and thymic tolerance

As discussed in more detail below, mouse APECED models in which the *Aire* gene has been inactivated or knocked out revealed that AIRE is specifically expressed in mature medullary thymic epithelial cells (mTECs, see Boxes 1 and 2) of the thymus (Derbinski et al., 2001; Rosatelli et al., 1998). mTECs are characterized by high expression levels of class II major histocompatibility complex (MHC class II) molecules and of a wide array of self-antigens (Danan-Gotthold et al., 2016), which they present to developing thymocytes. In mTECs, AIRE controls the expression of thousands of tissue-restricted antigens (TRAs) that normally are only expressed in one or a few peripheral tissues (Kyewski and Klein, 2006). Although many functional aspects of AIRE remain unknown, it certainly is involved in release of RNA polymerase II pausing at promoters of AIRE-dependent genes (Giraud et al., 2014; 2012) and in recruitment of chromatin-remodeling factors that facilitate transcriptional elongation (Abramson et al., 2010). Additionally, AIRE-dependent gene expression is regulated through a post-transcriptional mechanism that shortens the 3′ untranslated region of AIRE target transcripts to increase their stability (Guyon et al., 2020).

Impaired expression of AIRE-dependent TRAs in mouse models of APECED impedes the negative selection of developing self-reactive thymocytes (Liston et al., 2003). This has been demonstrated in transgenic mice that have thymocytes harboring T-cell receptors (TCRs) specific to the self-antigen hen egg lysosome (HEL) under the control of the rat insulin promoter (RIP), a promoter that depends on

Box 2. Specific markers and function of TECs

The role of the thymus in establishing immunological tolerance is based on the functional selection of T cells, a process that is orchestrated by thymic epithelial cells (TECs) (Takahama, 2006). Whereas cortical thymic epithelial cells (cTECs) are involved in thymocyte lineage commitment and in the positive selection of T cells based on the recognition of peptides-MHC molecules (Klein et al., 2014; Takahama, 2006), medullary epithelial cells (mTECs) mediate the negative selection of autoreactive T cells based on the unique ability of mTECs, to express and present tissue-restricted antigens (TRAs) to developing T cells and to eliminate the autoreactive ones (Anderson et al., 2002; Klein et al., 2014; Stritesky et al., 2012). Early markers of cTEC and mTEC lineages include the cytokeratins KRT8 (K8) and KRT5 (K5), respectively (Sekai et al., 2014). Mature mTECs also highly express CD80, MHC-II molecules and the autoimmune regulator AIRE, and are characterized by expressing a high numbers of AIRE-induced TRAs (Gäbler et al., 2007; Sekai et al., 2014).

action of AIRE in mTECs (Liston et al., 2003). In contrast to *Aire*-KO mice that do not express HEL in mTECs, few HEL-specific T cells were retrieved from wild-type (WT) mice, showing that AIRE-dependent HEL expression resulted in depletion of T cells able to recognize HEL peptides (Liston et al., 2004; 2003). However, the role of AIRE in shaping immunological tolerance (Box 1) appears to rely not only on the clonal deletion of autoreactive thymocytes but also on the generation of regulatory T cells (Tregs; see Box 1) (Yang et al., 2015). In addition, AIRE is also involved in the mechanisms that enable Tregs to suppress autoimmune manifestations in the periphery of the immune system (Aricha et al., 2011; Teh et al., 2010). These findings show that AIRE plays a key role in the establishment of immunological tolerance, by promoting the negative selection of developing autoreactive thymocytes and by generating Tregs that efficiently suppress autoreactive responses elicited by autoreactive T cells in their periphery. These findings have implications on how to treat APECED patients.

Current standard of care for APECED patients

Currently, APECED patients receive a combination of treatments tailored to their individual clinical profile. CMC is the most common clinical feature; it requires daily oral medication and close monitoring to avoid chronic *Candida* spp. infection, as it can lead to the development of oral squamous cell carcinoma (Böckle et al., 2010). Normally, CMC is treated with antifungal drugs such as fluconazole, topical ketonazole or amphotericin B for azole-resistant forms (Constantine and Lionakis, 2019; Humbert et al., 2018). APECED patients might also receive hormone replacement therapies comprising synthetic thyroid hormones, mineralo-corticoids, hydrocortisone or sex steroids (Jankowska, 2017; Napier and Pearce, 2012; Winer et al., 2008; Yeap et al., 2016) to treat hormone deficiencies resulting from HP, AD and/or gonadic failure (Box 1). Symptoms that are linked to an excessive response of autoreactive T cells, like autoimmune hepatitis, tubulo-interstitial nephritis or autoimmune enteropathy, are treated with immunosuppressants, such as azathioprine, mycophenolate or corticosteroids (Gentile et al., 2012; Manns et al., 2010; Ulinski et al., 2006). However, the long-term use of immunosuppressive drugs causes significant and unavoidable adverse reactions that can have life-long deleterious effects. For example, corticosteroid therapy in young APECED patients slows their growth and delays puberty (De Leonibus et al., 2016; Polito and Di Toro, 1992). In addition, immune inhibition caused by corticosteroid therapy in children and adults increases their susceptibility to infections – a significant issue in patients already prone to CMC. Hence, there is a profound need to develop more-targeted therapeutics to treat this disease. Recently, rituximab immunotherapy has been used with relative success to treat pneumonitis in the context of APECED; it leads to a clinical improvement without affecting the production of autoantibodies against potassium channel regulatory protein (KCNRG) (Ferré et al., 2019). Nevertheless, as APECED patients are still at risk of premature death (Borchers et al., 2020), their management is very complex and requires the collaboration of numerous specialists, such as dentists, dermatologists, endocrinologists and pediatricians.

The first significant step to improve our knowledge on the APECED syndrome and to evaluate the efficacy of new therapies was achieved only 20 years ago, when scientists generated the first rodent model of AIRE deficiency. We describe its details below.

Preclinical rodent models of APECED

To study the role of AIRE in the establishment and/or maintenance of immunological tolerance, several rodent models of APECED disease were generated by inactivating *Aire* in mice and rats. Here, we summarize all existing preclinical models of APECED, highlighting their strengths and limitations in relation to human APECED pathology. These models can be used in parrallel to study the heterogeneity and mechanisms underlying the APECED syndrome caused by different known human mutations.

Mouse APECED models: their strengths and limitations

The first available mouse models of APECED syndrome were generated from various mouse strains and genetic backgrounds (summarized in Table 1 and Fig. 2) using two main approaches: 1) engineering genetic mutations found in human APECED patients into the murine *Aire* locus and, 2) using exon targeting to delete exons that encode functional domains of Aire (Fig. 2B). The first APECED mouse, which we call model 1, was generated in the Peltonnen lab based on a mutation commonly found in Finnish APECED patients (Ramsey et al., 2002). This mutation corresponds to a cytosine→thymine nucleotide transition at position 889 (C→T, 889) that causes a premature stop codon, thereby truncating exon 6 of the human *AIRE* (Björses et al., 1998). To mimic this mutation, Peltonnen and colleagues designed a construct that targeted exon 6 through homologous recombination, leading to the insertion of a neomycin cassette at the beginning of exon 6 (Ramsey et al., 2002). The APECED mouse model 2, generated by the Mathis lab, uses a shorter *Aire* transcript in which the premature truncation of exon 1 caused the deletion of exon 2 and of some of the upstream and downstream introns, leading to a non-functional AIRE protein (Anderson et al., 2002). The APECED mouse model 3, generated in the Matsumoto lab, was also designed independently of any known human mutation. In this model, a neomycin cassette replaced exon 5 to exon 12 of the *Aire* locus, thus yielding a truncated AIRE protein that lacks a large segment of its functional domain (Kuroda et al., 2005). However, APECED mouse model 4 – containing a common human APECED-associated mutation found in the Anglo-American population (Hubert et al., 2009) – was generated in the Scott lab (Heino et al., 2001), comprising a 13 bp deletion in exon 8 (967–979), which disrupts the PHD1 domain of the protein.

The *Aire*-deficient mice described above have a range of infertility problems but present with normal weight and size compared with their littermates, both postnatally and at an age of ∼2–3 months (Anderson et al., 2002; Hubert et al., 2009; Kuroda et al., 2005; Ramsey et al., 2002). Most of their immunological traits, such as T cell proliferation, cytokine production, CD4:CD8 ratio, thymocyte

Table 1 . Overview of rodent APECED models

	Mouse											Rat
	Model 1 (Peltonnen lab)	**Model 2** (Mathis lab)						**Model 3** (Matsumoto lab)		**Model 4** (Scott lab)	**Model 5** (Anderson lab)		**Model 6** (Guillonneau lab)
Mutation in model	Premature stop codon in exon 6 (C→T, 889)	Deletion of exon 2 and portions of the upstream and downstream introns, causing the premature truncation of the protein shortly after exon 1						Replacement of exons 5–12 with a neomycin cassette, leading to formation of truncated AIRE protein		13 bp deletion within exon 8 (967-979)	Gly228Trp point mutation (G→T, 809 in exon 6)		17 bp deletion in exon 3
Corresponding human mutation	p.R257X (Finnish population 1:250, northern Italian and German population)	NA						NA		c.1094_1106del, p.L323fsX373 (Anglo-American population)	Gly228Trp autosomal dominant mutation (Italian population)		R139X (common in Sardinian patients)
Affected functional domain	PHD1, PHD2	CARD						PHD1, PHD2, SAND		PHD1	SAND		NLS
ESC strain	J129	Sv129						TT2		C57BL/6J (B6)	129/ola and Sv/129		NA
Mouse/rat strain	C57BL/6J (B6)	C57BL/6J (B6)	NOD and BALBc	C57BL/6J (B6)	BALB/cJ	NOD/LtJ	SJL/J	C57BL/6J (B6) and BALBc/J	NOD/Shi Jic	C57BL/6J (B6)	C57BL/6J (B6)	NOD	Brown Norway, Sprague Dawley, Lewis.1A
Phenotype	Infertility, sometimes associated with testicular and ovarian atrophies Autoimmune hepatitis Atrophy of the thymus/adrenal gland/reproductive organs Absence of adrenal glands	Infertility Retinal degeneration						Infertility Gastritis	Weight loss Infertility Pancreas atrophy	Male infertility Uveoretinitis Autoimmune uveitis Vitritis		Diabetes mellitus Insulitis Neuropathy (sciatic nerve) Thyroiditis	Infertility Pancreas and thymus early involution Nail hypertrophy Vitiligo Alopecia
	Lymphocytic infiltration	**Lymphocytic infiltration**						**Lymphocytic infiltration**			**Lymphocytic infiltration**		**Lymphocytic infiltration**
	Liver Testis Ovary Pancreas	Stomach Ovary Pancreas Thyroid Retina	Lung Prostate Eyes Salivary glands	Lung Prostate Ovary Eyes Stomach (gastritis) Salivary gland	Prostate Ovary Pancreas (pancreatitis) Thyroid (thyroiditis) Eyes Stomach Salivary gland Lung Liver	Stomach Eyes Salivary gland Lung Liver Prostate Ovary Pancreas (pancreatitis) Thyroid	Stomach Salivary gland Lung Liver Prostate Ovary Pancreas	Lachrymal gland Parotid glands Submandibular gland Stomach Pancreas	Pancreas (acinar cells) Liver Lung Salivary gland Thyroid Prostate	Salivary gland Lacrimal gland Parotid gland	Lacrimal gland Salivary glands	Lacrimal gland Salivary gland Eye/retina Exocrine Pancreas Stomach Lung	Testis Lung Pancreas Liver Kidney Skin Stomach
Organ-specific antibodies	Anti-spermatids (testis) Anti-pancreas Anti-hepatocytes (liver) Anti-GAD (pancreas) Anti-AADC (pancreas) Anti-adrenocortical (adrenal gland)	Anti-retina layer cells (epithelium, rod and cones) Anti-oocytes Anti-parietal layer cells	Anti-mucin 6	Anti-ovary Anti-eyes Anti-salivary gland Anti-stomach	Anti-eyes Anti-stomach	Anti-eyes Anti-pancreas Anti-stomach Anti-ovary		Anti-α fodrin (actin-binding protein) Anti-gastric mucosa	Anti-PDIp (acinar cells)	Anti-pancreas Anti-testis Anti-lung Anti-liver Anti-stomach	ND		Anti-hepatocytes Anti-pancreas Anti-intestines Anti-kidney Anti-liver Anti-testis Anti-adrenal gland Anti-thyroid Anti-Tgm4 (prostate antigen) Anti-Vegp2 (salivary gland antigen)
Cytokine-specific antibodies	NA	NA	NA	NA				NA	NA	Anti-IFNα2a Anti-IL-17 Anti-IL-22	NA		Anti-IFNω Anti-IFNα4 and Anti-IFNα11 Anti-IL17A and Anti-IL17F Anti-IL22
References	Ramsey et al., 2002	Anderson et al., 2002	Gavanescu et al., 2007	Jiang et al., 2005				Kuroda et al., 2005	Niki, 2006	Hubert et al., 2009; Kärner et al., 2013	Su et al., 2008		Ossart et al., 2018

NA, not applicable; ND, not determined; GAD, glutamate decarboxylase; AADC, aromatic L-amino acid decarboxylase; PDIp, protein-disulfide isomerase pancreas specific.

Disease Models & Mechanisms (2021) 14, dmm046359. doi:10.1242/dmm.046359

Disease Models & Mechanisms (2021) 14, dmm046359. doi:10.1242/dmm.046359

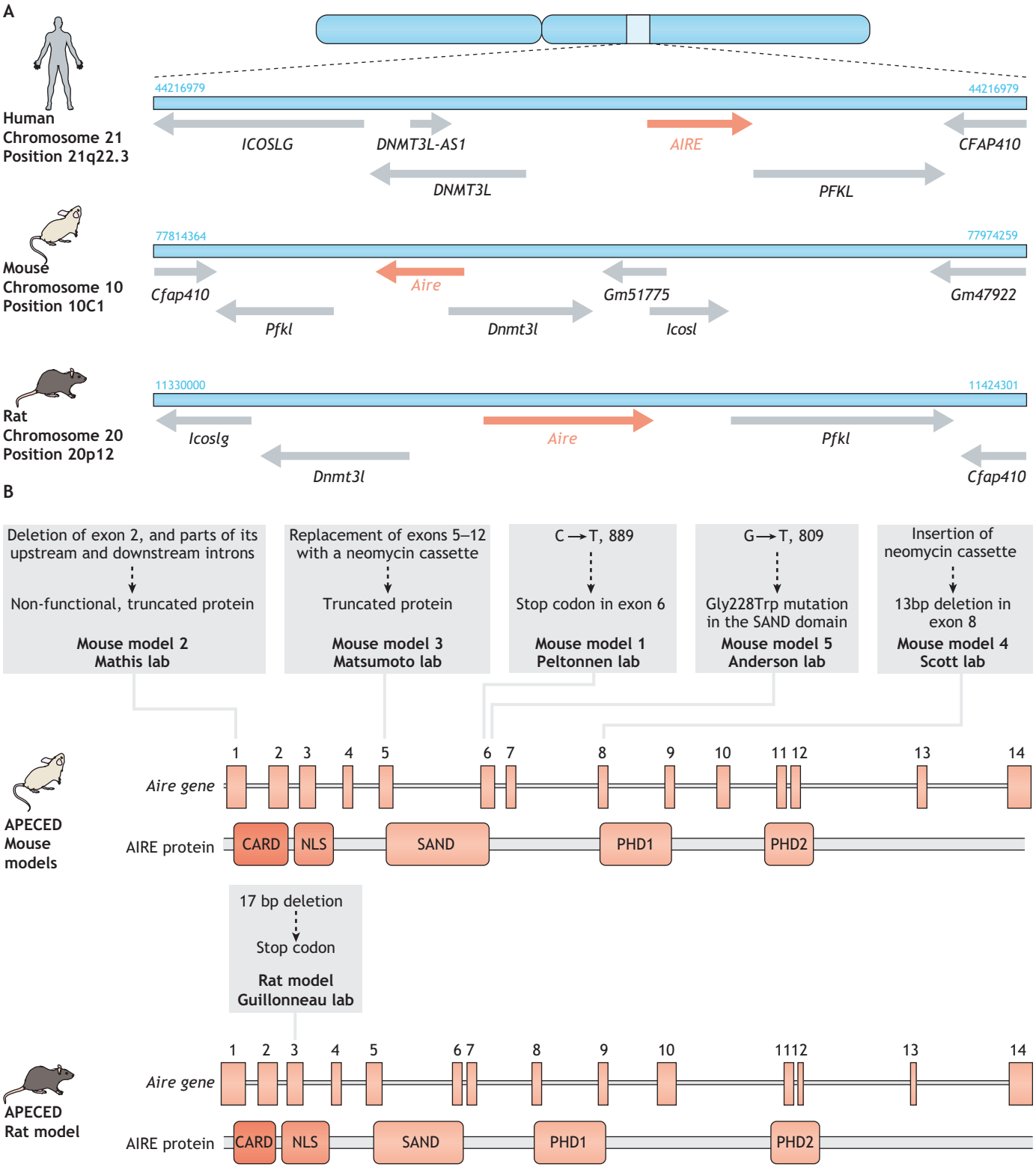

Fig. 2. Comparison of the *AIRE*/*Aire* locus in human, mouse and rat, and strategies to generate APECED rodent models. (A) Schematic representation of *AIRE*/*Aire* locus organization in human, mouse and rat, showing the different genetic contexts. (B) Summary of the strategies used to develop APECED mouse and rat models, providing the location of the genetic editing and its consequence for the Aire protein.

and lymphocyte numbers, expression of differentiation markers, and *in vitro* antigen presentation appear to be normal at birth and up to early adulthood. This is except mouse model 2 (Mathis lab); mice of this model present with increased numbers of activated/memory T cells ($CD44^{high}CD62L^{low}$) in peripheral lymphoid organs at the age of ∼2–3 months (Anderson et al., 2002). An increased number of mTECs was also observed in mice of models 1 and 4 at the age of ∼2–3 months (Anderson et al., 2002; Hubert et al., 2009). In models

2, 3 and 4, absence of AIRE is also associated with the loss or significantly reduced expression of several autoantigen genes, thus impairing the negative selection of autoreactive T cells usually mediated by AIRE in the thymus (Anderson et al., 2002; Derbinski et al., 2001; Kuroda et al., 2005; Niki, 2006; Su et al., 2008).

All these mouse APECED models display age-dependent organ lymphocytic infiltration, with variation in the targeted tissues possibly due to environmental factors and genetic backgrounds, as the original APECED mouse models 2 and 3 were back-crossed onto several different genetic backgrounds (Anderson et al., 2002; Gavanescu et al., 2007; Jiang et al., 2005; Kuroda et al., 2005; Niki, 2006). Numerous serum antibodies against different tissues were detected in early adulthood in most *Aire*-deficient mouse models, and the number and frequency of these antibodies progressively increases with age (Anderson et al., 2002; Hubert et al., 2009; Jiang et al., 2005; Kuroda et al., 2005).

Experiments involving thymic chimeras demonstrated that thymocytes derived from *Aire*-deficient mice are autoreactive and can transfer the autoimmune disease when transplanted to immuno-deficient recipients (Anderson et al., 2002; Kuroda et al., 2005). Initially, the number of Tregs (Box 1) and their function seemed to be normal in APECED mouse models 1, 2, 3 and 4, suggesting that only the overproduction of autoreactive T cells induces autoimmune manifestations (Kuroda et al., 2005). However, subsequent studies revealed that *Aire* deficiency also affects the function of Tregs. Indeed, an analysis of the T cell receptor (TCR; Box 1) repertoire of Tregs ($CD4^+Foxp3^+$ and $CD8^+CD28^{low}$) provided molecular evidence that AIRE is potentially involved in shaping the TCR repertoire of Tregs (Malchow et al., 2013a, 2016; Pomié et al., 2011). Moreover, a comparative analysis of $CD8^+CD28^{low}$ Tregs from WT and APECED model 4 mice (Hubert et al., 2009) revealed that, despite equal representation and similar immunosuppressive activity, the $CD8^+CD28^{low}$ Tregs from *Aire*-KO animals fail to control the onset of colitis when using adoptive cell transfer (ACT) in vivo together with colitogenic cells, a phenotypic feature of APECED patients (Pomié et al., 2011) – which is in contrast to $CD8^+CD28^{low}$ Tregs from WT mice.

Another mouse APECED model, hereafter, referred to as model 5, was developed in the Anderson lab (Su et al., 2008) (Table 1) and is based on an autosomal dominant mutation found in Italian patients, who show a heterozygous base substitution at position 809 of the cDNA sequence (G→T, 809 in exon 6) (Cetani et al., 2001). This nucleotide change leads to replacement of amino acid (aa) glycine with tryptophan at position 228 (Gly228Trp) in the SAND domain of human AIRE. Mice in model 5 present with autosomal dominant autoimmunity and a spectrum of disease manifestations that are different compared to those observed in the other mouse APECED models discussed above. This is because the AIRE protein carrying the Gly228Trp mutation appears to exert a dominant-negative effect that prevents WT AIRE protein to reach active transcription sites in mTECs (Su et al., 2008).

Despite the insights these mouse models provided regarding etiology and pathology of APECED, significant phenotypic and clinical differences exist between *Aire*-deficient mice and human APECED patients. For example, no animal of the APECED mouse models described here displayed the most common, visible autoimmune and ectodermal manifestations of APECED, i.e. CMC, HP and vitiligo – not even those of mouse models bred onto the non-obese diabetic (NOD) genetic background that exhibited a more severe autoimmune phenotype (Gavanescu et al., 2007; Jiang et al., 2005; Niki, 2006; Su et al., 2008). In addition, none of these models had autoantibodies directed against cytokines, such as type I IFNs, IL-22 and IL-17, which are commonly detected in APECED patients. However, a recent study reported that the APECED mouse model 4 (Hubert et al., 2009; Table 1) does have IFNα2a, IL-17 and IL-22-neutralizing autoantibodies (Kärner et al., 2013); and, whereas APECED remains a life-threatening autoimmune disease in humans, *Aire*-deficient mice have a life expectancy that matches that of their WT littermates, despite their organ-specific autoimmunity.

As such, none of these mouse APECED models have been able to recapitulate the severe clinical features seen in APECED patients. They have, nevertheless, provided important insights into the functional relationship between *Aire* and the cellular and molecular pathogenic mechanisms of this disease, enabling the function of AIRE to be investigated in the selection process of T cells and in the establishment of immunological tolerance. All the previously described AIRE-deficient mouse models also played an important role in understanding the role of AIRE in central immune tolerance. However, for proper clinical studies, there is still a need for an animal model that explicitly displays the phenotypical traits of APECED patient. In 2018, a potentially accurate rat model of the disease was designed in the Guillonneau lab (Ossart et al., 2018). The following section presents the strengths and limitations of this APECED rat model.

The rat model of APECED: strengths and limitations

As Fig. 2A shows, although organization of the *Aire* locus is similar in humans and rats, the murine *Aire* locus overlaps with another gene. As such, disrupting *Aire* in rats might more faithfully recapitulate the clinical features of APECED patients. To the best of our knowledge, only one *Aire*-deficient rat model exists, generated by our own group (Ossart et al., 2018) (Table 1). It was generated by targeting exon 3, which encodes the nuclear localization signal (NLS) sequence of *Aire*, to induce a 17 bp deletion that mimics the human Arg139X mutation commonly found in Sardinian APECED patients (Rosatelli et al., 1998). This mutation leads to an early stop codon, resulting in the premature termination of AIRE translation and reproduces in rats many of the main human characteristics of the APECED syndrome (Ossart et al., 2018). Three lines of these rats were generated by back-crossing the founder *Aire*-deficient Brown Norway rats with WT Sprague-Dawley or Lewis rats for several generations (Table 1). Despite some insignificant differences in terms of symptom severity, the overall phenotype of the rats was similar between each strain (Ossart et al., 2018). This observation supports the hypothesis that the consequences of *Aire* deficiency do not primarily depend on the genetic background but probably more on the layout of the *Aire* locus.

At approximately 6 months of age, animals of all *Aire*-deficient rat strains start to develop skin disorders, including patchy hair loss suggestive of alopecia, depigmentation (vitiligo), and nail overgrowth (nail dystrophy) – symptoms that are frequently seen in APECED patients (Collins et al., 2006). Moreover, several organs, including liver and kidney, show extensive lymphocytic infiltration in all strains of *Aire*-deficient rats, correlating with increased serum levels of alkaline phosphatase and creatinine, respectively (Ferre et al., 2016; Orlova et al., 2017). Both male and female *Aire*-deficient rats show reproductive defects, even when mated with WT animals, and even though testes and ovaries appear to be anatomically normal, thus recapitulating the fertility problems observed in APECED patients (Christin-Maitre et al., 1998; Schaller et al., 2008). In addition, exocrine pancreatic tissue destruction, a major clinical complication in some APECED patients, is a highly prevalent phenotype seen in >90% of *Aire*-

deficient rats (Perheentupa, 2006). Overall, histological analyses have revealed that 79% of *Aire*-deficient rats exhibit pancreatic fat accumulation, a decrease in acini, intralobular focal lymphocyte infiltration and hyperplasia of the islets of Langerhans (Ossart et al., 2018). However, glucose blood levels remain normal and they do not develop diabetes, in contrast to APECED patients (Paquette et al., 2010).

Thymopoiesis does occur in *Aire*-deficient rats, with the number and proportion of immune cells being similar to those in WT animals; an exception being decreased numbers of plasmacytoid dendritic cells and natural killer T cells, and increased numbers of effector T cells (Ossart et al., 2018). Transcriptomic comparisons of the thymus between *Aire*-deficient and WT rats and mice demonstrated that, in rats, AIRE does not regulate the expression of the same set of self-antigen genes, possibly explaining the difference in auto-reactivity observed between rodents (Ossart et al., 2018). Additionally, Fezf2 – another key factor involved in inducing the expression of TRAs in mTECs and potentially involved in the establishment of negative selection – is downregulated in the thymus of *Aire*-deficient rats but not in that of *Aire*-deficient mice (Takaba et al., 2015). This suggests that *Aire* deficiency decreases the complexity of the self-antigen repertoire presented in the rat thymus, resulting in the increased escape of autoreactive T cells and a larger array of autoimmune manifestations.

Aire-deficient rats also produce a large panel of autoantibodies against several antigens, including those found in the kidney, liver, testis, intestines, adrenal gland and pancreas (Ossart et al., 2018). As in humans, we found no correlation between the titers of these autoantibodies and the severity of the associated symptoms; as such, their importance in the etiology and pathology of APECED remains to be clearly established. Studies in *Aire*-deficient mice have reported the opposite result (DeVoss et al., 2008; Gavanescu et al., 2008), possibly due to the fact that the autoantibody repertoire in mice strongly differs from that of humans suffering from APECED (Pöntynen et al., 2006). In particular, APECED-specific autoantibodies, such as anti-IFNω, anti-IL-17 and anti-IL-22, are not found in most of *Aire*-deficient mouse models, except in model 4 (Kärner et al., 2013), but their levels in *Aire*-deficient rats are comparable to those in APECED patients (Ossart et al., 2018). This absence of spontaneous specific autoantibody production in mouse models of *Aire* deficiency further suggests that the immunopathological mechanisms that occur in these mouse models differ from those of the rat model and of APECED patients. Thus, the *Aire*-deficient rat seems to be an appropriate animal model in which to study autoantibodies in the context of APECED.

Although the rat model of *Aire* deficiency recapitulates many features of the APECED syndrome, the Whitaker's triad of symptoms remains to be observed in these animals. Whether those disparities are linked to *Aire* itself is still unknown. One hypothesis explaining the phenotypic differences between *Aire*-deficient mice and rats, and humans suffering from APECED states that each species has its own specificity in terms of immune system components, such as cytokines, complement system, B cell- and T cell-signaling pathways, γδ T cells, Th1/Th2 differentiation, etc (Mestas and Hughes, 2004). One particular example is that humans produce four subclasses of immunoglobulin G (IgG), i.e. IgG1, IgG2, IgG3 and IgG4, which have no direct homologues in mice and rats. Mice also lack expression of some Fc receptors (FcRs), such as FcαRI, FcγRIIA and FcrγRIIC, all of which play a crucial role in the immune response as they establish a link between adaptive immune cells that produce Igs and innate cells that express FcRs (Bruhns, 2012). Altogether, small divergences might be compounded by the central immune defect due to AIRE deficiency and result, *in fine*, in different phenotypes.

Mice have been extensively investigated for immunological research during the last decades, while the use of rat models for immunology-related investigation is more recent and, still, less frequent. As a consequence, most available techniques and tools are not tailored to rats. Despite this, rat models appear to be very useful as they better represent a number of human diseases, such as Duchenne muscular dystrophy (Ouisse et al., 2019) and, currently, the rat model is the most appropriate for preclinical studies of APECED. We foresee that *Aire*-deficient rat models will also benefit fundamental immunology studies regarding mechanisms of action of AIRE; particularly, because higher numbers of primary mTECs can be obtained from *Aire*-deficient rats as compared with *Aire*-deficient mice, as the availability of these cells is a limiting factor in *ex vivo* experiments. In combination with animal models, these *ex vivo* experiments – which are discussed in more detail below – are a great asset to study thymic mechanisms under pathological conditions.

Ex vivo models to assess mTEC function

Although animal models of APECED are invaluable to understand the events that link AIRE to the negative selection of autoreactive thymocytes and the selection of Tregs, we also need new models to gain further insights into the molecular mechanisms that underlie the mode of action of AIRE. As a result, *ex vivo* models, showing AIRE-mediated induction of TRAs and the impact AIRE has on T cell development, have been generated to investigate such mechanisms. Since primary TECs (see Box 2, Specific markers and function of TECs) die rapidly in standard culture systems *ex vivo*, TEC lines were initially used as *in vitro* systems in which to study induction of gene expression through AIRE. Although these TEC lines provided key findings (Abramson et al., 2010; Giraud et al., 2014), they also have several major limitations, including loss of *AIRE* expression, which has to be restored by transfecting these cells with an *AIRE* expression vector. To model induction of gene expression through AIRE in a more physiologically relevant manner, *ex vivo* models have been set up by using primary TECs in settings that better mimic the complex environment of the thymus, which keeps TECs alive and functional.

To date, only a few *ex vivo* culture systems of primary TECs in a 3D network have been established (Pinto et al., 2013; Villegas et al., 2018). In contrast to previously described two-dimensional (2D) models of TEC cultures (Bonfanti et al., 2010; Kont et al., 2008; Mohtashami and Zúñiga-Pflücker, 2006; Palumbo et al., 2006), 3D culture models preserve mTEC lineage functions, and the cells express TRAs under the control of AIRE and other transcription factors.

3D organotypic co-culture

Primary TECs show various biological similarities to keratinocytes in the skin (see Box 3, TECs and keratinocytes). As such, an *ex vivo* 3D organotypic co-culture (OTC) system that supports TEC survival and expansion has been developed, which draws on an *in vitro* model of skin development (Boehnke et al., 2007; Stark et al., 2006). The maturation process of both TECs and keratinocytes depends on their close interaction with stromal cells, such as fibroblasts, and on a 3D structural network of extracellular molecules – the extracellular matrix (ECM) (Depreter et al., 2008; He et al., 2002; Hunziker et al., 2011; Jenkinson et al., 2003; Ulyanchenko et al., 2016). The 3D OTC model mimics dermal tissue by using dermal fibroblasts that are embedded in an inert, semi-solid matrix of insoluble fibrin strands to mimic the ECM

Disease Models & Mechanisms (2021) 14, dmm046359. doi:10.1242/dmm.046359

Box 3. TECs and keratinocytes

Keratinocytes (skin cells) and TECs share many biological similarities (Petrie and Zúñiga-Pflücker, 2007). Indeed, TECs are organized into a 3D network that is crucial for the homeostatic maintenance of the thymic microenvironment and provide an excellent support for the education and maturation of functional thymocytes (Gordon and Manley, 2011). Keratinocytes form a multi-layer, tightly connected sheet that forms the outermost protective layer of the skin (Simpson et al., 2011). Both keratinocytes and TECs express the transcription factor FOXN1, which is necessary for their development and functional integrity (Baxter and Brissette, 2002; Bleul et al., 2006; Gordon and Manley, 2011; Nehls et al., 1996). In the thymus, FOXN1 is required to induce differentiation of both cTECs and mTECs (Gordon and Manley, 2011). In the epidermis, FOXN1 plays an important regulatory role in the development and homeostasis of keratinocytes, and their function in wound healing (Bukowska et al., 2018). Keratinocytes and TECs also express a set of similar cytokeratins (Bonfanti et al., 2010; Cabral et al., 2001; Langbein et al., 2003; Sekai et al., 2014) and differentiation factors, and their progenitors share similar markers, such as PLET-1, RAC1 and SMAD7, which play very important roles in the differentiation of these cells into specific subsets (Depreter et al., 2008; He et al., 2002; Hunziker et al., 2011).

(Fig. 3). The addition of TGF-β to this model induces the activation and proliferation of the dermal fibroblasts. Purified mature AIRE-positive mTECs extracted from young (4–6 weeks-old) mice are then seeded onto this matrix within a specific medium that contains the RANK ligand (RankL) (Fig. 3) – reportedly an essential factor for the terminal differentiation of AIRE-positive mTECs (Akiyama et al., 2008; Hikosaka et al., 2008; Rossi et al., 2007). The 3D matrix enables activated fibroblasts to secrete a number of key factors that establish a complex ECM (Fig. 3), which is key for mTEC integrity in this culture model (Boehnke et al., 2007; Stark et al., 2004). In this way, the OTC model preserves key features of mTEC function, such as expression of AIRE and its dependent TRAs, and has, therefore, been instrumental in the identification of the molecular mechanisms that underlie mTEC developmental features, such as the key differences between immature and mature mTECs, as reported for the intact thymus (Pinto et al., 2013). This model could also be used to identify the precise molecular mechanisms that underlie AIRE-dependent expression of TRAs.

However, although the OTC model provides an optimal environment for *ex vivo* TEC culture, its 3D organization might not be a perfect match for the thymus – it is still a model that sustains viable TECs for ∼1 week.

Human thymus-derived cell culture

A culture model was designed to allow the expansion of functional TECs from human thymic explants and to address a key problem of earlier versions of this type of model. Here, successive rounds of enzymatic digestion to isolate TECs from other types of thymic cell population (Fernández et al., 1994; Patel et al., 1995; Röpke, 1997; Skogberg et al., 2015) affected the expression of TEC surface molecules and impaired the viability of the cells (Autengruber et al., 2012; Shichkin et al., 2017). In contrast to these earlier approaches, the model reported by Villegas et al. involves an efficient, enzyme-free procedure that enables human primary mTECs to be extracted and, subsequently, expanded from fresh thymic explants (Villegas et al., 2018). Fresh thymic fragments were obtained from immunologically normal human babies (aged 2 days to 1 year) undergoing corrective cardiovascular surgery. Those thymic fragments were cultivated in a medium that supports the migration of various types of thymic cell population (Nancy and Berrih-Aknin, 2005; Nazzal et al., 2014; Wakkach et al., 1996), and the eventual migration and expansion of TECs around the explant. This expansion model was maintained for a few days and the functional properties of mTECs were assessed through expression of AIRE and of AIRE-dependent TRAs. The results of these studies show that the human-derived mTECs of this model retain their ability to secrete important signaling molecules, such as cytokines, chemokines and growth factors, that are essential for the differentiation and maturation of T cell subsets (Cowan et al., 2016; Hauri-Hohl et al., 2014; Kimura and Kishimoto, 2010; Kondo et al., 2019; Lkhagvasuren et al., 2013).

The human thymus-derived culture system is a short-term model that cannot be expanded beyond 7–8 days, which limits the types of study that can be performed (Villegas et al., 2018). Although *ex vivo* models of mTEC culture are a great way to assess mTEC function, they are also dependent on the availability of primary human thymic tissues. Organoid and stem cell-derived models might, therefore, be better suited to expand mTEC differentiation and functional TEC studies.

Organoids and stem cell-derived models

Thymic organoids are the next step towards a more realistic thymic model that would enable us to study the signals that trigger mTEC differentiation into their mature AIRE-positive state and to carry out T cell differentiation *ex vivo*. A 3D thymic organoid model would need to mimic the thymic microenvironment and have different types of cell population interacting within the ECM that, as discussed above, plays a key role in the survival and development of a thymic cell population. Significant progress in ECM modelling has recently been made using artificial ECMs (Seet et al., 2017) and decellularized tissues (Fan et al., 2015; Hun et al., 2017), which can support the generation of functional T cells *ex vivo* and are expected to greatly benefit research on stem cell-derived thymic models (Seet et al., 2017). Since induced pluripotent stem cells (iPSCs; Box 1) were first developed (Takahashi and Yamanaka, 2006), there has been growing interest in differentiating these cells into functional thymic tissue. Indeed, iPSCs are crucial to develop models with which to study the ontogeny and function of rare types of cell population, like mTECs, which are difficult to isolate and expand *ex vivo*. iPSC-derived cells also have the inherent capacity to harbor genetic diversity, an essential capacity for research in immunology. A key goal of APECED research is to derive iPSCs from the somatic cells of patients and then use gene editing to correct their endogenous *AIRE* gene mutations. The gene-edited iPSCs could then be differentiated into functional mTECs that express the restored AIRE protein and all the AIRE-dependent and -independent TRAs. This approach could result in promising clinical applications, notably cell therapies, where corrected syngeneic mTECs are transplanted to restore the functionality of thymic tissue.

A first step toward this goal has been achieved with the differentiation of mouse embryonic stem cells (ESCs) into $EpCAM^{+}K5^{+}K8^{+}$ TEC-like cells (Lai and Jin, 2009; Parent et al., 2013; Su et al., 2015), using a 14-day differentiation strategy (see Box 4). Here, two key markers of thymic lineage commitment, *FOXN1* and *HOXA3*, were expressed at similar levels in the resulting cells. After their transplantation into nude recipient mice, these ESC-derived TEC-like cells restored proper thymic organization, as evidenced by the formation of typical medullary and cortical structures. An increase in functional peripheral T cells was also observed, indicative of the transplanted differentiated cells showing normal thymic activity. TECs have also been differentiated from

Disease Models & Mechanisms (2021) 14, dmm046359. doi:10.1242/dmm.046359

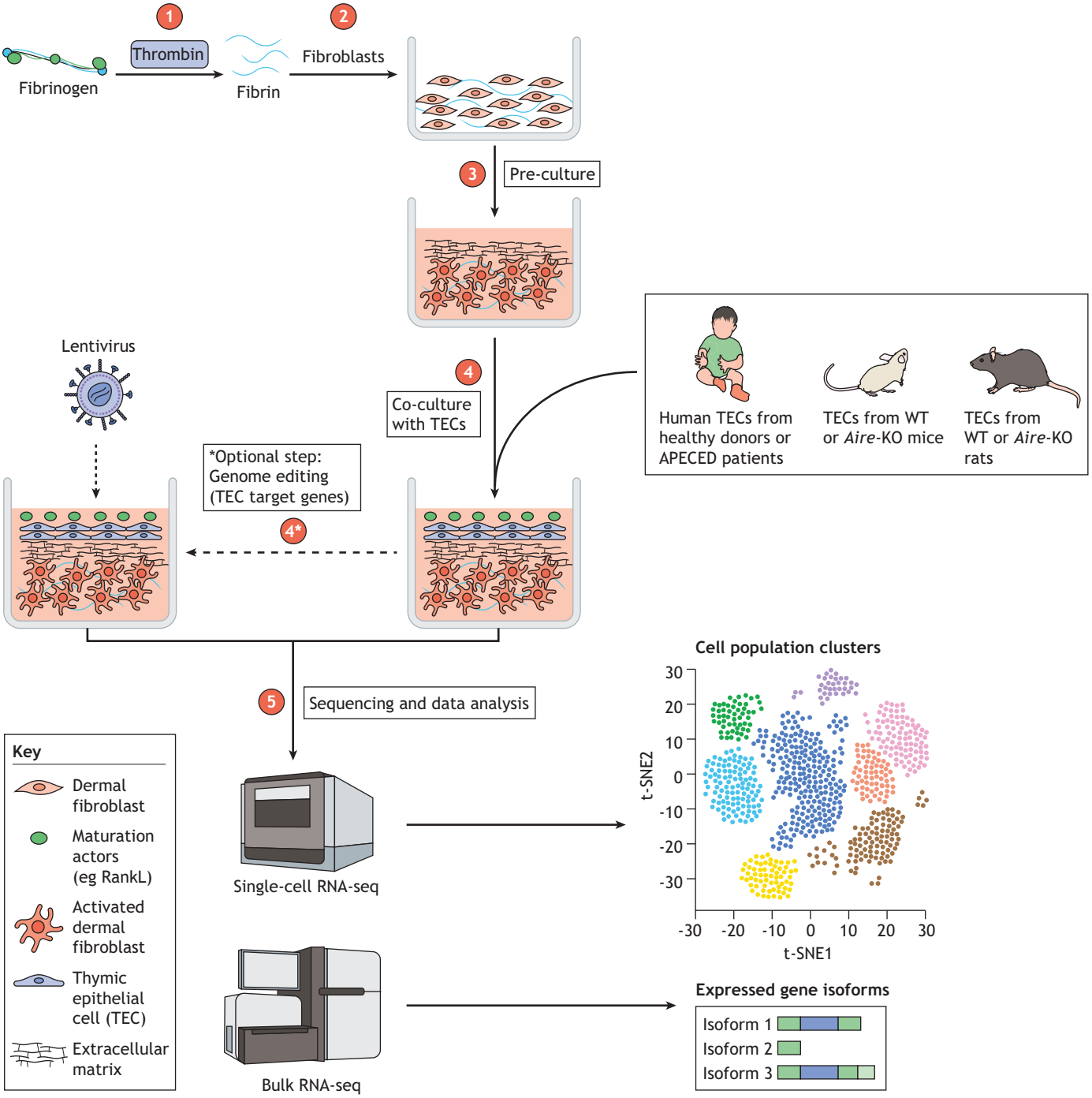

Fig. 3. TEC 3D organotypic co-culture model. (1) The scaffold of this tissue culture setup is the association of soluble fibrinogen polymerizing into insoluble strands of fibrin through the action of thrombin. (2) Dermal fibroblasts are added to fibrin strands. (3) A few days of pre-culture are required to activate the fibroblasts and to allow them to produce a unique extracellular matrix that is suitable for epithelial cell culture. (4) Freshly extracted thymic epithelial cells (TECs) from different species can be added to the culture together with certain maturation factors, such as the Rank ligand (RankL), which is key for the maintenance of mature and functional TECs. (4*) An optional, additional next step is lentiviral-based gene therapy or gene editing to correct *AIRE* deficiency or to knock down the expression of specific genes relevant to the particular APECED research question. (5) This model can also be used to perform sequencing experiments (bulk or single-cell RNA-seq) to analyze *AIRE*-dependent gene expression or to characterize TEC heterogeneity.

human iPSCs, with comparable results (Chhatta et al., 2019; Inami et al., 2011; Sun et al., 2013). More recently, the transplantation of reaggregated differentiated mouse iPSCs into nude recipient mice was shown to promote the tolerance of skin grafts and the generation of functional T cells (Otsuka et al., 2020). However, several challenges remain that hinder further refinements to this approach. First, the differentiation efficiency achieved by these culturing protocols remains low, with ∼10% of cells expressing the TEC marker epithelial cell adhesion molecule (EpCAM) (Box 1) (Otsuka et al., 2020; Soh et al., 2014), and so further studies are needed to optimize these protocols. Another priority is to develop robust protocols that can be adapted to different iPSC lines, as reproducibility remains a main issue. The difficulty of maintaining TECs in culture also jeopardizes the final stages of iPSC-derived

Disease Models & Mechanisms (2021) 14, dmm046359. doi:10.1242/dmm.046359

Box 4. iPSCs – thymic differentiation strategies

To differentiate iPSC lines derived from somatic cells such as fibroblasts or B cells (Otsuka et al., 2020; Su et al., 2015) into a functional thymic epithelium, cells must replicate the steps of thymic embryonic development, i.e. they must differentiate from definitive endoderm (DE) into anterior foregut endoderm and then into third pouch pharyngeal endoderm (Parent et al., 2013). Several protocols have been established and optimized to generate individual iPSC lines. Generally, DE is induced by culturing iPSCs for 5 days with activin A (INHBA) and, in some cases, with WNT3A and the GSK3 inhibitor CHIR99021 (Otsuka et al., 2020; Parent et al., 2013; Soh et al., 2014; Sun et al., 2013). The anteriorization stage relies on the effect of retinoic acid (RA) combined with that of BMP- and WNT-signal inhibitors, LDN193189 and IWR1, respectively (Inami et al., 2011; Otsuka et al., 2020; Parent et al., 2013; Soh et al., 2014). The TGF-β inhibitors SB431542 or LY364947 are also crucial at this stage. In the final steps of differentiation, cells are usually exposed to BMP4, WNT3A, RA, and FGF signals, such as FGF7, FGF8 and FGF10 (Otsuka et al., 2020; Parent et al., 2013). The sonic hedgehog inhibitor cyclopamine has also been shown to improve thymic differentiation. Since these differentiation protocols are highly susceptible to variability, they still need to be fine-tuned to achieve successful differentiation of the thymic epithelium and should be adapted for each individual iPSC line.

TEC differentiation. Hopefully, recent advances of TEC conservation in culture will make the co-culturing of TECs with T cells possible, in order to support crosstalk between these two cell types and to enable the induction of the cellular programs that lead to their respective maturation. In addition, recent findings have revealed a substantial and unrecognized degree of TEC heterogeneity (Bornstein et al., 2018; Dhalla et al., 2019 preprint). In the past, a relatively small marker set was used to define differentiated TECs, to distinguish few distinct types of TEC population. However, the recent application of single-cell transcriptomics revealed a substantial degree of TEC heterogeneity (Bornstein et al., 2018; Dhalla et al., 2019 preprint), providing us with a more precise way to identify a particular population of iPSC-derived TECs and its signaling pathways. Thus, thymic models based on iPSCs will benefit from new insights provided by single-cell transcriptomics and are expected to closely mimic the biological mechanisms that occur *in vivo*. In addition, over time, the differentiation of APECED patient-derived iPSCs into functional TECs is expected to lead to efficient cell therapies, e.g. transplantable TECs or Tregs obtained from an *ex vivo* T cell development system in which T cell precursors interact with iPSC-generated TECs.

From experiments to human trials

Gene and cell therapy to correct a mutant *AIRE* gene or to correct AIRE function represent a promising approach to cure APECED. In support of this, similar approaches have been employed to treat other rare diseases, by using CRISPR-Cas9- or adeno-associated virus-based gene therapy to restore the correct expression of mutated genes (see also Gene therapy: The ultimate cure for hereditary disease therapy, 2019). However, in the case of APECED, there are some pitfalls to restoring AIRE expression on a tissue-wide scale, since normal expression of AIRE is restricted to the mTEC lineage. Indeed, it has been shown that some tumor-associated antigens are AIRE-dependent and that immune responses to tumors are stronger in *Aire*-deficient mice (Bakhru et al., 2017; Malchow et al., 2013a,b; Träger et al., 2012), indicating that the widespread expression of a corrected *AIRE* gene in patients could increase the risk of an APECED patient to develop cancer. One study, employing a more targeted approach, indicates how this problem might be addressed (Ko et al., 2010) by using Aire-deficient mice, which only express reduced levels of TRA and, therefore, are more susceptible to TRA-induced experimental autoimmune encephalomyelitis (EAE). Retroviral transduction was then applied to overexpress AIRE *in vitro* in cell lines of thymic medullary or dendritic cell origin, as well as in bone marrow cells. In the cell lines, this approach showed reduced expression of TRAs. However, in bone marrow chimeras that had been generated using the transduced bone marrow cells, elevated expression of TRAs resulted in a delay of the symptomatic onset of EAE (Ko et al., 2010). Transplantation of the thymus from allogeneic sources remains under investigation, but has been successfully performed in pediatric patients with a severe primary immunodeficiency called DiGeorge syndrome, which is characterized by thymic hypoplasia or aplasia (Markert et al., 2010). In this study, sixty patients were transplanted with postnatal allogeneic cultured thymus tissues, resulting in >70% survival, and the successful reconstitution of recipient T cells and T cell function. However, the allogeneic origin of the transplanted thymic tissue might limit its long-term function due to anti-donor immune responses. In addition, only tissue from donors who were less than one year old was used to limit the risk of viral exposure to these immunodeficient patients (Markert et al., 2010). To the best of our knowledge, this approach has not been used to treat APECED patients.

Thanks to developments in tissue-engineering techniques, bioengineered artificial thymus organoids are also being developed with the aim of rejuvenating thymus function. Such organoids have been shown to successfully attract lymphocyte progenitors in nude mice, supporting the generation of a complex T cell repertoire and the induction of donor-specific tolerance (Fan et al., 2015; Tajima et al., 2016). However, thymic organoids will need to also mimic the complexity of a real thymus, which – despite recent advances (Fan et al., 2015) – is yet to be achieved. In addition, concomitant cytokine (such as IL-7 or IL-22) and growth factor (FGF7) therapies might be needed to maintain and promote the proliferation of thymic structures (Berent-Maoz et al., 2012; Dudakov et al., 2012).

Given the broad spectrum of symptoms in APECED, translating findings derived from animal models and from *ex vivo* and *in vitro* experiments to the clinic is a real challenge. To diagnose patients at an early stage is of key importance as it allows therapies to take place before irreversible organ lesions have occurred. In addition, monoclonal antibodies represent a tremendously powerful tool that could be used to target specific effector T cells while preserving Tregs. Indeed, they might represent the next-generation therapies for APECED and would also help to avoid the deleterious, long-term side effects of the immunosuppressive drugs currently used to manage APECED patients (Constantine and Lionakis, 2019). Indeed, we have shown that – for complications after transplantation (i.e. solid-organ rejection and graft-versus-host disease) and in patients with Duchene muscular dystrophy – treatment with anti-CD45RC mAb can restore the balance of Teff-to-Treg cells, inhibit transplant rejection and induce tolerance and, thus, protect against muscle loss in Duchene dystrophy (Boucault et al., 2020; Ouisse et al., 2019; Picarda et al., 2017). Treg cell therapy – either from allogeneic sources or genetically modified to restore their function – also represents a potential treatment (Bezie et al., 2019; Flippe et al., 2019). Moreover, the rat model of APECED could be used to develop such immunotherapies because it allows the visual assessment of disease-associate phenotypes, such as alopecia, weight loss and vitiligo.

Finally, although the absence of AIRE is a feature of APECED disease, significantly decreased levels of AIRE have also been observed in patients suffering from Omenn syndrome or Down

Disease Models & Mechanisms (2021) 14, dmm046359. doi:10.1242/dmm.046359

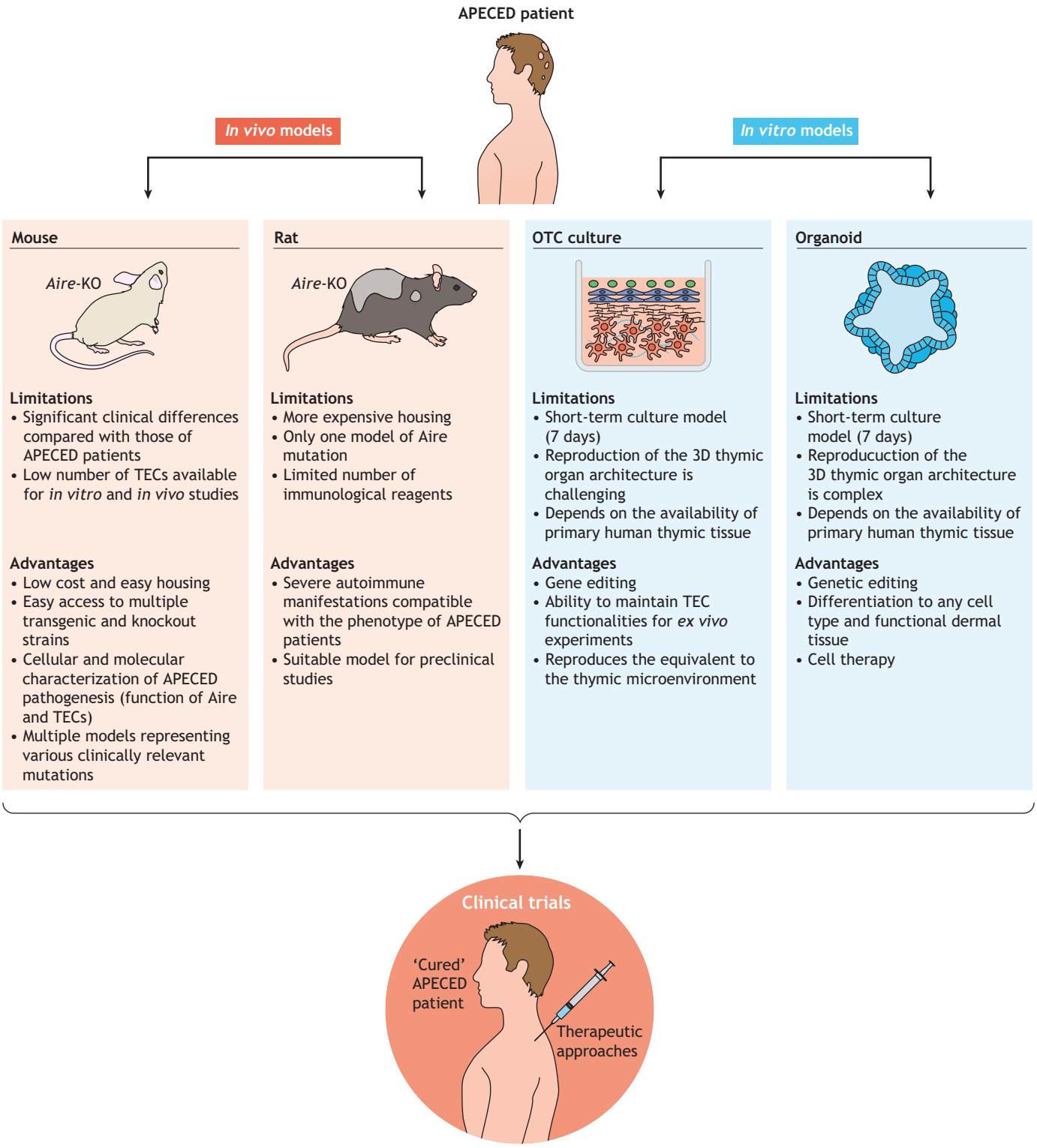

Fig. 4. Research strategies that employ *in vivo* and *in vitro* models of APECED to develop new therapies. This schematic highlights the advantages and limitations of each model.

syndrome, two disorders characterized by severe immunodeficiency and T-cell-mediated autoimmunity (Cavadini et al., 2005; Giménez-Barcons et al., 2014). This strong correlation between thymic AIRE expression and the susceptibility to a wide range of autoimmune manifestations suggest a 'dose-effect' of AIRE that may also provide clues for targeted therapeutics.

Conclusions

The different models generated to study APECED and the development of systems for culturing primary TECs have considerably improved our understanding of the mechanisms that underlie immunological tolerance in the thymus. In addition, they have enabled the development of several pre-clinical therapeutic

approaches for controlling autoimmunity in APECED (Fig. 4). However, the existing animal models of APECED do not recapitulate all of the specific aspects of the human disease in humans. Indeed, many mouse models recapitulate only a few aspects of human ACEPED pathology and its clinical features. Moreover, although the rat APECED model can recapitulate several pathological hallmarks of the human disease and will help the translation of drugs to the clinic, additional models are needed, including those of other known *Aire* point mutations that might be associated with specific disease phenotypes. The *ex vivo* 3D OTC and thymus-derived culture models also need to be adapted to the newly discovered broad spectrum of TEC sub-population (Kadouri et al., 2019) the specificities of species origin, i.e. mouse, rat and human. Further studies of these models will undoubtedly offer new insights into function thymic epithelium – notably, with respect to the effect AIRE has across human and murine samples – and will explain the phenotypical differences between APECED in mice, rats and humans. Differentiation of iPSCs into functional thymic tissue will enable functional T cells differentiation *ex vivo*, thereby providing a unique opportunity to restore a dysfunctional immune system through personalized cell therapy treatments. The comprehensive characterization of the complex molecular mechanisms that underlie the effect of AIRE on induction of TRAs, as well as the identification of additional molecular factors involved in the induction of central immune tolerance, will certainly be revealed by using newly developed single-cell transcriptomic and epigenetics approaches. Combined analyses of such new and existing data on TEC biology in human and rodent samples (Bornstein et al., 2018; Kernfeld et al., 2018; Miragaia et al., 2018; Park et al., 2020) are key to tackle TEC heterogeneity and function and, especially, the repertoire of Aire-dependent and independent TRAs. These approaches of deciphering the molecular mechanisms that underlie APECED by using different models and culture system are essential to ensure appropriate and efficient therapeutic measures.

Competing interests

The authors declare no competing or financial interests.

Funding

This work was funded by: the Labex IGO (project «Investissements d'Avenir», ANR-11-LABX-0016-01), IHU-Cesti (project funded by the «Investissements d'Avenir», ANR-10-IBHU-005 as well as by Nantes Metropole and Region Pays de la Loire). This work was supported by the Fondation Progreffe to N.P., Fondation pour la Recherche Médicale to C.G., EJP-Rare Disease JTC2019 program TARID project funded by the Agence Nationale de la Recherche (ANR-19-RAR4-0011-4) to C.G. and (ANR-19-RAR4-0011-5) to M.G.

References

Abramson, J., Giraud, M., Benoist, C. and Mathis, D. (2010). Aire's partners in the molecular control of immunological tolerance. *Cell* **140**, 123-135. doi:10.1016/j.cell.2009.12.030

Ahonen, P., Myllärniemi, S., Sipilä, I. and Perheentupa, J. (1990). Clinical variation of autoimmune polyendocrinopathy–candidiasis–ectodermal dystrophy (APECED) in a series of 68 patients. *N. Engl. J. Med*. **322**, 1829-1836. doi:10.1056/NEJM199006283222601

Akiyama, T., Shimo, Y., Yanai, H., Qin, J., Ohshima, D., Maruyama, Y., Asaumi, Y., Kitazawa, J., Takayanagi, H., Penninger, J. M. et al. (2008). The tumor necrosis factor family receptors RANK and CD40 cooperatively establish the thymic medullary microenvironment and self-tolerance. *Immunity* **29**, 423-437. doi:10.1016/j.immuni.2008.06.015

Anderson, M. S., Venanzi, E. S., Klein, L., Chen, Z., Berzins, S. P., Turley, S. J., von Boehmer, H., Bronson, R., Dierich, A., Benoist, C. et al. (2002). Projection of an immunological self shadow within the thymus by the aire protein. *Science* **298**, 1395-1401. doi:10.1126/science.1075958

Aricha, R., Feferman, T., Scott, H. S., Souroujon, M. C., Berrih-Aknin, S. and Fuchs, S. (2011). The susceptibility of Aire(−/−) mice to experimental myasthenia gravis involves alterations in regulatory T cells. *J. Autoimmun*. **36**, 16-24. doi:10.1016/j.jaut.2010.09.007

Autengruber, A., Gereke, M., Hansen, G., Hennig, C. and Bruder, D. (2012). Impact of enzymatic tissue disintegration on the level of surface molecule expression and immune cell function. *Eur. J. Microbiol. Immunol*. **2**, 112-120. doi:10.1556/EuJMI.2.2012.2.3

Bakhru, P., Zhu, M.-L., Wang, H.-H., Hong, L. K., Khan, I., Mouchess, M., Gulati, A. S., Starmer, J., Hou, Y., Sailer, D. et al. (2017). Combination central tolerance and peripheral checkpoint blockade unleashes antimelanoma immunity. *JCI Insight* **2**, e93265. doi:10.1172/jci.insight.93265

Baxter, R. M. and Brissette, J. L. (2002). Role of the nude gene in epithelial terminal differentiation. *J. Invest. Dermatol*. **118**, 303-309. doi:10.1046/j.0022-202x.2001.01662.x

Berent-Maoz, B., Montecino-Rodriguez, E., Signer, R. A. J. and Dorshkind, K. (2012). Fibroblast growth factor-7 partially reverses murine thymocyte progenitor aging by repression of Ink4a. *Blood* **119**, 5715-5721. doi:10.1182/blood-2011-12-400002

Bezie, S., Charreau, B., Vimond, N., Lasselin, J., Gerard, N., Nerriere-Daguin, V., Bellier-Waast, F., Duteille, F., Anegon, I. and Guillonneau, C. (2019). Human CD8+ Tregs expressing a MHC-specific CAR display enhanced suppression of human skin rejection and GVHD in NSG mice. *Blood Adv* **3**, 3522-3538. doi:10.1182/bloodadvances.2019000411

Björses, P., Aaltonen, J., Horelli-Kuitunen, N., Yaspo, M. L. and Peltonen, L. (1998). Gene defect behind APECED: a new clue to autoimmunity. *Hum. Mol. Genet*. **7**, 1547-1553. doi:10.1093/hmg/7.10.1547

Bleul, C. C., Corbeaux, T., Reuter, A., Fisch, P., Mönting, J. S. and Boehm, T. (2006). Formation of a functional thymus initiated by a postnatal epithelial progenitor cell. *Nature* **441**, 992-996. doi:10.1038/nature04850

Böckle, B. C., Wilhelm, M., Müller, H., Götsch, C. and Sepp, N. T. (2010). Oral mucous squamous cell carcinoma—an anticipated consequence of autoimmune polyendocrinopathy-candidiasis-ectodermal dystrophy (APECED). *J. Am. Acad. Dermatol*. **62**, 864-868. doi:10.1016/j.jaad.2009.06.061

Boehnke, K., Mirancea, N., Pavesio, A., Fusenig, N. E., Boukamp, P. and Stark, H.-J. (2007). Effects of fibroblasts and microenvironment on epidermal regeneration and tissue function in long-term skin equivalents. *Eur. J. Cell Biol*. **86**, 731-746. doi:10.1016/j.ejcb.2006.12.005

Bonfanti, P., Claudinot, S., Amici, A. W., Farley, A., Blackburn, C. C. and Barrandon, Y. (2010). Microenvironmental reprogramming of thymic epithelial cells to skin multipotent stem cells. *Nature* **466**, 978-982. doi:10.1038/nature09269

Borchers, J., Pukkala, E., Mäkitie, O. and Laakso, S. (2020). Patients with APECED have increased early mortality due to endocrine causes, malignancies and infections. *J. Clin. Endocrinol. Metab*. **105**, e2207-e2213. doi:10.1210/clinem/dgaa140

Bornstein, C., Nevo, S., Giladi, A., Kadouri, N., Pouzolles, M., Gerbe, F., David, E., Machado, A., Chuprin, A., Tóth, B. et al. (2018). Single-cell mapping of the thymic stroma identifies IL-25-producing tuft epithelial cells. *Nature* **559**, 622-626. doi:10.1038/s41586-018-0346-1

Boucault, L., Lopez Robles, M.-D., Thiolat, A., Bézie, S., Schmueck-Henneresse, M., Braudeau, C., Vimond, N., Freuchet, A., Autrusseau, E., Charlotte, F. et al. (2020). Transient antibody targeting of CD45RC inhibits the development of graft-versus-host disease. *Blood Adv*. **4**, 2501-2515. doi:10.1182/bloodadvances.2020001688

Bruhns, P. (2012). Properties of mouse and human IgG receptors and their contribution to disease models. *Blood* **119**, 5640-5649. doi:10.1182/blood-2012-01-380121

Bukowska, J., Kopcewicz, M., Walendzik, K. and Gawronska-Kozak, B. (2018). Foxn1 in skin development, homeostasis and wound healing. *Int. J. Mol. Sci*. **19**, 1956. doi:10.3390/ijms19071956

Burbelo, P. D., Browne, S. K., Sampaio, E. P., Giaccone, G., Zaman, R., Kristosturyan, E., Rajan, A., Ding, L., Ching, K. H., Berman, A. et al. (2010). Anti-cytokine autoantibodies are associated with opportunistic infection in patients with thymic neoplasia. *Blood* **116**, 4848-4858. doi:10.1182/blood-2010-05-286161

Cabral, A., Voskamp, P., Cleton-Jansen, A.-M., South, A., Nizetic, D. and Backendorf, C. (2001). Structural organization and regulation of the small proline-rich family of cornified envelope precursors suggest a role in adaptive barrier function. *J. Biol. Chem*. **276**, 19231-19237. doi:10.1074/jbc.M100336200

Cavadini, P., Vermi, W., Facchetti, F., Fontana, S., Nagafuchi, S., Mazzolari, E., Sediva, A., Marrella, V., Villa, A., Fischer, A. et al. (2005). AIRE deficiency in thymus of 2 patients with Omenn syndrome. *J. Clin. Invest*. **115**, 728-732. doi:10.1172/JCI200523087

Cetani, F., Barbesino, G., Borsari, S., Pardi, E., Cianferotti, L., Pinchera, A. and Marcocci, C. (2001). A novel mutation of the autoimmune regulator gene in an Italian kindred with autoimmune polyendocrinopathy-candidiasis-ectodermal dystrophy, acting in a dominant fashion and strongly cosegregating with hypothyroid autoimmune thyroiditis. *J. Clin. Endocrinol. Metab*. **86**, 4747-4752. doi:10.1210/jcem.86.10.7884

Chhatta, A. R., Cordes, M., Hanegraaf, M. A. J., Vloemans, S., Cupedo, T., Cornelissen, J. J., Carlotti, F., Salvatori, D., Pike-Overzet, K., Fibbe, W. E. et al. (2019). De novo generation of a functional human thymus from induced

pluripotent stem cells. *J. Allergy Clin. Immunol.* **144**, 1416-1419.e7. doi:10.1016/j.jaci.2019.05.042

Christin-Maitre, S., Vasseur, C., Portnoï, M.-F. and Bouchard, P. (1998). Genes and premature ovarian failure. *Mol. Cell. Endocrinol.* **145**, 75-80. doi:10.1016/S0303-7207(98)00172-5

Collins, S. M., Dominguez, M., Ilmarinen, T., Costigan, C. and Irvine, A. D. (2006). Dermatological manifestations of autoimmune polyendocrinopathy-candidiasis-ectodermal dystrophy syndrome. *Br. J. Dermatol.* **154**, 1088-1093. doi:10.1111/j.1365-2133.2006.07166.x

Constantine, G. M. and Lionakis, M. S. (2019). Lessons from primary immunodeficiencies: autoimmune regulator and autoimmune polyendocrinopathy-candidiasis-ectodermal dystrophy. *Immunol. Rev.* **287**, 103-120. doi:10.1111/imr.12714

Cowan, J. E., McCarthy, N. I. and Anderson, G. (2016). CCR7 controls thymus recirculation, but not production and emigration, of Foxp3+T cells. *Cell Rep.* **14**, 1041-1048. doi:10.1016/j.celrep.2016.01.003

Danan-Gotthold, M., Guyon, C., Giraud, M., Levanon, E. Y. and Abramson, J. (2016). Extensive RNA editing and splicing increase immune self-representation diversity in medullary thymic epithelial cells. *Genome Biol.* **17**, 219. doi:10.1186/s13059-016-1079-9

De Leonibus, C., Attanasi, M., Roze, Z., Martin, B., Marcovecchio, M. L., Di Pillo, S., Chiarelli, F. and Mohn, A. (2016). Influence of inhaled corticosteroids on pubertal growth and final height in asthmatic children. *Pediatr. Allergy Immunol.* **27**, 499-506. doi:10.1111/pai.12558

Depreter, M. G. L., Blair, N. F., Gaskell, T. L., Nowell, C. S., Davern, K., Pagliocca, A., Stenhouse, F. H., Farley, A. M., Fraser, A., Vrana, J. et al. (2008). Identification of Plet-1 as a specific marker of early thymic epithelial progenitor cells. *Proc. Natl. Acad. Sci. USA* **105**, 961-966. doi:10.1073/pnas.0711170105

Derbinski, J., Schulte, A., Kyewski, B. and Klein, L. (2001). Promiscuous gene expression in medullary thymic epithelial cells mirrors the peripheral self. *Nat. Immunol.* **2**, 1032-1039. doi:10.1038/ni723

DeVoss, J. J., Shum, A. K., Johannes, K. P. A., Lu, W., Krawisz, A. K., Wang, P., Yang, T., LeClair, N. P., Austin, C., Strauss, E. C. et al. (2008). Effector mechanisms of the autoimmune syndrome in the murine model of autoimmune polyglandular syndrome Type 1. *J. Immunol.* **181**, 4072-4079. doi:10.4049/jimmunol.181.6.4072

Dhalla, F., Baran-Gale, J., Maio, S., Chappell, L., Holländer, G. and Ponting, C. P. (2019). Biologically indeterminate yet ordered promiscuous gene expression in single medullary thymic epithelial cells. *EMBO J.* **39**, e101828. doi:10.15252/embj.2019101828

Dudakov, J. A., Hanash, A. M., Jenq, R. R., Young, L. F., Ghosh, A., Singer, N. V., West, M. L., Smith, O. M., Holland, A. M., Tsai, J. J. et al. (2012). Interleukin-22 drives endogenous thymic regeneration in mice. *Science* **336**, 91-95. doi:10.1126/science.1218004

Ekwall, O., Hedstrand, H., Grimelius, L., Haavik, J., Perheentupa, J., Gustafsson, J., Husebye, E., Kämpe, O. and Rorsman, F. (1998). Identification of tryptophan hydroxylase as an intestinal autoantigen. *The Lancet* **352**, 279-283. doi:10.1016/S0140-6736(97)11050-9

Esselborn, V. M., Landing, B. H., Whitaker, J. and Williams, R. R. (1956). The syndrome of familial juvenile hypoadrenocorticism, hypoparathyroidism and superficial moniliasis. *J. Clin. Endocrinol. Metab.* **16**, 1374-1387. doi:10.1210/jcem-16-10-1374

Fan, Y., Tajima, A., Goh, S. K., Geng, X., Gualtierotti, G., Grupillo, M., Coppola, A., Bertera, S., Rudert, W. A., Banerjee, I. et al. (2015). Bioengineering thymus organoids to restore thymic function and induce donor-specific immune tolerance to allografts. *Mol. Ther.* **23**, 1262-1277. doi:10.1038/mt.2015.77

Fernández, E., Vicente, A., Zapata, A., Brera, B., Lozano, J. J., Martínez, C. and Toribio, M. L. (1994). Establishment and characterization of cloned human thymic epithelial cell lines. Analysis of adhesion molecule expression and cytokine production. *Blood* **83**, 3245-3254. doi:10.1182/blood.V83.11.3245.3245

Ferre, E. M. N., Rose, S. R., Rosenzweig, S. D., Burbelo, P. D., Romito, K. R., Niemela, J. E., Rosen, L. B., Break, T. J., Gu, W., Hunsberger, S. et al. (2016). Redefined clinical features and diagnostic criteria in autoimmune polyendocrinopathy-candidiasis-ectodermal dystrophy. *JCI Insight* **1**, e88782. doi:10.1172/jci.insight.88782

Ferré, E. M. N., Break, T. J., Burbelo, P. D., Allgäuer, M., Kleiner, D. E., Jin, D., Xu, Z., Folio, L. R., Mollura, D. J., Swamydas, M., et al., (2019). Lymphocyte-driven regional immunopathology in pneumonitis caused by impaired central immune tolerance. *Sci. Transl. Med.* **11**, eaav5597. doi:10.1126/scitranslmed.aav5597

Fishman, D., Kisand, K., Hertel, C., Rothe, M., Remm, A., Pihlap, M., Adler, P., Vilo, J., Peet, A., Meloni, A. et al. (2017). Autoantibody repertoire in APECED patients targets two distinct subgroups of proteins. *Front. Immunol.* **8**, 976. doi:10.3389/fimmu.2017.00976

Flippe, L., Bézie, S., Anegon, I. and Guillonneau, C. (2019). Future prospects for CD8$^+$ regulatory T cells in immune tolerance. *Immunol. Rev.* **292**, 209-224. doi:10.1111/imr.12812

Gäbler, J., Arnold, J. and Kyewski, B. (2007). Promiscuous gene expression and the developmental dynamics of medullary thymic epithelial cells. *Eur. J. Immunol.* **37**, 3363-3372. doi:10.1002/eji.200737131

Gavanescu, I., Kessler, B., Ploegh, H., Benoist, C. and Mathis, D. (2007). Loss of Aire-dependent thymic expression of a peripheral tissue antigen renders it a target of autoimmunity. *Proc. Natl. Acad. Sci. USA* **104**, 4583-4587. doi:10.1073/pnas.0700259104

Gavanescu, I., Benoist, C. and Mathis, D. (2008). B cells are required for Aire-deficient mice to develop multi-organ autoinflammation: a therapeutic approach for APECED patients. *Proc. Natl. Acad. Sci. USA* **105**, 13009-13014. doi:10.1073/pnas.0806874105

Gene therapy: The ultimate cure for hereditary diseases. (2019). EBioMedicine 47, 1. https://doi.org/10.1016/j.ebiom.2019.09.018.

Gentile, N. M., Murray, J. A. and Pardi, D. S. (2012). Autoimmune enteropathy: a review and update of clinical management. *Curr. Gastroenterol. Rep.* **14**, 380-385. doi:10.1007/s11894-012-0276-2

Giménez-Barcons, M., Casteràs, A., Armengol, M. del P., Porta, E., Correa, P. A., Marín, A., Pujol-Borrell, R. and Colobran, R. (2014). Autoimmune predisposition in down syndorome may result from a partial central tolerance failure due to insufficient intrathymic expression of *AIRE* and peripheral antigens. *J. Immunol.* **193**, 3872-3879. doi:10.4049/jimmunol.1400223

Giraud, M., Yoshida, H., Abramson, J., Rahl, P. B., Young, R. A., Mathis, D. and Benoist, C. (2012). Aire unleashes stalled RNA polymerase to induce ectopic gene expression in thymic epithelial cells. *Proc. Natl. Acad. Sci. USA* **109**, 535-540. doi:10.1073/pnas.1119351109

Giraud, M., Jmari, N., Du, L., Carallis, F., Nieland, T. J. F., Perez-Campo, F. M., Bensaude, O., Root, D. E., Hacohen, N., Mathis, D. et al. (2014). An RNAi screen for Aire cofactors reveals a role for Hnrnpl in polymerase release and Aire-activated ectopic transcription. *Proc. Natl. Acad. Sci. USA* **111**, 1491-1496. doi:10.1073/pnas.1323535111

Gordon, J. and Manley, N. R. (2011). Mechanisms of thymus organogenesis and morphogenesis. *Development* **138**, 3865-3878. doi:10.1242/dev.059998

Guyon, C., Jmari, N., Padonou, F., Li, Y.-C., Ucar, O., Fujikado, N., Coulpier, F., Blanchet, C., Root, D. E. and Giraud, M. (2020). Aire-dependent genes undergo Clp1-mediated 3'UTR shortening associated with higher transcript stability in the thymus. *eLife* **9**, 2078. doi:10.7554/eLife.52985

Hauri-Hohl, M., Zuklys, S., Holländer, G. A. and Ziegler, S. F. (2014). A regulatory role for TGF-β signaling in the establishment and function of the thymic medulla. *Nat. Immunol.* **15**, 554-561. doi:10.1038/ni.2869

He, W., Li, A. G., Wang, D., Han, S., Zheng, B., Goumans, M.-J., Ten Dijke, P. and Wang, X.-J. (2002). Overexpression of Smad7 results in severe pathological alterations in multiple epithelial tissues. *EMBO J.* **21**, 2580-2590. doi:10.1093/emboj/21.11.2580

Heino, M., Peterson, P., Kudoh, J., Shimizu, N., Antonarakis, S. E., Scott, H. S. and Krohn, K. (2001). APECED mutations in the autoimmune regulator (AIRE) gene. *Hum. Mutat.* **18**, 205-211. doi:10.1002/humu.1176

Hikosaka, Y., Nitta, T., Ohigashi, I., Yano, K., Ishimaru, N., Hayashi, Y., Matsumoto, M., Matsuo, K., Penninger, J. M., Takayanagi, H. et al. (2008). The cytokine RANKL produced by positively selected thymocytes fosters medullary thymic epithelial cells that express autoimmune regulator. *Immunity* **29**, 438-450. doi:10.1016/j.immuni.2008.06.018

Hubert, F.-X., Kinkel, S. A., Crewther, P. E., Cannon, P. Z. F., Webster, K. E., Link, M., Uibo, R., O'Bryan, M. K., Meager, A., Forehan, S. P. et al. (2009). Aire-deficient C57BL/6 mice mimicking the common human 13-base pair deletion mutation present with only a mild autoimmune phenotype. *J. Immunol. Baltim. Md* **182**, 3902-3918. doi:10.4049/jimmunol.0802124

Humbert, L., Cornu, M., Proust-Lemoine, E., Bayry, J., Wemeau, J.-L., Vantyghem, M.-C. and Sendid, B. (2018). Chronic mucocutaneous candidiasis in autoimmune polyendocrine syndrome type 1. *Front. Immunol.* **9**, 2570. doi:10.3389/fimmu.2018.02570

Hun, M., Barsanti, M., Wong, K., Ramshaw, J., Werkmeister, J. and Chidgey, A. P. (2017). Native thymic extracellular matrix improves in vivo thymic organoid T cell output, and drives *in vitro* thymic epithelial cell differentiation. *Biomaterials* **118**, 1-15. doi:10.1016/j.biomaterials.2016.11.054

Hunziker, L., Benitah, S. A., Aznar Benitah, S., Braun, K. M., Jensen, K., McNulty, K., Butler, C., Potton, E., Nye, E., Boyd, R. et al. (2011). Rac1 deletion causes thymic atrophy. *PLoS ONE* **6**, e19292. doi:10.1371/journal.pone.0019292

Inami, Y., Yoshikai, T., Ito, S., Nishio, N., Suzuki, H., Sakurai, H. and Isobe, K.-I. (2011). Differentiation of induced pluripotent stem cells to thymic epithelial cells by phenotype. *Immunol. Cell Biol.* **89**, 314-321. doi:10.1038/icb.2010.96

Jankowska, K. (2017). Premature ovarian failure. *Menopausal Rev.* **2**, 51-56. doi:10.5114/pm.2017.68592

Jenkinson, W. E., Jenkinson, E. J. and Anderson, G. (2003). Differential requirement for mesenchyme in the proliferation and maturation of thymic epithelial progenitors. *J. Exp. Med.* **198**, 325-332. doi:10.1084/jem.20022135

Jiang, W., Anderson, M. S., Bronson, R., Mathis, D. and Benoist, C. (2005). Modifier loci condition autoimmunity provoked by Aire deficiency. *J. Exp. Med.* **202**, 805-815. doi:10.1084/jem.20050693

Kadouri, N., Nevo, S., Goldfarb, Y. and Abramson, J. (2019). Thymic epithelial cell heterogeneity: TEC by TEC. *Nat. Rev. Immunol.* **20**, 239-253. doi:10.1038/s41577-019-0238-0

Kärner, J., Meager, A., Laan, M., Maslovskaja, J., Pihlap, M., Remm, A., Juronen, E., Wolff, A. S. B., Husebye, E. S., Podkrajšek, K. T. et al. (2013). Anti-

cytokine autoantibodies suggest pathogenetic links with autoimmune regulator deficiency in humans and mice. *Clin. Exp. Immunol.* **171**, 263-272. doi:10.1111/cei.12024

Kernfeld, E. M., Genga, R. M. J., Neherin, K., Magaletta, M. E., Xu, P. and Maehr, R. (2018). A Single-cell transcriptomic atlas of thymus organogenesis resolves cell types and developmental maturation. *Immunity* **48**, 1258-1270.e6. doi:10.1016/j.immuni.2018.04.015

Kimura, A. and Kishimoto, T. (2010). IL-6: Regulator of Treg/Th17 balance. *Eur. J. Immunol.* **40**, 1830-1835. doi:10.1002/eji.201040391

Kisand, K. and Peterson, P. (2011). Autoimmune polyendocrinopathy candidiasis ectodermal dystrophy: known and novel aspects of the syndrome: APECED: known and novel aspects of the syndrome. *Ann. N. Y. Acad. Sci.* **1246**, 77-91. doi:10.1111/j.1749-6632.2011.06308.x

Kisand, K., Link, M., Wolff, A. S. B., Meager, A., Tserel, L., Org, T., Murumägi, A., Uibo, R., Willcox, N., Trebušak Podkrajšek, K. et al. (2008). Interferon autoantibodies associated with AIRE deficiency decrease the expression of IFN-stimulated genes. *Blood* **112**, 2657-2666. doi:10.1182/blood-2008-03-144634

Klein, L., Kyewski, B., Allen, P. M. and Hogquist, K. A. (2014). Positive and negative selection of the T cell repertoire: what thymocytes see (and don't see). *Nat. Rev. Immunol.* **14**, 377-391. doi:10.1038/nri3667

Ko, H.-J., Kinkel, S. A., Hubert, F.-X., Nasa, Z., Chan, J., Siatskas, C., Hirubalan, P., Toh, B.-H., Scott, H. S. and Alderuccio, F. (2010). Transplantation of autoimmune regulator-encoding bone marrow cells delays the onset of experimental autoimmune encephalomyelitis. *Eur. J. Immunol.* **40**, 3499-3509. doi:10.1002/eji.201040679

Kondo, K., Ohigashi, I. and Takahama, Y. (2019). Thymus machinery for T-cell selection. *Int. Immunol.* **31**, 119-125. doi:10.1093/intimm/dxy081

Kont, V., Laan, M., Kisand, K., Merits, A., Scott, H. S. and Peterson, P. (2008). Modulation of Aire regulates the expression of tissue-restricted antigens. *Mol. Immunol.* **45**, 25-33. doi:10.1016/j.molimm.2007.05.014

Kuroda, N., Mitani, T., Takeda, N., Ishimaru, N., Arakaki, R., Hayashi, Y., Bando, Y., Izumi, K., Takahashi, T., Nomura, T. et al. (2005). Development of autoimmunity against transcriptionally unrepressed target antigen in the thymus of Aire-deficient mice. *J. Immunol. Baltim. Md* **174**, 1862-1870. doi:10.4049/jimmunol.174.4.1862

Kyewski, B. and Klein, L. (2006). A central role for central tolerance. *Annu. Rev. Immunol.* **24**, 571-606. doi:10.1146/annurev.immunol.23.021704.115601

Lai, L. and Jin, J. (2009). Generation of thymic epithelial cell progenitors by mouse embryonic stem cells. *Stem Cells* **27**, 3012-3020. doi:10.1002/stem.238

Langbein, L., Pape, U.-F., Grund, C., Kuhn, C., Praetzel, S., Moll, I., Moll, R. and Franke, W. W. (2003). Tight junction-related structures in the absence of a lumen: Occludin, claudins and tight junction plaque proteins in densely packed cell formations of stratified epithelia and squamous cell carcinomas. *Eur. J. Cell Biol.* **82**, 385-400. doi:10.1078/0171-9335-00330

Liston, A., Lesage, S., Wilson, J., Peltonen, L. and Goodnow, C. C. (2003). Aire regulates negative selection of organ-specific T cells. *Nat. Immunol.* **4**, 350-354. doi:10.1038/ni906

Liston, A., Gray, D. H. D., Lesage, S., Fletcher, A. L., Wilson, J., Webster, K. E., Scott, H. S., Boyd, R. L., Peltonen, L. and Goodnow, C. C. (2004). Gene dosage–limiting role of Aire in thymic expression, clonal deletion, and organ-specific autoimmunity. *J. Exp. Med.* **200**, 1015-1026. doi:10.1084/jem.20040581

Lkhagvasuren, E., Sakata, M., Ohigashi, I. and Takahama, Y. (2013). Lymphotoxin β receptor regulates the development of CCL21-expressing subset of postnatal medullary thymic epithelial cells. *J. Immunol.* **190**, 5110-5117. doi:10.4049/jimmunol.1203203

Malchow, S., Leventhal, D. S., Nishi, S., Fischer, B. I., Shen, L., Paner, G. P., Amit, A. S., Kang, C., Geddes, J. E., Allison, J. P. et al. (2013a). Aire-dependent thymic development of tumor-associated regulatory T cells. *Science* **339**, 1219-1224. doi:10.1126/science.1233913

Malchow, S., Leventhal, D. S. and Savage, P. A. (2013b). Organ-specific regulatory T cells of thymic origin are expanded in murine prostate tumors. *OncoImmunology* **2**, e24898. doi:10.4161/onci.24898

Malchow, S., Leventhal, D. S., Lee, V., Nishi, S., Socci, N. D. and Savage, P. A. (2016). Aire enforces immune tolerance by directing autoreactive T cells into the regulatory T cell lineage. *Immunity* **44**, 1102-1113. doi:10.1016/j.immuni.2016.02.009

Manns, M. P., Czaja, A. J., Gorham, J. D., Krawitt, E. L., Mieli-Vergani, G., Vergani, D. and Vierling, J. M. (2010). Diagnosis and management of autoimmune hepatitis. *Hepatology* **51**, 2193-2213. doi:10.1002/hep.23584

Markert, M. L., Devlin, B. H. and McCarthy, E. A. (2010). Thymus transplantation. *Clin. Immunol.* **135**, 236-246. doi:10.1016/j.clim.2010.02.007

Mathis, D. and Benoist, C. (2009). Aire. *Annu. Rev. Immunol.* **27**, 287-312. doi:10.1146/annurev.immunol.25.022106.141532

Mestas, J. and Hughes, C. C.W., (2004). Of mice and not men: differences between mouse and human immunology. *J. Immunol.* **172**, 2731-2738. doi:10.4049/jimmunol.172.5.2731

Meyer, S., Woodward, M., Hertel, C., Vlaicu, P., Haque, Y., Kärner, J., Macagno, A., Onuoha, S. C., Fishman, D., Peterson, H. et al. (2016). AIRE-deficient patients harbor unique high-affinity disease-ameliorating autoantibodies. *Cell* **166**, 582-595. doi:10.1016/j.cell.2016.06.024

Miragaia, R. J., Zhang, X., Gomes, T., Svensson, V., Ilicic, T., Henriksson, J., Kar, G. and Lönnberg, T. (2018). Single-cell RNA-sequencing resolves self-antigen expression during mTEC development. *Sci. Rep.* **8**, 685. doi:10.1038/s41598-017-19100-4

Mohtashami, M. and Zúñiga-Pflücker, J. C. (2006). Three-dimensional architecture of the thymus is required to maintain delta-like expression necessary for inducing T cell development. *J. Immunol. Baltim. Md* **176**, 730-734. doi:10.1002/stem.238

Nancy, P. and Berrih-Aknin, S. (2005). Differential estrogen receptor expression in autoimmune myasthenia gravis. *Endocrinology* **146**, 2345-2353. doi:10.1210/en.2004-1003

Napier, C. and Pearce, S. H.S. (2012). Autoimmune Addison's disease. *Presse Médicale* **41**, e626-e635. doi:10.1016/j.lpm.2012.09.010

Nazzal, D., Gradolatto, A., Truffault, F., Bismuth, J. and Berrih-Aknin, S. (2014). Human thymus medullary epithelial cells promote regulatory T-cell generation by stimulating interleukin-2 production via ICOS ligand. *Cell Death Dis.* **5**, e1420-e1420. doi:10.1038/cddis.2014.377

Nehls, M., Kyewski, B., Messerle, M., Waldschutz, R., Schuddekopf, K., Smith, A. J. H. and Boehm, T. (1996). Two genetically separable steps in the differentiation of thymic epithelium. *Science* **272**, 886-889. doi:10.1126/science.272.5263.886

Neufeld, M., Maclaren, N. and Blizzard, R. (1980). Autoimmune polyglandular syndromes. *Pediatr. Ann.* **9**, 154-162. doi:10.3928/0090-4481-19800401-07

Niki, S. (2006). Alteration of intra-pancreatic target-organ specificity by abrogation of Aire in NOD mice. *J. Clin. Invest.* **116**, 1292-1301. doi:10.1172/JCI26971

Oftedal, B. E., Hellesen, A., Erichsen, M. M., Bratland, E., Vardi, A., Perheentupa, J., Kemp, E. H., Fiskerstrand, T., Viken, M. K., Weetman, A. P. et al. (2015). Dominant mutations in the autoimmune regulator AIRE are associated with common organ-specific autoimmune diseases. *Immunity* **42**, 1185-1196. doi:10.1016/j.immuni.2015.04.021

Orlova, E. M., Sozaeva, L. S., Kareva, M. A., Oftedal, B. E., Wolff, A. S. B., Breivik, L., Zakharova, E. Y., Ivanova, O. N., Kämpe, O., Dedov, I. I. et al. (2017). Expanding the phenotypic and genotypic landscape of autoimmune polyendocrine syndrome type 1. *J. Clin. Endocrinol. Metab.* **102**, 3546-3556. doi:10.1210/jc.2017-00139

Ossart, J., Moreau, A., Autrusseau, E., Ménoret, S., Martin, J. C., Besnard, M., Ouisse, L.-H., Tesson, L., Flippe, L., Kisand, K. et al. (2018). Breakdown of immune tolerance in AIRE-deficient rats induces a severe autoimmune polyendocrinopathy–candidiasis–ectodermal dystrophy–like autoimmune disease. *J. Immunol.* **201**, 874-887. doi:10.4049/jimmunol.1701318

Otsuka, R., Wada, H., Tsuji, H., Sasaki, A., Murata, T., Itoh, M., Baghdadi, M. and Seino, K. (2020). Efficient generation of thymic epithelium from induced pluripotent stem cells that prolongs allograft survival. *Sci. Rep.* **10**, 1-8. doi:10.1038/s41598-019-56847-4

Ouisse, L.-H., Remy, S., Lafoux, A., Larcher, T., Tesson, L., Chenouard, V., Guillonneau, C., Brusselle, L., Vimond, N., Rouger, K. et al. (2019). Immunophenotype of a rat model of Duchenne's disease and demonstration of improved muscle strength after anti-CD45RC antibody treatment. *Front. Immunol.* **10**, 2131. doi:10.3389/fimmu.2019.02131

Palumbo, M. O., Levi, D., Chentoufi, A. A. and Polychronakos, C. (2006). Isolation and characterization of proinsulin-producing medullary thymic epithelial cell clones. *Diabetes* **55**, 2595-2601. doi:10.2337/db05-1651

Paquette, J., Varin, D. S. E., Hamelin, C. E., Hallgren, Å., Kämpe, O., Carel, J.-C., Perheentupa, J. and Deal, C. L. (2010). Risk of autoimmune diabetes in APECED: association with short alleles of the 5′insulin VNTR. *Genes Immun.* **11**, 590-597. doi:10.1038/gene.2010.33

Parent, A. V., Russ, H. A., Khan, I. S., LaFlam, T. N., Metzger, T. C., Anderson, M. S. and Hebrok, M. (2013). Generation of functional thymic epithelium from human embryonic stem cells that supports host T cell development. *Cell Stem Cell* **13**. 219-229 doi:10.1016/j.stem.2013.04.004

Park, J.-E., Botting, R. A., Domínguez Conde, C., Popescu, D.-M., Lavaert, M., Kunz, D. J., Goh, I., Stephenson, E., Ragazzini, R., Tuck, E. et al. (2020). A cell atlas of human thymic development defines T cell repertoire formation. *Science* **367**, eaay3224. doi:10.1126/science.aay3224

Patel, D. D., Whichard, L. P., Radcliff, G., Denning, S. M. and Haynes, B. F. (1995). Characterization of human thymic epithelial cell surface antigens: phenotypic similarity of thymic epithelial cells to epidermal keratinocytes. *J. Clin. Immunol.* **15**, 80-92. doi:10.1007/BF01541736

Perheentupa, J. (1980). Autoimmune polyendocrinopathy-candidiasis-ectodermal dystrophy (APECED) (ed. A. W. Eriksson, H. R. Forsius, H. R. Nevanlinna, P. L. Workm and R. K. Norio), pp. 583-588. Popul. Struct. Genet. Disord. Lond. Acad. Press.

Perheentupa, J. (2002). APS-I/APECED: the clinical disease and therapy. *Endocrinol. Metab. Clin. North Am.* **31**, 295-320. doi:10.1016/S0889-8529(01)00013-5

Perheentupa, J. (2006). Autoimmune polyendocrinopathy-candidiasis-ectodermal dystrophy. *J. Clin. Endocrinol. Metab.* **91**, 2843-2850. doi:10.1210/jc.2005-2611

Petrie, H. T. and Zúñiga-Pflücker, J. C. (2007). Zoned out: functional mapping of stromal signaling microenvironments in the thymus. *Annu. Rev. Immunol.* **25**, 649-679. doi:10.1146/annurev.immunol.23.021704.115715

Picarda, E., Bézie, S., Boucault, L., Autrusseau, E., Kilens, S., Meistermann, D., Martinet, B., Daguin, V., Donnart, A., Charpentier, E. et al. (2017). Transient antibody targeting of CD45RC induces transplant tolerance and potent antigen-specific regulatory T cells. *JCI Insight* **2**. doi:10.1172/jci.insight.90088

Pinto, S., Schmidt, K., Egle, S., Stark, H.-J., Boukamp, P. and Kyewski, B. (2013). An organotypic coculture model supporting proliferation and differentiation of medullary thymic epithelial cells and promiscuous gene expression. *J. Immunol.* **190**, 1085-1093. doi:10.4049/jimmunol.1201843

Polito, C. and Di Toro, R. (1992). Delayed pubertal growth spurt in glomerulopathic boys receiving alternate-day prednisone. *Child Nephrol. Urol.* **12**, 202-207.

Pomié, C., Vicente, R., Vuddamalay, Y., Lundgren, B. A., van der Hoek, M., Enault, G., Kagan, J., Fazilleau, N., Scott, H. S., Romagnoli, P. et al. (2011). Autoimmune regulator (AIRE)-deficient CD8+CD28low regulatory T lymphocytes fail to control experimental colitis. *Proc. Natl. Acad. Sci. USA* **108**, 12437-12442. doi:10.1073/pnas.1107136108

Pöntynen, N., Miettinen, A., Petteri Arstila, T., Kämpe, O., Alimohammadi, M., Vaarala, O., Peltonen, L. and Ulmanen, I. (2006). Aire deficient mice do not develop the same profile of tissue-specific autoantibodies as APECED patients. *J. Autoimmun.* **27**, 96-104. doi:10.1016/j.jaut.2006.06.001

Ramsey, C., Winqvist, O., Puhakka, L., Halonen, M., Moro, A., Kämpe, O., Eskelin, P., Pelto-Huikko, M. and Peltonen, L. (2002). Aire deficient mice develop multiple features of APECED phenotype and show altered immune response. *Hum. Mol. Genet.* **11**, 397-409. doi:10.1093/hmg/11.4.397

Röpke, C. (1997). Thymic epithelial cell culture. *Microsc. Res. Tech.* **38**, 276-286. doi:10.1002/(SICI)1097-0029(19970801)38:3<276::AID-JEMT8>3.0.CO;2-K

Rosatelli, M. C., Meloni, A., Meloni, A., Devoto, M., Cao, A., Scott, H. S., Peterson, P., Heino, M., Krohn, K. J. E., Nagamine, K. et al. (1998). A common mutation in Sardinian autoimmune polyendocrinopathy-candidiasis-ectodermal dystrophy patients. *Hum. Genet.* **103**, 428-434. doi:10.1007/s004390050846

Rossi, S. W., Kim, M.-Y., Leibbrandt, A., Parnell, S. M., Jenkinson, W. E., Glanville, S. H., McConnell, F. M., Scott, H. S., Penninger, J. M., Jenkinson, E. J. et al. (2007). RANK signals from CD4(+)3(–) inducer cells regulate development of Aire-expressing epithelial cells in the thymic medulla. *J. Exp. Med.* **204**, 1267-1272. doi:10.1084/jem.20062497

Schaller, C. E., Wang, C. L., Beck-Engeser, G., Goss, L., Scott, H. S., Anderson, M. S. and Wabl, M. (2008). Expression of aire and the early wave of apoptosis in spermatogenesis. *J. Immunol.* **180**, 1338-1343. doi:10.4049/jimmunol.180.3.1338

Seet, C. S., He, C., Bethune, M. T., Li, S., Chick, B., Gschweng, E. H., Zhu, Y., Kim, K., Kohn, D. B., Baltimore, D. et al. (2017). Generation of mature T cells from human hematopoietic stem and progenitor cells in artificial thymic organoids. *Nat. Methods* **14**, 521-530. doi:10.1038/nmeth.4237

Sekai, M., Hamazaki, Y. and Minato, N. (2014). Medullary thymic epithelial stem cells maintain a functional thymus to ensure lifelong central T cell tolerance. *Immunity* **41**, 753-761. doi:10.1016/j.immuni.2014.10.011

Shichkin, V. P., Gorbach, O. I., Zuieva, O. A., Grabchenko, N. I., Aksyonova, I. A. and Todurov, B. M. (2017). Effect of cryopreservation on viability and growth efficiency of stromal-epithelial cells derived from neonatal human thymus. *Cryobiology* **78**, 70-79. doi:10.1016/j.cryobiol.2017.06.010

Simpson, C. L., Patel, D. M. and Green, K. J. (2011). Deconstructing the skin: cytoarchitectural determinants of epidermal morphogenesis. *Nat. Rev. Mol. Cell Biol.* **12**, 565-580. doi:10.1038/nrm3175

Skogberg, G., Lundberg, V., Berglund, M., Gudmundsdottir, J., Telemo, E., Lindgren, S. and Ekwall, O. (2015). Human thymic epithelial primary cells produce exosomes carrying tissue-restricted antigens. *Immunol. Cell Biol.* **93**, 727-734. doi:10.1038/icb.2015.33

Soh, C.-L., Giudice, A., Jenny, R. A., Elliott, D. A., Hatzistavrou, T., Micallef, S. J., Kianizad, K., Seach, N., Zúñiga-Pflücker, J. C., Chidgey, A. P. et al. (2014). FOXN1GFP/w reporter hESCs enable identification of integrin-β4, HLA-DR, and EpCAM as markers of human PSC-derived FOXN1^{+} thymic epithelial progenitors. *Stem Cell Rep.* **2**, 925-937. doi:10.1016/j.stemcr.2014.04.009

Stark, H.-J., Willhauck, M. J., Mirancea, N., Boehnke, K., Nord, I., Breitkreutz, D., Pavesio, A., Boukamp, P. and Fusenig, N. E. (2004). Authentic fibroblast matrix in dermal equivalents normalises epidermal histogenesis and dermoepidermal junction in organotypic co-culture. *Eur. J. Cell Biol.* **83**, 631-645. doi:10.1078/0171-9335-00435

Stark, H.-J., Boehnke, K., Mirancea, N., Willhauck, M. J., Pavesio, A., Fusenig, N. E. and Boukamp, P. (2006). Epidermal homeostasis in long-term scaffold-enforced skin equivalents. *J. Investig. Dermatol. Symp. Proc.* **11**, 93-105. doi:10.1038/sj.jidsymp.5650015

Stolarski, B., Pronicka, E., Korniszewski, L., Pollak, A., Kostrzewa, G., Rowińska, E., Włodarski, P., Skórka, A., Gremida, M., Krajewski, P. et al. (2006). Molecular background of polyendocrinopathy-candidiasis-ectodermal dystrophy syndrome in a Polish population: novel AIRE mutations and an estimate of disease prevalence. *Clin. Genet.* **70**, 348-354. doi:10.1111/j.1399-0004.2006.00690.x

Stritesky, G. L., Jameson, S. C. and Hogquist, K. A. (2012). Selection of self-reactive T cells in the thymus. *Annu. Rev. Immunol.* **30**, 95-114. doi:10.1146/annurev-immunol-020711-075035

Su, M. A., Giang, K., Zumer, K., Jiang, H., Oven, I., Rinn, J. L., DeVoss, J. J., Johannes, K. P. A., Lu, W., Gardner, J. et al. (2008). Mechanisms of an autoimmunity syndrome in mice caused by a dominant mutation in Aire. *J. Clin. Invest.* **118**, 1712-1726. doi:10.1172/JCI34523

Su, M. A., Hu, R., Jin, J., Yan, Y., Song, Y., Sullivan, R. and Lai, L. (2015). Efficient *in vitro* generation of functional thymic epithelial progenitors from human embryonic stem cells. *Sci. Rep.* **5**, 1-8. doi:10.1038/srep09882

Sun, X., Xu, J., Lu, H., Liu, W., Miao, Z., Sui, X., Liu, H., Su, L., Du, W., He, Q. et al. (2013). Directed differentiation of human embryonic stem cells into thymic epithelial progenitor-like cells reconstitutes the thymic microenvironment In Vivo. *Cell Stem Cell* **13**, 230-236. doi:10.1016/j.stem.2013.06.014

Tajima, A., Pradhan, I., Trucco, M. and Fan, Y. (2016). Restoration of thymus function with bioengineered thymus organoids. *Curr. Stem Cell Rep.* **2**, 128-139. doi:10.1007/s40778-016-0040-x

Takaba, H., Morishita, Y., Tomofuji, Y., Danks, L., Nitta, T., Komatsu, N., Kodama, T. and Takayanagi, H. (2015). Fezf2 orchestrates a thymic program of self-antigen expression for immune tolerance. *Cell* **163**, 975-987. doi:10.1016/j.cell.2015.10.013

Takahama, Y. (2006). Journey through the thymus: stromal guides for T-cell development and selection. *Nat. Rev. Immunol.* **6**, 127-135. doi:10.1038/nri1781

Takahashi, K. and Yamanaka, S. (2006). Induction of pluripotent stem cells from mouse embryonic and adult fibroblast cultures by defined factors. *Cell* **126**, 663-676. doi:10.1016/j.cell.2006.07.024

Teh, C. E., Daley, S. R., Enders, A. and Goodnow, C. C. (2010). T-cell regulation by casitas B-lineage lymphoma (Cblb) is a critical failsafe against autoimmune disease due to autoimmune regulator (Aire) deficiency. *Proc. Natl. Acad. Sci. USA* **107**, 14709-14714. doi:10.1073/pnas.1009209107

Thorpe, E. S. (1929). Chronic tetany and chronic mycelial stomatitis in a child aged four and one-half years. *Arch. Pediatr. Adolesc. Med.* **38**, 328. doi:10.1001/archpedi.1929.01930080104011

Träger, U., Sierro, S., Djordjevic, G., Bouzo, B., Khandwala, S., Meloni, A., Mortensen, M. and Simon, A. K. (2012). The immune response to melanoma is limited by thymic selection of self-antigens. *PLoS ONE* **7**, e35005. doi:10.1371/journal.pone.0035005

Trebušak Podkrajšek, K., Bratanič, N., Kržišnik, C. and Battelino, T. (2005). Autoimmune regulator-1 messenger ribonucleic acid analysis in a novel intronic mutation and two additional novel *AIRE* gene mutations in a cohort of autoimmune polyendocrinopathy-candidiasis-ectodermal dystrophy patients. *J. Clin. Endocrinol. Metab.* **90**, 4930-4935. doi:10.1210/jc.2005-0418

Ulinski, T., Perrin, L., Morris, M., Houang, M., Cabrol, S., Grapin, C., Chabbert-Buffet, N., Bensman, A., Deschênes, G. and Giurgea, I. (2006). Autoimmune polyendocrinopathy-candidiasis-ectodermal dystrophy syndrome with renal failure: impact of posttransplant immunosuppression on disease activity. *J. Clin. Endocrinol. Metab.* **91**, 192-195. doi:10.1210/jc.2005-1538

Ulyanchenko, S., O'Neill, K. E., Medley, T., Farley, A. M., Vaidya, H. J., Cook, A. M., Blair, N. F. and Blackburn, C. C. (2016). Identification of a bipotent epithelial progenitor population in the adult thymus. *Cell Rep.* **14**, 2819-2832. doi:10.1016/j.celrep.2016.02.080

Villalón-García, I., Álvarez-Córdoba, M., Suárez-Rivero, J. M., Povea-Cabello, S., Talaverón-Rey, M., Suárez-Carrillo, A., Munuera-Cabeza, M. and Sánchez-Alcázar, J. A. (2020). Precision medicine in rare diseases. *Diseases* **8**, 42. doi:10.3390/diseases8040042

Villasenor, J., Benoist, C. and Mathis, D. (2005). AIRE and APECED: molecular insights into an autoimmune disease. *Immunol. Rev.* **204**, 156-164. doi:10.1111/j.0105-2896.2005.00246.x

Villegas, J. A., Gradolatto, A., Truffault, F., Roussin, R., Berrih-Aknin, S., Le Panse, R. and Dragin, N. (2018). Cultured human thymic-derived cells display medullary thymic epithelial cell phenotype and functionality. *Front. Immunol.* **9**, 1663. doi:10.3389/fimmu.2018.01663

Wakkach, A., Guyon, T., Bruand, C., Tzartos, S., Cohen-Kaminsky, S. and Berrih-Aknin, S. (1996). Expression of acetylcholine receptor genes in human thymic epithelial cells: implications for myasthenia gravis. *J. Immunol. Baltim. Md* **157**, 3752-3760.

Winer, K. K., Sinaii, N., Peterson, D., Sainz, B. and Cutler, G. B. (2008). Effects of once versus twice-daily parathyroid hormone 1–34 therapy in children with hypoparathyroidism. *J. Clin. Endocrinol. Metab.* **93**, 3389-3395. doi:10.1210/jc.2007-2552

Yang, S., Fujikado, N., Kolodin, D., Benoist, C. and Mathis, D. (2015). Immune tolerance. Regulatory T cells generated early in life play a distinct role in maintaining self-tolerance. *Science* **348**, 589-594. doi:10.1126/science.aaa7017

Yeap, B. B., Grossmann, M., McLachlan, R. I., Handelsman, D. J., Wittert, G. A., Conway, A. J., Stuckey, B. G., Lording, D. W., Allan, C. A., Zajac, J. D et al. (2016). Endocrine Society of Australia position statement on male hypogonadism : assessment and indications for testosterone therapy. *Med. J. Aust.* **205**, 173-178. doi:10.5694/mja16.00393

Zlotogora, J. and Shapiro, M. S. (1992). Polyglandular autoimmune syndrome type I among Iranian Jews. *J. Med. Genet.* **29**, 824-826. doi:10.1136/jmg.29.11.824